P. E. El'yasberg

Introduction to the
THEORY OF FLIGHT OF
ARTIFICIAL EARTH SATELLITES

TRANSLATED FROM RUSSIAN

Series: *Mechanics of Space Flight*

P. E. EL'YASBERG

INTRODUCTION TO THE

Theory of Flight of Artificial Earth Satellites

(Vvedenie v teoriyu poleta iskusstvennykh sputnikov Zemli)

Translated from Russian

Translated by Z. Lerman

III/13/5

TABLE OF CONTENTS

iv

PREFACE

The dynamic space research programs of the Soviet Union and other countries, culminating in the launching of artificial satellites, space probes, and automatic interplanetary stations, have naturally resulted in a proliferation of various publications dealing with the theory of flight of space vehicles of all kinds. The great majority of these publications are short papers scattered in different periodicals, each discussing some limited aspect of the theory. Very few works have been published which present the theory of flight of artificial Earth satellites (or at least some of its major subdivisions) on a level suitable for the solution of practical problems. The need for a systematic exposition of this kind is very acute, since an ever increasing number of scientists and engineers in different branches of science and technology come into direct contact with fundamental problems of the theory of satellite dynamics. Furthermore, the elements of the theory of flight of space vehicles have by now been included in the curricula of some institutes of higher education.

The present book is an attempt to present the reader with a systematic treatment of the fundamental propositions of one of the principal subdivisions of the general theory of flight of artificial heavenly bodies, the theory of flight of artificial Earth satellites. The main emphasis is on the relations which should help the reader to visualize the general rules governing the coast of a satellite with its engines turned off. Continuity of presentation necessitated the inclusion of some chapters which are normally regarded as the subject matter of the classical celestial mechanics (the theory of unperturbed Kepler motion, derivation of the differential equations of perturbed motion in osculating elements). The bulk of the book, however, is concerned with various problems which are hardly ever touched upon in conventional textbooks, but which are nevertheless of great importance in the theory of flight of artificial Earth satellites. In this group we have the motion of a satellite in circular and nearly circular orbits; analysis of the alternative trajectories through two given points in space; the effect of initial firing conditions on the elements of an elliptical orbit; the effect of the Earth's flattening and aerodynamic drag on satellite motion; the influence of lunisolar perturbations on satellite orbits.

The motion of satellites in circular and nearly circular orbits constitutes the main point of interest in the book. These orbits are highly significant in the actual practice of satellite launching. The results obtained for circular and nearly circular motion are both simple and visual, greatly contributing to an overall understanding of the general laws of motion of artificial Earth satellites. It should be also kept in mind that many of the general relations describing elliptical motion cannot be used in the treatment of circular and nearly circular orbits without first being appropriately modified.

vii

INTRODUCTION

The theory of flight of artificial celestial bodies is closely related to classical celestial mechanics (or theoretical astronomy, as it is often called), one of the oldest and most highly developed branches of science. The equations which describe the coast of an artificial space vehicle (i.e., its flight with the engines turned off) are in principle identical with the equations of motion of natural celestial bodies. The theory of flight of artificial space vehicles therefore freely draws upon the results originally derived in classical celestial mechanics.

However, the scope of the theory of flight of artificial space vehicle and the methods applied for the solution of specific problems are inherently different from those of the classical celestial mechanics. Indeed, the latter is essentially a contemplative science, and its principal aim is to determine and to study the laws of motion of existing heavenly bodies. The theory of flight of artificial space vehicle, on the other hand, is an active engineering science which is concerned with the solution of the following principal problems:

    (a) choice of optimal orbits and trajectories;
    (b) determination of existing orbits;
    (c) calculation of midcourse corrections which change the established orbit.

Of the three problems above, only the second is common for both celestial mechanics and the theory of flight of artificial space vehicles. But even within this category the difference in approach between the two disciplines is pronounced. Classical celestial mechanics is primarily concerned with stationary orbits which have existed for a long time. Each orbit is investigated in its own right, as an independent phenomenon. The determination of these orbits extends over considerable periods of time, often taking as much as a few years. The artificial satellites, on the other hand, once launched move in nonstationary, short-lived orbits.

For example, most of the artificial Earth satellites are impacted after a comparatively short period (typically a few months or years). This is due mainly to the effect of air drag and the lunisolar gravitational perturbations. The theory of flight of artificial space vehicles thus operates with complex and rapidly changing orbits. The orbital calculations should therefore be completed in a very short time. Furthermore, a particular orbit is of no significance in itself: it is analyzed only from the viewpoint of the specific mission of the artificial space vehicle which moves in it.

A characteristic feature of the theory of flight of artificial space vehicles is that there we are always dealing with a great variety of alternative orbits trying to establish the optimal trajectory for the particular object that we have in mind. This involves the rapid solution of many laborious equations. All exact computations in the theory of flight of artificial space vehicles are therefore normally made on high-speed electronic computers, which

integrate numerically a fairly complete set of equations of motion of the space vehicle.

Speed of computations, however, is not enough for selecting the optimal trajectory from a multiparametric family of allowed orbits. Simple approximate relations should be found which permit rapid analysis of a variety of alternatives and help to visualize the effect of the principal parameters on the motion of the satellite. These relations reduce the number of parameters to be examined to a minimum and essentially restrict the allowed region of their variation. It is only after these simplifications that one may profitably proceed with exact calculations.

We see from the preceding that the following two approaches should be adopted in the theory of flight of artificial space vehicles: development of approximate methods of rapid and graphic analysis of the various factors influencing the motion of the vehicle and creation of exact numerical methods of orbit determination.

The classical methods of celestial mechanics are often inadequate for either purpose, since, on the one hand, they are too abstract and formalistic and, on the other hand, they are not adapted for computer work.

The present book is devoted entirely to the first of the two aspects mentioned above. Approximate formulas and techniques are discussed which permit simple and graphic evaluation of the effect of various factors on the motion of artificial Earth satellites.

Chapter 1

MOTION IN CIRCULAR ORBITS

1.1. STATEMENT OF THE PROBLEM
AND PRINCIPAL RELATIONS

Many of the artificial Earth satellites move in orbits which are close
to circular. Some of the principal features of their flight can be derived
from the theory of circular or nearly circular motion, which is most
illuminating as regards the general conclusions. It is this theory which
is developed in the present chapter. Here we shall deal with unperturbed
circular motion of a satellite. In Chapters 2 and 3 we shall consider various
perturbations of circular motion and describe the almost circular motion
resulting from these perturbations.

In our analysis of the unperturbed circular motion, we shall proceed
from the following simplifying assumptions.

1. The Earth is a sphere of radius

$$R = 6371 \text{ km.} \tag{1.1}$$

2. The Earth's gravitational pull is the only driving force on the
satellite.

3. The gravitational acceleration is invariably directed to the Earth's
center, and its magnitude g is defined by Newton's formula

$$g = \frac{\mu}{r^2}, \tag{1.2}$$

where r is the distance of the satellite from the Earth's center, μ a
coefficient equal to the gravitational constant multiplied by the Earth's mass.
With sufficient accuracy, we may take

$$\mu = 3.986 \cdot 10^5 \text{ km}^3/\text{sec}^2. \tag{1.3}$$

More exact values of the coefficients defining the terrestrial field
of gravity will be given in Chapter 12.

4. The satellite's injection velocity (the magnitude and the direction
of its initial velocity) ensures a circular orbit.

Let w be the velocity of the satellite in a circular orbit of radius r;
we call it the c i r c u l a r   v e l o c i t y of the satellite. From assumption 2
and expression (1.2) above, we have

$$\frac{w^2}{r} = \frac{\mu}{r^2}$$

and

$$w = \sqrt{\frac{\mu}{r}}.$$ (1.4)

The time required by the satellite to complete one revolution around the Earth is called the o r b i t a l   p e r i o d , or the p e r i o d   o f   r e v o l u t i o n of the satellite, P. Clearly

$$P = \frac{2\pi r}{w} = 2\pi \frac{r^{\frac{3}{2}}}{\sqrt{\mu}}.$$ (1.5)

The circular velocity w of a satellite and its orbital period P are thus functions of the distance r from the Earth's center, or equivalently of the flight altitude of the satellite above the surface of the Earth,

$$h = r - R.$$

As the flight altitude h increases, the circular velocity w decreases and the orbital period P becomes longer. Figure 1.1 plots the parameters w and P vs. h. We see from the graphs that for low-flying satellites, w and P vary between comparatively narrow limits. For $h < 2000$ km, the orbital period P does not exceed 2 hrs 7 min, and the circular velocity does not drop below 6.9 km/sec. On the other hand, we shall show in the following that prolonged existence of a satellite at heights $h < 100 - 150$ km is virtually impossible (on account of the rapidly increasing air resistance). These flight altitudes characterize the minimum allowed orbital period $P_{min} \approx 87$ min and the maximum circular velocity $w_{max} \approx 7.85$ km/sec. For satellites orbiting at altitudes $h < 2000$ km, the orbital period thus varies from 1 hr 27 min to 2 hrs 7 min, and the flight velocity from 6.9 to 7.85 km/sec.
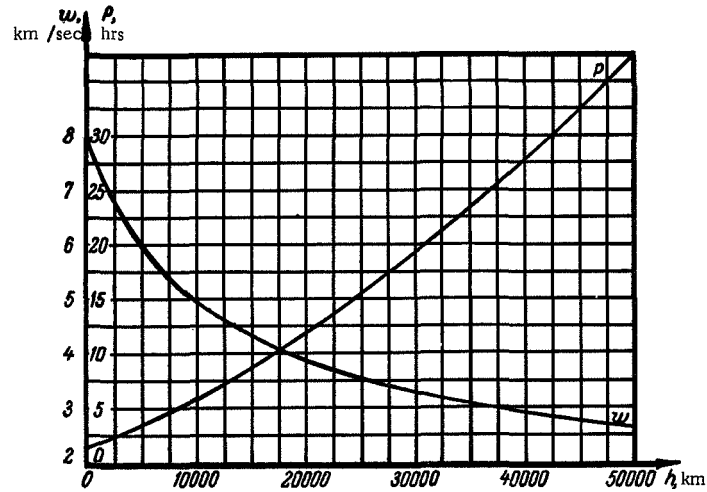
FIGURE 1.1. The orbital period P and the circular flight velocity w vs. the height h of the circular orbit.

2

Further increase in flight altitude produces a monotonic rise in orbital period. In particular, for $h = 36,000$ km, the orbital period is one sidereal day. If a satellite with this orbital period is launched along the equator in the direction of the Earth's spin, it will remain "hanging" above one point of the Earth's surface.

Let us now calculate the total mechanical energy Q which should be imparted per unit mass of the satellite in order to launch it into circular orbit from the Earth's surface. Applying relations (1.2) and (1.4), we can easily derive the following expressions for the kinetic Q_k and the potential Q_p energy per unit mass:

$$\left. \begin{array}{l} Q_k = \dfrac{w^2}{2} = \dfrac{\mu}{2r}, \\[2mm] Q_p = \displaystyle\int_R^r g\, dr = \mu\left(\dfrac{1}{R} - \dfrac{1}{r}\right). \end{array} \right\} \tag{1.6}$$

The total energy per unit mass of the satellite is

$$Q = Q_k + Q_p = \mu\left(\frac{1}{R} - \frac{1}{2r}\right). \tag{1.7}$$

The total mechanical energy of a satellite in circular orbit increases with the distance from the Earth's surface (although the flight velocity, and therefore the kinetic energy, both decrease). As the orbit recedes to infinity, its energy approaches a constant limit

$$Q_\infty = \frac{\mu}{R}. \tag{1.8}$$

From equality (1.4) we see that in this case $w = 0$, i.e., the entire mechanical energy of the satellite is concentrated as potential energy.

A satellite launched from the surface of the Earth will have the energy Q_∞ if it is fired with the initial velocity

$$V_R = \sqrt{2Q_\infty} = \sqrt{2\frac{\mu}{R}} = \sqrt{2}\, w_R, \tag{1.9}$$

where w_R is the circular velocity of the satellite for $h = 0$, i.e., for $r = R$ (this case, as we have previously observed, is unfeasible in practice, but numerically $w_R \approx 7.9$ km/sec).

In what follows we shall show that any projectile propelled with an initial velocity V_R on the Earth's surface will overcome the Earth's gravitational pull escaping to infinity along a parabolic trajectory. The parameter $V_R \approx 11.2$ km/sec is called the escape (or parabolic) velocity.

In conclusion, let us estimate the rate of change in the energy of a satellite traveling in a circular orbit as its flight altitude varies. Differentiating (1.7) and applying (1.2), we find

$$\frac{dQ}{dh} = \frac{dQ}{dr} = \frac{\mu}{2r^2} = \frac{g}{2} < 5 \text{ m/sec}^2. \tag{1.10}$$

We shall show in the following that a close satellite constantly loses height due to friction with the upper atmosphere. Its mechanical energy is

converted to heat. From (1.10) it follows that the thermal energy ΔT released as the satellite drops by Δh can be evaluated from the expression

$$\Delta T \approx \frac{G}{g_0} \frac{dQ}{dh} \Delta h = \frac{G \Delta h}{2} \frac{g}{g_0} < \frac{G \Delta h}{2},$$

where G is the weight of the satellite, and g_0 the gravitational acceleration at the surface of the Earth. Taking $G = 1$ kg and $\Delta h = 1$ km, we have $\Delta T < 500$ kgm ≈ 1.2 kcal.

It is shown in Chapter 14 that the flight altitude of a satellite diminishes comparatively slowly due to atmospheric drag. The greater part of the released heat is therefore dissipated. The temperature of the satellite hardly changes, or changes very slowly as the satellite decelerates and drops toward the Earth's surface. Abrupt heating occurs only at the very last stages of flight, when the satellite enters the dense atmosphere and starts falling rapidly.

1.2. SPACE MOTION IN A CIRCULAR ORBIT

We know from theoretical mechanics that in virtue of our assumption of a central gravitational field, the satellite orbits in one plane. We call this plane the orbital plane of the satellite (it will be shown later on that the noncentral components of the Earth's gravitational field produce a continuous variation in the orientation of the orbital plane).
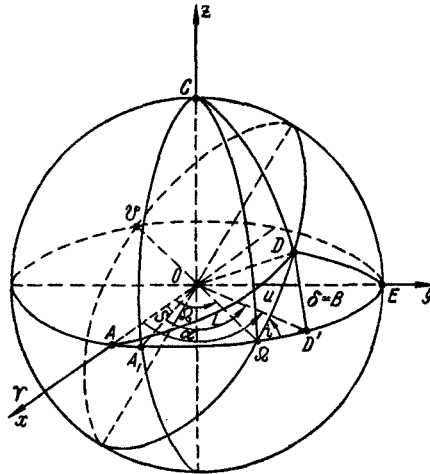
FIGURE 1.2. The elements defining the space motion of a satellite in a circular orbit.

The line of intersection of the orbital plane with the Earth's equatorial plane is called the line of nodes. The point where the orbit meets the equatorial plane as the satellite moves from south to north is the ascending node Ω. The diametrically opposite point of the orbit (relative to the Earth's center) is the descending node Υ (Figure 1.2).

4

The location of the ascending node is specified by the angle between the line $O\Omega$ and a certain fixed direction in the equatorial plane. This angle is called the l o n g i t u d e   o f   t h e   a s c e n d i n g   n o d e; it is denoted by the same symbol Ω. The longitude Ω is generally reckoned counterclockwise (viewing from the direction of the north pole) from the axis through the point of vernal equinox Υ (also known as the first point in Aries). If this definition is adopted, the longitude of the ascending node is equal to the right ascension of the point Ω /9/.

The second angle defining the orientation of the orbit is the angle i between the equatorial and the orbital planes: this is the i n c l i n a t i o n   o f   t h e   o r b i t (see Figure 1.2). The apex of the angle i is the ascending node Ω, and this angle is reckoned counterclockwise from the eastern direction on the equator. The inclination i of the orbit varies from 0 to π (when the orbital plane has rotated through an angle $i > \pi$, the ascending and the descending nodes are switched). The range $0 \leqslant i < \pi/2$ corresponds to west-east motion of the satellite, and the range $\pi/2 < i \leqslant \pi$ corresponds to east-west motion.

The position D of the satellite in orbit is defined by the angle u between the lines $O\Omega$ and OD. It is reckoned in the direction of satellite's flight. Since the flight velocity of a satellite in a circular orbit is constant, we have

$$u = \frac{2\pi}{P}(t - t_\Omega),\tag{1.11}$$

where t is the epoch, t_Ω the time of nodal passage of the satellite.

The angles Ω, i, u and the distance r of the satellite from the Earth's center fully define the satellite's position in space. The only exception is the case $i = 0$ (or π), since here the orbit is coplanar with the equator, and the node is indeterminate. To avoid this ambiguity, we take $\Omega = 0$, and the angles u are reckoned from the axis $O\Upsilon$.

As an example, let us find the position of a satellite in a spherical system of coordinates $r\alpha\delta$, where α is the right ascension of the satellite, i.e., the angle between the line $O\Upsilon$ from the Earth's center to the point of vernal equinox and the meridianal plane through the satellite (this angle is reckoned to the east from the point Υ), and δ is the declination, i.e., the angle between the line OD and the equatorial plane (positive angles are reckoned to the north from the equator). From the spherical right triangle $\Omega DD'$ (see Figure 1.2), we have

$$\left.\begin{aligned}\alpha &= \Omega + \operatorname{arctg}(\operatorname{tg} u \cos i), \\ \delta &= \arcsin(\sin u \sin i).\end{aligned}\right\}\tag{1.12}$$

From (1.12) we see that as the satellite moves in its orbit, the angle α continuously runs from 0 to 2π, while δ varies between the limits

$$\left.\begin{aligned}-i \leqslant \delta \leqslant i &\quad \text{for } 0 \leqslant i \leqslant \frac{\pi}{2}, \\ i - \pi \leqslant \delta \leqslant \pi - i &\quad \text{for } \frac{\pi}{2} \leqslant i \leqslant \pi.\end{aligned}\right\}\tag{1.13}$$

In many cases, the position of the satellite can be conveniently determined in a right-hand rectangular frame $Oxyz$, where the axis Oz points along the Earth's spin axis, and Ox is directed to the point of vernal equinox (see

Figure 1.2). Let A, E, and C be the intersection points of the axes with the sphere which has the orbit as one of its great circles. From the spherical triangles $AD\Omega, ED\Omega$, and $CD\Omega$, we have

$$\cos \widetilde{AD} = \cos \Omega \cos u - \sin \Omega \sin u \cos i,$$

$$\cos \widetilde{ED} = \sin \Omega \cos u + \cos \Omega \sin u \cos i,$$

$$\cos \widetilde{CD} = \sin u \sin i,$$

whence

$$
\left.
\begin{aligned}
x &= r(\cos \Omega \cos u - \sin \Omega \sin u \cos i), \\
y &= r(\sin \Omega \cos u + \cos \Omega \sin u \cos i), \\
z &= r \sin u \sin i, \\
v_x &= \dot{x} = v_r(\cos \Omega \cos u - \sin \Omega \sin u \cos i) - \\
&\quad - v_u(\cos \Omega \sin u + \sin \Omega \cos u \cos i), \\
v_y &= \dot{y} = v_r(\sin \Omega \cos u + \cos \Omega \sin u \cos i) - \\
&\quad - v_u(\sin \Omega \sin u - \cos \Omega \cos u \cos i), \\
v_z &= \dot{z} = v_r \sin u \sin i + v_u \cos u \sin i,
\end{aligned}
\right\}
\tag{1.14}
$$

where x, y, z are the coordinates of the satellite, r the radius of the orbit, v_x, v_y, v_z the projections of the current velocity vector on the coordinate axes, $v_r = \dot{r}$ and $v_u = r\dot{u}$ are the projections of this vector on the radius r and the in-plane normal to this radius, respectively. For a circular orbit,

$$v_r = 0, \quad v_u = \omega.$$

From (1.4), (1.5), (1.11), and (1.14) it follows that the position and the velocity of a satellite in a circular orbit can be determined at any time if the following four parameters are known: the longitude Ω of the ascending node, the inclination i of the orbit, the time t_Ω of nodal passage, and the orbital period P (or the radius r of the orbit). These parameters, which fully describe a circular orbit, will be called the o r b i t a l e l e m e n t s . Note that motion in circular orbit is a particular case of space motion of a point mass in a given force field. This general motion, as we know, is described by a sixth-order system of ordinary differential equations, and it is therefore defined by six independent parameters (e. g., the initial conditions). In our case, the two missing parameters are derived from the conditions of circular orbit. The flight velocity is determined from (1.4), and the direction of the velocity vector is found from the condition that it is directed at right angles to the vertical at the given point of the orbit.

1.3. MOTION RELATIVE TO THE ROTATING EARTH

The foregoing relations define the motion of a satellite relative to a fixed ("absolute") frame of reference. The earthbound observer, however, is more concerned with the motion relative to the geocentric system of axes which rotates with the Earth. We therefore introduce a spherical system of coordinates hBL, where h is the flight altitude of the satellite

above the Earth's surface, B the geocentric latitude of the point D occupied by the satellite at the given time, and L the longitude of this point to the east from the Greenwich meridian. Let A_1 (see Figure 1.2) be the point where the Greenwich meridian meets the equator, and S the angle AOA_1. Note that this angle is equal to the sidereal time on the Greenwich meridian /9/, and it can be determined from the relation

$$S = S_0 + \Omega t,$$

where S_0 is the sidereal time at a certain Greenwich midnight (according to the Astronomical Almanac), $\Omega = 7.29211 \cdot 10^{-5}$ sec^{-1} is the angular velocity of the Earth's spin, and t the time which has elapsed from that standard midnight.

Applying this equality, we write

$$h = r - R, \quad B = \delta, \quad L = \alpha - (S_0 + \Omega t). \tag{1.15}$$

From (1.15), making use of (1.11) and (1.12), we can plot the projection of the satellite's orbit on the surface of the Earth (i.e., the locus of ground points where the satellite is observed in zenith). This projection is called the g r o u n d t r a c k o f t h e s a t e l l i t e . Its shape is entirely specified by the parameters i and P. Any variation in the other orbital elements (Ω and t_Ω) only produces a certain displacement of the ground track in latitude, and also shifts the satellite's projection along the track.
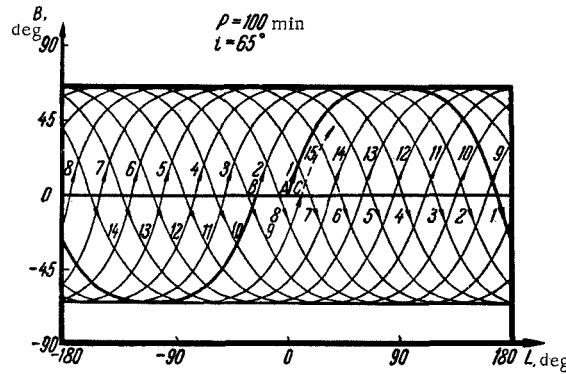
FIGURE 1.3. The ground track of a satellite moving in a circular orbit with $P = 100$ min and $i = 65°$.

Figures 1.3 — 1.7 depict various ground tracks. The abscissa marks the longitude of the satellite's projection on the ground, and the ordinate gives the latitude. Figure 1.3 shows the ground track of a satellite with an orbital period $P = 100$ min and inclination $i = 65°$. The bold trajectory is the projection of the first circuit of revolution (a circuit is the part of the orbit corresponding to one complete revolution of the satellite around the Earth; the origin of each circuit is identified with the passage of the satellite

7

across the equator). The distance in longitude between the first A and
the last B points of this circuit is equal to the angle through which the Earth
rotates during one revolution. It is found from the equality

$$\Delta L = 2\pi \frac{P}{P_s} = P\Omega, \tag{1.16}$$

where P_s is the sidereal day /9/.

The distance ΔL is the displacement of the satellite in
longitude during one circuit of revolution. This displacement
is reckoned from east to west, i.e., in the direction of decreasing eastern
longitude.

Note that the actual ΔL is somewhat different from the displacement
defined by (1.16). This is attributable to the continuous movement of the
orbital plane in the Earth's noncentral field of gravity. It will be shown
in the following that the resulting relative change in ΔL does not exceed
$1 - 1.5\%$.

All the subsequent circuits of the ground track can be obtained by
successively moving the first track from east to west by amounts of ΔL.
In Figure 1.3 the upper-row figures are the numbers of the ascending
circuit branches (i.e., the parts of the corresponding circuits with the
satellite traveling from south to north), while the lower-row figures
are the numbers of the descending branches (with the satellite moving from
north to south).

Let N be the nearest whole number corresponding to the formula

$$N \approx \frac{2\pi}{\Delta L} \approx \frac{P_s}{P}. \tag{1.17}$$

For the case depicted in Figure 1.3, $N = 14$. From (1.17) it follows
that the satellite completes N circuits approximately in one day. N is
therefore called the diurnal number of circuits. For low-altitude
satellites $(h < 2000 \text{ km})$, the diurnal circuit number varies from 12 to 17.
At the beginning of circuit $N + 1$, (point C in Figure 1.3), the satellite is
clearly nearest to its point of origin A. The distance in longitude between
the points A and C is the diurnal displacement of the orbit
ΔL_d; it is calculated from the equality

$$\Delta L_d = 2\pi - N\Delta L.$$

Positive ΔL_d correspond to increasing eastern longitude, and negative
to decreasing eastern longitude. From the definition of N, we have

$$|\Delta L_d| \leqslant \frac{\Delta L}{2}.$$

All the circuits from $N + 1$ to $2N$, inclusive, can obviously be obtained
from the first N circuits if these are displaced in longitude by ΔL_d. An
additional displacement by the same amount gives the satellite circuits
from $2N + 1$ to $3N$, etc. If the ratio $\frac{2\pi}{\Delta L}$ is an integer, we have

8

$\Delta L_d = 0$, and the satellite returns to the point of origin approximately* after one day. If this ratio is a rational fraction

$$\frac{2\pi}{\Delta L} = \frac{n}{m},$$

where n and m are whole numbers, the satellite returns to the point of origin having completed n circuits, i.e., approximately after m days.

In the general case of an irrational $\frac{2\pi}{\Delta L}$ the satellite never returns to the point of origin. The ground track eventually covers the entire belt between the latitudes

$$-i \leqslant B \leqslant i \qquad \text{for} \quad 0 \leqslant i \leqslant \frac{\pi}{2},$$

$$i - \pi \leqslant B \leqslant \pi - i \quad \text{for} \quad \frac{\pi}{2} \leqslant i \leqslant \pi.$$

The ground track shown in Figure 1.3 corresponds to a comparatively small orbital period $(P \ll 0.5\,P_s)$. If the orbital period is increased substantially, the ground track geometry changes. Figures 1.4 − 1.7 depict ground tracks for the same inclination $i = 65°$ (west-east flight) and comparatively long orbital periods. In Figure 1.4, the curve AB is the ground track of the first circuit of revolution with $\Delta L = \pi\,(P \approx 0.5 P_s)$. Figure 1.5 is the ground track of several orbital circuits with $P = 20\,\text{hrs}$. The displacement per circuit in this case lies in the interval

$$\pi < \Delta L < 2\pi,$$

and, as we see from Figure 1.5, the terminal point B of the first circuit is to the east of the point of origin A.

For the ground track in Figure 1.6 (orbital period $P = 30\,\text{hrs}$), we have

$$2\pi < \Delta L < 3\pi.$$

In this case the orbit moves from east to west (as for small orbital periods), but the ground tracks of the successive circuits are looped.

As the orbital period is further increased, the northern and the southern loops of the track gradually diminish, and eventually they disappear. In Figure 1.4, the curve $A_1 B_1$ is the ground track with $\Delta L = 4\pi$ $(P \approx 2P)$.

The curve $A_2 B_2$ in Figure 1.4 deserves special mention: it is the ground track with $\Delta L = 2\pi$ $(P \approx P_s)$. We see that this satellite retraces a stationary "figure-of-eight" track. This "figure-of-eight" contracts in latitude as the inclination i decreases. For $i = 0$, the track reduces to a single point. Note that this orbit can be realized only if the orbital period remains constant with a very high accuracy. Active correction of the orbit should therefore be continuously applied if a satellite is to remain for any length of time over one region.

The shape of the ground track varies, not only with the period P, but

---

* The qualification "approximately" is essential, since equality (1.17) is approximate.
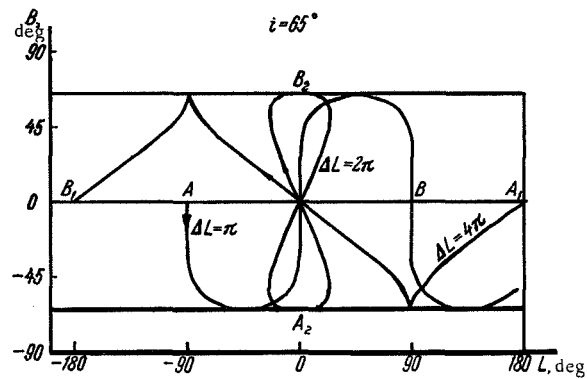
FIGURE 1.4. Ground tracks of satellites in circular orbits with $i = 65°$ for $\Delta L = \pi, 2\pi, 4\pi$.
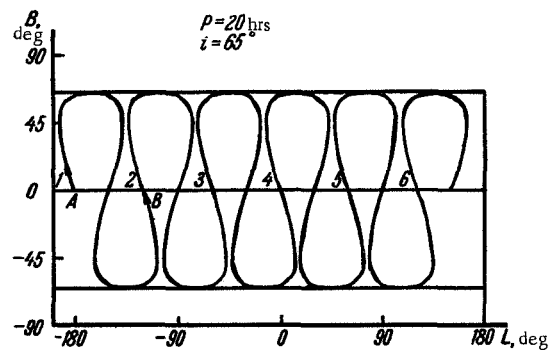
FIGURE 1.5. Ground track of a satellite in a circular orbit with $P = 20$ hrs and $i = 65°$.
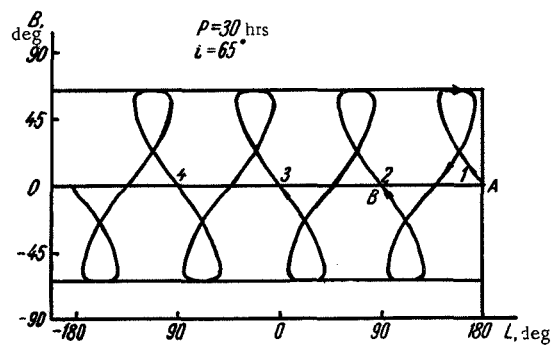
FIGURE 1.6. Ground track of a satellite in a circular orbit with $P = 30$ hrs and $i = 65°$.

10

also with the inclination i. For east-west flight $\left(\frac{\pi}{2} < i < \pi\right)$, we no longer have the characteristic eastward-moving looped tracks. As an example, Figure 1.7 shows a ground track for $P = 30\,\text{hrs}$, $i = 115°$. The satellite
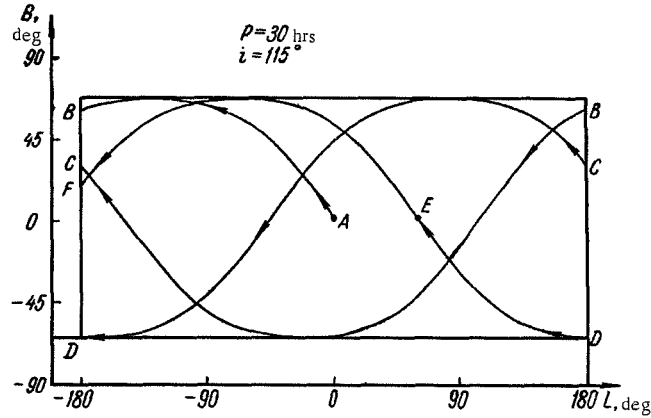
FIGURE 1.7. The ground track of a satellite in a circular orbit with $P = 30\,\text{hrs}$ and $i = 115°$.

successively covers the points $ABCDEF$ (the interval from A to E corresponds to a single circuit of revolution). Comparison of Figures 1.6 and 1.7 shows that changing over from $i = 65°$ to $i = 115° = 180° - 65°$ radically alters the ground track of the satellite.

11

Chapter 2

SMALL PERTURBATIONS OF CIRCULAR ORBITS

2.1. STATEMENT OF THE PROBLEM

In Chapter 1 we considered the principal features of motion in circular
orbit proceeding from the simplifying assumptions of Sec. 1.1. In reality,
however, these assumptions are never satisfied exactly, so that the actual
orbit always deviates from the ideal circular. The deviations are produced
by various perturbations, which fall in the following groups.

1. Deviation of the initial flight conditions from the ideal conditions
specifying motion in circular orbit.

2. Additional forces acting on the satellite in orbit. These mainly
include the aerodynamic drag in the upper atmosphere, the noncentral
components of the Earth's gravitational field, the pull of the Sun, the Moon,
and the planets, electrodynamic forces arising as the satellite moves in the
Earth's magnetic field, solar radiation pressure.

3. Forces contributed by the payload. These forces are connected with
the peculiarities of mass distribution in the satellite.

The foregoing factors produce substantial distortions in the satellite
orbit, and in some cases they may entirely change the character of motion.
This occurs either if the deviation in the initial conditions is excessive,
or if the perturbation forces are comparable with the Earth's pull (e. g.,
when the satellite enters dense atmospheric layers, approaches the Moon,
moves through the region of space where the gravitational pull of the Sun
balances the Earth's pull, or is subjected to midcourse thrust, etc.).
Small perturbation forces may also cause substantial disturbances if they
act systematically for a sufficiently long time. However, in various cases
which are of considerable applied significance, the orbit is nearly circular
despite the perturbations, and it can be analyzed (at least qualitatively)
by means of the linearized equations of motion. In the present chapter
we shall confine the discussion to this comparatively simple case. Problems
relating to highly distorted orbits will be considered in subsequent chapters.

2.2. EQUATIONS OF PERTURBED MOTION

We shall operate in the cylindrical coordinates *ruz*, where *r* is the
distance from the Earth's center to the projection of the satellite on the
normal, unperturbed orbital plane, *u* the angle reckoned in the normal
orbital plane in the direction of satellite flight from a certain fixed axis *Ox*,

z the vertical distance from the normal orbital plane to the satellite. The satellite, viewed in the direction of increasing , appears to move clockwise. The passage of the satellite through the point with $u = 0$ is regarded as the starting time, $t = 0$ (Figure 2.1).
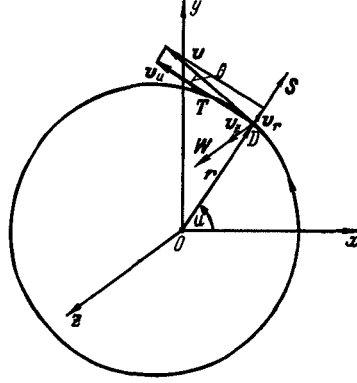
FIGURE 2.1. Cylindrical system of coordinates connected with the satellite's position in orbit.

By perturbing acceleration we shall mean the total acceleration caused by the various forces on the satellite, with the exception of the Earth's normal pull, defined in Sec. 1.1. Let S, T and W be the projections of the perturbing acceleration on the continuation of the radius-vector r, on the in-plane normal (i.e., the direction perpendicular to the radius-vector in the unperturbed normal orbital plane), and on the axis z, respectively (Figure 2.1). Then, assuming a small $\frac{z}{r}$ ratio and ignoring all terms of second order of smallness, we may write for the equations of motion of the satellite in cylindrical coordinates /28/

$$
\left.
\begin{aligned}
S - g &= \ddot{r} - r\dot{u}^2, \\
T &= \frac{1}{r}\frac{d}{dt}(r^2\dot{u}), \\
W &= \ddot{z} + g\frac{z}{r},
\end{aligned}
\right\}
\tag{2.1.}
$$

where g is the Earth's normal gravitational acceleration calculated from (1.2). (Dots will henceforth denote the time derivatives of scalar or vector functions: $\dot{r} = \frac{dr}{dt}$, $\ddot{r} = \frac{d^2r}{dt^2}$, $\dddot{r} = \frac{d^3r}{dt^3}$, etc.)

As we have previously observed, we shall only consider the case of small perturbing accelerations S, T, W (small in comparison with the normal gravitational acceleration g of the Earth) and small deviations from circular motion (small in comparison with r and w). The reciprocal influence of orbital perturbations on S, T, W is ignored to terms of the first order of smallness, and the perturbing accelerations are defined on this approximation as corresponding to the normal circular orbit, where the coordinates and the velocity components are known functions of flight

time. The first two equations in (2.1) are thus integrated independently of the third equation, since the accelerations S and T, to terms of the first order of smallness, do not depend on the lateral displacement z.

Let

$$v_r = \dot{r} \quad \text{and} \quad v_u = r\dot{u}$$

be the projections of the velocity vector on the continuation of the radius-vector r and on the normal to the radius-vector in the unperturbed orbital plane. Inserting these quantities in the first two equations in (2.1), and also substituting (1.2), we find after simple manipulations

$$
\left.
\begin{aligned}
\dot{v}_r &= S - \frac{\mu}{r^3} + \frac{v_u^2}{r}, \\
\dot{v}_u &= T - \frac{v_r v_u}{r}, \\
\dot{r} &= v_r.
\end{aligned}
\right\}
\tag{2.2}
$$

This set of three differential equations in the variables r, v_r, and v_u is not integrable in a finite form for arbitrary perturbing accelerations S and T (the solution of this set for $S = T = 0$ will be found in Chapter 4). To find an approximate solution of the set (2.2), we assume that the principal characteristics of the satellite's motion over the relevant periods do not deviate much from the corresponding characteristics of motion in a certain circular orbit of radius r_0 (in the following we shall call it the unperturbed or normal orbit, in distinction from the perturbed orbit that we seek). Let Δr, Δu, Δv_r, and Δv_u denote the variations in the corresponding quantities which differentiate between the normal and the perturbed orbits. Clearly,

$$
\left.
\begin{aligned}
r &= r_0 + \Delta r, \\
v_r &= \Delta v_r, \\
v_u &= w + \Delta v_u, \\
\dot{v}_u &= \Delta \dot{v}_u,
\end{aligned}
\right\}
\tag{2.3}
$$

where w is the velocity of the satellite in unperturbed circular orbit.

Note that for the unperturbed orbit the first equation in (2.2) takes the form

$$0 = -\frac{\mu}{r_0^2} + \frac{w^2}{r_0}. \tag{2.4}$$

Substituting (2.3) in (2.2), we subtract (2.4) from the first of the three equations. Then, applying (1.4) and assuming small $\Delta r, \Delta v_r$, and Δv_u, we may write (to within terms of the first order of smallness)

$$
\left.
\begin{aligned}
\Delta \dot{v}_r - 2\lambda \Delta v_u - \lambda^2 \Delta r &= S, \\
\Delta \dot{v}_u + \lambda \Delta v_r &= T, \\
\Delta \dot{r} - \Delta v_r &= 0,
\end{aligned}
\right\}
\tag{2.5}
$$

14

where λ is the angular velocity of the satellite in normal circular orbit, defined as

$$\lambda = \frac{w}{r_0}.$$ (2.6)

We now have a set of three linear differential equations with constant coefficients in the unknowns Δr, Δv_r, and Δv_u. We shall show that the solution of this set reduces to the solution of one second-order linear differential equation and one quadrature. Take the third equation in (2.5)

$$\Delta v_r = \Delta \dot{r}$$ (2.7)

and insert it in the second equation in (2.5). Integrating, we have

$$\Delta v_u = \int_0^t T \, dt - \lambda \Delta r + C,$$ (2.8)

where C is a constant.

Substituting (2.7) and (2.8) in the first equation in (2.5), we obtain the final equation for Δr:

$$\Delta \ddot{r} + \lambda^2 \Delta r = F,$$ (2.9)

where

$$F = 2\lambda \left(\int_0^t T \, dt + C \right) + S.$$ (2.9')

The general solution of this equation has the form

$$\Delta r = A \sin \lambda t + B \cos \lambda t + \frac{1}{\lambda} \int_0^t F(\xi) \sin \lambda (t - \xi) \, d\xi,$$ (2.10)

where A and B are constants.

Applying (2.9'), we have

$$\frac{1}{\lambda} \int_0^t F(\xi) \sin \lambda (t - \xi) \, d\xi = 2 \int_0^t \sin \lambda (t - \xi) \, d\xi \int_0^\xi T(\eta) \, d\eta +$$

$$+ \frac{1}{\lambda} \int_0^t S(\xi) \sin \lambda (t - \xi) \, d\xi + \frac{2C}{\lambda} (1 - \cos \lambda t).$$ (2.11)

Seeing that

$$\sin \lambda (t - \xi) = \frac{1}{\lambda} \frac{d}{d\xi} \cos (t - \xi)$$

we now integrate by parts the first term in the right-hand side of (2.11). We find

$$\frac{1}{\lambda} \int_0^t F(\xi) \sin \lambda (t - \xi) \, d\xi = \frac{2}{\lambda} \int_0^t T(\xi) [1 - \cos \lambda (t - \xi)] \, d\xi +$$

$$+ \frac{1}{\lambda} \int_0^t S(\xi) \sin \lambda (t - \xi) \, d\xi + \frac{2C}{\lambda} (1 - \cos \lambda t).$$

15

Substituting in (2.10), we have

$$\Delta r = A \sin \lambda t + B_1 \cos \lambda t + \frac{2C}{\lambda} +$$

$$+ \frac{2}{\lambda} \int_0^t T(\xi)[1 - \cos \lambda(t - \xi)]\, d\xi +$$

$$+ \frac{1}{\lambda} \int_0^t S(\xi) \sin \lambda(t - \xi)\, d\xi, \tag{2.12}$$

where

$$B_1 = B - \frac{2C}{\lambda}. \tag{2.13}$$

Let Δr_0, Δv_{r0}, and Δv_{u0} be the initial values of the corresponding perturbations. Setting $t = 0$ in (2.8) and (2.12), we obtain expressions for the constants B_1 and C. To find the constant A, we first differentiate (2.12) and then put $t = 0$. Thus,

$$\left.\begin{aligned}
C &= \Delta v_{u0} + \lambda\, \Delta r_0, \\
A &= \frac{\Delta v_{r0}}{\lambda}, \\
B_1 &= - \Delta r_0 - \frac{2\Delta v_{u0}}{\lambda}.
\end{aligned}\right\} \tag{2.14}$$

Substituting these constants in (2.12), we obtain a final expression for Δr; applying (2.7), (2.8), and (2.14), we then find Δv_r and Δv_u. Now, taking the variation of $v_u = r\dot{u}$ and applying (2.6), we find

$$\Delta \dot{u} = \frac{1}{r_0}(\Delta v_u - \lambda\, \Delta r),$$

where Δu is the perturbation in the coordinate u.

Inserting the perturbations Δv_u, Δr in the right-hand side of this equality and integrating, we find Δu. Double integrals are converted into simple integrals with the aid of the equalities

$$\int_0^t S(\xi) \sin \lambda(t - \xi)\, d\xi = \frac{1}{\lambda} \frac{d}{dt} \int_0^t S(\xi)[1 - \cos \lambda(t - \xi)]\, d\xi,$$

$$\int_0^t T(\xi)[3 - 4\cos \lambda(t - \xi)]\, d\xi = \frac{1}{\lambda} \frac{d}{dt} \int_0^t T(\xi)[3\lambda(t - \xi) - 4 \sin \lambda(t - \xi)]\, d\xi.$$

Finally, to find the displacement at right angles to the orbital plane, z, and $v_z = \dot{z}$, we take the third equation in (2.1). Seeing that the second term in the right-hand side of this equation is small, we substitute for r and g their normal, unperturbed values r_0 and $g_0 = \frac{\mu}{r_0^2}$. Making use of (1.4) and (2.6), we write

$$\ddot{z} + \lambda^2 z = W. \tag{2.15}$$

Applying the general solution (2.10) of equations of this type, we obtain the required expressions for the perturbations z and v_z.

To sum up, we have the following expressions for the various orbital perturbations:

$$\Delta r = (2 - \cos \lambda t) \Delta r_0 + \frac{\sin \lambda t}{\lambda} \Delta v_{r0} +$$

$$+ \frac{2(1 - \cos \lambda t)}{\lambda} \Delta v_{u0} + \frac{1}{\lambda} \int_0^t S(\xi) \sin \lambda (t - \xi) d\xi +$$

$$+ \frac{2}{\lambda} \int_0^t T(\xi) [1 - \cos \lambda (t - \xi)] d\xi,$$

$$\Delta v_r = \lambda \sin \lambda t \cdot \Delta r_0 + \cos \lambda t \cdot \Delta v_{r0} + 2 \sin \lambda t \cdot \Delta v_{u0} +$$

$$+ \int_0^t S(\xi) \cos \lambda (t - \xi) d\xi +$$

$$+ 2 \int_0^t T(\xi) \sin \lambda (t - \xi) d\xi,$$

$$\Delta u = \Delta u_0 - \frac{3\lambda t - 2 \sin \lambda t}{r_0} \Delta r_0 - \frac{2(1 - \cos \lambda t)}{w} \Delta v_{r0} -$$

$$- \frac{3\lambda t - 4 \sin \lambda t}{w} \Delta v_{u0} - \frac{2}{w} \int_0^t S(\xi) [1 - \cos (t - \xi)] d\xi -$$

$$- \frac{1}{w} \int_0^t T(\xi) [3\lambda (t - \xi) - 4 \sin \lambda (t - \xi)] d\xi,$$

$$\Delta v_u = - \lambda (1 - \cos \lambda t) \Delta r_0 - \sin \lambda t \cdot \Delta v_{r0} -$$

$$- (1 - 2 \cos \lambda t) \Delta v_{u0} - \int_0^t S(\xi) \sin \lambda (t - \xi) d\xi -$$

$$- \int_0^t T(\xi) [1 - 2 \cos \lambda (t - \xi)] d\xi,$$

$$z = \cos \lambda t \cdot z_0 + \frac{\sin \lambda t}{\lambda} v_{z0} +$$

$$+ \frac{1}{\lambda} \int_0^t W(\xi) \sin \lambda (t - \xi) d\xi,$$

$$v_z = - \lambda \sin \lambda t \cdot z_0 + \cos \lambda t \cdot v_{z0} +$$

$$+ \int_0^t W(\xi) \cos \lambda (t - \xi) d\xi.$$

(2.16)

In these expressions, the extra-integral terms characterize the dependence of orbital perturbations on deviations in the initial conditions, while the integrands represent the contribution from disturbing forces on the satellite.

2.3. SMALL INITIAL PERTURBATIONS

To analyze the effect of small initial perturbations Δr_0, Δv_{r0}, Δu_0, Δv_{u0}, z_0 and v_{z0}, we put $S = T = W = 0$ in (2.16) and write the resulting expressions

17

in a nondimensional form:

$$\frac{\Delta r}{r_0} = k_{11}\frac{\Delta r_0}{r_0} + k_{12}\frac{\Delta v_{r0}}{w} + k_{13}\frac{\Delta v_{u0}}{w},$$

$$\frac{\Delta v_r}{w} = k_{21}\frac{\Delta r_0}{r_0} + k_{22}\frac{\Delta v_{r0}}{w} + k_{23}\frac{\Delta v_{u0}}{w},$$

$$\frac{\Delta v_u}{w} = k_{31}\frac{\Delta r_0}{r_0} + k_{32}\frac{\Delta v_{r0}}{w} + k_{33}\frac{\Delta v_{u0}}{w},$$

$$\Delta u = k_{41}\frac{\Delta r_0}{r_0} + k_{42}\frac{\Delta v_{r0}}{w} + k_{43}\frac{\Delta v_{u0}}{w} + k_{44}\Delta u_0,$$

$$\frac{z}{r_0} = k_{55}\frac{z_0}{r_0} + k_{56}\frac{v_{z0}}{w},$$

$$\frac{v_z}{w} = k_{65}\frac{z_0}{r_0} + k_{66}\frac{v_{z0}}{w}.$$

$$(2.17)$$

Here k_{ij} $(i, j = 1, 2, \ldots, 6)$ are dimensionless coefficients defined by

$$
\begin{aligned}
&k_{11} = 2 - \cos\varphi, && k_{12} = \sin\varphi, && k_{13} = 2(1 - \cos\varphi), \\
&k_{21} = \sin\varphi, && k_{22} = \cos\varphi, && k_{23} = 2\sin\varphi, \\
&k_{31} = -(1 - \cos\varphi), && k_{32} = -\sin\varphi, && k_{33} = -(1 - 2\cos\varphi), \\
&k_{41} = -(3\varphi - 2\sin\varphi), && k_{42} = -2(1 - \cos\varphi), && k_{43} = -(3\varphi - 4\sin\varphi), \\
&k_{55} = \cos\varphi, && k_{56} = \sin\varphi, && k_{44} = 1, \\
&k_{65} = -\sin\varphi, && k_{66} = \cos\varphi,
\end{aligned}
$$

$$(2.18)$$

where $\varphi = \lambda t$ is the unperturbed u.

From these relations we see that the orbital perturbations fall in two groups.

A. Periodic perturbations, which repeat themselves after each complete revolution of the satellite (i.e., as the angle φ goes through 2π). A characteristic feature of these perturbations is that, for fairly small initial disturbances, they do not produce a substantial change in the satellite's position.

B. Secular perturbations, which increase monotonically with the angle φ (i.e., with flight time t). Even if the initial disturbances are arbitrarily small, these perturbations will eventually cause a substantial displacement of the satellite. In our case, secular perturbations occur in the angle u only, and they are attributable to a variation in the satellite's orbital period P. In the following we shall show that disturbing forces may produce secular perturbations in other coordinates also.

From the expression for the perturbations in r we see that a change in the initial conditions, in general, will result in a noncircular orbit. The corresponding small perturbations are proportional to $\sin\varphi$ and $\cos\varphi$. It can be shown that, to terms of the first order of smallness, the perturbed orbit is an ellipse, with one of its foci at the Earth's center (it will be shown in the following that the perturbed orbits resulting from a variation in the initial conditions are exact ellipses: the nearly elliptical shape of the orbit is a direct consequence of the solution being accurate only to terms of the first order of smallness).

We now proceed with a more detailed analysis of the contribution from various initial perturbations.

2.4. PERTURBATION OF THE INITIAL DISTANCE OF THE SATELLITE FROM THE EARTH'S CENTER ($\Delta r_0 > 0$)

Variation in the initial radius r_0 produces perturbations which are represented by the coefficients k_{i1} ($i = 1, 2, 3, 4$). These perturbations cause elliptical distortion of the orbit, as shown in Figure 2.2 a. The point nearest to the Earth (perigee) corresponds to the initial value $\varphi = 0$, and the point farthest from the Earth (apogee), to $\varphi = \pi$. The variations
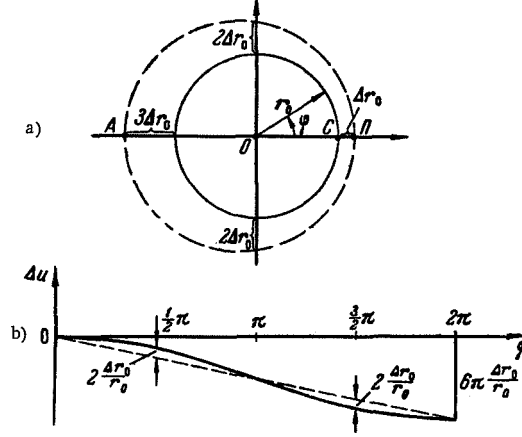
FIGURE 2.2. Perturbation of circular orbit resulting from variation of the initial distance to the gravitational center.

in flight altitude in perigee Δr_p and in apogee Δr_a are given by the equalities

$$\Delta r_p = \Delta r_0, \quad \Delta r_a = 3\Delta r_0. \tag{2.19}$$

Radial velocity perturbation Δv_r varies sinusoidally, with maxima (in absolute value) at the points $\varphi = \pi/2$ and $\varphi = 3\pi/2$. The peak magnitude of this perturbation is

$$|\Delta v_r|_{max} = \frac{w}{r_0}|\Delta r_0|. \tag{2.20}$$

The perturbation Δu along the orbit produces a systematic lag in the actual position of the satellite relative to its position in unperturbed motion. This perturbation displays a linear secular component and a sinusoidal periodic component (Figure 2.2 b). The displacement of the satellite increases by the following amount during each revolution around the Earth:

$$\Delta u (2\pi) = - 6\pi \frac{\Delta r_0}{r_0}. \tag{2.21}$$

19

Hence, applying (1.5), we obtain an expression for the rate of secular displacement $(\Delta v_\varphi)_{sec}$ of the central projection of the satellite on the normal orbit and for the variation of the orbital period ΔP:

$$\left.\begin{array}{l}(\Delta v_\varphi)_{sec} = \dfrac{r_0 \Delta u\,(2\pi)}{P} = -3w\dfrac{\Delta r_0}{r_0}, \\[2mm] \Delta P = -\dfrac{r_0 \Delta u\,(2\pi)}{w} = 3P\dfrac{\Delta r_0}{r_0}. \end{array}\right\} \qquad (2.22)$$

The perturbation Δv_u in the longitudinal velocity varies from

$$(\Delta v_u)_{min} = 0 \qquad \text{for} \quad \varphi = 0,\ 2\pi \qquad (2.23)$$

to

$$(\Delta v_u)_{max} = -2w\frac{\Delta r_0}{r_0} \quad \text{for} \quad \varphi = \pi. \qquad (2.24)$$

Note that the mean in-orbit velocity perturbation $(\Delta v_u)_m = -\dfrac{w}{r_0}\Delta r_0$ is not equal to the velocity (2.22) of secular movement along the orbit, $(\Delta v_\varphi)_{sec}$. This is so because $(\Delta v_u)_m$ is determined by the variation in the actual velocity v_u of the satellite, while $(\Delta v_\varphi)_{sec}$ represents the change in the speed of the satellite's projection on a normal circular orbit of radius r_0. Let this velocity be v_φ. Clearly,

$$v_u = r\frac{v_\varphi}{r_0}.$$

Differentiating this equality and seeing that for unperturbed orbit $r = r_0$ and $v_\varphi = w$, we have

$$\Delta v_u = \Delta v_\varphi + \frac{\Delta r}{r_0}w.$$

In particular, this equality is satisfied if Δr is replaced with the mean value

$$\Delta r_m = \frac{1}{2}(\Delta r_p + \Delta r_a) = 2\Delta r_0,$$

and Δv_u and Δv_φ with the preceding expressions for $(\Delta v_u)_m$ and $(\Delta v_\varphi)_{sec}$.

2.5. INITIAL PERTURBATION OF RADIAL VELOCITY ($\Delta v_{r0} > 0$)

A change in the initial radial velocity produces perturbations represented by the coefficients $k_{i2}\,(i = 1, 2, 3, 4)$. The orbit is distorted as shown in Figure 2.3 a. The apogee is at the point with $\varphi = \dfrac{\pi}{2}$, and the perigee at the point with $\varphi = \dfrac{3\pi}{2}$. The magnitude of the radial displacements in apogee and in perigee is

$$|\Delta r_a| = |\Delta r_p| = \frac{r_0}{w}\Delta r_{r0}. \qquad (2.25)$$

20

The radial velocity is proportional to $\cos\varphi$, and the longitudinal velocity to $\sin\varphi$. The peak magnitude of velocity perturbations is equal to the initial disturbance Δv_{r0}.
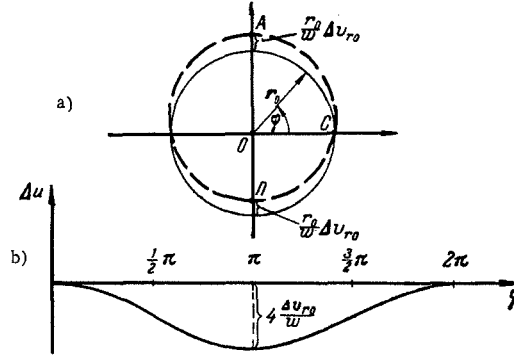
FIGURE 2.3. Perturbations of circular orbit resulting from variation of the radial velocity.

In-orbit perturbation causes a certain lag of the satellite relative to its position in the normal orbit. This displacement is periodic, and has no secular component (Figure 2.3 b). The orbital period P therefore remains unaffected. The maximum displacement of the satellite along the orbit occurs at the point $\varphi = \pi$, and it is given by the equality

$$\Delta u\,(\pi) = -4\,\frac{\Delta v_{r0}}{w}\,. \tag{2.26}$$

2.6. INITIAL PERTURBATION ALONG THE ORBIT

From (2.17) and (2.18) we see that an initial angular displacement $\Delta u_0{}'$ rotates the entire orbit around the Earth's center through the angle $\Delta u = \Delta u_0$.

Variation in the initial longitudinal velocity Δv_{u0} is represented by the coefficients k_{i3} $(i = 1, 2, 3, 4)$. For $\Delta v_{u0} > 0$, the perigee is at the point $\varphi = 0$, and the apogee at the point $\varphi = \pi$ (Figure 2.4 a). The radial displacement in perigee and in apogee is given by the equalities

$$\Delta r_p = 0 \quad \text{and} \quad \Delta r_a = 4\,\frac{r_0}{w}\,\Delta v_{u0}. \tag{2.27}$$

Radial velocity perturbation Δv_r varies sinusoidally. The peak magnitude of this perturbation is

$$\left|\Delta v_r\left(\tfrac{\pi}{2}\right)\right| = \left|\Delta v_r\left(\tfrac{3\pi}{2}\right)\right| = 2\Delta v_{u0}. \tag{2.28}$$

In-orbit perturbations have both periodic and secular components (Figure 2.4 b). Initially, the displacement Δu along the orbit has the same

21

sign as the original velocity perturbation Δv_{u0}. This displacement is maximal for $\varphi = 41°24'35''$. The corresponding maximum value of Δu is

$$\Delta u_{max} \approx 0.4776 \frac{\Delta v_{u0}}{w}.$$

The separation between the perturbed and the normal positions of the satellite subsequently decreases, and for $\varphi = 73°05'32''$, we have $\Delta u = 0$.
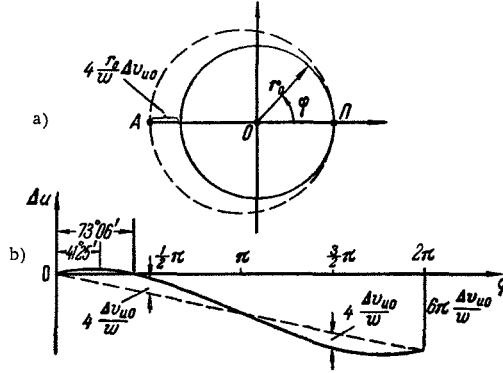
FIGURE 2.4. Perturbations of circular orbit resulting from variation of the longitudinal velocity.

Now the perturbed satellite starts lagging behind its normal position (for $\Delta v_{u0} > 0$). The lag per one circuit of revolution is

$$\Delta u (2\pi) = -6\pi \frac{\Delta v_{u0}}{w}. \tag{2.29}$$

Hence, by analogy with (2.22), we find the mean rate of secular movement of the satellite along the orbit and the change in the orbital period:

$$\left. \begin{array}{l} (\Delta v_\varphi)_{sec} = -3\Delta v_{u0}, \\ \Delta P = 3P \dfrac{\Delta v_{u0}}{w}. \end{array} \right\} \tag{2.30}$$

We see that if the initial velocity of the satellite along the orbit is perturbed, the satellite will eventually regress at a rate equal to three times the initial velocity perturbation. Later on, we shall consider the energy aspects of this seemingly paradoxical phenomenon.

The longitudinal velocity perturbation Δv_u is periodic. It is positive for $-\pi/3 < \varphi < \pi/3$ and negative for $\pi/3 < \varphi < 5\pi/3$. The extreme values of this perturbation are

$$\Delta v_u (0) = \Delta v_{u0} \quad \text{and} \quad \Delta v_u (\pi) = -3\Delta v_{u0}. \tag{2.31}$$

22

2.7. PERTURBATIONS AT RIGHT ANGLES TO THE ORBITAL PLANE

Initial disturbances at right angles to the orbital plane are periodic; they are represented by the coefficients k_{ij} ($i, j = 5, 6$). To terms of the first order of smallness, these perturbations can be shown to reduce to certain rotations of the orbital plane. Let us consider the rotation of the orbital plane through a small angle ψ (Figure 2.5) around the axis MN,
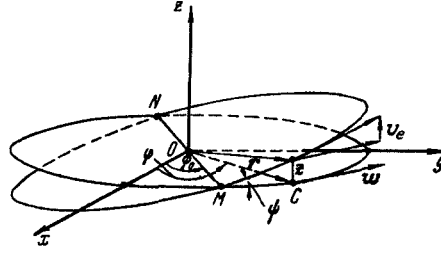
FIGURE 2.5. Initial perturbations at right angles to the plane of circular orbit.

making an angle φ_0 with the line Ox from which the angles are reckoned. Let C be a point of the unperturbed orbit whose position is specified by the angle $COx = \varphi$. The radius-vector r of this point and the corresponding velocity vector w of the satellite make angles $\varphi - \varphi_0$ and $\frac{\pi}{2} + \varphi - \varphi_0$ with the axis of orbit rotation MN. As these vectors rotate with the orbital plane, they acquire nonzero projections on the normal Oz to the unperturbed orbital plane; to terms of the first order of smallness, these orbit-plane normal components are given by

$$\left. \begin{array}{l} z = r\psi \sin(\varphi - \varphi_0), \\ v_z = w\psi \cos(\varphi - \varphi_0). \end{array} \right\} \tag{2.32}$$

Hence, applying (2.17) and (2.18), we find that the elevation z_0 of the satellite above the orbital plane corresponds to a rotation of the entire orbit around an axis through the points $\varphi = \pi/2$ and $\varphi = 3\pi/2$; the initial velocity perturbation v_{z0} similarly corresponds to a rotation of the orbital plane around an axis through $\varphi = 0$ and $\varphi = \pi$. The angles through which the orbital plane rotates around the two axes are given by

$$\psi(z_0) = \frac{z_0}{r_0} \quad \text{and} \quad \psi(v_{z0}) = \frac{v_{z0}}{w}. \tag{2.33}$$

To sum up, small perturbations Δr_0, Δv_{r0}, Δu_0, and Δv_{u0} in the initial conditions of motion distort the shape of the orbit and also cause periodic and secular displacement of the satellite along the orbit. The orbital plane, however, remains fixed. Small disturbances z_0 and v_{z0} at right angles to the orbital plane alter the orientation of this plane.

We have already remarked that secular perturbations are much more effective than periodic perturbations and, unlike the latter, they eventually produce substantial inequalities in the motion of the satellite, even if the initial disturbances are very small. As an example, let us consider the motion of a satellite in circular orbit at a height $h = 630$ km, which corresponds to $r = 7000$ km, $w \approx 7.5$ km/sec, $P = 98$ min. The initial velocity and the initial position of the satellite are slightly perturbed: $\Delta v_0 = 1$ m/sec, $= 1$ km. Table 2.1 lists the corresponding maximum magnitudes of the periodic and the secular displacements in the satellite's position resulting from variously directed initial perturbations.

TABLE 2.1.

Initial perturbations		Satellite displacement, km					Perturbation of orbital period, sec
		maximum periodic			secular, along the orbit		
description and magnitude	direction	from the Earth's center	along the orbit	at right angles to the orbital plane	per circuit	per day	
Initial velocity perturbation $\Delta v_0 = 1$ m/sec	from the Earth's center	0.9	3.7	–	–	–	–
	along the orbit	3.7	3.7	–	17.6	260	2.3
	at right angles to the orbital plane	–	–	0.9	–	–	–
Initial position perturbations $\Delta l_0 = 1$ km	from the Earth's center	3	2	–	18.8	280	2.5
	along the orbit	–	1	–	–	–	–
	at right angles to the orbital plane	–	–	1	–	–	–

This table illustrates the relation between secular and periodic displacements of the satellite. It should be borne in mind that secular displacements increase monotonically with flight time, whereas periodic deviations do not exceed the maximum values indicated in the table.

2.8. ALMOST CIRCULAR MOTION

In the preceding section we have established that small perturbations in the initial conditions cause a certain distortion of the circular orbit. The motion in this distorted orbit is almost circular or nearly circular. It follows from the preceding that this is plane motion. The motion in the orbital plane is derived by adding to the coordinates and the velocity components of the unperturbed circular orbit the corrections calculated from the first four relations in (2.16), for $S = T = W = 0$. The

principal features of almost circular motion can be established from these relations. We introduce the concept of m e a n c i r c u l a r m o t i o n, which is defined as motion in a circular orbit of some mean radius r_m. This radius is selected so that the period of revolution for the mean circular orbit is equal to the period of revolution P for the particular nearly circular orbit.

Applying (1.5), we write, to terms of the first order of smallness,

$$P = P_0 + \Delta P, \quad \Delta P = \frac{3}{2} P_0 \frac{\Delta r_m}{r_0},$$

where P_0 is the orbital period of the unperturbed orbit of radius r_0, and

$$\Delta r_m = r_m - r_0.$$

Adding up the orbital period corrections obtaining from (2.22) and (2.30), we find

$$\Delta P = 3P\left(\frac{\Delta r_0}{r_0} + \frac{\Delta v_{u0}}{w_0}\right),$$

where w_0 is the satellite's velocity in unperturbed orbit.

Comparing this expression to the foregoing equalities, we see that

$$r_m = r_0 + 2\left(\Delta r_0 + \frac{\Delta v_{u0}}{\lambda_0}\right), \tag{2.34}$$

where

$$\lambda_0 = \frac{w_0}{r_0} \tag{2.35}$$

is the angular velocity of the satellite in the normal orbit.

Let now $w_m = w_0 + \Delta w_m$ and u_m stand respectively for the flight velocity and the angular movement of the satellite in the mean circular orbit. From (1.4) we have

$$\Delta w_m = -\frac{1}{2} \lambda_0 \Delta r_m.$$

Hence, making use of (2.34), we write, to terms of the first order of smallness,

$$w_m = w_0 - \frac{1}{2} \lambda_0 (r_m - r_0) = w_0 - (\lambda_0 \Delta r_0 + \Delta v_{u0}). \tag{2.36}$$

In a circular orbit,

$$u = u_0 + \frac{w}{r} t,$$

where u_0 is the initial position angle. Varying this relation, we apply expressions (2.34)—(2.36). The motion of the satellite in the mean circular orbit is furthermore assumed to satisfy the following initial condition:

$$(u_m)_0 = \Delta u_0 - 2 \frac{\Delta v_{r0}}{w_0}.$$

In other words, the initial angle $(u_m)_0$ is determined by the time-independent terms in the right-hand side of the corresponding equation in (2.17). The final result gives

$$u_m = \Delta u_0 - 2\frac{\Delta v_{r0}}{w_0} + \varphi_0 + \left(\frac{\Delta w_m}{w_0} - \frac{\Delta r_m}{r_0}\right)\varphi_0 =$$
$$= \Delta u_0 - 2\frac{\Delta v_{r0}}{w_0} + \varphi_0 - 3\varphi_0\left(\frac{\Delta v_{u0}}{w_0} + \frac{\Delta r_0}{r_0}\right), \qquad (2.37)$$

where $\varphi_0 = \lambda_0 t$.

From (2.34), (2.36), and (2.37) it follows that

$$r_0 = r_m - 2\left(\Delta r_0 + \frac{\Delta v_{u0}}{\lambda_0}\right),$$
$$w_0 = w_m + (\lambda_0\,\Delta r_0 + \Delta v_{u0}),$$
$$\varphi_0 = u_m - \Delta u_0 + 2\frac{\Delta v_{r0}}{w_0} + 3\varphi_0\left(\frac{\Delta w_0}{w_0} + \frac{\Delta r_0}{r_0}\right).$$

We substitute these expressions, together with the first four equalities from (2.16), in the right-hand sides of the relations

$$r = r_0 + \Delta r, \quad v_r = \Delta v_{r0}, \quad u = \varphi_0 + \Delta u, \quad v_u = w_0 + \Delta w.$$

Zero perturbing accelerations are assumed $(S = T = W = 0)$. In terms defining small periodic deviations from the mean circular motion, we take

$$\varphi_0 = u_m = \varphi, \quad r_0 = r_m, \quad w_0 = w_m.$$

The resulting error is of the second order of smallness. After elementary manipulations, carried out to first order of smallness, we obtain the following equations of almost circular motion:

$$\left.\begin{array}{l} r = r_m(1 - e_1\cos\varphi - e_2\sin\varphi), \\ v_r = w_m(e_1\sin\varphi - e_2\cos\varphi), \\ u = \varphi + 2(e_1\sin\varphi - e_2\cos\varphi), \\ v_u = w_m(1 + e_1\cos\varphi + e_2\sin\varphi), \\ w_m = \sqrt{\dfrac{\mu}{r_m}}, \\ \varphi = \dfrac{w_m}{r_m}(t - t_0), \end{array}\right\} \qquad (2.38)$$

where t_0 is the time of passage of the satellite moving in the mean circular orbit (we call it the *mean satellite*) through the point of origin $u = 0$, and the parameters e_1 and e_2 are expressed in terms of the initial perturbations Δr_0, Δv_{r0}, and Δu_0:

$$e_1 = \frac{\Delta r_0}{r_0} + 2\frac{\Delta v_{u0}}{w_0}, \quad e_2 = -\frac{\Delta v_{r0}}{w_0}. \qquad (2.39)$$

Expressions (2.38) can be somewhat modified by substituting the parameters e and ω from the equalities

$$\left.\begin{array}{l} e_1 = e\cos\omega, \quad e_2 = e\sin\omega, \\ e = \sqrt{e_1^2 + e_2^2}, \quad \omega = \text{arctg}\,\dfrac{e_2}{e_1}. \end{array}\right\} \qquad (2.40)$$

This gives

$$r = r_{\mathrm{m}}[1 - e\cos(\varphi - \omega)],$$
$$v_r = w_{\mathrm{m}}e\sin(\varphi - \omega),$$
$$u = \varphi + 2e\sin(\varphi - \omega),$$
$$v_u = w_{\mathrm{m}}[1 + e\cos(\varphi - \omega)]. \tag{2.41}$$

Let v be the flight velocity of the satellite, and the angle which the velocity vector makes with the local horizon. Clearly (see Figure 2.1)

$$v = \sqrt{v_u^2 + v_r^2},$$
$$\operatorname{tg}\theta = \frac{v_r}{v_u}.$$

Applying (2.41), we may write, to terms of the first order of smallness,

$$v = v_u = w_{\mathrm{m}}[1 + e\cos(\varphi - \omega)],$$
$$\theta = e\sin(\varphi - \omega). \tag{2.42}$$

From (2.41) and (2.42) we see that the mean values of the principal characteristics of satellite motion in a nearly circular orbit are equal to the corresponding parameters for the mean circular orbit (r_{m}, $u_{\mathrm{m}} = \varphi$, $v_{\mathrm{m}} = v_{u\,\mathrm{m}} = w_{\mathrm{m}}$, $v_{r\,\mathrm{m}} = 0$, $\theta_{\mathrm{m}} = 0$).

The point of the nearly circular orbit closest to the Earth (perigee) corresponds to $\varphi = \omega$, and the farthest point (apogee), to $\varphi = \omega + \pi$. Assigning the subscripts "p" and "a" to the values of the corresponding parameters in perigee and in apogee, respectively, we write

$$r_{\mathrm{p}} = r_{\mathrm{m}}(1 - e), \qquad r_{\mathrm{a}} = r_{\mathrm{m}}(1 + e),$$
$$v_{r\mathrm{p}} = v_{r\mathrm{a}} = 0, \qquad \theta_{\mathrm{p}} = \theta_{\mathrm{a}} = 0,$$
$$v_{\mathrm{p}} = v_{u\mathrm{p}} = w_{\mathrm{m}}(1 + e), \qquad v_{\mathrm{a}} = v_{u\mathrm{a}} = w_{\mathrm{m}}(1 - e). \tag{2.43}$$

The perigee point thus corresponds to maximum velocity v, and the apogee to minimum velocity. The angle θ at these points is zero. It reaches its maximum $\theta_{\max} = e$ at the point $\varphi = \omega + \frac{\pi}{2}$ and its minimum $\theta_{\min} = -e$ at the point $\varphi = \omega + \frac{3}{2}\pi$.

From (2.41) and (2.42) we see that the magnitude of the deviations from the mean circular orbit is determined by the parameter e, whereas the position of the perigee is specified by the angle ω. The parameter e is therefore called the e c c e n t r i c i t y of the orbit, and the angle ω a r g u m e n t o f p e r i g e e .

In the analysis of nearly circular motion, it is advisable to treat the eccentricity of the orbit as a vector of magnitude e pointing along the axis $\varphi = \omega$. From (2.40) it follows that the parameters e_1 and e_2 are the projections of this vector on the directions $u = 0$ and $u = \frac{\pi}{2}$ (the axes Ox and Oy in Figure 2.1). If the coordinate system is rotated through a certain angle γ in the direction of motion of the satellite (which is always assumed to travel counterclockwise, as indicated by the choice of the axis Oz in Figure 2.1),

the eccentricity components are transformed according to the general transformation formulas for a two-dimensional vector:

$$e_1' = e_1 \cos \gamma + e_2 \sin \gamma,$$
$$e_2' = -e_1 \sin \gamma + e_2 \cos \gamma,$$

where e_1' and e_2' are the projections of the eccentricity vector on the axes of the rotated system.

Applying (2.38), we can derive the following simple relations among the parameters of satellite motion at the point $\varphi = 0$ and the components e_1 and e_2 of the eccentricity vector:

$$r(0) = r_{\mathrm{m}}(1 - e_1), \quad v_r(0) = -w_{\mathrm{m}}e_2,$$
$$u(0) = -2e_2, \qquad v_u(0) = w_{\mathrm{m}}(1 + e_1).$$

To find the parameters of space motion in nearly circular orbit, relations (2.38) and (2.41) must be supplemented with expression (1.14). In this case, it is advisable to reckon the angle u from the line joining the Earth's center with the ascending node of the orbit; the time t_0 in (2.38) should then be replaced with the time t_Ω of nodal passage of the mean satellite.

2.9. THE ELEMENTS OF ALMOST CIRCULAR ORBIT

From (1.14) and (2.41) it follows that motion in nearly circular orbit is fully defined by the following six parameters: the mean radius r_{m}, the time of mean satellite nodal passage t_Ω, the eccentricity e, the argument of perigee ω, the node Ω, the inclination i. If these parameters are known, then the coordinates and the velocity components of the satellite at any epoch can be determined. These six parameters are therefore regarded as the elements of almost circular orbit. From (2.38) we see that the eccentricity e and the argument of perigee ω can be replaced with the projections e_1 and e_2 of the eccentricity vector on two axes (in particular, the line of nodes and the line perpendicular to it). This substitution is very convenient in our case. The argument of perigee ω is expressed in terms of the ratio of two small parameters (2.40). In some cases, even for very small initial perturbations, the perigee may therefore show a substantial displacement, although the distortion of the orbit is negligible. The position of the perigee in a nearly circular orbit is therefore fairly uncertain. This uncertainty increases as the real orbit approaches the ideal circular orbit, for which the very concept of perigee is meaningless (by uncertainty in ω we mean, not the mathematical uncertainty, which obtains for an exactly circular orbit only, but practical uncertainty resulting from the inevitable errors of measurement and calculation: because of these errors, the perigee cannot be pinpointed with any accuracy). On the other hand, small variations of the orbit are always reflected in small variations of the parameters e_1 and e_2. An exactly circular orbit is characterized by well defined values of the two projections of the eccentricity vector: $e_1 = e_2 = 0$. The accuracy in the determination of these parameters therefore does not decrease as we approach the ideal circular orbit.

From (2.34) and (2.39) it follows that r_m, e_1 and e_2 are linear functions of the initial perturbations. For $i \neq 0$ it can be shown that, to terms of the first order of smallness, this is so for the other orbital elements (t_Ω, Ω, and i) also. The total distortion of the orbit under several small perturbations can therefore be found by adding the contributions from the individual perturbations. The uncertainty in the position of the node obtaining for small inclinations i can be eliminated by changing over from the equatorial plane to any other plane of reference for the definition of the orbit. As regards the parameters e and ω, they follow the rules of vector addition under compound perturbations.

The number of elements defining an almost circular orbit is equal to the number of initial conditions needed to specify the motion of a point mass in a given force field. We thus arrive at the problem of calculating the orbital elements from known initial conditions. This problem will be solved in the right-hand rectangular system of coordinates $Oxyz$, shown in Figure 1.2. Let D denote the position of the satellite at the epoch $t = t_0$, and let r_0 and v_0, respectively, be the initial radius-vector and the initial velocity vector of the satellite:

$$r_0 = x_0 i + y_0 j + z_0 k, \quad v_0 = v_{x0} i + v_{y0} j + v_{z0} k,$$

where x_0, y_0, z_0 and v_{x0}, v_{y0}, v_{z0} are the known initial values of the coordinates and the velocity components, i, j, k are the unit vectors of the triad $Oxyz$.
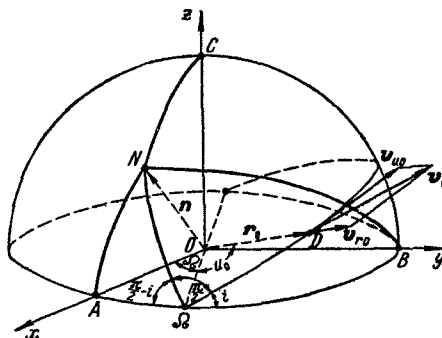
FIGURE 2.6. Determination of the node and the inclination from the initial conditions of motion.

The orbital plane is defined as the plane through r_0 and v_0. A unit vector at right angles to this plane (Figure 2.6) is correspondingly defined by the equality

$$n = \frac{r_0 \times v_0}{|r_0 \times v_0|},$$

where

$$[r_0 \times v_0] = \begin{vmatrix} i & j & k \\ x_0 & y_0 & z_0 \\ v_{x0} & v_{y0} & v_{z0} \end{vmatrix} = C_1 i + C_2 j + C_3 k,$$

$$\left. \begin{array}{l} C_1 = y_0 v_{z0} - z_0 v_{y0}, \quad C_2 = z_0 v_{x0} - x_0 v_{z0}, \\ C_3 = x_0 v_{y0} - y_0 v_{x0}. \end{array} \right\} \tag{2.44}$$

29

The projections of the vector n on the axes of the frame $Oxyz$ are therefore given by the formulas

$$n_x = \frac{C_1}{C}, \quad n_y = \frac{C_2}{C}, \quad n_z = \frac{C_3}{C},$$
$$C = \sqrt{C_1^2 + C_2^2 + C_3^2}. \tag{2.45}$$

On the other hand, these projections can be expressed in terms of the angles Ω and i. To this end, let A, B, C, N stand for the intersection points of the coordinate axes and the orbit-plane normal with a unit sphere; take the spherical triangles $A\Omega N$ and $B\Omega N$ (see Figure 2.6), where

$$A\overset{\smile}{\Omega} = \Omega, \quad B\overset{\smile}{\Omega} = \frac{\pi}{2} - \Omega, \quad \angle N\Omega B = \frac{\pi}{2} + i,$$

$$\angle N\Omega A = \frac{\pi}{2} - i, \quad \overset{\smile}{\Omega N} = \frac{\pi}{2}.$$

Also note that $\overset{\smile}{CN} = i$ (since the angle between the normals to two planes is equal to the angle between these planes). Thus,

$$n_x = \cos A\overset{\smile}{N} = \sin\Omega \sin i,$$
$$n_y = \cos B\overset{\smile}{N} = -\cos\Omega \sin i, \tag{2.45'}$$
$$n_z = \cos C\overset{\smile}{N} = \cos i.$$

Comparing these expressions to (2.45), we see that

$$\operatorname{tg}\Omega = -\frac{C_1}{C_2}, \quad \cos i = \frac{C_3}{C}. \tag{2.46}$$

The inclination i is uniquely defined from the condition

$$0 \leqslant i < \pi. \tag{2.47}$$

To find the ascending node Ω without ambiguity, note that $\sin i \geqslant 0$. The signs of $\sin\Omega$ and $\cos\Omega$ are therefore those of the constants C_1 and $-C_2$, respectively.

We now proceed with the determination of r_m, e_1, e_2, t_Ω. First, we calculate the distance r_0 from the initial point D to the Earth's center, and also the projections v_{r0} and v_{u0} on the vector r_0 and on its in-plane normal. We have

$$r_0 = \sqrt{x_0^2 + y_0^2 + z_0^2},$$
$$v_{r0} = \frac{x_0 v_{x0} + y_0 v_{y0} + z_0 v_{z0}}{r_0}, \tag{2.48}$$
$$v_{u0} = \sqrt{v_{x0}^2 + v_{y0}^2 + v_{z0}^2 - v_{r0}^2}.$$

The circular velocity corresponding to r_0 is

$$w_0 = \sqrt{\frac{\mu}{r_0}} \tag{2.49}$$

and we thus have for the perturbation of the longitudinal velocity

$$\Delta v_{u0} = v_{u0} - w_0. \tag{2.50}$$

30

Applying (2.34), (2.35), and (2.39) and putting $\Delta r_0 = 0$, we find

$$
\left.
\begin{aligned}
r_{\mathrm{m}} &= r_0\left(1 + 2\frac{\Delta v_{u0}}{w_0}\right), \\
e_1' &= 2\frac{\Delta v_{u0}}{w_0}, \\
e_2' &= -\frac{v_{r0}}{w_0},
\end{aligned}
\right\}
\tag{2.51}
$$

where e_1' and e_2' are the projections of the eccentricity vector on r_0 and at right angles to it.

Making use of (1.14), we find expressions for the angle u_0 between the line of nodes and the vector r_0. Multiplying the first equality in (1.14) by $\cos \Omega$ and the second by $\sin \Omega$ and adding them up, we find

$$
\left.
\begin{aligned}
\sin u_0 &= \frac{z_0}{r_0 \sin i}, \\
\cos u_0 &= \frac{x_0 \cos \Omega + y_0 \sin \Omega}{r_0}.
\end{aligned}
\right\}
\tag{2.52}
$$

Hence, making use of (2.45) and (2.45'), we find

$$
\operatorname{tg} u_0 = \frac{z_0 C}{y_0 C_1 - x_0 C_2};
\tag{2.52'}
$$

the sign of $\sin u_0$ is that of the numerator in the right-hand side of (2.52'), and the sign of $\cos u_0$ is that of the denominator.

To find the parameters e_1', e_2', and u_0, we first calculate the projections of the eccentricity vector on the line of nodes and at right angles to it:

$$
\left.
\begin{aligned}
e_1 &= e_2' \cos u_0 - e_2' \sin u_0, \\
e_2 &= e_1' \sin u_0 + e_2' \cos u_0.
\end{aligned}
\right\}
\tag{2.53}
$$

Applying (2.38), we obtain the initial value of the angle φ (apart from terms of higher order of smallness), and the time of nodal passage of the mean satellite t_Ω:

$$
\left.
\begin{aligned}
\varphi_0 &= u_0 - 2(e_1 \sin u_0 - e_2 \cos u_0), \\
t_\Omega &= t_0 - \varphi_0 \frac{r_{\mathrm{m}}^{\frac{3}{2}}}{\sqrt{\mu}}.
\end{aligned}
\right\}
\tag{2.54}
$$

The initial conditions thus uniquely specify the elements of a nearly circular orbit. It must be borne in mind, however, that these results are meaningful only if the ratios $\frac{\Delta v_{u0}}{w_0}$ and $\frac{v_{r0}}{w_0}$ are small. Otherwise, the orbit is not almost circular, and the methods of the next chapter should be applied for its determination.

2.10. TOTAL MECHANICAL ENERGY OF NEARLY CIRCULAR MOTION

Let us determine the total mechanical energy per unit mass for a satellite in nearly circular orbit. Applying the expression for the potential

energy (1.6), we write

$$Q = \frac{v^2}{2} + \mu \left(\frac{1}{R} - \frac{1}{r} \right).$$

Substituting (2.41), (2.42), and (1.4), we obtain, to terms of the first order of smallness,

$$Q = \mu \left(\frac{1}{R} - \frac{1}{2r_m} \right). \tag{2.55}$$

Comparison of this expression with (1.7) shows that the total mechanical energy of a satellite in nearly circular orbit is equal to the energy of the satellite in the mean circular orbit.

In conclusion we should stress that all the equations describing almost circular motion are inherently approximate. The accuracy of these equations will be estimated in what follows.

Chapter 3

PERTURBING ACCELERATIONS IN CIRCULAR
AND NEARLY CIRCULAR ORBITS

3.1. IMPULSIVE PERTURBATIONS

Perturbing accelerations are estimated from the integral terms in the right-hand sides of (2.16).

These expressions are linear, so that (to terms of the first order of smallness) they apply to perturbations in both circular and nearly circular orbits. It is advisable to take an orbit of radius $r = r_{\rm m}$ (where $r_{\rm m}$ is the mean radius of the actual nearly circular orbit) as the standard circular orbit of our calculations: there will be no growing secular deviations of the ideal circular orbit from the real nearly circular one. The angular and the linear velocities of the circular satellite entering (2.16) are then written as

$$\lambda = \frac{2\pi}{P}, \quad w = \frac{2\pi r_{\rm m}}{P},$$
(3.1)

where P is the orbital period of the satellite in nearly circular orbit.

In accordance with the preceding, we put in (2.16)

$$\Delta r_0 = \Delta v_{r0} = \Delta u_0 = \Delta v_{u0} = z_0 = v_{z0} = 0$$
(3.2)

and proceed to consider the influence of short impulsive perturbations. The accelerations S, T, and W do not vanish in a small interval

$$t_1 - \varkappa \leqslant t \leqslant t_1 + \varkappa,$$

where t_1 is a certain epoch, and $\varkappa$ a small (in comparison with the satellite's orbital period) quantity.

We introduce the following notations for the total impulsive perturbing accelerations:

$$\Delta v_{r1} = \int_{t_1 - \varkappa}^{t_1 + \varkappa} S\, dt,$$

$$\Delta v_{u1} = \int_{t_1 - \varkappa}^{t_1 + \varkappa} T\, dt,$$

$$\Delta v_{z1} = \int_{t_1 - \varkappa}^{t_1 + \varkappa} W\, dt.$$

33

Assuming $\sin \lambda(t - \xi)$ and $\cos \lambda(t - \xi)$ to remain constant in the relevant time interval, we write (2.16) in the form

$$\Delta r = \frac{\sin(\varphi - \varphi_1)}{\lambda} \Delta v_{r1} + 2 \frac{1 - \cos(\varphi - \varphi_1)}{\lambda} \Delta v_{u1},$$

$$\Delta v_r = \cos(\varphi - \varphi_1) \Delta v_{r1} + 2 \sin(\varphi - \varphi_1) \Delta v_{u1},$$

$$\Delta u = -2 \frac{1 - \cos(\varphi - \varphi_1)}{w} \Delta v_{r1} -$$

$$- \frac{3(\varphi - \varphi_1) - 4\sin(\varphi - \varphi_1)}{w} \Delta v_{u1},$$ \qquad (3.3)

$$\Delta v_u = -\sin(\varphi - \varphi_1) \Delta v_{r1} - [1 - 2\cos(\varphi - \varphi_1)] \Delta v_{u1},$$

$$\Delta z = \frac{\sin(\varphi - \varphi_1)}{\lambda} \Delta v_{z1},$$

$$\Delta v_z = \cos(\varphi - \varphi_1) \Delta v_{z1},$$

where

$$\varphi = \lambda t, \quad \varphi_1 = \lambda t_1.$$

Comparison of these relations with (2.17) and (2.18) shows that impulsive perturbing accelerations are equivalent to the corresponding perturbations in the components of the velocity vector at the time $t = t_1$. The nature of these perturbations can be analyzed on the basis of the conclusions in Sections 2.5 — 2.7. We thus arrive at the following principal results.

A. An impulse Δv_{u1} in the direction of increasing flight velocity simultaneously raises the flight altitude. Some kinetic energy is converted to potential energy, and the flight velocity decreases. Over most of the orbit (for $\varphi_1 + \frac{1}{3}\pi < \varphi < \varphi_1 + \frac{5}{3}\pi$) this reduction in flight velocity more than offsets the acceleration produced by the initial impulse. The mean flight velocity decreases ($\Delta u_m = -\Delta v_{u1}$), so that the final outcome of this impulsive perturbation is a lengthening of the orbital period and a growing secular lag of the satellite behind its position in unperturbed orbit. This seemingly paradoxical result is explained by the increase in the net mechanical energy due to the impulsive acceleration. In accordance with (2.55), this leads to an increase in the mean orbital radius r_m by an amount $\Delta r_m = r_m \frac{2\Delta v_{u1}}{w}$, which in turn lowers the mean flight velocity w_m and raises the orbital period P by an amount $\Delta P = 3 \frac{\Delta v_{u1}}{w} P$. Impulsive deceleration will obviously produce an opposite effect.

B. Impulses Δv_r and Δv_z at right angles to the orbit displace the satellite in the direction of their action for $\varphi_1 < \varphi < \varphi_1 + \pi$ only. For $\varphi_1 + \pi < \varphi < \varphi_1 + 2\pi$, the satellite is displaced in the opposite direction.

Orbit perturbations are thus characterized by a peculiar retrograde effect: over the greater part of the orbit, the satellite is displaced against the direction of the impulsive perturbations.

3.2. CONTINUOUS PERTURBING ACCELERATIONS

In our analysis of continuous perturbations, we shall consider perturbing accelerations S, T, and W dependent on the satellite's parameters of motion

(position and velocity): the time t does not enter the dependences explicitly. We also ignore the reciprocal influence of the orbital perturbations on S, T, and W (with secular perturbations this is possible, in general, only if the discussion is limited to comparatively few circuits of revolution). Under these simplifying assumptions, the perturbing accelerations are periodic functions of the angle

$$\varphi = \lambda t \qquad (3.4)$$

and they can be conveniently expanded in Fourier series:

$$
\left.
\begin{aligned}
S(\varphi) &= S_0 + \sum_{i=1}^{\infty} S_i \sin i(\varphi - \varphi_{Si}), \\
T(\varphi) &= T_0 + \sum_{i=1}^{\infty} T_i \sin i(\varphi - \varphi_{Ti}), \\
W(\varphi) &= W_0 + \sum_{i=1}^{\infty} W_i \sin i(\varphi - \varphi_{Wi}),
\end{aligned}
\right\} \qquad (3.5)
$$

where S_i, T_i, W_i $(i = 0, 1, 2, \ldots)$ are the expansion coefficients, and φ_{Si}, φ_{Ti}, φ_{Wi} are the phase shifts of the component harmonics.

To simplify future manipulations, we transform (2.16) with the aid of (3.1) and (3.2). Thus,

$$
\left.
\begin{aligned}
\Delta r(\varphi) &= P_1^2 \int_0^{\varphi} \{S(\psi) \sin(\varphi - \psi) + \\
&\qquad + 2T(\psi)[1 - \cos(\varphi - \psi)]\} \, d\psi, \\
\Delta v_r(\varphi) &= P_1 \int_0^{\varphi} [S(\psi) \cos(\varphi - \psi) + \\
&\qquad + 2T(\psi) \sin(\varphi - \psi)] \, d\psi, \\
\Delta u(\varphi) &= -\frac{P_1^2}{r_m} \int_0^{\varphi} \{2S(\psi)[1 - \cos(\varphi - \psi)] + \\
&\qquad + T(\psi)[3(\varphi - \psi) - 4\sin(\varphi - \psi)]\} \, d\psi, \\
\Delta v_u(\varphi) &= -P_1 \int_0^{\varphi} \{S(\psi) \sin(\varphi - \psi) + \\
&\qquad + T(\psi)[1 - 2\cos(\varphi - \psi)]\} \, d\psi, \\
\Delta z(\varphi) &= P_1^2 \int_0^{\varphi} W(\psi) \sin(\varphi - \psi) \, d\psi \\
\Delta v_z &= P_1 \int_0^{\varphi} W(\psi) \cos(\varphi - \psi) \, d\psi,
\end{aligned}
\right\} \qquad (3.6)
$$

where

$$P_1 = \frac{P}{2\pi} = \frac{1}{\lambda} = \frac{r_m^{\frac{3}{2}}}{\sqrt{\mu}}, \quad \psi = \lambda \xi = \frac{\xi}{P_1}. \qquad (3.7)$$

Note that P_1 is the time during which the satellite travels in orbit through the angle $\varphi = 1$.

3.3. CONSTANT PERTURBING ACCELERATIONS

We now proceed to calculate the orbital variations produced by the first terms in (3.5), i.e., by constant perturbing accelerations. Setting in (3.6) $S = S_0, T = T_0, \ W = W_0$ and integrating, we find

$$
\left.
\begin{aligned}
\Delta r(\varphi) &= P_1^2 [S_0(1 - \cos\varphi) + 2T_0(\varphi - \sin\varphi)], \\
\Delta v_r(\varphi) &= P_1 [S_0 \sin\varphi + 2T_0(1 - \cos\varphi)], \\
\Delta u(\varphi) &= - \frac{P_1^2}{r_m} \Big\{ 2S_0(\varphi - \sin\varphi) + \\
&\qquad + T_0 \Big[\frac{3}{2}\varphi^2 - 4(1 - \cos\varphi)\Big] \Big\}, \\
\Delta v_u(\varphi) &= - P_1 [S_0(1 - \cos\varphi) + T_0(\varphi - 2\sin\varphi)], \\
\Delta z(\varphi) &= P_1^2 W_0(1 - \cos\varphi), \\
\Delta v_z(\varphi) &= P_1 W_0 \sin\varphi.
\end{aligned}
\right\}
\tag{3.8}
$$

The influence of the constant perturbing accelerations can be analyzed from these relations. The analysis leads to the following conclusions.

A. Constant perturbing acceleration $S = S_0$ along the radius causes periodic perturbation in r, v_r, u, v_u and secular perturbation $(\Delta u)_{sec}$ along the orbit. The maximum magnitudes of the periodic perturbations are given by

$$
\left.
\begin{aligned}
|\Delta r|_{max} &= |\Delta l|_{max} = 2P_1^2 |S_0| = 2r_m \frac{|S_0|}{g_m}, \\
|\Delta v_r|_{max} &= P_1 |S_0| = w \frac{|S_0|}{g_m}, \\
|\Delta v_u|_{max} &= 2P_1 |S_0| = 2w \frac{|S_0|}{g_m},
\end{aligned}
\right\}
\tag{3.9}
$$

where $\Delta l = r_m \Delta u$ is the in-orbit displacement of the satellite, w and g_m are respectively the orbital velocity and the gravitational acceleration in mean circular orbit.

Comparison of (2.17), (2.18), and (3.9) shows that periodic perturbations in r and v_r, which are the orbit distorting factors with constant S_0, are equivalent to analogous perturbations arising as the initial longitudinal velocity is disturbed by an amount

$$
\Delta v_{u0} = \frac{P_1 S_0}{2} = \frac{w}{2} \frac{S_0}{g_m}.
$$

The distorted orbit is depicted in Figure 2.4a (the preceding refers to perturbation along the orbit).

The secular displacement of the satellite per one circuit, $\Delta l(2\pi)$, the rate of this displacement $(\Delta v_\varphi)_{sec}$, and the corresponding change ΔP in the orbital period can be calculated from the expressions

$$
\left.
\begin{aligned}
\Delta l(2\pi) &= r_m \Delta u(2\pi) = - 4\pi P_1^2 S_0 = - 4\pi r_m \frac{S_0}{g_m}. \\
(\Delta v_\varphi)_{sec} &= \frac{\Delta l(2\pi)}{2\pi P_1} = - 2P_1 S_0 = - 2w \frac{S_0}{g_m}, \\
\Delta P &= - \frac{\Delta l(2\pi)}{w} = \frac{4\pi P_1^3}{r_m} S_0 = 2P \frac{S_0}{g_m}.
\end{aligned}
\right\}
\tag{3.10}
$$

36

Constant radial acceleration S_0 thus causes a certain distortion of the orbit, but introduces no secular perturbations along the radius. Secular displacement occurs only along the orbit, i.e., at right angles to the line of action of the perturbing acceleration. This perturbation is attributable to changes in the mean radius and the mean flight velocity:

$$\Delta r_{\mathrm{m}} = P_1^2 S_0 = r_{\mathrm{m}} \frac{S_0}{g_{\mathrm{m}}}, \quad \Delta v_{\mathrm{m}} = -P_1 S_0 = -w \frac{S_0}{g_{\mathrm{m}}}.$$

B. Constant perturbing acceleration $T = T_0$ along the orbit causes periodic perturbations in r, v_r, u, v_u and secular perturbations $(\Delta r)_{\mathrm{sec}}$, $(\Delta u)_{\mathrm{sec}}$, and $(\Delta v_u)_{\mathrm{sec}}$. The maximum magnitudes of the periodic perturbations are

$$\left.\begin{aligned}
|\Delta r|_{\max} &= 2P_1^2 |T_0| = 2r_{\mathrm{m}} \frac{|T_0|}{g_{\mathrm{m}}}, \\
|\Delta v_r|_{\max} &= 4P_1 |T_0| = 4w \frac{|T_0|}{g_{\mathrm{m}}}, \\
|\Delta l|_{\max} &= |\Delta u|_{\max} r_{\mathrm{m}} = 8P_1^2 |T_0| = 8r_{\mathrm{m}} \frac{|T_0|}{g_{\mathrm{m}}}, \\
|\Delta v_u|_{\max} &= 2P_1 |T_0| = 2w \frac{|T_0|}{g_{\mathrm{m}}}.
\end{aligned}\right\} \tag{3.11}$$

The secular displacement along the radius per one circuit, $\Delta r(2\pi)$, and the rate of this displacement $(\Delta v_r)_{\mathrm{sec}}$, are defined by

$$\left.\begin{aligned}
\Delta r(2\pi) &= 4\pi P_1^2 T_0 = 4\pi r_{\mathrm{m}} \frac{T_0}{g_{\mathrm{m}}}, \\
(\Delta v_r)_{\mathrm{sec}} &= 2P_1 T_0 = 2w \frac{T_0}{g_{\mathrm{m}}}.
\end{aligned}\right\} \tag{3.12}$$

The secular perturbation Δl along the orbit is proportional to the square of the angle φ (or the flight time $t = P_1 \varphi$). The orbital period varies monotonically: it is a linear function of the circuit number n. The mean rate of the in-orbit secular displacement, $(\Delta v_\varphi)_{\mathrm{m}}$, the corresponding acceleration $\frac{d}{dt}[(\Delta v_\varphi)_{\mathrm{m}}]$, the linear displacement $\Delta l(2\pi n)$ at the end of the n-th circuit, the perturbation $\Delta P(n)$ in the orbital period during the n-th circuit, and the change δP in the orbital period per circuit are given by the relations

$$\left.\begin{aligned}
(\Delta v_\varphi)_{\mathrm{sec}} &= \frac{d}{dt}\left(-\frac{3}{2}P_1^2 T_0 \varphi^2\right) = \frac{1}{P_1} \frac{d}{d\varphi}\left[-\frac{3}{2}P_1^2 T_0 \varphi^2\right] = \\
&= -3P_1 T_0 \varphi = -3T_0 t, \\
\frac{d}{dt}[(\Delta v_\varphi)_{\mathrm{sec}}] &= -3T_0, \\
\Delta l(2\pi n) &= -6\pi^2 P_1^2 n^2 T_0 = -6\pi^2 n^2 r_{\mathrm{m}} \frac{T_0}{g_{\mathrm{m}}}, \\
\Delta P(n) &= -\frac{\Delta l(2\pi n) - \Delta l[2\pi(n-1)]}{w} = \\
&= \frac{6\pi^2 (2n-1) P_1^3}{r_{\mathrm{m}}} T_0 = 3\pi(2n-1)P \frac{T_0}{g_{\mathrm{m}}}, \\
\delta P &= \Delta P(n) - \Delta P(n-1) = \frac{12\pi^2 P_1^3}{r_{\mathrm{m}}} T_0 = 6\pi P \frac{T_0}{g_{\mathrm{m}}},
\end{aligned}\right\} \tag{3.13}$$

37

where $t = P_1\varphi$ is the time reckoned from injection (or from the initial application of the perturbing acceleration).

The secular perturbation $\Delta v_u(2\pi)$ in longitudinal velocity per circuit and the secular acceleration $(\Delta \dot{v}_u)_{sec}$ along the orbit are given by

$$\begin{aligned}\Delta v_u(2\pi) &= -2\pi P_1 T_0 = -2\pi w \frac{T_0}{g_m}, \\[6pt] (\Delta \dot{v}_u)_{sec} &= \frac{\Delta v_u(2\pi)}{P} = -T_0.\end{aligned} \right\} \tag{3.14}$$

Note that $\Delta v_u(2\pi)$ and $(\Delta \dot{v}_u)_{sec}$ are not equal to $(\Delta v_\varphi)_{sec}(2\pi)$ and $\frac{d}{dt}[(\Delta v_\varphi)_{sec}]$.

The former characterize the change in the actual flight velocity, whereas the latter represent variation in the speed of the satellite's projection on the unperturbed mean circular orbit.

Constant in-orbit perturbation makes the satellite trace an evolute spiral (with slight periodic oscillations about the mean spiral path). The flight velocity constantly decreases, the orbital period increases. Both parameters are linear functions of time or the number of circuits. The mean (secular) variation in the flight velocity is equal to minus the perturbing acceleration. The secular lag of the satellite behind its position in unperturbed orbit is proportional to time squared (or to the square of the circuit number). Oppositely directed perturbing acceleration produces a convolute spiral orbit. The flight velocity increases, and the orbital period decreases.

This seemingly paradoxical motion is attributable to the increase in the satellite's mechanical energy due to perturbation forces. In accordance with (2.55), the increase in the mechanical energy leads to an increase in flight altitude, which in turn entails a reduction in orbital speed. An oppositely directed acceleration produces a reverse effect. Note that the "retrograde" influence of the longitudinal acceleration (analogous to the retrograde displacement due to the previously considered impulsive perturbation in longitudinal velocity v_u) is manifested, not immediately, but only after some time. At first, the longitudinal acceleration displaces the satellite in the direction of its action. Indeed, if the angle φ in (3.8) is small, we have (to terms of higher order of smallness)

$$\Delta u \approx \frac{P_1^2}{r_m} \frac{\varphi^2}{2} T_0 = \frac{t^2}{2r_m} T_0,$$

$$\Delta v_u \approx P_1 \varphi T_0 = t T_0.$$

This initial perturbation, however, rapidly decays as the flight altitude changes. For $\varphi > 108°36'14''$ the velocity variation Δv_u reverses its sign, and for $\varphi > 104°55'6''$, the sense of the displacement Δu is reversed.

C. Constant perturbing acceleration $W = W_0$ at right angles to the orbital plane produces periodic disturbances in z and v_z. From (2.32) and (3.8) it follows that these perturbations amount to a mean displacement of the orbital plane by

$$(\delta z)_m = P_1^2 W_0 = r_m \frac{W_0}{g_m} \tag{3.15}$$

38

and its rotation around the axis MN which makes an angle $\varphi_0 = \pi/2$ with the x axis (see Figure 2.5). The rotation angle of the orbital plane is

$$\psi = \frac{P_1^2 W_0}{r_m} = \frac{W_0}{g_m}.$$ (3.16)

The resultant displacement of the orbital plane is equivalent to its rotation through the angle ψ around the axis MN tangent at the initial point
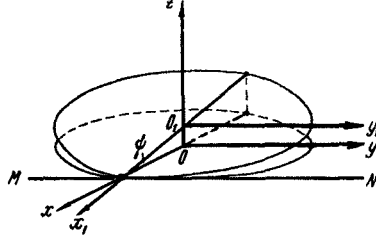
FIGURE 3.1. The effect of constant perturbing accelerations at right angles to the orbital plane.

of the unperturbed circular orbit (Figure 3.1). The satellite is farthest from the unperturbed orbital plane at the point $\varphi = \pi$, deviating by

$$(\delta z)_{max} = 2 P_1^2 W_0 = 2 r_m \frac{W_0}{g_m}.$$ (3.17)

Comparison of these results with the preceding analysis of the effects produced by constant radial acceleration (see under A above) shows that constant acceleration applied at right angles to the orbit (whether along the radius or along the normal to the orbital plane) introduces no secular perturbations along the line of its action. It only "stretches" the orbit in this direction. The maximum displacement of the orbit occurs at the point $\varphi = \pi$: it is calculated from (3.9) and (3.17). The change in the orbital period and the resulting secular displacement along the orbit produced by the radial acceleration S_0 are attributable to the variation in the mean orbital radius (which clearly does not apply for normal acceleration W_0).

3.4. PERIODIC PERTURBATIONS WITH SATELLITE'S ORBITAL FREQUENCY

We now proceed with the analysis of periodic perturbing accelerations whose frequency is equal to the satellite's orbital frequency. Substituting the second terms from the right-hand sides of (3.5) in (3.6), we obtain

39

the following expressions for the corresponding orbital perturbations:

$$
\begin{aligned}
\Delta r(\varphi) &= P_1^2 \int_0^{\varphi} \{S_1 \sin(\psi - \varphi_{S1}) \sin(\varphi - \psi) + \\
&\quad + 2T_1 \sin(\psi - \varphi_{T1})[1 - \cos(\varphi - \psi)]\} \, d\psi, \\
\Delta v_r(\varphi) &= P_1 \int_0^{\varphi} \{S_1 \sin(\psi - \varphi_{S1}) \cos(\varphi - \psi) + \\
&\quad + 2T_1 \sin(\psi - \varphi_{T1}) \sin(\varphi - \psi)] \, d\psi, \\
\Delta u(\varphi) &= -\frac{P_1^2}{r_{\mathrm{m}}} \int_0^{\varphi} \{2S_1 \sin(\psi - \varphi_{S1})[1 - \cos(\varphi - \psi)] + \\
&\quad + T_1 \sin(\psi - \varphi_{T1})[3(\varphi - \psi) - 4\sin(\varphi - \psi)]\} \, d\psi, \\
\Delta v_u(\varphi) &= -P_1 \int_0^{\varphi} \{S_1 \sin(\psi - \varphi_{S1}) \sin(\varphi - \psi) + \\
&\quad + T_1 \sin(\psi - \varphi_{T1})[1 - 2\cos(\varphi - \psi)]\} \, d\psi, \\
\Delta z(\varphi) &= P_1^2 \int_0^{\varphi} W_1 \sin(\psi - \varphi_{W1}) \sin(\varphi - \psi) \, d\psi, \\
\Delta v_z(\varphi) &= P_1 \int_0^{\varphi} W_1 \sin(\psi - \varphi_{W1}) \cos(\varphi - \psi) \, d\psi.
\end{aligned}
\qquad (3.18)
$$

The right-hand sides of these relations reduce to integrals of the form

$$
\begin{aligned}
J_1 &= \int_0^{\varphi} \sin(\psi - \varphi_1) \sin(\varphi - \psi) \, d\psi, \\
J_2 &= \int_0^{\varphi} \sin(\psi - \varphi_1) \cos(\varphi - \psi) \, d\psi, \\
J_3 &= \int_0^{\varphi} \sin(\psi - \varphi_1)(\varphi - \psi) \, d\psi, \\
J_4 &= \int_0^{\varphi} \sin(\psi - \varphi_1) \, d\psi.
\end{aligned}
\qquad (3.19)
$$

After some manipulations, applying the equality

$$
\int x \sin x \, dx = \sin x - x \cos x, \qquad (3.20)
$$

we find

$$
\begin{aligned}
J_1 &= \frac{1}{2} \int_0^{\varphi} [\cos(2\psi - \varphi_1 - \varphi) - \cos(\varphi - \varphi_1)] \, d\psi = \\
&= \frac{1}{2} [\sin\varphi \cos\varphi_1 - \varphi \cos(\varphi - \varphi_1)], \\
J_2 &= \frac{1}{2} \int_0^{\varphi} [\sin(\varphi - \varphi_1) + \sin(2\psi - \varphi_1 - \varphi)] \, d\psi = \\
&= \frac{1}{2} [\varphi \sin(\varphi - \varphi_1) - \sin\varphi \sin\varphi_1], \\
J_3 &= \int_0^{\varphi} [(\varphi - \varphi_1) - (\psi - \varphi_1)] \sin(\psi - \varphi_1) \, d\psi = \\
&= \varphi \cos\varphi_1 - \sin(\varphi - \varphi_1) - \sin\varphi_1, \\
J_4 &= \cos\varphi_1 (1 - \cos\varphi) - \sin\varphi \sin\varphi_1.
\end{aligned}
\qquad (3.21)
$$

40

Inserting these expressions in (3.18) (after substituting $\varphi_{S1}, \varphi_{T1}$, and φ_{W1} for φ_1), we find

$$
\begin{aligned}
\Delta r\,(\varphi) &= P_1^2 \left\{ \frac{S_1}{2}\,[\sin\varphi\cos\varphi_{S1} - \varphi\cos(\varphi - \varphi_{S1})] + \right. \\
&\quad + T_1\,[2\cos\varphi_{T1}\,(1 - \cos\varphi) - \\
&\quad \left. - \sin\varphi\sin\varphi_{T1} - \varphi\sin(\varphi - \varphi_{T1})]\right\}, \\
\Delta v_r\,(\varphi) &= P_1 \left\{ \frac{S_1}{2}\,[\varphi\sin(\varphi - \varphi_{S1}) - \sin\varphi\sin\varphi_{S1}] + \right. \\
&\quad \left. + T_1\,[\sin\varphi\cos\varphi_{T1} - \varphi\cos(\varphi - \varphi_{T1})]\right\}, \\
\Delta u\,(\varphi) &= -\frac{P_1^2}{r_m}\left\{ S_1\,[2\cos\varphi_{S1}\,(1 - \cos\varphi) - \right. \\
&\quad - \sin\varphi\sin\varphi_{S1} - \varphi\sin(\varphi - \varphi_{S1})] + \\
&\quad + T_1\,[3\varphi\cos\varphi_{T1} - 3\sin(\varphi - \varphi_{T1}) - \\
&\quad \left. - 3\sin\varphi_{T1} + 2\varphi\cos(\varphi - \varphi_{T1}) - 2\sin\varphi\cos\varphi_{T1}]\right\}, \\
\Delta v_u\,(\varphi) &= -P_1 \left\{ \frac{S_1}{2}\,[\sin\varphi\cos\varphi_{S1} - \varphi\cos(\varphi - \varphi_{S1})] + \right. \\
&\quad \left. + T_1\,[\cos\varphi_{T1}\,(1 - \cos\varphi) - \varphi\sin(\varphi - \varphi_{T1})]\right\}, \\
\Delta z\,(\varphi) &= \frac{1}{2}\,P_1^2 W_1\,[\sin\varphi\cos\varphi_{W1} - \varphi\cos(\varphi - \varphi_{W1})], \\
\Delta v_z\,(\varphi) &= \frac{1}{2}\,P_1 W_1\,[\varphi\sin(\varphi - \varphi_{W1}) - \sin\varphi\sin\varphi_{W1}].
\end{aligned}
\tag{3.22}
$$

These expressions contain secular and periodic terms. We shall not analyze the periodic disturbances, since their contribution is overshadowed by the secular effects (this analysis, however, can be easily made on the basis of the foregoing relations).

Let $\Delta_{sec}r$, $\Delta_{sec}v_r$, $\Delta_{sec}u$, $\Delta_{sec}v_u$, $\Delta_{sec}z$ and $\Delta_{sec}v_z$ be the secular variations in the corresponding orbital elements. These variations are produced by those terms in the right-hand sides of (3.22) which contain the monotonically increasing factor φ. We have

$$
\begin{aligned}
\Delta_{sec}r &= P_1^2 \left[-\frac{S_1}{2}\,\varphi\cos(\varphi - \varphi_{S1}) - T_1\varphi\sin(\varphi - \varphi_{T1}) \right], \\
\Delta_{sec}v_r &= P_1 \left[\frac{S_1}{2}\,\varphi\sin(\varphi - \varphi_{S1}) - T_1\varphi\cos(\varphi - \varphi_{T1}) \right], \\
\Delta_{sec}u &= \frac{P_1^2}{r_m}\left\{ S_1\varphi\sin(\varphi - \varphi_{S1}) - \right. \\
&\quad \left. - T_1\,[3\varphi\cos\varphi_{T1} + 2\varphi\cos(\varphi - \varphi_{T1})]\right\}, \\
\Delta_{sec}v_u &= P_1 \left[\frac{S_1}{2}\,\varphi\cos(\varphi - \varphi_{S1}) + T_1\varphi\sin(\varphi - \varphi_{T1}) \right], \\
\Delta_{sec}z &= -\frac{1}{2}\,P_1^2 W_1\,\varphi\cos(\varphi - \varphi_{W1}), \\
\Delta_{sec}v_z &= \frac{1}{2}\,P_1 W_1\varphi\sin(\varphi - \varphi_{W1}).
\end{aligned}
\tag{3.23}
$$

A characteristic feature of these expressions is that they all contain terms which are proportional to the angle φ (or the flight time $t = P_1\varphi$) multiplied by trigonometric functions of the angles $\varphi - \varphi_{S1}$, $\varphi - \varphi_{T1}$ and $\varphi - \varphi_{W1}$. The rate of secular variation is different at different points of the orbit, and this results in continuous systematic distortions of the orbit. We shall determine the nature of these distortions for various periodic perturbing accelerations.

41

3.5. PERIODIC PERTURBING ACCELERATION
ALONG THE RADIUS $r(S_1 \neq 0, \; T_1 = W_1 = 0)$

Comparison of (2.41) and (3.23) shows that this radial perturbation produces a nearly circular orbit with eccentricity e and argument of perigee ω, defined by

$$e = \frac{P_1^2 S_1}{2r_m} \, \varphi = \frac{1}{2} \frac{S_1}{g_m} \varphi, \quad \omega = \varphi_{S_1}, \tag{3.24}$$

where r_m is the mean radius of unperturbed orbit, and $g_m = g(r_m)$.

Applying (2.43), which defines the distance of the perigee (r_p) and of the apogee (r_a) from the center of attraction, and seeing that

$$\varphi = \frac{t}{P_1}, \tag{3.25}$$

we find the secular rate of change of e, r_p, and r_a (for $S_1 > 0$):

$$\left. \begin{array}{l} \dfrac{dr_a}{dt} = -\dfrac{dr_p}{dt} = \dfrac{P_1 S_1}{2} = \dfrac{w}{2} \dfrac{S_1}{g_m}, \\[2mm] \dfrac{de}{dt} = \dfrac{P_1 S_1}{2r_m} = \dfrac{1}{2P_1} \dfrac{S_1}{g_m}. \end{array} \right\} \tag{3.26}$$

For $S_1 < 0$, r_a and r_p are switched.

The secular rate of change in the radius r at any point of the orbit can be found from the relation

$$\frac{d}{dt} (\Delta_{sec} r) = \frac{P_1 S_1}{2} \sin \left[\varphi - \left(\varphi_{S_1} + \frac{\pi}{2} \right) \right] = \frac{w}{2} \frac{S_1}{g_m} \sin \left[\varphi - \left(\varphi_{S_1} + \frac{\pi}{2} \right) \right]. \tag{3.27}$$

This secular perturbation thus reduces to a monotonically increasing distortion of the orbit. The radial rate of growth of this distortion fluctuates with a period equal to the satellite's orbital period. The distortion lags by $\pi/2$ behind the initial perturbing acceleration. This aspect is graphically illustrated in Figure 3.2, where the solid arrows mark the direction of the perturbing acceleration, while the dashed arrows point in the direction of the corresponding orbital distortion (the large arrow inside the circle points in the direction of motion of the satellite).
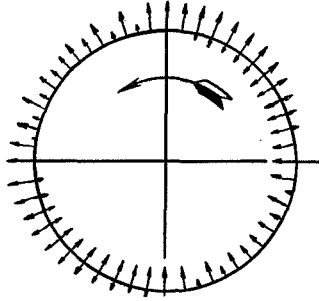
FIGURE 3.2. Radial periodic perturbing accelerations in circular orbit.

3.6. PERIODIC PERTURBING ACCELERATION
ALONG THE ORBIT $(T_1 \neq 0, S_1 = W_1 = 0)$

The secular perturbation in this case is conveniently represented as a sum of two component perturbations. The first term is defined by the equalities

$$\left.\begin{aligned}
\Delta_1 r &= -P_1^2 T_1 \varphi \sin(\varphi - \varphi_{T_1}), \\
\Delta_1 v_r &= -P_1 T_1 \varphi \cos(\varphi - \varphi_{T_1}), \\
\Delta_1 u &= -\frac{2P_1^2}{r_m} T_1 \varphi (\cos \varphi - \varphi_{T_1}), \\
\Delta_1 v_u &= P_1 T_1 \varphi \sin(\varphi - \varphi_{T_1}),
\end{aligned}\right\} \qquad (3.28)$$

and the second term by

$$\left.\begin{aligned}
\Delta_2 r &= \Delta_2 v_r = \Delta_2 v_u = 0, \\
\Delta_2 u &= -\frac{3P_1^2}{r_m} T_1 \varphi \cos \varphi_{T_1}.
\end{aligned}\right\} \qquad (3.29)$$

From (2.41) and (3.28) it follows that the first of the two component perturbations produces a nearly circular orbit with the following eccentricity and argument of perigee:

$$e = \frac{P_1^2 T_1}{r_m} \varphi = \frac{T_1}{g_m} \varphi, \quad \omega = \varphi_{T_1} + \frac{\pi}{2}. \qquad (3.30)$$

Hence, applying (3.25), we obtain expressions for the secular rate of change in e, r_p, r_a, and $r(\varphi)$ (for $T_1 > 0$):

$$\left.\begin{aligned}
\frac{dr_a}{dt} &= -\frac{dr_p}{dt} = P_1 T_1 = w \frac{T_1}{g_m}, \\
\frac{de}{dt} &= \frac{P_1 T_1}{r_m} = \frac{1}{P_1} \frac{T_1}{g_m}, \\
\frac{d}{dt}(\Delta_1 r) &= P_1 T_1 \sin[\varphi - (\varphi_{T_1} - \pi)] = w \frac{T_1}{g_m} \sin[\varphi - (\varphi_{T_1} - \pi)].
\end{aligned}\right\} \qquad (3.31)$$

The orbit in this case undergoes monotonically growing distortion at a rate which varies periodically with the satellite's orbital period. The distortion of the orbit lags by π behind the initial perturbing acceleration. This is illustrated in Figure 3.3, which is entirely analogous to Figure 3.2.
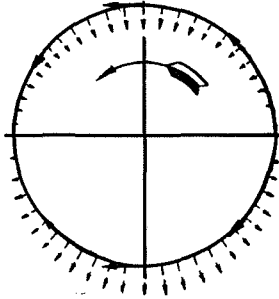
FIGURE 3.3. Longitudinal periodic perturbing accelerations in circular orbit.

The second secular perturbation defined by (3.29) has nothing to do with orbital distortion: it somewhat alters the period of revolution. The change in the orbital period is given by

$$\Delta P = \frac{6\pi P_1^3}{r_m} T_1 \cos \varphi_{T1} = 3P \frac{T_1}{g_m} \cos \varphi_{T1}.$$ (3.32)

Note that this change in the orbital period is associated with a certain variation Δr_m in the mean orbital radius. The magnitude of this variation is determined by the periodic terms in the right-hand side of (3.22):

$$\Delta r_m = 2P_1^2 T_1 \cos \varphi_{T1} = 2r_m \frac{T_1}{g_m} \cos \varphi_{T1}.$$ (3.33)

3.7. PERIODIC PERTURBING ACCELERATIONS AT RIGHT ANGLES TO THE ORBITAL PLANE ($W_1 \neq 0$, $S_1 = T_1 = 0$)

From (2.32) and (3.23) it follows that the secular displacement of the orbit in this case reduces to rotation of the orbital plane about an axis pointing at an angle

$$\varphi_0 = \varphi_{W1} + \frac{\pi}{2}.$$ (3.34)

The rotation angle of the orbital plane is

$$\psi = \frac{P_1^2 W_1}{2r_m} \varphi = \frac{1}{2} \frac{W_1}{g_m} \varphi.$$ (3.35)

Hence, applying (3.25), we find the angular rate of rotation of the orbital plane:

$$\frac{d\psi}{dt} = \frac{P_1 W_1}{2r_m} = \frac{\lambda}{2} \frac{W_1}{g_m},$$ (3.36)

where $\lambda = \frac{1}{P_1}$ is the mean angular velocity of the satellite in orbit.

The relation between the perturbing accelerations and the rotation of the orbital plane is depicted in Figure 3.4, where the vertical arrows mark the perturbing accelerations, is the direction of flight of the satellite, and N is the sense in which the orbital plane rotates; the line AO points in the direction $\varphi = \varphi_{W1}$, and the line CD is the axis of rotation of the orbital plane.
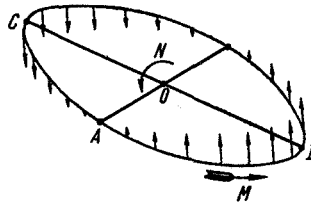
FIGURE 3.4. Periodic perturbing acceleration at right angles to the orbital plane

44

3.8. PERIODIC PERTURBATIONS WITH A FREQUENCY WHICH IS AN INTEGER MULTIPLE OF THE SATELLITE'S ORBITAL FREQUENCY

We now estimate the influence of the higher harmonics in (3.5), corresponding to $i \geqslant 2$. The expressions for the orbital perturbations resulting from these harmonics are analogous to relations (3.18) with $\sin(\psi - \varphi_{Si})$, $\sin(\psi - \varphi_{Ti})$ and $\sin(\psi - \varphi_{Wi})$ for $\sin i(\psi - \varphi_{Si})$, $\sin i(\psi - \varphi_{Ti})$ and $\sin i(\psi - \varphi_{Wi})$. This substitution reduces the problem to evaluation of integrals of the form

$$
\left.
\begin{aligned}
J_1^{(i)} &= \int_0^\varphi \sin i(\psi - \varphi_1) \sin(\varphi - \psi)\, d\psi, \\[2mm]
J_2^{(i)} &= \int_0^\varphi \sin i(\psi - \varphi_1) \cos(\varphi - \psi)\, d\psi, \\[2mm]
J_3^{(i)} &= \int_0^\varphi (\varphi - \psi) \sin i(\psi - \varphi_1)\, d\psi, \\[2mm]
J_4^{(i)} &= \int_0^\varphi \sin i(\psi - \varphi_1)\, d\psi.
\end{aligned}
\right\}
\qquad (3.37)
$$

We only consider secular perturbations of the orbit. From

$$
\sin i(\psi - \varphi_1)\sin(\varphi - \psi) = \tfrac{1}{2}\{\cos[(i+1)\psi - i\varphi_1 - \varphi] - \cos[(i-1)\psi - i\varphi_1 + \varphi]\},
$$

$$
\sin i(\psi - \varphi_1)\cos(\varphi - \psi) = \tfrac{1}{2}\{\sin[(i-1)\psi - i\varphi_1 + \varphi] + \sin[(i+1)\psi - i\varphi_1 - \varphi]\}
$$

it follows immediately that the integrals $J_1^{(i)}$ and $J_2^{(i)}$ do not introduce secular terms for $i \geqslant 2$. The fourth integral $J_4^{(i)}$ does not contribute secular terms either. We shall therefore concentrate on the third integral $J_3^{(i)}$. Applying (3.20), we have

$$
\begin{aligned}
J_3^{(i)} &= \int_0^\varphi [(\varphi - \varphi_1) - (\psi - \varphi_1)] \sin i(\psi - \varphi_1)\, d\psi = \\[2mm]
&= \frac{1}{i} \int_{-i\varphi_1}^{i(\varphi - \varphi_1)} \left(\varphi - \varphi_1 - \frac{x}{i}\right) \sin x\, dx = \frac{\varphi \cos i\varphi_1}{i} - \frac{\sin i(\varphi - \varphi_1) + \sin i\varphi_1}{i^2}, \quad (3.38)
\end{aligned}
$$

where $x = i(\psi - \varphi_1)$.

Only the first term in the right-hand side of this expression corresponds to secular perturbations of the orbit. Making use of (3.18), we conclude that only u is disturbed by these secular perturbations, and they are therefore given by

$$
\Delta_{\mathrm{sec}} u = -\frac{3P_1^2}{ir_{\mathrm{m}}} T_i \varphi \cos i\varphi_{Ti} = -\frac{3}{i}\frac{T_i}{g_{\mathrm{m}}} \varphi \cos i\varphi_{Ti}. \qquad (3.39)
$$

This secular perturbation does not involve growing distortion of the orbit: it only alters the orbital period by

$$
\Delta P = \frac{6\pi P_1^3}{ir_{\mathrm{m}}} T_i \cos i\varphi_{Ti} = 3\frac{P}{i}\frac{T_i}{g_{\mathrm{m}}} \cos i\varphi_{Ti}. \qquad (3.40)
$$

This variation in the orbital period decreases as the order i of the perturbation harmonic becomes higher. It is also fairly sensitive to the initial phase $\varphi_{\tau i}$ of the perturbation.

3.9. CLASSIFICATION OF ORBITAL PERTURBATIONS

It follows from the preceding that small perturbing accelerations which are periodic functions of the angle $\varphi = \lambda t$ may cause secular orbital perturbations of three different kinds.

1. Secular perturbations which produce growing distortion of the orbit (eventually leading to orbit decay — the satellite falls to the Earth or escapes from the sphere of the Earth's pull). These perturbations are attributable to constant accelerations along the orbit (or in the opposite direction), and also to periodic accelerations in the orbital plane whose frequency is equal to the satellite's orbital frequency around the center of attraction. In-orbit constant accelerations make the satellite move in an evolute (convolute) spiral with a monotonically increasing (decreasing) period of revolution. Periodic accelerations, on the other hand, cause monotonic growth of orbit eccentricity, and the shape of the orbit is eventually distorted to a considerable extent.

2. Secular perturbations resulting in constant rotation of the orbital plane around an axis through the center of attraction. These perturbations are caused by periodic accelerations at right angles to the orbital plane, whose frequency is equal to the satellite's orbital frequency.

3. Secular perturbations which change the orbital period of the satellite without distorting its orbit. These perturbations are caused by constant accelerations along the radius r and by periodic accelerations along the orbit. The contribution from the periodic accelerations is smaller for the higher harmonics in (3.39).

Perturbing accelerations whose frequency is equal to the orbital frequency of the satellite have an essentially different effect from the "overtones". When the acceleration frequency matches the orbital frequency of the satellite, a certain resonance occurs which is responsible for the growing distortions of the orbit. The nature of this resonance can be investigated with the aid of expressions (3.3), which describe the effect of impulsive perturbations. To this end, it suffices to consider impulses which are systematically applied as the satellite passes through two diametrically opposite points of the orbit. The perturbing impulses in diametrically opposite points must have the same magnitude and opposite directions. From (3.3) it follows that the in-plane impulsive perturbations will produce a continuous growth of eccentricity. If the impulsive perturbations are directed along the normal to the orbital plane, the plane will rotate. Any perturbing acceleration whose period is equal to the satellite's orbital period can obviously be treated as a combination of those impulsive perturbations.

Chapter 4

GENERAL CASE OF MOTION IN A NEWTONIAN FIELD OF GRAVITY

4.1. STATEMENT OF THE PROBLEM

In the previous chapters we have considered motion in circular and nearly circular orbits. It has been shown that these orbits are possible only if the initial conditions meet certain specifications.

We shall show in what follows that in the general case (for arbitrary initial conditions), the orbits may substantially depart from circular. Various results of the preceding chapters then become meaningless. In this chapter we shall therefore consider the general case of motion around a gravitational center (the Earth or any other primary). The only force in this analysis will be the gravitational pull pointing exactly to the Earth's center (or, in general, to the center of the primary). The acceleration produced by this force will be defined by Newton's formula (1.2). It will be shown in Chapter 16 that (in the absence of large active forces) this is the principal driving force on a satellite moving inside the sphere of the Earth's gravitational pull and beyond the effective range of the Moon's pull (at distances less than $9 \cdot 10^5$ km from the Earth's center and greater than $7 \cdot 10^4$ from the Moon's center), at altitudes of $100-150$ km.

The motion produced by the Newtonian gravitation only is therefore generally regarded as u n p e r t u r b e d motion. The problems connected with the superposition of various perturbing forces are considered in what follows.

4.2. EQUATIONS OF MOTION

We shall operate in the previously defined right-hand rectangular system $Oxyz$, with the axis Oz pointing along the Earth's spin axis, and Ox directed to the point of vernal equinox. In Figure 4.1, C denotes the position of the satellite. Consider a rectangular parallelepiped M, with the center of attraction O and the point C at its opposite vertices, and its edges parallel to the axes of the $Oxyz$ frame. These edges are obviously equal to the rectangular coordinates x, y, z of the satellite. The diagonal of this parallelepiped is

$$OC = r = \sqrt{x^2 + y^2 + z^2}.$$

The gravitational acceleration vector g is laid off along the diagonal CO, and a second rectangular parallelepiped N is drawn, with the vector g as
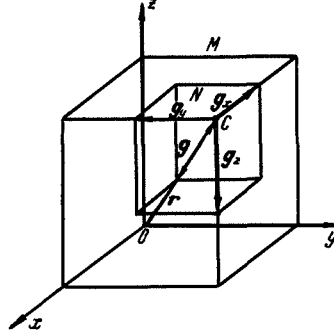
FIGURE 4.1. Projections of the gravitational acceleration on rectangular coordinate axes.

its diagonal; the edges of this parallelepiped are the projections g_x, g_y, g_z of the vector g on the coordinate axes. The parallelepipeds M and N are similar. Applying (1.2), we write

$$\left.\begin{aligned} g_x &= -g\frac{x}{r} = -\mu\frac{x}{r^3}, \\ g_y &= -g\frac{y}{r} = -\mu\frac{y}{r^3}, \\ g_z &= -g\frac{z}{r} = -\mu\frac{z}{r^3} \end{aligned}\right\} \tag{4.1}$$

or, in vector notations,

$$g = -\frac{\mu}{r^3}r, \tag{4.2}$$

where r is the vector which defines the position of the point C in the $Oxyz$ frame.

From (4.2), we have the vector equation of motion

$$\ddot{r} = -\frac{\mu}{r^3}r. \tag{4.3}$$

This vector equation is clearly equivalent to a set of three second-order scalar differential equations.

4.3. FIRST INTEGRALS OF MOTION

Vector-multiplying equation (4.3) by r and seeing that $r \times r = 0$, we have

$$r \times \ddot{r} = 0.$$

Hence, seeing that $\dot{r} \times \dot{r} = 0$, we write

$$\tfrac{d}{dt}(r \times \dot{r}) = r \times \ddot{r} = 0.$$

Integrating this equality, we find the so-called a r e a l i n t e g r a l in vector form:

$$r \times v = C, \qquad (4.4)$$

where $v = \dot{r}$ is the satellite's velocity vector, C some constant vector (for the given unperturbed orbit). The vector integral (4.4) is equivalent to a set of three scalar integrals:

$$yv_z - zv_y = C_1, \ zv_x - xv_z = C_2, \ xv_y - yv_x = C_3, \qquad (4.5)$$

where v_x, v_y, v_z and C_1, C_2, C_3 are the projections of the vectors v and C, respectively, on the coordinate axes of $Oxyz$. C_1, C_2, C_3 are clearly constant for the given orbit.

From (4.4) it follows that the vectors r and v remain in a certain fixed plane through the center of attraction, at right angles to the vector C. The satellite in our case is seen to move in one plane, which is called the o r b i t a l p l a n e .

Let C be the magnitude of the vector C:

$$C = \sqrt{C_1^2 + C_2^2 + C_3^2}. \qquad (4.6)$$

Applying the well-known expression for the magnitude of vector product /15/, we write

$$C = rv \sin \alpha, \qquad (4.7)$$

where v is the magnitude of the satellite's velocity vector, α the angle between the vectors v and r (Figure 4.2).

Let ds be the elementary displacement of the satellite in time dt. For small dt, we have

$$ds = v \, dt.$$

Expression (4.7) takes the form

$$C \, dt = r \sin \alpha \, ds.$$

But from Figure 4.2 we see that $r \sin \alpha \, ds = 2d\sigma$ (to terms of higher order of smallness) is twice the area of the elementary orbital sector OAA_1. Hence,

$$2 \tfrac{d\sigma}{dt} = C. \qquad (4.8)$$

Integrating, we find

$$2\sigma = Ct + C_4, \qquad (4.9)$$

49

where σ is the area enclosed by the segment $A_0 A$ of the orbit and the radii $O A_0$ and $O A$ (here A_0 is an initial position of the satellite).
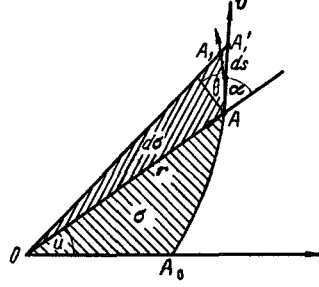
FIGURE 4.2. Illustrating the definition of areal velocity.

C_4 is a new constant which depends on the choice of the point of origin for σ and t. From (4.4) and (4.8) it follows that the satellite moves in a plane through the gravitational center. The areas swept by the radius-vector in equal times are equal; in other words, the so-called areal velocity is constant, being equal to $\frac{C}{2}$.

We now take the scalar product of equation (4.3) and the vector $\dot{r}$:

$$\ddot{r} \cdot \dot{r} = -\frac{\mu}{r^3}(r \cdot \dot{r}).\tag{4.10}$$

The distance r from the center of attraction and the velocity v are clearly given by the relations

$$r = \sqrt{r \cdot r}, \quad v = \sqrt{\dot{r} \cdot \dot{r}}.$$

Then,

$$\ddot{r} \cdot \dot{r} = \frac{1}{2}\frac{d}{dt}(\dot{r} \cdot \dot{r}) = \frac{1}{2}\frac{d}{dt}(v^2),$$

$$\frac{1}{r}(r \cdot \dot{r}) = \frac{d}{dt}\sqrt{r \cdot r} = \frac{dr}{dt}.$$

Substituting in (4.10), we have

$$\frac{1}{2}\frac{d}{dt}(v^2) = -\frac{\mu}{r^2}\frac{dr}{dt}.$$

Integrating this expression, we find another first integral

$$v^2 - \frac{2\mu}{r} = C_5,\tag{4.11}$$

where C_5 is a constant.

From (1.6) it follows that (4.11) is a particular case of the general principle of constancy of mechanical energy in a conservative force field

/28/. It is generally called the energy integral. The constant C_5 is equal to twice the amount of mechanical energy per unit mass.

A direct consequence of the energy integral is that the velocity decreases with distance from the center of attraction.

4.4. SHAPE OF ORBIT

To find the shape of the orbit, we introduce a polar system of coordinates r, u, where u is the angular distance from a certain fixed direction through the center of attraction in the orbital plane. In these coordinates, equations (4.8) and (4.11) take the form

$$r^2 \dot{u} = C, \quad \dot{r}^2 + r^2 \dot{u}^2 = \frac{2\mu}{r} + C_5. \tag{4.12}$$

In this chapter we shall only consider orbits with

$$C \neq 0.$$

The case $C = 0$, corresponding to vertical motion, will be discussed in Chapter 7.

To eliminate the independent variable t from (4.12), we take the first equation of the set, which gives

$$\dot{u} = \frac{C}{r^2}, \quad \dot{r} = \frac{dr}{du} \dot{u} = \frac{dr}{du} \frac{C}{r^2}. \tag{4.13}$$

Substituting in the second equation of (4.12), we obtain a differential equation which describes the orbit:

$$\left(\frac{C}{r^2} \frac{dr}{du} \right)^2 + \frac{C^2}{r^2} = \frac{2\mu}{r} + C_5. \tag{4.14}$$

Substituting a new variable r

$$\rho = \frac{C}{r}, \tag{4.15}$$

we have

$$r = \frac{C}{\rho}, \quad \frac{dr}{du} = -\frac{C}{\rho^2} \frac{d\rho}{du}. \tag{4.16}$$

Inserting in (4.14), we find

$$\left(\frac{d\rho}{du} \right)^2 + \rho^2 = \frac{2\mu}{C} \rho + C_5,$$

$$\frac{d\rho}{du} = \pm \sqrt{C_5 + \frac{2\mu}{C} \rho - \rho^2} = \pm \sqrt{C_5 + \frac{\mu^2}{C^2} - \left(\rho - \frac{\mu}{C} \right)^2}.$$

Hence

$$u = \pm \int \frac{d\rho}{\sqrt{C_5 + \frac{\mu^2}{C^2} - \left(\rho - \frac{\mu}{C} \right)^2}} = \pm \arccos \frac{\rho - \frac{\mu}{C}}{\sqrt{C_5 + \frac{\mu^2}{C^2}}} + C_6.$$

51

where C_6 is a new integration constant.

From (4.15) we have

$$\frac{C}{r} - \frac{\mu}{C} = \sqrt{C_5 + \frac{\mu^2}{C^2}} \cos(u - C_6),$$

$$r = \frac{\frac{C^2}{\mu}}{1 + \sqrt{1 + \frac{C^2 C_5}{\mu^2}} \cos(u - C_6)}.$$

Changing over to a new variable

$$\vartheta = u - C_6, \tag{4.17}$$

we also introduce two new constants

$$p = \frac{C^2}{\mu} \quad \text{and} \quad e = \sqrt{1 + \frac{C^2 C_5}{\mu^2}}. \tag{4.18}$$

These substitutions give the final equation of the orbit in polar coordinates:

$$r = \frac{p}{1 + e \cos \vartheta}. \tag{4.19}$$

This is clearly an equation of a conical section (ellipse, hyperbola, or parabola) with a focal parameter p and eccentricity e. The center of attraction is located at one of the foci of the conic. Our result is known as Kepler's second law (in generalized form). The angle ϑ is generally called the t r u e a n o m a l y.

4.5. SHAPE OF THE ORBIT AS A FUNCTION OF FLIGHT VELOCITY

From (4.19) it follows that for $0 \leqslant e < 1$, the orbit is an ellipse (for $e = 0$, this ellipse reduces to a circle of radius $r = $const). For $e = 1$, the orbit is a parabola, and for $e > 1$ a hyperbola.

Let θ be the angle between the direction of the velocity vector and the in-plane normal to the radius-vector at the point A (see Figure 4.2). Clearly,

$$\theta = \frac{\pi}{2} - \alpha \tag{4.20}$$

and (4.7) takes the form

$$C = rv \cos \theta. \tag{4.21}$$

Hence, applying (4.11) and (4.18), we find

$$e = \sqrt{1 - k(2 - k) \cos^2 \theta}, \tag{4.22}$$

52

where

$$k = \frac{rv^2}{\mu} = \frac{v^2}{w^2} = \frac{2v^2}{V^2}.$$ (4.23)

In accordance with (1.4) and (1.9), $w = \sqrt{\frac{\mu}{r}}$ is the circular velocity at a distance r from the center of attraction, and

$$V = \sqrt{2}\, w = \sqrt{\frac{2\mu}{r}}$$ (4.24)

is the so-called escape velocity for the particular primary being considered.

From (4.22) and (4.24) it follows that if $v < V$, then $k < 2$ and $e < 1$. The orbit is an ellipse. If now $v = V$, then $k = 2$ and $e = 1$, and the orbit is parabolic. If $v > V$, then $k > 2$, $e > 1$, and the orbit is a hyperbola. To sum up, if a body moves at any time with a velocity which is less than the escape velocity V, it will continue moving in an elliptical orbit (providing, of course, that it does not collide at the end of its path with the Earth's surface). If the velocity of the body is equal to the escape velocity, it will move in a parabola, and if its velocity is greater than the escape velocity, its path is a hyperbola. In either of the last two cases, the body recedes to infinity, i.e., escapes from its primary. This conclusion is fully consistent with the corresponding result which has been derived in Sec. 1.1 from energy considerations. Since without perturbations the eccentricity e remains constant, the conditions $v < V$, $v = V$ or $v > V$ are conserved in the course of motion in unperturbed orbit.

In conclusion, note that (4.22) may be written as

$$e = \sqrt{\sin^2\theta + (k-1)^2 \cos^2\theta}.$$ (4.25)

Hence it follows that a circular orbit $(e = 0)$ is possible only if

$$v = w \quad \text{and} \quad \theta = 0,$$ (4.26)

which is consistent with the results of Chapter 1.

53

Chapter 5

ELLIPTICAL ORBITS

5.1. PRINCIPAL GEOMETRICAL PROPERTIES
OF ELLIPTICAL ORBITS

Let us consider in greater detail motion in elliptical orbit $(0 \leqslant e < 1, \; v < V)$. In our analysis, we shall apply the well-known geometrical properties of ellipses.

From (4.19) it follows that the p e r i c e n t e r Π is located at the point with $\vartheta = 0$ (the pericenter is the point of the orbit which is closest to the center of attraction; for orbits around the Earth this point is the p e r i g e e, for orbits around the Sun it is the p e r i h e l i o n). The point farthest from the center of attraction (the a p o c e n t e r A; this is the a p o g e e of orbits around the Earth and the a p h e l i o n of solar orbits) corresponds to a true
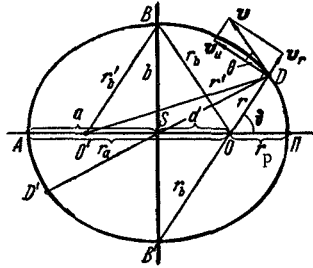
FIGURE 5.1. Geometrical parameters
of elliptical orbit.

anomaly $\vartheta = \pi$ (Figure 5.1). Putting $\vartheta = 0$ and $\vartheta = \pi$ in the right-hand side of (4.19), we find the pericenter (minimum) and the apocenter (maximum) distances of the center of attraction O (the f i r s t f o c u s of the elliptical orbit):

$$r_{\mathrm{p}} = \frac{p}{1+e}, \quad r_{\mathrm{a}} = \frac{p}{1-e}. \tag{5.1}$$

The points A and Π are the two farthest points of the elliptical orbit. The line $A\Pi$ is therefore called the m a j o r a x i s of the orbit. Half the length of $A\Pi$ is the s e m i m a j o r a x i s, a; it is given by the expression

$$a = \frac{r_{\mathrm{p}} + r_{\mathrm{a}}}{2} = \frac{p}{1-e^2}, \tag{5.2}$$

where p is the focal parameter.

If a and e are known, the parameters p, r_p, and r_a are determined from the relations

$$p = a(1 - e^2), \quad r_p = a(1 - e), \quad r_a = a(1 + e). \tag{5.3}$$

Hence

$$e = \frac{r_a - r_p}{2a}.$$

Let h_a and h_p be the apogee and the perigee heights of the orbit above the Earth's surface. If the Earth is a sphere of radius R, so that $r_p = R + h_p$, $r_a = R + h_a$, we have

$$a = R + \frac{h_a + h_p}{2}, \quad e = \frac{h_a - h_p}{2R + h_a + h_p}.$$

The midpoint S of the semimajor axis is the center of the elliptical orbit. The distance $d = OS$ is the linear eccentricity, defined by

$$d = a - r_p = ae. \tag{5.4}$$

The point O', which is the symmetrical image point of O on the major axis (i.e., $O'S = OS = d$) is the second focus of the orbit. We know from analytical geometry that the ellipse is a locus of points satisfying the equality

$$r + r' = 2a, \tag{5.5}$$

where r and r' are the distances of an arbitrary point of the orbit from the foci O and O'.

Any straight line through the center S meets the ellipse at two points D and D'. Any segment between these two points is the diameter of the ellipse. The center of the ellipse is the midpoint of all the diameters, i.e.,

$$SD = SD'.$$

The largest diameter of the ellipse is its major axis $A\Pi$. The least diameter BB' is at right angles to the axis $A\Pi$; this is the minor axis, while the segment $b = SB = SB'$ is the semiminor axis. Since the ellipse is symmetrical, we see that the distances r_b and r_b' from the points B and B' to the two foci are equal. From (5.5) we have

$$r_b = a. \tag{5.6}$$

From (5.4) we have the length of the semiminor axis

$$b = \sqrt{a^2 - d^2} = a\sqrt{1 - e^2}. \tag{5.7}$$

From (4.19) we see that as the satellite moves from the pericenter Π to the apocenter A (i.e., as the true anomaly goes from 0 to π), the distance r continually increases, whereas from point A to point Π it

decreases. The points B and B' therefore divide the entire orbit into two parts: $B'\Pi B$, where $r \leqslant a$, and $B'AB$, where $r \geqslant a$.

From the above relations we see that all elliptical orbits of equal eccentricity e are similar. As e increases, the elliptical orbit becomes progressively more elongated, and for $e \rightarrow 1$, we have

$$\frac{r_a}{r_p} = \frac{1+e}{1-e} \rightarrow \infty. \tag{5.8}$$

The apocenter recedes to infinity, and the orbit reduces to a parabola.

5.2. FLIGHT VELOCITY AND ENERGY

We now find the components of the velocity vector v at any point of the orbit. Let v_r and v_u be the projections of this vector on the radius and its in-plane normal (Figure 5.1). Applying (4.21) and seeing that

$$v_u = v \cos \theta, \tag{5.9}$$

we have

$$v_u = \frac{C}{r}.$$

On the other hand, from (4.18) we see that

$$C = \sqrt{\mu p}; \tag{5.10}$$

hence

$$v_u = \frac{\sqrt{\mu p}}{r} = \sqrt{\frac{\mu}{p}}(1 + e \cos \vartheta). \tag{5.11}$$

To find v_r, we differentiate (4.19):

$$v_r = \dot{r} = \frac{pe \sin \vartheta}{(1 + e \cos \vartheta)^2}\dot{\vartheta}.$$

From (4.19) and (5.11) we obtain

$$\dot{\vartheta} = \frac{v_u}{r} = \frac{\sqrt{\mu p}}{p^2}(1 + e \cos \vartheta)^2. \tag{5.12}$$

Substituting in the preceding equality, we finally have

$$v_r = \sqrt{\frac{\mu}{p}}e \sin \vartheta. \tag{5.13}$$

To find the magnitude of the velocity vector v, we make use of relations (4.11), (4.18), (5.3), and (5.10). After simple manipulations, we have

$$\left. \begin{array}{l} v^2 = \frac{2\mu}{r} + C_5, \\[2mm] C_5 = -\frac{(1-e^2)\mu^2}{C^2} = -\frac{\mu}{a} \end{array} \right\} \tag{5.14}$$

or finally

$$v^2 = \frac{2\mu}{r} - \frac{\mu}{a}. \tag{5.15}$$

From (5.11), (5.13), and from Figure 5.1 it follows that the angle θ (the inclination of the velocity vector to the local horizon) is given by

$$\text{tg } \theta = \frac{v_r}{v_u} = \frac{r}{p} e \sin \vartheta = \frac{e \sin \vartheta}{1 + e \cos \vartheta}. \tag{5.16}$$

We see that the flight velocity decreases as the body recedes from the center of attraction (i.e., as the angle ϑ goes from 0 to π) and increases as it approaches the center (for ϑ going from π to 2π). The flight velocity is maximal and minimal at the pericenter and the apocenter, respectively. Applying (5.3) and (5.15), we find the corresponding velocities v_p and v_a:

$$\left. \begin{array}{l} v_p = \sqrt{\dfrac{1+e}{1-e} \dfrac{\mu}{a}} = w_m \sqrt{\dfrac{1+e}{1-e}} = w_p \sqrt{1+e}, \\[2mm] v_a = \sqrt{\dfrac{1-e}{1+e} \dfrac{\mu}{a}} = w_m \sqrt{\dfrac{1-e}{1+e}} = w_a \sqrt{1-e}, \\[2mm] \dfrac{v_p}{v_a} = \dfrac{1+e}{1-e}, \end{array} \right\} \tag{5.17}$$

where $w_m = \sqrt{\dfrac{\mu}{a}}$ is the circular velocity for the radius $r=a$; $w_p = \sqrt{\dfrac{\mu}{r_p}}$ and $w_a = \sqrt{\dfrac{\mu}{r_a}}$ are the circular velocities in perigee and in apogee.

From (1.4), (5.6), and (5.15) it follows that the flight velocity at the extreme points B and B' of the minor axis is

$$v_b = w_m = w_b,$$

where w_b is the circular velocity at these points.

Expression (5.15) may be written as

$$v^2 = w^2 + \mu \left(\frac{1}{r} - \frac{1}{a} \right),$$

where $w = \sqrt{\dfrac{\mu}{r}}$ is the circular velocity at the current point of the orbit.

Since over the part $B'\Pi B$ of the orbit $r<a$, then clearly $v>w$. Conversely, over the path $B'AB$ we have $r>a$, so that $v<w$.

The minor axis BB' is seen to divide the elliptical orbit into two similar parts. The one nearer to the pericenter ($B\Pi B'$) is characterized by the inequalities

$$r<a, \quad v>w.$$

The other (BAB'), which is closer to the apocenter, has

$$r>a, \quad v<w.$$

As regards the angle θ between the velocity vector and the horizon (i.e., the inclination of the tangent to the orbit), we see from (5.16) that at the pericenter and the apocenter

$$\theta_p = \theta_a = 0. \tag{5.18}$$

As the body moves from pericenter to apocenter, $\theta > 0$, and on its way from apocenter to pericenter, $\theta < 0$.

To find the extrema (the maximum and the minimum values) of the angle θ, we differentiate (5.16) and make use of the condition

$$\frac{d}{d\vartheta}(\text{tg } \theta) = \frac{\cos \vartheta + e}{(1 + e \cos \vartheta)^2}\, e = 0, \tag{5.19}$$

which for $e \neq 0$ (i.e., a noncircular orbit) is equivalent to

$$\cos \vartheta = -e. \tag{5.20}$$

The two roots of this equation, ϑ_1 and ϑ_2, are defined by

$$\sin \vartheta_1 = +\sqrt{1 - e^2} \quad \text{and} \quad \sin \vartheta_2 = -\sqrt{1 - e^2}.$$

Substituting these roots in (5.16), we obtain the maximum and the minimum values of the angle θ:

$$\theta_{max} = \arcsin e, \quad \theta_{min} = -\arcsin e. \tag{5.21}$$

Applying (5.20) and Figure 5.1, we can show that these extremal values are attained at the end points of the minor axis, B and B'.

Let us calculate the total mechanical energy per unit mass, Q, which should be imparted to an artificial Earth satellite launched into a given elliptical orbit. Applying (1.6), (1.7), and (5.15), we find

$$Q = \mu \left(\frac{1}{R} - \frac{1}{2a} \right). \tag{5.22}$$

This expression is identical to relations (1.7) and (2.55) for circular and nearly circular orbits, with semimajor axis substituted for the radius of circular orbit (the mean radius of nearly circular orbit).
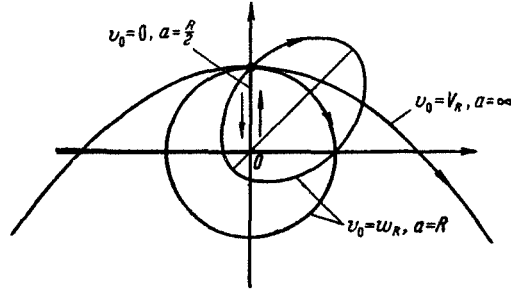
FIGURE 5.2. Various elliptical orbits.

There is thus a single-valued relation between the total mechanical energy per unit mass and the semimajor axis a of the orbit. In particular, if $Q = 0$, we have $a = \frac{R}{2}$, if $Q = \frac{\mu}{2R}$, we have $a = R$, and if $Q = \frac{\mu}{R}$, we have $a = \infty$ (the elliptical orbit is transformed into a parabola). The first of the three cases represents free fall, the second is the launch of a satellite with the ground

circular velocity w_R, and the third is the launch with the escape velocity V_P (see Sec. 1.1). The corresponding orbits are shown in Figure 5.2.

5.3. FLIGHT TIME AND ORBITAL PERIOD

Making use of the areal integral (4.9) and relation (5.10), we can find the time of passage through a given point D of the orbit. After some manipulations, we have

$$t = \frac{2\sigma}{\sqrt{\mu p}} + \tau, \tag{5.23}$$

where τ is the epoch of pericenter passage, and σ the area of the elliptical sector ΠOD (Figure 5.3).
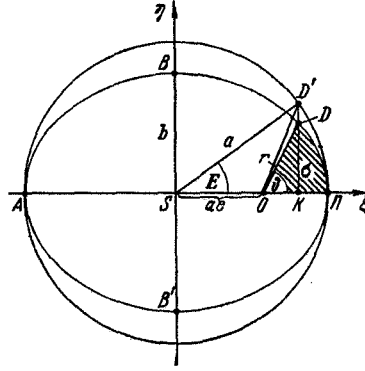
FIGURE 5.3. The relation between true and eccentric anomalies.

To find the area σ, we draw a circle of radius a around the center S of the elliptical orbit. The ellipse being considered can be obtained from this so-called a u x i l i a r y   c i r c l e   by uniform compression in a ratio b/a along the semiminor axis. Therefore, if a straight line parallel to the semiminor axis is drawn through the point D, K and D' being the intersection points of this line with the semimajor axis and the auxiliary circle, we may write

$$\frac{DK}{D'K} = \frac{b}{a}, \tag{5.24}$$

$$\sigma = \frac{b}{a}(S_1 - S_2), \tag{5.25}$$

where S_1 and S_2 are respectively the areas of the circular sector $\Pi SD'$ and the triangle OSD'.

Making use of Figure 5.3 and seeing that according to (5.4) $SO = ae$, we write the following expressions for the areas S_1 and S_2:

$$S_1 = \frac{a^2}{2} E, \quad S_2 = \frac{a^2}{2} e \sin E, \tag{5.26}$$

59

where $E = \angle D'S\Pi$ is the eccentric anomaly (in distinction from the true anomaly $\vartheta = \angle DO\Pi$).

Substituting (5.3), (5.7), (5.25), and (5.26) in (5.23), we find

$$t = \tau + \frac{E - e \sin E}{\lambda}, \tag{5.27}$$

where

$$\lambda = \frac{\sqrt{\mu}}{a^{3/2}}. \tag{5.28}$$

The problem thus reduces to the determination of the eccentric anomaly E (see Figure 5.3). Applying (5.3), (5.7), and (5.24), we find

$$\left. \begin{array}{l} r \cos \vartheta = OK = a (\cos E - e), \\ r \sin \vartheta = \frac{b}{a} D'K = a \sqrt{1 - e^2} \sin E. \end{array} \right\} \tag{5.29}$$

Squaring these equalities and adding, we find

$$r = a(1 - e \cos E). \tag{5.30}$$

From this relation and from the first equality in (5.29), we have

$$\left. \begin{array}{l} r(1 + \cos \vartheta) = a(1 - e)(1 + \cos E), \\ r(1 - \cos \vartheta) = a(1 + e)(1 - \cos E). \end{array} \right\} \tag{5.31}$$

Dividing the second equality by the first, we obtain the final expression for the eccentric anomaly:

$$\text{tg} \frac{E}{2} = \sqrt{\frac{1 - e}{1 + e}} \, \text{tg} \frac{\vartheta}{2}. \tag{5.32}$$

In calculating E from this formula, we must keep in mind that the angles $\frac{E}{2}$ and $\frac{\vartheta}{2}$ are always in one quadrant. Moreover, from the above relation we see that $E = \vartheta$ at the pericenter and the apocenter (i.e., for $\vartheta = k\pi$, where k is a whole number). Along the path from pericenter to apocenter $(0 < \vartheta < \pi)$, $E < \vartheta$, and along the path from apocenter to pericenter $(\pi < \vartheta < 2\pi)$, $E > \vartheta$.

From relations (5.27), (5.28), and (5.32) we can find the epoch t corresponding to any point of the orbit (as specified by the angles ϑ or E).

It is often necessary to solve the inverse problem — to find the position of the satellite (i.e., the angle ϑ) at a known time t. From (5.27) and (5.32) we see that this problem is reduced to the determination of the eccentric anomaly E from Kepler's equation

$$E - e \sin E = M, \tag{5.33}$$

where M is the so-called mean anomaly,

$$M = \lambda(t - \tau). \tag{5.34}$$

60

We shall show that Kepler's equation always has a single real solution. Consider the function

$$F(E, M) = E - e \sin E - M.$$

Clearly,

$$F(-\infty, M) = -\infty, \quad F(\infty, M) = \infty, \quad \frac{dF}{dE} = 1 - e \cos E > 0.$$

Hence it follows that for any M there is always an E, such that $F(E, M) = 0$, which corresponds to a solution of Kepler's equation.

There are a great many techniques for approximate solution of Kepler's equation. One of these is the method of successive approximations, where the calculations are made according to the scheme

$$E_n = M + e \sin E_{n-1}, \tag{5.35}$$

where E_{n-1} and E_n are the preceding and the current approximations of E. As the first approximation, we can always take $E_1 = M$.

Let us now find the orbital period P. We must calculate the change in time t as the angle ϑ goes through 2π. From (5.32) it follows that the angle E also goes through 2π. Then, applying (5.27), we find

$$P = \frac{2\pi}{\lambda} = 2\pi \frac{a^{3/2}}{\sqrt{\mu}}. \tag{5.36}$$

This expression is analogous to the corresponding relation (1.5) for circular orbit, with the major semiaxis a substituted for the radius r. The orbital period of a satellite in elliptical orbit with semimajor axis a is thus equal to the orbital period of a hypothetical satellite in circular orbit of radius $r = a$. From (5.28) and (5.34) we see that λ is the angular velocity of the satellite (equal to the mean angular velocity in elliptical orbit), while the mean anomaly M gives the angular distance of the hypothetical satellite from the perigee point of the elliptical orbit.

From (5.36) we see that the orbital period P increases with the semimajor axis a. Numerical estimates of the P vs. a dependence can be obtained from the graph in Figure 1.1: the flight altitude $h = r - R$ of the circular satellite should of course be replaced with the mean altitude $h_m = a - R$ of the elliptical orbit.

Comparison of (5.22) and (5.36) shows that there is a one-to-one correspondence between the semimajor axis a of elliptical orbit, the total mechanical energy per unit mass Q, and the orbital period P.

5.4. ELEMENTS OF ELLIPTICAL ORBIT

Motion in elliptical orbit is a particular case of motion of a point mass in a given force field. As we have previously observed, this motion is described by a sixth-order set of ordinary differential equations. Hence it follows that an elliptical orbit is fully defined by six independent parameters. These are, for instance, the initial conditions of motion, i.e., the rectangular coordinates x_0, y_0, z_0 of the mass center and the components v_{x0}, v_{y0}, v_{z0} of the velocity vector at a certain epoch $t = t_0$.

61

Another set of independent parameters fully describing the orbit is provided by the six constants C_1, C_2, ..., C_6 introduced in the previous chapter in the integration of the equations of motion (4.3). A one-to-one correspondence can be established between the set of initial conditions of motion and the set of integration constants C_1, C_2, ..., C_6. A set of any six independent parameters which are in one-to-one correspondence with the initial conditions of motion (or, in virtue of the preceding remark, with the integration constants C_1, C_2, ..., C_6) can obviously be used as orbit characteristics. We call it a c o m p l e t e   s e t   o f   o r b i t a l   e l e m e n t s. A criterion of its completeness is that it completely defines the orbit, i.e., makes it possible to find the coordinates and the velocity components of the mass center at any point of the orbit (or, alternatively, at any time t).

As an example, let us consider the following set of orbital elements:

inclination i,

longitude of the ascending node Ω,

argument of pericenter ω,

semimajor axis a,

eccentricity e,

epoch of pericenter passage τ.

The parameters i and Ω characterize the orientation of the orbital plane. Their definition is given in Sec. 1.2 (see Figures 1.2 and 5.4).
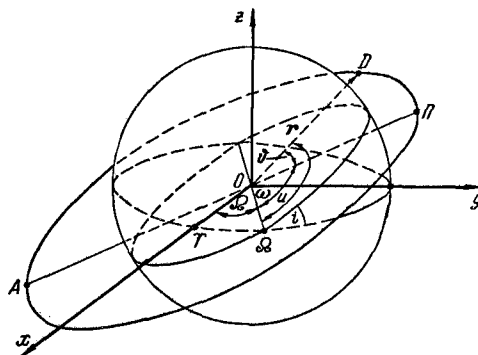
FIGURE 5.4. Elements of elliptical orbit.

The argument of the pericenter, ω, is the angular distance from the ascending node Ω to the pericenter Π, reckoned in the direction of motion of the satellite (see Figure 5.4). This angle specifies the direction of the semimajor axis of the orbit and the position of the pericenter; it is defined by

$$\omega = u - \vartheta.$$

where u and ϑ are respectively the angular distance from the ascending node and the true anomaly of any point D of the orbit. The elements a and e specify the extent and the shape of the orbit, while the epoch τ is used as a reference point on the time scale.

5.5. POSITION AND VELOCITY FROM ORBITAL ELEMENTS

We list the formulas which are used in determining the coordinates x, y, z and the velocity components v_x, v_y, v_z from known values of the orbital elements i, Ω, ω, a, e, τ. Applying relations (1.14), (4.19), (5.3), (5.11), (5.13), (5.27), (5.28), (5.30), and (5.32), we write

$$
\begin{aligned}
&r = \frac{p}{1 + e\cos\vartheta} = a(1 - e\cos E), \quad p = a(1 - e^2), \\[4pt]
&u = \omega + \vartheta, \\[4pt]
&t = \tau + \frac{E - e\sin E}{\lambda}, \quad \lambda = \frac{\sqrt{\mu}}{a^{3/2}}, \\[4pt]
&\operatorname{tg}\frac{E}{2} = \sqrt{\frac{1 - e}{1 + e}}\,\operatorname{tg}\frac{\vartheta}{2}, \\[4pt]
&v_r = \sqrt{\frac{\mu}{p}}\,e\sin\vartheta, \\[4pt]
&v_u = \sqrt{\frac{\mu p}{r}} = \sqrt{\frac{\mu}{p}}(1 + e\cos\vartheta), \\[4pt]
&x = r(\cos\Omega\cos u - \sin\Omega\sin u\cos i), \\
&y = r(\sin\Omega\cos u + \cos\Omega\sin u\cos i), \\
&z = r\sin u\sin i, \\
&v_x = v_r(\cos\Omega\cos u - \sin\Omega\sin u\cos i) - \\
&\qquad\quad - v_u(\cos\Omega\sin u + \sin\Omega\cos u\cos i), \\
&v_y = v_r(\sin\Omega\cos u + \cos\Omega\sin u\cos i) - \\
&\qquad\quad - v_u(\sin\Omega\sin u - \cos\Omega\cos u\cos i), \\
&v_z = v_r\sin u\sin i + v_u\cos u\sin i.
\end{aligned}
\qquad (5.37)
$$

These formulas unambiguously give the values of x, y, z, v_x, v_y, v_z at any point of the orbit (that the procedure is single-valued follows from the unique solvability of Kepler's equation (5.33) and also from the fact that the angles $\frac{E}{2}$ and $\frac{\vartheta}{2}$ are in the same quadrant). The time t, the true anomaly ϑ, or the eccentric anomaly E can be assumed as the argument specifying the position of the body in orbit. If the time t is adopted as argument, Kepler's equation (5.33) must first be solved, in order to find the eccentric anomaly E (a technique for the solution of this equation has been outlined in the previous section). If ϑ or E are chosen as argument, Kepler's equation need not be solved.
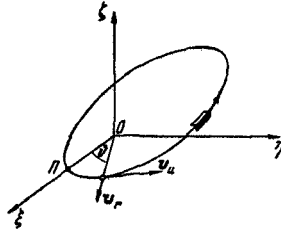
FIGURE 5.5. A frame of reference connected with the orbital plane and the perigee point of elliptical orbit.

If the position of the satellite in orbit is defined in terms of E (or t), it is advisable to eliminate the true anomaly ϑ among the relations in (5.37). To this end, consider a right-hand rectangular frame $O\xi\eta\zeta$ with its origin at the center of attraction O. The axis $O\xi$ is directed to the pericenter, the plane $O\xi\eta$ is the orbital plane, and the axis $O\zeta$ points at right angles to the orbital plane so that the satellite appears to move clockwise if viewed in the positive direction of this axis (Figure 5.5).

From (5.37) and Figure 5.5 we have

$$
\left.
\begin{aligned}
\xi &= r\cos\vartheta = a\,(1-e\cos E)\cos\vartheta, \\
\eta &= r\sin\vartheta = a\,(1-e\cos E)\sin\vartheta, \\
v_\xi &= v_r\cos\vartheta - v_u\sin\vartheta = \sqrt{\tfrac{\mu}{p}}\,[e\sin\vartheta\cos\vartheta - \\
&\quad -(1+e\cos\vartheta)\sin\vartheta] = -\sqrt{\tfrac{\mu}{p}}\sin\vartheta, \\
v_\eta &= v_r\sin\vartheta + v_u\cos\vartheta = \sqrt{\tfrac{\mu}{p}}\,[e\sin^2\vartheta + \\
&\quad +(1+e\cos\vartheta)\cos\vartheta] = \sqrt{\tfrac{\mu}{p}}\,(e+\cos\vartheta), \\
\zeta &= v_\zeta = 0.
\end{aligned}
\right\}
\tag{5.38}
$$

On the other hand, from (5.29) and (5.30) we have

$$
\sin\vartheta = \frac{\sqrt{1-e^2}\,\sin E}{1-e\cos E}, \quad \cos\vartheta = \frac{\cos E-e}{1-e\cos E},
\tag{5.39}
$$

and finally, making use of (5.3),

$$
\left.
\begin{aligned}
\xi &= a\,(\cos E - e), \\
\eta &= a\,\sqrt{1-e^2}\,\sin E, \\
\zeta &= 0, \\
v_\xi &= -\sqrt{\tfrac{\mu}{a}}\,\frac{\sin E}{1-e\cos E}, \\
v_\eta &= \sqrt{\tfrac{\mu}{a}}\,\frac{\sqrt{1-e^2}\,\cos E}{1-e\cos E}, \\
v_\zeta &= 0.
\end{aligned}
\right\}
\tag{5.40}
$$

The frame $O\xi\eta\zeta$ is transformed to the previously defined frame $Oxyz$ by the following matrix of direction cosines:

	ξ	η	ζ
x	$\cos\Omega\cos\omega -$ $-\sin\Omega\sin\omega\cos i$	$-\cos\Omega\sin\omega -$ $-\sin\Omega\cos\omega\cos i$	$\sin\Omega\sin i$
y	$\sin\Omega\cos\omega +$ $+\cos\Omega\sin\omega\cos i$	$-\sin\Omega\sin\omega +$ $+\cos\Omega\cos\omega\cos i$	$-\cos\Omega\sin i$
z	$\sin\omega\sin i$	$\cos\omega\sin i$	$\cos i$

The first column of this matrix is easily derived from (5.37). To this end, it suffices to find the ratios $\frac{x}{r}$, $\frac{y}{r}$, $\frac{z}{r}$, substituting ω for the angle u

64

in the corresponding relations. The second column is obtained from the first by substituting $\omega + \pi/2$ for ω. The third column is determined making use of (2.45').

5.6. ORBITAL ELEMENTS FROM INITIAL CONDITIONS OF MOTION

The relations of the previous section enable us to find the initial conditions of motion x_0, y_0, z_0, v_{x0}, v_{y0}, v_{z0} at a certain epoch $t = t_0$ from the orbital elements a, e, τ, i, Ω, ω; the procedure is single-valued. Let us now consider the reverse problem, namely how to determine the orbital elements from the initial conditions.

The elements Ω and i can be found from (2.44) and (2.46).

To find the semimajor axis a and the eccentricity e, we should first determine the initial distance r_0 from the gravitational center, the magnitude of the initial velocity vector v_0, and the angle θ_0 between the velocity vector and the in-plane normal to the radius vector joining the gravitational center with the point in orbit. We have

$$
\left.
\begin{aligned}
r_0 &= \sqrt{x_0^2 + y_0^2 + z_0^2}, \\
v_0 &= \sqrt{v_{x0}^2 + v_{y0}^2 + v_{z0}^2}, \\
\sin \theta_0 &= \frac{x_0 v_{x0} + y_0 v_{y0} + z_0 v_{z0}}{r_0 v_0}, \\
\cos \theta_0 &= \frac{\sqrt{r_0^2 v_0^2 - (x_0 v_{x0} + y_0 v_{y0} + z_0 v_{z0})^2}}{r_0 v_0} = \\
&= \frac{\sqrt{(x_0 v_{y0} - y_0 v_{x0})^2 + (y_0 v_{z0} - z_0 v_{y0})^2 + (z_0 v_{x0} - x_0 v_{z0})^2}}{r_0 v_0}.
\end{aligned}
\right\} \tag{5.41}
$$

We invariably assume

$$\cos \theta_0 > 0.$$

This is so because the angle θ is reckoned in the direction of satellite motion (see Figure 4.2), and therefore

$$-\frac{\pi}{2} \leqslant \theta_0 \leqslant \frac{\pi}{2}, \tag{5.42}$$

which ensures unambiguous definition of the angle.

From (4.22), (4.23), and (5.15), we have

$$
\left.
\begin{aligned}
a &= \frac{r_0}{2 - k_0}, \\
e &= \sqrt{1 - k_0(2 - k_0)\cos^2 \theta_0} = \\
&\qquad = \sqrt{(1 - k_0) + k_0(2 - k_0)\sin^2 \theta_0}, \\
k_0 &= \frac{r_0 v_0^2}{\mu}.
\end{aligned}
\right\} \tag{5.43}
$$

65

To find ω and τ, we should first determine the true anomaly ϑ at the point of origin. From (5.37) we have

$$
\left.
\begin{aligned}
v_{r0} &= v_0 \sin\theta_0 = \sqrt{\frac{\mu}{p}}\, e \sin\vartheta_0, \\
v_{u0} &= v_0 \cos\theta_0 = \sqrt{\frac{\mu}{p}}\,(1 + e \cos\vartheta_0),
\end{aligned}
\right\}
\tag{5.44}
$$

where v_{r0} and v_{u0} are the initial values of the two velocity components.

On the other hand, from (4.18) and (4.21) we have

$$
\sqrt{\frac{\mu}{p}} = \frac{\mu}{C} = \frac{\mu}{r_0 v_0 \cos\theta_0}.
$$

Substituting this expression in the right-hand sides of (5.44) and applying expression (5.43) for the coefficient k_0, we have

$$
\left.
\begin{aligned}
\sin\vartheta_0 &= \frac{k_0 \sin\theta_0 \cos\theta_0}{e}, \\
\cos\vartheta_0 &= \frac{k_0 \cos^2\theta_0 - 1}{e}.
\end{aligned}
\right\}
\tag{5.45}
$$

Hence

$$
\operatorname{tg}\vartheta_0 = \frac{k_0 \sin\theta_0 \cos\theta_0}{k_0 \cos^2\theta_0 - 1}.
\tag{5.46}
$$

The true anomaly ϑ_0 is uniquely determined from (5.45). A verification is possible using the identity $\sin^2\vartheta_0 + \cos^2\vartheta_0 = 1$ (this simultaneously verifies the calculated eccentricity e). From (5.46), on the other hand, the true anomaly is determined uniquely only if we remember that $\sin\vartheta_0$ has the same sign as the numerator in the right-hand side of (5.46), and $\cos\vartheta_0$ the same sign as the denominator (since $e > 0$).

To find the argument ω, we make use of the third equality in (5.37), according to which

$$
\omega = u_0 - \vartheta_0,
\tag{5.47}
$$

where u_0 is the initial value of the angle u, defined by (2.52).

The expression for the last element τ can be obtained from (5.37):

$$
\left.
\begin{aligned}
\tau &= t_0 = \frac{E_0 - e \sin E_0}{\lambda}, \\
\operatorname{tg}\frac{E_0}{2} &= \sqrt{\frac{1 - e}{1 + e}}\,\operatorname{tg}\frac{\vartheta_0}{2},
\end{aligned}
\right\}
\tag{5.48}
$$

where E_0 is the eccentric anomaly at the point of origin.

We list all the formulas which are used in calculation of the orbital elements a, e, τ, Ω, i, ω from the initial conditions x_0, y_0, z_0, v_{x0}, v_{y0}, v_{z0} at

a certain epoch $t = t_0$:

$$C_1 = y_0 v_{z0} - z_0 v_{y0},$$

$$C_2 = z_0 v_{x0} - x_0 v_{z0},$$

$$C_3 = x_0 v_{y0} - y_0 v_{x0},$$

$$C = \sqrt{C_1^2 + C_2^2 + C_3^2},$$

$$\operatorname{tg} \Omega = -\frac{C_1}{C_2}, \quad \cos i = \frac{C_3}{C}, \quad 0 \leqslant i < \pi,$$

$$v_0 = \sqrt{v_{x0}^2 + v_{y0}^2 + x_{z0}^2}, \quad r_0 = \sqrt{x_0^2 + y_0^2 + z_0^2},$$

$$\sin \theta_0 = \frac{x_0 v_{x0} + y_0 v_{y0} + z_0 v_{z0}}{r_0 v_0}, \quad -\frac{\pi}{2} \leqslant \theta_0 \leqslant \frac{\pi}{2},$$

$$\cos \theta_0 = \frac{\sqrt{r_0^2 v_0^2 - (x_0 v_{x0} + y_0 v_{y0} + z_0 v_{z0})^2}}{r_0 v_0} =$$

$$= \frac{\sqrt{(x_0 v_{y0} - y_0 v_{x0})^2 + (y_0 v_{z0} - z_0 v_{y0})^2 + (z_0 v_{x0} - x_0 v_{z0})^2}}{r_0 v_0},$$

$$k_0 = \frac{r_0 v_0^2}{\mu}, \quad a = \frac{r_0}{2 - k_0},$$

$$e = \sqrt{1 - k_0 (2 - k_0) \cos^2 \theta_0} =$$

$$= \sqrt{(1 - k_0)^2 + k_0 (2 - k_0) \sin^2 \theta_0},$$

$$\sin \vartheta_0 = \frac{k_0 \sin \theta_0 \cos \theta_0}{e}, \quad \cos \vartheta_0 = \frac{k_0 \cos^2 \theta_0 - 1}{e},$$

$$\operatorname{tg} \vartheta_0 = \frac{k_0 \sin \theta_0 \cos \theta_0}{k_0 \cos^2 \theta_0 - 1},$$

$$\omega = u_0 - \vartheta_0,$$

$$\cos u_0 = \frac{x_0 \cos \Omega + y_0 \sin \Omega}{r_0}, \quad \sin u_0 = \frac{z_0}{r_0 \sin i},$$

$$\tau = t_0 - \frac{E_0 - e \sin E_0}{\lambda}, \quad \lambda = \frac{\sqrt{\mu}}{a^{3/2}},$$

$$\operatorname{tg} \frac{E_0}{2} = \sqrt{\frac{1 - e}{1 + e}} \operatorname{tg} \frac{\vartheta_0}{2}.$$

(5.49)

When using these formulas, we must always remember that the sign of $\sin \Omega$ is the sign of C_1, whereas the sign of $\cos \Omega$ is the sign of minus C_2. Furthermore, the angles $\frac{E_0}{2}$ and $\frac{\vartheta_0}{2}$ lie in one quadrant.

Relations (5.49) are suitable for unambiguous determination of the orbital elements from known initial coordinates and velocity components, which satisfy the condition of elliptical orbit

$$k_0 = \frac{r_0 v_0^2}{\mu} < 2. \tag{5.50}$$

In conclusion, note that when solving our problem from (5.49), we need not carry the process to explicit determination of θ_0: either $\sin \theta_0$ or $\cos \theta_0$ will suffice.

We have thus established a reciprocal one-to-one correspondence between the initial conditions of motion and the orbital elements. The particular set of orbital elements introduced in Sec. 5.4 completely defines the entire orbit, and is therefore complete.

There is clearly an infinity of different complete sets of orbital elements. In particular, the semimajor axis a can be replaced with the period P, or the focal parameter p can be substituted for either of the parameters

67

a or e. In celestial mechanics the epoch of perigee passage τ is often replaced with the mean anomaly

$$M_0 = \lambda(t_0 - \tau) = E_0 - e \sin E_0, \tag{5.51}$$

at a certain given instant of time t_0 (E_0 is the corresponding eccentric anomaly).

Kepler's equation (5.33) then takes the form

$$M = M_0 + \lambda(t - t_0) = E - e \sin E_0. \tag{5.52}$$

5.7. SERIES FOR APPROXIMATE DETERMINATION OF LOW-ECCENTRICITY ELLIPTICAL ORBITS

It follows from the preceding results that to establish a relation among the polar coordinates r, ϑ and the flight time t, we must introduce a new intermediary quantity — the eccentric anomaly E — and solve Kepler's transcendental equation (5.33). This often prevents us from performing a rapid qualitative analysis of motion in elliptical orbit. In the analysis of low-eccentricity orbits, this obstacle is easily overcome by introducing series expansions with the eccentricity e as a small parameter. In this section, we consider some of the approximation series. The true anomaly ϑ, and then the time t will be used as the independent variables in the expansions.

A series for the function $r(\vartheta)$ is obtained by expanding the right-hand side of (4.19) in powers of the small quantity $e \cos \vartheta$:

$$r = p(1 - e \cos \vartheta + e^2 \cos^2 \vartheta - e^3 \cos^3 \vartheta + e^4 \cos^4 \vartheta - \ldots). \tag{5.53}$$

A series expansion of $t(\vartheta)$ is derived from (5.2), (5.12), and (5.36). We have

$$t = \tau + P_1 \int_0^\vartheta (1 - e^2)^{3/2} (1 + e \cos \vartheta)^{-2} \, d\vartheta, \tag{5.54}$$

where P_1 is determined from (3.7):

$$P_1 = \frac{P}{2\pi} = \frac{1}{\lambda} = \frac{a^{3/2}}{\sqrt{\mu}}.$$

We now expand the integrand in the right-hand side of (5.54) in powers of e. To this end, note that

$$(1 + e \cos \vartheta)^{-2} = 1 - 2e \cos \vartheta + 3e^2 \cos^2 \vartheta - 4e^3 \cos^3 \vartheta + 5e^4 \cos^4 \vartheta - \ldots,$$

$$(1 - e^2)^{3/2} = 1 \qquad - \frac{3}{2} e^2 \qquad + \frac{3}{8} e^4 + \cdots$$

68

Multiplying these series term by term, we find

$$(1 - e^2)^{1/2}(1 + e \cos \vartheta)^{-2} = 1 - 2e \cos \vartheta +$$
$$+ 3e^2 \left(\cos^2 \vartheta - \frac{1}{2}\right) - e^3 (4 \cos^3 \vartheta - 3 \cos \vartheta) +$$
$$+ e^4 \left(5 \cos^4 \vartheta - \frac{9}{2} \cos^2 \vartheta + \frac{3}{8}\right) + \cdots$$

Now,

$$\cos^2 \vartheta = \frac{\cos 2\vartheta + 1}{2},$$
$$\cos^3 \vartheta = \frac{\cos 3\vartheta + 3 \cos \vartheta}{4},$$
$$\cos^4 \vartheta = \frac{\cos 4\vartheta + 4 \cos 2\vartheta + 3}{8},$$
$$\cdots \cdots \cdots \cdots \cdots$$

Then,

$$(1 - e^2)^{3/2}(1 + e \cos \vartheta)^{-2} = 1 - 2e \cos \vartheta + \frac{3}{2} e^2 \cos 2\vartheta -$$
$$- e^3 \cos 3\vartheta + \frac{1}{8} e^4 (5 \cos 4\vartheta + 2 \cos 2\vartheta) - \cdots$$

Substituting in the right-hand side of (5.54) and integrating, we find the series

$$t = \tau + P_1 \left[\vartheta - 2e \sin \vartheta + \frac{3}{4} e^2 \sin 2\vartheta - \frac{e^3}{3} \sin 3\vartheta +\right.$$
$$\left. + \frac{e^4}{32} (5 \sin 4\vartheta + 4 \sin 2\vartheta) - \cdots \right]. \tag{5.55}$$

Let us now write the series expansions of $\vartheta(t)$ and $r(t)$. The mean anomaly

$$M = 2\pi \frac{t - \tau}{P} = \frac{t - \tau}{P_1} = \lambda (t - \tau) \tag{5.56}$$

is used as the independent variable, rather than the time t.

We apply Lagrange's formula for a function $f(y)$, where y is a root of the equation

$$y = a + x\varphi(y). \tag{5.57}$$

Here a, x, y are arbitrary complex numbers, and $\varphi(y)$ meanwhile is an arbitrary function. Lagrange's formula in this case has the form /2, 30/

$$f(y) = f(a) + x\varphi(a) f'(a) + \frac{x^2}{2!} \frac{d}{da} [\varphi^2(a) f'(a)] + \cdots$$
$$\cdots + \frac{x^n}{n!} \frac{d^{n-1}}{da^{n-1}} [\varphi^n(a) f'(a)] + \cdots \tag{5.58}$$

Let s be a closed contour (in the complex plane) inside which $f(y)$ and $\varphi(y)$ are holomorphous functions. If at any point of the contour s

$$\left|\frac{x\varphi(y)}{y - x}\right| < 1, \tag{5.59}$$

the series (5.58) converges to $f(y)$ for any a from the region inside s.

Kepler's equation (5.33) is clearly a particular case of equation (5.57). Here

$$y = E, \; \varphi(E) = \sin E, \; x = e, \; a = M. \qquad (5.60)$$

Hence, putting

$$f(E) = E,$$

and applying Lagrange's series (5.58), we obtain the following expansion for the eccentric anomaly:

$$E = M + e \sin M + \frac{e^2}{2!} \frac{d}{dM} \sin^2 M + \frac{e^3}{3!} \frac{d^2}{dM^2} \sin^3 M + \frac{e^4}{4!} \frac{d^3}{dM^3} \sin^4 M + \dots \qquad (5.61)$$

Now,

$$\sin^2 M = \frac{1 - \cos 2M}{2},$$

$$\sin^3 M = \frac{3 \sin M - \sin 3M}{4},$$

$$\sin^4 M = \frac{\cos 4M - 4 \cos 2M + 3}{8},$$

$$\dots \dots \dots \dots \dots \dots$$

Differentiating and substituting in (5.61), we obtain a final expression for E, the solution of Kepler's equation (5.33):

$$E = M + e \sin M + \frac{e^2}{2} \sin 2M + \frac{e^3}{8} (3 \sin 3M - \sin M) +$$

$$+ \frac{e^4}{6} (2 \sin 4M - \sin 2M) + \dots \qquad (5.62)$$

To obtain $\vartheta(M)$, we make use of (5.2), (5.11), (5.12), (5.28), (5.30), and (5.56), whence

$$\frac{d\vartheta}{dM} = \frac{d\vartheta}{dt} \frac{dt}{dM} = \frac{a^{3/2}}{\sqrt{\mu}} \frac{d\vartheta}{dt} = \frac{a^{3/2} \sqrt{p}}{r^2} = \frac{\sqrt{1 - e^2}}{(1 - e \cos E)^2}. \qquad (5.63)$$

On the other hand, differentiating Kepler's equation (5.33), we have

$$\frac{dE}{dM}(1 - e \cos E) = 1, \quad \frac{dE}{dM} = \frac{1}{1 - e \cos E}. \qquad (5.64)$$

Comparing (5.64) to (5.63), we see that

$$\vartheta = \sqrt{1 - e^2} \int_0^M \left(\frac{dE}{dM}\right)^2 dM. \qquad (5.65)$$

Differentiating (5.62) and squaring the series, we find

$$\frac{dE}{dM} = 1 + e \cos M + e^2 \cos 2M + \frac{e^3}{8} (9 \cos 3M - \cos M) + \frac{e^4}{3} (4 \cos 4M - \cos 2M) + \dots,$$

$$\left(\frac{dE}{dM}\right)^2 = 1 + 2e \cos M + e^2 (2 \cos 2M + \cos^2 M) + \frac{e^3}{4} (9 \cos^3 M - \cos M + 8 \cos M \cos 2M) + \dots =$$

$$= 1 + 2e \cos M + \frac{e^2}{2} (5 \cos 2M + 1) + \frac{e^3}{4} (13 \cos 3M + 3 \cos M) + \dots$$

Substituting in (5.65), integrating, and inserting for $\sqrt{1-e^2}$ its binomial expansion

$$\sqrt{1-e^2} = 1 - \frac{1}{2}e^2 - \frac{1}{8}e^4 - \ldots,$$

we obtain the final series

$$\vartheta = M + 2e\sin M + \frac{5}{4}e^2 \sin 2M + \frac{e^3}{12}(13\sin 3M - 3\sin M) + \ldots \qquad (5.66)$$

We now proceed to determine $r(M)$ with the aid of Lagrange's formula (5.58) and equalities (5.60). From (5.30) we have

$$f(E) = \frac{r}{a} = 1 - e\cos E, \quad f'(E) = e\sin E.$$

Hence,

$$\frac{r}{a} = 1 - e\cos M + e^2 \sin^2 M + \frac{e^3}{2!}\frac{d}{dM}\sin^3 M + \frac{e^4}{3!}\frac{d^2}{dM^2}\sin^4 M + \ldots$$

or, finally,

$$r = a\left[1 - e\cos M + \frac{e^2}{2}(1 - \cos 2M) + \right.$$
$$\left. + \frac{3}{8}e^3(\cos M - \cos 3M) + \frac{e^4}{3}(\cos 2M - \cos 4M) + \ldots\right]. \qquad (5.67)$$

As regards the convergence of the series (5.53), (5.55), (5.62), (5.66), and (5.67), we should note that the derivation of (5.53) and (5.55) is based on the binomial expansion of $(1+\alpha)^n$, where α is a fairly small number, and n an arbitrary power. The binomial series is known to converge for any $\alpha < 1$. The series (5.53) and (5.55) are thus convergent for any ϑ if

$$e < 1. \qquad (5.68)$$

More detailed analyses /2/ bases on inequality (5.59) show that the series (5.62), (5.66), and (5.67) converge for all real M if

$$e < 0.6627\ldots \qquad (5.69)$$

The series expansions of this section can be profitably used in the analysis of orbits with eccentricity not greater than $0.2 - 0.3$. In this case, the series converge very rapidly, and only a few of the leading terms need be retained. The first term of the truncated series provides an estimate for the accuracy of the results.

A more detailed discussion of the theory will be found in Duboshin's book /2/. This book also gives expressions for the general terms of the series (5.62), (5.66), and (5.67).

5.8. ESTIMATING THE ACCURACY OF THE EXPRESSIONS OF THE THEORY OF NEARLY CIRCULAR MOTION

If only the first two terms are retained in the right-hand sides of (5.66) and (5.67), we arrive at equation (2.41) of a nearly circular orbit whose $P, e, \omega,$ and τ are equal to those of the elliptical orbit. Thus,

$$a = r_m, \quad M = \varphi - \omega, \quad \vartheta = u - \omega. \tag{5.70}$$

The sums of all the terms in the right-hand sides of (5.66) and (5.67) which contain the higher powers of e (i.e., starting with the third term) can be applied to evaluate the errors introduced by the equations of nearly circular orbits (2.38) and (2.41). In practice (for fairly small eccentricities), the accuracy can be estimated by the third term in the right-hand sides of the expansions (5.66) and (5.67). We obtain the following estimates for the errors in the equations of nearly circular orbit:

$$|\Delta r| \leqslant e^2 r_m, \quad |\Delta l| \leqslant \frac{5}{4} e^2 r_m, \tag{5.71}$$

where Δr and Δl are respectively the linear errors in satellite position along the radius r and along the in-plane normal l to the radius.

We shall show in the following that the errors of the "exact" elliptical theory, which ignores the noncentral components of the gravitational field, the pull of the Moon and the Sun, and various other factors, are as large as a few tens and even hundreds of kilometers. The transition from the theory of elliptical motion to the theory of nearly circular motion is therefore fully justified, in so far as Δl and Δr are of the order of $5 - 10$ km. From (5.71) it follows that for low-flying satellites ($r_m < 10,000$ km) this requirement is satisfied if

$$e < 0.02. \tag{5.72}$$

We recall that, for low eccentricities, the introduction of the nearly circular theory is further justified, not only by the exceptional simplicity of the relations, but also by the uncertainty in the position of the pericenter. As we have observed in Sec. 2. 8, it is advisable to use formulas (2.38) in this case, since they are independent of the pericenter point.

Chapter 6

HYPERBOLIC ORBITS

6.1. PRINCIPAL GEOMETRICAL PROPERTIES
OF HYPERBOLIC ORBITS

As we have observed in Sec. 4.5, a body moves in hyperbolic orbit if its flight velocity is greater than the escape velocity V from the primary, i.e., if

$$v > V = \sqrt{\frac{2\mu}{r}}.$$
<div align="right">(6.1)</div>

The eccentricity e and the coefficient k from (4.22) and (4.23) satisfy the inequalities

$$e > 1 \quad \text{and} \quad k > 2.$$
<div align="right">(6.2)</div>

It is known from analytical geometry that for $e > 1$ the equation of orbit (4.19) in polar coordinates is the equation of a hyperbola with a focal parameter p and eccentricity e. In a rectangular frame $S\xi\eta$, this equation takes the form

$$\frac{\xi^2}{\alpha^2} - \frac{\eta^2}{\beta^2} = 1,$$
<div align="right">(6.3)</div>

where α and β are the semiaxes of the hyperbola defined by

$$\alpha = \frac{p}{e^2 - 1}, \quad \beta = \alpha \sqrt{e^2 - 1} = \frac{p}{\sqrt{e^2 - 1}}.$$
<div align="right">(6.4)</div>

In the frame $S\xi\eta$, the axis $S\xi$ points in the direction $\vartheta = 0$ through the center of attraction O, and the origin S (the center of the hyperbola) is distant

$$\gamma = \alpha e = \frac{pe}{e^2 - 1}$$
<div align="right">(6.5)</div>

from the gravitational center O (Figure 6.1).

The gravitational center O is the f i r s t f o c u s of the hyperbola. The s e c o n d f o c u s O' is on the $O\xi$ axis in the symmetric point about the center of the hyperbola:

$$SO' = SO = \gamma.$$

If r and r' are the distance from a point D of the orbit to the foci O and O', then the principal property of the hyperbola (in fact, its definition) is given by the equality

$$|r' - r| = 2\alpha. \tag{6.6}$$

The hyperbola defined by (6.3) or (6.6) is a curve with two branches. The first branch, shown by the solid line in Figure 6.1, curves around the gravitational center O, while the second branch (the dashed curve) curves away from the center. It is only the first branch which is physically meaningful in our problem, since it corresponds to orbital motion
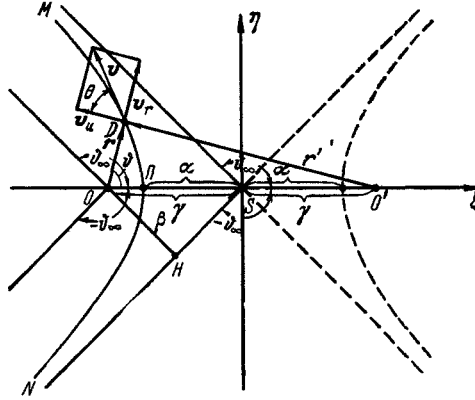
FIGURE 6.1. Geometrical parameters of hyperbolic orbit.

accelerated toward the center of attraction O, i.e., in the field of an attractive force through this center. The second branch represents motion in the field of a repulsive force, and we shall henceforth ignore it. Note that in accordance with (4.19), the second branch of the hyperbola corresponds to negative distances r, which is clearly impossible. Along the first branch of the hyperbola, relation (6.6) takes the form

$$r' - r = 2\alpha. \tag{6.7}$$

Unlike the ellipse, hyperbolic orbit is an open trajectory beginning and ending outside the sphere of attraction of the primary (i.e., outside the region where the gravitational pull of the primary constitutes the main driving force). In our analysis of hyperbolic motion, we shall regard the portions of the orbit outside the sphere of gravitational pull of the primary as lying "at infinity". The hyperbolic orbit can be shown to approach a straight line "at infinity". We rewrite expression (6.3) as

$$\eta = \pm \frac{\beta}{\alpha} \xi \sqrt{1 - \frac{\alpha^2}{\xi^2}}. \tag{6.8}$$

74

For $\xi \to \infty$, we have $\frac{\alpha^2}{\xi^2} \to 0$. We can therefore expand the right-hand side of (6.8) in a binomial series. Thus,

$$\eta = \pm \frac{\beta}{\alpha}\xi \mp \frac{1}{2}\frac{\alpha\beta}{\xi} + \cdots = \pm \frac{\beta}{\alpha}\xi + O\left(\frac{1}{\xi}\right). \tag{6.9}$$

For $\xi \to \infty$, we have $O\left(\frac{1}{\xi}\right) \to 0$, and the hyperbola asymptotically approaches one of the straight lines

$$\eta = \pm \frac{\beta}{\alpha}\xi. \tag{6.10}$$

These lines are the a s y m p t o t e s of the hyperbolic orbit. One of these (the segment NS in Figure 6.1) is the entry trajectory of the body into the sphere of attraction of the primary, while the other (the segment SM) is the path of escape of the body from the primary.

We now return to the equation of the orbit (4.19) in polar coordinates. Seeing that

$$r > 0,$$

we have

$$-\frac{1}{e} < \cos \vartheta < 1. \tag{6.11}$$

This inequality may be written as

$$-\vartheta_\infty < \vartheta < \vartheta_\infty, \tag{6.12}$$

where

$$\frac{\pi}{2} < \vartheta_\infty = \arccos\left(-\frac{1}{e}\right) < \pi. \tag{6.13}$$

The angle $\pm \vartheta_\infty$ is clearly the limiting value of the true anomaly ϑ as the body recedes to infinity.

Applying (6.4) and (6.13), we write

$$\operatorname{tg} \vartheta_\infty = -\sqrt{e^2 - 1} = -\frac{\beta}{\alpha}. \tag{6.14}$$

The limiting values of the true anomaly, $\pm \vartheta_\infty$, are thus the angles between the asymptotes of the hyperbola to its axis $S\xi$ (see Figure 6.1).

We see from Figure 6.1 that for a body moving in hyperbolic orbit, the true anomaly monotonically increases. Motion in the interval $N\Pi$, defined by the inequality

$$-\vartheta_\infty < \vartheta \leqslant 0, \tag{6.15}$$

corresponds to a monotonic rise of $\cos \vartheta$ from $\cos(-\vartheta_\infty) = -\frac{1}{e}$ to $\cos(0) = 1$;

in the interval ΠM, defined by the inequality

$$0 \leqslant \vartheta < \vartheta_\infty, \tag{6.16}$$

75

$\cos\vartheta$ monotonically decreases from $\cos(0)=1$ to $\cos(\vartheta_\infty)=-\frac{1}{e}$.

Applying (4.19), we see that in the interval $N\Pi$, the distance r monotonically decreases and the body approaches the gravitational center O, while in the interval ΠM, r increases and the body moves away from the center O. The section $N\Pi$ is therefore called the descending branch of hyperbolic orbit, and the section ΠM, the ascending branch. Note that a moving body will trace both branches of hyperbolic orbit only if it travels from "infinity". In particular, this applies to an artificial Earth satellite trapped by the Moon's pull. If, however, a body is injected into hyperbolic orbit inside the sphere of gravitational pull of the primary (e.g., a satellite launched from the Earth with a velocity greater than the escape velocity), it will only describe the path from the injection point D to the terminal point M, where it escapes to "infinity" (see Figure 6.1).

The point closest to the center of attraction O (corresponding to $\vartheta=0$) is the pericenter (perigee, perihelion, etc., as the case may be) of the orbit. Its distance r_p from the center of attraction is called the pericenter (perigee, perihelion) distance. From (4.19), (6.4), and (6.5) we have

$$r_{\mathrm{p}}=\frac{p}{1+e}=\alpha(e-1)=\gamma-\alpha. \tag{6.17}$$

From Figure 6.1 we now can find the distance from the pericenter Π to the center S of the orbit:

$$\Pi S=\gamma-r_p=\alpha. \tag{6.18}$$

To establish the geometrical meaning of the second semiaxis β, we calculate the distance OH from the gravitational center to one of the asymptotes (see Figure 6.1). From the right triangle OSH, making use of (6.4), (6.5), and (6.13), we have

$$OH=\gamma\cos\left(\vartheta_\infty-\frac{\pi}{2}\right)=ae\sqrt{1-\frac{1}{e^2}}=\beta. \tag{6.19}$$

The first semiaxis α of hyperbolic orbit is equal to the distance from the pericenter Π (the vertex of the hyperbola) to the center S of the hyperbola. The second semiaxis β is equal to the distance from the gravitational center O (the first focus of the hyperbola) to either asymptote. The β-to-α ratio is the absolute value of the slope of the asymptote to the $O\xi$ axis.

For any hyperbolic orbit, from relations (5.2), (5.7), and (6.4), we can define the semiaxes of an equivalent ellipse

$$a=-\alpha,\; b=-i\beta,\; \alpha=|a|,\; \beta=|b|. \tag{6.20}$$

In other words, hyperbolic orbit corresponds to an ellipse with a negative semimajor axis and an imaginary semiminor axis. From (5.36) and (6.20) it follows that the orbital period P for this ellipse is imaginary. Although this imaginary elliptical orbit is physically meaningless, equalities (6.20) can be applied for formal extension of the relations derived for elliptical orbits to the case of motion in hyperbolic orbit.

The validity of this generalization can be verified in each particular case by repeating the corresponding manipulations.

6.2. FLIGHT VELOCITY AND ENERGY

The velocity components v_u and v_r, the magnitude v of the velocity vector, its inclination θ to the local horizon, and the mechanical energy Q per unit mass can be obtained from relations (5.11), (5.13), (5.15), (5.16), and (5.22). Substitution of (6.20) in these relations gives

$$\left.\begin{array}{l} v_u = \frac{\sqrt{\mu p}}{r} = \sqrt{\frac{\mu}{p}}\,(1 + e\cos\vartheta), \\[2mm] v_r = \sqrt{\frac{\mu}{p}}\,e\sin\vartheta, \\[2mm] v^2 = \frac{2\mu}{r} - \frac{\mu}{a} = \frac{2\mu}{r} + \frac{\mu}{a}, \\[2mm] \mathrm{tg}\,\theta = \frac{v_r}{v_u} = \frac{r}{p}\,e\sin\vartheta = \frac{e\sin\vartheta}{1 + e\cos\vartheta}, \\[2mm] Q = \mu\left(\frac{1}{R} - \frac{1}{2a}\right) = \mu\left(\frac{1}{R} + \frac{1}{2a}\right). \end{array}\right\} \tag{6.21}$$

From (6.21) we see that the velocity v in hyperbolic orbit monotonically increases along the descending branch $N\varPi$ and decreases along the ascending branch $\varPi M$ (see Figure 6.1). The minimum velocity (we call it the **asymptotic velocity**) corresponding to infinite recession of the satellite from the primary is given by

$$v_\infty = \sqrt{\frac{\mu}{a}}. \tag{6.22}$$

There is thus a one-to-one correspondence between the asymptotic velocity v_∞, the semiaxis a of the hyperbola, and the mechanical energy Q. Figure 6.2 plots the semiaxis a vs. v_∞ for satellite encounter with the Earth and the Moon. (Here a_δ denotes the semiaxis of hyperbolic orbit around the Earth, and $a_{\mathbb{C}}$ that around the Moon).
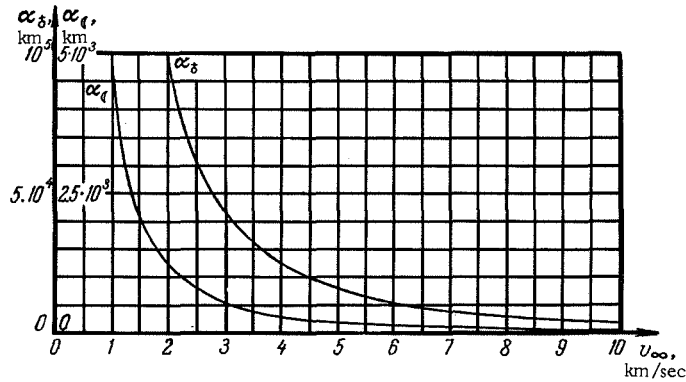
FIGURE 6.2. Semiaxis a of hyperbolic orbit vs. asymptotic velocity v_∞ for satellite encounter with the Earth and the Moon.

The maximum velocity v_p is attained at the pericenter. From (6.17) and (6.21) we have for this pericenter velocity

$$v_{\mathrm{p}} = \sqrt{\frac{\mu}{a} \frac{e+1}{e-1}} = v_{\infty} \sqrt{\frac{e+1}{e-1}} = w_{\mathrm{p}} \sqrt{e+1}, \tag{6.23}$$

where $w_{\mathrm{p}} = \sqrt{\frac{\mu}{a(e-1)}}$ is the circular velocity at the pericenter Π.

Applying (4.24) and (6.22), we write for the flight velocity

$$v^2 = V^2 + v_{\infty}^2. \tag{6.24}$$

This equality lends itself to a simple energy interpretation. Here v^2 is twice the amount of kinetic energy per unit mass of the body at the particular point of the orbit, V^2 is twice the kinetic energy which is converted to potential energy as each unit mass recedes to infinity, v_{∞}^2 is twice the kinetic energy per unit mass at infinity.

Expression (6.21) for the mechanical energy Q required to inject a unit mass into hyperbolic orbit around the Earth may be analogously written in the form

$$Q = \frac{V_R^2}{2} + \frac{v_{\infty}^2}{2}, \tag{6.25}$$

where $V_R = \sqrt{\frac{2\mu}{R}}$ is the velocity of escape from the Earth's surface.

Let us now consider the variation in the angle θ between the velocity vector and the local horizon (see Figure 6.1). From (5.19) and conditions (6.2), (6.11) we see that in hyperbolic orbit

$$\frac{d}{d\vartheta} (\mathrm{tg}\ \theta) > 0. \tag{6.26}$$

Hence, applying expression (6.21) for $\mathrm{tg}\,\theta$, we see that in hyperbolic orbit the angle θ monotonically increases between the limits

$$-\frac{\pi}{2} < \theta < \frac{\pi}{2}. \tag{6.27}$$

As we move to infinity in the retrograde sense, i.e., along the path of approach of the satellite to the primary, $\theta \to -\frac{\pi}{2}$, which corresponds to a head-on collision between the satellite and the primary. Along the receding path, however, $\theta \to \frac{\pi}{2}$, which corresponds to motion away from the primary. At the pericenter Π, $\theta = 0$.

6.3. FLIGHT TIME

The flight time in hyperbolic orbit is obtained from (4.19) and (5.12), which give

$$d\vartheta = \frac{\sqrt{\mu p}}{r^2} dt. \qquad (6.28)$$

To integrate this equation, we change over in (6.28) from the true anomaly ϑ to a variable H, the analog of the eccentric anomaly E in elliptical orbit. We should first note that the equation of elliptical orbit in rectangular coordinates is

$$\frac{\xi^2}{a^2} + \frac{\eta^2}{b^2} = 1. \qquad (6.29)$$

The origin S of the rectangular frame $S\xi\eta$ is at the center of the ellipse, the axis $S\xi$ pointing along the semimajor axis, and $S\eta$ along the semiminor axis (see Figure 5.3). From Figure 5.3 and relation (5.24), we write (6.29) in parametric form:

$$\xi = a \cos E, \quad \eta = b \sin E. \qquad (6.30)$$

Simple substitution shows that the coordinates ξ and η defined by (6.30) satisfy the equation of the ellipse (6.29).

Substituting hyperbolic functions for the trigonometric functions in (6.30) and applying the identity

$$\text{ch}^2 x - \text{sh}^2 x = 1,$$

we write the equation (6.3) of the left branch of the hyperbola (see Figure 6.1) in the parametric form

$$\xi = -\alpha \, \text{ch} \, H, \quad \eta = \beta \, \text{sh} \, H, \qquad (6.31)$$

where H is an analog of the eccentric anomaly E of elliptical orbit.

From Figure 6.1 and relations (6.4), (6.5), we have

$$\left.\begin{array}{l} r \cos \vartheta = \gamma + \xi = \alpha (e - \text{ch} \, H), \\ r \sin \vartheta = \eta = \beta \, \text{sh} \, H = \alpha \sqrt{e^2 - 1} \, \text{sh} \, H. \end{array}\right\} \qquad (6.32)$$

Squaring and adding, we have

$$r = \alpha (e \, \text{ch} \, H - 1). \qquad (6.33)$$

Hence, from the first equality in (6.32),

$$\left.\begin{array}{l} r(1 + \cos \vartheta) = \alpha (e - 1)(\text{ch} \, H + 1), \\ r(1 - \cos \vartheta) = \alpha (e + 1)(\text{ch} \, H - 1). \end{array}\right\} \qquad (6.34)$$

Taking the ratio of these relations and seeing that

$$\frac{\text{ch} \, H + 1}{2} = \text{ch}^2 \frac{H}{2}, \quad \frac{\text{ch} \, H - 1}{2} = \text{sh}^2 \frac{H}{2}, \quad \frac{\text{ch} \, H - 1}{\text{sh} \, H + 1} = \text{th}^2 \frac{H}{2},$$

we arrive at the following definition of H:

$$\text{th} \frac{H}{2} = \sqrt{\frac{e-1}{e+1}} \, \text{tg} \frac{\vartheta}{2}.$$ (6.35)

Differentiating (6.35), we find

$$d\vartheta = \frac{\cos^2 \frac{\vartheta}{2}}{\text{ch}^2 \frac{H}{2}} \sqrt{\frac{e+1}{e-1}} \, dH.$$

On the other hand, from the first equality in (6.34), we write

$$\frac{\cos^2 \frac{\vartheta}{2}}{\text{ch}^2 \frac{H}{2}} = \frac{a(e-1)}{r}.$$

Hence,

$$d\vartheta = \sqrt{e^2-1} \, \frac{a}{r} \, dH.$$

Substituting in (6.28) and applying (6.4), we find

$$dt = r \sqrt{\frac{a}{\mu}} \, dH.$$

Finally, making use of (6.33), we write

$$dt = \frac{a^{3/2}}{\sqrt{\mu}} (e \, \text{ch} \, H - 1) dH.$$ (6.36)

Integrating (6.36) in the interval from the pericenter to any point of the orbit, and seeing that in accordance with (6.35) at the pericenter

$$\text{th} \, H = H = \vartheta = 0,$$

we obtain Kepler's equation for hyperbolic orbit:

$$e \, \text{sh} \, H - H = \nu(t-\tau),$$ (6.37)

where $\nu = \frac{\sqrt{\mu}}{a^{3/2}}$, and τ is the epoch of pericenter passage.

Note that relations (6.32), (6.33), (6.35), and (6.37) can be derived for the corresponding relations (5.29), (5.30), (5.32), and (5.27) of elliptical orbit on substitution

$$H = iE, \quad \text{sh} \, H = i \sin E, \quad \text{ch} \, H = \cos E$$ (6.38)

(making use of (6.20)).

We shall show that equation (6.37) has a single real solution for any

$$N = \nu(t-\tau).$$ (6.39)

80

Consider the function

$$F(H, N) = e \operatorname{sh} H - H - N.$$

For any N, we clearly have

$$F(-\infty, N) = -\infty \quad \text{and} \quad F(\infty, N) = \infty.$$

Furthermore,

$$\frac{dF}{dH} = e \operatorname{ch} H - 1 > 0.$$

Hence it follows that for any N there is a single H, such that $F(H, N) = 0$, which is in fact the solution of Kepler's equation.

In solving Kepler's equation for hyperbolic orbit by the method of successive approximations, it is advisable to replace scheme (5.35) with the relation

$$\operatorname{sh} H_n = \frac{N + H_{n-1}}{e}, \tag{6.40}$$

where H_{n-1} and H_n are the preceding and the current approximations of H. As the first approximation, we may always take $H_0 = 0$.

Let us now consider how H varies along the orbit. We shall apply relation (6.35) and the fact that the angle ϑ monotonically increases between the limits $-\vartheta_\infty < \vartheta < \vartheta_\infty$. Hence it follows that $\operatorname{th} \frac{H}{2}$ monotonically increases from -1 to 0 on the descending branch of the orbit and from 0 to $+1$ on the ascending branch. H should also monotonically increase, ranging from $-\infty$ to 0 on the descending branch and from 0 to $+\infty$ on the ascending branch.

6.4. ELEMENTS OF HYPERBOLIC ORBIT

Like elliptical orbit, hyperbolic orbit is completely defined by six independent orbital elements (see Sec. 5.4). As an example, let us consider the set of hyperbolic elements comprising the parameters α, e, τ, i, Ω, ω. All the elements, with the exception of the semiaxis α, are the same as for elliptical orbit. We shall list the relations which are used in calculating the orbit (i.e., the coordinates and the velocity components of a body at any point) from known values of the orbital elements. In collecting these relations, we proceed from expressions (4.19), (6.4), (6.21), (6.33), (6.35), (6.37), operating in the coordinate system Oru of Figure 5.4.

We have:

$$\left.\begin{aligned}
&r = \frac{p}{1 + e \cos \vartheta} = \alpha(e \operatorname{ch} H - 1), \quad p = \alpha(e^2 - 1), \\
&u = \omega + \vartheta, \\
&t = \tau + \frac{e \operatorname{sh} H - H}{\nu}, \quad \nu = \frac{\sqrt{\mu}}{\alpha^{3/2}}, \\
&\qquad \operatorname{th} \frac{H}{2} = \sqrt{\frac{e-1}{e+1}} \operatorname{tg} \frac{\vartheta}{2}, \\
&v_r = \sqrt{\frac{\mu}{p}}\, e \sin \vartheta, \\
&v_u = \frac{\sqrt{\mu p}}{r} = \sqrt{\frac{\mu}{p}} (1 + e \cos \vartheta).
\end{aligned}\right\} \tag{6.41}$$

These formulas define the motion of the body in the orbital plane. The last six formulas in (5.37) can be applied to reconstruct the motion in the three-dimensional rectangular frame $Oxyz$ (see Figure 5.4).

Any of the three parameters ϑ, t, and H may be assumed, in conjunction with the set (6.41), as the argument which defines the position of the body in hyperbolic orbit. The true anomaly ϑ, however, is somewhat inconvenient if we are to determine the motion at large distance from the primary; in this case the true anomaly approaches the asymptotic values $\pm\vartheta_\infty$, so that small changes in ϑ correspond to considerable displacements along the orbit, which inevitably lowers the accuracy of the calculations in terms of this argument.

In certain cases, when the coordinates and the velocity components are determined as functions of the arguments H or t, it is unnecessary to proceed with the explicit calculation of ϑ. From (6.4), (6.32), and (6.33) we have

$$\sin\vartheta = \frac{\sqrt{e^2-1}\,\mathrm{sh}\,H}{e\,\mathrm{ch}\,H-1}, \qquad \cos\vartheta = \frac{e-\mathrm{ch}\,H}{e\,\mathrm{ch}\,H-1}. \tag{6.42}$$

From these relations, making use of (6.21), (6.32) and passing to the rectangular frame $O\xi\eta\zeta$ of Figure 5.5, we have

$$\left.\begin{aligned}
\xi &= a(e-\mathrm{ch}\,H),\\
\eta &= a\sqrt{e^2-1}\,\mathrm{sh}\,H,\\
\zeta &= 0,\\
v_\xi &= -\sqrt{\frac{\mu}{a}}\,\frac{\mathrm{sh}\,H}{e\,\mathrm{ch}\,H-1},\\
v_\eta &= \sqrt{\frac{\mu}{a}}\,\frac{\sqrt{e^2-1}\,\mathrm{ch}\,H}{e\,\mathrm{ch}\,H-1},\\
v_\zeta &= 0.
\end{aligned}\right\} \tag{6.43}$$

The transformation from $O\xi\eta\zeta$ to $Oxyz$ is defined by the matrix of direction cosines in Sec. 5.5.

The above relations are suitable for calculating the initial conditions of motion (the coordinates and the velocity components at the epoch $t=t_0$) from the elements of hyperbolic orbit. The solution of the reverse problem, i.e., determination of the elements a, e, τ, i, Ω, ω of hyperbolic orbit from the initial conditions x_0, y_0, z_0, v_{x0}, v_{y0}, v_{z0}, can be obtained from (5.49). It suffices to put $a=-\alpha$ in these equations, substituting the following expressions for the last three equalities in (5.49):

$$\left.\begin{aligned}
\tau &= t_0 - \frac{e\,\mathrm{sh}\,H_0 - H_0}{\nu},\\
\nu &= \frac{\sqrt{\mu}}{\alpha^{3/2}},\\
\mathrm{th}\frac{H_0}{2} &= \sqrt{\frac{e-1}{e+1}}\,\mathrm{tg}\frac{\vartheta_0}{2}.
\end{aligned}\right\} \tag{6.44}$$

Note that if the point of origin (corresponding to the epoch $t-t_0$) is far from the primary, formulas (6.44) are not quite convenient for the calculation of H_0 and τ, since for $\mathrm{th}\frac{H_0}{2}\to 1$, H_0 is determined with low accuracy. In this case, the last equality in (6.44) should preferably be

replaced with the relation

$$\operatorname{ch} H_0 = \frac{\frac{r_0}{a} + 1}{e},$$

(6.45)

which follows directly from (6.33).

6.5. GROUND TRACKS OF HYPERBOLIC ORBITS

Ground tracks of hyperbolic orbits (i.e., the projections of these orbits on the surface of the rotating Earth) are essentially different from the ground tracks of circular orbits described in Sec. 1.3. To find the ground track of hyperbolic orbit, we calculate drom (1.12), (1.15), and (6.41) the height h of the body above the Earth's surface, the latitude B and the longitude L of its projection on the Earth's surface, and then plot the calculated points on a map.

As an example, Figures 6.3 and 6.4 show ground tracks of orbits with the elements $\alpha = 16,000\,\text{km}$, $e = 1.5$, $\tau = \omega = 0$. Figure 6.3 corresponds to an orbit with inclination $i = 65°$ (direct west-east motion), and Figure 6.4 to an orbit with $i = 135°$ (retrograde east-west motion); Ω has been chosen setting $L = 0$ for $t = 0$. In the two graphs, the ordinate gives the latitude B, and the abscissa the longitude L. The flight height h in kilometers is marked for the various points of the ground track.

From the graphs in Figures 6.3 and 6.4 we see that when the body is at large distances from the Earth, its ground track is close to some parallel. From (1.12), (1.15), (6.12), and (6.41) it follows that in the limit, with the body at infinity, the latitude of this parallel approaches the value

$$B_\infty = \arcsin[\sin(\omega \pm \vartheta_\infty)\sin i],$$

(6.46)

where ϑ_∞ is defined by (6.13); the sign $+$ corresponds to the ascending branch of the orbit, and the sign $-$ to the descending branch. Note that the angular rate of displacement of the ground track in longitude approaches the spin rate of the Earth (i.e., $15°2'28''$ per hour from east to west).

As the body approaches the Earth, its ground track progressively deviates from the limiting parallel. Near the perigee, the ground track evolves into a curve of the type shown in Figures 6.3 and 6.4. For $0 \leqslant i \leqslant \frac{\pi}{2}$, the ground tracks are confined to the belt $-i \leqslant B \leqslant i$, and for $\frac{\pi}{2} \leqslant i \leqslant \pi$ they lie inside the region $i - \pi \leqslant B \leqslant \pi - i$. The ground tracks are tangent at one point to the northern boundary of the belt, and at one point to the southern boundary.

The ground tracks in Figures 6.3 and 6.4 are clearly those of bodies approaching the Earth from infinity. The ground tracks of bodies injected into hyperbolic orbit near the Earth will show only part of the curves depicted in Figures 6.3 and 6.4 (from injection point to recession to infinity).

83
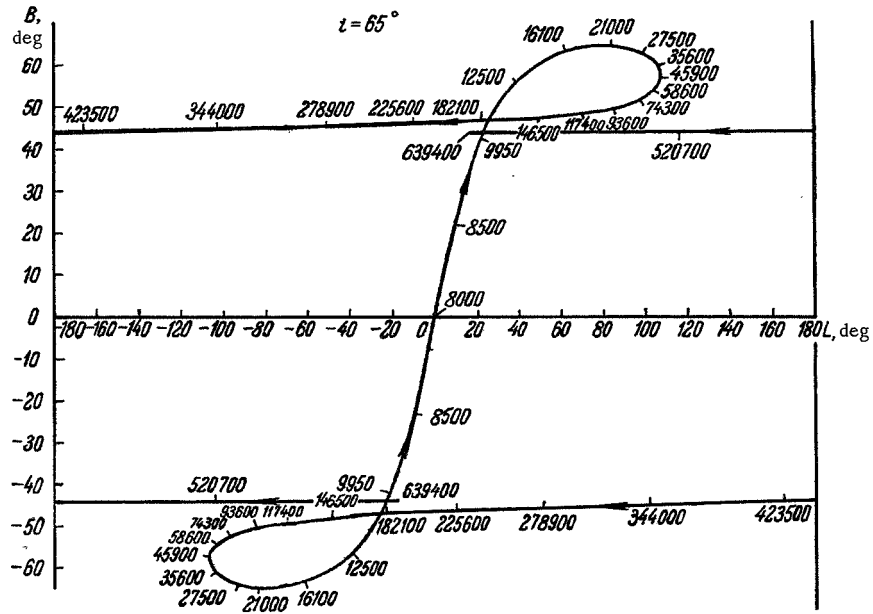
FIGURE 6.3. Ground track of a hyperbolic orbit with semiaxis α= 16,000 km, eccentricity e= 1.5, and inclination i= 65°.
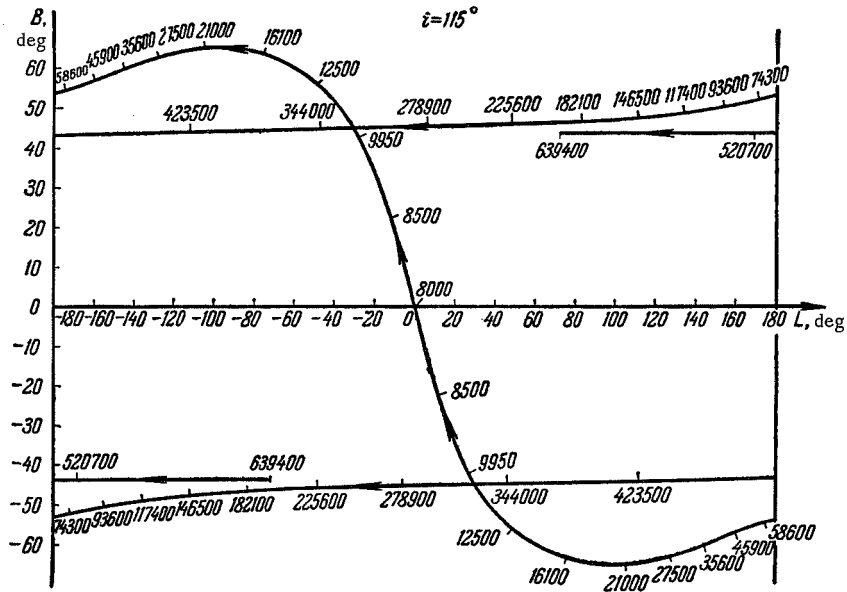
FIGURE 6.4. Ground track of a hyperbolic orbit with semiaxis α = 16,000 km, eccentricity e = 1.5, and inclination i = 115°.

84

6.6. HYPERBOLIC FLY-BY ORBITS

In this section we shall consider the influence of a center of attraction on the motion of a body which approaches from infinity. The initial velocity of the body relative to the gravitational center and the direction of the incoming asymptote NS (the initial unperturbed path of the body) are known. It follows from the preceding that near the gravitational center the body will move in hyperbolic orbit. The plane of this orbit is the plane through the center of attraction O and the line NS.
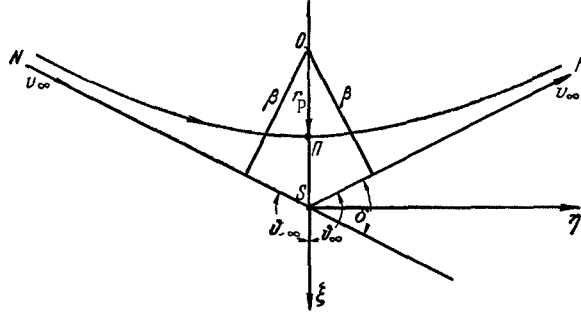
FIGURE 6.5. Hyperbolic fly-by orbit.

Let us consider in greater detail the principal characteristics of motion in this plane. The distance β from the incoming asymptote NS to the gravitational center O is known (Figure 6.5): we have shown in the preceding that β is the second semiaxis of the hyperbolic orbit.

From (6.4), (6.5), (6.13), (6.14), (6.17), and (6.22) we obtain expressions for the first semiaxis α of the hyperbola, the eccentricity e, the pericenter distance $r_p = O\Pi$, the distance $\gamma = OS$ from the gravitational center to the center of the hyperbola, and the angle $\vartheta_\infty = \angle NS\xi$ between the initial direction of motion and the axis of the hyperbola:

$$
\left.
\begin{aligned}
\alpha &= \frac{\mu}{v_\infty^2}, \\
e &= \sqrt{\frac{\beta^2}{\alpha^2} + 1}, \\
r_p &= \alpha(e - 1) = \sqrt{\beta^2 + \alpha^2} - \alpha, \\
\gamma &= \alpha e = \sqrt{\beta^2 + \alpha^2}, \\
\vartheta_\infty &= \arccos\left(-\frac{1}{e}\right) = \operatorname{arctg}\left(-\frac{\beta}{\alpha}\right).
\end{aligned}
\right\}
\tag{6.47}
$$

The parameters α and e define the shape and the size of the hyperbolic orbit, whereas γ and ϑ_∞ specify the direction of the hyperbola axis $O\xi$ and the position of its center S.

After its encounter with the gravitational center, the body will escape to infinity along the second asymptote SM through the center S of the hyperbola. The relative velocity v_∞ of this asymptotic motion and the distance β from the asymptote SM to the center O are equal to the

85

corresponding values for the initial (unperturbed) motion. The encounter has only altered the direction of the relative velocity. From relations (6.47) and Figure 6.5, we find an expression for the angle between the initial and final velocity vectors:

$$\delta = 2\left(\vartheta_\infty - \frac{\pi}{2}\right) = 2 \arcsin\left(\frac{1}{e}\right) = 2 \arcsin\frac{\alpha}{\sqrt{\beta^2 + \alpha^2}}.$$ (6.48)

Let

$$\varkappa = \frac{\alpha}{\beta} = \frac{1}{\sqrt{e^2-1}} = \frac{w_\beta^2}{v_\infty^2},$$ (6.49)

where

$$w_\beta = \sqrt{\frac{\mu}{\beta}}.$$ (6.50)

Physically, w_β is the circular velocity at the distance $r = \beta$.
From (6.47)—(6.49) we have

$$\left.\begin{array}{l}\delta = 2 \arcsin\dfrac{\varkappa}{\sqrt{1+\varkappa^2}} = 2 \operatorname{arctg}\varkappa,\\[2mm] r_p = \beta(\sqrt{1+\varkappa^2} - \varkappa).\end{array}\right\}$$ (6.51)

Differentiating,

$$\left.\begin{array}{l}\dfrac{d\delta}{d\varkappa} = \dfrac{2}{1+\varkappa^2} > 0,\\[2mm] \dfrac{d}{d\varkappa}\left(\dfrac{r_p}{\beta}\right) = \dfrac{\varkappa}{\sqrt{\varkappa^2+1}} - 1 < 0.\end{array}\right\}$$ (6.52)

Hence it follows that as $\varkappa$ increases from 0 to ∞, the angle of rotation monotonically rises from 0 to 2π, whereas the ratio $\frac{r_p}{\beta}$ monotonically decreases from 1 to 0.

The parameter $\varkappa$ numerically characterizes the degree of perturbation produced by the center of attraction. Small $\varkappa$ correspond to the case of a brief encounter at a large distance from the center O. The initial path is hardly distorted, and the pericenter distance r_p scarcely departs from β. For a close encounter ($\varkappa \gg 1$), the direction of the initial velocity is almost reversed, and the pericenter distance sharply diminishes ($r_p \ll \beta$).

Note that for $\varkappa \ll 1$ (brief remote encounter), expressions (6.51) can often be replaced with the approximate relations

$$\delta \approx 2\varkappa = \frac{2\alpha}{\beta}, \quad r_p \approx \beta(1 - \varkappa) = \beta - \alpha.$$ (6.53)

To illustrate the influence of the primary on a fly-by orbit, let us consider Figures 6.6 and 6.7. The first figure depicts a bunch of orbits with $\beta = $ const and various v_∞. The second figure shows a bunch of orbits with $v_\infty = $ const and various β. We see from these figures that the gravitational center produces a characteristic scattering effect. This point is of considerable applied significance. For example, in close encounter, comparatively small errors in the parameters of initial motion multiply

out of all proportion, and the determination of the final motion is hopelessly inaccurate. After the encounter, the orbital elements must often be determined anew, and in case of mission flight, midcourse trajectory correction is inevitable.
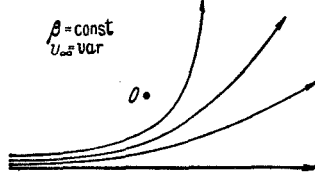
FIGURE 6.6. Scattering of a bunch of hyperbolic orbits with $\beta =$ const and various v_∞
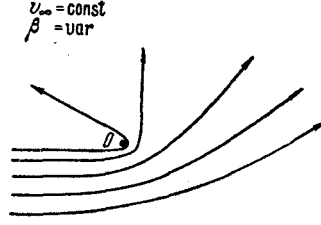
FIGURE 6.7. Scattering of a bunch of hyperbolic orbits with $v_\infty =$ const and various β.

Aside from the scattering of orbits, which becomes particularly pronounced at large distances from the gravitational center, the bunch is often compressed near the pericenter. To establish this effect, we first consider the relation between the variations $\Delta\beta$ in the distance from the incoming asymptote to the center of attraction and the variations Δr_p in pericenter distance. Differentiating the equation for r_p in (6.47) and applying (6.49), we find

$$\Delta r_p = \frac{\partial r_p}{\partial \beta} \Delta\beta, \quad \frac{\partial r_p}{\partial \beta} = \frac{1}{\sqrt{1+x^2}} < 1. \tag{6.54}$$

Hence it follows that $\Delta r_p < \Delta\beta$. A bunch of orbits with various β (and $v_\infty =$ const) is thus compressed near the pericenter. This compression is particularly distinct for $x \gg 1$ (i.e., in the case of close prolonged encounter). The probability of the body reaching a certain neighborhood of the pericenter is therefore correspondingly higher.

6.7. HYPERBOLIC ESCAPE ORBITS

Let us consider the motion of a body which, at the point D, has been injected into hyperbolic orbit with a sufficiently high velocity v_0 (Figure 6.8). We have shown in the preceding that the final outcome of motion in this orbit is the escape of the body from the Earth's pull along the asymptote SM (S being the center of the hyperbolic orbit). The motion along this straight line is characterized by the velocity v, the inclination θ_∞ of the line SM to the horizontal at the injection point D, and the distance β from the line SM to the Earth's center O. In this section we shall consider the dependence of these quantities on the initial values of the velocity v_0, the inclination θ_0 of the velocity vector to the horizon, the distance r_0 of the injection point D from the Earth's center, and the coefficient

$$k_0 = \frac{r_0 v_0^2}{\mu} = \frac{2v_0^2}{V_0^2}, \tag{6.55}$$

87

where $V_0 = \sqrt{\frac{2\mu}{r_0}}$ is the velocity of escape from the Earth at the injection point D.

Note that for hyperbolic orbit

$$v_0 > V_0, \quad k_0 > 2, \tag{6.56}$$

whereas the case $v_0 = V_0$, $k_0 = 2$ corresponds to a parabolic trajectory.

Applying (5.49), (6.20), and (6.22), we have

$$v_\infty = v_0 \sqrt{\frac{k_0 - 2}{k_0}}. \tag{6.57}$$

We see from this relation that as k_0 increases from 2 to ∞ the ratio $\frac{v_\infty}{v_0}$ monotonically rises from 0 to 1. The case $k_0 = 2$, $v_\infty = 0$ corresponds to a projectile which loses its entire initial kinetic energy to overcome the Earth's gravitational pull (parabolic orbit), whereas the case $k_0 \to \infty$, $v_\infty \to v_0$ represents injection with a very large velocity v_0, so that the Earth's gravity has hardly any influence on the motion of the body.
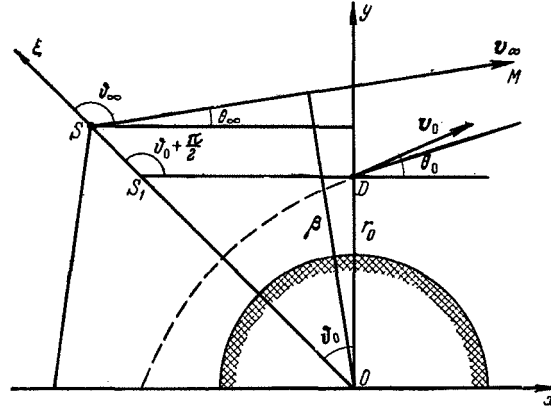
FIGURE 6.8. Hyperbolic escape orbit.

To find the angle θ_∞, let S_1 in Figure 6.8 be the intersection point of the hyperbola axis $S\xi$ with the horizontal at the injection point D. Then,

$$\angle DS_1\xi = \frac{\pi}{2} + \vartheta_0, \quad \angle MS\xi = \vartheta_\infty, \quad \theta_\infty = \angle DS_1\xi - \angle MS\xi,$$

whence

$$\theta_\infty = \vartheta_0 - \left(\vartheta_\infty - \frac{\pi}{2}\right), \tag{6.58}$$

where ϑ_0 and ϑ_∞ are the initial and the asymptotic values of the true anomaly, defined by (5.49) and (6.13).

Figure 6.9 plots the angle θ_∞ as a function of θ_0 and k_0. We see from the graphs that the angle θ_∞ monotonically increases with θ_0 and k_0. For small k_0 ($k_0 \approx 2$), θ_∞ vs. θ_0 is almost the linear function characteristic of
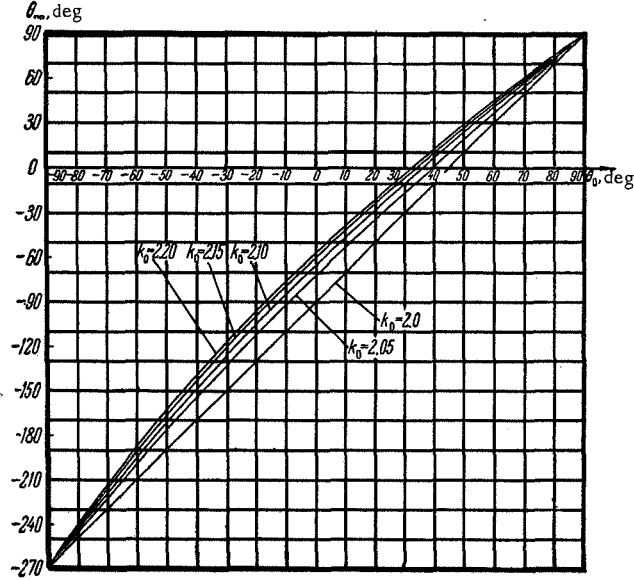
FIGURE 6.9. The asymptotic inclination θ_∞ of the velocity vector to the horizon vs. the injection angle θ_0 for hyperbolic orbits with various $k_0 = \dfrac{r_0 v_0^2}{\mu}$.

parabolic orbit $(k_0 = 2)$. From (5.49) and (6.13) we have for the limiting values of the angle θ_∞

$$\left.\begin{aligned}
\theta_\infty &= -\arcsin\frac{1}{k_0-1} \quad \text{for} \quad \theta_0 = 0, \\
\theta_\infty &= \frac{\pi}{2} \quad \text{for} \quad \theta_0 = \pm\frac{\pi}{2}, \\
\theta_\infty &= 2\theta_0 - \frac{\pi}{2} \quad \text{for} \quad k_0 = 2, \\
\theta_\infty &\to \theta_0 \quad \text{for} \quad k_0 \to \infty.
\end{aligned}\right\} \qquad (6.59)$$

From (5.49), (6.4), (6.19), and (6.57), we find the following relation for the distance β from the asymptote to the Earth's center:

$$\beta = r_0 \cos\theta_0 \sqrt{\frac{k_0}{k_0-2}} = \frac{v_0}{v_\infty} r_0 \cos\theta_0. \qquad (6.60)$$

We see from this expression that the distance β monotonically decreases with the increase in the coefficient k_0. If $k_0 \to 2$, we have $\beta \to \infty$, and if $k_0 \to \infty$, then $\beta \to r_0 \cos\theta_0$.

89

Chapter 7

PARABOLIC AND VERTICAL ORBITS

7.1. PRINCIPAL GEOMETRICAL PROPERTIES
OF PARABOLIC ORBITS

We have observed in Sec. 4.5 that for $k = 2$ the orbit is parabolic. From (4.22) it follows that the eccentricity of this orbit is $e = 1$, and equation (4.19) takes the form

$$r = \frac{p}{1 + \cos \vartheta} = \frac{p}{2 \cos^2 \frac{\vartheta}{2}} . \qquad (7.1)$$

This is the equation of a parabola with its focus at the origin (i.e., at the center of attraction O). We see from this equation that all parabolas are similar, differing only in the linear magnitude of the parameter p
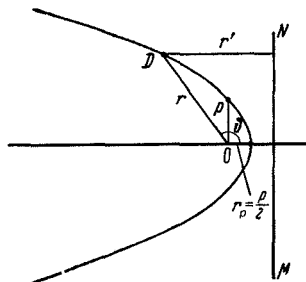
FIGURE 7.1. Geometrical parameters
of parabolic orbit.

(Figure 7.1). The line $\vartheta = 0$ through the focus is the a x i s o f t h e
p a r a b o l a (it is the symmetry axis of the curve). The main geometrical
property of a parabola (which may be regarded as its definition) is

$$r = r' , \qquad (7.2)$$

where r is the distance from a current point D on the parabola to the focus,
and r' the distance from D to the directrix, i.e., the line MN perpendicular
to the axis of the parabola and distant p from the focus.

From (5.2) and (6.4) we see that, upon passing from an ellipse to a
parabola, the semimajor axis $a \to \infty$, while upon passing from hyperbolic

90

orbit to a parabola $\alpha \to \infty$. In other words, for parabolic orbit we may take

$$a = \pm \infty.$$

From (7.1) it follows that for motion in parabolic orbit, the true anomaly ϑ varies between the limits

$$-\pi < \vartheta < \pi. \tag{7.3}$$

As ϑ approaches $\pm \pi$, the distance $r \to \infty$. Hence it follows that parabolic orbit, like hyperbola, is an open curve: for $-\pi < \vartheta < 0$ the body approaches the gravitational center (the descending branch of the orbit), and for $0 < \vartheta < \pi$ it recedes from the center (the ascending branch of the orbit). The pericenter point corresponds to zero true anomaly, $\vartheta = 0$. The pericenter (minimum) distance from the center

$$r_p = \frac{p}{2}. \tag{7.4}$$

The lack of asymptotes is a distinctive feature of the parabola, distinguishing it from the hyperbola. This follows directly from (6.4) and (6.60), which imply that for $e \to 1$ and $k \to 2$, we have $\beta \to \infty$ (for $p \neq 0$ and $r_0 \cos \theta_0 \neq 0$).

7.2. FLIGHT VELOCITY AND ENERGY

The velocity components v_u and v_r in parabolic orbit, the magnitude of the velocity vector v, the angle θ between the velocity vector and the local horizon, and the mechanical energy Q per unit mass are obtained from (6.21), where we set $e = 1$, $a = \infty$. Thus,

$$\left. \begin{array}{l} v_u = \sqrt{\frac{\mu}{p}} \, (1 + \cos \vartheta), \\[2mm] v_r = \sqrt{\frac{\mu}{p}} \sin \vartheta, \\[2mm] v^2 = \frac{2\mu}{r} = V^2, \\[2mm] \theta = \frac{\vartheta}{2}, \\[2mm] Q = \frac{\mu}{R} = \frac{V_R^2}{2}. \end{array} \right\} \tag{7.5}$$

We see from these expressions that the velocity v in parabolic orbit is constantly equal to the velocity of escape V of the body from the primary. This velocity increases from 0 to $v_p = 2\sqrt{\frac{\mu}{p}}$ as the body travels down the descending branch, and again decreases to 0 as the body moves up the ascending branch of the orbit. A characteristic feature of parabolic orbits (as distinct from hyperbolas) is the vanishingly small velocity at large distances from the gravitational center.

The angle θ between the velocity vector and the local horizon monotonically increases from $-\pi/2$ to $+\pi/2$ in parabolic orbit.

The energy Q per unit mass, which is expended when the body is injected into a given orbit from the Earth's surface, is constant for all parabolic orbits: it is equal to the energy which should be imparted to a body if it is to escape to infinity from the ground.

7.3. FLIGHT TIME

The flight time in parabolic orbit is found from (6.28) and (7.1), which give

$$\frac{d\vartheta}{\cos^4\frac{\vartheta}{2}} = \frac{4\sqrt{\mu}}{p^{3/2}}\,dt. \tag{7.6}$$

Note that

$$\int \frac{d\vartheta}{\cos^4\frac{\vartheta}{2}} = 2\int \left(1 + \mathrm{tg}^2\frac{\vartheta}{2}\right) d\left(\mathrm{tg}\frac{\vartheta}{2}\right) = 2\left(\mathrm{tg}\frac{\vartheta}{2} + \frac{1}{3}\mathrm{tg}^3\frac{\vartheta}{2}\right).$$

Applying this expression and integrating equation (7.6) in the interval from the pericenter to an arbitrary point of the orbit, we obtain Kepler's equation for parabolic orbit:

$$\frac{2\sqrt{\mu}}{p^{3/2}}(t - \tau) = \mathrm{tg}\frac{\vartheta}{2} + \frac{1}{3}\mathrm{tg}^3\frac{\vartheta}{2}. \tag{7.7}$$

where τ is the epoch of pericenter passage.
Let

$$\mathrm{tg}\frac{\vartheta}{2} = \xi, \quad \frac{2\sqrt{\mu}}{p^{3/2}}(t - \tau) = M. \tag{7.8}$$

The determination of the true anomaly ϑ at a given instant t clearly reduces to the solution of the cubic

$$F(\xi) = \frac{\xi^3}{3} + \xi - M = 0. \tag{7.9}$$

This equation has a single real solution, since

$$F(-\infty, M) = -\infty, \quad F(\infty, M) = \infty, \quad \frac{dF}{d\xi} = \xi^2 + 1 > 0.$$

7.4. ELEMENTS OF PARABOLIC ORBIT

Motion in parabolic orbit imposes a certain a priori restriction on the trajectory of the body (in virtue of the condition $v = V$), so that all parabolic orbits (unlike elliptical and hyperbolic ones) are described by five, and not six, elements. As an example of a complete set of orbital elements, let us consider the parameters, $p, \tau, i, \Omega, \omega$. Applying (7.1), (7.5), and (7.7), we list the formulas used in determining the coordinates

and the velocity components in parabolic orbit from known orbital elements:

$$r = \frac{p}{1+\cos\vartheta} = \frac{p}{2\cos^2\frac{\vartheta}{2}} = \frac{p}{2}\left(1 + \operatorname{tg}^2\frac{\vartheta}{2}\right),$$

$$u = \omega + \vartheta, \quad t = \tau + \frac{p^{3/2}}{2\sqrt{\mu}}\left(\operatorname{tg}\frac{\vartheta}{2} + \frac{1}{3}\operatorname{tg}^3\frac{\vartheta}{2}\right),$$

$$v_r = \sqrt{\frac{\mu}{p}}\sin\vartheta = \sqrt{\frac{\mu}{p}}\,\frac{2\operatorname{tg}\frac{\vartheta}{2}}{1+\operatorname{tg}^2\frac{\vartheta}{2}},$$

$$v_u = \sqrt{\frac{\mu}{p}}(1+\cos\vartheta) = \sqrt{\frac{\mu}{p}}\,\frac{2}{1+\operatorname{tg}^2\frac{\vartheta}{2}}.$$

(7.10)

These formulas define the motion of a body in the orbital plane. The transformation to the space frame $Oxyz$ (see Figure 5.4) is effected with the aid of the last six relations in (5.37). Note that in calculations based on the set (7.10) it is often advisable to take $\xi = \operatorname{tg}\frac{\vartheta}{2}$, and not the true anomaly ϑ, as the independent variable: this quantity monotonically varies from $-\infty$ to $+\infty$ in orbit. This substitution of variables is justified by the fact that, at large distances from the primary, small changes in the angle ϑ correspond to considerable displacements along the orbit.

When determining the elements of a parabolic orbit from known initial conditions of motion (i.e., the parameters x_0, y_0, z_0, v_{x0}, v_{y0}, v_{z0} at the epoch $t = t_0$), k_0 must be calculated from (5.49) in order to verify that the condition of launch into parabolic orbit is in fact satisfied ($k_0 = 2$). Then, from (5.49), the elements Ω, i, u_0, θ_0, r_0 are calculated. Further computations proceed from the relations

$$p = 2r_0\cos^2\theta_0, \quad \omega = u_0 - 2\theta_0,$$

$$\tau = t_0 - \frac{p^{3/2}}{2\sqrt{\mu}}\left(\operatorname{tg}\theta_0 + \frac{1}{3}\operatorname{tg}^3\theta_0\right),$$

(7.11)

which are derived directly from (4.18), (7.1), (7.5), and (7.7).

7.5. TYPES OF VERTICAL ORBIT

As we have observed in Sec. 4.4, the equation of the orbit (4.19) is derived under the assumption that the integration constant (4.21) is not zero:

$$C = rv\cos\theta \neq 0.$$

In this section, we shall consider motion with zero integration constant:

$$C = rv\cos\theta = 0.$$

(7.12)

This condition holds true if at least one of the following equalities is satisfied: $r = 0$, $v = 0$ or $\theta = \pm\frac{\pi}{2}$. Any one of these exact equalities obtaining at an arbitrary point of unperturbed orbit (at a finite distance from the

gravitational center) is a sufficient condition for the orbit to coincide with a certain vertical straight line (i.e., a straight line through the center of attraction).

In our analysis of vertical rectilinear motion, we shall take $v>0$ for a body receding from the gravitational center ($\theta = \pi/2$) and $v<0$ for a body approaching the gravitational center ($\theta = -\pi/2$). Let r_0 and v_0 be the initial radius and velocity at a certain starting time $t=t_0$. Applying the energy integral, we write for any point of the vertical orbit

$$v^2 = \frac{2\mu}{r} - \left(\frac{2\mu}{r_0} - v_0^2\right) = \frac{2\mu}{r} - \frac{\mu}{a}, \qquad (7.13)$$

where

$$a = \frac{r_0}{2-k_0}, \quad k_0 = \frac{r_0 v_0^2}{\mu} = \frac{v_0^2}{w_0^2}, \quad w_0^2 = \frac{\mu}{r_0}. \qquad (7.14)$$

It follows from these expressions that three distinct cases of vertical motion are possible, depending on the initial value k_0.

(1) $k_0<2, a>0$. From (7.13) and the condition $v^2>0$ we have

$$0 \leqslant r \leqslant 2a. \qquad (7.15)$$

This case corresponds to oscillatory vertical motion from the center of attraction to a maximum (apocenter) height of

$$r_a = 2a.$$

From (7.13) we have for this case

$$\left.\begin{array}{ll} v=0 & \text{for} \quad r=2a, \\ v \to \infty & \text{for} \quad r \to 0. \end{array}\right\} \qquad (7.16)$$

This motion can be interpreted as a limiting case of elliptical orbit with $a=\text{const}, b \to 0, e \to 1$. We therefore refer to it as vertical elliptical motion.

(2) $k_0=2, a=\infty$. Here the distance of the satellite from the gravitational center varies between the limits

$$0 \leqslant r < \infty, \qquad (7.17)$$

and the flight velocity

$$\left.\begin{array}{ll} v \to 0 & \text{for} \quad r \to \infty, \\ v \to \infty & \text{for} \quad r \to 0. \end{array}\right\} \qquad (7.18)$$

This is a case of vertical parabolic motion, i.e., flight in parabolic orbit with $p \to 0$.

(3) $k_0>2, a<0$. The distance r varies between the same limits (7.17), and the flight velocity is

$$\left.\begin{array}{l} v \to v_\infty = \sqrt{v_0^2 - \frac{2\mu}{r_0}} = \sqrt{\frac{\mu}{-a}} \quad \text{for} \quad r \to \infty, \\ v \to \infty \quad \text{for} \quad r \to 0. \end{array}\right\} \qquad (7.19)$$

This motion obtains as the limiting case of hyperbolic orbit with $a=$const, $e \to 1$. We call it vertical hyperbolic motion.

7.6. VERTICAL ELLIPTICAL MOTION

We proceed with a more detailed analysis of vertical elliptical motion. To find the distance r as a function of flight time t, we substitute the eccentric anomaly E as the new independent variable (compare with the procedure adopted in the analysis of curvilinear elliptical motion). Taking $e \to 1$ in (5.30), we find

$$r = a(1 - \cos E),$$ (7.20)

whence

$$v = \frac{dr}{dt} = a \sin E \frac{dE}{dt}.$$ (7.21)

Substituting (7.20) and (7.21) in (7.13), we obtain after some manipulations

$$\frac{dE}{dt} = \frac{\sqrt{\mu}}{a^{3/2}} \frac{1}{1 - \cos E}.$$ (7.22)

Integrating, we obtain Kepler's differential equation of vertical elliptical motion:

$$E - \sin E = \frac{\sqrt{\mu}}{a^{3/2}} (t - \tau),$$ (7.23)

where τ is the epoch corresponding to $E=0$, $r=0$.

Applying the method suggested in Sec. 5.3, we can show that this equation is uniquely solvable. In other words, for any t there is a single E. The parameter E may therefore be introduced as the independent variable of vertical elliptical motion. From (7.20)–(7.23) we obtain the parametric equation of the orbit:

$$\left. \begin{array}{l} t = \tau + \dfrac{a^{3/2}}{\sqrt{\mu}} (E - \sin E), \\[2mm] r = a(1 - \cos E), \\[2mm] v = \sqrt{\dfrac{\mu}{a}} \dfrac{\sin E}{1 - \cos E} = \sqrt{\dfrac{\mu}{a}} \operatorname{ctg} \dfrac{E}{2}. \end{array} \right\}$$ (7.24)

As the eccentric anomaly E goes from 0 to π, the distance r increases from 0 to $2a$, and as E goes from π to 2π (or from $-\pi$ to 0), the distance r decreases from $2a$ to 0.

Vertical elliptical motion thus reduces to linear oscillations between the points O and A (Figure 7.2). At the apocenter point A, the velocity $v=0$. The pericenter is located at the center of attraction O. Here $v = \infty$. Note that in reality the approach to the center of attraction is limited by the size of the primary. The part OB of the orbit, which lies inside the primary body, is therefore physically unfeasible. The entire orbit falls into two parts: the ascending branch BA and the descending branch AB.

95

In practice, the body may pass only once from the ascending to the descending branch, at the apocenter A. Reverse transition is virtually impossible.
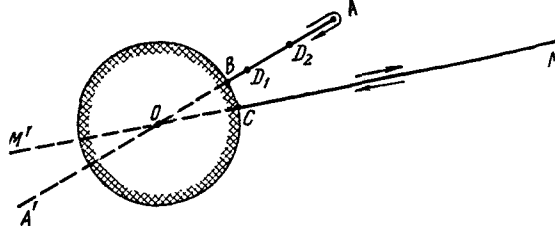
FIGURE 7.2. Types of vertical orbits.

From (7.24) it follows that vertical elliptical orbit is fully described by four elements: the parameters a, τ, and two angles specifying the direction of the straight line of motion.

The elements of vertical orbit can be determined from the initial conditions by making use of expression (7.14) for u. The epoch τ is obtained from (7.24):

$$\tau = t_0 - \frac{a^{3/2}}{\sqrt{\mu}}(E_0 - \sin E_0),$$

$$\text{ctg}\,\frac{E_0}{2} = v_0 \sqrt{\frac{a}{\mu}}.$$

$$(7.25)$$

7.7. HYPERBOLIC AND PARABOLIC VERTICAL MOTION

Vertical hyperbolic orbit is investigated like its elliptical analog. A new independent variable H is defined by

$$r = \alpha(\text{ch}\,H - 1),$$

$$(7.26)$$

where

$$\alpha = -a = \frac{r_0}{k_0 - 2} > 0.$$

$$(7.27)$$

From (7.13), we have

$$v = \alpha\,\text{sh}\,H\,\frac{dH}{dt},$$

$$\frac{dH}{dt} = \frac{\sqrt{\mu}}{\alpha^{3/2}}\frac{1}{\text{ch}\,H - 1}.$$

$$(7.28)$$

Integrating, we obtain Kepler's equation for vertical hyperbolic orbit:

$$\text{sh}\,H - H = \frac{\sqrt{\mu}}{\alpha^{3/2}}(t - \tau),$$

$$(7.29)$$

where τ is the epoch corresponding to $H = 0$, $r = 0$.

Like in Sec. 6.3, it can be shown that equation (7.29) is always uniquely solvable.

H is adopted as the independent variable. Then, from (7.26), (7.28), and (7.29), we obtain the following equations of vertical hyperbolic orbit:

$$\left.\begin{array}{l} t=\tau+\dfrac{a^{3/2}}{\sqrt{\mu}}(\operatorname{sh}H-H), \\[2mm] r=a(\operatorname{ch}H-1), \\[2mm] v=\sqrt{\dfrac{\mu}{a}}\,\dfrac{\operatorname{sh}H}{\operatorname{ch}H-1}=\sqrt{\dfrac{\mu}{a}}\operatorname{cth}\dfrac{H}{2}. \end{array}\right\} \qquad (7.30)$$

As H goes from $-\infty$ to 0, the distance r decreases from ∞ to 0, and as H varies from 0 to $-\infty$, the distance r increases from 0 to ∞.

From (7.30) we see that hyperbolic vertical orbit is fully defined by four elements: the parameters a, τ, and two angles specifying the direction of the straight line of motion.

To find the time τ from known initial conditions, we make use of the relations

$$\left.\begin{array}{l} \tau=t_0-\dfrac{a^{3/2}}{\sqrt{\mu}}(\operatorname{sh}H_0-H_0), \\[2mm] \operatorname{cth}\dfrac{H_0}{2}=\sqrt{\dfrac{a}{\mu}}\,v_0. \end{array}\right\} \qquad (7.31)$$

In parabolic vertical motion, equation (7.13) takes the form

$$v^2=\frac{2\mu}{r}, \qquad (7.32)$$

whence

$$\frac{dr}{dt}=v=\pm\sqrt{\frac{2\mu}{r}}. \qquad (7.33)$$

The sign + corresponds to recession from the primary, and the sign − to approach.

Integrating, we find

$$\frac{2}{3}r^{3/2}=\pm\sqrt{2\mu}\,(t-\tau), \qquad (7.34)$$

where τ is the epoch corresponding to $r=0$.

Relations (7.33) and (7.34) define the vertical parabolic orbit, which is described by three elements: the epoch τ and two angles.

It follows from the preceding that hyperbolic and parabolic vertical orbits represent motion along an infinite half-line OM (Figure 7.2). The pericenters of these orbits are at the center of the primary body O. The pericenter velocity $v=\infty$. A certain section OC of the orbit lies inside the primary, so that any transition from the descending branch MC to the ascending branch CM or back is virtually impossible.

In conclusion note that we approached vertical motion as a limiting case of the respective conical orbits. An immediate consequence of this approach is that after encounter with the center of attraction, the direction of flight is reversed, changing by 180°. Although in reality circumnavigation

97

of the gravitational center is unfeasible, these vertical orbits are of some
applied interest for the investigation of the asymptotic properties of motion
in highly elongated curvilinear orbits. The equations of vertical motion
also apply, with sufficient accuracy, to the analysis of motion in curvilinear
orbits at great distances from the primary. It must be borne in mind,
however, that in reality, proper vertical motion (i. e., motion exactly
through the center of attraction) does not result in reversal of the velocity
vector. Having passed through the point O, the body will move on along
the lines OA' or OM'. This solution of the equations of vertical motion,
though mathematically correct, is clearly meaningless in practice.

Chapter 8

DETERMINATION OF ORBIT FROM TWO
KNOWN POSITIONS OF THE SATELLITE

8.1. STATEMENT OF THE PROBLEM

A common problem in the determination of orbits or transfer trajectories of artificial Earth satellites and other space vehicles calls for orbit inference from two known positions D_1 and D_2 in space at the times t_1 and t_2. Each of the points D_1 and D_2 is defined by three coordinates, which are functions of the six orbital elements. The problem therefore reduces to the solution of a set of six transcendental equations in six unknown orbital elements. The aim of the present chapter is to investigate this set of equations. We determine the number and the nature of its solutions, and also describe one of the numerical techniques of solution. In our analysis we shall assume the following basic set of orbital elements q_i $(i = 1, 2, \ldots, 6)$: the longitude of the ascending node Ω, the inclination of the orbit i, the semimajor axis a, the parameter p, the argument of the pericenter ω, and the epoch of pericenter passage τ.

This is a universal set of elements, which is very convenient for all kinds of orbits. The numerical values of a and p define the type of the orbit in accordance with the list in Table 8.1.

TABLE 8.1

Orbital elements	Type of orbit	Orbital elements	Type of orbit
$a > 0, \ p > 0$	Elliptical	$a > 0, \ p = 0$	Vertical elliptical
$a = \infty, p > 0$	Parabolic	$a = \infty, p = 0$	Vertical parabolic
$a < 0, \ p > 0$	Hyperbolic	$a < 0, \ p = 0$	Vertical hyperbolic

The epoch t_1 is assumed as the starting instant, and the flight time $\Delta t = t_2 - t_1$ between the two positions is known; the polar coordinates $r_1, \ u_1$ and $r_2, \ u_2$ of the points D_1 and D_2 in the orbital plane are also given (Figure 8.1). Without loss of generality, we take $0 \leqslant u_2 - u_1 < 2\pi$. This condition can always be satisfied if the angle u_1 or u_2 is adjusted by a multiple of 2π.

There are two paths from point D_1 to D_2: by circumnavigating the center of attraction counterclockwise along the trajectory $D_1 A D_2$ or clockwise along the trajectory $D_1 B D_2$. Furthermore, if the body moves in elliptical

orbit, it may have completed one or several revolutions around the primary
O before arriving at the point D_2 at the time t_2. The angular distance $\Delta\vartheta$ to
be covered by the body on its way from point D_1 to D_2 in the time $\Delta t = t_2 - t_1$,
may therefore take any of the values

$$\Delta\vartheta = |2\pi n + (u_2 - u_1)|, \tag{8.1}$$

where n is a certain integer, the values $n = 0, 1, 2, 3, \ldots$ corresponding to
motion in the direction of increasing u, and the values $n = -1, -2, -3, \ldots$
to motion in the direction of decreasing u.
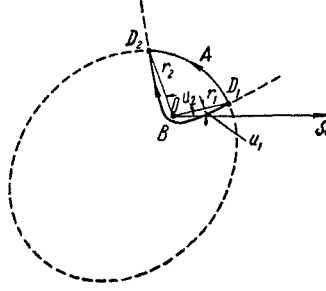
FIGURE 8.1. Transfer trajectories
between two points.

It is clear that each $\Delta\vartheta$ from (8.1) in general corresponds to a different
orbit. It is therefore advisable to state the problem as follows: given the
coordinates of the points D_1 and D_2 and the intervals $\Delta\vartheta$ and Δt, find the
type of the orbit (whether elliptical, hyperbolic, or parabolic) and calculate
its elements.

We shall first consider the case when the points D_1, D_2, and the primary
O are not colinear. Since the points D_1, D_2, and O always lie in the orbital
plane, then, given the coordinates of these points, we can easily find the
orientation of the plane and hence the elements Ω and i. Depending on the
particular value of $\Delta\vartheta$, the following two cases are possible.

(1) For $0 < \Delta\vartheta - 2\pi n < \pi$, the elements Ω and i are calculated from (5.49),
substituting the coordinates x_1, y_1, z_1 of the first point for x_0, y_0, z_0 and the
coordinates x_2, y_2, z_2 of the second point for v_{x0}, v_{y0}, v_{z0}.

(2) For $\pi < \Delta\vartheta - 2\pi n < 2\pi$, the coordinates x_2, y_2, z_2 of the second point are
substituted for x_0, y_0, z_0 and the coordinates x_1, y_1, z_1 of the first point are
substituted for v_{x0}, v_{y0}, v_{z0}. Here n is the number of complete revolutions
contained in the angle $\Delta\vartheta$.

If the elements a, p, ω, and the time of passage of the body through one of
the two points $(D_1$ or $D_2)$ are known, the epoch τ can be determined from
(5.49), (6.44), and (7.10). The problem thus reduces to an investigation
of motion in the orbital plane and determination of the parameters a, p, ω
for known $r_1, r_2, u_1, \Delta\vartheta$, and Δt.

In our treatment of this problem, we shall proceed from the method
developed by M. F. Subbotin /26/ for orbit determination; this method is
based on the solution of the Euler—Lambert equation. This equation, as
we know, gives the time Δt as a function of the parameters $r_1, r_2, \Delta\vartheta$, and a.

By solving this equation, we find the semimajor axis a without previous knowledge of the other orbital elements. In Sec. 8.2 we therefore assume that a is known, and proceed to determine the elements p and ω from known values of r_1, r_2, u_1, $\Delta\vartheta$, and a. The subsequent sections are devoted to derivation and investigation of the Euler —Lambert equation. At the end of this chapter, we consider various particular cases obtaining for colinear disposition of the points D_1, D_2, O (specifically, the case when the points D_1 and D_2 coincide).

8.2. DETERMINATION OF THE ORBIT WHEN a IS KNOWN

When a is known, and the flight time Δt is arbitrary, the orbit through two given points can be found with the aid of a geometrical construction. The following cases are possible.
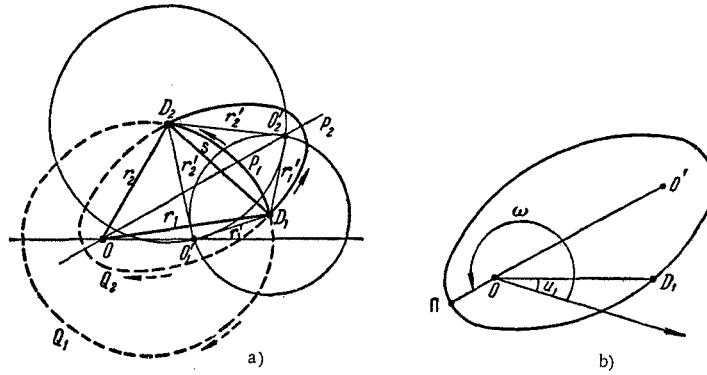
FIGURE 8.2. Determination of elliptical orbit through two given points when the semimajor axis a is known.

A. $a > 0$. The orbit is an ellipse. Let O' be the second focus of the ellipse, and r_1', r_2' the distances of the points D_1 and D_2 from this focus (Figure 8.2 a). From (5.5) we have

$$r_1' = 2a - r_1, \quad r_2' = 2a - r_2.$$

(8.2)

The parameters r_1' and r_2' define the position of the focus O'. By drawing a circle of radius r_1' around the point D_1 and a circle of radius r_2' around the point D_2, we arrive at one of the following three cases:

(1) $r_1' + r_2' < s$, where s is the distance between the points D_1 and D_2. From (8.2) we see that this is equivalent to the condition

$$a < \frac{r_1 + r_2 + s}{4}.$$

(8.3)

The circles do not intersect and the problem is unsolvable.

101

(2) $r_1' + r_2' = s$, which is equivalent to the condition

$$a = \frac{r_1 + r_2 + s}{4}.\qquad(8.4)$$

The circles have a common tangent, and the second focus O' is at the point of tangency, on the line $D_1 D_2$.

(3) $r_1' + r_2' > s$, which is equivalent to the condition

$$a > \frac{r_1 + r_2 + s}{4}.\qquad(8.5)$$

The circles intersect and two orbits are obtained, with the second foci at the intersection points O_1' and O_2', respectively.

Having found the position of the second focus O', we can easily calculate the parameters p and ω. The calculations are made from the expressions

$$p = a(1 - e^2), \quad e = \frac{OO'}{2a}, \quad \omega = u_1 + \angle\, D_1 O O' \pm \pi,\qquad(8.6)$$

whose derivation is obvious from Figure 8.2 b, and also from relations (5.2) and (5.4).

There are thus four possible transfer trajectories between the points D_1 and D_2, which are all arcs of elliptical orbit with semimajor axis a; the possible trajectories are $D_1 P_1 D_2$, $D_1 P_2 D_2$, $D_1 Q_1 D_2$, $D_1 Q_2 D_2$ (see Figure 8.2 a). If the sense of motion around the gravitational center O is specified (or if $\Delta\vartheta$, $\Delta\vartheta \neq \pi$, is known), the number of possible trajectories is reduced to two (in Figure 8.2 a, counterclockwise motion and $\Delta\vartheta < \pi$ corresponds to the paths $D_1 P_1 D_2$ and $D_1 P_2 D_2$, while clockwise motion and $\Delta\vartheta > \pi$ to the trajectories $D_1 Q_1 D_2$ and $D_1 Q_2 D_2$). The elliptical trajectories $D_1 P_1 D_2$ and $D_1 Q_2 D_2$ both correspond to a case when the second focus is located outside the elliptical segment enclosed by the line $D_1 D_2$ and the trajectory. Paths of this type will be called e l l i p t i c a l   t r a j e c t o r i e s   (o r b i t s)   o f t h e   f i r s t   k i n d . If the second focus is located inside the corresponding elliptical segment (the paths $D_1 P_2 D_2$ and $D_1 Q_1 D_2$), we speak of e l l i p t i c a l t r a j e c t o r i e s   (o r b i t s)   o f   t h e   s e c o n d   k i n d . If a is defined by (8.4), the trajectories of the first and the second kind merge into one, so-called l i m i t i n g   t r a j e c t o r y .

B. $a < 0$. The orbit is a hyperbola. To locate the second focus O', we apply equation (6.7), which gives

$$r_1' = 2\alpha + r_1, \quad r_2' = 2\alpha + r_2,\qquad(8.7)$$

where $\alpha = -a$, r_1' and r_2' are the distances of the points D_1 and D_2 from the second focus O'.

To find the point O', we draw a circle of radius r_1' around the point D_1 and another circle of radius r_2' around D_2 (Figure 8.3 a). These circles always meet at two points O_1' and O_2', since

$$r_1' + r_2' = 4\alpha + r_1 + r_2 > s.\qquad(8.8)$$

The intersection points represent two possible positions of the second focus of the hyperbola. From elementary geometrical properties of

hyperbola we see that $\Delta\vartheta<\pi$ corresponds to a case with the foci O and O_2' on the two sides of the line D_1D_2, while $\Delta\vartheta>\pi$ corresponds to a case with the foci O and O_1' on one side of that line. For $\Delta\vartheta=\pi$ the position of the second focus cannot be determined unambiguously, unless the sense of motion
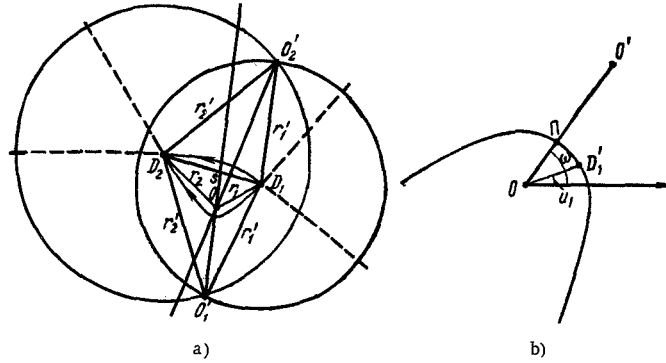
FIGURE 8.3. Determination of hyperbolic orbit through two given points when the semimajor axis a is known.

from D_1 to D_2 around the center O is known. If the direction of motion is known, then, seeing that it is the convex side of the hyperbola which always faces the second focus, we obtain a single-valued solution of the problem. The parameters p and ω can be determined from Figure 8.3 b, and also from relations (6.4) and (6.5), which give

$$p=a(e^2-1), \quad a=-a, \quad e=\frac{OO'}{2a}, \quad \omega=u_1+\angle D_1OO' \qquad (8.9)$$

C. $a=\pm\infty$. The orbit is a parabola. To find the directrix MN of this parabola, we draw a circle of radius r_1 around the point D_1 and another circle of radius r_2 around D_2 (Figure 8.4). From (7.2) it follows that the
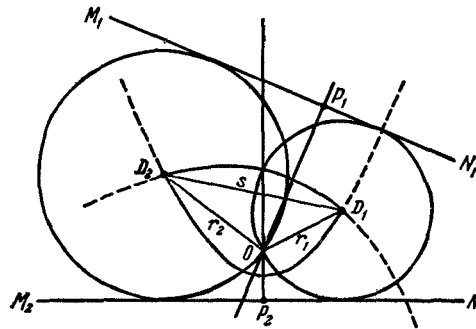
FIGURE 8.4. Determination of parabolic orbit through two given points.

directrix of the parabola is the common tangent of the two circles. Two such tangents can be drawn (M_1N_1 and M_2N_2), on the two sides of the

103

gravitational center O. These two directrixes define two parabolic orbits, circumnavigating the center O in two different directions (the parabola always turns the convex side to its directrix). If the sense of orbital motion is known (or if $\Delta\vartheta$, $\Delta\vartheta \neq \pi$, is given), the problem is uniquely solvable.

The elements p and ω of the parabolic orbit can be calculated once the axis of the parabola has been found. The axis is the line OP through the center of attraction at right angles to the directrix MN. (P is the intersection point of the axis with the directrix.) As for hyperbolic orbit, we have

$$p = OP, \quad \omega = u_1 + \angle D_1 OP. \tag{8.10}$$

8.3. AREA OF ELLIPTICAL SECTOR

As we have previously observed, the Euler — Lambert equation relates the flight time $\Delta t = t_2 - t_1$ with the parameters r_1, r_2, $\Delta\vartheta$, and a. To find this relation, we proceed from expression (5.23), which gives

$$\Delta t = \frac{2(\sigma_2 - \sigma_1)}{\sqrt{\mu p}} = \frac{F}{\sqrt{\mu p}}, \tag{8.11}$$

where σ_1 and σ_2 are the areas described by the radius-vector as the orbiting body moves from the perigee Π to the points D_1 and D_2 (the sectors $\Pi O D_1$ and $\Pi O D_2$ in Figure 8.5), and $F = 2(\sigma_2 - \sigma_1)$ is twice the area of the sector $O D_1 D_2$ (described in the direction of motion around the center O).
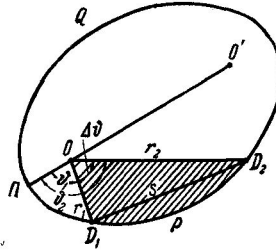
FIGURE 8.5. Elliptical sectors of the first and second kind.

The problem thus reduces to the determination of F. Let us first calculate the area of an elliptical sector. From (5.25) and (5.26) we have

$$F = 2(\sigma_2 - \sigma_1) = ab[E_2 - E_1 - e(\sin E_2 - \sin E_1)], \tag{8.12}$$

where E_1 and E_2 are the eccentric anomalies at the points D_1 and D_2.

These formulas are inadequate for the solution of our problem, since E_1 and E_2 are functions of e and ω, which must not enter the final expression. We therefore write

$$F = ab \left(E_2 - E_1 - 2e \sin\frac{E_2 - E_1}{2} \cos\frac{E_2 + E_1}{2} \right) = 2ab(g - \sin g \cos h), \tag{8.13}$$

104

where

$$g = \frac{E_2 - E_1}{2},$$
$$\cos h = e \cos \frac{E_2 + E_1}{2} \qquad (0 < h < \pi). \qquad (8.14)$$

Let

$$\varepsilon = h + g, \quad \delta = h - g. \qquad (8.15)$$

Then

$$h = \frac{\varepsilon + \delta}{2}, \quad g = \frac{\varepsilon - \delta}{2} \qquad (8.15')$$

and equality (8.13) is written as

$$F = ab[\varepsilon - \sin \varepsilon - (\delta - \sin \delta)]. \qquad (8.16)$$

We now express the angles ε and δ in terms of $r_1 = OD_1$, $r_2 = OD_2$, $s = D_1 D_2$, and a (see Figure 8.5), which are independent of e, ω. From (5.30) we have

$$r_1 = a(1 - e \cos E_1), \quad r_2 = a(1 - e \cos E_2). \qquad (8.17)$$

Hence, applying (8.14),

$$r_1 + r_2 = 2a(1 - \cos g \cos h). \qquad (8.18)$$

On the other hand, from Figure 8.5 we see that

$$s^2 = r_1^2 + r_2^2 - 2r_1 r_2 \cos \Delta\vartheta = (r_1 + r_2)^2 - 4r_1 r_2 \cos^2 \frac{\Delta\vartheta}{2}. \qquad (8.19)$$

Note that relations (5.31) between the trigonometric functions of the true anomaly ϑ and the eccentric anomaly E can be written in the form

$$\sqrt{r} \sin \frac{\vartheta}{2} = \sqrt{a(1 + e)} \sin \frac{E}{2},$$
$$\sqrt{r} \cos \frac{\vartheta}{2} = \sqrt{a(1 - e)} \cos \frac{E}{2}. \qquad (8.20)$$

Now, seeing that $\Delta\vartheta = \vartheta_2 - \vartheta_1$ (here ϑ_1 and ϑ_2 are the true anomalies at the points D_1 and D_2, respectively) and also applying (8.14), we write

$$\sqrt{r_1 r_2} \cos \frac{\Delta\vartheta}{2} = \sqrt{r_1 r_2} \left(\cos \frac{\vartheta_1}{2} \cos \frac{\vartheta_2}{2} + \sin \frac{\vartheta_1}{2} \sin \frac{\vartheta_2}{2} \right) =$$
$$= a(1 - e) \cos \frac{E_1}{2} \cos \frac{E_2}{2} + a(1 + e) \sin \frac{E_1}{2} \sin \frac{E_2}{2} =$$
$$= a \cos \frac{E_2 - E_1}{2} - ae \cos \frac{E_2 + E_1}{2} = a(\cos g - \cos h). \qquad (8.21)$$

Substituting (8.18) and (8.21) in the right-hand side of (8.19), we have

$$s = 2a \sin g \sin h. \qquad (8.22)$$

From (8.18) and 8.22) we find

$$r_1 + r_2 + s = 2a[1 - \cos (g+h)],$$
$$r_1 + r_2 - s = 2a[1 - \cos (g-h)].$$

Hence, applying (8.15), we find

$$\sin^2 \frac{\varepsilon}{2} = \frac{r_1 + r_2 + s}{4a}, \quad \sin^2 \frac{\delta}{2} = \frac{r_1 + r_2 - s}{4a}. \tag{8.23}$$

If we are to calculate the parameter F from (8.16), (8.19), and (8.23), we should first establish in what quadrants the angles $\frac{\varepsilon}{2}$ and $\frac{\delta}{2}$ are located. To this end, it suffices to find the signs of $\sin \frac{\varepsilon}{2}$, $\cos \frac{\varepsilon}{2}$, $\sin \frac{\delta}{2}$, $\cos \frac{\delta}{2}$.

Take the case

$$0 < \Delta \vartheta < 2\pi.$$

From the geometrical definition of eccentric anomaly (see Figure 5.3) we have

$$0 < E_2 - E_1 < 2\pi.$$

Therefore, making use of (8.14), we write

$$0 < g < \pi.$$

Now, from (8.14) we have

$$0 < h < \pi.$$

Hence, applying (8.15),

$$0 < \frac{\varepsilon}{2} = \frac{g+h}{2} < \pi, \quad \sin \frac{\varepsilon}{2} > 0.$$

Note that with the aid of (8.15'), expression (8.21) may be written as

$$\sqrt{r_1 r_2} \cos \frac{\Delta\vartheta}{2} = 2a \sin \frac{\varepsilon}{2} \sin \frac{\delta}{2},$$

whence it follows that $\sin \frac{\delta}{2}$ has the same sign as $\cos \frac{\Delta\vartheta}{2}$. In other words,

$$\sin \frac{\delta}{2} > 0 \quad \text{for} \quad 0 < \Delta\vartheta < \pi$$
$$\sin \frac{\delta}{2} < 0 \quad \text{for} \quad 2\pi > \Delta\vartheta > \pi.$$

To find the sign of $\cos \frac{\varepsilon}{2}$ and $\cos \frac{\delta}{2}$, we first consider an infinitesimally narrow sector, where $2g = E_2 - E_1 = 0$ and $\varepsilon = \delta = h$. In this sector

$$0 < \frac{\varepsilon}{2} = \frac{\delta}{2} = \frac{h}{2} < \frac{\pi}{2},$$
$$\cos \frac{\varepsilon}{2} > 0, \quad \cos \frac{\delta}{2} > 0.$$

106

The quantities $\cos\frac{\varepsilon}{2}$ and $\cos\frac{\delta}{2}$ cannot reverse their sign upon gradual expansion of the sector unless they pass through 0. But if $\cos\frac{\varepsilon}{2}=0$, then clearly $\sin^2\frac{\varepsilon}{2}=1$. From (8.23) we see that in this case

$$r_1+r_2+s=4a, \tag{8.24}$$

which corresponds to the condition (8.4) of the previous section, according to which the second focus O' is on the line DD'.

In what follows, an elliptical sector of the first kind is a sector OD_1PD_2, where the second focus O' lies outside the segment D_1PD_2 (see Figure 8.5), i.e., a sector corresponding to an elliptical orbit of the first kind, as defined in Sec. 8.2. This sector can obviously be obtained from an infinitesimally narrow sector by continuous expansion, while the second focus O' never crosses the chord D_1D_2. Hence it follows that

$$\cos\frac{\varepsilon}{2}>0.$$

For the angle δ we always have

$$\cos\frac{\delta}{2}>0,$$

since the condition $\cos\frac{\delta}{2}=0$ leads to the impossible equalities

$$r_1+r_2-s=4a, \quad r_1'+r_2'=-s,$$

where r_1' and r_2' are the distances of the points D_1 and D_2 from the second focus O', as defined by (8.2).

It follows from the preceding that for an elliptical sector of the first kind, with $0<\Delta\vartheta<2\pi$, the angle $\frac{\varepsilon}{2}$ is always in the first quadrant. The angle $\frac{\delta}{2}$ is in the first quadrant for $0<\Delta\vartheta<\pi$ and in the fourth quandrant for $\pi<\Delta\vartheta<2\pi$. Expression (8.16) is thus written in the form

$$F=ab[\varepsilon_0-\sin\varepsilon_0\mp(\delta_0-\sin\delta_0)], \tag{8.25}$$

where

$$\sin\frac{\varepsilon_0}{2}=\sqrt{\frac{r_1+r_2+s}{4a}}, \quad \sin\frac{\delta_0}{2}=\sqrt{\frac{r_1+r_2-s}{4a}}, \\ 0<\frac{\varepsilon_0}{2}<\frac{\pi}{2}, \qquad 0<\frac{\delta_0}{2}<\frac{\pi}{2}. \tag{8.26}$$

The sign $-$ corresponds to $0<\Delta\vartheta<\pi$, and the sign $+$ to $\pi<\Delta\vartheta<2\pi$. We see from the second relation in (8.23) that $\delta=\sin\delta=0$ for $\Delta\vartheta=\pi$ (since $r_1+r_2=s$). In this case, either sign may be assumed in (8.25).

We now proceed to determine the area of an elliptical sector of the second kind, i.e., a sector where the second focus O' is inside the corresponding elliptical segment (this is consistent with the previous definition of elliptical orbit of the second kind). Twice the area of this

sector (the sector D_1QD_2O in Figure 8.5) can be obtained from the expression

$$F(\Delta\vartheta) = F(2\pi) - F(2\pi - \Delta\vartheta),$$

where $F(2\pi)$ is twice the area of the ellipse (i.e., of a sector with $\Delta\vartheta = 2\pi$), and $F(2\pi - \Delta\vartheta)$ is twice the area of the complementary sector. From Figure 8.5 we see that the complementary sector is a sector of the first kind. $F(2\pi)$ is obtained from

$$F(2\pi) = 2\pi ab, \tag{8.27}$$

where πab is the area of the ellipse. Hence, applying (8.25), we see that for an elliptical sector of the second kind, with $0 < \Delta\vartheta < 2\pi$,

$$F = ab[2\pi - (\varepsilon_0 - \sin\varepsilon_0) \mp (\delta_0 - \sin\delta_0)]. \tag{8.28}$$

The parameters ε_0 and δ_0 are obtained from (8.26), and the sign in the right-hand side of (8.28) is chosen from the same considerations as the sign in (8.25).

For a limiting elliptical sector (where the second focus lies on the line D_1D_2; this corresponds to the case of a limiting elliptical orbit) condition (8.24) is satisfied. From (8.26) we see that $\varepsilon_0 = \pi$ in this case, and the area formulas (8.25) and (8.28) take the form

$$F = ab[\pi \mp (\delta_0 - \sin\delta_0)]. \tag{8.29}$$

From (8.27) we see that for

$$\Delta\vartheta > 2\pi,$$

the expression

$$F(2\pi n) = 2\pi n ab, \tag{8.30}$$

where n is the number of complete revolutions contained in the angle $\Delta\vartheta$, must be added to (8.25), (8.27), and (8.29). The nature of the sector (whether of the first or second kind or limiting) and the sign in the right-hand sides of (8.25), (8.28), and (8.29) are determined in this case by the parameter

$$\Delta\vartheta' = \Delta\vartheta - 2\pi n. \tag{8.31}$$

8.4. AREA OF HYPERBOLIC AND PARABOLIC SECTORS

Since hyperbolic and parabolic trajectories are open, we always have

$$0 < \Delta\vartheta < 2\pi. \tag{8.32}$$

Moreover, it is only sectors of the first kind that need be considered (for a parabola no sectors of the second kind are possible, since the second focus is at infinity, while for a hyperbola they correspond to the second branch, which is of no relevance for the solution of our problem).

In determining the area of a hyperbolic sector OD_1D_2 $(a<0)$, we shall proceed from relations (6.4), (6.37), and (8.11), which give

$$F = \alpha\beta\left[e\left(\operatorname{sh}H_2 - \operatorname{sh}H_1\right) - (H_2 - H_1)\right] =$$
$$= \alpha\beta\left[2e\operatorname{sh}\frac{H_2-H_1}{2}\operatorname{ch}\frac{H_2+H_1}{2} - (H_2 - H_1)\right],$$

where H_1 and H_2 are the values of the variable H at the points D_1 and D_2. Let

$$g = \frac{H_2-H_1}{2}, \quad \operatorname{ch}h = e\operatorname{ch}\frac{H_2+H_1}{2}, \quad h>0, \Big\}$$
$$\varepsilon = h+g, \qquad \delta = h-g, \tag{8.33}$$

whence

$$h = \frac{\varepsilon+\delta}{2}, \quad g = \frac{\varepsilon-\delta}{2}. \tag{8.33'}$$

Then, making use of the identity

$$\operatorname{sh}\xi\operatorname{ch}\eta = \frac{1}{2}\left[\operatorname{sh}(\xi+\eta)+\operatorname{sh}(\xi-\eta)\right],$$

where ξ and η are arbitrary quantities, we have

$$F = 2\alpha\beta(\operatorname{sh}g\operatorname{ch}h - g) =$$
$$= \alpha\beta\left[\operatorname{sh}\varepsilon - \varepsilon - (\operatorname{sh}\delta - \delta)\right]. \tag{8.34}$$

To find the angles ε and δ entering this expression, we make use of (6.33), which gives (see Figure 8.3 a)

$$OD_1 = r_1 = \alpha(e\operatorname{ch}H_1 - 1), \Big\}$$
$$OD_2 = r_2 = \alpha(e\operatorname{ch}H_2 - 1). \Big\} \tag{8.35}$$

Adding these expressions and applying the identity

$$\operatorname{ch}\xi + \operatorname{ch}\eta = 2\operatorname{ch}\frac{\xi+\eta}{2}\operatorname{ch}\frac{\xi-\eta}{2}$$

with relations (8.33), we find

$$r_1 + r_2 = 2\alpha(\operatorname{ch}g\operatorname{ch}h - 1). \tag{8.36}$$

We now return to expressions (8.19) for the distance s between the points D_1 and D_2 and proceed to determine the angle

$$\Delta\vartheta = \vartheta_2 - \vartheta_1$$

in the right-hand side of these expressions (ϑ_1 and ϑ_2 are the true anomalies at the points D_1 and D_2). Applying relations (6.34) and the identities

$$\operatorname{ch}\xi + 1 = 2\operatorname{ch}^2\frac{\xi}{2}, \quad \operatorname{ch}\xi - 1 = 2\operatorname{sh}^2\frac{\xi}{2},$$

109

we find

$$\sqrt{r}\sin\frac{\vartheta}{2} = \sqrt{\alpha(e+1)}\,\mathrm{sh}\,\frac{H}{2},$$

$$\sqrt{r}\cos\frac{\vartheta}{2} = \sqrt{\alpha(e-1)}\,\mathrm{ch}\,\frac{H}{2},$$

$$\sqrt{r_1 r_2}\cos\frac{\Delta\vartheta}{2} = \sqrt{r_1 r_2}\left(\cos\frac{\vartheta_1}{2}\cos\frac{\vartheta_2}{2} + \sin\frac{\vartheta_1}{2}\sin\frac{\vartheta_2}{2}\right) =$$

$$= \alpha(e-1)\,\mathrm{ch}\,\frac{H_1}{2}\,\mathrm{ch}\,\frac{H_2}{2} + \alpha(e+1)\,\mathrm{sh}\,\frac{H_1}{2}\,\mathrm{ch}\,\frac{H_2}{2}.$$

Now, making use of relations (8.33') and the identities

$$\mathrm{ch}\,(\xi+\eta) = \mathrm{ch}\,\xi\,\mathrm{ch}\,\eta + \mathrm{sh}\,\xi\,\mathrm{sh}\,\eta,$$
$$\mathrm{ch}\,(\xi-\eta) = \mathrm{ch}\,\xi\,\mathrm{ch}\,\eta - \mathrm{sh}\,\xi\,\mathrm{sh}\,\eta,$$

we find

$$\sqrt{r_1 r_2}\cos\frac{\Delta\vartheta}{2} = \alpha\,(\mathrm{ch}\,h - \mathrm{ch}\,g). \tag{8.37}$$

Substituting (8.37) and (8.36) in (8.19), we find

$$s = 2\alpha\,\mathrm{sh}\,g\,\mathrm{sh}\,h. \tag{8.38}$$

From (8.36) and (8.38) it follows that

$$r_1 + r_2 + s = 2\alpha\,[\mathrm{ch}\,(g+h) - 1],$$
$$r_1 + r_2 - s = 2\alpha\,[\mathrm{ch}\,(g-h) - 1],$$

whence, applying (8.33), we find

$$\mathrm{sh}^2\frac{\varepsilon}{2} = \frac{r_1 + r_2 + s}{4\alpha}, \quad \mathrm{sh}^2\frac{\delta}{2} = \frac{r_1 + r_2 - s}{4\alpha}. \tag{8.39}$$

The parameters ε and δ can be determined from these formulas only if their sign is known. From (8.33), seeing that the variable H monotonically increases with flight time (see Sec. 6.3), we find

$$g = \frac{H_2 - H_1}{2} > 0, \quad h > 0, \quad \varepsilon > 0. \tag{8.40}$$

On the other hand, making use of relations (8.33) and the identity

$$\mathrm{ch}\,\xi - \mathrm{ch}\,\eta = 2\,\mathrm{sh}\,\frac{\xi+\eta}{2}\,\mathrm{sh}\,\frac{\xi-\eta}{2},$$

we write for (8.37)

$$\sqrt{r_1 r_2}\cos\frac{\Delta\vartheta}{2} = \alpha\,\mathrm{sh}\,\frac{\varepsilon}{2}\,\mathrm{sh}\,\frac{\delta}{2}.$$

Hence, making use of inequalities (8.40), we find

$$\delta \geqslant 0 \quad \text{for} \quad \Delta\vartheta \leqslant \pi,$$
$$\delta \leqslant 0 \quad \text{for} \quad \Delta\vartheta \geqslant \pi.$$

110

Comparing relations (8.34), (8.39), and (8.40), we obtain the following final expression for twice the area of a hyperbolic sector:

$$F = \alpha\beta[\text{sh}\,\varepsilon_1 - \varepsilon_1 \mp (\text{sh}\,\delta_1 - \delta_1)],$$ (8.41)

where

$$\text{sh}\,\frac{\varepsilon_1}{2} = \sqrt{\frac{r_1 + r_2 + s}{4a}}, \quad \text{sh}\,\frac{\delta_1}{2} = \sqrt{\frac{r_1 + r_2 - s}{4a}},$$

$$\varepsilon_1 \geqslant 0, \quad \delta_1 \geqslant 0.$$

Here — corresponds to $\Delta\vartheta < \pi$ and + to $\Delta\vartheta > \pi$ (for $\Delta\vartheta = \pi$, $\delta_1 = 0$).

Note that (8.14) can also be derived from (8.25) and (8.26) on substitution

$$\varepsilon_0 = i\varepsilon_1, \quad \delta_0 = i\delta_1,$$

where $i = \sqrt{-1}$. This approach, however, leaves open the question of the signs of ε and δ.

To find the area of a parabolic sector $(a = \pm\infty)$, we expand (8.25) and (8.26) in powers of $\frac{1}{a}$. Let

$$m = \sqrt{\frac{r_1 + r_2 + s}{4a}}.$$

Then from (8.26) we have

$$\frac{\varepsilon_0}{2} = \arcsin m = m + \frac{1}{3}\frac{1}{2}m^3 + \frac{1}{5}\frac{1\cdot 3}{2\cdot 4}m^5 + \frac{1}{7}\frac{1\cdot 3\cdot 5}{2\cdot 4\cdot 6}m^7 + \cdots,$$

whence

$$\frac{\sin \varepsilon_0}{2} = m\sqrt{1 - m^2} = m - \frac{1}{2}m^3 - \frac{1\cdot 1}{2\cdot 4}m^5 - \frac{1\cdot 1\cdot 3}{2\cdot 4\cdot 6}m^7 - \cdots,$$

$$\varepsilon_0 - \sin \varepsilon_0 = 4\left(\frac{1}{3}m^3 + \frac{1}{5}\frac{1}{2}m^5 + \frac{1}{7}\frac{1\cdot 3}{2\cdot 4}m^7 + \cdots\right).$$

Analogous expansion can be obtained for $\delta_0 - \sin \delta_0$. Inserting these expansions in (8.25), (8.28) and making use of (5.3) and (5.7), we obtain for elliptical sectors of the first kind

$$F = \sqrt{p}\left\{\frac{1}{3}\frac{1}{2}[(r_1 + r_2 + s)^{3/2} \mp (r_1 + r_2 - s)^{3/2}] + \right.$$

$$+ \frac{1}{5}\frac{1}{2^3}\frac{1}{2}\frac{1}{a}[(r_1 + r_2 + s)^{5/2} \mp (r_1 + r_2 - s)^{5/2}] +$$

$$\left. + \frac{1}{7}\frac{1}{2^5}\frac{1\cdot 3}{2\cdot 4}\frac{1}{a^2}[(r_1 + r_2 + s)^{7/2} \mp (r_1 + r_2 - s)^{7/2}] + \cdots\right\};$$ (8.42)

for elliptical sectors of the second kind

$$F = \sqrt{p}\left\{2\pi a^{3/2} + \frac{1}{3}\frac{1}{2}[-(r_1 + r_2 + s)^{3/2} \mp (r_1 + r_2 - s)^{3/2}] + \right.$$

$$+ \frac{1}{5}\frac{1}{2^3}\frac{1}{2}\frac{1}{a}[-(r_1 + r_2 + s)^{5/2} \mp (r_1 + r_2 - s)^{5/2}] +$$

$$\left. + \frac{1}{7}\frac{1}{2^5}\frac{1\cdot 3}{2\cdot 4}\frac{1}{a^2}[-(r_1 + r_2 + s)^{7/2} \mp (r_1 + r_2 - s)^{7/2}] + \cdots\right\}.$$ (8.43)

The first of these formulas can be shown to apply, not only for elliptical, but also for hyperbolic sectors. It must be borne in mind, however, that

the series converge only if $\sqrt{\frac{r_1 + r_2 + s}{4|a|}} < 1$. From (8.3) it follows that this condition holds true for elliptical orbits (with the exception of limiting orbits, with $m = 1$). For hyperbolic orbits, however, this may not be true, and (8.42) is then meaningless. For $a \rightarrow \infty$, expression (8.42) reduces to the formula for twice the area of a parabolic sector:

$$F = \frac{\sqrt{p}}{6} [(r_1 + r_2 + s)^{3/2} \mp (r_1 + r_2 - s)^{3/2}], \tag{8.44}$$

where $-$ corresponds to $\Delta \vartheta < \pi$ and $+$ to $\Delta \vartheta > \pi$.

8.5. EULER — LAMBERT EQUATION

Substituting (8.25), (8.28), (8.29), (8.41), and (8.44) in (8.11) and making use of (5.3), (5.7), (6.4), and (8.30), we find:
for hyperbolic orbits ($a < 0$)

$$\Delta t = \frac{a^{3/2}}{\sqrt{\mu}} [\mathrm{sh}\, \varepsilon_1 - \varepsilon_1 \mp (\mathrm{sh}\, \delta_1 - \delta_1)], \tag{8.45}$$

where

$$\left.\begin{array}{l} \mathrm{sh}\, \dfrac{\varepsilon_1}{2} = \sqrt{\dfrac{r_1 + r_2 + s}{4\alpha}}, \\[2mm] \mathrm{sh}\, \dfrac{\delta_1}{2} = \sqrt{\dfrac{r_1 + r_2 - s}{4\alpha}}, \\[2mm] \varepsilon_1 \geqslant 0, \quad \delta_1 \geqslant 0, \quad \alpha = -a; \end{array}\right\} \tag{8.45'}$$

for parabolic orbits ($a = \pm\infty$)

$$\Delta t = \frac{1}{6\sqrt{\mu}} [(r_1 + r_2 + s)^{3/2} \mp (r_1 + r_2 - s)^{3/2}]; \tag{8.46}$$

for elliptical orbits of the first kind $\left(a > \frac{r_1 + r_2 + s}{4}\right)$

$$\Delta t = \frac{a^{3/2}}{\sqrt{\mu}} [2\pi n + \varepsilon_0 - \sin \varepsilon_0 \mp (\delta_0 - \sin \delta_0)], \tag{8.47}$$

where

$$\left.\begin{array}{ll} \sin \dfrac{\varepsilon_0}{2} = \sqrt{\dfrac{r_1 + r_2 + s}{4a}}, & \sin \dfrac{\delta_0}{2} = \sqrt{\dfrac{r_1 + r_2 - s}{4a}}, \\[2mm] \dfrac{\pi}{2} \geqslant \dfrac{\varepsilon_0}{2} \geqslant 0, & \dfrac{\pi}{2} \geqslant \dfrac{\delta_0}{2} \geqslant 0; \end{array}\right\} \tag{8.47'}$$

for limiting elliptical orbits $\left(a = \frac{r_1 + r_2 + s}{4}\right)$

$$\Delta t = \frac{a^{3/2}}{\sqrt{\mu}} [\pi(2n + 1) \mp (\delta_0 - \sin \delta_0)], \tag{8.48}$$

where

$$\sin\frac{\delta_0}{2} = \sqrt{\frac{r_1+r_2-s}{r_1+r_2+s}}, \quad \left.\right\}$$
$$\frac{\pi}{2} \geqslant \frac{\delta_0}{2} \geqslant 0; \quad \left.\right\}$$

(8.48')

for elliptical orbits of the second kind $\left(a > \frac{r_1+r_2+s}{4}\right)$

$$\Delta t = \frac{a^{3/2}}{\sqrt{\mu}} [2\pi(n+1) - (\varepsilon_0 - \sin\varepsilon_0) \mp (\delta_0 - \sin\delta_0)].$$

(8.49)

In (8.45'), (8.46), (8.47') and (8.48'), s is determined from (8.19) (always $s \geqslant 0$), n is the number of times 2π goes into $\Delta\vartheta$ (for hyperbolic and parabolic orbits $n = 0$), the sign − corresponds to $\Delta\vartheta - 2\pi n < \pi$, the sign + to $\Delta\vartheta - 2\pi n > \pi$.

The preceding relations constitute the so-called Euler—Lambert equations for the various kinds of orbits. Numerical solution of the Euler—Lambert equation (i.e., determination of a from r_1, r_2, $\Delta\vartheta$, and Δt) can be carried out without difficulty, if the type of the orbit and the number of allowed solutions are known. Any of the conventional techniques for the solution of transcendental equations is adequate. As we have shown in Sec. 8.2, all the elements can be unambiguously determined once the type of the orbit and the parameter a are known.

Our problem thus reduces to the determination of the type of the orbit and the number of solutions of the Euler—Lambert equation for various values of the parameters r_1, r_2, $\Delta\vartheta$, and Δt. In the following sections we therefore proceed with an investigation of the Euler—Lambert equation.

8.6. TYPE OF ORBIT FOR $\Delta\vartheta < 2\pi$

If the body does not complete at least one revolution around the primary ($\Delta\vartheta < 2\pi$), any of the foregoing orbits may apply. To establish the actual type of the orbit in each particular case, we introduce a new variable

$$\varkappa = \frac{1}{a} = -\frac{1}{\alpha}.$$

(8.50)

As this variable monotonically increases, we gradually progress from hyperbolic to parabolic, and eventually to elliptical orbits. Hyperbola corresponds to $\varkappa < 0$, parabola to $\varkappa = 0$, and ellipse to $\varkappa > 0$.

Let us consider the dependence $\Delta t(\varkappa)$ for various types of orbits.

From (8.45) and from the known properties of hyperbolic functions, we see that for $\varkappa \to -\infty$,

$$\Delta t = 2\frac{(-\varkappa)^{-3/2}}{\sqrt{\mu}}\left[\operatorname{sh}\frac{\varepsilon_1}{2}\sqrt{\operatorname{sh}^2\frac{\varepsilon_1}{2}+1} - \frac{\varepsilon_1}{2}\mp\right.$$

$$\left.\mp\left(\operatorname{sh}\frac{\delta_1}{2}\sqrt{\operatorname{sh}^2\frac{\delta_1}{2}+1} - \frac{\delta_1}{2}\right)\right]\to$$

$$\to 2\frac{(-\varkappa)^{-3/2}}{\sqrt{\mu}}\left(\operatorname{sh}^2\frac{\varepsilon_1}{2}\mp\operatorname{sh}^2\frac{\delta_1}{2}\right) = \frac{r_1+r_2+s\mp(r_1+r_2-s)}{2\sqrt{-\mu\varkappa}}\to 0.$$

113

Let us establish the sign of the derivative

$$\frac{d}{dx}(\Delta t) = \frac{1}{x^2}\frac{d}{d\alpha}(\Delta t) = \frac{1}{2x^2}\sqrt{\frac{\alpha}{\mu}}\Big\{3[\mathrm{sh}\,\varepsilon_1 - \varepsilon_1 \mp (\mathrm{sh}\,\delta_1 - \delta_1)] +$$
$$+ 2\alpha\Big[(\mathrm{ch}\,\varepsilon_1 - 1)\frac{d\varepsilon_1}{d\alpha} \mp (\mathrm{ch}\,\delta_1 - 1)\frac{d\delta_1}{d\alpha}\Big]\Big\}$$

in hyperbolic orbit. Differentiating expressions (8.45') for ε_1 and δ_1, we find

$$\frac{1}{2}\mathrm{ch}\,\frac{\varepsilon_1}{2}\frac{d\varepsilon_1}{d\alpha} = -\frac{1}{2\alpha}\sqrt{\frac{r_1 + r_2 + s}{4\alpha}} = -\frac{1}{2\alpha}\mathrm{sh}\,\frac{\varepsilon_1}{2},$$
$$\frac{d\varepsilon_1}{d\alpha} = -\frac{1}{\alpha}\mathrm{th}\,\frac{\varepsilon_1}{2}.$$

Similarly,

$$\frac{d\delta_1}{d\alpha} = -\frac{1}{\alpha}\mathrm{th}\,\frac{\delta_1}{2}.$$

Hence

$$\frac{d}{dx}(\Delta t) = \frac{1}{2x^2}\sqrt{\frac{\alpha}{\mu}}[\Phi(\varepsilon_1) \mp \Phi(\delta_1)], \qquad (8.51)$$

where

$$\Phi(x) = 3(\mathrm{sh}\,x - x) - 2(\mathrm{ch}\,x - 1)\mathrm{th}\,\frac{x}{2}.$$

Clearly,

$$\Phi(0) = 0.$$

Also

$$\frac{d\Phi}{dx} = 3(\mathrm{ch}\,x - 1) - \frac{\mathrm{ch}\,x - 1}{\mathrm{ch}^2\frac{x}{2}} - 2\,\mathrm{sh}\,x\,\mathrm{th}\,\frac{x}{2} = 2\,\mathrm{sh}^2\frac{x}{2}\Big(1 - \frac{1}{\mathrm{ch}^2\frac{x}{2}}\Big) \geqslant 0.$$

We see that $\Phi(x)$ monotonically increases with x, and $\Phi(x) \geqslant 0$ for $x \geqslant 0$. Hence, applying (8.51) and seeing that

$$\varepsilon_1 > \delta_1 > 0,$$

we obtain in our case

$$\frac{d}{dx}(\Delta t) > 0.$$

In hyperbolic orbits, the time Δt monotonically increases as x rises from $-\infty$ to 0. For $x = -\infty$ we have $\Delta t = 0$ (flight with "infinite" velocity), and for $x = 0$ we have the flight time Δt_{par} defined by expression (8.46) for parabolic orbit.

The function $\Delta t(x)$ for elliptical orbits can be analyzed making use of expansions (8.42) and (8.43), which on substitution in (8.11) (in conjunction with (8.27)) give the following expressions:

for elliptical orbits of the first kind

$$\Delta t = \frac{1}{\sqrt{\mu}}\Big\{2\pi n x^{-3/2} + \frac{1}{6}[(r_1 + r_2 + s)^{3/2} \mp (r_1 + r_2 - s)^{3/2}] +$$
$$+ \frac{x}{80}[(r_1 + r_2 + s)^{5/2} \mp (r_1 + r_2 - s)^{5/2}] + \frac{3x^2}{1792}[(r_1 + r_2 + s)^{7/2} \mp (r_1 + r_2 - s)^{7/2}] + \ldots\Big\}; \quad (8.52)$$

114

for elliptical orbits of the second kind

$$\Delta t = \frac{1}{\sqrt{\mu}} \left\{ 2\pi(n+1)\varkappa^{-3/2} + \right.$$

$$+ \frac{1}{6} \left[-(r_1 + r_2 + s)^{3/2} \mp (r_1 + r_2 - s)^{3/2} \right] +$$

$$+ \frac{\varkappa}{80} \left[-(r_1 + r_2 + s)^{5/2} \mp (r_1 + r_2 - s)^{5/2} \right] +$$

$$\left. + \frac{3\varkappa^2}{1792} \left[-(r_1 + r_2 + s)^{7/2} \mp (r_1 + r_2 - s)^{7/2} \right] + \dots \right\}. \tag{8.53}$$

In our case, the number of complete revolutions

$$n = 0.$$

Moreover,

$$r_1 + r_2 + s > r_1 + r_2 - s,$$

and for elliptical orbits the parameter $\varkappa$ varies between the limits

$$0 < \varkappa \leqslant \varkappa_{\lim} = \frac{4}{r_1 + r_2 + s}. \tag{8.54}$$

As $\varkappa$ increases, the time Δt monotonically increases for elliptical orbits of the first kind and decreases for orbits of the second kind.

For $\varkappa \to 0$, we have $\Delta t \to \Delta t_{\text{par}}$ in orbits of the first kind, and $\Delta t \to \infty$ in orbits of the second kind. For $\varkappa \to \varkappa_{\lim} = \frac{4}{r_1 + r_2 + s}$, we have $\Delta t \to \Delta t_{\lim}$ in elliptical orbits of either kind, where $\Delta t_{\lim}$ is defined by (8.48).
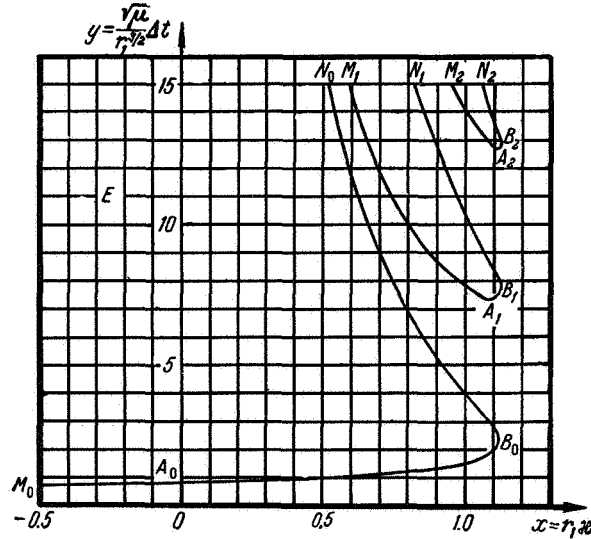
FIGURE 8.6. Flight time Δt between two given points vs. $\varkappa = \frac{1}{a}$.

115

We see that for $\Delta\vartheta<2\pi$, the function $\Delta t(\varkappa)$ follows the curve $M_0A_0B_0N_0$ of Figure 8.6, where the abscissa gives a dimensionless number $x=\frac{r_1}{a}=r_1\varkappa$, which is proportional to $\varkappa$, and the ordinate the dimensionless number $y=\frac{\sqrt{\mu}}{r_1^{3/2}}\Delta t$, which is proportional to Δt (the curve plotted in Figure 8.6 corresponds to the case $r=1.5\,r_1, \Delta\vartheta=45°$).

On this curve, the interval M_0A_0 corresponds to hyperbolic orbits, the point A_0 to parabolic orbits, the interval A_0B_0 to elliptical orbits of the first kind, the point B_0 to limiting elliptical orbits, and the interval B_0N_0 to elliptical orbits of the second kind. As the points M_0 and N_0 recede to infinity, the curve A_0M_0 asymptotically approaches the abscissa axis ($\Delta t = 0$), and the curve B_0N_0 moves to the ordinate axis ($\varkappa = 0$).

We see from the curve $M_0A_0B_0N_0$ that for $\Delta\vartheta<2\pi$, to each Δt there always corresponds a single $\varkappa$. Since $\varkappa$ and a are unambiguously related by (8.50), the Euler—Lambert equation (and therefore our problem as a whole) is uniquely solvable in this case. To find the type of the orbit, it suffices to calculate the parameters Δt_{par} and Δt_{lim} from (8.46) and (8.48).

For hyperbolic orbit

$$\Delta t<\Delta t_{par}\,;$$

for parabolic orbit

$$\Delta t=\Delta t_{par}\,;$$

for elliptical orbit of the first kind

$$\Delta t_{lim}>\Delta t>\Delta t_{par}\,;$$

for limiting elliptical orbit

$$\Delta t=\Delta t_{lim}\,;$$

for elliptical orbit of the second kind

$$\Delta t>\Delta t_{lim}\,;$$

8.7. TYPE OF ORBIT FOR $\Delta\vartheta>2\pi$

If the body completes several revolutions around the primary ($\Delta\vartheta>2\pi$, $n\geqslant1$), the orbit is of necessity elliptic. To establish the type of the orbit and the number of solutions of the Euler—Lambert equation, we proceed with an analysis of the function $\Delta t(\varkappa)$ for these orbits.

Differentiating (8.52) we see that for elliptical orbits of the first kind

$$\frac{d}{d\varkappa}(\Delta t)=-F_1(\varkappa)+F_2(\varkappa),$$

116

where

$$F_1(x) = \frac{3\pi n}{\sqrt{\mu}} x^{-\frac{5}{2}},$$

$$F_2(x) = \frac{1}{\sqrt{\mu}} \left\{ \frac{1}{80} [(r_1 + r_2 + s)^{\frac{5}{2}} \mp (r_1 + r_2 - s)^{\frac{5}{2}}] + \right.$$

$$\left. + \frac{3x}{896} [(r_1 + r_2 + s)^{\frac{7}{2}} \mp (r_1 + r_2 - s)^{\frac{7}{2}}] + \ldots \right\}.$$

We see from these expressions that as x increases between the limits (8.54),
the function $F_1(x)$ monotonically decreases from ∞ to $F_1(x_{\lim}) = \frac{3\pi n}{\sqrt{\mu}} x_{\lim}^{-\frac{5}{2}}$, and
the function $F_2(x)$ increases from $F_2(0) = \frac{1}{80\sqrt{\mu}} [(r_1 + r_2 + s)^{\frac{5}{2}} \mp (r_1 + r_2 - s)^{\frac{5}{2}}]$.
The derivative $\frac{d}{dx}(\Delta t)$ monotonically increases from $\frac{d}{dx}(\Delta t) = -\infty$ for $x = 0$.
From (8.47) and (8.50) we have

$$\frac{d}{dx}(\Delta t) = \frac{1}{x^2} \sqrt{\frac{a}{\mu}} \left\{ \left(1 - \cos \varepsilon_0 \right) \operatorname{tg} \frac{\varepsilon_0}{2} \mp \right.$$

$$\left. \mp (1 - \cos \delta_0) \operatorname{tg} \frac{\delta_0}{2} - \frac{3}{2} [2\pi n + \varepsilon_0 - \sin \varepsilon_0 \mp (\delta_0 - \sin \delta_0)] \right\}.$$

From (8.47), (8.50), and (8.54) we see that for $x \to x_{\lim}$, $\varepsilon_0 \to \pi$ and $\delta_0 < \pi$.
Hence,

$$\frac{d}{dx}(\Delta t) \to \infty \quad \text{for} \quad x \to x_{\lim}.$$

We see that for elliptical orbits of the first kind, the derivative $\frac{d}{dx}(\Delta t)$
monotonically increases from $-\infty$ to $+\infty$ in the entire interval (8.54),
passing once through zero. Hence it follows that for elliptical orbits
of the first kind $\Delta t(x)$ monotonically decreases with increasing x from
∞ to a certain minimum Δt, and then rises to $\Delta t_{\lim}$, as defined by (8.48).

The function $\Delta t(x)$ for elliptical orbits of the second kind, as we see
from (8.53), monotonically decreases with increasing x from ∞ to $\Delta t_{\lim}$.
Hence, for $n \geqslant 1$, the function $\Delta t(x)$ is represented in Figure 8.6 by the
curves $M_n A_n B_n N_n$ ($n = 1, 2, 3, \ldots$). In these curves, the intervals $M_n B_n$
correspond to elliptical orbits of the first kind, the points B_n to limiting
elliptical orbits, and the intervals $B_n N_n$ to elliptical orbits of the second
kind. The points A_n correspond to orbits of the first kind with the minimum
time $\Delta t = \Delta t_n$. As the points M_n and N_n recede to infinity, the curves $B_n M_n$
and $B_n N_n$ asymptotically approach the ordinate axis ($x = 0$).

From the curves $M_n A_n B_n N_n$ we see that for

$$\Delta t < \Delta t_n$$

the problem is unsolvable.
For

$$\Delta t = \Delta t_n$$

the problem has one solution (in the region of orbits of the first kind);
for

$$\Delta t_{\lim} > \Delta t > \Delta t_n$$

there are two solutions in the region of orbits of the first kind;
for

$$\Delta t = \Delta t_{\text{lim}}$$

there are again two solutions, one corresponding to an orbit of the first kind, the other to a limiting orbit.

Finally, for

$$\Delta t > \Delta t_{\text{lim}}$$

there are two solutions corresponding to orbits of the first and the second kind.

To find the numerical value of the minimum time $\Delta t = \Delta t_n$, we must solve the equation

$$\frac{d}{da}(\Delta t) = 0. \tag{8.54'}$$

Differentiating (8.47), we see that the solution of equation (8.54') is equivalent to the solution of the equation

$$3 \left[2\pi n + \varepsilon_0 - \sin \varepsilon_0 \mp (\delta_0 - \sin \delta_0) \right] -$$
$$- 2 \left[(1 - \cos \varepsilon_0) \operatorname{tg} \frac{\varepsilon_0}{2} \mp (1 - \cos \delta_0) \operatorname{tg} \frac{\delta_0}{2} \right] = 0. \tag{8.55}$$

Solving this equation by any of the common approximate techniques, we find the corresponding $a = a_n$, and substitution in (8.47) gives Δt_n.

It can be shown that for fixed points D_1 and D_2 (i.e., for constant values of the parameters r_1, r_2, and s), the time Δt_n increases with increasing n. Hence it follows that if with given positions of the points D_1 and D_2 and with a given time Δt, the problem is solvable for some $n = n_0$, it is also solvable for any $n < n_0$.

In the preceding analysis we invariably assumed that the number of complete revolutions around the primary was known. We shall now try to do without this assumption, i.e., we shall seek the possible paths between the points D_1 and D_2 with a constant flight time Δt. The sense of motion around the gravitational center is known.

In other words, the n in expression (8.1) is arbitrary, but one of the ± signs is specified. Graphically, each solution of this problem corresponds to an intersection of the horizontal line

$$y = \frac{\sqrt{\mu}}{r_1^{3/2}} \Delta t$$

(the line EF) with one of the curves $M_n A_n B_n N_n$ (Figure 8.6). Let N be the largest of the integers n for which the problem is solvable, i.e., let N be defined from the condition

$$\Delta t_N \leqslant \Delta t, \ \Delta t_{N+1} > \Delta t,$$

where Δt_N is the minimum allowed value of Δt for

$$n = N \ (\Delta t_0 = 0).$$

Having thus found the number N, we can easily find the number of solutions k. From (8.6) we have

$$k = \begin{cases} 2N+1 & \text{for} \quad \Delta t_N < \Delta t, \\ 2N & \text{for} \quad \Delta t_N = \Delta t. \end{cases}$$

8.8. PARTICULAR CASES OF ORBIT DETERMINATION

We have invariably assumed in the preceding that the points D_1, D_2' and the gravitational center O were not colinear. If these points are on one line, the solutions of our problem acquire the following peculiar features.

(1) Besides the curvilinear motion defined by (4.19), there is also a possibility of vertical motion along the line $D_1 D_2 O$.

(2) In curvilinear motion, the orientation of the orbital plane is indeterminate. The orbit may lie in any plane through the straight line $D_1 D_2 O$.

In general, there are three different colinear dispositions of the points D_1, D_2, and O.

A. The points D_1 and D_2 are on the two sides of O.

B. The points D_1 and D_2 are on one side of O, but they do not coincide.

C. The points D_1 and D_2 coincide.

The case when one of the points D_1 and D_2 (or both) coincides with the gravitational center O is of no practical value.

When the points D_1 and D_2 are on the two sides of the primary, only curvilinear orbits are possible. Vertical motion is ruled out since vertical trajectories are invariably confined to one side of the gravitational center (see Secs. 7.5—7.7). To determine the curvilinear orbit, we should first decide on the orientation of the orbital plane through the line $D_1 O D_2$; the Euler—Lambert equations (8.45)—(8.49) are then applied, putting

$$\left. \begin{array}{l} \Delta\vartheta = \pi(2n+1), \quad s = r_1 + r_2, \\ r_1 + r_2 + s = 2(r_1 + r_2), \quad r_1 + r_2 - s = 0, \\ \sin\dfrac{\varepsilon_0}{2} = \sqrt{\dfrac{r_1 + r_2}{2a}}, \quad \operatorname{sh}\dfrac{\varepsilon_1}{2} = \sqrt{\dfrac{r_1 + r_2}{2a}}, \\ \delta_0 = \delta_1 = 0. \end{array} \right\} \tag{8.56}$$

All the alternative solutions of the Euler—Lambert equation listed in Secs. 8.6 and 8.7 apply in this case. However, for $\Delta\vartheta = \pi(2n+1)$, to each of these alternatives there correspond, not one, but two trajectories in any orbital plane, differing in the sense of motion around the gravitational center (the trajectories $D_1 P_1 D_2$ and $D_1 P_2 D_2$ in Figure 8.7). The orbit $D_1 P_2 D_2$ clearly obtains from the orbit $D_1 P_1 D_2$ by rotating the orbital plane through π around the line $D_1 D_2$. The ambiguity can therefore be eliminated if, given the position of the orbital plane Σ, we define its "positive side" as the side where the orbital motion is clockwise. In this case, the orientation of the plane Σ can be defined by the dihedral angle γ between the orbital plane and a given reference plane Σ_0. This angle increases as the orbital plane rotates in the positive direction. The trajectories $D_1 P_1 D_2$ and $D_1 P_2 D_2$ then correspond to different orientations of the plane Σ, defined by the angles γ_1 and $\gamma_2 = \gamma_1 + \pi$.

We see that when the points D_1 and D_2 are on the line D_1OD_2, on the two sides of O, all the different cases of Secs. 8.6 and 8.7 apply. Each solution of the Euler—Lambert equation corresponds to a one-parametric family
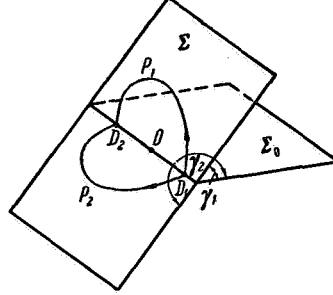
FIGURE 8.7. Motion between two given points D_1 and D_2 colinear with the center of attraction O.

of orbits, with different orientations of the orbital plane. The parameter specifying the orientation of the orbital plane is the angle γ, which varies between the limits

$$0 \leqslant \gamma < 2\pi.$$

If two distinct points D_1 and D_2 are on one side of the center of attraction O, no curvilinear transfer trajectory is possible. Indeed, in this case $\Delta\vartheta = 2\pi n$. Hence, applying (4.19), we have $r_1 = r_2$, which is at variance with the assumption that the points D_1 and D_2 are distinct.

A vertical orbit is permitted. Its direction is along the line OD_1D_2. Since no circumnavigation of the gravitational center is possible with vertical orbits (see Secs. 7.6 and 7.7), we must take

$$\Delta\vartheta = 0. \tag{8.57}$$

To find the parameter a, we make use of Euler—Lambert equations (8.45)—(8.49), applying condition (8.57) and also the condition

$$s = r_{\text{max}} - r_{\text{min}},$$

where r_{max} and r_{min} are respectively the larger and the smaller of the two distances r_1 and r_2.
Hence

$$r_1 + r_2 + s = 2r_{\text{max}}, \quad r_1 + r_2 - s = 2r_{\text{min}}. \tag{8.58}$$

As we have observed in Sec. 7.5, vertical elliptical orbit is the limiting case of a curvilinear trajectory with $a = $ const and $e \rightarrow 1$. The second focus coincides with the vertex A of the vertical orbit (see Figure 7.2). Hence, elliptical orbits of the first kind degenerate into vertical trajectories, with the body moving from point D_1 to point D_2 without passing through the vertex A. Orbits of the second kind degenerate into trajectories D_1AD_2,

where the body passes through the vertex. From (8.24) and (8.25) it follows that for limiting vertical elliptical orbits

$$2a = r_{max}, \qquad (8.59)$$

which corresponds to a case with one of the points (D_1 or D_2) at the vertex.

Substituting (8.57)—(8.59) in the right-hand sides of (8.45)—(8.49), we write Euler—Lambert equations in the following form:

for vertical hyperbolic orbits ($a<0$)

$$\left. \begin{array}{c} \Delta t = \dfrac{a'^{h}}{\sqrt{\mu}} [\operatorname{sh}\varepsilon_1 - \varepsilon_1 - (\operatorname{sh}\delta_1 - \delta_1)], \\[2mm] \operatorname{sh}\dfrac{\varepsilon_1}{2} = \sqrt{\dfrac{r_{max}}{2\alpha}}, \quad \operatorname{sh}\dfrac{\delta_1}{2} = \sqrt{\dfrac{r_{min}}{2\alpha}}, \\[2mm] \varepsilon_1 \geqslant 0, \quad \delta_1 \geqslant 0, \quad \alpha = -a; \end{array} \right\} \qquad (8.60)$$

for vertical parabolic orbits ($a = \infty$)

$$\Delta t = \dfrac{1}{6\sqrt{\mu}} [(2r_{max})^{3/2} - (2r_{min})^{3/2}]; \qquad (8.61)$$

for vertical elliptical orbits of the first kind $\left(a > \dfrac{r_{max}}{2}\right)$

$$\left. \begin{array}{c} \Delta t = \dfrac{a'^{h}}{\sqrt{\mu}} [\varepsilon_0 - \sin\varepsilon_0 - (\delta_0 - \sin\delta_0)], \\[2mm] \sin\dfrac{\varepsilon_0}{2} = \sqrt{\dfrac{r_{max}}{2a}}, \quad \sin\dfrac{\delta_0}{2} = \sqrt{\dfrac{r_{min}}{2a}}, \\[2mm] \dfrac{\pi}{2} \geqslant \dfrac{\varepsilon_0}{2} \geqslant 0, \quad \dfrac{\pi}{2} \geqslant \dfrac{\delta_0}{2} \geqslant 0; \end{array} \right\} \qquad (8.62)$$

for limiting vertical elliptical orbits $\left(a = \dfrac{r_{max}}{2}\right)$

$$\left. \begin{array}{c} \Delta t = \dfrac{a'^{h}}{\sqrt{\mu}} [\pi - (\delta_0 - \sin\delta_0)], \\[2mm] \sin\dfrac{\delta_0}{2} = \sqrt{\dfrac{r_{min}}{r_{max}}}, \quad \dfrac{\pi}{2} \geqslant \dfrac{\delta_0}{2} \geqslant 0; \end{array} \right\} \qquad (8.63)$$

for vertical elliptical orbits of the second kind $\left(a > \dfrac{r_{max}}{2}\right)$

$$\Delta t = \dfrac{a'^{h}}{\sqrt{\mu}} [2\pi - (\varepsilon_0 - \sin\varepsilon_0) - (\varepsilon_0 - \sin\delta_0)]. \qquad (8.64)$$

All the conclusions obtained in Sec. 8.6 for the general Euler—Lambert equation with $\Delta\vartheta<2\pi$ remain in force. It follows that if the points D_1 and D_2 are distinct, the Euler—Lambert equation is always uniquely solvable. To find the type of the vertical orbit, we should calculate from (8.61) and (8.63) the flight time Δt_{par} in parabolic orbit and Δt_{lim} in limiting elliptical orbit. The type of the orbit is then determined as at the end of Sec. 8.6.

Having established the type of the orbit and calculated the parameter a by numerically solving the Euler—Lambert equation, we can find the second element τ of the vertical orbit from the known time of passage through one of the points D_1 or D_2. The relations in Secs. 7.6 and 7.7 are

121

adequate for this purpose. To sum up, if two distinct points D_1 and D_2 lie on the line OD_1D_2, on one side of the gravitational center O, the problem has a unique solution, which corresponds to a certain vertical trajectory.

If the points D_1 and D_2 coincide, different cases are possible with $\Delta t = 0$ and $\Delta t \neq 0$. The case $\Delta t = 0$ is the trivial problem of orbit determination through a given point D_1. The solution of this problem is clearly a three-parametric family of possible orbits (the parameters specifying each orbit of this family are, say, the velocity components at the point D_1).

In the case

$$\Delta t \neq 0, \ \Delta\vartheta = 2\pi n \ (n = 0, 1, 2, \ldots), \ r_1 = r_2, \tag{8.65}$$

on the other hand, both vertical and curvilinear orbits are possible.

As we have previously observed, for vertical trajectories we need only consider the case $n = \Delta\vartheta = 0$. Then

$$r_1 = r_2, \ s = 0, \ r_1 + r_2 + s = r_1 + r_2 - s = 2r_1, \ \epsilon_0 = \delta_0, \ \epsilon_1 = \delta_1.$$

Hyperbolic vertical orbits, parabolic vertical orbits, elliptical vertical orbits of the first kind, and limiting elliptical vertical orbits are all impossible in this case, since from (8.60) — (8.64) we have $\Delta t = 0$.

We are therefore left with elliptical vertical orbits of the second kind, and the Euler — Lambert equation (8.64) takes the form

$$\left.\begin{array}{l} \Delta t = \dfrac{2a^{3/2}}{\sqrt{\mu}} (\pi - \epsilon_0 + \sin \epsilon_0), \\[2mm] \sin\dfrac{\epsilon_0}{2} = \sqrt{\dfrac{r_1}{2a}}, \ \dfrac{\pi}{2} > \dfrac{\epsilon_0}{2} \geqslant 0. \end{array}\right\} \tag{8.66}$$

From (8.66) we see that Δt monotonically increases with a. As a varies between the limits $\frac{r_1}{2} < a < \infty$, Δt varies in the interval $0 < \Delta t < \infty$. The Euler — Lambert equation is therefore uniquely solvable in our case. This solution defines the orbit.

Aside from the vertical trajectory, there are also curvilinear orbits. Here

$$n \geqslant 1, \ \Delta\vartheta = 2\pi n.$$

These are ellipses with an orbital period

$$P = \frac{\Delta t}{n} = 2\pi \frac{\Delta t}{\Delta\vartheta}. \tag{8.67}$$

Hence, making use of (5.36), we obtain the semimajor axis

$$a = \sqrt[3]{\mu \left(\frac{\Delta t}{2\pi n}\right)^2} = \sqrt[3]{\mu \left(\frac{\Delta t}{\Delta\vartheta}\right)^2}. \tag{8.68}$$

These orbits are possible only if

$$a = \sqrt[3]{\mu \left(\frac{\Delta t}{\Delta\vartheta}\right)^2} > \frac{r_1}{2}. \tag{8.69}$$

This condition may be written as

$$\Delta t > \Delta t_n, \quad \Delta t_n = \Delta \vartheta \frac{r_1^{3/2}}{\sqrt{8\mu}} = \pi n \frac{r_1^{3/2}}{\sqrt{2\mu}} \, . \tag{8.70}$$

For $\Delta t = \Delta t_n$, the closed elliptical orbit degenerates into a vertical trajectory. The solution becomes unfeasible, since it presupposes circumnavigation of the gravitational center. From (5.15) it follows that the desired orbit is attained if the velocity at the given point is

$$v_1 = \sqrt{\frac{2\mu}{r_1} - \frac{\mu}{a}} \, .$$

The direction of the velocity v_1 remains indeterminate. Hence it follows that if condition (8.70) is satisfied, the solution of our problem is a two-parametric family of elliptical orbits. The parameters defining each orbit of this family are, say, the two angles specifying the direction of the velocity vector at the point D_1. If condition (8.70) is not satisfied, the problem is unsolvable.

8.9. LIST OF THE DIFFERENT CASES OF ORBIT DETERMINATION FOR TWO FIXED POINTS

We are now in a position to list all the different cases in the determination of orbits through two given points D_1 and D_2, when the flight time Δt between the points and the circumnavigation angle $\Delta \vartheta$ are known. This list is given in Table 8.2, which shows how the number and the type of solutions depend on the relative disposition of the points O, D_1, D_2, and also on the particular values of Δt and $\Delta \vartheta$. By unfeasible solutions we mean those which require passage through the gravitational center O.

In conclusion we should note that in many-valued cases, the accuracy of orbit determination is lowered because of the significant increase in the contribution from errors of measurement and calculation. It follows from Table 8.2 that this loss of accuracy occurs in the following cases:

(i) $\Delta \vartheta \rightarrow 0$, $\Delta t \rightarrow 0$;

(ii) $\Delta \vartheta \rightarrow \pi n$ $(n = 1, 2, 3, \ldots)$, $\Delta t \neq 0$;

(iii) $\Delta \vartheta > 2\pi$, $\Delta t \rightarrow \Delta t_n$.

The case of large $\Delta \vartheta$, close to $\Delta \vartheta = \pi n + \frac{\pi}{2}$ $(n = 0, 1, 2, \ldots)$, is optimal as regards the solution of the problem.

8.10. CALCULATION OF THE ELEMENTS p AND ω

Once the type of the orbit has been determined and the parameter a calculated, the problem reduces to the determination of the elements p and ω (see Sec. 8.1). We have shown in Sec. 8.2 that this problem is

TABLE 8.2.

No.	Disposition of the points O, D_1, and D_2	$\Delta\vartheta$	Δt	Solution	Orbit
1	Not colinear	$0 < \Delta\vartheta < 2\pi$	$\Delta t < \Delta t_{par}$	One	Hyperbolic
2	"	"	$\Delta t = \Delta t_{par}$	"	Parabolic
3	"	"	$\Delta t_{lim} > \Delta t > \Delta t_{par}$	"	Elliptical first kind
4	"	"	$\Delta t = \Delta t_{lim}$	"	Limiting elliptical
5	"	"	$\Delta t > \Delta t_{lim}$	"	Elliptical second kind
6	"	$\Delta\vartheta > 2\pi$	$\Delta t < \Delta t_n$	None	–
7	"	"	$\Delta t = \Delta t_n$	One	Elliptical first kind
8	"	"	$\Delta t_{lim} > \Delta t > \Delta t_n$	Two	"
9	"	"	$\Delta t = \Delta t_{lim}$	"	Elliptical first kind and limiting elliptical
10			$\Delta t > \Delta t_{lim}$	"	Elliptical first and second kind
11–20	Colinear: D_1 and D_2 on the two sides of O	All the solutions from 1 through 10 are possible, depending on the particular values of $\Delta\vartheta$ and Δt. Each of the solutions 1 through 10 corresponds to a one-parametric family of orbits			
21–25	Colinear: D_1 and D_2 on one side of O	$\Delta\vartheta = 0$	All the solutions from 1 through 5 are possible, depending on the particular values of Δt. Each of these solutions uniquely defines a vertical orbit		
26		$\Delta\vartheta = 2\pi n$ $(n = 1, 2, 3, \ldots)$	Arbitrary	Impossible or unfeasible	Vertical elliptical
27	D_1 and D_2 coincide	$\Delta\vartheta = 0$	$\Delta t = 0$	Three-parametric family	Any
28	"	"	$\Delta t > 0$	One	Vertical elliptical second kind
29	"	$\Delta\vartheta = 2\pi n$ $(n = 1, 2, 3, \ldots)$	$\Delta t < \Delta t_n$	None	–
30		"	$\Delta t = \Delta t_n$	Unfeasible	Limiting vertical elliptical
31			$\Delta t > \Delta t_n$	Two-parametric family	Elliptical

124

always uniquely solvable, and that the solution can be obtained by geometrical construction. In the present section we derive analytical expressions for these elements.

In the case of elliptical orbit, we proceed from relations (8.17). Adding and subtracting, we obtain

$$\frac{r_2+r_1}{2a} = 1 - e\cos\frac{E_2+E_1}{2}\cos\frac{E_2-E_1}{2},$$

$$\frac{r_2-r_1}{2a} = e\sin\frac{E_2+E_1}{2}\sin\frac{E_2-E_1}{2},$$

whence

$$\left. \begin{aligned} e\sin\frac{E_2+E_1}{2} &= \frac{r_2-r_1}{2a\sin\frac{E_2-E_1}{2}}, \\ e\cos\frac{E_2+E_1}{2} &= \left(1 - \frac{r_2+r_1}{2a}\right)\frac{1}{\cos\frac{E_2-E_1}{2}}. \end{aligned} \right\} \qquad (8.71)$$

On the other hand, from (8.14) and (8.15) we have

$$E_2 - E_1 = \varepsilon - \delta. \qquad (8.72)$$

Changing over from ε and δ to ε_0 and δ_0 $(0 \leqslant \varepsilon_0,\ \delta_0 \leqslant \pi)$, we note that the angle 2π goes into $E_2 - E_1$ the same number of times as into $\Delta\vartheta = \vartheta_2 - \vartheta_1 = u_2 - u_1$.

On the basis of the preceding analysis of the signs of $\frac{\varepsilon}{2}$ and $\frac{\delta}{2}$, we find that

$$E_2 - E_1 = \left\{ \begin{aligned} &2\pi n + \varepsilon_0 \mp \delta_0 \quad \text{for elliptical orbits of the first kind,} \\ &\pi(2n+1) \mp \delta_0 \quad \text{for limiting elliptical orbits,} \\ &2\pi(n+1) - \varepsilon_0 \mp \delta_0 \quad \text{for elliptical orbits of the second kind,} \end{aligned} \right\} (8.73)$$

where the sign $-$ corresponds to $0 \leqslant \Delta\vartheta - 2\pi n < \pi$, and the sign $+$ to $2\pi > \Delta\vartheta - 2\pi n \geqslant \pi$.

If $E_2 - E_1$ is known, we can easily find the eccentricity e. It suffices to square the equalities (8.71) and add them up. Thus

$$e = \sqrt{\left(\frac{r_2-r_1}{2a\sin\frac{E_2-E_1}{2}}\right)^2 + \left(1 - \frac{r_2+r_1}{2a}\right)^2\frac{1}{\cos^2\frac{E_2-E_1}{2}}}. \qquad (8.74)$$

Having calculated $E_2 - E_1$ and e, we can find $E_2 + E_1$ from (8.71), and then determine E_2 and E_1 separately. Now, from (5.49) we have

$$\left. \begin{aligned} \operatorname{tg}\frac{\vartheta_{1,2}}{2} &= \sqrt{\frac{1+e}{1-e}}\,\operatorname{tg}\frac{E_{1,2}}{2}, \\ \omega &= u_1 - \vartheta_1 = u_2 - \vartheta_2. \end{aligned} \right\} \qquad (8.75)$$

The angles $\frac{\vartheta_{1,2}}{2}$ are in the same quadrants as the corresponding angles $\frac{E_{1,2}}{2}$. The last equality in (8.75) can be applied for verification.

The elements of hyperbolic orbit are calculated in the same way. From (8.35) we have

$$\frac{r_2+r_1}{2a} = e\,\mathrm{ch}\,\frac{H_2+H_1}{2}\,\mathrm{ch}\,\frac{H_2-H_1}{2} - 1,$$

$$\frac{r_2-r_1}{2a} = e\,\mathrm{sh}\,\frac{H_2+H_1}{2}\,\mathrm{sh}\,\frac{H_2-H_1}{2},$$

where

$$\left.\begin{array}{l} e\,\mathrm{sh}\,\dfrac{H_2+H_1}{2} = \dfrac{r_2-r_1}{2a\,\mathrm{sh}\,\dfrac{H_2-H_1}{2}}\,. \\[4mm] e\,\mathrm{ch}\,\dfrac{H_2+H_1}{2} = \left(1 + \dfrac{r_2+r_1}{2a}\right)\dfrac{1}{\mathrm{ch}\,\dfrac{H_2-H_1}{2}}, \end{array}\right\} \tag{8.76}$$

$$e = \sqrt{\left(1 + \frac{r_2+r_1}{2a}\right)^2 \frac{1}{\mathrm{ch}^2\,\dfrac{H_2-H_1}{2}} - \left(\frac{r_2-r_1}{2a\,\mathrm{sh}\,\dfrac{H_2-H_1}{2}}\right)^2}\,. \tag{8.77}$$

The difference $H_2 - H_1$ entering the right-hand side of these expressions is determined from (8.33), (8.41):

$$H_2 - H_1 = \varepsilon_1 \mp \delta_1. \tag{8.78}$$

The parameters ε_1 and δ_1 are calculated from (8.41); the sign $-$ corresponds to $\Delta\vartheta \leqslant \pi$, the sign $+$ to $\Delta\vartheta \geqslant \pi$.

Having found $H_2 - H_1$ and e, we can determine p and $H_2 + H_1$ from (6.4) and (8.76), and then H_2 and H_1 separately. Now, from (6.41) we have

$$\left.\begin{array}{l} \mathrm{tg}\,\dfrac{\vartheta_{1,2}}{2} = \sqrt{\dfrac{e+1}{e-1}}\,\mathrm{th}\,\dfrac{H_{1,2}}{2}, \\[3mm] \omega = u_1 - \vartheta_1 = u_2 - \vartheta_2. \end{array}\right\} \tag{8.79}$$

The angles $\dfrac{\vartheta_{1,2}}{2}$ in these formulas are in the first or the fourth quadrant (since for hyperbolic orbit $-\pi < \vartheta < \pi$).

The elements of parabolic orbit $(a = \infty)$ are determined from (7.1), which gives

$$r_1 = \frac{p}{2\cos^2\dfrac{\vartheta_1}{2}}\,, \quad r_2 = \frac{p}{2\cos^2\dfrac{\vartheta_2}{2}}\,,$$

whence

$$\cos\frac{\vartheta_1}{2} = \sqrt{\frac{p}{2r_1}}\,, \quad \cos\frac{\vartheta_2}{2} = \cos\left(\frac{\vartheta_1 + \Delta\vartheta}{2}\right) = \sqrt{\frac{p}{2r_2}}\,. \tag{8.80}$$

From these equalities, after some manipulations, we find

$$\sin\frac{\vartheta_1}{2} = \mathrm{ctg}\,\frac{\Delta\vartheta}{2}\sqrt{\frac{p}{2r_1}} - \frac{1}{\sin\dfrac{\Delta\vartheta}{2}}\sqrt{\frac{p}{2r_2}}\,. \tag{8.81}$$

From (8.80) and (8.81) we have

$$p = \frac{2}{\dfrac{1}{r_1} + \left(\dfrac{\mathrm{ctg}\,\dfrac{\Delta\vartheta}{2}}{\sqrt{r_1}} - \dfrac{1}{\sin\dfrac{\Delta\vartheta}{2}\sqrt{r_2}}\right)^2}\,. \tag{8.82}$$

The angle ϑ_1 is calculated from (8.80) and (8.81), and the argument ω is determined from (8.79).

Chapter 9

THE INFLUENCE OF VARIATIONS IN THE INITIAL
CONDITIONS OF MOTION ON THE ELEMENTS OF
ELLIPTICAL ORBIT

9.1. STATEMENT OF THE PROBLEM

In Chapters 5 — 7 we derived expressions for the orbital elements in terms of the initial conditions of motion. In the solution of various applied problems, we often have to consider the influence of variations in the initial conditions on the orbital elements. For nearly circular orbits, this problem has been dealt with in Chapter 2.

The present chapter investigates this question in application to the elliptical orbits of artificial Earth satellites. We first consider in-plane perturbations of the elements (which do not alter the orientation of the orbital plane), and then proceed to analyze orbit-plane perturbations (assuming unperturbed motion in the orbital plane).

The motion of a satellite in the orbital plane is determined by four initial conditions: two coordinates and two velocity components. The initial position of the satellite in polar coordinates can be defined by the distance r_0 from the center of attraction and the angular distance u_0 from some fixed direction (e. g., the line joining the center of attraction with the ascending node Ω). The initial velocity vector can be characterized by its magnitude v_0 and by the angle θ_0 between its direction and the local horizon (Figure 9.1).
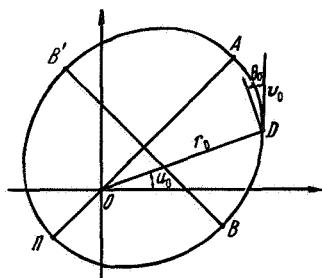
FIGURE 9.1. Initial conditions of motion
in polar coordinates.

The time is reckoned from the passage of the satellite through the point of origin of its orbit (i. e., its initial position).

127

Since any variation in the angle u_0 rotates the orbit around the center of attraction, we shall be concerned with the contribution from variations in r_0, v_0, and θ_0 only. We shall particularly concentrate on the following in-orbit perturbations:

> perturbation of the semimajor axis a,
> perturbation of the orbital period P,
> perturbation of the eccentricity e,
> perturbation of the angular distance ϑ_0 from the pericenter
>   to the point of origin,
> perturbation of the pericenter and apocenter distances r_p and r_a.

The results of this chapter are also applicable in the analysis of various impulsive perturbations. To this end, it suffices to conceive of the point of application of the impulsive perturbation as the point of origin, interpreting the impulsive perturbation as a corresponding variation in the initial velocity vector.

9.2. VARIATIONS OF SEMIMAJOR AXIS
AND ORBITAL PERIOD

We have shown in Chapter 5 that the semimajor axis a of an elliptical orbit and the orbital period P are related by a single-valued expression (5.36). Hence a relation between the variations Δa and ΔP of these parameters:

$$\frac{\Delta P}{P} = \frac{3}{2}\frac{\Delta a}{a}.$$ (9.1)

In virtue of this relation, the two variations should preferably be considered simultaneously.

From (5.43) we see that a and P are functions of r_0 and

$$k_0 = \frac{v_0^2 r_0}{\mu}$$ (9.2)

while being independent of the angle θ_0. Differentiating (5.43) and applying (9.1), we see that a variation Δr_0 in the initial distance r_0 produces variations Δa and ΔP, which are defined by

$$\left.\begin{aligned}\Delta a = a_r \Delta r_0, \quad a_r = \frac{2}{(2-k_0)^2}, \\ \frac{\Delta P}{P} = P_r \frac{\Delta r_0}{a}, \quad P_r = \frac{3}{(2-k_0)^2},\end{aligned}\right\}$$ (9.3)

For a variation Δv_0 in the initial velocity v_0, we similarly have

$$\left.\begin{aligned}\frac{\Delta a}{a} = a_v \frac{\Delta v_0}{v_0}, \quad a_v = \frac{2k_0}{2-k_0}, \\ \frac{\Delta P}{P} = P_v \frac{\Delta v_0}{v_0}, \quad P_v = \frac{3k_0}{2-k_0},\end{aligned}\right\}$$ (9.4)

In circular orbit $k_0 = 1$, so that $a_r = a_v = 2$, $P_r = P_v = 3$, which is fully consistent with the results of Chapter 2 for circular orbits.

For elliptical orbits, these coefficients are functions of k_0. From (4.19), (4.23), (5.2), (5.15), and (5.30) we see that

$$k_0 = 2 - \frac{r_0}{a} = 1 + e \cos E_0 = \frac{1 + 2e \cos \vartheta_0 + e^2}{1 + e \cos \vartheta_0}.$$ (9.5)

Hence it follows that as the point of origin is displaced from pericenter to apocenter, the coefficient k_0 monotonically decreases (since the eccentric anomaly E_0 monotonically increases from 0 to π). At the pericenter $(E_0 = \vartheta_0 = 0)$ $k_0 = 1 + e$, at the point of intersection of the orbit with the semiminor axis $\left(E_0 = \frac{\pi}{2} \right)$ $k_0 = 1$, and at the apocenter $(E_0 = \vartheta_0 = \pi)$ $k_0 = 1 - e$.

Substituting (9.5) in (9.3) and (9.4), we find

$$a_r = \frac{2}{(1 - e \cos E_0)^2} = \frac{2 (1 + e \cos \vartheta_0)^2}{(1 - e^2)^2},$$ (9.6)

$$a_v = 2 \frac{1 + e \cos E_0}{1 - e \cos E_0} = 2 \frac{1 + 2e \cos \vartheta_0 + e^2}{1 - e^2}.$$ (9.7)

Analogous expressions are obtained for the coefficients P_r and P_v (the factor 3 is substituted for 2 in the right-hand sides).

The coefficients a_r, P_r, a_v, and P_v monotonically decrease as the point of origin is displaced from pericenter to apocenter. At the pericenter,

$$a_r = \frac{2}{(1 - e)^2}, \quad P_r = \frac{3}{(1 - e)^2}, \quad a_v = 2 \frac{1 + e}{1 - e}, \quad P_v = 3 \frac{1 + e}{1 - e},$$

at the intersection point of the orbit with the semiminor axis,

$$a_r = a_v = 2, \quad P_r = P_v = 3 ,$$

and at the apocenter,

$$a_r = \frac{2}{(1 + e)^2}, \quad P_r = \frac{3}{(1 + e)^2}, \quad a_v = 2 \frac{1 - e}{1 + e}, \quad P_v = 3 \frac{1 - e}{1 + e}.$$

In elliptical orbits, the influence of initial (or impulsive) perturbations on the semimajor axis a and the period P is thus greatest when the point of origin is at the pericenter, and least when it is at the apocenter. As the eccentricity increases (the orbit becomes progressively more "elongated"), the difference between the maximum and the minimum perturbations becomes more pronounced. With the point of origin near the pericenter and $e \to 1$, the coefficients a_r, a_v, P_r, and P_v are infinitely large, which corresponds to a transition from elliptical to parabolic orbit $(a, P = \infty)$. If an artificial Earth satellite traveling in a highly elongated elliptical orbit is subjected to comparatively small perturbations near the perigee point (these perturbations may be attributed to injection errors, to Earth's flattening, to aerodynamic drag, etc.), its orbit will be highly distorted. These disturbances may entail a change in the orbital period P, and they are therefore classified as secular, growing effects.

9.3. VARIATIONS OF ECCENTRICITY

From (5.43) it follows that the eccentricity of an orbit is a function of k_0 and , i.e., in the final analysis, of r_0, v_0, and θ_0.

To establish the dependence of e on k_0, we write the second equality in (5.43) as

$$e^2 = 1 - k_0(2 - k_0)\cos^2\theta_0 = (k_0 - 1)^2\cos^2\theta_0 + \sin^2\theta_0, \qquad (9.8)$$

whence

$$\frac{e^2}{\sin^2\theta_0} - \frac{(k_0-1)^2}{\operatorname{tg}^2\theta_0} = 1. \qquad (9.9)$$

The dependence of the eccentricity e on the coefficient k_0 is thus described by a hyperbola (Figure 9.2) whose axis points along the line $k_0 = 1$, and whose semiaxes are equal to $|\sin\theta_0|$ (along the ordinate axis e) and $|\operatorname{tg}\theta_0|$
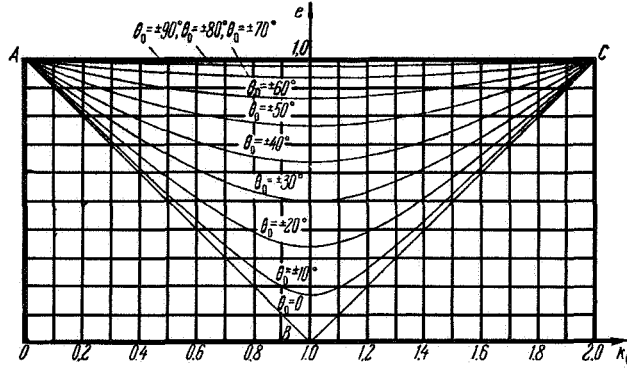
FIGURE 9.2. Eccentricity e vs. $k_0 = \dfrac{r_0 v_0^2}{\mu}$ for various θ_0.

(along the abscissa axis k_0). For elliptical orbits, only the part of the hyperbola between the following limits is meaningful:

$$0 \leqslant k_0 \leqslant 2, \quad 0 \leqslant e < 1. \qquad (9.10)$$

For $\theta_0 = 0$, the hyperbola degenerates into a polygonal line ABC defined by the equality

$$e = |k_0 - 1|, \qquad (9.11)$$

and for $\theta_0 = \pm\frac{\pi}{2}$, into the straight line $e = 1$.

For other values of the angle θ_0, we obtain a family of hyperbolas which fill the entire triangle ABC in Figure 9.2. The hyperbolas corresponding to θ_0 of opposite signs merge into a single line. All the hyperbolas meet at the points A and C of the triangle $(e = 1, k_0 = 0; 2)$, and for $k_0 = 1$ they all

pass through points with

$$e = |\sin \theta_0|, \qquad\qquad (9.12)$$

which correspond to minimum eccentricity for each given θ_0.

To find a relation between small variations in k_0 and e, we calculate the derivative $\frac{\partial e}{\partial k_0}$. From (9.8) we have

$$\frac{\partial e}{\partial k_0} = \frac{k_0 - 1}{e} \cos^2 \theta_0. \qquad\qquad (9.13)$$

From this relation and from Figure 9.2 we see that for $k_0 < 1$, $\frac{\partial e}{\partial k_0} < 0$, and for $k_0 > 1$, $\frac{\partial e}{\partial k_0} > 0$. For $k_0 = 1$, $\frac{\partial e}{\partial k_0} = 0$ for all orbits, except circular $(k_0 = 1, \theta_0 = 0)$. Circular orbit, for which in accordance with (9.11) $\frac{\partial e}{\partial k_0} = \pm 1$, constitutes an exceptional case.

Let B and B' in Figure 9.1 be the points of the orbit on the minor axis. From the geometrical definition of the eccentric anomaly E (see Figure 5.3) we see that $|E| < \frac{\pi}{2}$ over the path $B\Pi B'$ and $|E| > \frac{\pi}{2}$ over the path $B'AB$. At the end points of these trajectories, $|E| = \frac{\pi}{2}$. Hence, applying (9.5), we find that $k_0 > 1$ for $B\Pi B'$ and $k_0 < 1$ for BAB'. At the points B and B', $k_0 = 1$.

Comparison of these results shows for the path $B\Pi B'$ near the pericenter Π of elliptical orbit, $\frac{\partial e}{\partial k_0} > 0$. Along this part of the orbit, any increase in k_0 (for constant θ_0) entails an increase in the eccentricity e. As k_0 decreases, the eccentricity first decreases, passes through the minimum $e_{\min} = |\sin \theta_0|$, and then starts increasing. Along the path BAB', $\frac{\partial e}{\partial k_0} < 0$, and any decrease in k_0 entails an increase in eccentricity. As k_0 increases, e first decreases, passes through a minimum, and then increases.

At the points B and B', where the orbit meets the minor axis, $\frac{\partial e}{\partial k_0} = 0$.

At these points, the first variations of e corresponding to small variations of k_0 are zero. Higher-order variations, however, are positive, and to any change in k_0 (for constant θ_0) corresponds an increase of eccentricity.

For circular orbits, any change in k_0 entails an increase of eccentricity. Since the function $e(k_0)$ in this case is a polygonal line, the first variations of e do not vanish. Infinitesimal eccentricity variations in circular orbit therefore correspond to the singular point in Figure 9.2 $(e = 0, k = 1)$. As the eccentricity decreases, the e vs. k_0 hyperbolas of Figure 9.2 become progressively more pointed, approaching the polygonal line ABC. In low-eccentricity orbits, the linear relation

$$\Delta e \approx \frac{\partial e}{\partial k_0} \Delta k_0$$

therefore applies for very small variations Δe and Δk_0 only.

If we are dealing with larger finite variations Δe and Δk_0 in low-eccentricity orbits, the above linear relation should preferably be replaced with an

approximate formula, which is exact for circular orbits:

$$\Delta e \approx |\Delta k_0|. \tag{9.14}$$

In conclusion note that, in accordance with (9.2),

$$\frac{\partial k_0}{\partial v_0} > 0, \qquad \frac{\partial k_0}{\partial r_0} > 0. \tag{9.15}$$

Hence it follows that our remarks on the function $e(k_0)$ can be extended without modification to the functions $e(v_0)$ and $e(r_0)$.

Passing to the function $e(\theta_0)$, we write (9.8) in the form

$$e^2 = (1 - k_0)^2 + k_0(2 - k_0) \sin^2 \theta_0, \tag{9.16}$$

whence

$$\frac{e^2}{(1 - k_0)^2} - \frac{k_0(2 - k_0)}{(1 - k_0)^2} \sin^2 \theta_0 = 1. \tag{9.17}$$

For various k_0, the function $e(\sin \theta_0)$ is represented by the family of hyperbolas plotted in Figure 9.3. All these hyperbolas meet at the points A and C, where

$$\sin \theta_0 = \pm 1, \quad e = 1.$$

For $\sin \theta_0 = 0$, these hyperbolas pass through points with

$$e = |1 - k_0|. \tag{9.18}$$

These points correspond to minimum eccentricity for each given k_0.
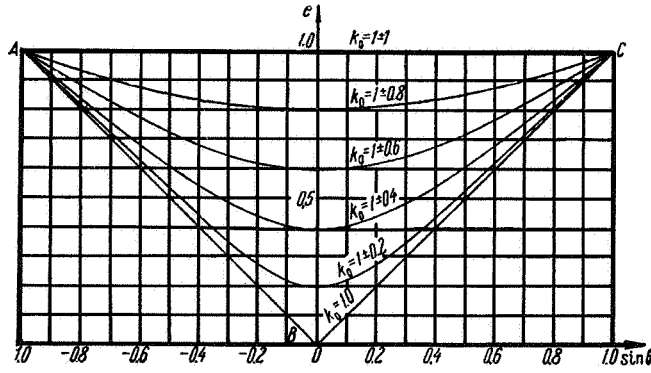
FIGURE 9.3. Eccentricity e vs. θ_0 for various $k_0 = \dfrac{r_0 v_0^2}{\mu}$.

The hyperbolas coincide for any two values of k_0 (k_0' and k_0'') which are symmetric about $k_0 = 1$ and are related by the equality

$$1 - k_0' = k_0'' - 1, \text{ i.e., } k_0' + k_0'' = 2. \tag{9.19}$$

132

For $k_0 = 1$, the hyperbolas degenerate into the polygonal line

$$e = |\sin \theta_0|,\tag{9.20}$$

and for $k_0 = 0, 2$ into the straight line $e = 1$.

Differentiating (9.16), we obtain

$$\frac{\partial e}{\partial \theta_0} = \frac{k_0 (2 - k_0)}{2e} \sin 2\theta_0.\tag{9.21}$$

For $\theta_0 < 0$, $\frac{\partial e}{\partial \theta_0} < 0$, and for $\theta_0 > 0$, $\frac{\partial e}{\partial \theta_0} > 0$. For $\theta_0 = 0$, $\frac{\partial e}{\partial \theta_0} = 0$ for all orbits, except circular. For circular orbit $(\theta_0 = 0, k_0 = 1)$, $\frac{\partial e}{\partial \theta_0} = \pm 1$.

It follows from the preceding that in elliptical orbits, along the path from pericenter to apocenter $(\theta_0 > 0)$, any increase in the angle θ_0 (for constant k_0) corresponds to an increase in the eccentricity e. As the angle θ_0 decreases in this interval, e first decreases, reaches its minimum (9.18), and then starts increasing. Along the path from apocenter to pericenter $(\theta_0 < 0)$, the situation is reversed. A decrease in θ_0 entails an increase in e, while an increase in θ_0 produces a decrease in eccentricity, which eventually gives way to an increase in e.

At the apocenter and the pericenter points, $\theta_0 = 0$. Therefore, $\frac{\partial e}{\partial \theta_0} = 0$ at these points, and the first variations of e corresponding to small variations of θ_0 are zero. Higher-order variations of eccentricity, however, are positive, so that any change in the angle θ_0 (for constant k_0) entails an increase in eccentricity.

For circular orbits, any change in θ_0 leads to an increase in e. Since $e(\theta_0)$ in this case is represented by a polygonal line, the first variations of e do not vanish. Therefore, infinitesimal variations of eccentricity in circular orbits are represented by the singular point of the family of elliptical orbits.

9.4. VARIATIONS OF ANGULAR DISTANCE FROM PERICENTER TO INITIAL POSITION

To find the variations in the angular distance ϑ_0 from the pericenter to the point of origin, we proceed from expressions (5.49):

$$\left. \begin{aligned} \sin \vartheta_0 &= \frac{k_0 \sin \theta_0 \cos \theta_0}{e}, \\ \cos \vartheta_0 &= \frac{k_0 \cos^2 \theta_0 - 1}{e}, \\ \operatorname{tg} \vartheta_0 &= \frac{k_0 \sin \theta_0 \cos \theta_0}{k_0 \cos^2 \theta_0 - 1}. \end{aligned} \right\} \tag{9.22}$$

The angle ϑ_0 is assumed to vary between the limits

$$-\pi \leqslant \vartheta_0 \leqslant \pi,\tag{9.23}$$

the points $\vartheta_0 = \pm \pi$ coinciding.

133

The function $\vartheta_0(\theta_0)$ is shown in Figure 9.4 for various k_0. From (9.8) and (9.22) we have

$$\vartheta_0 = \begin{cases} \pm \pi & \text{for} \quad k_0 = 0, \\ 2\theta_0 & \text{for} \quad k_0 = 2. \end{cases}$$

(9.24)

For the extreme values of the coefficient k_0, the functions $\vartheta_0(\theta_0)$ are linear. We see from Figure 9.4 that for all the intermediate values $0 < k_0 < 2$, the
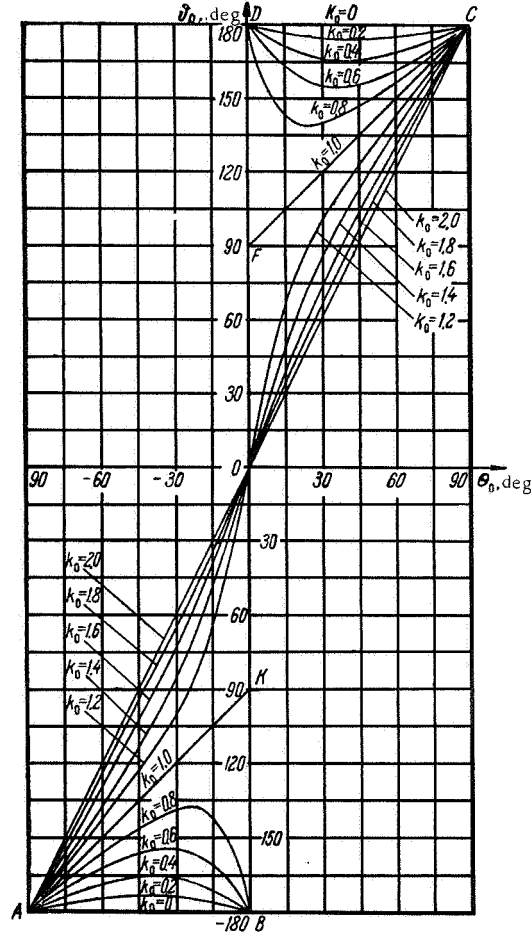
FIGURE 9.4. Angular distance ϑ_0 between the point of origin and the pericenter vs. θ_0 for various $k_0 = \dfrac{r_0 v_0^2}{\mu}$.

curves $\vartheta_0(\theta_0)$ lie inside the triangles ABO and DCO between these straight lines and the ordinate axis.

For $k_0 = 1$, the eccentricity e can be obtained from (9.20). From (9.22) we have:

for $k_0 = 1$ and $\theta_0 < 0$

$$\sin \vartheta_0 = -\cos \theta_0, \quad \cos \vartheta_0 = \sin \theta_0, \quad \vartheta_0 = \theta_0 - \frac{\pi}{2}; \qquad (9.25)$$

for $k_0 = 1$ and $\theta_0 > 0$

$$\sin \vartheta_0 = \cos \theta_0, \quad \cos \vartheta_0 = -\sin \theta_0, \quad \vartheta_0 = \theta_0 + \frac{\pi}{2}. \qquad (9.26)$$

It follows from these expressions that for $k_0 = 1$ the function is represented by the polygonal line $AKFC$ (Figure 9.4). At the point $\theta_0 = 0$ the function is discontinuous, ϑ_0 changing abruptly from $-\frac{\pi}{2}$ to $+\frac{\pi}{2}$. This discontinuity is attributable to the uncertainty in the position of the pericenter point in circular orbits (see Sec. 2.9).

We see from Figure 9.4 that the polygonal line $AKFC$ divides the entire region of allowed ϑ_0 into two parts:

the part inside the triangles AKB and DFC, where $k_0 < 1$;
the part inside the triangles AKO and OFC, where $k_0 > 1$.

The curves $\vartheta_0(\theta_0)$ in these two different regions are entirely different. For $k_0 > 1$, ϑ_0 monotonically increases with the angle θ_0, running through the entire range of allowed values (from $\vartheta_0 = -\pi$ for $\theta_0 = -\frac{\pi}{2}$ to $\vartheta_0 = +\pi$ for $\theta_0 = +\frac{\pi}{2}$). For $k_0 < 1$, the curve has a maximum $\vartheta_{max}(k_0)$ for $\theta_0 < 0$ and a minimum $\vartheta_{min}(k_0)$ for $\theta_0 > 0$ (it should be kept in mind that the curves with $\theta_0 < 0$ continuously merge into curves with $\theta_0 > 0$, since the points B and D in Figure 9.4 are in fact a single point). Here

$$|\vartheta_{max}(k_0)| = |\vartheta_{min}(k_0)| = |\vartheta_0(k_0)|_{min} > \frac{\pi}{2}, \qquad (9.27)$$

where $\vartheta_0(k_0)|_{min}$ is the minimum value $|\vartheta|_0$ for constant $k_0 < 1$.

Hence it follows that for $k_0 < 1$, ϑ_0 does not take values in the entire range (9.23). The allowed values are restricted by the conditions

$$\pi \geqslant |\vartheta_0(k_0)| \geqslant |\vartheta_0(k_0)|_{min} > \frac{\pi}{2}. \qquad (9.28)$$

To find $|\vartheta_0(k_0)|_{min}$, we differentiate the last equality in (9.22). Making use of the second equality in (9.22), we then obtain

$$\frac{\partial \vartheta_0}{\partial \theta_0} = \frac{k_0^2 - (2 - k_0) k_0 \cos 2\theta_0}{2e^2}. \qquad (9.29)$$

Setting the right-hand side equal to zero, we find

$$\cos 2\theta_{ext} = \frac{k_0}{2 - k_0}, \quad \cos \theta_{ext} = -\frac{1}{\sqrt{2 - k_0}}, \quad \sin \theta_{ext} = \pm \sqrt{\frac{1 - k_0}{2 - k_0}},$$

where θ_{ext} are the angles θ_0 corresponding to the extremal values of ϑ_0.

Substituting in the third equality in (9.22), we find

$$|\vartheta_0(k_0)|_{\min} = \text{arctg}\left(-\frac{k_0}{2\sqrt{1-k_0}}\right).$$ (9.30)

The function $\vartheta_0(k_0)$ is plotted in Figure 9.5 for various angles θ_0. In
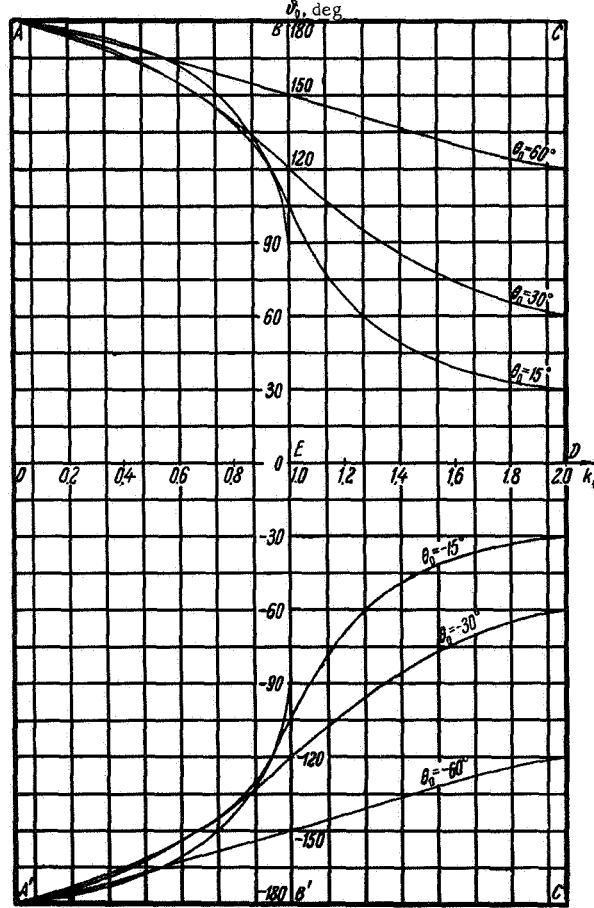
FIGURE 9.5. Angular distance ϑ_0 between the point of origin and the pericenter vs. $k_0 = \dfrac{r_0 v_0^2}{\mu}$ for various θ_0.

particular, from (9.8) and (9.22), we have:
for $\theta_0 = 0$ and $k_0 < 1$

$$e = 1 - k_0, \quad \cos\vartheta_0 = -1, \quad \sin\vartheta_0 = 0, \quad \vartheta_0 = \pm\pi;$$

for $\theta_0 = 0$ and $k_0 > 1$

$$e = k_0 - 1, \quad \cos\vartheta_0 = 1, \quad \sin\vartheta_0 = 0, \quad \vartheta_0 = 0;$$

136

for $\theta_0 = \pm \frac{\pi}{2}$

$$e = 1, \quad \cos \vartheta_0 = -1, \quad \sin \vartheta_0 = 0, \quad \vartheta_0 = \pm \pi.$$

For $\theta_0 = 0$, the function $\vartheta_0(k_0)$ is the polygonal line $ABED$ (or $A'B'ED$) in Figure 9.5. For $\theta_0 = \pm \frac{\pi}{2}$, this function is represented by the straight line AC (or $A'C'$). For all other values of θ_0, the functions are smooth curves.

Differentiating the third equality in (9.22) with respect to k_0 and applying the second equality, we find

$$\frac{\partial \vartheta_0}{\partial k_0} = -\frac{\sin 2\theta_0}{2e^2}. \tag{9.31}$$

It follows from this expression that for $\theta_0 < 0$, ϑ_0 monotonically increases with k_0, while for $\theta_0 > 0$ it monotonically decreases.

As we have previously observed, for $k_0 > 1$, the parameter ϑ_0 may take values in the entire range (9.23). Hence it follows that the $\vartheta_0(k_0)$ curves corresponding to various θ_0 fill the entire rectangle $B'BCC'$ in Figure 9.5.

For $k_0 < 1$, the allowed values of ϑ_0 are defined by condition (9.28). Hence it follows that for $k_0 < 1$, the $\vartheta_0(k_0)$ curves lie outside the region defined by the inequality

$$|\vartheta_0(k_0)| \leqslant |\vartheta_0(k_0)|_{\min},$$

where $|\vartheta_0(k_0)|_{\min}$ is obtained from (9.30). The boundary of this region is marked in Figure 9.5 by the curve $A'EA$.

9.5. VARIATION OF PERICENTER AND APOCENTER HEIGHTS

From (5.3) we can write a general expression for the apocenter and the pericenter heights, r_a and r_p:

$$\tilde{r} = a(1 \pm e), \tag{9.32}$$

where the sign + corresponds to the apocenter point $(\tilde{r} = r_a)$, and − to the pericenter point $(\tilde{r} = r_p)$.

Thus

$$\left(\frac{\tilde{r}}{a} - 1 \right)^2 = e^2.$$

Inserting a and e from (5.43) and (9.16), we find

$$\left[\frac{\tilde{r}}{r_0} (2 - k_0) - 1 \right]^2 = (1 - k_0)^2 + k_0(2 - k_0) \sin^2 \theta_0. \tag{9.33}$$

137

This equality may be written as

$$\frac{\left(\frac{\tilde{r}}{r_0} - \frac{1}{2-k_0}\right)^2}{\left(\frac{1-k_0}{2-k_0}\right)^2} - \frac{\sin^2\theta_0}{\frac{(1-k_0)^2}{k_0(2-k_0)}} = 1. \tag{9.34}$$

Hence it follows that the curve of $\frac{\tilde{r}}{r_0}$ vs. $\sin\theta_0$ (for constant k_0) is a hyperbola centered at the point

$$\frac{\tilde{r}}{r_0} = \frac{1}{2-k_0}, \quad \sin\theta_0 = 0$$

and with the semiaxes $\frac{1-k_0}{2-k_0}$ and $\frac{1-k_0}{\sqrt{k_0(2-k_0)}}$. The branch of the hyperbola corresponding to $\frac{\tilde{r}}{r_0} \gg 1$ gives $\frac{r_a}{r_0}$ vs. $\sin\theta_0$, and the second branch $(\frac{\tilde{r}}{r_0} < 1)$ gives $\frac{r_p}{r_0}$ vs. $\sin\theta_0$.
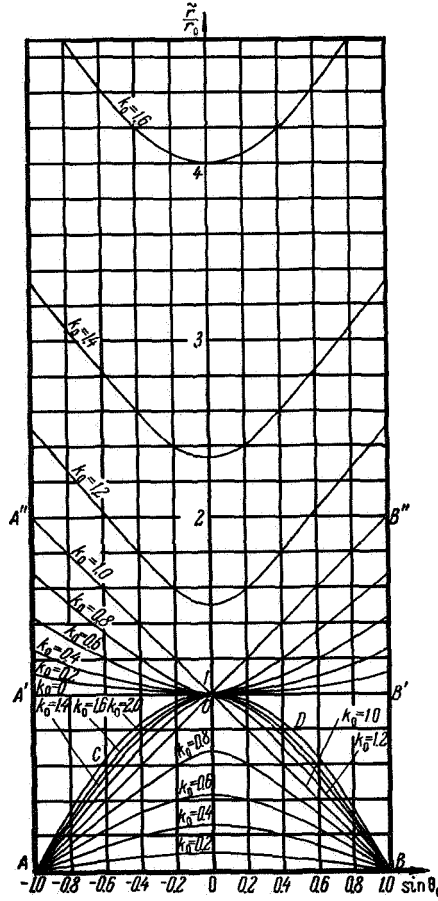
FIGURE 9.6. Pericenter and apocenter heights vs. θ_0 for various $k_0 = \dfrac{r_0 v_0^2}{\mu}$.

138

Figure 9.6 plots the function $\frac{\tilde{r}}{r_0}(\sin\theta_0)$ for various k_0. The curves above the straight line $A'B'$ (i.e., above the line $\frac{\tilde{r}}{r_0}=1$) correspond to the function $\frac{r_a}{r_0}(\sin\theta_0)$, and the curves below this straight line represent the function $\frac{r_p}{r_0}(\sin\theta_0)$. In particular, for $k_0=0$, we have from (9.33) or (9.34)

$$2\frac{\tilde{r}}{r_0}-1=\pm 1, \quad \frac{r_a}{r_0}=1, \quad \frac{r_p}{r_0}=0. \tag{9.35}$$

In this case, $\frac{r_p}{r_0}$ and $\frac{r_a}{r_0}$ vs. $\sin\theta_0$ are represented in Figure 9.6 by the horizontal lines AB and $A'B'$.

For $k_0=1$, relation (9.33) takes the form

$$\frac{\tilde{r}}{r_0}=1\pm\sin\theta_0, \tag{9.36}$$

which is plotted in Figure 9.6 as a pair of intersecting straight lines $A''OB$ and AOB''. The polygonal line AOB gives the function $\frac{r_p}{r_0}(\sin\theta_0)$, and the polygonal line $A''OB''$ plots the function $\frac{r_a}{r_0}(\sin\theta_0)$.

For $k_0=2$, relations (9.33) and (9.34) are indeterminate. To eliminate the indeterminacy, we write (9.33) in the form

$$\frac{\tilde{r}}{r_0}=\frac{1}{2-k_0}\left[1\pm(k_0-1)\sqrt{1+\frac{k_0(2-k_0)}{(k_0-1)^2}\sin^2\theta_0}\right],$$

where + corresponds to $\tilde{r}=r_a$, and − to $\tilde{r}=r_p$.

For $k_0\to 2$, the second term under the radical is small. Expanding the radicand in a binomial series, we may write

$$\frac{\tilde{r}}{r_0}=\frac{1}{2-k_0}\left\{1\pm(k_0-1)\left[1+\frac{k_0(2-k_0)}{2(k_0-1)^2}\sin^2\theta_0+(2-k_0)^2 R(k_0,\ \sin\theta_0)\right]\right\},$$

where $R(k_0,\sin\theta_0)$ is a bounded function of k_0 and $\sin\theta_0$. Hence

$$\frac{r_a}{r_0}=\frac{k_0}{2-k_0}+\frac{k_0\sin^2\theta_0}{2(k_0-1)}+(2-k_0)(k_0-1)R(k_0,\ \sin\theta_0),$$

$$\frac{r_p}{r_0}=1-\frac{k_0}{2(k_0-1)}\sin^2\theta_0-(2-k_0)(k_0-1)R(k_0,\ \sin\theta_0).$$

For $k_0=2$,

$$\frac{r_a}{r_0}=\infty, \quad \frac{r_p}{r_0}=1-\sin^2\theta_0, \tag{9.37}$$

i.e., the curve $\frac{r_p}{r_0}(\sin\theta_0)$ degenerates into a parabola ($ACODB$ in Figure 9.6).

For all other values of k_0, the curves $\frac{\tilde{r}}{r_0}(\sin\theta_0)$ are hyperbolas. The point $\theta_0=0$ is the maximum of the ratio $\frac{r_p}{r_0}$ and the minimum of $\frac{r_a}{r_0}$.

From (9.33) we see that for $\theta_0=0$,

$$\tilde{r}=r_0\frac{1\pm|1-k_0|}{2-k_0}, \tag{9.38}$$

139

where + corresponds to $\tilde{r}=r_a$, and $-$ to $\tilde{r}=r_p$. Hence

$$\frac{r_a}{r_0} = \begin{cases} 1 & \text{for } \theta_0=0, \quad k_0 \leqslant 1, \\ \dfrac{k_0}{2-k_0} > 1 & \text{for } \theta_0=0, \quad k_0 > 1; \end{cases}$$

$$\frac{r_p}{r_0} = \begin{cases} \dfrac{k_0}{2-k_0} < 1 & \text{for } \theta_0=0, \quad k_0 < 1, \\ 1 & \text{for } \theta_0=0, \quad k_0 \geqslant 1. \end{cases} \tag{9.39}$$

These relations reflect the obvious fact that for $\theta_0=0$ and $k_0<1$, the apogee point of the orbit coincides with the point of origin, and the perigee lies below this point $(r_a=r_0,\ r_p<r_0)$. For $\theta_0=0$ and $k_0>1$, it is the perigee which coincides with the point of origin, and the apogee is located at a greater altitude $(r_a>r_0,\ r_p=r_0)$.

For $\theta_0 = \pm\frac{\pi}{2}$, we have from (9.33)

$$\frac{r_a}{r_0} = \frac{2}{2-k_0}, \quad r_a=2a, \\ \frac{r_p}{r_0}=0. \tag{9.40}$$

Comparing the various results, we see that for $k_0<1$, the function $\frac{r_p}{r_0}$ (sin θ_0) is a hyperbola through the points A, B, which lies inside the triangle AOB (Figure 9.6). The function $\frac{r_a}{r_0}$ (sin θ_0), on the other hand, is a hyperbola through the point O, which lies inside the triangles $A'OA''$ and $B'OB''$.

For $k_0>1$, the curves $\frac{r_p}{r_0}$ (sin θ_0) are hyperbolas through the points A, O, B. These curves lie inside the region enclosed by the parabola $ACODB$ and the polygonal line AOB. Since all the $\frac{r_p}{r_0}$ (sin θ_0) curves pass below the parabola $ACODB$, this parabola, defined by (9.37), gives the largest possible value of the ratio $\frac{r_p}{r_0}$ for a given θ_0 and an arbitrary k_0. The hyperbolas $\frac{r_a}{r_0}$ (sin θ_0), for $k_0>1$, pass above the polygonal line $A''OB''$.

We shall show in what follows that the deceleration of a low-flying satellite in the Earth's atmosphere (and therefore its total lifetime) is mainly determined by the pericenter distance r_p. When a satellite is orbited, an attempt is therefore always made to attain a maximum perigee height. It is moreover essential that the parameter r_p should remain stable irrespective of various deviations in the initial conditions of motion (injection errors). It follows from the preceding that both these requirements are satisfied if $\theta_0=0$. The satellites should therefore be launched into their final orbit so that this equality is observed with the greatest possible precision.

We see from Figure 9.6 that the point O of circular orbit $(k_0=1,\ \theta_0=0)$ is a singular point of the family $\frac{\tilde{r}}{r_0}$ $(k_0,\ \theta_0)$. As we approach this point, the $\frac{\tilde{r}}{r_0}$ $(k_0,\ \theta_0)$ curves become progressively more pointed, moving closer to the two intersecting lines. The distance r_p becomes progressively more sensitive to errors in the injection angle θ_0 (in comparison to orbits with

140

$\theta_0 = 0$ and $k_0 \neq 0$). These factors are among the main reasons interfering with the launching of satellites into exactly circular orbits.

To determine the influence of small deviations in the initial conditions on the distances r_a and r_p, we derive expressions for the corresponding derivatives. Differentiating (9.32) with respect to some parameter q ($q = \theta_0$, v_0, r_0), we obtain

$$\frac{\partial \tilde{r}}{\partial q} = \frac{\partial a}{\partial q}(1 \pm e) \pm a \frac{\partial e}{\partial q},$$ (9.41)

where $+$ corresponds to $\tilde{r} = r_a$, and $-$ to $\tilde{r} = r_p$.

Hence, making use of (5.43), (9.2), (9.3), (9.13), and (9.21), we find

$$\left.\begin{array}{l} \dfrac{\partial \tilde{r}}{\partial \theta_0} = \pm \dfrac{r_0 k_0}{2e} \sin 2\theta_0, \\[2ex] \dfrac{\partial^2 \tilde{r}}{\partial \theta_0^2} = \pm \left[\dfrac{r_0 k_0}{e} \cos 2\theta_0 - \dfrac{r_0 k_0^2(2-k_0)}{4e^3} \sin^2 2\theta_0 \right], \\[2ex] \dfrac{\partial \tilde{r}}{\partial r_0} = \dfrac{1}{2-k_0} \left[\dfrac{2(1 \pm e)}{2-k_0} \pm \dfrac{k_0-1}{e} k_0 \cos^2 \theta_0 \right], \\[2ex] \dfrac{\partial \tilde{r}}{\partial v_0} = \dfrac{2ak_0}{v_0} \left(\dfrac{1 \pm e}{2-k_0} \pm \dfrac{k_0-1}{e} \cos^2 \theta_0 \right). \end{array}\right\}$$ (9.42)

Let us consider in greater detail the case $\theta_0 = 0$. From (9.18), we see that for $k_0 \neq 1$

$$\left.\begin{array}{l} \dfrac{\partial \tilde{r}}{\partial \theta_0} = 0, \\[2ex] \dfrac{\partial^2 \tilde{r}}{\partial \theta_0^2} = \pm \dfrac{r_0 k_0}{e} = \pm \dfrac{r_0 k_0}{|k_0-1|}, \\[2ex] \dfrac{\partial r_a}{\partial r_0} = \left\{ \begin{array}{ll} 1 & \text{for } k_0 < 1, \\[1ex] \left(\dfrac{2}{2-k_0}\right)^2 - 1 & \text{for } k_0 > 1; \end{array} \right. \\[4ex] \dfrac{\partial r_p}{\partial r_0} = \left\{ \begin{array}{ll} \left(\dfrac{2}{2-k_0}\right)^2 - 1 & \text{for } k_0 < 1, \\[1ex] 1 & \text{for } k_0 > 1; \end{array} \right. \\[4ex] \dfrac{\partial r_a}{\partial v_0} = \left\{ \begin{array}{ll} 0 & \text{for } k_0 < 1, \\[1ex] \dfrac{4ak_0}{(2-k_0)v_0} & \text{for } k_0 > 1; \end{array} \right. \\[4ex] \dfrac{\partial r_p}{\partial v_0} = \left\{ \begin{array}{ll} \dfrac{4ak_0}{(2-k_0)v_0} & \text{for } k_0 < 1, \\[1ex] 0 & \text{for } k_0 > 1. \end{array} \right. \end{array}\right\}$$ (9.43)

It follows from these expressions that the derivatives are discontinuous at the point $\theta_0 = 0$, $k_0 = 1$. Let $\left(\dfrac{\partial \tilde{r}}{\partial q}\right)_+$ be the value of these derivatives to the "right" from the discontinuity (i.e., the values obtaining as we move from the direction of large q) and $\left(\dfrac{\partial \tilde{r}}{\partial q}\right)_-$ their value to the "left" from the discontinuity (i.e., the values obtaining as we move from the direction of small q). Also note that for $\theta_0 = 0$ and $k_0 = 1$, relation (9.42) for $\dfrac{\partial \tilde{r}}{\partial \theta_0}$ becomes indeterminate. To eliminate the indeterminacy, we make use of (9.20).

Finally, for $\theta_0 = 0$ and $k_0 = 1$ we obtain

$$
\left.\begin{array}{ll}
\left(\dfrac{\partial r_a}{\partial \theta_0}\right)_+ = r_0, & \left(\dfrac{\partial r_a}{\partial \theta_0}\right)_- = -r_0, \\[2mm]
\left(\dfrac{\partial r_p}{\partial \theta_0}\right)_+ = -r_0, & \left(\dfrac{\partial r_p}{\partial \theta_0}\right)_- = r_0, \\[2mm]
\left(\dfrac{\partial r_a}{\partial r_0}\right)_+ = 3, & \left(\dfrac{\partial r_a}{\partial r_0}\right)_- = 1, \\[2mm]
\left(\dfrac{\partial r_p}{\partial r_0}\right)_+ = 1, & \left(\dfrac{\partial r_p}{\partial r_0}\right)_- = 3, \\[2mm]
\left(\dfrac{\partial r_a}{\partial v_0}\right)_+ = 4\,\dfrac{r_0}{v_0}, & \left(\dfrac{\partial r_a}{\partial v_0}\right)_- = 0, \\[2mm]
\left(\dfrac{\partial r_p}{\partial v_0}\right)_+ = 0, & \left(\dfrac{\partial r_p}{\partial v_0}\right)_- = 4\,\dfrac{r_0}{v_0}, \\[2mm]
\multicolumn{2}{c}{\dfrac{\partial^2 \tilde{r}}{\partial \theta_0^2} = \infty.}
\end{array}\right\}
\qquad (9.44)
$$

These relations can be derived from the results of Sec. 2.3. Let φ_a and φ_p stand for the angular distances of the apocenter and the pericenter from the point of origin. From Sec. 2.4 we have

$$
\left.\begin{array}{llll}
\varphi_a = \dfrac{\pi}{2}, & \varphi_p = -\dfrac{\pi}{2} & \text{for} \quad k_0 = 1, & \theta_0 > 0; \\[2mm]
\varphi_a = -\dfrac{\pi}{2}, & \varphi_p = \dfrac{\pi}{2} & \text{for} \quad k_0 = 1, & \theta_0 < 0; \\[2mm]
\varphi_a = \pi, & \varphi_p = 0 & \text{for} \quad k_0 > 1, & \theta_0 = 0; \\[2mm]
\varphi_a = 0, & \varphi_p = \pi & \text{for} \quad k_0 < 1, & \theta_0 = 0.
\end{array}\right\}
\qquad (9.45)
$$

We now determine the derivatives

$$
\frac{\partial r}{\partial \theta_0}, \quad \frac{\partial r}{\partial r_0}, \quad \text{and} \quad \frac{\partial r}{\partial v_0}
$$

at the points $\varphi = \pm\dfrac{\pi}{2}$, 0, and π. To this end, we make use of equalities (2.17) and (2.18). Note that in circular orbit $\Delta v_0 = \Delta v_{u0}$, and the variation $\Delta\theta_0$ is equivalent to a variation $\Delta v_{r0} = w\Delta\theta_0$ in the radial velocity. Thus,

$$
\left.\begin{array}{ll}
\dfrac{\partial r}{\partial \theta_0}\left(\dfrac{\pi}{2}\right) = r_0, & \dfrac{\partial r}{\partial \theta_0}\left(-\dfrac{\pi}{2}\right) = -r_0, \\[2mm]
\dfrac{\partial r}{\partial r_0}(0) = 1, & \dfrac{\partial r}{\partial r_0}(\pi) = 3, \\[2mm]
\dfrac{\partial r}{\partial v_0}(0) = 0, & \dfrac{\partial r}{\partial v_0}(\pi) = 4\,\dfrac{r_0}{v_0}.
\end{array}\right\}
\qquad (9.46)
$$

We see that at the given points of the orbit (those specified by the angle φ), the derivatives are finite. If, however, we apply equalities (9.45) and remember that the pericenter point changes discontinuously in nearly circular orbit, the derivatives become indeterminate and (9.44) obtain directly from (9.46).

From (9.38) and (9.43) it follows that for small θ_0, with $k_0 \neq 1$, the distances r_a and r_p can be determined from the approximate relation

$$
\tilde{r} \approx \tilde{r}\,(\theta_0 = 0) + \frac{1}{2}\,\frac{\partial^2 r}{\partial \theta_0^2}\,\theta_0^2 = r_0 \left(\frac{1 \pm |k_0 - 1|}{2 - k_0} \pm \frac{k_0}{|k_0 - 1|}\,\theta_0^2 \right).
\qquad (9.47)
$$

142

This relation is meaningless as $k_0 \to 1$ (orbits close to circular), since

here $\dfrac{\partial^2 r}{\partial \theta_0^2} \to \infty$. For nearly circular orbits $(k_0 \approx 1)$ this relation should therefore be replaced with the approximate equality

$$\tilde{r} = r_0 (1 \pm |\theta_0|), \tag{9.48}$$

which obtains directly from (9.44).

9.6. VARIATIONS OF ELEMENTS WHICH DEFINE THE ORIENTATION OF THE ORBITAL PLANE

Let r_0 be the vector specifying the initial position (i.e., the point of origin) D in orbit, and v_0 the initial velocity vector at that point. Any change in the orientation of the orbital plane entails a change in the projections of these vectors along the normal to the original orbital plane (for unperturbed orbital plane, these projections are of course zero). Let the projections of the disturbed vectors r_0 and v_0 on the orbit-plane normal be ζ_0 and $v_{\zeta 0}$. We assume that these quantities are small (in comparison with the distance r to the primary and the flight velocity v) and proceed to investigate the influence of these perturbations on the orientation of the orbital plane. All calculations will be made to terms of the first order of smallness. The positive directions for ζ_0 and $v_{\zeta 0}$ are so chosen that the satellite appears to move counterclockwise in unperturbed orbit, if viewed from the positive tip of the vector ζ_0 or $v_{\zeta 0}$.

In our analysis of the deviations ζ_0 of the initial position from unperturbed orbital plane, we take the initial velocity vector v_0 to be unperturbed $(v_{\zeta 0} = 0)$. Let D and D_1 be the initial and the displaced positions of the point of origin, and r_1 the vector which defines the position of the point D_1 in space (Figure 9.7). The initial and the perturbed orbital planes are defined as the planes through the vectors r_0, v_0 and r_1, v_0 respectively (the origin of the vectors r_0 and r_1 is fixed at the gravitational center O, while v_0 is a sliding vector). These planes intersect along the line MN through the center of attraction O, parallel to the vector v_0. The orbital perturbation therefore reduces to a rotation of the orbital plane through some angle ψ around the axis MN. Let u_0 be the angle ΩOD which specifies the angular distance of the point D from the node Ω, and u_1' the angle ΩOM which defines the orientation of the axis MN (the angles u_0 and u_1 are reckoned in the direction of satellite motion, and the point M is so chosen that an observer at this point sees the orbital plane as rotating counterclockwise for a positive perturbation ζ_0). Making use of Figure 9.7, we can show that

$$u_1 = u_0 - \left(\theta_0 + \frac{\pi}{2}\right). \tag{9.49}$$

To find the angle ψ, a normal DK is dropped from the point D on the axis MN. Since $\angle ODK = \theta_0$ (θ_0 being the angle between the vector v_0 and the in-plane normal to the vector r_0), we have

$$DK = r_0 \cos \theta_0,$$

where r_0 is the magnitude of the vector r_0. Hence, to terms of the first order of smallness,

$$\psi = \frac{\zeta_0}{r_0 \cos \theta_0} \, , \qquad (9.50)$$

Let us now consider the influence of the initial velocity perturbation $v_{\zeta 0}$ (for constant r_0). From Figure 9.8 we see that in this case the orbital plane is rotated around the axis OD through the center of attraction O and the point of origin D. The angle u_1 which defines the direction of the rotation axis and the angle of rotation ψ are obtained from the relations

$$u_1 = u_0, \quad \psi = \frac{v_{\zeta 0}}{v_0 \cos \theta_0} \, . \qquad (9.51)$$

The orbital plane is thus rotated through a small angle ψ around an axis through the gravitational center, which makes an angle u_1 with the orbit's line of nodes. Let us consider the influence of this rotation on the position of the ascending node Ω, on the inclination i of the orbit, and on the angular distance u to the ascending node. Figure 9.9 is a diagram showing the
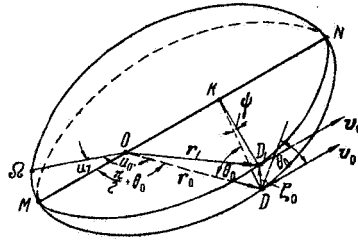
FIGURE 9.7. Rotation of the orbital plane as the initial position is displaced at right angles to this plane.
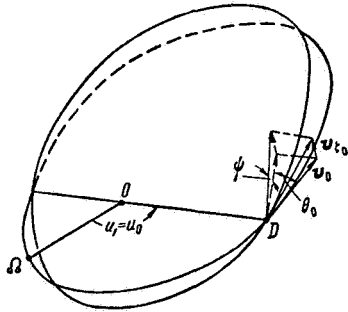
FIGURE 9.8. A change in the orientation of the orbital plane as the initial velocity vector is rotated at right angles to this plane.
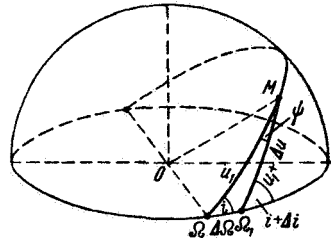
FIGURE 9.9. A change in the position of the node Ω and in the inclination i as the orbit is rotated around an in-plane axis.

intersection of the perturbed and the unperturbed orbital planes with some sphere described about the center of attraction O. The points Ω and Ω_1 are the ascending nodes of the unperturbed and the perturbed orbits, and the line OM is the axis of rotation of the orbital plane (the point M is so chosen that an observer at this point sees the orbital plane as rotating counterclockwise). Let Δi, $\Delta\Omega$, and Δu be the variations of the elements i, Ω, and u_1 on rotation. From the spherical triangle $\Omega M\Omega_1$ we have

$$\left.\begin{aligned}
&\cos(i+\Delta i) = \cos i \cos\psi - \sin i \sin\psi\cos u_1, \\
&\sin\Delta\Omega = \frac{\sin u_1}{\sin(i+\Delta i)}\sin\psi, \\
&\cos(u_1+\Delta u) = \cos u_1\cos\Delta\Omega + \sin u_1\sin\Delta\Omega\,\cos i.
\end{aligned}\right\} \tag{9.52}$$

Linearizing these relations (for small ψ, $\Delta\Omega$, Δi, and Δu), we obtain approximate equalities

$$\left.\begin{aligned}
&\Delta i = \psi\cos u_1, \\
&\Delta\Omega = \psi\frac{\sin u_1}{\sin i}, \\
&\Delta u = -\Delta\Omega\cos i = -\frac{\sin u_1}{\mathrm{tg}\,i}\psi.
\end{aligned}\right\} \tag{9.53}$$

Expressions (9.53) are clearly meaningless for $i\to 0$. Note that in the absence of in-plane perturbations, the variation Δu characterizes the displacement of the node Ω relative to all the points of the orbit. The angular distance of any point of the orbit from the node therefore changes by Δu; this of course applies also to the angular distance ω of the pericenter. Thus,

$$\Delta\omega = \Delta u = -\Delta\Omega\cos i = -\frac{\sin u_1}{\mathrm{tg}\,i}\psi. \tag{9.54}$$

Substituting (9.49) and (9.50) in (9.53) and (9.54), we find for the variations of the elements i, Ω and ω when the point of origin deviates from the orbital plane

$$\begin{aligned}
&\Delta i = \frac{\sin(u_0-\theta_0)}{r_0\cos\theta_0}\zeta_0, \\
&\Delta\Omega = -\frac{\cos(u_0-\theta_0)}{r_0\cos\theta_0\sin i}\zeta_0, \\
&\Delta\omega = \frac{\cos(u_0-\theta_0)}{r_0\cos\theta_0\,\mathrm{tg}\,i}\zeta_0.
\end{aligned}$$

Hence

$$\left.\begin{aligned}
&\frac{\partial i}{\partial\zeta_0} = \frac{\sin(u_0-\theta_0)}{r_0\cos\theta_0}, \\
&\frac{\partial\Omega}{\partial\zeta_0} = -\frac{\cos(u_0-\theta_0)}{r_0\cos\theta_0\sin i}, \\
&\frac{\partial\omega}{\partial\zeta_0} = \frac{\cos(u_0-\theta_0)}{r_0\cos\theta_0\,\mathrm{tg}\,i}.
\end{aligned}\right\} \tag{9.55}$$

Applying (9.51), (9.53), and (9.54), we similarly write

$$\left.\begin{aligned}
&\frac{\partial i}{\partial v_{\zeta 0}} = \frac{\cos u_0}{v_0\cos\theta_0}, \\
&\frac{\partial\Omega}{\partial v_{\zeta 0}} = \frac{\sin u_0}{v_0\cos\theta_0\sin i}, \\
&\frac{\partial\omega}{\partial v_{\zeta 0}} = -\frac{\sin u_0}{v_0\cos\theta_0\,\mathrm{tg}\,i}.
\end{aligned}\right\} \tag{9.56}$$

Chapter 10

RELATIONSHIP BETWEEN VARIATIONS IN
CURRENT PARAMETERS AND IN INITIAL
CONDITIONS OF MOTION

10.1. BASIC RELATIONS

Any point D of the orbit can be defined by a single parameter s which varies continuously in the course of motion, such as the flight time t, the angular distance u from a fixed point, the eccentric anomaly E, the distance r from the primary, the flight velocity v, etc. The main requirement governing our choice of the orbit parameter s is that there should be a one-to-one correspondence between the position of D and the value of s. This correspondence must hold true either along the entire orbit (for $s = t, u, E, \ldots$) or over a certain partial trajectory (for $s = r, v, \ldots$).

The position of the center of mass of a body at a parametrically defined point of the orbit is completely specified by six independent elements p_i ($i = 1, 2, \ldots, 6$), which are sufficient for calculating the future course of motion. For $s = t$, the coordinates and the velocity components of the mass center may be adopted as the p_i. If s is one of the coordinates, p_i comprise the other two coordinates, time, and velocity components. We call these p_i the c u r r e n t   p a r a m e t e r s   o f   m o t i o n . Different sets of current parameters are generally interchanged without difficulty. Furthermore, if the initial conditions of motion (or the orbital elements) q_j ($j = 1, 2, \ldots, 6$) are known, then the parameters p_i for a given s can be easily calculated from the relations in Chapters 4 — 7. A more difficult, though no less important, problem is to establish a relationship between the variations Δq_j and Δp_i of these parameters.

If the variations Δp_i and Δq_j are small, then to terms of higher order of smallness,

$$
\left.
\begin{aligned}
\Delta_s p_1 &= \left(\tfrac{\partial p_1}{\partial q_1}\right)_s \Delta q_1 + \left(\tfrac{\partial p_1}{\partial q_2}\right)_s \Delta q_2 + \cdots + \left(\tfrac{\partial p_1}{\partial q_6}\right)_s \Delta q_6, \\
\Delta_s p_2 &= \left(\tfrac{\partial p_2}{\partial q_1}\right)_s \Delta q_1 + \left(\tfrac{\partial p_2}{\partial q_2}\right)_s \Delta q_2 + \cdots + \left(\tfrac{\partial p_2}{\partial q_6}\right)_s \Delta q_6, \\
&\cdots\cdots\cdots\cdots\cdots\cdots\cdots\cdots\cdots\cdots\cdots\cdots \\
\Delta_s p_6 &= \left(\tfrac{\partial p_6}{\partial q_1}\right)_s \Delta q_1 + \left(\tfrac{\partial p_6}{\partial q_2}\right)_s \Delta q_2 + \cdots + \left(\tfrac{\partial p_6}{\partial q_6}\right)_s \Delta q_6.
\end{aligned}
\right\}
\qquad (10.1)
$$

Here the subscript s in the variations, $\Delta_s p_i$, and in the partial derivatives, $\left(\frac{\partial p_i}{\partial q_j}\right)_s$, indicates that variation and differentiation is carried out for $s = \text{const}$.

146

Relations (10.1) can be written in matrix form:

$$(\Delta p)_s = \left\| \frac{\partial p_1,\ p_2,\ \ldots,\ p_6}{\partial q_1,\ q_2,\ \ldots,\ q_6} \right\|_s (\Delta q), \qquad (10.2)$$

where

$$(\Delta p)_s = \left\| \begin{matrix} \Delta_s p_1 \\ \Delta_s p_2 \\ \cdot \\ \cdot \\ \cdot \\ \Delta_s p_6 \end{matrix} \right\|, \qquad (\Delta q) = \left\| \begin{matrix} \Delta q_1 \\ \Delta q_2 \\ \cdot \\ \cdot \\ \cdot \\ \Delta q_6 \end{matrix} \right\|,$$

$$\left\| \frac{\partial p_1,\ p_2,\ \ldots,\ p_6}{\partial q_1,\ q_2,\ \ldots,\ q_6} \right\|_s = \left\| \begin{matrix} \left(\frac{\partial p_1}{\partial q_1}\right)_s & \left(\frac{\partial p_1}{\partial q_2}\right)_s & \cdots & \left(\frac{\partial p_1}{\partial q_6}\right)_s \\ \left(\frac{\partial p_2}{\partial q_1}\right)_s & \left(\frac{\partial p_2}{\partial q_2}\right)_s & \cdots & \left(\frac{\partial p_2}{\partial q_6}\right)_s \\ \cdot & \cdot & \cdots & \cdot \\ \left(\frac{\partial p_6}{\partial q_1}\right)_s & \left(\frac{\partial p_6}{\partial q_2}\right)_s & \cdots & \left(\frac{\partial p_6}{\partial q_6}\right)_s \end{matrix} \right\|.$$

The problem thus reduces to the determination of the partial derivatives $\left(\frac{\partial p_i}{\partial q_j}\right)_s$ $(i, j = 1, 2, \ldots, 6)$.

Let the matrix $\left\| \frac{\partial p_1,\ p_2,\ \ldots,\ p_6}{\partial q_1,\ q_2,\ \ldots,\ q_6} \right\|_s$ be known. This matrix relates the variations in the initial conditions $q_1, q_2, \ldots, q_6$ with the variations in the parameters of motion $p_1, p_2, \ldots, p_6$ for $s = $ const, and it is now required to write an analogous matrix for some other set of initial conditions $q_1', q_2', \ldots, q_6'$ and parameters of motion $p_1'\ p_2', \ldots, p_6'$. The variations of the original parameters are related with the variations of the modified parameters by equalities of the form

$$(\Delta p') = \left\| \frac{\partial p_1',\ p_2',\ \ldots,\ p_6'}{\partial p_1,\ p_2,\ \ldots,\ p_6} \right\| (\Delta p), \left. \begin{matrix} \\ \\ \end{matrix} \right\}$$

$$(\Delta q) = \left\| \frac{\partial q_1,\ q_2,\ \ldots,\ q_6}{\partial q_1',\ q_2',\ \ldots,\ q_6'} \right\| (\Delta q'). \quad (10.3)$$

The matrices $\left\| \frac{\partial p_1',\ p_2',\ \ldots,\ p_6'}{\partial p_1,\ p_2,\ \ldots,\ p_6} \right\|$ and $\left\| \frac{\partial q_1,\ q_2,\ \ldots,\ q_6}{\partial q_1',\ q_2',\ \ldots,\ q_6'} \right\|$ in the right-hand sides of these

relations can be determined without much difficulty by a transformation of coordinates at the point of origin D_0 and the current point D. Multiplying

(10.2) by $\left\| \frac{\partial p_1',\ p_2',\ \ldots,\ p_6'}{\partial p_1,\ p_2,\ \ldots,\ p_6} \right\|$ and making use of (10.3), we find

$$(\Delta p')_s = \left\| \frac{\partial p_1',\ p_2',\ \ldots,\ p_6'}{\partial q_1',\ q_2',\ \ldots,\ q_6'} \right\|_s (\Delta q'), \qquad (10.4)$$

where

$$\left\| \frac{\partial p_1',\ p_2',\ \ldots,\ p_6'}{\partial q_1',\ q_2',\ \ldots,\ q_6'} \right\|_s = \left\| \frac{\partial p_1',\ p_2',\ \ldots,\ p_6'}{\partial p_1,\ p_2,\ \ldots,\ p_6} \right\| \left\| \frac{\partial p_1,\ p_2,\ \ldots,\ p_6}{\partial q_1,\ q_2,\ \ldots,\ q_6} \right\|_s \left\| \frac{\partial q_1,\ q_2,\ \ldots,\ q_6}{\partial q_1',\ q_2',\ \ldots,\ q_6'} \right\|. \qquad (10.5)$$

147

Let us now consider how the partial derivatives $\left(\frac{\partial p_i}{\partial q_j}\right)_s$ are transformed when we pass from the parameter s to some other parameter σ in defining the position of the current point D in orbit. Take a path D_0D along the unperturbed orbit and a slightly deviating perturbed path $D_0D'D''$ (Figure 10.1).
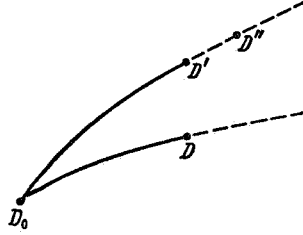
FIGURE 10.1. Positions of a perturbed point
for different choices of the orbit parameter.

Let s_1, σ_1, p_{i1} be the values of the parameters s, σ, p_i at the current point D of unperturbed orbit. For a constant s, the point D is mapped into some point D' of the perturbed orbit, and for a constant σ, it is mapped into some point D''. The relevant parameters take the following values at these perturbed points:

$$s(D') = s_1, \qquad \sigma(D') = \sigma_1 + \Delta_s\sigma, \quad p_i(D') = p_{i1} + \Delta_s p_i,$$
$$s(D'') = s_1 + \Delta_\sigma s, \quad \sigma(D'') = \sigma_1, \qquad p_i(D'') = p_{i1} + \Delta_\sigma p_i,$$

where $\Delta_s p_i$ and $\Delta_s\sigma$ are the variations of p_i and σ for $s = $ const, and $\Delta_\sigma p_i$ and $\Delta_\sigma s$ are the variations of p_i and s for $\sigma = $ const. Hence, to terms of higher order of smallness,

$$p_i(D') = p_i(D'') + \frac{dp_i}{d\sigma}\,\Delta_s\sigma,$$

where the derivative $\frac{dp_i}{d\sigma}$ is taken along the unperturbed trajectory.

Inserting $p_i(D')$ and $p_i(D'')$ from the previous expressions, we find

$$\Delta_s p_i = \Delta_\sigma p_i + \frac{dp_i}{d\sigma}\,\Delta_s\sigma.$$

Dividing the right- and the left-hand sides of this equality by the increment Δq_j in any of the initial conditions and taking the limit, we find

$$\left(\frac{\partial p_i}{\partial q_j}\right)_\sigma = \left(\frac{\partial p_i}{\partial q_j}\right)_s - \left(\frac{\partial \sigma}{\partial q_j}\right)_s \frac{dp_i}{d\sigma}, \tag{10.6}$$

where $\left(\frac{\partial \sigma}{\partial q_j}\right)_s$ is the partial derivative $\frac{\partial \sigma}{\partial q_j}$ for $s = $ const.

From (10.5) and (10.6) it follows that if the matrix $\left\|\frac{\partial p_1,\ p_2,\ \ldots,\ p_6}{\partial q_1,\ q_2,\ \ldots,\ q_6}\right\|_s$ is known for some set of the parameters p_i, q_j, s (i, $j = 1, 2, \ldots, 6$), the corresponding matrix can always be found for any other set of parameters.

148

Some current parameters of motion in unperturbed orbit may meet the condition

$$p_i = \text{const.} \tag{10.6a}$$

This applies, in particular, for the following parameters:

(a) in any orbit, for the displacement ζ at right angles to the orbital plane and for the normal projection v_ζ of the velocity vector;

(b) in unperturbed circular orbit, for the radius r, the longitudinal velocity component v_u, and the radial velocity component v_r (this, of course, in addition to ζ and v_ζ).

Then in unperturbed orbit $\frac{dp_i}{d\sigma} = 0$, and relation (10.6) takes the form

$$\left(\frac{\partial p_i}{\partial q_j}\right)_\sigma = \left(\frac{\partial p_i}{\partial q_j}\right)_s.$$

In other words, for current parameters of motion which satisfy condition (10.6 a), the derivatives $\frac{\partial p_i}{\partial q_j}$ are independent of the choice of the parameter s. We shall henceforth omit the parametric subscript when dealing with derivatives of this kind.

10.2. VARIATIONS IN THE PARAMETERS OF MOTION FOR CONSTANT ANGULAR DISTANCE FROM THE POINT OF ORIGIN

We shall operate in cylindrical coordinates $Oru\zeta$ (the axis ζ perpendicular to the plane of the drawing, pointing toward the reader; see Figure 10.2). The point of origin is some point D_0 of the orbit corresponding to the starting instant $t = t_0$; the initial conditions of motion are the coordinates r_0, u_0, ζ_0
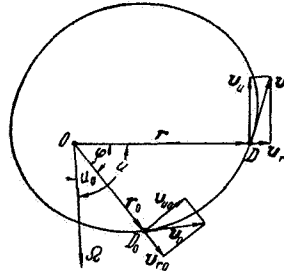
FIGURE 10.2. Initial conditions and current parameters of motion in cylindrical coordinates.

and the corresponding velocity components $v_{r0} = \dot{r}_0$, $v_{u0} = r_0 \dot{u}_0$, $v_{\zeta 0} = \dot{\zeta}_0$ at the point D_0 (in unperturbed orbit $\zeta_0 = v_{\zeta 0} = 0$). The current point D in perturbed and unperturbed orbits is defined by assuming constant angular distance from the point of origin,

$$\varphi = u - u_0, \tag{10.7}$$

149

where u_0 is the angular coordinate of the unperturbed point of origin (it need not be the same for the perturbed orbit, since the point D_0 is determined from the condition $t_0 = \text{const}$).

The current parameters of motion are the time of arrival t at the particular point, the coordinates r, ζ and the velocity components v_r, v_u, v_ζ at that point.

In calculating the matrix elements of

$$\left\| \frac{\partial r,\ t,\ \zeta,\ v_r,\ v_u,\ v_\zeta}{\partial r_0,\ u_0,\ \zeta_0,\ v_{r0},\ v_{u0},\ v_{\zeta0}} \right\|_\varphi,$$

we make use of the fact that small perturbations in the orbital plane are independent of perturbations at right angles to that plane. Thus,

$$\frac{\partial p_i}{\partial q_j} = 0 \quad \text{for} \quad \begin{cases} p_i = r,\ t,\ v_r,\ v_u; & q_j = \zeta_0,\ v_{\zeta0}; \\ p_i = \zeta,\ v_\zeta; & q_j = r_0,\ u_0,\ v_{r0},\ v_{u0}. \end{cases} \tag{10.8}$$

Moreover, the partial derivatives with respect to u_0 are easily found by rotating the orbit through an angle Δu_0 in its plane around the gravitational center O; the derivatives with respect to ζ_0 and $v_{\zeta0}$ are obtained by rotating the orbital plane (see Sec. 9.6). This being so, we first calculate the derivatives $\left(\frac{\partial p_i}{\partial q_j}\right)_\varphi$ for $p_i = r,\ t,\ v_r,\ v_u$ and $q_j = r_0,\ v_{r0},\ v_{u0}$.

10.3. PARTIAL DERIVATIVES OF THE CURRENT RADIUS FOR $\varphi = \text{const}$

We shall make use of relation (4.19) and the equality

$$\varphi = \vartheta - \vartheta_0, \tag{10.9}$$

where ϑ_0 and ϑ are the true anomalies at the point of origin and at the current point. We obtain

$$r = \frac{p}{1 + e \cos(\vartheta_0 + \varphi)} = \frac{p}{1 + e \cos\vartheta_0 \cos\varphi - e \sin\vartheta_0 \sin\varphi}. \tag{10.10}$$

On the other hand, from (4.18), (4.21), and (5.45), we have

$$\begin{aligned} p &= r_0 k_0 \cos^2\theta_0, \quad e \sin\vartheta_0 = k_0 \sin\theta_0 \cos\theta_0, \\ e \cos\vartheta_0 &= k_0 \cos^2\theta_0 - 1, \quad k_0 = \frac{r_0 v_0^2}{\mu}, \end{aligned} \tag{10.11}$$

where v_0 and θ_0 are the magnitude of the initial velocity vector and its inclination to the local horizon at the point of origin; thus,

$$v_0^2 = v_{r0}^2 + v_{u0}^2, \quad u_0 \cos\theta_0 = v_{u0}, \quad v_0 \sin\theta_0 = v_{r0}. \tag{10.12}$$

Substituting (10.11) in (10.10), we find

$$r = \frac{r_0 k_0 \cos^2\theta_0}{1 + (k_0 \cos^2\theta_0 - 1)\cos\varphi - k_0 \sin\theta_0 \cos\theta_0 \sin\varphi} = \frac{r_0 k_0 \cos^2\theta_0}{1 - \cos\varphi + k_0 \cos\theta_0 \cos(\varphi + \theta_0)},$$

whence

$$k_0 = \frac{1 - \cos\varphi}{\dfrac{r_0}{r}\cos\theta_0 - \cos\theta_0\cos(\varphi+\theta_0)}. \tag{10.13}$$

From (10.11) and (10.12), k_0, v_0, θ_0 are expressed in terms of v_{r0}, v_{u0}, r_0, and μ, so that (10.13) takes the form

$$(1 - \cos\varphi)\,\mu + r_0(v_{u0}^2\cos\varphi - v_{u0}v_{r0}\sin\varphi) - \frac{r_0^2}{r}v_{u0}^2 = 0. \tag{10.14}$$

Differentiating this equality for $\varphi = \text{const}$, we have

$$\left(v_{u0}^2\cos\varphi - v_{u0}v_{r0}\sin\varphi - \frac{2r_0}{r}v_{u0}^2\right)dr_0 +$$
$$+ \left[2\left(r_0\cos\varphi - \frac{r_0^2}{r}\right)v_{u0} - r_0 v_{r0}\sin\varphi\right]dv_{u0} -$$
$$- r_0 v_{u0}\sin\varphi\,dv_{r0} = -\frac{r_0^2}{r^2}v_{u0}^2\,dr.$$

Hence the expressions for the partial derivatives

$$\left.\left(\frac{\partial r}{\partial r_0}\right)\right._\varphi = \frac{r^2}{r_0^2}\left(\frac{v_{r0}}{v_{u0}}\sin\varphi - \cos\varphi\right) + 2\frac{r}{r_0},$$

$$\left.\left(\frac{\partial r}{\partial v_{r0}}\right)\right._\varphi = \frac{r^2}{r_0 v_{u0}}\sin\varphi, \tag{10.15}$$

$$\left.\left(\frac{\partial r}{\partial v_{u0}}\right)\right._\varphi = \frac{r^2}{r_0 v_{u0}}\left(\frac{v_{r0}}{v_{u0}}\sin\varphi - 2\cos\varphi\right) + 2\frac{r}{v_{u0}}.$$

Making use of (5.44) and (10.9), we write

$$\frac{v_{r0}}{v_{u0}}\sin\varphi - \cos\varphi = \frac{e\sin\vartheta_0\sin\varphi - (1 + e\cos\vartheta_0)\cos\varphi}{v_{u0}}\sqrt{\frac{\mu}{p}} = -\sqrt{\frac{\mu}{p}}\,\frac{e\cos\vartheta + \cos\varphi}{v_{u0}}.$$

On the other hand, from (4.19) we have

$$e\cos\vartheta = \frac{p}{r} - 1. \tag{10.16}$$

Hence

$$\frac{v_{r0}}{v_{u0}}\sin\varphi - \cos\varphi = -\frac{1}{v_{u0}}\sqrt{\frac{\mu}{p}}\left(\frac{p}{r} - 1 + \cos\varphi\right). \tag{10.17}$$

Furthermore, applying (10.11) and (10.12), we write

$$p = \frac{r_0^2 v_{u0}^2}{\mu}, \quad \sqrt{p\mu} = r_0 v_{u0}, \quad \sqrt{\frac{\mu}{p}} = \frac{\mu}{r_0 v_{u0}}. \tag{10.18}$$

Substituting (5.11), (10.17), and (10.18) in (10.15), we find

$$\left.\left(\frac{\partial r}{\partial r_0}\right)\right._\varphi = \frac{r}{r_0}\left[1 + \frac{r}{p}(1 - \cos\varphi)\right],$$

$$\left.\left(\frac{\partial r}{\partial v_{r0}}\right)\right._\varphi = \frac{r^2}{\sqrt{\mu p}}\sin\varphi = \frac{r}{v_u}\sin\varphi, \tag{10.19}$$

$$\left.\left(\frac{\partial r}{\partial v_{u0}}\right)\right._\varphi = \frac{r}{v_{u0}}\left[1 + \frac{r}{p} - \left(\frac{r}{p} + \frac{r}{r_0}\right)\cos\varphi\right].$$

151

10.4. PARTIAL DERIVATIVES OF THE VELOCITY
COMPONENTS v_r AND v_u FOR $\varphi = \text{const}$

To find the partial derivatives of the longitudinal velocity component v_u, we make use of (5.11) and (10.18), which give

$$v_u = \frac{r_0 v_{u0}}{r}.\tag{10.20}$$

Differentiating, we obtain

$$\left(\frac{\partial v_u}{\partial r_0}\right)_\varphi = \frac{v_{u0}}{r} - \frac{r_0 v_{u0}}{r^2}\left(\frac{\partial r}{\partial r_0}\right)_\varphi,$$

$$\left(\frac{\partial v_u}{\partial v_{r0}}\right)_\varphi = -\frac{r_0 v_{u0}}{r^2}\left(\frac{\partial r}{\partial v_{r0}}\right)_\varphi,$$

$$\left(\frac{\partial v_u}{\partial v_{u0}}\right)_\varphi = \frac{r_0}{r} - \frac{r_0 v_{u0}}{r^2}\left(\frac{\partial r}{\partial v_{u0}}\right)_\varphi$$

Inserting from (10.15) in the right-hand sides of these equalities, we find

$$\left.\begin{aligned}
\left(\frac{\partial v_u}{\partial r_0}\right)_\varphi &= \frac{v_{u0}}{r_0}\left(\cos\varphi - \frac{v_{r0}}{v_{u0}}\sin\varphi\right) - \frac{v_{u0}}{r}, \\
\left(\frac{\partial v_u}{\partial v_{r0}}\right)_\varphi &= -\sin\varphi, \\
\left(\frac{\partial v_u}{\partial v_{u0}}\right)_\varphi &= 2\cos\varphi - \frac{v_{r0}}{v_{u0}}\sin\varphi - \frac{r_0}{r}.
\end{aligned}\right\}\tag{10.21}$$

Hence, applying (5.11), (10.17), and (10.18), we have

$$\left.\begin{aligned}
\left(\frac{\partial v_u}{\partial r_0}\right)_\varphi &= -\sqrt{\frac{\mu}{p}}\,\frac{1-\cos\varphi}{r_0} = \frac{v_{u0}}{p}(1-\cos\varphi), \\
\left(\frac{\partial v_u}{\partial v_{r0}}\right)_\varphi &= -\sin\varphi, \\
\left(\frac{\partial v_u}{\partial v_{u0}}\right)_\varphi &= -\frac{r_0}{p} + \left(1 + \frac{r_0}{p}\right)\cos\varphi.
\end{aligned}\right\}\tag{10.22}$$

To find the radial velocity component v_r, we make use of relations (5.13) and (10.9), which give

$$v_r = \sqrt{\frac{\mu}{p}}\,e\sin(\varphi+\vartheta_0) = \sqrt{\frac{\mu}{p}}\,e\cos\vartheta_0\sin\varphi + v_{r0}\cos\varphi.$$

On the other hand, from (5.11) and (10.18), we have

$$\sqrt{\frac{\mu}{p}}\,e\cos\vartheta = v_u - \sqrt{\frac{\mu}{p}} = v_u - \frac{\mu}{rv_u}.\tag{10.23}$$

Thus

$$v_r = v_{r0}\cos\varphi + \left(v_{u0} - \frac{\mu}{r_0 v_{u0}}\right)\sin\varphi.\tag{10.24}$$

Differentiating for $\varphi = \text{const}$ and applying (10.18), we have

$$
\left.\begin{aligned}
\left(\frac{\partial v_r}{\partial r_0}\right)_\varphi &= \frac{\mu}{r_0^2 v_{a0}}\sin\varphi = \frac{v_{u0}}{p}\sin\varphi = \sqrt{\frac{\mu}{p}}\,\frac{\sin\varphi}{r_0}, \\
\left(\frac{\partial v_r}{\partial v_{r0}}\right)_\varphi &= \cos\varphi, \\
\left(\frac{\partial v_r}{\partial v_{u0}}\right)_\varphi &= \left(1 + \frac{\mu}{r_0 v_{u0}^2}\right)\sin\varphi = \left(1 + \frac{r_0}{p}\right)\sin\varphi.
\end{aligned}\right\}
\tag{10.25}
$$

10.5. PARTIAL DERIVATIVES OF
FLIGHT TIME t FOR $\varphi = \text{const}$

To determine the flight time t from the point of origin D_0 to the current point D, we make use of (6.28) and (10.18), which give

$$
t = \frac{1}{\sqrt{\mu p}}\int_0^\varphi r^2\,du = \frac{1}{r_0 v_{u0}}\int_0^\varphi r^2\,du.
\tag{10.26}
$$

Here the current angle u is reckoned from the point D_0 ($u_0 = 0$).
Differentiating (10.26) for $\varphi = \text{const}$, we find

$$
\left.\begin{aligned}
\left(\frac{\partial t}{\partial r_0}\right)_\varphi &= -\frac{t}{r_0} + \frac{2}{\sqrt{\mu p}}\int_0^\varphi r\left(\frac{\partial r}{\partial r_0}\right)_\varphi du, \\
\left(\frac{\partial t}{\partial v_{r0}}\right)_\varphi &= \frac{2}{\sqrt{\mu p}}\int_0^\varphi r\left(\frac{\partial r}{\partial v_{r0}}\right)_\varphi du, \\
\left(\frac{\partial t}{\partial v_{u0}}\right)_\varphi &= -\frac{t}{v_{u0}} + \frac{2}{\sqrt{\mu p}}\int_0^\varphi r\left(\frac{\partial r}{\partial v_{u0}}\right)_\varphi du.
\end{aligned}\right\}
\tag{10.27}
$$

Inserting from (10.15) in the right-hand sides of these relations and applying (10.18) and (10.26), we find

$$
\left.\begin{aligned}
\left(\frac{\partial t}{\partial r_0}\right)_\varphi &= \frac{1}{r_0}\left[3t + \frac{2}{\mu p}\left(v_{r0}\int_0^\varphi r^3\sin u\,du - v_{u0}\int_0^\varphi r^3\cos u\,du\right)\right], \\
\left(\frac{\partial t}{\partial v_{r0}}\right)_\varphi &= \frac{2}{\mu p}\int_0^\varphi r^3\sin u\,du, \\
\left(\frac{\partial t}{\partial v_{u0}}\right)_\varphi &= \frac{1}{v_{u0}}\left[3t + \frac{2}{\mu p}\left(v_{r0}\int_0^\varphi r^3\sin u\,du - 2v_{u0}\int_0^\varphi r^3\cos u\,du\right)\right].
\end{aligned}\right\}
\tag{10.28}
$$

The problem thus reduces to the evaluation of the integrals

$$
J_1 = \int_0^\varphi r^3\sin u\,du, \quad J_2 = \int_0^\varphi r^3\cos u\,du.
\tag{10.29}
$$

Applying (10.9), we write

$$J_1 = \int_{\vartheta_0}^{\vartheta} r^3 \sin(\xi - \vartheta_0) \, d\xi = \cos \vartheta_0 \int_{\vartheta_0}^{\vartheta} r^3 \sin \xi \, d\xi - \sin \vartheta_0 \int_{\vartheta_0}^{\vartheta} r^3 \cos \xi \, d\xi, \qquad (10.30)$$

where ξ is the current true anomaly, defined by

$$\xi = \vartheta_0 + u. \qquad (10.31)$$

Now, making use of (4.19), we write

$$\int_{\vartheta_0}^{\vartheta} r^3 \sin \xi \, d\xi = p^3 \int_{\vartheta_0}^{\vartheta} \frac{\sin \xi}{(1 + e \cos \xi)^3} \, d\xi.$$

Seeing that

$$\sin \xi = -\frac{1}{e} \frac{d}{d\xi} (1 + e \cos \xi),$$

we have

$$\int_{\vartheta_0}^{\vartheta} r^3 \sin \xi \, d\xi = \frac{p^3}{2e} \frac{1}{(1 + e \cos \xi)^2} \Big|_{\vartheta_0}^{\vartheta} = \frac{p}{2e} (r^2 - r_0^2). \qquad (10.32)$$

To evaluate the second integral in the right-hand side of (10.30), we write it as a sum of two integrals

$$\int_{\vartheta_0}^{\vartheta} r^3 \cos \xi \, d\xi = \frac{p^3}{e} \int_{\vartheta_0}^{\vartheta} \frac{e \cos \xi}{(1 + e \cos \xi)^3} \, d\xi = \frac{p^3}{e} \left(\int_{\vartheta_0}^{\vartheta} \frac{d\xi}{(1 + e \cos \xi)^2} - \int_{\vartheta_0}^{\vartheta} \frac{d\xi}{(1 + e \cos \xi)^3} \right). \qquad (10.33)$$

Now, taking the well-known recursive formula /25/

$$\int \frac{dx}{(a + b \cos x)^n} = \frac{1}{(n-1)(a^2 - b^2)} \left[-\frac{b \sin x}{(a + b \cos x)^{r-1}} + \right.$$
$$\left. + (2n - 3) a \int \frac{dx}{(a + b \cos x)^{n-1}} - (n - 2) \int \frac{dx}{(a + b \cos x)^{n-2}} \right]$$

and putting

$$x = \xi, \quad a = 1, \quad b = e, \quad n = 2, 3,$$

we find

$$\left. \begin{array}{l} \displaystyle \int \frac{d\xi}{(1 + e \cos \xi)^2} = \frac{1}{1 - e^2} \left(-\frac{e \sin \xi}{1 + e \cos \xi} + \int \frac{d\xi}{1 + e \cos \xi} \right), \\[3mm] \displaystyle \int \frac{d\xi}{(1 + e \cos \xi)^3} = \frac{1}{2(1 - e^2)} \left[-\frac{e \sin \xi}{(1 + e \cos \xi)^2} + 3 \int \frac{d\xi}{(1 + e \cos \xi)^2} - \int \frac{d\xi}{1 + e \cos \xi} \right]. \end{array} \right\} (10.34)$$

Hence

$$\int \frac{d\xi}{(1 + e \cos \xi)^2} - \int \frac{d\xi}{(1 + e \cos \xi)^3} = \frac{1}{2(1 - e^2)} \left\{ \frac{e \sin \xi}{(1 + e \cos \xi)^2} - \frac{2e \sin \xi}{1 + e \cos \xi} + \right.$$
$$\left. + 3 \left[\int \frac{d\xi}{1 + e \cos \xi} - \int \frac{d\xi}{(1 + e \cos \xi)^2} \right] \right\}.$$

154

On the other hand, from (10.34) we have

$$\int \frac{d\xi}{1+e\cos\xi} - \int \frac{d\xi}{(1+e\cos\xi)^2} = \frac{e\sin\xi}{1+e\cos\xi} - e^2 \int \frac{d\xi}{(1+e\cos\xi)^2}.$$

Substituting this expression in the preceding equality, we find

$$\int \frac{d\xi}{(1+e\cos\xi)^2} - \int \frac{d\xi}{(1+e\cos\xi)^3} = \frac{1}{2(1-e^2)}\left[\frac{e\sin\xi}{(1+e\cos\xi)^2} + \frac{e\sin\xi}{1+e\cos\xi} - 3e^2\int \frac{d\xi}{(1+e\cos\xi)^2}\right].$$

Equality (10.33) is now written as

$$\int_{\vartheta_0}^{\vartheta} r^3\cos\xi\,d\xi = \frac{p^3}{2e(1-e^2)}\left\{-3e^2\int_{\vartheta_0}^{\vartheta} \frac{d\xi}{(1+e\cos\xi)^2} + \left[\frac{e\sin\xi}{(1+e\cos\xi)^2} + \frac{e\sin\xi}{1+e\cos\xi}\right]_{\vartheta_0}^{\vartheta}\right\}. \quad (10.35)$$

Note that from (4.19), (10.9), (10.26), and (10.31),

$$p^2\int_{\vartheta_0}^{\vartheta} \frac{d\xi}{(1+e\cos\xi)^2} = \int_{0}^{\varphi} r^2\,du = t\sqrt{\mu p}. \quad (10.36)$$

Substituting (4.19), (5.13), and (10.36) in (10.35) and making use of (5.2), we find

$$\int_{0}^{\vartheta} r^3\cos\xi\,d\xi = \frac{a}{2}\left\{-3e\sqrt{\mu p}\,t + \frac{1}{e}\sqrt{\frac{\mu}{p}}[rv_r(r+p) - r_0v_{r0}(r_0+p)]\right\}. \quad (10.37)$$

Applying (10.30), (10.32), and (10.37), we write for the first integral in (10.29)

$$J_1 = \frac{p}{2e}(r^2 - r_0^2)\cos\vartheta_0 - \frac{a}{2}\left\{-3e\sqrt{\mu p}\,t + \frac{1}{e}\sqrt{\frac{p}{\mu}}[rv_r(r+p) - r_0v_{r0}(r_0+p)]\right\}\sin\vartheta_0. \quad (10.38)$$

We should now eliminate the true anomaly ϑ_0 from this expression and ensure that no indeterminate forms obtain as $e \to 0$ (i.e., on passing to circular orbits). Making use of (5.2), (5.11), (5.13), (10.9), and (10.16), we have

$$J_1 = \frac{a}{2}\Big[3pv_{r0}t + \frac{1-e^2}{e}(r^2 - r_0^2)\cos\vartheta_0 -$$

$$- r(r+p)\sin\vartheta\sin\vartheta_0 + r_0(r_0+p)\sin^2\vartheta_0\Big] =$$

$$= \frac{a}{2}[3pv_{r0}t - r(r+p)\cos\varphi + r(r+p)\cos\vartheta\cos\vartheta_0 +$$

$$+ r_0(r_0+p) - r_0(r_0+p)\cos^2\vartheta_0 +$$

$$+ \frac{r^2-r_0^2}{e}\cos\vartheta_0 - (r^2-r_0^2)e\cos\vartheta_0\Big] =$$

$$= \frac{a}{2}\left\{3pv_{r0}t - r(r+p)\cos\varphi + r_0(r_0+p) - (r^2-r_0^2)\left(\frac{p}{r_0}-1\right) +\right.$$

$$\left. + \frac{\cos\vartheta_0}{e}\left[r(r+p)\left(\frac{p}{r}-1\right) - r_0(r_0+p)\left(\frac{p}{r_0}-1\right) + r^2 - r_0^2\right]\right\} =$$

$$= \frac{a}{2}\Big[3pv_{r0}t - r(r+p)\cos\varphi + r_0^2 + r_0p -$$

$$- \frac{r^2p}{r_0} + r_0p + r^2 - r_0^2 + \frac{\cos\vartheta_0}{e}(p^2 - r^2 - p^2 + r_0^2 + r^2 - r_0^2)\Big] =$$

$$= \frac{a}{2}\left[3pv_{r0}t - r(r+p)\cos\varphi + 2r_0p - \frac{r^2p}{r_0} + r^2\right],$$

155

or finally

$$J_1 = \frac{apr}{2}\left[\frac{3v_{r_0}t}{r} - \left(1 + \frac{r}{p}\right)\cos\varphi + 2\frac{r_0}{r} - \frac{r}{p}\left(\frac{p}{r_0} - 1\right)\right].\qquad(10.39)$$

The second integral in (10.29) is evaluated analogously. From (5.13), (10.9), (10.16), (10.31), (10.32), and (10.37), we have

$$J_2 = \int\limits_{\vartheta_0}^{\vartheta} r^3 \cos(\xi - \vartheta_0)\, d\xi =$$

$$= \cos\vartheta_0 \int\limits_{\vartheta_0}^{\vartheta} r^3 \cos\xi\, d\xi + \sin\vartheta_0 \int\limits_{\vartheta_0}^{\vartheta} r^3 \sin\xi\, d\xi =$$

$$= \frac{a}{2}\Big\{-3e\,\sqrt{\mu p}\,t +$$

$$+ \frac{1}{e}\sqrt{\frac{p}{\mu}}\,[rv_r(r+p) - r_0 v_{r_0}(r_0 + p)]\Big\}\cos\vartheta_0 +$$

$$+ \frac{p}{2e}(r^2 - r_0^2)\sin\vartheta_0 =$$

$$= \frac{a}{2}\Big[-3\left(\frac{p}{r_0} - 1\right)\sqrt{\mu p}\,t + r(r+p)\sin\vartheta\cos\vartheta_0 -$$

$$- r_0(r_0+p)\sin\vartheta_0\cos\vartheta_0 + \frac{1-e^2}{e}(r^2 - r_0^2)\sin\vartheta_0\Big] =$$

$$= \frac{a}{2}\Big[-3\left(\frac{p}{r_0} - 1\right)\sqrt{\mu p}\,t + r(r+p)\sin\varphi +$$

$$+ r(r+p)\cos\vartheta\sin\vartheta_0 - r_0(r_0+p)\sin\vartheta_0\cos\vartheta_0 +$$

$$+ \frac{r^2 - r_0^2}{e}\sin\vartheta_0 - (r^2 - r_0^2)e\sin\vartheta_0\Big] =$$

$$= \frac{a}{2}\Big\{-3\left(\frac{p}{r_0} - 1\right)\sqrt{\mu p}\,t +$$

$$+ r(r+p)\sin\varphi - \sqrt{\frac{p}{\mu}}(r^2 - r_0^2)v_{r_0} +$$

$$+ \frac{\sin\vartheta_0}{e}\Big[r(r+p)\left(\frac{p}{r} - 1\right) - r_0(r_0+p)\left(\frac{p}{r_0} - 1\right) + r^2 - r_0^2\Big]\Big\},$$

or finally,

$$J_2 = \frac{a}{2}\Big[-3\left(\frac{p}{r_0} - 1\right)\sqrt{\mu p}\,t + r(r+p)\sin\varphi - \sqrt{\frac{p}{\mu}}(r^2 - r_0^2)v_{r_0}\Big].\qquad(10.40)$$

We now calculate the derivatives $\left(\frac{\partial t}{\partial r_0}\right)_\varphi$, $\left(\frac{\partial t}{\partial v_{r_0}}\right)_\varphi$ and $\left(\frac{\partial t}{\partial v_{u_0}}\right)_\varphi$. To find the first derivative, we make use of relations (5.16), (10.9) and write expression (10.15) for $\left(\frac{\partial r}{\partial r_0}\right)_\varphi$ in the form

$$\left(\frac{\partial r}{\partial r_0}\right)_\varphi = \frac{r^2}{r_0^2}\left(\frac{e\sin\vartheta_0}{1+e\cos\vartheta_0}\sin\varphi - \cos\varphi\right) + 2\frac{r}{r_0} =$$

$$= \frac{r^2}{r_0^2}\,\frac{e(\sin\vartheta_0\sin\varphi - \cos\vartheta_0\cos\varphi) - \cos\varphi}{1+e\cos\vartheta_0} + 2\frac{r}{r_0} =$$

$$= -\frac{r^2}{r_0 p}(e\cos\vartheta + \cos\varphi) + 2\frac{r}{r_0}.\qquad(10.41)$$

Substituting this equality in the third expression in (10.27), we have

$$\left(\frac{\partial t}{\partial r_0}\right)_\varphi = -\frac{t}{r_0} + \frac{2}{\sqrt{\mu p}}\left(-\frac{e}{r_0 p}\int\limits_{\vartheta_0}^{\vartheta} r^3\cos\xi\, d\xi - \frac{1}{r_0 p}\int\limits_0^\varphi r^3\cos u\, du + \frac{2}{r_0}\int\limits_0^\varphi r^2\, du\right).$$

156

Inserting for the integrals their expressions (10.26), (10.29), (10.37), and (10.40), we find

$$\left(\frac{\partial t}{\partial r_0}\right)_\varphi = \frac{3t}{r_0} + \frac{a}{r_0 p \sqrt{\mu p}}\left\{3e^2\sqrt{\mu p}\,t - \sqrt{\frac{p}{\mu}}[rv_r(r+p) - r_0 v_{r0}(r_0+p)] + \right.$$

$$\left. + 3\sqrt{\mu p}\left(\frac{p}{r_0}-1\right)t - r(r+p)\sin\varphi + \sqrt{\frac{p}{\mu}}(r^2-r_0^2)v_{r0}\right\} = \frac{3ta}{r_0^2}\left(\frac{r_0}{a}+\frac{e^2 r_0}{p}+\frac{p-r_0}{p}\right) - $$

$$- \frac{ra}{\mu}\left(\frac{rv_r}{r_0 p}+\frac{v_r}{r_0}-\frac{r_0 v_{r0}}{rp}-\frac{v_{r0}}{r}-\frac{rv_{r0}}{r_0 p}+\frac{r_0 v_{r0}}{rp}\right) - \frac{ra}{r_0\sqrt{\mu p}}\left(1+\frac{r}{p}\right)\sin\varphi.$$

Now, from (5.2)

$$\frac{r_0}{a}+\frac{e^2 r_0}{p}+\frac{p-r_0}{p} = 1+\frac{r_0}{p}(1-e^2+e^2-1) = 1.$$

Thus,

$$\left(\frac{\partial t}{\partial r_0}\right)_\varphi = a\left\{\frac{3t}{r_0^2}-\frac{r}{\mu}\left[\frac{v_r}{r_0}-\frac{v_{r0}}{r}+\frac{r}{r_0 p}(v_r-v_{r0})\right]-\frac{r}{r_0\sqrt{\mu p}}\left(1+\frac{r}{p}\right)\sin\varphi\right\}. \quad (10.42)$$

To find the derivative $\left(\frac{\partial t}{\partial v_{r0}}\right)_\varphi$ we make use of relations (10.28), (10.29), and (10.39), which give

$$\left(\frac{\partial t}{\partial v_{r0}}\right)_\varphi = \frac{ar}{\mu}\left[\frac{3v_{r0}}{r}t-\left(1+\frac{r}{p}\right)\cos\varphi+2\frac{r_0}{r}-\frac{r}{p}\left(\frac{p}{r_0}-1\right)\right]. \quad (10.43)$$

To obtain the derivative $\left(\frac{\partial t}{\partial v_{u0}}\right)_\varphi$ we note that in accordance with (10.15), (10.18), and (10.27)

$$\left(\frac{\partial t}{\partial v_{u0}}\right)_\varphi = \frac{r_0}{v_{u0}}\left(\frac{\partial t}{\partial r_0}\right)_\varphi - \frac{2}{\mu p}J_2,$$

where J_2 is defined by (10.29). Thus, making use of (10.40) and (10.42), we find

$$\left(\frac{\partial t}{\partial v_{u0}}\right)_\varphi = \frac{r_0^2}{\sqrt{\mu p}}a\left\{\frac{3t}{r_0^2}-\frac{r}{\mu}\left[\frac{v_r}{r_0}-\frac{v_{r0}}{r}+\frac{r}{r_0 p}(v_r-v_{r0})\right]-\right.$$

$$\left. -\frac{r}{r_0\sqrt{\mu p}}\left(1+\frac{r}{p}\right)\sin\varphi\right\}-\frac{a}{\mu p}\left[-3\sqrt{\mu p}\left(\frac{p}{r_0}-1\right)t+\right.$$

$$\left.+r(r+p)\sin\varphi+\sqrt{\frac{p}{\mu}}(r_0^2-r^2)v_{r0}\right] = \frac{ar}{\mu}\left\{\frac{3t}{r}\sqrt{\frac{\mu}{p}}+\frac{3t}{r}\sqrt{\frac{\mu}{p}}\left(\frac{p}{r_0}-1\right)-\right.$$

$$-\frac{r_0^2}{\sqrt{\mu p}}\left[\frac{v_r}{r_0}-\frac{v_{r0}}{r}+\frac{r}{r_0 p}(v_r-v_{r0})\right]-\frac{1}{r\sqrt{\mu p}}(r_0^2-r^2)v_{r0}-\frac{r_0}{p}\left(1+\frac{r}{p}\right)\sin\varphi-\left(1+\frac{r}{p}\right)\sin\varphi\right\}=$$

$$=\frac{a}{\mu}\left[3\sqrt{\frac{\mu p}{r_0}}t-r\left(1+\frac{r}{p}\right)\left(1+\frac{r_0}{p}\right)\sin\varphi-\frac{r}{\sqrt{\mu p}}\left(r_0 v_r-\frac{r_0^2 v_{r0}}{r}+\frac{rr_0}{p}v_r-\frac{rr_0}{p}v_{r0}+\frac{r_0^2 v_{r0}}{r}-rv_{r0}\right)\right],$$

or finally, applying (5.11)

$$\left(\frac{\partial t}{\partial v_{u0}}\right)_\varphi = \frac{a}{\mu}\left\{3v_{u0}t-r\left(1+\frac{r_0}{p}\right)\left(1+\frac{r}{p}\right)\sin\varphi-\right.$$

$$\frac{r}{\sqrt{\mu p}}\left[\left(1+\frac{r}{p}\right)r_0 v_r-\left(1+\frac{r_0}{p}\right)rv_{r0}\right]\right\}. \quad (10.44)$$

10.6. DERIVATIVES WITH RESPECT
TO THE ANGULAR COORDINATE u_0

If the point of origin D_0 is displaced by Δu_0, the entire orbit rotates in its plane around the gravitational center O through the same angle (Figure 10.3). The path $D_0 D$ of unperturbed orbit is transformed into the path $D_0' D'$ of the perturbed (rotated) orbit. The condition $\varphi = $ const for the perturbed orbit defines a point D_1' on the radius OD. All the parameters of motion at this
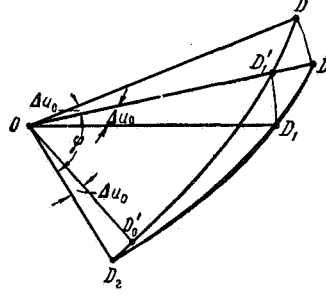
FIGURE 10.3. Variation in current parameters of motion when the point of origin is displaced by Δu_0.

point are identical with the parameters of motion at some point D_1 of unperturbed orbit. This unperturbed point is displaced from the initial position of the point D by $-\Delta u_0$ (the sign $-$ is introduced since the angle Δu_0 is reckoned against the rotation of the orbit). We thus obtain for the partial derivative of any parameter of motion p_i at the current point with $\varphi = $ const:

$$\left(\frac{\partial p_i}{\partial u_0}\right)_\varphi = -\frac{dp_i}{du} = -\frac{\dot{p}_i}{\dot{u}}, \tag{10.45}$$

where the derivatives $\frac{dp_i}{du}$, $\dot{p}_i$, and $\dot{u}$ are taken for unperturbed orbit.

From (2.2) and (5.11) we see that in unperturbed orbit (for $S = T = 0$)

$$\left. \begin{aligned} \dot{r} &= v_r, \quad \dot{t} = 1, \quad \dot{u} = \frac{v_u}{r}, \\ \dot{v}_r &= -\frac{\mu}{r^2} + \frac{v_u^2}{r} = \frac{\mu}{r^2}\left(\frac{p}{r} - 1\right), \\ \dot{v}_u &= -\frac{v_r v_u}{r}. \end{aligned} \right\} \tag{10.46}$$

Substituting these equalities in (10.45) (and putting successively $p_i = r$, t, v_r, v_u), we find

$$\left. \begin{aligned} \left(\frac{\partial r}{\partial u_0}\right)_\varphi &= -\frac{r v_r}{v_u}, \\ \left(\frac{\partial t}{\partial u_0}\right)_\varphi &= -\frac{r}{v_u}, \\ \left(\frac{\partial v_r}{\partial u_0}\right)_\varphi &= \frac{\mu}{r v_u} - v_u = \sqrt{\frac{\mu}{p}}\left(1 - \frac{p}{r}\right), \\ \left(\frac{\partial v_u}{\partial u_0}\right)_\varphi &= v_r. \end{aligned} \right\} \tag{10.47}$$

158

10.7. PARTIAL DERIVATIVES OF PARAMETERS
DESCRIBING THE DISPLACEMENT OF THE SATELLITE
AT RIGHT ANGLES TO UNPERTURBED ORBITAL PLANE

We have shown in Sec. 9.6 that normal perturbations rotate the orbital
plane around some axis through the gravitational center O. The lateral
displacement $\Delta\zeta$ of the current point D is defined by the displacement of
the radius-vector r joining the center of attraction O with the point D
(Figure 10.4). The lateral velocity perturbation* Δv_ζ is equal to the
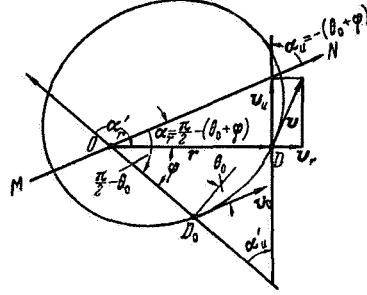
FIGURE 10.4. The position of the rotation axis MN of the
orbital plane for lateral displacement of the point of origin D_0.

corresponding displacement of the tip of the velocity vector v at the current
point. Let A stand for either of the vectors r and v, and let α be the angle**
between this vector and the axis of rotation of the orbital plane, MN. As
the orbital plane rotates through a small angle ψ, the tip of the vector A
is displaced by

$$\Delta A = \psi \mid A \mid \sin \alpha. \qquad (10.48)$$

From Sec. 9.6 it follows that lateral displacement $\Delta\zeta$ of the point D_0
corresponds to a rotation of the orbital plane around an axis parallel to
the velocity vector at that point, through an angle defined by equality (9.50):

$$\psi = \frac{\Delta\zeta_0}{r_0 \cos\theta_0}, \qquad (10.49)$$

where θ_0 is the angle between the initial velocity vector and the local horizon.

We see from Figure 10.4 that in this case the angle α_r between the axis
of rotation MN and the radius-vector r of the current point is

$$\alpha_r = \frac{\pi}{2} - (\theta_0 + \varphi). \qquad (10.50)$$

Hence, applying (10.48) and (10.49), we find an expression for the lateral
displacement of the current point:

$$\Delta\zeta = \frac{r \cos(\theta_0 + \varphi)}{r_0 \cos\theta_0} \Delta\zeta_0.$$

* The positive direction for $\Delta\zeta$ and Δv_ζ is at right angles to the plane of the drawing, toward the reader.
** This angle is positive if the vector A rotates clockwise.

159

Thus,

$$\frac{\partial \zeta}{\partial \zeta_0} = \frac{r \cos (\theta_0 + \varphi)}{r_0 \cos \theta_0} = \frac{r}{r_0} (\cos \varphi - \sin \varphi \; \mathrm{tg} \; \theta_0) = \frac{r}{r_0} \left(\cos \varphi - \frac{v_{r0}}{v_{u0}} \sin \varphi \right). \qquad (10.51)$$

Making use of (4.19), (5.16), (10.9), and (10.16), we transform this expression, writing

$$\frac{\partial \zeta}{\partial \zeta_0} = \frac{r}{r_0} \left(\cos \varphi - \frac{r_0}{p} e \sin \vartheta_0 \sin \varphi \right) =$$

$$= \frac{r}{p} \left(\frac{p}{r_0} \cos \varphi - e \sin \vartheta_0 \sin \varphi \right) =$$

$$= \frac{r}{p} [(1 + e \cos \vartheta_0) \cos \varphi - e \sin \vartheta_0 \sin \varphi] =$$

$$= \frac{r}{p} (\cos \varphi + e \cos \vartheta) = \frac{r}{p} \left(\cos \varphi + \frac{p}{r} - 1 \right),$$

where

$$\vartheta = \vartheta_0 + \varphi,$$

or finally

$$\frac{\partial \zeta}{\partial \zeta_0} = 1 - \frac{r}{p} (1 - \cos \varphi). \qquad (10.52)$$

The derivative $\frac{\partial v_\zeta}{\partial \zeta_0}$ is found analogously. The velocity vector $\boldsymbol{v}$ at the current point is conveniently represented as a sum of its components in the directions r and u (see Figure 10.4):

$$\boldsymbol{v} = \boldsymbol{v}_r + \boldsymbol{v}_u. \qquad (10.53)$$

Expression (10.48) takes the form

$$\Delta v_\zeta = \psi (v_r \sin \alpha_r + v_u \sin \alpha_u), \qquad (10.54)$$

where α_u is the angle between the rotation axis MN of the orbital plane and the vector v_u.

From Figure 10.4 we see that*

$$\alpha_u = \alpha_r - \frac{\pi}{2} = -(\theta_0 + \varphi).$$

Hence, applying (10.49) and (10.50), we find

$$\frac{\partial v_\zeta}{\partial \zeta_0} = \frac{v_r \cos (\varphi + \theta_0) - v_u \sin (\varphi + \theta_0)}{r_0 \cos \theta_0} =$$

$$= \frac{1}{r_0} [v_r (\cos \varphi - \sin \varphi \; \mathrm{tg} \; \theta_0) - v_u (\sin \varphi + \cos \varphi \; \mathrm{tg} \; \theta_0)] =$$

$$= \frac{1}{r_0} \left[v_r \left(\cos \varphi - \frac{v_{r0}}{v_{u0}} \sin \varphi \right) - v_u \left(\sin \varphi + \frac{v_{r0}}{v_{u0}} \cos \varphi \right) \right].$$

---

* The minus sign in front of the expression $(\theta_0 + \varphi)$ indicates that the vector v_u deviates counterclockwise from the axis MN, i.e., in the direction of negative α.

Making use of (4.19), (5.11), (5.13), (5.16), (10.9), and (10.16), we write for this formula

$$\frac{\partial v_\xi}{\partial \zeta_0} = \frac{1}{r_0} \sqrt{\frac{\mu}{p}} \left[e \sin \vartheta \left(\cos \varphi - \frac{r_0}{p} e \sin \vartheta_0 \sin \varphi \right) - \right.$$
$$\left. - (1 + e \cos \vartheta) \left(\sin \varphi + \frac{r_0}{p} \sin \vartheta_0 \cos \varphi \right) \right] =$$

$$= \frac{1}{p} \sqrt{\frac{\mu}{p}} \left[e \sin \vartheta \left(\frac{p}{r_0} \cos \varphi - e \sin \vartheta_0 \sin \varphi \right) - \right.$$
$$\left. - (1 + e \cos \vartheta) \left(\frac{p}{r_0} \sin \varphi + e \sin \vartheta_0 \cos \varphi \right) \right] =$$

$$= \frac{1}{p} \sqrt{\frac{\mu}{p}} \{ e \sin \vartheta [(1 + e \cos \vartheta_0) \cos \varphi - e \sin \vartheta_0 \sin \varphi] - $$
$$- (1 + e \cos \vartheta) [(1 + e \cos \vartheta_0) \sin \varphi + e \sin \vartheta_0 \cos \varphi)] \} =$$

$$= \frac{1}{p} \sqrt{\frac{\mu}{p}} \{ (1 + e \cos \vartheta_0) [e \sin \vartheta \cos \varphi - (1 + e \cos \vartheta) \sin \varphi] - $$
$$- e^2 \sin \vartheta \sin \vartheta_0 \sin \varphi - (1 + e \cos \vartheta) e \sin \vartheta_0 \cos \varphi \} =$$

$$= -\frac{1}{p} \sqrt{\frac{\mu}{p}} [(1 + e \cos \vartheta_0)(\sin \varphi - e \sin \vartheta_0) + $$
$$+ e^2 \sin \vartheta_0 \cos \vartheta_0 + e \sin \vartheta_0 \cos \varphi] =$$

$$= -\frac{1}{p} \sqrt{\frac{\mu}{p}} [(1 + e \cos \vartheta_0) \sin \varphi - e \sin \vartheta_0 + e \cos \varphi \sin \vartheta_0] =$$

$$= -\frac{1}{p} \sqrt{\frac{\mu}{p}} (\sin \varphi + e \sin \vartheta - e \sin \vartheta_0),$$

or finally,

$$\frac{\partial v_\xi}{\partial \zeta_0} = -\frac{1}{p} \left(v_r - v_{r0} + \sqrt{\frac{\mu}{p}} \sin \varphi \right). \tag{10.55}$$

Lateral perturbation $\Delta v_{\zeta 0}$ of the initial velocity rotates the orbital plane around the axis $D_0 O$ joining the point of origin with the center of attraction. The rotation angle is obtained from the second equality in (9.51):

$$\psi = \frac{\Delta v_{\zeta 0}}{v_0 \cos \theta_0} = \frac{\Delta v_{\zeta 0}}{v_{u0}}. \tag{10.56}$$

The angles between the rotation axis $D_0 O$ and the vectors $\mathbf{r}$ (or $\mathbf{v}_r$) and $\mathbf{v}_u$, respectively, are

$$\alpha_r' = \pi - \varphi, \quad \alpha_u' = \frac{\pi}{2} - \varphi.$$

Hence, applying (10.48), and (10.54), we obtain

$$\left. \begin{array}{l} \dfrac{\partial \zeta}{\partial v_{\zeta 0}} = \dfrac{r}{v_{u0}} \sin \varphi = \dfrac{r_0 r}{\sqrt{\mu p}} \sin \varphi, \\[3mm] \dfrac{\partial v_\xi}{\partial v_{\zeta 0}} = \dfrac{v_r \sin \varphi + v_u \cos \varphi}{v_{u0}}. \end{array} \right\} \tag{10.57}$$

The second equality can be transformed making use of (5.11), (5.13), and (10.9). We write

$$\frac{\partial v_\xi}{\partial v_{\zeta 0}} = \frac{\sqrt{\frac{\mu}{p}} [e \sin \vartheta \sin \varphi + (1 + e \cos \vartheta) \cos \varphi]}{\sqrt{\mu p}} r_0 = \frac{r_0}{p} (\cos \varphi + e \cos \vartheta_0),$$

161

or finally, from (10.16),

$$\frac{\partial v_\xi}{\partial v_{\xi 0}} = 1 - \frac{r_0}{p}(1 - \cos\varphi).$$

(10.58)

10.8. LIST OF THE PARTIAL DERIVATIVES OF THE CURRENT PARAMETERS WITH RESPECT TO THE INITIAL CONDITIONS OF MOTION FOR φ = const

From (10.8) we see that the matrix $\left\| \dfrac{\partial r,\ t,\ v_r,\ v_u,\ \zeta,\ v_\xi}{\partial r_0,\ u_0,\ v_{r0},\ v_{u0},\ \zeta_0,\ v_{\xi 0}} \right\|_\varphi$ can be written as

$$\left\| \frac{\partial r,\ t,\ v_r,\ v_u,\ \zeta,\ v_\xi}{\partial r_0,\ u_0,\ v_{r0},\ v_{u0},\ \zeta_0,\ v_{\xi 0}} \right\|_\varphi = \left\| \begin{array}{cc} \left\| \dfrac{\partial r,\ t,\ v_r,\ v_u}{\partial r_0,\ u_0,\ v_{r0},\ v_{u0}} \right\|_\varphi & 0 \\ 0 & \left\| \dfrac{\partial \zeta,\ v_\xi}{\partial \zeta_0,\ v_{\xi 0}} \right\| \end{array} \right\|,$$

(10.59)

where the matrix $\left\| \dfrac{\partial r,\ t,\ v_r,\ v_u}{\partial r_0,\ u_0,\ v_{r0},\ v_{u0}} \right\|_\varphi$ comprises the partial derivatives which specify in-orbit variations, whereas the matrix $\left\| \dfrac{\partial \zeta,\ v_\xi}{\partial \zeta_0,\ v_{\xi 0}} \right\|$ consists of partial derivatives which correspond to displacements at right angles to the orbital plane. Tables 10.1 and 10.2 present a summary of the matrix elements, obtained from expressions (10.19), (10.22), (10.25), (10.42), (10.43), (10.44), (10.47), (10.52), (10.55), (10.57), and (10.58).

TABLE 10.1

	$/\partial r_0$	$/\partial u_0$	$/\partial v_{r0}$	$/\partial v_{u0}$
$\partial r/$	$\dfrac{r}{r_0}\left[1 + \dfrac{r}{p}(1 - \cos\varphi)\right]$	$-\dfrac{r v_r}{v_u}$	$\dfrac{r}{v_u}\sin\varphi$	$\dfrac{r}{v_{u0}}\left[1 + \dfrac{r}{p} - \left(\dfrac{r}{p} + \dfrac{r}{r_0}\right)\cos\varphi\right]$
$\partial t/$	$a\left\{\dfrac{3t}{r_0^2} - \dfrac{r}{\mu}\left[\dfrac{v_r}{r_0} - \dfrac{v_{r0}}{r} + \right.\right.$ $\left. + \dfrac{r}{r_0 p}(v_r - v_{r0})\right] -$ $\left. - \dfrac{r}{r_0\sqrt{\mu p}}\left(1 + \dfrac{r}{p}\right)\sin\varphi\right\}$	$-\dfrac{r}{v_u}$	$\dfrac{a}{\mu}\left[3v_{r0}t - r\times\right.$ $\times\left(1 + \dfrac{r}{p}\right)\cos\varphi +$ $\left. + 2r_0 - \dfrac{r^2}{p}\left(\dfrac{p}{r_0} - 1\right)\right]$	$\dfrac{a}{\mu}\left\{3v_{u0}t - r\left(1 + \dfrac{r}{p}\right)\times\right.$ $\times\left(1 + \dfrac{r_0}{p}\right)\sin\varphi - \dfrac{r}{\sqrt{\mu p}}\times$ $\times\left[\left(1 + \dfrac{r}{p}\right)r_0 v_r -\right.$ $\left.\left. - \left(1 + \dfrac{r_0}{p}\right)r v_{r0}\right]\right\}$
$\partial v_r/$	$\dfrac{v_{u0}}{p}\sin\varphi$	$\sqrt{\dfrac{\mu}{p}}\left(1 - \dfrac{p}{r}\right)$	$\cos\varphi$	$\left(1 + \dfrac{r_0}{p}\right)\sin\varphi$
$\partial v_u/$	$-\dfrac{v_{u0}}{p}(1 - \cos\varphi)$	v_r	$-\sin\varphi$	$-\dfrac{r_0}{p} + \left(1 + \dfrac{r_0}{p}\right)\cos\varphi$

162

TABLE 10.2

	$/\partial \zeta_0$	$/\partial v_{\xi 0}$
$\partial \zeta /$	$1 - \dfrac{r}{p}(1 - \cos \varphi)$	$\dfrac{r_0 r}{\sqrt{\mu p}} \sin \varphi$
$\partial v_\xi /$	$-\dfrac{1}{p}\left(v_r - v_{r0} + \sqrt{\dfrac{\mu}{p}} \sin \varphi\right)$	$1 - \dfrac{r_0}{p}(1 - \cos \varphi)$

The formulas listed in the table apply for circular, elliptical, and hyperbolic orbits. For parabolic orbits, the expressions defining the derivatives $\left(\dfrac{\partial t}{\partial r_0}\right)_\varphi$, $\left(\dfrac{\partial t}{\partial v_{r0}}\right)_\varphi$ and $\left(\dfrac{\partial t}{\partial v_{u0}}\right)_\varphi$, become indeterminate and further calculations are required.

10.9. PARTIAL DERIVATIVES OF THE CURRENT PARAMETERS WITH RESPECT TO THE INITIAL CONDITIONS OF MOTION FOR φ = const AND FIXED ANGULAR POSITION OF THE POINT OF ORIGIN

In some problems it is often advisable to define the point of origin D_0 not as a point corresponding to some epoch $t = t_0$, but preferably as a point at constant angular distance $u = u_0$ from the zero-point axis. In this case the time of arrival at this point, t_0, is interpreted as an initial condition of motion, i.e., the set of initial conditions r_0, u_0, v_{r0}, v_{u0}, ζ_0, $v_{\xi 0}$ accepted in Sec. 10.2 is replaced with the set r_0, t_0, v_{r0}, v_{u0}, ζ_0, $v_{\xi 0}$. The matrix $\left\| \dfrac{\partial \zeta,\ v_\xi}{\partial \zeta_0,\ v_{\xi 0}} \right\|$ for the displacements at right angles to the orbital plane remains as before. For the matrix of in-plane displacements, we write (making use of (10.5))

$$\left\| \frac{\partial r,\ t,\ v_r,\ v_u}{\partial r_0,\ t_0,\ v_{r0},\ v_{u0}} \right\|_\varphi = \left\| \frac{\partial r,\ t,\ v_r,\ v_u}{\partial r_0,\ u_0,\ v_{r0},\ v_{u0}} \right\|_\varphi \left\| \frac{\partial r_0,\ u_0,\ v_{r0},\ v_{u0}}{\partial r_0,\ t_0,\ v_{r0},\ v_{u0}} \right\|.$$

On the other hand, from (10.46) we have

$$\left\| \frac{\partial r_0,\ u_0,\ v_{r0},\ v_{u0}}{\partial r_0,\ t_0,\ v_{r0},\ v_{u0}} \right\| = \left\| \begin{array}{cccc} 1 & -v_{r0} & 0 & 0 \\ 0 & -\dfrac{v_{u0}}{r_0} & 0 & 0 \\ 0 & -\dfrac{\mu}{r_0^2}\left(\dfrac{p}{r_0} - 1\right) & 1 & 0 \\ 0 & \dfrac{v_{r0} v_{u0}}{r_0} & 0 & 1 \end{array} \right\|.$$

Substituting this expression in the preceding equality, we find that only the second column of the matrix is altered under this transformation. The

163

entries in this column can be obtained from formulas of the form

$$\left(\frac{\partial p_i}{\partial t_0}\right)_{\varphi} = - v_{r0}\left(\frac{\partial p_i}{\partial r_0}\right)_{\varphi} - \frac{v_{u0}}{r_0}\left(\frac{\partial p_i}{\partial u_0}\right)_{\varphi} -$$
$$- \frac{\mu}{r_0^2}\left(\frac{p}{r_0} - 1\right)\left(\frac{\partial p_i}{\partial v_{r0}}\right)_{\varphi} + \frac{v_{r0}v_{u0}}{r_0}\left(\frac{\partial p_i}{\partial v_{u0}}\right)_{\varphi}, \quad p_i = r, t, v_r, v_u.$$

These partial derivatives, however, are obtained much more simply if we remember that the shape of the orbit is insensitive to changes in the time t_0. Then

$$\left(\frac{\partial p_i}{\partial t_0}\right)_{\varphi} = 0 \quad \text{for} \quad p_i = r, v_r, v_u,$$
$$\left(\frac{\partial p_i}{\partial t_0}\right)_{\varphi} = 1 \quad \text{for} \quad p_i = t.$$

$$(10.60)$$

The matrix elements of

$$\left\| \frac{\partial r, t, v_r, v_u}{\partial r_0, t_0, v_{r0}, v_{u0}} \right\|_{\varphi}$$

are thus obtained from Table 10.1 if expressions (10.60) are substituted in the second column of this table.

10.10. PARTIAL DERIVATIVES OF THE CURRENT
PARAMETERS WITH RESPECT TO THE INITIAL
CONDITIONS OF MOTION FOR t = const

Let $r, u, v_r, v_u, \zeta, v_\zeta$ be the set of the current parameters of motion. Our problem is to find the matrix of the partial derivatives of these parameters with respect to the initial conditions $r_0, u_0, v_{r0}, v_{u0}, \zeta_0, v_{\zeta 0}$ for $t=$const. By analogy with (10.59), we write

$$\left\| \frac{\partial r, u, v_r, v_u, \zeta, v_\zeta}{\partial r_0, u_0, v_{r0}, v_{u0}, \zeta_0, v_{\zeta 0}} \right\|_t = \left\| \begin{array}{cc} \left\| \frac{\partial r, u, v_r, v_u}{\partial r_0, u_0, v_{r0}, v_{u0}} \right\|_t & 0 \\ 0 & \left\| \frac{\partial \zeta, v_\zeta}{\partial \zeta_0, v_{\zeta 0}} \right\| \end{array} \right\|.$$

The problem thus reduces to calculating the matrix elements of $\left\| \frac{\partial r, u, v_r, v_u}{\partial r_0, u_0, v_{r0}, v_{u0}} \right\|_t$.
We make use of relations (10.6), which give

$$\left(\frac{\partial p_i}{\partial q_j}\right)_t = \left(\frac{\partial p_i}{\partial q_j}\right)_{\varphi} - \left(\frac{\partial t}{\partial q_j}\right)_{\varphi}\dot{p}_i.$$

$$(10.61)$$

Applying (10.46), (10.47), (10.61) and seeing that from (10.7) $\left(\frac{\partial u}{\partial q_j}\right)_{\varphi} = 0,$

we find

$$\left\|\frac{\partial r,\ u,\ v_r,\ v_u}{\partial r_0,\ u_0,\ v_{r0},\ v_{u0}}\right\|_t = \begin{Vmatrix} \left(\frac{\partial r}{\partial r_0}\right)_\varphi - v_r\left(\frac{\partial t}{\partial r_0}\right)_\varphi & 0 & \left(\frac{\partial r}{\partial v_{r0}}\right)_\varphi - v_r\left(\frac{\partial t}{\partial v_{r0}}\right)_\varphi & \left(\frac{\partial r}{\partial v_{u0}}\right)_\varphi - v_r\left(\frac{\partial t}{\partial v_{u0}}\right)_\varphi \\ -\frac{v_u}{r}\left(\frac{\partial t}{\partial r_0}\right)_\varphi & 1 & -\frac{v_u}{r}\left(\frac{\partial t}{\partial v_{r0}}\right)_\varphi & -\frac{v_u}{r}\left(\frac{\partial t}{\partial v_{u0}}\right)_\varphi \\ \left[\left(\frac{\partial v_r}{\partial r_0}\right)_\varphi - \frac{\mu}{r^2}\left(\frac{p}{r}-1\right)\left(\frac{\partial t}{\partial r_0}\right)_\varphi\right] & 0 & \left[\left(\frac{\partial v_r}{\partial v_{r0}}\right)_\varphi - \frac{\mu}{r^2}\left(\frac{p}{r}-1\right)\left(\frac{\partial t}{\partial v_{r0}}\right)_\varphi\right] & \left[\left(\frac{\partial v_r}{\partial v_{u0}}\right)_\varphi - \frac{\mu}{r^2}\left(\frac{p}{r}-1\right)\left(\frac{\partial t}{\partial v_{u0}}\right)_\varphi\right] \\ \left(\frac{\partial v_u}{\partial r_0}\right)_\varphi + \frac{v_r v_u}{r}\left(\frac{\partial t}{\partial r_0}\right)_\varphi & 0 & \left(\frac{\partial v_u}{\partial v_{r0}}\right)_\varphi + \frac{v_r v_u}{r}\left(\frac{\partial t}{\partial v_{r0}}\right)_\varphi & \left(\frac{\partial v_u}{\partial v_{u0}}\right)_\varphi + \frac{v_r v_u}{r}\left(\frac{\partial t}{\partial v_{u0}}\right)_\varphi \end{Vmatrix}. \quad (10.62)$$

On passing from the initial conditions $r_0,\ u_0,\ v_{r0},\ v_{u0}, \zeta_0,\ v_{\zeta 0}$ to $r_0,\ t_0,\ v_{r0},\ v_{u0},\ \zeta_0,\ v_{\zeta 0},$ we alter only the second column of the matrix (see Sec. 10.9). From (10.46), (10.60), and (10.61) it follows that the entries in this column are defined by

$$\left.\begin{array}{ll}\left(\dfrac{\partial r}{\partial t_0}\right)_t = -v_r, & \left(\dfrac{\partial u}{\partial t_0}\right)_t = -\dfrac{v_u}{r}, \\[2mm] \left(\dfrac{\partial v_r}{\partial t_0}\right)_t = -\dfrac{\mu}{r^2}\left(\dfrac{p}{r}-1\right), & \left(\dfrac{\partial v_u}{\partial t_0}\right)_t = \dfrac{v_r v_u}{r}. \end{array}\right\} \quad (10.62\,\mathrm{a})$$

Making use of relations (10.62), (10.62 a) and Table 10.1, we can always find the matrix elements of $\left\|\frac{\partial r,\ u,\ v_r,\ v_u}{\partial r_0,\ u_0,\ v_{r0},\ v_{u0}}\right\|_t$ and $\left\|\frac{\partial r,\ u,\ v_r,\ v_u}{\partial r_0,\ t_0,\ v_{r0},\ v_{u0}}\right\|_t$. In some cases, however, it is desirable to follow a simpler course.

To find the derivative $\left(\frac{\partial r}{\partial r_0}\right)_t$, we make use of (10.19), (10.42), and (10.62), which give

$$\left(\frac{\partial r}{\partial r_0}\right)_t = \frac{r}{r_0}\left[1 + \frac{r}{p}(1-\cos\varphi)\right] - av_r\left\{\frac{3t}{r_0^2} - \frac{r}{\mu}\left[\frac{v_r}{r_0} - \right.\right.$$
$$\left.\left. - \frac{v_{r0}}{r} + \frac{r}{r_0 p}(v_r - v_{r0})\right] - \frac{r}{r_0\sqrt{\mu p}}\left(1+\frac{r}{p}\right)\sin\varphi\right\}.$$

Applyi. g (4.19), (5.2), (5.11), (5.13), and (10.16), we write

$$\left(\frac{\partial r}{\partial r_0}\right)_t = -a\left(\frac{3v_r}{r_0^2}t + \frac{v_r v_{r0}}{\mu}\right) + \frac{a}{r_0}\left(\frac{r}{p}\right)^2 F, \quad (10.63)$$

where

$$F = (1 - e^2)(2 + e\cos\vartheta - \cos\varphi) + (1 + e\cos\vartheta)e^2\sin^2\vartheta + $$
$$+ e^2\sin^2\vartheta - e^2\sin\vartheta\sin\vartheta_0 + (2 + e\cos\vartheta)e\sin\vartheta\sin\varphi.$$

Note that in accordance with (10.9)

$$\left.\begin{array}{l} \sin\vartheta\sin\vartheta_0 = \cos\varphi - \cos\vartheta\cos\vartheta_0, \\[1mm] \sin\vartheta\sin\varphi = \cos\vartheta_0 - \cos\vartheta\cos\varphi. \end{array}\right\} \quad (10.64)$$

Thus

$$F = 2 + e\cos\vartheta - \cos\varphi - 2e^2 - e^3\cos\vartheta + e^2\cos\varphi + $$
$$+ 2e^2\sin^2\vartheta + e^3\cos\vartheta\sin^2\vartheta - e^2\cos\varphi + e^2\cos\vartheta\cos\vartheta_0 + $$
$$+ 2e\cos\vartheta_0 - 2e\cos\vartheta\cos\varphi + e^2\cos\vartheta\cos\vartheta_0 - $$
$$- e^2\cos^2\vartheta\cos\varphi = 2(1 + e\cos\vartheta + e\cos\vartheta_0 + e^2\cos\vartheta\cos\vartheta_0) - $$
$$- \cos\varphi(1 + e\cos\vartheta)^2 - e\cos\vartheta - 2e^2\cos^2\vartheta - e^3\cos^3\vartheta = $$
$$= 2(1 + e\cos\vartheta)(1 + e\cos\vartheta_0) - $$
$$- (\cos\varphi + e\cos\vartheta)(1 + e\cos\vartheta)^2 = \frac{p^2}{r^2}\left(2\frac{r}{r_0} + 1 - \frac{p}{r} - \cos\varphi\right).$$

Substituting in (10.63), we obtain

$$\left(\frac{\partial r}{\partial r_0}\right)_t = a\left[-\frac{3v_r}{r_0^2}\,t + \frac{1}{r_0}\left(2\,\frac{r}{r_0}+1-\frac{p}{r}-\cos\varphi\right)-\frac{v_r v_{r0}}{\mu}\right]. \qquad (10.65)$$

The derivatives $\left(\frac{\partial r}{\partial v_{r0}}\right)_t$ and $\left(\frac{\partial r}{\partial v_{u0}}\right)_t$ are determined analogously. From (10.43) we have

$$\left(\frac{\partial r}{\partial v_{r0}}\right)_t = \frac{r}{v_u}\sin\varphi - \frac{av_r}{\mu}\left[3v_{r0}t - r\left(1+\frac{r}{p}\right)\cos\varphi + 2r_0 - \frac{r^2}{p}\left(\frac{p}{r_0}-1\right)\right] =$$

$$= -a\left(\frac{3v_r v_{r0}}{\mu}\,t + \frac{2r_0 v_r}{\mu}\right) + a\,\frac{r^2}{p^2}\,\sqrt{\frac{p}{\mu}}\,F,$$

where

$$F = (1-e^2)\sin\varphi + (2+e\cos\vartheta)e\sin\vartheta\cos\varphi + e^2\cos\vartheta_0\sin\vartheta =$$
$$= (1-e^2)\sin\varphi + e(2+e\cos\vartheta)(\cos\vartheta\sin\varphi+\sin\vartheta_0) +$$
$$+ e^2(\sin\varphi + \cos\vartheta\sin\vartheta_0) = \sin\varphi(1+e\cos\vartheta)^2 +$$
$$+ 2e\sin\vartheta_0(1+e\cos\vartheta) = \frac{p^2}{r^2}\left(\sin\varphi + 2\,\sqrt{\frac{\mu}{p}}\,\frac{rv_{r0}}{\mu}\right).$$

Hence

$$\left(\frac{\partial r}{\partial v_{r0}}\right)_t = a\left[-\frac{3v_r v_{r0}}{\mu}\,t + \frac{2}{\mu}(rv_{r0}-r_0 v_r) + \sqrt{\frac{p}{\mu}}\,\sin\varphi\right]. \qquad (10.66)$$

Making use of (10.44), we write

$$\left(\frac{\partial r}{\partial v_{u0}}\right)_t = \frac{r}{v_{u0}}\left[1+\frac{r}{p}-\left(\frac{r}{p}+\frac{r}{r_0}\right)\cos\varphi\right] - \frac{av_r}{\mu}\left\{3v_{u0}t - r\left(1+\frac{r}{p}\right)\left(1+\frac{r_0}{p}\right)\sin\varphi - \right.$$

$$\left. - \frac{r}{\sqrt{\mu p}}\left[\left(1+\frac{r}{p}\right)r_0 v_r - \left(1+\frac{r_0}{p}\right)rv_{r0}\right]\right\} = a\,\sqrt{\frac{p}{\mu}}\left(-\frac{3v_r}{r_0}\,t + \frac{r^2 r_0}{p^3}\,F\right), \qquad (10.67)$$

where

$$F = \left[\frac{p}{r}+1-\left(1+\frac{p}{r_0}\right)\cos\varphi\right](1-e^2) +$$
$$+ \left(\frac{p}{r}+1\right)\left(\frac{p}{r_0}+1\right)e\sin\vartheta\sin\varphi + \left(\frac{p}{r}+1\right)e^2\sin^2\vartheta -$$
$$- \left(\frac{p}{r_0}+1\right)e^2\sin\vartheta\sin\vartheta_0 =$$
$$= \left[\frac{p}{r}+1-\left(1+\frac{p}{r_0}\right)\cos\varphi\right](1-e^2) +$$
$$+ \left(\frac{p}{r}+1\right)\left(\frac{p}{r_0}+1\right)e(\cos\vartheta_0 - \cos\vartheta\cos\varphi) +$$
$$+ \left(\frac{p}{r}+1\right)e^2(1-\cos^2\vartheta) - \left(\frac{p}{r_0}+1\right)e^2(\cos\varphi-\cos\vartheta\cos\vartheta_0) =$$
$$= \left(\frac{p}{r}+1\right)(1-e^2) + \left(\frac{p}{r}+1\right)\left(\frac{p}{r_0}+1\right)e\cos\vartheta_0 +$$
$$+ \left(\frac{p}{r}+1\right)e^2(1-\cos^2\vartheta) + \left(\frac{p}{r_0}+1\right)e^2\cos\vartheta\cos\vartheta_0 -$$
$$- \cos\varphi\left[\left(1+\frac{p}{r_0}\right)(1-e^2) + \left(\frac{p}{r}+1\right)\left(\frac{p}{r_0}+1\right)e\cos\vartheta +\right.$$
$$\left. + \left(\frac{p}{r_0}+1\right)e^2\right] = \frac{p}{r}+1+\left(\frac{p}{r}+1\right)\left(\frac{p^2}{r_0^2}-1\right) -$$
$$- \left(\frac{p}{r}-1\right)\left(\frac{p^2}{r^2}-1\right) + \left(\frac{p^2}{r_0^2}-1\right)\left(\frac{p}{r}-1\right) -$$
$$- \cos\varphi\left[1+\frac{p}{r_0}+\left(\frac{p^2}{r^2}-1\right)\left(1+\frac{p}{r_0}\right)\right] =$$
$$= 2\,\frac{p^3}{r_0^2 r} - \frac{p^2}{r^2}\left(\frac{p}{r_0}+1\right)\cos\varphi - \frac{p^2}{r^2}\left(\frac{p}{r}-1\right).$$

166

Substituting in (10.67), we find

$$\left(\frac{\partial r}{\partial v_{u0}}\right)_t = a\sqrt{\frac{p}{\mu}}\left[-\frac{3v_r t}{r_0} - \left(\frac{r_0}{p}+1\right)\cos\varphi + 2\frac{r}{r_0} - \frac{r_0}{p}\left(\frac{p}{r}-1\right)\right]. \qquad (10.68)$$

Making use of (4.19), (5.2), (5.11), (5.13), (10.9), (10.25), (10.42), and (10.62), we find

$$\left(\frac{\partial v_r}{\partial r_0}\right)_t = \sqrt{\frac{\mu}{p}}\,\frac{\sin\varphi}{r_0} - a\frac{\mu}{r^2}\left(\frac{p}{r}-1\right)\times$$

$$\times\left\{\frac{3t}{r_0^2} - \frac{r}{\mu}\left[\frac{v_r}{r_0} - \frac{v_{r0}}{r} + \frac{r}{r_0 p}(v_r - v_{r0})\right] - \frac{r}{r_0\sqrt{\mu p}}\left(1+\frac{r}{p}\right)\sin\varphi\right\} =$$

$$= a\left\{-\frac{3\mu}{r^2 r_0^2}\left(\frac{p}{r}-1\right)t + \sqrt{\frac{\mu}{p}}\,\frac{\sin\varphi}{p r_0}(1-e^2) + \right.$$

$$+\frac{1}{r}\left[\frac{v_r}{r_0} - \frac{v_{r0}}{r} + \frac{r}{r_0 p}(v_r - v_{r0})\right]\left(\frac{p}{r}-1\right) +$$

$$\left.+\frac{1}{rr_0}\sqrt{\frac{\mu}{p}}\left(1+\frac{r}{p}\right)\left(\frac{p}{r}-1\right)\sin\varphi\right\} =$$

$$= a\left\{-\frac{3\mu}{r^2 r_0^2}\left(\frac{p}{r}-1\right)t + \sqrt{\frac{\mu}{p}}\sin\varphi\left[\frac{1}{pr_0} + \frac{p}{r_0 r^2}\left(1-\frac{r^2}{p^2}\right)\right] + \right.$$

$$+\frac{1}{pr_0}\sqrt{\frac{\mu}{p}}\,e^2(\sin\vartheta_0\cos\vartheta - \cos\vartheta_0\sin\vartheta) +$$

$$\left.+\frac{1}{r}\left[\frac{v_r}{r_0} - \frac{v_{r0}}{r} + \frac{r}{r_0 p}(v_r - v_{r0})\right]\left(\frac{p}{r}-1\right)\right\} =$$

$$= a\left\{-\frac{3\mu}{r^2 r_0^2}\left(\frac{p}{r}-1\right)t + \frac{v_u}{rr_0}\sin\varphi + \right.$$

$$\left.+\frac{1}{pr_0}\left[v_{r0}\left(\frac{p}{r}-1\right) - v_r\left(\frac{p}{r_0}-1\right)\right] + \left(\frac{v_r}{rr_0} - \frac{v_{r0}}{r^2} + \frac{v_r}{r_0 p} - \frac{v_{r0}}{r_0 p}\right)\left(\frac{p}{r}-1\right)\right\}$$

or finally

$$\left(\frac{\partial v_r}{\partial r_0}\right)_t = a\left[-\frac{3\mu}{r^2 r_0^2}\left(\frac{p}{r}-1\right)t + \frac{v_u}{rr_0}\sin\varphi + \frac{v_{r0}}{r^2} - \frac{v_r}{r_0^2} + \frac{p}{r^2}\left(\frac{v_r}{r_0} - \frac{v_{r0}}{r}\right)\right]. \qquad (10.69)$$

From (10.43) we similarly have

$$\left(\frac{\partial v_r}{\partial v_{r0}}\right)_t = \cos\varphi - \frac{a}{r^2}\left(\frac{p}{r}-1\right)\left[3v_{r0}t - r\left(1+\frac{r}{p}\right)\cos\varphi + \right.$$

$$+2r_0 - \frac{r^2}{p}\left(\frac{p}{r_0}-1\right)\right] = a\left[-\frac{3v_{r0}}{r^2}\left(\frac{p}{r}-1\right)t + \right.$$

$$+\frac{1-e^2}{p}\cos\varphi + \frac{p}{r^2}\left(1-\frac{r^2}{p^2}\right)\cos\varphi -$$

$$\left.-\frac{2r_0}{r^2}\left(\frac{p}{r}-1\right) + \frac{1}{p}\left(\frac{p}{r}-1\right)\left(\frac{p}{r_0}-1\right)\right] =$$

$$= a\left[-\frac{3v_{r0}}{r^2}\left(\frac{p}{r}-1\right)t + \frac{p}{r^2}\cos\varphi - \frac{e^2}{r^2}(\cos\vartheta\cos\vartheta_0 + \right.$$

$$\left.+\sin\vartheta\sin\vartheta_0) - \frac{2r_0}{r^2}\left(\frac{p}{r}-1\right) + \frac{e^2}{p}\cos\vartheta\cos\vartheta_0\right].$$

Hence

$$\left(\frac{\partial v_r}{\partial v_{r0}}\right)_t = a\left[-\frac{3v_{r0}}{r^2}\left(\frac{p}{r}-1\right)t + \frac{p}{r^2}\cos\varphi - \frac{2r_0}{r^2}\left(\frac{p}{r}-1\right) - \frac{v_r v_{r0}}{\mu}\right]. \qquad (10.70)$$

167

TABLE 10.3

	$/\partial r_0$	$/\partial u_0$	$/\partial v_{r0}$	$/\partial v_{u0}$
$\partial r/$	$a\left[-\dfrac{3v_r}{r_0^2}t+\dfrac{1}{r_0}\left(2\dfrac{r}{r_0}+1-\right.\right.$ $\left.\left.-\dfrac{p}{r}-\cos\varphi\right)-\dfrac{v_rv_{r0}}{\mu}\right]$	0	$a\left[-\dfrac{3v_rv_{r0}}{\mu}t+\right.$ $+\dfrac{2}{\mu}(rv_{r0}-r_0v_r)+$ $\left.+\sqrt{\dfrac{p}{\mu}}\sin\varphi\right]$	$a\sqrt{\dfrac{p}{\mu}}\left[-\dfrac{3v_r}{r_0}t-\right.$ $-\left(\dfrac{r_0}{p}+1\right)\cos\varphi+$ $\left.+2\dfrac{r}{r_0}-\dfrac{r_0}{p}\left(\dfrac{p}{r}-1\right)\right]$
$\partial u/$	$\dfrac{a}{r}\left\{-\dfrac{3v_u}{r_0^2}t+\sqrt{\dfrac{p}{\mu}}\times\right.$ $\times\left[\dfrac{v_r}{r_0}-\dfrac{v_{r0}}{r}+\dfrac{r}{r_0p}(v_r-v_{r0})\right]+$ $\left.+\dfrac{1}{r_0}\left(1+\dfrac{r}{p}\right)\sin\varphi\right\}$	1	$\dfrac{av_u}{\mu}\left[-\dfrac{3v_{r0}}{r}t+\left(1+\dfrac{r}{p}\right)\cos\varphi-\right.$ $\left.-2\dfrac{r_0}{r}+\dfrac{r}{p}\left(\dfrac{p}{r_0}-1\right)\right]$	$\dfrac{av_u}{\mu}\left\{-\dfrac{3v_{u0}}{\cdot}t+\right.$ $+\left(1+\dfrac{r}{p}\right)\left(1+\dfrac{r_0}{p}\right)\sin\varphi+$ $+\dfrac{1}{\sqrt{\mu p}}\left[\left(1+\dfrac{r}{p}\right)r_0v_r-\right.$ $\left.\left.-\left(1+\dfrac{r_0}{p}\right)rv_{r0}\right]\right\}$
$\partial v_r/$	$a\left[-\dfrac{3\mu}{r^2r_0^2}\left(\dfrac{p}{r}-1\right)t+\right.$ $+\dfrac{v_u}{rr_0}\sin\varphi+\dfrac{v_{r0}}{r^2}-\dfrac{v_r}{r_0^2}+$ $\left.+\dfrac{p}{r^2}\left(\dfrac{v_r}{r_0}-\dfrac{v_{r0}}{r}\right)\right]$	0	$a\left[-\dfrac{3v_{r0}}{r^2}\left(\dfrac{p}{r}-1\right)t+\dfrac{p}{r^2}\cos\varphi-\right.$ $\left.-\dfrac{2r_0}{r^2}\left(\dfrac{p}{r}-1\right)-\dfrac{v_rv_{r0}}{\mu}\right]$	$\dfrac{a}{r}\left[-\dfrac{3v_u}{r_0}\left(\dfrac{p}{r}-1\right)t+\right.$ $+\dfrac{p}{r}\left(1+\dfrac{r_0}{p}\right)\sin\varphi+$ $\left.+v_r\sqrt{\dfrac{p}{\mu}}\left(\dfrac{r_0}{r}-\dfrac{r}{r_0}\right)\right]$
$\partial v_u/$	$\dfrac{av_r}{r}\left\{\dfrac{3v_u}{r_0^2}t-\sqrt{\dfrac{p}{\mu}}\times\right.$ $\times\left[\dfrac{v_r}{r_0}-\dfrac{v_{r0}}{r}+\dfrac{r}{r_0p}(v_r-v_{r0})\right]-$ $\left.-\dfrac{1}{r_0}\left(1+\dfrac{r}{p}\right)\sin\varphi\right\}-$ $-\dfrac{v_{u0}}{p}(1-\cos\varphi)$	0	$\dfrac{av_rv_u}{\mu}\left[\dfrac{3v_{r0}}{r}t-\left(1+\dfrac{r}{p}\right)\cos\varphi+\right.$ $\left.+2\dfrac{r_0}{r}-\dfrac{r}{p}\left(\dfrac{p}{r_0}-1\right)\right]-\sin\varphi$	$\dfrac{av_rv_u}{\mu}\left\{\dfrac{3v_{u0}}{r}t-\right.$ $-\left(1+\dfrac{r}{p}\right)\left(1+\dfrac{r_0}{p}\right)\sin\varphi-$ $-\dfrac{1}{\sqrt{\mu p}}\left[\left(1+\dfrac{r}{p}\right)r_0v_r-\right.$ $\left.\left.-\left(1+\dfrac{r_0}{p}\right)rv_{r0}\right]\right\}-$ $-\dfrac{r_0}{p}+\left(1+\dfrac{r_0}{p}\right)\cos\varphi$

168

From (10.44) we have

$$\left(\frac{\partial v_r}{\partial v_{u0}}\right)_t = \left(1 + \frac{r_0}{p}\right)\sin\varphi - \frac{a}{r^2}\left(\frac{p}{r} - 1\right)\times$$

$$\times\left\{3v_{u0}t - r\left(1 + \frac{r}{p}\right)\left(1 + \frac{r_0}{p}\right)\sin\varphi - \right.$$

$$\left. - \frac{r}{\sqrt{\mu p}}\left[\left(1 + \frac{r}{p}\right)r_0 v_r - \left(1 + \frac{r_0}{p}\right)r v_{r0}\right]\right\} =$$

$$= a\left\{-\frac{3v_u}{rr_0}\left(\frac{p}{r} - 1\right)t + \frac{1 - e^2}{p}\left(1 + \frac{r_0}{p}\right)\sin\varphi + \right.$$

$$\left. + \frac{1}{r}\left(1 + \frac{r}{p}\right)\left(1 + \frac{r_0}{p}\right)\left(\frac{p}{r} - 1\right)\sin\varphi + \right.$$

$$\left. + \frac{1}{r\sqrt{\mu p}}\left[\left(1 + \frac{r}{p}\right)r_0 v_r - \left(1 + \frac{r_0}{p}\right)r v_{r0}\right]\left(\frac{p}{r} - 1\right)\right\} =$$

$$= a\left\{-\frac{3v_u}{rr_0}\left(\frac{p}{r} - 1\right)t + \left[\frac{1}{p} + \frac{p}{r^2}\left(1 - \frac{r^2}{p^2}\right)\right]\left(1 + \frac{r_0}{p}\right)\sin\varphi + F\right\}, \qquad (10.71)$$

where

$$F = -\frac{e^2}{p}\left(1 + \frac{r_0}{p}\right)(\sin\vartheta\cos\vartheta_0 - \sin\vartheta_0\cos\vartheta) + $$

$$+ \frac{1}{r\sqrt{\mu p}}\left[\left(1 + \frac{r}{p}\right)r_0 v_r - \left(1 + \frac{r_0}{p}\right)r v_{r0}\right]\left(\frac{p}{r} - 1\right) = $$

$$= \frac{1}{\sqrt{p\mu}}\left[-\left(1 + \frac{r_0}{p}\right)\left(\frac{p}{r_0} - 1\right)v_r + \left(1 + \frac{r_0}{p}\right)\left(\frac{p}{r} - 1\right)v_{r0} + \right.$$

$$\left. + \frac{r_0}{r}\left(1 + \frac{r}{p}\right)\left(\frac{p}{r} - 1\right)v_r - \left(1 + \frac{r_0}{p}\right)\left(\frac{p}{r} - 1\right)v_{r0}\right] = $$

$$= \sqrt{\frac{p}{\mu}}\,v_r\left[\frac{r_0}{r^2}\left(1 - \frac{r^2}{p^2}\right) - \frac{1}{r_0}\left(1 - \frac{r_0^2}{p^2}\right)\right] = \frac{v_r}{r}\sqrt{\frac{p}{\mu}}\left(\frac{r_0}{r} - \frac{r}{r_0}\right).$$

Substituting in (10.71), we find

$$\left(\frac{\partial v_r}{\partial v_{u0}}\right)_t = \frac{a}{r}\left[-\frac{3v_u}{r_0}\left(\frac{p}{r} - 1\right)t + \frac{p}{r}\left(1 + \frac{r_0}{p}\right)\sin\varphi + v_r\sqrt{\frac{\mu}{p}}\left(\frac{r_0}{r} - \frac{r}{r_0}\right)\right]. \qquad (10.72)$$

The other matrix elements of $\left(\frac{\partial r,\ u,\ v_r,\ v_u}{\partial r_0,\ u_0,\ v_{r0},\ v_{u0}}\right)_t$ are determined analogously The final expressions for the matrix elements are listed in Table 10.3.

In conclusion we should note that as the orbit eccentricity decreases, the partial derivatives listed in Tables 10.2 and 10.3 continuously approach the corresponding quantities defined by (2.17) and (2.18). To obtain the limiting expressions, it suffices to put in Tables 10.2 and 10.3

$$\left.\begin{array}{ll} a \to p \to r \to r_0, & v_u \to v_{u0} \to \sqrt{\frac{\mu}{p}} \to w, \\[2mm] \varphi \to \frac{wt}{r_0}, & v_r \to v_{r0} \to 0. \end{array}\right\} \qquad (10.73)$$

10.11. PARTIAL DERIVATIVES OF THE CURRENT PARAMETERS WITH RESPECT TO THE INITIAL CONDITIONS OF MOTION IN THE RECTANGULAR FRAME (FOR t = const)

In various applied problems, the results are often required, not in cylindrical coordinates, but preferably in some rectangular frame. The transformation from cylindrical to rectangular coordinates need be

calculated for one particular frame only, and any further transformation to other nonrotating rectangular frames can be realized with the aid of equality (10.5) and the relation

$$\left\|\frac{\partial x,\ y,\ z,\ v_x,\ v_y,\ v_z}{\partial \xi,\ \eta,\ \zeta,\ v_\xi,\ v_\eta,\ v_\zeta}\right\| = \left\|\begin{matrix} A & 0 \\ 0 & A \end{matrix}\right\|,$$

(10.74)

where xyz and $\xi\eta\zeta$ are two rectangular frames, $v_x,\ v_y,\ v_z$ and $v_\xi,\ v_\eta, v_\zeta$ are the corresponding velocity components, A the matrix of direction cosines for the two rectangular frames.

Note that the sets of current parameters and initial conditions of motion may change upon transformation to rectangular coordinates. Invariance of the parametric set can always be ensured by making use of expressions (10.5) and (10.74).
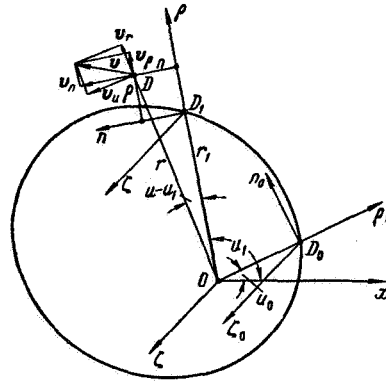
FIGURE 10.5. Current parameters and initial conditions of motion in rectangular frames connected with the satellite's position in orbit.

In the present section we shall operate in right-hand rectangular frames $\rho_0 n_0 \zeta_0$ and $\rho n \zeta$ (Figure 10.5). The origin of the two frames is at the points D_0 and D_1 of the unperturbed orbit, respectively. The axes $D_0\rho_0$ and $D_1\rho$ point along the radii joining the center of attraction O with the points D_0 and D_1, the axes $D_0 n_0$ and $D_1 n$ are in the orbital plane, pointing in the direction of motion, and the axes $D_0\zeta_0$ and $D_1\zeta$ are perpendicular to the orbital plane.

Here the axes $D_0\zeta_0$ and $D_1\zeta$ of the rectangular frames are parallel to the axis $O\zeta$ of the previously used cylindrical system $ru\zeta$. Therefore, on passing from the matrix $\left\|\dfrac{\partial r,\ u,\ v_r,\ v_u,\ \zeta,\ v_\zeta}{\partial r_0,\ u_0,\ v_{r_0},\ v_{u_0},\ \zeta_0,\ v_{\zeta_0}}\right\|_t$ to the matrix $\left\|\dfrac{\partial \rho,\ n,\ v_\rho,\ v_n,\ \zeta,\ v_\zeta}{\partial \rho_0,\ n_0,\ v_{\rho_0},\ v_{n_0},\ \zeta_0,\ v_{\zeta_0}}\right\|_t$, the variations which specify displacements in the orbital plane remain independent of the variations representing displacements at right angles to the orbital plane. In other words, like in (10.59), we may write

$$\left\|\frac{\partial \rho,\ n,\ v_\rho,\ v_n,\ \zeta,\ v_\zeta}{\partial \rho_0,\ n_0,\ v_{\rho_0},\ v_{n_0},\ \zeta_0,\ v_{\zeta_0}}\right\|_t = \left\|\begin{matrix} \left\|\dfrac{\partial \rho,\ n,\ v_\rho,\ v_n}{\partial \rho_0,\ n_0,\ v_{\rho_0},\ v_{n_0}}\right\|_t & 0 \\ 0 & \left\|\dfrac{\partial \zeta,\ v_\zeta}{\partial \zeta_0,\ v_{\zeta_0}}\right\| \end{matrix}\right\|.$$

(10.75)

170

The matrix $\left\| \frac{\partial \zeta, \; v_\zeta}{\partial \zeta_0, \; v_{\zeta_0}} \right\|$ is not altered, and its elements are obtained from Table 10.2.

The problem thus reduces to the calculation of the matrix elements of $\left\| \frac{\partial \rho, \; n, \; v_\rho, \; v_n}{\partial \rho_0, \; n_0, \; v_{\rho_0}, \; u_{n_0}} \right\|_k$, which by analogy with (10.5) is written as

$$\left\| \frac{\partial \rho, \; n, \; v_\rho, \; v_n}{\partial \rho_0, \; n_0, \; v_{\rho_0}, \; v_{n_0}} \right\|_k = \left\| \frac{\partial \rho, \; n, \; v_\rho, \; v_n}{\partial r, \; u, \; v_r, \; v_u} \right\| \left\| \frac{\partial r, \; u, \; v_r, \; v_u}{\partial r_0, \; u_0, \; v_{r0}, \; v_{u0}} \right\|_k \left\| \frac{\partial r_0, \; u_0, \; v_{r0}, \; v_{u0}}{\partial \rho_0, \; n_0, \; v_{\rho_0}, \; v_{n_0}} \right\|. \qquad (10.76)$$

To calculate the transformation matrices in the right-hand side of (10.76), we should first establish a relationship among the parameters of motion $\rho, \; n, \; v_\rho, \; v_n$ and $r, \; u, \; v_r, \; v_u$ at the current point. From Figure 10.5 we have

$$\left. \begin{aligned} \rho &= r \cos(u - u_1) - r_1, \\ n &= r \sin(u - u_1), \\ v_\rho &= v_r \cos(u - u_1) - v_u \sin(u - u_1), \\ v_n &= v_r \sin(u - u_1) + v_u \cos(u - u_1), \end{aligned} \right\} \qquad (10.77)$$

where $r_1, \; u_1$ are the polar coordinates of the unperturbed current point D_1. Hence

$$\left. \begin{aligned} \frac{\partial \rho}{\partial r} &= \cos(u - u_1), & \frac{\partial \rho}{\partial u} &= -r \sin(u - u_1), \\ \frac{\partial \rho}{\partial v_r} &= \frac{\partial \rho}{\partial v_u} = 0, \\ \frac{\partial n}{\partial r} &= \sin(u - u_1), & \frac{\partial n}{\partial u} &= r \cos(u - u_1), \\ \frac{\partial n}{\partial v_r} &= \frac{\partial n}{\partial v_u} = 0, \\ \frac{\partial v_\rho}{\partial r} &= 0, & \frac{\partial v_\rho}{\partial u} &= -v_r \sin(u - u_1) - v_u \cos(u - u_1), \\ \frac{\partial v_\rho}{\partial v_r} &= \cos(u - u_1), & \frac{\partial v_\rho}{\partial v_u} &= -\sin(u - u_1), \\ \frac{\partial v_n}{\partial r} &= 0, & \frac{\partial v_n}{\partial u} &= v_r \cos(u - u_1) - v_u \sin(u - u_1), \\ \frac{\partial v_n}{\partial v_r} &= \sin(u - u_1), & \frac{\partial v_n}{\partial v_u} &= \cos(u - u_1). \end{aligned} \right\} \qquad (10.78)$$

From (10.77) and (10.78) we see that at the unperturbed current point (for $r = r_1, \; u = u_1$),

$$\rho = n = 0, \quad v_\rho = v_r, \quad v_n = v_u, \qquad (10.79)$$

$$\left\| \frac{\partial \rho, \; n, \; v_\rho, \; v_n}{\partial r, \; u, \; v_r, \; v_n} \right\| = \begin{vmatrix} 1 & 0 & 0 & 0 \\ 0 & r & 0 & 0 \\ 0 & -v_u & 1 & 0 \\ 0 & v_r & 0 & 1 \end{vmatrix}. \qquad (10.80)$$

Making use of (10.80), we write the following relations among the variations of the relevant parameters:

$$\begin{aligned} \Delta \rho &= \Delta r, \\ \Delta n &= r \Delta u, \\ \Delta v_\rho &= -v_u \Delta u + \Delta v_r, \\ \Delta v_n &= v_r \Delta u + \Delta v_u, \end{aligned}$$

171

whence

$$\Delta r = \Delta\rho,$$

$$\Delta u = \frac{1}{r}\Delta n,$$

$$\Delta v_r = \Delta v_\rho + \frac{v_u}{r}\Delta n,$$

$$\Delta v_u = \Delta v_n - \frac{v_r}{r}\Delta n.$$

Thus

$$\left\| \frac{\partial r,\ u,\ v_r,\ v_u}{\partial \rho,\ n,\ v_\rho,\ v_n} \right\| = \left\| \begin{array}{cccc} 1 & 0 & 0 & 0 \\ 0 & \dfrac{1}{r} & 0 & 0 \\ 0 & \dfrac{v_u}{r} & 1 & 0 \\ 0 & -\dfrac{v_r}{r} & 0 & 1 \end{array} \right\|. \qquad (10.81)$$

The matrices $\left\| \dfrac{\partial \rho_0,\ n_0,\ v_{\rho_0},\ v_{n_0}}{\partial r_0,\ u_0,\ v_{r0},\ v_{u0}} \right\|$ and $\left\| \dfrac{\partial r_0,\ u_0,\ v_{r0},\ v_{u0}}{\partial \rho_0,\ n_0,\ v_{\rho_0},\ v_{n_0}} \right\|$ are determined similarly.

Substituting these expressions in (10.76) and omitting the subscript t of the derivatives, we find

$$\left\| \frac{\partial \rho,\ n,\ v_\rho,\ v_n}{\partial \rho_0,\ n_0,\ v_{\rho_0},\ v_{n_0}} \right\| = \left\| \begin{array}{cccc} 1 & 0 & 0 & 0 \\ 0 & r & 0 & 0 \\ 0 & -v_u & 1 & 0 \\ 0 & v_r & 0 & 1 \end{array} \right\| \left\| \begin{array}{cccc} \dfrac{\partial r}{\partial r_0} & \dfrac{\partial r}{\partial u_0} & \dfrac{\partial r}{\partial v_{r0}} & \dfrac{\partial r}{\partial v_{u0}} \\[4pt] \dfrac{\partial u}{\partial r_0} & \dfrac{\partial u}{\partial u_0} & \dfrac{\partial u}{\partial v_{r0}} & \dfrac{\partial u}{\partial v_{u0}} \\[4pt] \dfrac{\partial v_r}{\partial r_0} & \dfrac{\partial v_r}{\partial u_0} & \dfrac{\partial v_r}{\partial v_{r0}} & \dfrac{\partial v_r}{\partial v_{u0}} \\[4pt] \dfrac{\partial v_u}{\partial r_0} & \dfrac{\partial v_u}{\partial u_0} & \dfrac{\partial v_u}{\partial v_{r0}} & \dfrac{\partial v_u}{\partial v_{u0}} \end{array} \right\| \left\| \begin{array}{cccc} 1 & 0 & 0 & 0 \\ 0 & \dfrac{1}{r_0} & 0 & 0 \\ 0 & \dfrac{v_{u0}}{r_0} & 1 & 0 \\ 0 & -\dfrac{v_{r0}}{r_0} & 0 & 1 \end{array} \right\| =$$

$$= \left\| \begin{array}{cccc} \dfrac{\partial r}{\partial r_0} & \dfrac{\partial r}{\partial u_0} & \dfrac{\partial r}{\partial v_{r0}} & \dfrac{\partial r}{\partial v_{u0}} \\[4pt] r\dfrac{\partial u}{\partial r_0} & r\dfrac{\partial u}{\partial u_0} & r\dfrac{\partial u}{\partial v_{r0}} & r\dfrac{\partial u}{\partial v_{u0}} \\[4pt] -v_u\dfrac{\partial u}{\partial r_0}+\dfrac{\partial v_r}{\partial r_0} & -v_u\dfrac{\partial u}{\partial u_0}+\dfrac{\partial v_r}{\partial u_0} & -v_u\dfrac{\partial u}{\partial v_{r0}}+\dfrac{\partial v_r}{\partial v_{r0}} & -v_u\dfrac{\partial u}{\partial v_{u0}}+\dfrac{\partial v_r}{\partial v_{u0}} \\[4pt] v_r\dfrac{\partial u}{\partial r_0}+\dfrac{\partial v_u}{\partial r_0} & v_r\dfrac{\partial u}{\partial u_0}+\dfrac{\partial v_u}{\partial u_0} & v_r\dfrac{\partial u}{\partial v_{r0}}+\dfrac{\partial v_u}{\partial v_{r0}} & v_r\dfrac{\partial u}{\partial v_{u0}}+\dfrac{\partial v_u}{\partial v_{u0}} \end{array} \right\| \left\| \begin{array}{cccc} 1 & 0 & 0 & 0 \\ 0 & \dfrac{1}{r_0} & 0 & 0 \\ 0 & \dfrac{v_{u0}}{r_0} & 1 & 0 \\ 0 & -\dfrac{v_{r0}}{r_0} & 0 & 1 \end{array} \right\| =$$

$$= \left\| \begin{array}{cccc} \dfrac{\partial r}{\partial r_0} & \dfrac{1}{r_0}\left(\dfrac{\partial r}{\partial u_0}+v_{u0}\dfrac{\partial r}{\partial v_{r0}}-v_{r0}\dfrac{\partial r}{\partial v_{u0}}\right) & \dfrac{\partial r}{\partial v_{r0}} & \dfrac{\partial r}{\partial v_{u0}} \\[6pt] r\dfrac{\partial u}{\partial r_0} & \dfrac{r}{r_0}\left(\dfrac{\partial u}{\partial u_0}+v_{u0}\dfrac{\partial u}{\partial v_{r0}}-v_{r0}\dfrac{\partial u}{\partial v_{u0}}\right) & r\dfrac{\partial u}{\partial v_{r0}} & r\dfrac{\partial u}{\partial v_{u0}} \\[6pt] \left[-v_u\dfrac{\partial u}{\partial r_0}+\right. & \left[-\dfrac{v_u}{r_0}\left(\dfrac{\partial u}{\partial u_0}+v_{u0}\dfrac{\partial u}{\partial v_{r0}}-\right.\right. & \left[-v_u\dfrac{\partial u}{\partial v_{r0}}+\right. & \left[-v_u\dfrac{\partial u}{\partial v_{u0}}+\right. \\[4pt] \left.+\dfrac{\partial v_r}{\partial r_0}\right] & \left.\left.-v_{r0}\dfrac{\partial u}{\partial v_{u0}}\right)+\dfrac{1}{r_0}\left(\dfrac{\partial v_r}{\partial u_0}+\right.\right. & \left.+\dfrac{\partial v_r}{\partial v_{r0}}\right] & \left.+\dfrac{\partial v_r}{\partial v_{u0}}\right] \\[4pt] & \left.\left.+v_{u0}\dfrac{\partial v_r}{\partial v_{r0}}-v_{r0}\dfrac{\partial v_r}{\partial v_{u0}}\right)\right] & & \\[6pt] \left[v_r\dfrac{\partial u}{\partial r_0}+\right. & \left[\dfrac{v_r}{r_0}\left(\dfrac{\partial u}{\partial u_0}+v_{u0}\dfrac{\partial u}{\partial v_{r0}}-\right.\right. & \left[v_r\dfrac{\partial u}{\partial v_{r0}}+\right. & \left[v_r\dfrac{\partial u}{\partial v_{u0}}+\right. \\[4pt] \left.+\dfrac{\partial v_u}{\partial r_0}\right] & \left.\left.-v_{r0}\dfrac{\partial u}{\partial v_{u0}}\right)+\dfrac{1}{r_0}\left(\dfrac{\partial v_u}{\partial u_0}+\right.\right. & \left.+\dfrac{\partial v_u}{\partial v_{r0}}\right] & \left.+\dfrac{\partial v_u}{\partial v_{u0}}\right] \\[4pt] & \left.\left.+v_{u0}\dfrac{\partial v_u}{\partial v_{r0}}-v_{r0}\dfrac{\partial v_u}{\partial v_{u0}}\right)\right] & & \end{array} \right\| \qquad (10.82)$$

Inserting for the derivatives their expressions from Table 10.3, we obtain a table of the matrix elements of $\left\|\dfrac{\partial \rho,\ n,\ v_\rho,\ v_n}{\partial \rho_0,\ n_0,\ v_{\rho_0},\ v_{n_0}}\right\|_t$. However, we should first simplify the expressions for some of these derivatives. In particular,

$$\left(\frac{\partial r}{\partial n_0}\right)_t = \frac{1}{r_0}\left[\left(\frac{\partial r}{\partial u_0}\right)_t + v_{u0}\left(\frac{\partial r}{\partial v_{r0}}\right)_t - v_{r0}\left(\frac{\partial r}{\partial v_{u0}}\right)_t\right] =$$

$$= \frac{a}{r_0}\left[- \frac{3v_r v_{r0} v_{u0}}{\mu} t + \frac{2}{\mu} v_{u0}(rv_{r0} - r_0 v_r) + \right.$$

$$+ \sqrt{\frac{p}{\mu}}\, v_{u0}\sin\varphi + \sqrt{\frac{p}{\mu}}\frac{3v_r v_{r0}}{r_0} t + v_{r0}\sqrt{\frac{p}{\mu}}\left(\frac{r_0}{p}+1\right)\cos\varphi - $$

$$\left. - 2\sqrt{\frac{p}{\mu}}\frac{r}{r_0} v_{r0} + \sqrt{\frac{p}{\mu}}\, v_{r0}\frac{r_0}{p}\left(\frac{p}{r}-1\right)\right].$$

Hence, applying (4.19), (5.2), (5.11), (5.13), and (10.9), we obtain

$$\left(\frac{\partial r}{\partial n_0}\right)_t = \frac{a}{r_0}\sqrt{\frac{p}{\mu}}\left[-2v_r + v_{u0}\sin\varphi + v_{r0}\left(\frac{r_0}{p}+1\right)\cos\varphi + \right.$$

$$\left. + v_{r0}\frac{r_0}{p}\left(\frac{p}{r}-1\right)\right] = \frac{a}{p}\left[-2\frac{p}{r_0} e \sin\vartheta + \right.$$

$$+ \left(\frac{p}{r_0}\right)^2\sin\varphi + e\sin\vartheta_0\left(1+\frac{p}{r_0}\right)\cos\varphi + e\sin\vartheta_0\left(\frac{p}{r}-1\right)\right] =$$

$$= \frac{a}{p}\left[-2e\sin\vartheta\,(1+e\cos\vartheta_0) + (1+e\cos\vartheta_0)^2\sin\varphi + \right.$$

$$\left. + e\sin\vartheta_0(2+e\cos\vartheta_0)\cos\varphi + e^2\sin\vartheta_0\cos\vartheta\right] =$$

$$= \frac{a}{p}\left[\sin\varphi + e(-2\sin\vartheta + 2\cos\vartheta_0\sin\varphi + 2\sin\vartheta_0\cos\varphi) + \right.$$

$$+ e^2(-2\sin\vartheta\cos\vartheta_0 + \cos^2\vartheta_0\sin\varphi +$$

$$\left. + \sin\vartheta_0\cos\vartheta_0\cos\varphi + \sin\vartheta_0\cos\vartheta)\right] =$$

$$= \frac{a}{p}\left\{\sin\varphi + e^2\left[-2(\sin\varphi\cos\vartheta_0 + \cos\varphi\sin\vartheta_0)\cos\vartheta_0 + \right.\right.$$

$$+ \cos^2\vartheta_0\sin\varphi + \sin\vartheta_0\cos\vartheta_0\cos\varphi +$$

$$\left.\left. + \sin\vartheta_0(\cos\varphi\cos\vartheta_0 - \sin\varphi\sin\vartheta_0)\right]\right\} =$$

$$= \frac{a}{p}\left[\sin\varphi + e^2(-\sin\varphi\cos^2\vartheta_0 - \sin\varphi\sin^2\vartheta_0)\right] =$$

$$= \frac{a}{p}(1 - e^2)\sin\varphi = \sin\varphi. \tag{10.83}$$

Similarly,

$$\left(\frac{\partial n}{\partial n_0}\right)_t = \frac{r}{r_0}\left[\left(\frac{\partial u}{\partial u_0}\right)_t + v_{u0}\left(\frac{\partial u}{\partial v_{r0}}\right)_t - v_{r0}\left(\frac{\partial u}{\partial v_{u0}}\right)_t\right] =$$

$$= \frac{r}{r_0} + \frac{r}{r_0}\frac{av_u}{\mu}\left\{- \frac{3v_{r0}v_{u0}}{r} t + v_{u0}\left(1+\frac{r}{p}\right)\cos\varphi - 2v_{u0}\frac{r_0}{r} + \right.$$

$$+ v_{u0}\frac{r}{p}\left(\frac{p}{r_0}-1\right) + \frac{3v_{r0}v_{u0}}{r} t - v_{r0}\left(1+\frac{r}{p}\right)\left(1+\frac{r_0}{p}\right)\sin\varphi - $$

$$\left. - \frac{v_{r0}}{\sqrt{\mu p}}\left[\left(1+\frac{r}{p}\right)r_0 v_r - \left(1+\frac{r_0}{p}\right)rv_{r0}\right]\right\} =$$

$$= \frac{r}{r_0} + \frac{a}{r_0}\left\{\frac{p}{r_0}\left(1+\frac{r}{p}\right)\cos\varphi - 2\frac{p}{r} + \frac{r}{r_0}\left(\frac{p}{r_0}-1\right) - \right.$$

$$- e\sin\vartheta_0\left(1+\frac{r}{p}\right)\left(1+\frac{r_0}{p}\right)\sin\varphi - $$

$$\left. - e\sin\vartheta_0\left[\left(1+\frac{r}{p}\right)\frac{r_0}{p} e\sin\vartheta - \left(1+\frac{r_0}{p}\right)\frac{r}{p} e\sin\vartheta_0\right]\right\} =$$

$$= \frac{ra}{p^2}\left[\frac{p^2}{r_0 a} + \left(\frac{p}{r_0}\right)^2\left(\frac{p}{r}+1\right)\cos\varphi - 2\left(\frac{p}{r}\right)^2\frac{p}{r_0} + \right.$$

$$+ \left(\frac{p}{r_0}\right)^2\left(\frac{p}{r_0}-1\right) - \left(\frac{p}{r}+1\right)\left(\frac{p}{r_0}+1\right)e\sin\vartheta_0\sin\varphi - $$

$$- \left(\frac{p}{r}+1\right)e^2\sin\vartheta\sin\vartheta_0 + \left(\frac{p}{r_0}+1\right)e^2\sin^2\vartheta_0\right] = \frac{ra}{p^2}\left[(1-e^2)(1+e\cos\vartheta_0) + \right.$$

173

$$+ (1 + 2e\cos\vartheta_0 + e^2\cos^2\vartheta_0)\left(\frac{p}{r} + 1\right)\cos\varphi -$$

$$- 2(1 + e\cos\vartheta)^2(1 + e\cos\vartheta_0) + (1 + e\cos\vartheta_0)^2 e\cos\vartheta_0 -$$

$$- (2 + e\cos\vartheta)(2 + e\cos\vartheta_0)e\sin\vartheta_0\sin\varphi -$$

$$- \left(\frac{p}{r} + 1\right)e^2(\cos\vartheta\cos\vartheta_0 + \sin\vartheta\sin\vartheta_0) +$$

$$+ \left(\frac{p}{r} + 1\right)e^2\cos\vartheta\cos\vartheta_0 + (2 + e\cos\vartheta_0)e^2\sin^2\vartheta_0\Big] =$$

$$= \frac{ra}{p^2}\Big[(1 - e^2)\left(\frac{p}{r} + 1\right)\cos\varphi + (1 - e^2)(1 + e\cos\vartheta_0) +$$

$$+ (2e\cos\vartheta_0 + e^2\cos^2\vartheta_0)(2 + e\cos\vartheta)\cos\varphi -$$

$$- 2(1 + 2e\cos\vartheta + e^2\cos^2\vartheta)(1 + e\cos\vartheta_0) +$$

$$+ (1 + 2e\cos\vartheta_0 + e^2\cos^2\vartheta_0)e\cos\vartheta_0 -$$

$$- (4 + 2e\cos\vartheta + 2e\cos\vartheta_0 + e^2\cos\vartheta\cos\vartheta_0)e\sin\vartheta_0\sin\varphi +$$

$$+ (2 + e\cos\vartheta)e^2\cos\vartheta\cos\vartheta_0 +$$

$$+ (2 + e\cos\vartheta_0)e^2\sin^2\vartheta_0\Big] = \left(1 + \frac{r}{p}\right)\cos\varphi +$$

$$+ \frac{ra}{p^2}[-1 + e(\cos\vartheta_0 + 4\cos\vartheta_0\cos\varphi - 2\cos\vartheta_0 - 4\cos\vartheta +$$

$$+ \cos\vartheta_0 - 4\sin\vartheta_0\sin\varphi) + e^2(-1 + 2\cos^2\vartheta_0\cos\varphi +$$

$$+ 2\cos\vartheta\cos\vartheta_0\cos\varphi - 2\cos^2\vartheta - 4\cos\vartheta\cos\vartheta_0 +$$

$$+ 2\cos^2\vartheta_0 - 2\cos\vartheta\sin\vartheta_0\sin\varphi - 2\cos\vartheta_0\sin\vartheta_0\sin\varphi +$$

$$+ 2\cos\vartheta\cos\vartheta_0 + 2\sin^2\vartheta_0) + e^3(-\cos\vartheta_0 +$$

$$+ \cos^2\vartheta_0\cos\vartheta\cos\varphi - 2\cos^2\vartheta\cos\vartheta_0 + \cos^3\vartheta_0 +$$

$$+ \cos\vartheta\cos\vartheta_0\sin\vartheta_0\sin\varphi + \cos^2\vartheta\cos\vartheta_0 + \cos\vartheta_0\sin^2\vartheta_0)] =$$

$$= \left(1 + \frac{r}{p}\right)\cos\varphi + \frac{ra}{p^2}\{-1 + 4e[\cos(\varphi + \vartheta_0) - \cos\vartheta] +$$

$$+ e^2[-1 + 2\cos\vartheta_0\cos(\varphi + \vartheta_0) + 2\cos\vartheta\cos(\varphi + \vartheta_0) -$$

$$- 2\cos^2\vartheta - 2\cos\vartheta\cos\vartheta_0 + 2\cos^2\vartheta_0 + 2\sin^2\vartheta_0] +$$

$$+ e^3[-\cos\vartheta_0 + \cos\vartheta\cos\vartheta_0\cos(\varphi + \vartheta_0) -$$

$$- \cos^2\vartheta\cos\vartheta_0 + \cos^3\vartheta_0 + \cos\vartheta_0\sin^2\vartheta_0]\} =$$

$$= \left(1 + \frac{r}{p}\right)\cos\varphi - \frac{ra}{p^2}(1 - e^2) = \left(1 + \frac{r}{p}\right)\cos\varphi - \frac{r}{p}, \qquad (10.84)$$

$$\left(\frac{\partial v_p}{\partial n_0}\right)_t = F - \frac{v_u}{r}\left(\frac{\partial n}{\partial n_0}\right)_t, \qquad (10.85)$$

where

$$F = \frac{1}{r_0}\left[\left(\frac{\partial v_r}{\partial u_0}\right)_t + v_{u0}\left(\frac{\partial v_r}{\partial v_{r0}}\right)_t - v_{r0}\left(\frac{\partial v_r}{\partial v_{u0}}\right)_t\right] =$$

$$= \frac{a}{r_0}\left[-\frac{3v_{r0}v_{u0}}{r^2}\left(\frac{p}{r} - 1\right)t + v_{u0}\frac{p}{r^2}\cos\varphi - v_{u0}\frac{2r_0}{r^2}\left(\frac{p}{r} - 1\right) -$$

$$- \frac{v_r v_{r0}v_{u0}}{\mu} + \frac{3v_u v_{r0}}{rr_0}\left(\frac{p}{r} - 1\right)t - v_{r0}\frac{p}{r^2}\left(1 + \frac{r_0}{p}\right)\sin\varphi -$$

$$- \frac{v_r v_{r0}}{r}\sqrt{\frac{p}{\mu}}\left(\frac{r_0}{r} - \frac{r}{r_0}\right)\right] = \frac{a}{r_0}\left[v_{u0}\frac{p}{r^2}\cos\varphi -$$

$$- v_{u0}\frac{2r_0}{r^2}\left(\frac{p}{r} - 1\right) - v_{r0}\frac{p}{r^2}\left(1 + \frac{r_0}{p}\right)\sin\varphi - \frac{r_0 v_r v_{r0}}{r^2}\sqrt{\frac{p}{\mu}}\right] =$$

$$= \frac{a}{p}\frac{v_u}{r}\left[\left(\frac{p}{r_0}\right)^2\cos\varphi - 2\frac{p}{r_0}\left(\frac{p}{r} - 1\right) - e\sin\vartheta_0\left(\frac{p}{r_0} + 1\right)\sin\varphi -$$

$$- e^2\sin\vartheta\sin\vartheta_0\right] = \frac{a}{p}\frac{v_u}{r}[(1 + 2e\cos\vartheta_0 + e^2\cos^2\vartheta_0)\cos\varphi -$$

$$- 2(1 + e\cos\vartheta_0)e\cos\vartheta - (2 + e\cos\vartheta_0)e\sin\vartheta_0\sin\varphi - e^2\sin\vartheta\sin\vartheta_0] =$$

$$= \frac{a}{p}\frac{v_u}{r}[\cos\varphi + 2e(\cos\vartheta_0\cos\varphi - \cos\vartheta - \sin\vartheta_0\sin\varphi) + e^2(\cos^2\vartheta_0\cos\varphi - 2\cos\vartheta\cos\vartheta_0 -$$

$$- \cos\vartheta_0\sin\vartheta_0\sin\varphi - \sin\vartheta\sin\vartheta_0)] = \frac{a}{p}\frac{v_u}{r}\{\cos\varphi +$$

$$+ e^2[\cos\vartheta_0\cos(\varphi + \vartheta_0) - 2\cos\vartheta\cos\vartheta_0 - \sin\vartheta\sin\vartheta_0]\} = \frac{a}{p}\frac{v_u}{r}\cos\varphi(1 - e^2) = \frac{v_u}{r}\cos\varphi.$$

174

Substituting this expression in (10.85) and making use of (10.84), we find

$$\left(\frac{\partial v_\rho}{\partial n_0}\right)_t = \frac{v_u}{p}(1-\cos\varphi) = \frac{1}{r}\sqrt{\frac{\mu}{p}}\,(1-\cos\varphi).$$

(10.86)

To determine the derivative $\left(\frac{\partial v_n}{\partial n_0}\right)_t$, we make use of equality (10.62), which gives

$$\left(\frac{\partial v_u}{\partial v_{r0}}\right)_t = \left(\frac{\partial v_u}{\partial v_{r0}}\right)_\varphi + \frac{v_r v_u}{r}\left(\frac{\partial t}{\partial v_{r0}}\right)_\varphi, \quad \left(\frac{\partial u}{\partial v_{r0}}\right)_t = -\frac{v_u}{r}\left(\frac{\partial t}{\partial v_{r0}}\right)_\varphi,$$

$$\left(\frac{\partial v_u}{\partial v_{u0}}\right)_t = \left(\frac{\partial v_u}{\partial v_{u0}}\right)_\varphi + \frac{v_r v_u}{r}\left(\frac{\partial t}{\partial v_{u0}}\right)_\varphi, \quad \left(\frac{\partial u}{\partial v_{u0}}\right)_t = -\frac{v_u}{r}\left(\frac{\partial t}{\partial v_{u0}}\right)_\varphi.$$

(10.87)

Thus

$$\left(\frac{\partial v_u}{\partial v_{r0}}\right)_t = \left(\frac{\partial v_u}{\partial v_{r0}}\right)_\varphi - v_r\left(\frac{\partial u}{\partial v_{r0}}\right)_t, \quad \left(\frac{\partial v_u}{\partial v_{u0}}\right)_t = \left(\frac{\partial v_u}{\partial v_{u0}}\right)_\varphi - v_r\left(\frac{\partial u}{\partial v_{u0}}\right)_t.$$

(10.88)

Seeing that $\left(\frac{\partial v_u}{\partial u_0}\right)_t = 0$, we find

$$\left(\frac{\partial v_n}{\partial n_0}\right)_t = \frac{v_r}{r_0}\left[\left(\frac{\partial u}{\partial u_0}\right)_t + v_{u0}\left(\frac{\partial u}{\partial v_{r0}}\right)_t - v_{r0}\left(\frac{\partial u}{\partial v_{u0}}\right)_t\right] +$$

$$+ \frac{1}{r_0}\left\{v_{u0}\left[\left(\frac{\partial v_u}{\partial v_{r0}}\right)_\varphi - v_r\left(\frac{\partial u}{\partial v_{r0}}\right)_t\right] - v_{r0}\left[\left(\frac{\partial v_u}{\partial v_{u0}}\right)_\varphi - v_r\left(\frac{\partial u}{\partial v_{u0}}\right)_t\right]\right\} =$$

$$= \frac{1}{r_0}\left[v_r\left(\frac{\partial u}{\partial u_0}\right)_t + v_{u0}\left(\frac{\partial v_u}{\partial v_{r0}}\right)_\varphi - v_{r0}\left(\frac{\partial v_u}{\partial v_{u0}}\right)_\varphi\right].$$

Substituting the corresponding derivatives from Tables 10.1 and 10.3, we obtain

$$\left(\frac{\partial v_n}{\partial n_0}\right)_t = \frac{1}{r_0}\left\{v_r - v_{u0}\sin\varphi + v_{r0}\left[\frac{r_0}{p} - \left(1 + \frac{r_0}{p}\right)\cos\varphi\right]\right\} =$$

$$= \frac{1}{p}\left[\frac{p}{r_0}v_r - \left(\frac{p}{r_0}\right)^2\sqrt{\frac{\mu}{p}}\,\sin\varphi + v_{r0} - v_{r0}\left(\frac{p}{r_0} + 1\right)\cos\varphi\right] =$$

$$= \frac{1}{p}\left\{v_r - \sqrt{\frac{\mu}{p}}\,\sin\varphi + v_{r0} + \sqrt{\frac{\mu}{p}}\,[e^2\cos\vartheta_0\sin\vartheta -$$

$$- (2e\cos\vartheta_0 + e^2\cos^2\vartheta_0)\sin\varphi - e\sin\vartheta_0(2 + e\cos\vartheta_0)\cos\varphi]\right\} =$$

$$= \frac{1}{p}\left\{v_r - \sqrt{\frac{\mu}{p}}\,\sin\varphi + v_{r0} + \sqrt{\frac{\mu}{p}}\,[-2e\sin(\vartheta_0 + \varphi) +$$

$$+ e^2\sin\vartheta\cos\vartheta_0 - e^2\cos\vartheta_0\sin(\vartheta_0 + \varphi)]\right\} =$$

$$= -\frac{1}{p}\left(v_r - v_{r0} + \sqrt{\frac{\mu}{p}}\,\sin\varphi\right).$$

(10.89)

The derivatives $\left(\frac{\partial v_\rho}{\partial \rho_0}\right)_t$, $\left(\frac{\partial v_\rho}{\partial v_{\rho_0}}\right)_t$ and $\left(\frac{\partial v_\rho}{\partial v_{n_0}}\right)_t$ are determined similarly:

$$\left(\frac{\partial v_\rho}{\partial \rho_0}\right)_t = -v_u\left(\frac{\partial u}{\partial r_0}\right)_t + \left(\frac{\partial v_r}{\partial r_0}\right)_t =$$

$$= a\left\{\frac{3v_u^2}{rr_0^2}t - \frac{v_u}{r}\sqrt{\frac{p}{\mu}}\left[\frac{v_r}{r_0} - \frac{v_{r0}}{r} + \frac{r}{r_0 p}(v_r - v_{r0})\right] -$$

$$- \frac{v_u}{rr_0}\left(1 + \frac{r}{p}\right)\sin\varphi - \frac{3\mu}{r^2 r_0^2}\left(\frac{p}{r} - 1\right)t + \frac{v_u}{rr_0}\sin\varphi + \frac{v_{r0}}{r^2} - \frac{v_r}{r_0^2} + \frac{p}{r^2}\left(\frac{v_r}{r_0} - \frac{v_{r0}}{r}\right)\right\} =$$

$$= a\left(\frac{3\mu}{r^2 r_0^2}t - \frac{v_r - v_{r0}}{rr_0} - \frac{v_u}{r_0 p}\sin\varphi + \frac{v_{r0}}{r^2} - \frac{v_r}{r_0^2}\right) =$$

$$= a\left[\frac{3\mu}{r^2 r_0^2}t - \sqrt{\frac{\mu}{p}}\,\frac{\sin\varphi}{rr_0} + \left(\frac{1}{r_0} + \frac{1}{r}\right)\left(\frac{v_{r0}}{r} - \frac{v_r}{r_0}\right)\right].$$

(10.90)

175

TABLE 10.4

	$/\partial\rho_0$	$/\partial n_0$	$/\partial v_{\rho_0}$	$/\partial v_{n_0}$
$\partial\rho/$	$a\left[-\dfrac{3v_\rho}{r_0^2}t + \dfrac{1}{r_0}\left(2\dfrac{r}{r_0} - \dfrac{p}{r} + 1 - \cos\varphi\right) - \dfrac{v_\rho v_{\rho_0}}{\mu}\right]$	$\sin\varphi$	$a\left[-\dfrac{3v_\rho v_{\rho_0}}{\mu}t + \dfrac{2}{\mu}(rv_{\rho_0} - r_0 v_\rho) + \sqrt{\dfrac{p}{\mu}}\sin\varphi\right]$	$a\sqrt{\dfrac{p}{\mu}}\left[-\dfrac{3v_\rho}{r_0}t - \left(1+\dfrac{r_0}{p}\right)\cos\varphi + 2\dfrac{r}{r_0} - \dfrac{r_0}{p}\left(\dfrac{p}{r}-1\right)\right]$
$\partial n/$	$a\left\{-\dfrac{3v_n}{r_0^2}t + \sqrt{\dfrac{p}{\mu}}\left[\dfrac{v_\rho}{r_0} - \dfrac{v_{\rho_0}}{r} + \dfrac{r}{r_0 p}(v_\rho - v_{\rho_0})\right] + \dfrac{1}{r_0}\left(1+\dfrac{r}{p}\right)\sin\varphi\right\}$	$\left(1+\dfrac{r}{p}\right)\cos\varphi - \dfrac{r}{p}$	$a\sqrt{\dfrac{p}{\mu}}\left[-\dfrac{3v_{\rho_0}}{r}t + \left(1+\dfrac{r}{p}\right)\cos\varphi - 2\dfrac{r_0}{r} + \dfrac{r}{p}\left(\dfrac{p}{r_0}-1\right)\right]$	$a\sqrt{\dfrac{p}{\mu}}\left\{-\dfrac{3v_{n_0}}{r}t + \left(1+\dfrac{r}{p}\right)\left(1+\dfrac{r_0}{p}\right)\sin\varphi + \dfrac{1}{\sqrt{\mu p}}\left[\left(1+\dfrac{r}{p}\right)r_0 v_\rho - \left(1+\dfrac{r_0}{p}\right)r v_{\rho_0}\right]\right\}$
$\partial v_\rho/$	$a\left[\dfrac{3\mu}{r^2 r_0^2}t - \sqrt{\dfrac{\mu}{p}}\dfrac{\sin\varphi}{r r_0} + \left(\dfrac{1}{r_0}+\dfrac{1}{r}\right)\left(\dfrac{v_{\rho_0}}{r}-\dfrac{v_\rho}{r_0}\right)\right]$	$\dfrac{1}{r}\sqrt{\dfrac{\mu}{p}}\times(1-\cos\varphi)$	$a\left[\dfrac{3v_{\rho_0}}{r^2}t - \dfrac{1}{r}\left(\dfrac{p}{r_0}+\cos\varphi-1\right) + 2\dfrac{r_0}{r^2} - \dfrac{v_\rho v_{\rho_0}}{\mu}\right]$	$a\left\{\dfrac{3v_{n_0}}{r^2}t - \dfrac{1}{r}\left(1+\dfrac{r_0}{p}\right)\sin\varphi + \sqrt{\dfrac{p}{\mu}}\left[\dfrac{v_{\rho_0}}{r}-\dfrac{v_\rho}{r_0} + \dfrac{r_0}{pr}(v_{\rho_0}-v_\rho)\right]\right\}$
$\partial v_n/$	$-\dfrac{v_{n_0}}{p}(1-\cos\varphi)$	$-\dfrac{1}{p}\left(v_\rho - v_{\rho_0} + \sqrt{\dfrac{\mu}{p}}\sin\varphi\right)$	$-\sin\varphi$	$\left(1+\dfrac{r_0}{p}\right)\cos\varphi - \dfrac{r_0}{p}$

$$\left(\frac{\partial v_\rho}{\partial v_{\rho_0}}\right)_t = -v_u\left(\frac{\partial u}{\partial v_{r0}}\right)_t + \left(\frac{\partial v_r}{\partial v_{r0}}\right)_t = a\left[\frac{3v_{r0}v_u^2}{\mu r}t - \frac{v_u^2}{\mu}\left(1+\frac{r}{p}\right)\cos\varphi + \frac{2v_u^2}{\mu}\frac{r_0}{r} - \frac{v_u^2}{\mu}\frac{r}{p}\left(\frac{p}{r_0}-1\right) - \right.$$

$$\left. - \frac{3v_{r0}}{r^2}\left(\frac{p}{r}-1\right)t + \frac{p}{r^2}\cos\varphi - \frac{2r_0}{r^2}\left(\frac{p}{r}-1\right) - \frac{v_r v_{r0}}{\mu}\right] =$$

$$= a\left[\frac{3v_{r0}}{r^2}t - \frac{\cos\varphi}{r} - \frac{1}{r}\left(\frac{p}{r_0}-1\right) + 2\frac{r_0}{r^2} - \frac{v_r v_{r0}}{\mu}\right] =$$

$$= a\left[\frac{3v_{r0}}{r^2}t - \frac{1}{r}\left(\frac{p}{r_0}+\cos\varphi-1\right) + 2\frac{r_0}{r^2} - \frac{v_r v_{r0}}{\mu}\right]. \tag{10.91}$$

$$\left(\frac{\partial v_\rho}{\partial v_{n_0}}\right)_t = -v_u\left(\frac{\partial u}{\partial v_{u0}}\right)_t + \left(\frac{\partial v_r}{\partial v_{u0}}\right)_t =$$

$$= a\left\{\frac{3v_u^2 v_{u0}}{\mu r}t - \frac{v_u^2}{\mu}\left(1+\frac{r}{p}\right)\left(1+\frac{r_0}{p}\right)\sin\varphi - \right.$$

$$- \frac{v_u^2}{\mu\sqrt{\mu p}}\left[\left(1+\frac{r}{p}\right)r_0 v_r - \left(1+\frac{r_0}{p}\right)r v_{r0}\right] - \frac{3v_u}{rr_0}\left(\frac{p}{r}-1\right)t +$$

$$+ \frac{p}{r^2}\left(1+\frac{r_0}{p}\right)\sin\varphi + \frac{v_r}{r}\sqrt{\frac{\mu}{p}}\left(\frac{r_0}{r}-\frac{r}{r_0}\right)\right\} =$$

$$= a\left\{\frac{3v_{u0}}{r^2}t - \frac{1}{r}\left(1+\frac{r_0}{p}\right)\sin\varphi + \sqrt{\frac{p}{\mu}}\left[-\left(1+\frac{r}{p}\right)\frac{r_0 v_r}{r^2} + \right.\right.$$

$$\left.\left. + \left(1+\frac{r_0}{p}\right)\frac{v_{r0}}{r} + \frac{v_r}{r}\left(\frac{r_0}{r}-\frac{r}{r_0}\right)\right]\right\} =$$

$$= a\left\{\frac{3v_{u0}}{r^2}t - \frac{1}{r}\left(1+\frac{r_0}{p}\right)\sin\varphi + \sqrt{\frac{p}{\mu}}\left[\frac{v_{r0}}{r} - \frac{v_r}{r_0} + \frac{r_0}{pr}(v_{r0}-v_r)\right]\right\}. \tag{10.92}$$

In calculating the derivatives $\left(\frac{\partial v_n}{\partial q_j}\right)_t$ $(q_j = \rho_0,\, v_{\rho_0},\, v_{n_0})$, we make use of relations (10.88) and the analogous equality

$$\left(\frac{\partial v_u}{\partial r_0}\right)_t = \left(\frac{\partial v_u}{\partial r_0}\right)_\varphi - v_r\left(\frac{\partial u}{\partial r_0}\right)_t. \tag{10.93}$$

Substituting in the last row in the right-hand side of (10.82), we find

$$\left(\frac{\partial v_n}{\partial \rho_0}\right)_t = \left(\frac{\partial v_u}{\partial r_0}\right)_\varphi,\quad \left(\frac{\partial v_n}{\partial v_{\rho_0}}\right)_t = \left(\frac{\partial v_u}{\partial v_{r0}}\right)_\varphi,\quad \left(\frac{\partial v_n}{\partial v_{n_0}}\right)_t = \left(\frac{\partial v_u}{\partial v_{u0}}\right)_\varphi. \tag{10.94}$$

Hence it follows that the derivatives can be determined from the last row in Table 10.1.

Substituting (in accordance with (10.79)) v_ρ and v_n for v_r and v_u in the resulting expressions for the matrix elements of $\left\|\frac{\partial \rho,\, n,\, v_\rho,\, v_n}{\partial \rho_0,\, n_0,\, v_{\rho_0},\, v_{n_0}}\right\|_t$, we obtain the final formulas listed in Table 10.4. Note that the expressions for these matrix elements can be directly derived by the method proposed by V. I. Charnyi /31/.

10.12. THE CASE OF MOTION IN ELLIPTICAL ORBIT

We see from Tables 10.1 — 10.4 that in elliptical orbit, any of the derivatives of the current parameters with respect to the initial conditions of motion can be written in the general form

$$\left(\frac{\partial p_i}{\partial q_j}\right)_s = \left(\frac{\partial p_i}{\partial q_j}\right)_s^{\text{sec}} + \left(\frac{\partial p_i}{\partial q_j}\right)_s^{\text{mix}} + \left(\frac{\partial p_i}{\partial q_j}\right)_s^{\text{per}}. \tag{10.95}$$

where $\left(\dfrac{\partial p_i}{\partial q_j}\right)_s^{\text{sec}}$ is the secular term which increases linearly with flight

time t,

$\left(\dfrac{\partial p_i}{\partial q_j}\right)^{\text{per}}$ is the periodic term with a period equal to the orbital

period P of the body,

$\left(\dfrac{\partial p_i}{\partial q_j}\right)_s^{\text{mix}}$ a mixed term, which is a product of some periodic

function and flight time t.

As we have shown in Chapter 2 for the particular case of circular orbits, secular perturbing terms are much more effective than the periodic terms and, unlike the latter, they eventually cause substantial displacement of the satellite even if the initial perturbations are very small (see Table 2.1). The mixed perturbing terms may possess a similar property.

We see from Table 10.2 that the matrix $\left\|\dfrac{\partial \zeta,\ v_\zeta}{\partial \zeta_0,\ v_{\zeta_0}}\right\|$ is composed entirely of

periodic terms. The periodic displacements from the orbital plane described by this matrix have been analyzed in adequate detail in Sec. 9.6.

We shall therefore concentrate on the matrices $\left\|\dfrac{\partial r,\ t,\ v_r,\ v_u}{\partial r_0,\ u_0,\ v_{r0},\ v_{u0}}\right\|_\varphi$, $\left\|\dfrac{\partial r,\ t,\ v_r,\ v_u}{\partial r_0,\ t_0,\ v_{r0},\ v_{u0}}\right\|_\varphi$,

$\left\|\dfrac{\partial r,\ u,\ v_r,\ v_u}{\partial r_0,\ u_0,\ v_{r0},\ v_{u0}}\right\|_t$, and $\left\|\dfrac{\partial p,\ n,\ v_p,\ v_n}{\partial p_0,\ n_0,\ v_{p_0},\ v_{n_0}}\right\|_t$, which describe in-plane displacements.

We see from Tables 10.1, 10.3, 10.4 and from expressions (10.60) that the elements of these matrices contain secular and mixed terms. The matrices

$\left\|\dfrac{\partial r,\ t,\ v_r,\ v_u}{\partial r_0,\ u_0,\ v_{r0},\ v_{u0}}\right\|_\varphi$ and $\left\|\dfrac{\partial r,\ t,\ v_r,\ v_u}{\partial r_0,\ t_0,\ v_{r0},\ v_{u0}}\right\|_\varphi$ are the simplest: they contain no mixed

terms, while secular terms enter the derivatives $\left(\dfrac{\partial t}{\partial r_0}\right)_\varphi$, $\left(\dfrac{\partial t}{\partial v_{r0}}\right)_\varphi$, and $\left(\dfrac{\partial t}{\partial v_{u0}}\right)_\varphi$

only. This is so because small variations in the initial conditions of motion slightly distort the original orbit Σ into a perturbed orbit Σ' (Figure 10.6). Therefore, if the unperturbed and the perturbed points
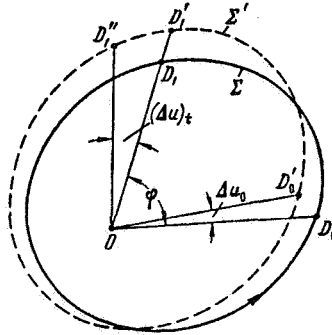
FIGURE 10.6. Relationship between the variations in current parameters of motion for constant time and constant distance from the initial position.

D_t and D_t' are on one radius through the center of attraction O (i.e., $\varphi = \text{const}$), perturbations in most of the parameters at the current point remain small, varying periodically in time. However, perturbation of the orbital period introduces a secular increment in the time of arrival at the perturbed

point D_1'. The distance between the perturbed point D_1' with $\varphi = \text{const}$ and the perturbed point D_1'' with $t = \text{const}$ increases monotonically. This in turn is responsible for the secular and the mixed components of the variations in the parameters of motion at the point D_1''.

Many of the mixed perturbations which obtain for $t = \text{const}$ are in fact long-periodic effects. Indeed, it follows from the preceding that the angle $(\Delta u)_t$ between the radii OD_1 and OD_1'' monotonically increases in time. When it becomes equal to $2\pi n$ (n an arbitrary integer), the variations in most of the parameters of motion for $t = \text{const}$ resume the initial small values, which are equal to the corresponding variations for $\varphi = \text{const}$. The only exception is the variation $(\Delta u)_t$, which is a pure secular, monotonically growing perturbation. Eventually, the distance between the points D_1 and D_1'' becomes substantial even if the initial perturbations are arbitrarily small. The linear relations (10.1) among the perturbations in the current parameters and the initial conditions of motion are therefore rendered meaningless. In other words, in elliptical orbit, relations (10.1) with $s = t$ apply only during some limited period. If $s = \varphi$, this time restriction is lifted, since under small initial perturbations the points D_1 and D_1'' are always close to each other. The perturbation $(\Delta t)_\varphi$ in the time of arrival at the current point is determined by varying relation (10.26), and the variations of all the parameters in the integrand are invariably small. Therefore, although the perturbation $(\Delta t)_\varphi$ increases indefinitely, the relative error of its determination from the linear relations remains small, provided the initial perturbations are fairly small.

It follows from the preceding that the matrices $\left\| \dfrac{\partial r,\ t,\ v_r,\ v_u}{\partial r_0,\ u_0,\ v_{r0},\ v_{u0}} \right\|_\varphi$ and

$\left\| \dfrac{\partial r,\ t,\ v_r,\ v_u}{\partial r_0,\ t_0,\ v_{r0},\ v_{u0}} \right\|_\varphi$ are more convenient than the matrices $\left\| \dfrac{\partial r,\ u,\ v_r,\ v_u}{\partial r_0,\ u_0,\ v_{r0},\ v_{u0}} \right\|_t$ and

$\left\| \dfrac{\partial p,\ n,\ v_p,\ v_n}{\partial p_0,\ n_0,\ v_{p_0},\ v_{n_0}} \right\|_t$ for the analysis of the effect of small initial perturbations.

Moreover, as we see from Tables 10.1, 10.3, 10.4 and relations (10.60), the expressions for most of the entries in the first pair of matrices are simpler. As regards the matrices for $t = \text{const}$, they should be used in determining the variations in parameters which are definitely known to be related to a certain epoch (e. g., in treatment and analysis of orbital measurements).

In analyzing the influence of initial perturbations on motion in elliptical orbit, we often consider the contribution from secular terms only, as these are decisive. In such cases it is convenient to replace the previous set of initial conditions r_0, u_0, v_{r0}, v_{u0} with the set r_0, u_0, a, θ_0, where a and θ_0 are respectively the semimajor axis of the orbit and the inclination of the initial velocity vector to the local horizon:

$$ a = \frac{r_0}{2 - \dfrac{r_0 (v_{r0}^2 + v_{u0}^2)}{\mu}}, \quad \mathrm{tg}\,\theta_0 = \frac{v_{r0}}{v_{u0}}, \quad -\frac{\pi}{2} \leqslant \theta_0 \leqslant \frac{\pi}{2}. \tag{10.96} $$

Making use of (10.5), we obtain an expression for the corresponding matrix:

$$ \left\| \frac{\partial r,\ t,\ v_r,\ v_u}{\partial r_0,\ u_0,\ a,\ \theta_0} \right\|_\varphi = \left\| \frac{\partial r,\ t,\ v_r,\ v_u}{\partial r_0,\ u_0,\ v_{r0},\ v_{u0}} \right\|_\varphi \left\| \frac{\partial r_0,\ u_0,\ v_{r0},\ v_{u0}}{\partial r_0,\ u_0,\ a,\ \theta_0} \right\|. \tag{10.97} $$

To calculate the matrix elements of $\left\|\dfrac{\partial r_0,\ u_0,\ v_{r0},\ v_{u0}}{\partial r_0,\ u_0,\ a,\ \theta_0}\right\|$, we make use of the relations

$$v_0^2 = \frac{2\mu}{r_0} - \frac{\mu}{a}, \quad v_{r0} = v_0 \sin\theta_0, \quad v_{u0} = v_0 \cos\theta_0,$$

where $v_0 = \sqrt{v_{r0}^2 + v_{u0}^2}$ is the magnitude of the initial velocity vector. Hence

$$\frac{\partial v_0}{\partial r_0} = -\frac{\mu}{v_0 r_0^2}, \quad \frac{\partial v_0}{\partial a} = \frac{\mu}{2v_0 a^2}, \quad \frac{\partial v_0}{\partial u_0} = \frac{\partial v_0}{\partial \theta_0} = 0,$$

$$\frac{\partial v_{r0}}{\partial v_0} = \frac{v_{r0}}{v_0}, \quad \frac{\partial v_{r0}}{\partial \theta_0} = v_{u0}, \quad \frac{\partial v_{u0}}{\partial v_0} = \frac{v_{u0}}{v_0}, \quad \frac{\partial v_{u0}}{\partial \theta_0} = -v_{r0}.$$

Thus

$$\frac{\partial v_{r0}}{\partial r_0} = \frac{\partial v_{r0}}{\partial v_0}\frac{\partial v_0}{\partial r_0} = -\frac{\mu v_{r0}}{v_0^2 r_0^2}, \quad \frac{\partial v_{r0}}{\partial a} = \frac{\partial v_{r0}}{\partial v_0}\frac{\partial v_0}{\partial a} = \frac{\mu v_{r0}}{2 v_0^2 a^2},$$

$$\frac{\partial v_{r0}}{\partial \theta_0} = v_{u0}, \quad \frac{\partial v_{r0}}{\partial u_0} = 0,$$

$$\frac{\partial v_{u0}}{\partial r_0} = \frac{\partial v_{u0}}{\partial v_0}\frac{\partial v_0}{\partial r_0} = -\frac{\mu v_{u0}}{v_0^2 r_0^2}, \quad \frac{\partial v_{u0}}{\partial a} = \frac{\partial v_{u0}}{\partial v_0}\frac{\partial v_0}{\partial a} = \frac{\mu v_{u0}}{2 v_0^2 a^2},$$

$$\frac{\partial v_{u0}}{\partial \theta_0} = -v_{r0}, \quad \frac{\partial v_{u0}}{\partial u_0} = 0.$$

Finally

$$\left\|\frac{\partial r_0,\ u_0,\ v_{r0},\ v_{u0}}{\partial r_0,\ u_0,\ a,\ \theta_0}\right\| = \left\|\begin{matrix} 1 & 0 & 0 & 0 \\ 0 & 1 & 0 & 0 \\ -\dfrac{\mu v_{r0}}{v_0^2 r_0^2} & 0 & \dfrac{\mu v_{r0}}{2 v_0^2 a^2} & v_{u0} \\ -\dfrac{\mu v_{u0}}{v_0^2 r_0^2} & 0 & \dfrac{\mu v_{r0}}{2 v_0^2 a^2} & -v_{r0} \end{matrix}\right\|. \tag{10.98}$$

Substituting this matrix in the right-hand side of (10.97) and applying Table 10.1, we see that the secular terms appear in none of the matrix elements of $\left\|\dfrac{\partial r_0,\ t_0,\ v_{r0},\ v_{u0}}{\partial r_0,\ u_0,\ a,\ \theta_0}\right\|_\varphi$, with the exception of the derivative $\left(\dfrac{\partial t}{\partial a}\right)_\varphi$. The secular component of this derivative is calculated from

$$\left(\frac{\partial t}{\partial a}\right)_\varphi^{\text{sec}} = \frac{3}{2}\frac{t}{a}. \tag{10.99}$$

If the orbital period P from (5.36), and not the semimajor axis a, is introduced as the independent initial condition, it follows from (10.99) that

$$\left(\frac{\partial t}{\partial P}\right)_\varphi^{\text{sec}} = \left(\frac{\partial t}{\partial a}\right)_\varphi^{\text{sec}}\frac{\partial a}{\partial P} = \frac{t}{P}. \tag{10.100}$$

10.13. INVERSION OF MATRICES

In some problems, we seek the variations Δq_j in the initial conditions from known small disturbances $(\Delta p_i)_s$ in the current parameters of motion. Left-multiplying equality (10.2) by the inverse of the matrix $\left\| \dfrac{\partial p_1,\ p_2,\ \ldots,\ p_6}{\partial q_1,\ q_2,\ \ldots,\ q_6} \right\|_s$, we find

$$(\Delta q) = \left\| \frac{\partial q_1,\ q_2,\ \ldots,\ q_6}{\partial p_1,\ p_2,\ \ldots,\ p_6} \right\|_s (\Delta p)_s, \tag{10.101}$$

where

$$\left\| \frac{\partial q_1,\ q_2,\ \ldots,\ q_6}{\partial p_1,\ p_2,\ \ldots,\ p_6} \right\|_s = \left\| \frac{\partial p_1,\ p_2,\ \ldots,\ p_6}{\partial q_1,\ q_2,\ \ldots,\ q_6} \right\|_s^{-1}. \tag{10.102}$$

The problem thus reduces to the inversion of a matrix whose elements are partial derivatives of the current parameters with respect to the initial conditions.

If the sets of current parameters and initial conditions are symmetric, i.e., if they are defined in one system of coordinates, for the same initial and current positions, as the case is for the matrices

$$\left\| \frac{\partial r,\ t,\ v_r,\ v_u}{\partial r_0,\ t_0,\ v_{r0},\ v_{u0}} \right\|_\varphi, \quad \left\| \frac{\partial r,\ u,\ v_r,\ v_u}{\partial r_0,\ u_0,\ v_{r0},\ v_{u0}} \right\|_t \quad \text{and} \quad \left\| \frac{\partial \rho,\ n,\ v_\rho,\ v_n}{\partial \rho_0,\ n_0,\ v_{\rho_0},\ v_{n_0}} \right\|_t,$$

the problem can be solved without going into the cumbersome calculation of inverse matrices. It suffices to make use of the fact that the initial equations of motion (4.3) can be solved not only for positive, but also for negative time. All the previous relations remain in force (since it is only the coordinates of the body and their second derivatives which explicitly enter equations (4.3); these equations do not contain the time and any of the odd derivatives of position). If negative time is introduced, the current parameters and the initial conditions of motion are interchanged. Hence it follows that the expressions for the matrix elements of the inverse (i.e., for the partial derivatives of the initial conditions with respect to the current parameters of motion) can be obtained from the expressions for the elements of the original matrix on substitution of $-t$ for t, $-\varphi$ for φ, q_j for p_i, p_i for q_j. In other words,

$$\frac{\partial q_i}{\partial p_j}(t,\ \varphi,\ p_k,\ q_l) = \frac{\partial p_i}{\partial q_j}(-t,\ -\varphi,\ q_l,\ p_k) \quad (k,\ l = 1,\ 2,\ \ldots,\ 6). \tag{10.103}$$

For example, from Table 10.4 we have

$$\left. \begin{aligned} \frac{\partial \rho_0}{\partial \rho} &= a\left[\frac{3v_{\rho_0}}{r^2}t + \frac{1}{r}\left(2\frac{r_0}{r} - \frac{p}{r_0} + 1 - \cos\varphi \right) - \frac{v_\rho v_{\rho_0}}{\mu} \right], \\ \frac{\partial \rho_0}{\partial n} &= -\sin\varphi, \\ \frac{\partial \rho_0}{\partial v_\rho} &= a\left[\frac{3v_\rho v_{\rho_0}}{\mu}t + \frac{2}{\mu}\left(r_0 v_\rho - r v_{\rho_0} \right) - \sqrt{\frac{p}{\mu}}\sin\varphi \right], \ \text{etc.} \end{aligned} \right\} \tag{10.104}$$

Charnyi /31/ has shown that the calculation of the inverse is considerably simplified if the problems are solved in rectangular coordinates for constant

time. In this case, the matrix elements of the inverse need not be computed. They are derived from the entries in the original matrix by a sequence of transpositions and permutations. Transposing some of the rows and the columns in the matrices, we write

$$\left\| \frac{\partial \rho,\, n,\, \zeta,\, v_\rho,\, v_n,\, v_\zeta}{\partial \rho_0,\, n_0,\, \zeta_0,\, v_{\rho_0},\, v_{n_0},\, v_{\zeta_0}} \right\|_t = \left\|\begin{array}{cc} \left\| \dfrac{\partial \rho,\, n,\, \zeta}{\partial \rho_0,\, n_0,\, \zeta_0} \right\|_t & \left\| \dfrac{\partial \rho,\, n,\, \zeta}{\partial v_{\rho_0},\, v_{n_0},\, v_{\zeta_0}} \right\|_t \\[2mm] \left\| \dfrac{\partial v_\rho,\, v_n,\, v_\zeta}{\partial \rho_0,\, n_0,\, \zeta_0} \right\|_t & \left\| \dfrac{\partial v_\rho,\, v_n,\, v_\zeta}{\partial v_{\rho_0},\, v_{n_0},\, v_{\zeta_0}} \right\|_t \end{array}\right\| ,$$

$$\left\| \frac{\partial \rho_0,\, n_0,\, \zeta_0,\, v_{\rho_0},\, v_{n_0},\, v_{\zeta_0}}{\partial \rho,\, n,\, \zeta,\, v_\rho,\, v_n,\, v_\zeta} \right\|_t = \left\|\begin{array}{cc} \left\| \dfrac{\partial \rho_0,\, n_0,\, \zeta_0}{\partial \rho,\, n,\, \zeta} \right\|_t & \left\| \dfrac{\partial \rho_0,\, n_0,\, \zeta_0}{\partial v_\rho,\, v_n,\, v_\zeta} \right\|_t \\[2mm] \left\| \dfrac{\partial v_{\rho_0},\, v_{n_0},\, v_{\zeta_0}}{\partial \rho,\, n,\, \zeta} \right\|_t & \left\| \dfrac{\partial v_{\rho_0},\, v_{n_0},\, v_{\zeta_0}}{\partial v_\rho,\, v_n,\, v_\zeta} \right\|_t \end{array}\right\| ,$$

where

$$\left\| \frac{\partial \rho,\, n,\, \zeta}{\partial \rho_0,\, n_0,\, \zeta_0} \right\|_t = \left\| \begin{array}{ccc} \left(\dfrac{\partial \rho}{\partial \rho_0}\right)_t & \left(\dfrac{\partial \rho}{\partial n_0}\right)_t & 0 \\[2mm] \left(\dfrac{\partial n}{\partial \rho_0}\right)_t & \left(\dfrac{\partial n}{\partial n_0}\right)_t & 0 \\[2mm] 0 & 0 & \left(\dfrac{\partial \zeta}{\partial \zeta_0}\right)_t \end{array} \right\| ,$$

$$\left\| \frac{\partial \rho,\, n,\, \zeta}{\partial v_{\rho_0},\, v_{n_0},\, v_{\zeta_0}} \right\|_t = \left\| \begin{array}{ccc} \left(\dfrac{\partial \rho}{\partial v_{\rho_0}}\right)_t & \left(\dfrac{\partial \rho}{\partial v_{n_0}}\right)_t & 0 \\[2mm] \left(\dfrac{\partial n}{\partial v_{\rho_0}}\right)_t & \left(\dfrac{\partial n}{\partial v_{n_0}}\right)_t & 0 \\[2mm] 0 & 0 & \left(\dfrac{\partial \zeta}{\partial v_{\zeta_0}}\right)_t \end{array} \right\| , \quad \text{etc.}$$

Then

$$\left\| \frac{\partial \rho_0,\, n_0,\, \zeta_0}{\partial \rho,\, n,\, \zeta} \right\|_t = \left\| \frac{\partial v_\rho,\, v_n,\, v_\zeta}{\partial v_{\rho_0},\, v_{n_0},\, v_{\zeta_0}} \right\|_t^* ,$$

$$\left\| \frac{\partial v_{\rho_0},\, v_{n_0},\, v_{\zeta_0}}{\partial v_\rho,\, v_n,\, v_\zeta} \right\|_t = \left\| \frac{\partial \rho,\, n,\, \zeta}{\partial \rho_0,\, n_0,\, \zeta_0} \right\|_t^* ,$$

$$\left\| \frac{\partial \rho_0,\, n_0,\, \zeta_0}{\partial v_\rho,\, v_n,\, v_\zeta} \right\|_t = -\left\| \frac{\partial \rho,\, n,\, \zeta}{\partial v_{\rho_0},\, v_{n_0},\, v_{\zeta_0}} \right\|_t^* ,$$

$$\left\| \frac{\partial v_{\rho_0},\, v_{n_0},\, v_{\zeta_0}}{\partial \rho,\, n,\, \zeta} \right\|_t = -\left\| \frac{\partial v_\rho,\, v_n,\, v_\zeta}{\partial \rho_0,\, n_0,\, \zeta_0} \right\|_t^* ,$$

(10.105)

where the asterisk $*$ denotes the transposed matrix.

Equalities (10.105) give the numerical values of the matrix elements of $\left\| \dfrac{\partial \rho_0,\, n_0,\, \zeta_0,\, v_{\rho_0},\, v_{n_0},\, v_{\zeta_0}}{\partial \rho,\, n,\, \zeta,\, v_\rho,\, v_n,\, v_\zeta} \right\|_t$ if the matrix elements of $\left\| \dfrac{\partial \rho,\, n,\, \zeta,\, v_\rho,\, v_n,\, v_\zeta}{\partial \rho_0,\, n_0,\, \zeta_0,\, v_{\rho_0},\, v_{n_0},\, v_{\zeta_0}} \right\|_t$ are known, and vice versa. The validity of relations (10.105) is easily proved on the basis of Tables 10.2, 10.4 and equality (10.103).

Chapter 11

THE INFLUENCE OF PERTURBING ACCELERATIONS
ON ORBITAL ELEMENTS

11.1. STATEMENT OF THE PROBLEM
AND FUNDAMENTAL RELATIONS

In previous chapters we have considered motion in a central gravitational field, defined by (1.2). As we have observed in Sec. 4.1, central gravity is the main driving force on a satellite which moves close to the Earth (or to any other primary), so that the orbital parameters computed for the ideal central force describe the main features of real motion of artificial satellites and other space vehicles. However, a more detailed analysis cannot ignore the contribution from the so-called pe rtu rb in g forces, the main ones being:

    (i)   noncentral components of the Earth's gravity which depart (in
          magnitude and direction) from the central force defined in (1.2);
   (ii)   air drag and other aerodynamic forces;
  (iii)   the pull of the Sun, the Moon, and the planets;
  (iv)   radiation pressure, etc.

In the sphere of the Earth's gravitational pull (and outside the dense atmosphere), these perturbing forces are small in comparison with the main central gravity component, but they nevertheless have a substantial influence on the orbital motion of satellites. The most significant effects include the so-called secular perturbations of the orbit, which eventually cause a substantial change in the nature of motion (even if the perturbing forces are very small; see Sec. 2.3).

The present chapter deals with the effect of various perturbing forces on the orbital motion. In our analysis we ignore the exact nature of these disturbing forces assuming, in general, that the satellite experiences two accelerations: the gravitational acceleration g defined by (4.2) and some perturbing acceleration j. The vector equation of motion (4.3) is then written in the form

$$\ddot{r} = -\frac{\mu}{r^3} r + j. \tag{11.1}$$

The contribution from each particular perturbing factor (producing a definite perturbing acceleration j) is considered in the chapters that follow.

Equations (11.1), in general, are not integrable in finite form. They are mostly solved by numerical integration. Numerical techniques, however, though highly useful for exact computations, are much too complicated to satisfy the requirements of qualitative analysis. Various approximate

183

methods of solution are much more convenient for qualitative investigation of (11.1). We shall use here the method of osculating elements, which essentially amounts to the following.

In practice, an orbit which corresponds to some solution of equation (11.1) is fully described by the dependence of the vectors r and $v=\dot{r}$ on flight time t. At any point D of the orbit, at some epoch $t=t_1$, we can always construct the so-called osculating orbit which is described by the vectors $\rho(t)$ and $\dot{\rho}(t)$ defined as follows:

$$\left.\begin{array}{l} \rho(t_1)=r(t_1), \\ \dot{\rho}(t_1)=\dot{r}(t_1), \\ \ddot{\rho}=-\frac{\mu}{\rho^3}\rho, \end{array}\right\} \tag{11.2}$$

where $\rho=|\rho|$.

These conditions clearly define a unique orbit at each point D, which differs from point to point. The osculating orbit satisfies the equations of unperturbed motion (4.3) and it is therefore elliptical, hyperbolic, parabolic, or vertical (see Chapter 4). At the particular point D, it touches the actual orbit and both orbits have the same flight velocity $v=|\dot{r}|$. In the course of motion, however, the actual and the osculating orbits diverge. If the perturbing acceleration j is small in comparison with the Newtonian

acceleration $g=\frac{\mu}{r^3}r$, this divergence will be insignificant in a certain

neighborhood of the point D. The osculating orbit can therefore be used as a characteristic of actual motion near the point D. This point, where the actual and the osculating orbits coincide, is the point of osculation, and the corresponding time $t=t_1$ is the instant of osculation.

An osculating orbit can be constructed for each point of the real orbit, considered as the point of osculation. According to Sec. 5.4, each of these osculating orbits is described by six elements $q_i(t)$ $(i=1, 2, 3, \ldots, 6)$. Each point of the real orbit is thus in correspondence with a set of elements q_i which describe some osculating orbit; these elements are the osculating elements of the real orbit being considered. The elements q_i are constant along the corresponding osculating orbit, but they change if the instant of osculation is changed. In other words, for the real orbit we have the dependence $q_i=q_i(t)$, where t is the instant of osculation. It follows from Sec. 5.4 that the magnitudes of the osculating elements at some instant $t=t_1$ are uniquely determined by the components of the vectors ρ and $\dot{\rho}$ at that time. Hence, making use of (11.2), we find that $q_i(t_1)$ uniquely define the vectors $r(t_1)$ and $\dot{r}(t_1)$. In other words, the determination of the osculating elements as a function of flight time, $q_i=q_i(t)$, is thus equivalent to the determination of the functions $r(t)$ and $\dot{r}(t)$ which define the real orbit.

The set of osculating elements $q_i(t)$ $(i=1, 2, \ldots, 6)$ can therefore be applied as a set of variables uniquely defining an orbit in an arbitrary force field. In the equations of motion (11.1) we may change over from x, y, z, v_x, v_y, v_z (i.e., from the components of the vectors r and $v=r$) to q_i. The equations then take the form

$$\frac{dq_i}{ds}=f_i(q_1, q_2, \ldots, q_6, s, j_1, j_2, j_3), \quad i=1, 2, \ldots, 6, \tag{11.3}$$

where s is an independent variable (say, the flight time t), and j_1, j_2, j_3 are the projections of the perturbing acceleration j on the axes of some (as yet arbitrary) system of coordinates.

The set (11.3) are the equations of motion in osculating elements. They are more convenient than the starting equations (11.1) for qualitative analysis of small perturbing accelerations on account of the following features.

(1) For small perturbing accelerations ($|j| \ll g$), the elements $q_i(t)$ vary slowly along the orbit (since for $j = 0$, $q_i = $ const), so that an approximate solution of (11.3) can be readily obtained by the method of the small parameter.

(2) The osculating elements q_i obtained from the solution of (11.3) have an obvious kinematic meaning, which facilitates the qualitative analysis.

The principal problem of this chapter is to derive the equations of motion in osculating elements. The approximate solution of these equations will be considered in subsequent chapters in connection with various particular perturbing accelerations j.

11.2. DERIVATIVES FOR FUNCTIONS
OF POSITION AND VELOCITY

Before proceeding with the actual derivation of the equations of motion in osculating elements, let us consider some function of position and velocity

$$F = F(x, y, z, v_x, v_y, v_z),$$

where x, y, z are the coordinates of the satellite and v_x, v_y, v_z its velocity components.

Let ξ, η, ζ, v_ξ, v_η, v_ζ be the coordinates and the velocity components in osculating orbit. From (11.3) we see that at the instant of osculation

$$F(x, y, z, v_x, v_y, v_z) = F(\xi, \eta, \zeta, v_\xi, v_\eta, v_\zeta). \tag{11.4}$$

In any orbit, F is a function of flight time t. Let $\dfrac{dF}{dt}$ be the derivative of F with respect to t for motion in real orbit, and $\left(\dfrac{dF}{dt}\right)_o$ the same derivative for motion in osculating orbit. Then, from (11.1) and (11.2), we write

$$\frac{dF}{dt} = \frac{\partial F}{\partial x} v_x + \frac{\partial F}{\partial y} v_y + \frac{\partial F}{\partial z} v_z + \frac{\partial F}{\partial v_x}(g_x + j_x) + \frac{\partial F}{\partial v_y}(g_y + j_y) + \frac{\partial F}{\partial v_z}(g_z + j_z),$$

$$\left(\frac{dF}{dt}\right)_o = \frac{\partial F}{\partial x} v_\xi + \frac{\partial F}{\partial y} v_\eta + \frac{\partial F}{\partial z} v_\zeta + \frac{\partial F}{\partial v_x} g_x + \frac{\partial F}{\partial v_y} g_y + \frac{\partial F}{\partial v_z} g_z,$$

where g_x, g_y, g_z, j_x, j_y, j_z are the projections of the vectors g and j.

From (11.2) we see that at the instant of osculation

$$\frac{dF}{dt} = \left(\frac{dF}{dt}\right)_o + \frac{d\tilde{F}}{dt}. \tag{11.5}$$

185

where

$$\frac{d\tilde{F}}{dt} = \frac{\partial F}{\partial v_x} j_x + \frac{\partial F}{\partial v_y} j_y + \frac{\partial F}{\partial v_z} j_z. \tag{11.6}$$

We call $\frac{dF}{dt}$ the total derivative, and $\frac{d\tilde{F}}{dt}$ the special derivative of the function F.

In particular, if F is some element q of the osculating orbit (or an integration constant of the equations of unperturbed motion), we have for the osculating orbit

$$q\,(\xi,\ \eta,\ \zeta,\ v_\xi,\ v_\eta,\ v_\zeta) = \text{const},\quad \left(\frac{dq}{dt}\right)_o = 0. \tag{11.7}$$

Hence, for the real orbit

$$\frac{dq}{dt} = \frac{d\tilde{q}}{dt} = \frac{\partial q}{\partial v_x} j_x + \frac{\partial q}{\partial v_y} j_y + \frac{\partial q}{\partial v_z} j_z. \tag{11.8}$$

This relation will be widely used in what follows in the derivation of the equations of motion in osculating elements. Let us consider it in some detail. Note that during a fairly short period Δt, the effect produced by the perturbing acceleration j can be replaced, to first approximation, by an impulsive increment in the velocity vector,

$$\Delta v = j\,\Delta t. \tag{11.9}$$

The orbital elements $q = q\,(r,\ v)$ then change, to first approximation, by an amount

$$\Delta q = \frac{\partial q}{\partial v_x}\Delta v_x + \frac{\partial q}{\partial v_y}\Delta v_y + \frac{\partial q}{\partial v_z}\Delta v_z = \left(\frac{\partial q}{\partial v_x} j_x + \frac{\partial q}{\partial v_y} j_y + \frac{\partial q}{\partial v_z} j_z\right)\Delta t. \tag{11.10}$$

Hence, passing to the limit as $\Delta t \to 0$, we recover (11.8).

Relation (11.8) is thus easily derived as the limit when the continuous perturbing acceleration is replaced with an infinity of infinitesimal impulsive increments of the velocity vector.

11.3. THE DERIVATIVES $\frac{d\Omega}{dt}$, $\frac{di}{dt}$ AND $\frac{d\tilde{u}}{dt}$

In deriving the expressions for the derivatives of various osculating elements, we shall invariably refer to the system of cylindrical coordinates $r,\ u,\ z$ depicted in Figure 2.1. The origin of this system is at the center of attraction O, the plane ru coincides with the osculating orbital plane (for the instant of osculation being considered), the angles u are reckoned from the line through the ascending node Ω of the osculating orbit, and the axis z points at right angles to the osculating orbital plane. Let $S,\ T,\ W$ be the projections of the perturbing acceleration in the directions $r,\ u,\ z,$

186

respectively. Then (11.6) and (11.8) take the form

$$\frac{dF}{dt} = \frac{\partial F}{\partial v_r}\,S + \frac{\partial F}{\partial v_u}\,T + \frac{\partial F}{\partial v_z}\,W,$$
$$\frac{dq}{dt} = \frac{\widetilde{dq}}{dt} = \frac{\partial q}{\partial v_r}\,S + \frac{\partial q}{\partial v_u}\,T + \frac{\partial q}{\partial v_z}\,W,$$

(11.11)

where v_r, v_u, and v_z are the corresponding projections of the velocity vector.

We first derive the expressions for the derivatives of the elements Ω and i, which define the orientation of the orbital plane. Since the perturbations S and T cannot alter the orientation of this plane, we need only consider the contribution from the perturbing acceleration component W. Proceeding from the remarks at the end of the previous section, we shall substitute for the continuous perturbing acceleration an infinity of infinitesimal impulsive increments

$$\Delta v_z = W\Delta t.$$

Making use of (9.51), we see that this velocity increment rotates the orbital plane around an axis through the gravitational center O and the point of osculation D, by an angle

$$\psi = \frac{W}{v_u}\,\Delta t.$$

(11.12)

Hence, applying (5.11) and (9.53), we find for the corresponding variations of Ω, i, and u

$$\Delta\Omega = W\sqrt{\frac{p}{\mu}}\,\frac{r}{p}\,\frac{\sin u}{\sin i}\,\Delta t,$$
$$\Delta i = W\sqrt{\frac{p}{\mu}}\,\frac{r}{p}\cos u\,\Delta t,$$
$$\Delta\widetilde{u} = -W\sqrt{\frac{p}{\mu}}\,\frac{r}{p}\,\frac{\sin u}{\mathrm{tg}\,i}\,\Delta t.$$

(11.13)

Note that here $\Delta\Omega$ and Δi are the total variations of the corresponding orbital elements, while $\Delta\widetilde{u}$ is a special variation, neglecting the change in the angle u in the course of motion in osculating orbit.

Passing in (11.13) to the limit for $\Delta t \to 0$, we find

$$\frac{d\Omega}{dt} = W\sqrt{\frac{p}{\mu}}\,\frac{r}{p}\,\frac{\sin u}{\sin i},$$
$$\frac{di}{dt} = W\sqrt{\frac{p}{\mu}}\,\frac{r}{p}\cos u,$$

(11.14)

$$\frac{d\widetilde{u}}{dt} = -W\sqrt{\frac{p}{\mu}}\,\frac{r}{p}\,\frac{\sin u}{\mathrm{tg}\,i},$$

(11.15)

11.4. THE DERIVATIVES $\frac{dp}{dt}$ AND $\frac{de}{dt}$

To find the derivatives of p and e, we make use of relations (4.18), (4.21), (4.22), and (4.23), remembering that $v\cos\theta = v_u$ and $v\sin\theta = v_r$.

187

Thus,

$$p = \frac{r^2 v_u^2}{\mu},$$
$$e^2 = 1 - 2\frac{r}{\mu}v_u^2 + \frac{r^2}{\mu^2}v_u^4 + \frac{r^2}{\mu^2}v_u^2 v_r^2. \qquad (11.16)$$

Differentiating and applying (4.19), (5.11), (5.13), we find

$$\frac{\partial p}{\partial v_u} = \sqrt{\frac{p}{\mu}}\,2r, \quad \frac{\partial p}{\partial v_r} = 0,$$
$$\frac{\partial e}{\partial v_u} = \frac{1}{e}\sqrt{\frac{p}{\mu}}\left(-2 + 2\frac{p}{r} + \frac{r}{p}e^2\sin^2\vartheta\right) =$$
$$= \sqrt{\frac{p}{\mu}}\left(2\cos\vartheta - \frac{r}{p}e\cos^2\vartheta + e\frac{r}{p}\right) =$$
$$= \sqrt{\frac{p}{\mu}}\left[\left(1 + \frac{r}{p}\right)\cos\vartheta + e\frac{r}{p}\right], \qquad (11.17)$$
$$\frac{\partial e}{\partial v_r} = \sqrt{\frac{p}{\mu}}\sin\vartheta, \quad \frac{\partial p}{\partial v_z} = \frac{\partial e}{\partial v_z} = 0.$$

Substituting in (11.11), we have

$$\frac{dp}{dt} = T\sqrt{\frac{p}{\mu}}\,2r,$$
$$\frac{de}{dt} = \sqrt{\frac{p}{\mu}}\left\{S\sin\vartheta + T\left[\left(1 + \frac{r}{p}\right)\cos\vartheta + e\frac{r}{p}\right]\right\}. \qquad (11.18)$$

11.5. THE DERIVATIVES $\frac{d\omega}{dt}$, $\frac{du}{dt}$ AND $\frac{d\vartheta}{dt}$

To find the derivative of the argument of the pericenter ω, we make use of expression (5.49):

$$\omega = u - \vartheta. \qquad (11.19)$$

Taking the special derivatives of the left- and the right-hand sides and seeing that $\frac{d\omega}{dt} = \frac{d\tilde{\omega}}{dt}$ (since ω is one of the orbital elements), we write

$$\frac{d\omega}{dt} = \frac{d\tilde{u}}{dt} - \frac{d\tilde{\vartheta}}{dt}. \qquad (11.20)$$

To obtain the derivative $\frac{d\tilde{\vartheta}}{dt}$, we write (4.19) in the form

$$\frac{p}{r} = 1 + e\cos\vartheta \qquad (11.21)$$

and take the special derivatives of the left- and the right-hand sides of this equality. Seeing that

$$\frac{d\tilde{p}}{dt} = \frac{dp}{dt}, \quad \frac{d\tilde{e}}{dt} = \frac{de}{dt}, \quad \frac{d\tilde{r}}{dt} = 0,$$

we have

$$\frac{1}{r}\frac{dp}{dt} = -e\sin\vartheta\,\frac{d\tilde{\vartheta}}{dt} + \cos\vartheta\,\frac{de}{dt}.$$

Hence, applying (11.18), we write

$$\sqrt{\frac{\mu}{p}}\,e\sin\vartheta\,\frac{d\tilde{\vartheta}}{dt} = S\sin\vartheta\cos\vartheta + T\left\{\left[\left(1+\frac{r}{p}\right)\cos\vartheta + e\frac{r}{p}\right]\cos\vartheta - 2\right\}.$$

Making use of (4.19), we write for the expression in braces

$$\left[\left(1+\frac{r}{p}\right)\cos\vartheta + e\frac{r}{p}\right]\cos\vartheta - 2 =$$
$$= \left(1+\frac{r}{p}\right)\cos^2\vartheta + \frac{e\cos\vartheta}{1+e\cos\vartheta} - 2 =$$
$$= \left(1+\frac{r}{p}\right)\cos^2\vartheta - \left(\frac{r}{p}+1\right) = -\left(1+\frac{r}{p}\right)\sin^2\vartheta.$$

Then

$$\frac{d\tilde{\vartheta}}{dt} = \frac{1}{e}\sqrt{\frac{p}{\mu}}\left[S\cos\vartheta - T\left(1+\frac{r}{p}\right)\sin\vartheta\right]. \tag{11.22}$$

Substituting (11.15) and (11.22) in (11.20), we obtain the final expression for the derivative $\frac{d\omega}{dt}$:

$$\frac{d\omega}{dt} = \sqrt{\frac{p}{\mu}}\left\{\frac{1}{e}\left[-S\cos\vartheta + T\left(1+\frac{r}{p}\right)\sin\vartheta\right] - W\frac{r}{p}\operatorname{ctg}i\sin u\right\}. \tag{11.23}$$

From (11.15) and (11.22), we obtain expressions for the total derivatives $\frac{d\vartheta}{dt}$ and $\frac{du}{dt}$. Let us first determine the derivatives of these elements for motion in osculating orbit. Applying (11.19) and seeing that in osculating orbit $\omega=\mathrm{const}$, we have from (5.11) and (5.12)

$$\left(\frac{du}{dt}\right)_o = \left(\frac{d\vartheta}{dt}\right)_o = \frac{v_u}{r} = \sqrt{\frac{\mu p}{r^2}}. \tag{11.24}$$

Hence, making use of (11.5), (11.15), and (11.22), we have

$$\frac{du}{dt} = \left(\frac{du}{dt}\right)_o + \frac{d\tilde{u}}{dt} = \sqrt{\frac{p}{\mu}}\left(\frac{\mu}{r^2} - W\frac{r}{p}\operatorname{ctg}i\sin u\right), \tag{11.25}$$

$$\frac{d\vartheta}{dt} = \left(\frac{d\vartheta}{dt}\right)_o + \frac{d\tilde{\vartheta}}{dt} = \sqrt{\frac{p}{\mu}}\left[\frac{\mu}{r^2} + S\frac{\cos\vartheta}{e} - T\frac{1}{e}\left(1+\frac{r}{p}\right)\sin\vartheta\right]. \tag{11.26}$$

Thus, with perturbing accelerations, $\frac{du}{dt} \neq \frac{v_u}{r}$, $\frac{d\vartheta}{dt} \neq \frac{v_u}{r}$. This is so because the displacement of the point of osculation produces simultaneous displacement of the point of origin from which the angles u and ϑ are reckoned (i.e., the node and the pericenter of the osculating orbit both shift).

11.6. THE DERIVATIVES $\frac{da}{dt}$, $\frac{dr_p}{dt}$, AND $\frac{dP}{dt}$

To find the derivative of the semimajor axis a of the orbit, we make use of relation (5.15), which can be written as

$$\frac{1}{a} = \frac{2}{r} - \frac{v_u^2 + v_r^2}{\mu}.$$

Differentiating and applying (5.2), (5.11), and (5.13), we find

$$\left.\begin{array}{l}
\frac{\partial a}{\partial v_u} = \frac{2a^2}{\mu} v_u = \sqrt{\frac{p}{\mu}} \frac{2a^2}{r} = \sqrt{\frac{p}{\mu}} \frac{2a}{1-e^2} \frac{p}{r}, \\[2mm]
\frac{\partial a}{\partial v_r} = \frac{2a^2}{\mu} v_r = \sqrt{\frac{p}{\mu}} \frac{2a}{1-e^2} e \sin \vartheta.
\end{array}\right\} \tag{11.27}$$

Hence putting $q = a$ in (11.11), we have

$$\frac{da}{dt} = \sqrt{\frac{p}{\mu}} \frac{2a}{1-e^2} \left(S e \sin \vartheta + T \frac{p}{r} \right). \tag{11.28}$$

To find the change in the osculating orbital period P and in the osculating pericenter distance r_p (i.e., in the elements P and r_p as computed for osculating orbit), we differentiate the second expression in (5.3) and relation (5.36). Thus

$$\frac{dr_p}{dt} = (1 - e) \frac{da}{dt} - a \frac{de}{dt}, \qquad \frac{dP}{dt} = \frac{3}{2} \frac{P}{a} \frac{da}{dt}. \tag{11.29}$$

Inserting (11.18) and (11.28), we find

$$\frac{dr_p}{dt} = \sqrt{\frac{p}{\mu}} a \left\{ -S \frac{1-e}{1+e} \sin \vartheta + \right.$$
$$\left. + T \left[\frac{2}{1+e} \frac{p}{r} - \left(1 + \frac{r}{p} \right) \cos \vartheta - e \frac{r}{p} \right] \right\}, \tag{11.30}$$

$$dP = \sqrt{\frac{p}{\mu}} \frac{3P}{1-e^2} \left(S e \sin \vartheta + T \frac{p}{r} \right). \tag{11.31}$$

Perturbing accelerations thus cause continuous variation of the osculating orbital period P and the osculating pericenter distance r_p in the course of orbital motion. Therefore, strictly speaking, these two quantities cannot be assumed as characteristic of any particular circuit of revolution. A more exact definition is required: the orbital period may be defined as the nodical period of revolution P_Ω (the time of revolution from ascending node to ascending node; see Sec. 13.6), and the pericenter distance should be taken as the minimum (for the particular circuit) distance r_{min} from the center of attraction.

The parameter r_{min} is often conveniently replaced with the minimum height h_{min} of the satellite above the Earth's surface (on account of the Earth's flattening, the parameters r_{min} and h_{min} in general correspond to different points of the orbit). With small perturbing accelerations, the osculating values of P and r_p are close to P_Ω and r_{min}. Secular perturbations in these osculating parameters are therefore fairly representative of the secular perturbations in P_Ω and r_{min}.

11.7. DIFFERENTIAL EQUATIONS OF MOTION IN OSCULATING ELEMENTS

We first introduce a somewhat generalized definition of osculating orbital elements. By an osculating orbital element we mean not only an element of the osculating orbit, but any parameter characterizing motion in osculating orbit. This parameter may vary in the course of motion in osculating orbit, and it is its value at the point of osculation which is adopted as the osculating element. Under this definition, $\mu(t)$ and $\vartheta(t)$ may also be regarded as osculating elements of the real orbit (although strictly speaking they are not elements of the osculating orbit, along which they are variable).

A complete set of osculating elements $q_i(t)$ $(i = 1, 2, \ldots, 6)$ is a set of parameters unambiguously defining the orbit, e.g., the vectors $r(t)$ and $v(t)$. If some complete set of elements $q_i(t)$ $(i = 1, 2, \ldots, 6)$ is known, all other osculating orbital elements can be easily determined. Therefore, any set of differential equations which define some complete set of osculating elements may be regarded as the differential equations of motion in osculating elements. It would be easiest to write the differential equations for $p(t)$, $e(t)$, $\omega(t)$, $\Omega(t)$, $i(t)$ and $\vartheta(t)$. From (5.37), (6.41), and (7.10) it follows that these parameters uniquely define any point of the real orbit (irrespective of whether the osculating orbit is elliptical, hyperbolic or parabolic).

Making use of relations (11.14), (11.18), (11.23), and (11.26), we write the following set of equations in these osculating elements:

$$
\left.
\begin{aligned}
\frac{dp}{dt} &= T\sqrt{\frac{p}{\mu}}\,2r, \\
\frac{de}{dt} &= \sqrt{\frac{p}{\mu}}\left\{S\sin\vartheta + T\left[\left(1+\frac{r}{p}\right)\cos\vartheta + e\frac{r}{p}\right]\right\}, \\
\frac{d\omega}{dt} &= \sqrt{\frac{p}{\mu}}\left[-S\frac{\cos\vartheta}{e} + T\frac{1}{e}\left(1+\frac{r}{p}\right)\sin\vartheta - \right. \\
&\qquad\qquad\qquad\left. - W\frac{r}{p}\operatorname{ctg} i \sin u\right], \\
\frac{d\Omega}{dt} &= W\sqrt{\frac{p}{\mu}}\,\frac{r}{p}\,\frac{\sin u}{\sin i}, \\
\frac{di}{dt} &= W\sqrt{\frac{p}{\mu}}\,\frac{r}{p}\cos u, \\
\frac{d\vartheta}{dt} &= \sqrt{\frac{p}{\mu}}\left[\frac{\mu}{r^2} + S\frac{\cos\vartheta}{e} - T\frac{1}{e}\left(1+\frac{r}{p}\right)\sin\vartheta\right],
\end{aligned}
\right\} \qquad (11.32)
$$

where

$$
r = \frac{p}{1+e\cos\vartheta}, \quad \frac{r}{p} = \frac{1}{1+e\cos\vartheta}, \quad u = \omega + \vartheta. \qquad (11.33)
$$

In deriving equations (11.32), we never actually used the assumption of small perturbing accelerations S, T, W. However, if the accelerations S, T, W are comparable in magnitude with the Newtonian acceleration $g = \frac{\mu}{r^2}$, the elements p, e, ω, Ω, i vary rapidly along the orbit, and equations (11.32) therefore lose their advantage in comparison with the starting set (11.1), which is much simpler.

11.8. SOLUTION OF THE DIFFERENTIAL EQUATIONS OF MOTION IN OSCULATING ELEMENTS BY THE METHOD OF SUCCESSIVE APPROXIMATIONS

If the ratios $\frac{S}{g}$, $\frac{T}{g}$ and $\frac{W}{g}$ are small, equations (11.32) can be solved by the method of successive approximations. Changing over to ϑ as the independent variable in (11.32), we write for the equations of motion

$$\frac{dp}{d\vartheta} = TF2r.$$

$$\frac{de}{d\vartheta} = F\left\{ S \sin\vartheta + T\left[\left(1+\frac{r}{p}\right)\cos\vartheta + e\frac{r}{p}\right]\right\},$$

$$\frac{d\omega}{d\vartheta} = F\left[-S\frac{\cos\vartheta}{e} + T\frac{1}{e}\left(1+\frac{r}{p}\right)\sin\vartheta -\right.$$
$$\left. - W\frac{r}{p}\operatorname{ctg} i \sin u\right],$$

$$\frac{d\Omega}{d\vartheta} = WF\frac{r}{p}\frac{\sin u}{\sin i},$$

$$\frac{di}{d\vartheta} = WF\frac{r}{p}\cos u,$$

where
$$\frac{dt}{d\vartheta} = \sqrt{\frac{\mu}{p}}\,F,$$

(11.34)

$$F = \frac{1}{\frac{\mu}{r^2}+S\frac{\cos\vartheta}{e} - T\frac{1}{e}\left(1+\frac{r}{p}\right)\sin\vartheta}.$$

(11.35)

We shall only consider the cases when the perturbing accelerations S, T, W are functions of the vectors r, v and do not depend explicitly on the time t. Then only five equations in the set (11.34) must be solved simultaneously. The sixth equation can be subsequently applied to determine the flight time t by quadrature.

In our presentation of the method of successive approximations for the simultaneous solution of five equations in (11.34), we shall write $\tilde{p}$, $\tilde{e}$, $\tilde{\omega}$, $\tilde{\Omega}$, $\tilde{i}$ for the initial values of the osculating elements at the point $\vartheta=\vartheta_0$. The symbols $\Delta p(\vartheta)$, $\Delta e(\vartheta)$, $\Delta \omega(\vartheta)$, $\Delta\Omega(\vartheta)$, $\Delta i(\vartheta)$ stand for the perturbations of these elements in the course of orbital motion. The osculating elements of the real orbit are thus written in the form

$$p(\vartheta) = \tilde{p} + \Delta p(\vartheta), \quad e(\vartheta) = \tilde{e} + \Delta e(\vartheta),$$
$$\omega(\vartheta) = \tilde{\omega} + \Delta\omega(\vartheta), \quad \Omega(\vartheta) = \tilde{\Omega} + \Delta\Omega(\vartheta),$$
$$i(\vartheta) = \tilde{i} + \Delta i(\vartheta).$$

(11.36)

Making use of (11.36) and seeing that $\tilde{p}$, $\tilde{e}$, $\tilde{\omega}$, $\tilde{\Omega}$, $\tilde{i}$ are constant, we write for the first five equations in (11.34)

$$\frac{d}{d\vartheta}(\Delta p) = TF2r,$$

$$\frac{d}{d\vartheta}(\Delta e) = F\left\{ S \sin\vartheta + T\left[\left(1+\frac{r}{p}\right)\cos\vartheta + e\frac{r}{p}\right]\right\},$$

$$\frac{d}{d\vartheta}(\Delta\omega) = F\left[-S\frac{\cos\vartheta}{e} + T\frac{1}{e}\left(1+\frac{r}{p}\right)\sin\vartheta -\right.$$
$$\left. - W\frac{r}{p}\operatorname{ctg} i \sin u\right],$$

$$\frac{d}{d\vartheta}(\Delta\Omega) = WF\frac{r}{p}\frac{\sin u}{\sin i},$$

$$\frac{d}{d\vartheta}(\Delta i) = WF\frac{r}{p}\cos u,$$

(11.37)

which is solved with the aid of (11.33), (11.35), and (11.36).

Let us consider the integration of these equations in an interval of ϑ-values where the perturbations Δp, Δe, $\Delta\omega$, $\Delta\Omega$, and Δi remain small. Then, to first approximation, we may set $p=\tilde{p}$, $e=\tilde{e}$, $\omega=\tilde{\omega}$, $\Omega=\tilde{\Omega}$, $i=\tilde{i}$ in the right-hand sides of (11.37). Each of the five equations is integrated separately, and the perturbations Δp, Δe, $\Delta\omega$, $\Delta\Omega$, and Δi are found from quadratures. Substituting these perturbations in (11.36), we find the osculating orbital elements to second approximation, and so on, until the desired accuracy is attained.

In our qualitative analysis of the various particular perturbations, we shall stop after the first approximation. We shall also take the ratios $\dfrac{S}{eg}$ and $\dfrac{T}{eg}$ to be small. Equality (11.35) is then reduced to the approximate

$$F \approx \frac{r^2}{\mu}. \tag{11.38}$$

As we have shown in Chapter 3, small perturbations have a substantial influence on the motion of artificial satellites only if they cause growing, secular disturbances of the orbital elements. The secular effects can be characterized by the change in the orbital elements during one period, δp, δe, $\delta\omega$, $\delta\Omega$, δi. We write the following approximate expressions for these perturbations:

$$\left. \begin{aligned}
\delta p &= \int_0^{2\pi} \frac{T}{g}\, 2r\, d\vartheta, \\[6pt]
\delta e &= \int_0^{2\pi} \left\{ \frac{S}{g}\sin\vartheta + \frac{T}{g}\Big[\Big(1+\frac{r}{p}\Big)\cos\vartheta + e\,\frac{r}{p}\Big]\right\} d\vartheta, \\[6pt]
\delta\omega &= \int_0^{2\pi} \left[-\frac{S}{g}\frac{\cos\vartheta}{e} + \frac{T}{g}\frac{1}{e}\Big(1+\frac{r}{p}\Big)\sin\vartheta - \frac{W}{g}\frac{r}{p}\operatorname{ctg} i \sin u \right] d\vartheta, \\[6pt]
\delta\Omega &= \int_0^{2\pi} \frac{W}{g}\frac{r}{p}\frac{\sin u}{\sin i}\, d\vartheta, \\[6pt]
\delta i &= \int_0^{2\pi} \frac{W}{g}\frac{r}{p}\cos u\, d\vartheta, \\[6pt]
r &= \frac{p}{1+e\cos\vartheta}, \quad \frac{r}{p} = \frac{1}{1+e\cos\vartheta}, \\[6pt]
u &= \omega+\vartheta, \quad g = \frac{\mu}{r^2}.
\end{aligned} \right\} \tag{11.39}$$

For simplicity, we have omitted the tilde $\sim$ in the notations of the initial osculating (i.e., unperturbed) orbit.

In deriving (11.39), the ratios $\dfrac{S}{eg}$, $\dfrac{T}{eg}$ and $\dfrac{W}{g}$ were assumed to be small. Hence it follows that for nearly circular orbits ($e\to 0$) these expressions may become meaningless even if the perturbing accelerations are very small. In the analysis of perturbations in circular and nearly circular orbits, we shall therefore resort to the methods of Chapter 3.

Chapter 12

THE GRAVITATIONAL FIELD OF THE EARTH

12.1. STATEMENT OF THE PROBLEM

In the previous chapters we assumed that the vector g of the Earth's gravitational acceleration always pointed to the Earth's center, and that its magnitude was as defined by (1.2).

In accordance with Newton's law of universal gravitation, this assumption is true if the entire mass of the Earth is concentrated at one point, namely its center. Then,

$$\mu = fM, \qquad (12.1)$$

where M is the Earth's mass, and f the so-called gravitational constant.

The assumption of point mass is justified in the motion of remote celestial bodies, whose distance from the Earth is much greater than the Earth's radius. However, even the Moon is not far enough for this assumption to apply: the finite mass distribution of the Earth must be introduced in the exact lunar theory. This factor is therefore much more significant for the analysis of motion of close satellites, which move in the immediate Earth environment.

The gravitational pull of bodies of various sizes, shapes, and internal structures is the subject of a separate scientific discipline — the theory of potential. Various theoretical problems that can be applied to the determination of the force of gravity are the province of gravimetry. It is closely related with the theory of the Earth's figure, which studies the shape and the size of our planet. The present chapter describes the principal results of these disciplines in so far as they are needed in the analysis of motion of artificial Earth satellites. Some propositions are presented without derivation. The reader is referred to specialized literature for a more detailed and rigorous treatment of these topics /4, 8, 21, 27/.

12.2. GRAVITATIONAL POTENTIAL

The gravitational acceleration of a body may be treated as the sum total of gravitational accelerations of the elementary particles comprising the body. The attraction of each of these elementary particles is defined by Newton's law. Let dg be the vector of gravitational acceleration of

some elementary particle. From (4.1) and (12.1) we see that the projections of this vector on the axes of some rectangular frame $Oxyz$ are

$$dg_x = -f\,\frac{x-\xi}{|r-\rho|^3}\,dm,$$

$$dg_y = -f\,\frac{y-\eta}{|r-\rho|^3}\,dm,$$

$$dg_z = -f\,\frac{z-\zeta}{|r-\rho|^3}\,dm,$$

where dm is the mass of the attracting elementary particle, ρ and r are respectively the vectors which define the position of the attracting particle and the test particle for which the gravitational acceleration g is being calculated, ξ, η, ζ and x, y, z are the projections of these vectors on the rectangular axes.

We introduce a function

$$dU = \frac{f\,dm}{|r-\rho|}.$$

From the previous equalities we have

$$dg_x = \frac{\partial}{\partial x}\,dU,\quad dg_y = \frac{\partial}{\partial y}\,dU,\quad dg_z = \frac{\partial}{\partial z}\,dU$$

or

$$dg = \mathrm{grad}\,(dU).$$

To find the gravitational acceleration due to the entire body, the elementary accelerations dg must be integrated. The total gravitational acceleration g is given by

$$g = \mathrm{grad}\,U, \tag{12.2}$$

where

$$U = f\int \frac{dm}{|r-\rho|}. \tag{12.3}$$

Here the integral is taken over the entire volume occupied by the attracting body.

The function $U = U(x,y,z)$ is the gravitational potential (or the potential function of gravity) of the body in question. By definition,

$$U \to 0 \quad \text{for} \quad |r| \to \infty. \tag{12.4}$$

Let Q_{AB} be the energy expended as a test body of unit mass is moved against the gravitational pull from point A to some other point B. From (12.2) we have

$$Q_{AB} = -\int_A^B g\cdot dS = -\int_A^B \mathrm{grad}\,U\cdot dS = -\int_{U(A)}^{U(B)} dU = U(A) - U(B),$$

195

where $d\mathbf{S}$ is the vector of elementary displacement of the test body moving from point A to point B, dU the change in the function U corresponding to the displacement $d\mathbf{S}$.

Now, making use of (12.4), we see that as the point B recedes to infinity, the energy $Q_{AB} \rightarrow U(A)$. In other words, the function $U(x, y, z)$ is the potential energy which is acquired by a body of unit mass as it moves from a given field point to infinity (i.e., escaping from the sphere of gravitational pull of the primary).

12.3. EARTH'S GRAVITATION AS A FUNCTION OF EARTH'S FIGURE

From (12.2) it follows that the gravitational field of any body can be determined if its gravitational potential $U(x, y, z)$ is known at any point external to the body. The potential function can be computed from (12.3). This approach, however, necessitates advance knowledge of the mass distribution in the body interior, and is therefore hardly practicable at present. The problem is considerably simplified by the following fundamental theorem of the potential theory: *to find the gravitational potential in the entire external space around an attracting body which rotates with constant angular velocity, it suffices to know the total mass of the body, the angular velocity of its rotation, and the shape of its surface*. The body surface here is the surface of some hypothetical ocean which covers the body completely. This surface can be shown to satisfy the equality

$$U(x, y, z) + U_1(x, y, z) = \text{const,}$$

where $U_1(x, y, z)$ is the potential of the centrifugal force, defined as

$$U_1 = \frac{\Omega^2 r_1^2}{2},$$

where Ω is the angular velocity of rotation of the body, r_1 the distance from the test point to the spin axis.

It follows from this theorem that the mass distribution in the Earth's interior is irrelevant for the calculation of the Earth's gravitational potential: it suffices to establish the shape of the Earth's surface, the so-called Earth's figure. In particular, if the Earth's spin is neglected, and the Earth is assumed to be a regular sphere, the gravitational potential is easily found from

$$U = \frac{\mu}{r}, \quad \mu = fM, \tag{12.5}$$

where r is the distance of the test point from the Earth's center.

This potential corresponds to a gravitational acceleration through the Earth's center, defined by (1.2). In other words, the gravitational pull of a spherical nonspinning Earth is the same as the pull of the corresponding point mass. The Earth's surface is actually close to a sphere, and the rotational effects are comparatively small (the centrifugal acceleration on the Earth's surface is small in comparison with the gravitational

196

acceleration). In the approximate analysis of motion of artificial Earth satellites we may therefore conceive of the Earth's mass as concentrated at the Earth's center (although the distance from the artificial satellite to the Earth's surface is often much less than the Earth's radius). This assumption, however, is inadmissible in more exact investigations, where the Earth's nonspherical figure and its spin must be taken into consideration.

12.4. THE GEOCENTRIC REFERENCE ELLIPSOID AND THE NORMAL GRAVITATIONAL FIELD OF THE EARTH

The Earth's figure is a fairly complex surface, which is conventionally called a g e o i d . The exact shape of the geoid has not been determined yet, and its refinement is one of the aims of gravimetry and the theory of Earth's figure. In some cases, however, the geoid can be replaced with fair accuracy by an oblate ellipsoid of revolution, whose center of mass is at the Earth's center and whose minor axis points along the Earth's spin axis. This ellipsoid provides the best approximation to the surface of the real geoid, and it is called the g e o c e n t r i c r e f e r e n c e e l l i p s o i d .
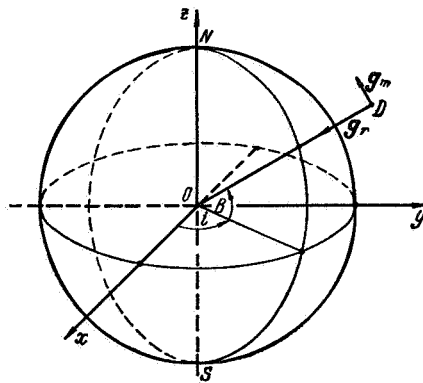
FIGURE 12.1. Components of the normal gravitational acceleration.

As we have previously observed, the gravitational field is completely defined by the Earth's figure (for given mass and spin rate of the Earth). In gravimetry, the gravitational field of the reference ellipsoid is called the n o r m a l f i e l d , whereas the deviation of the real geoid field from normal is called the f i e l d o f g r a v i t y a n o m a l i e s , or in short the a n o m a l o u s f i e l d .

The geocentric reference ellipsoid is a surface of revolution with an axis along the Earth's spin axis, so that the normal gravitational field is symmetric about the Earth's axis. The acceleration vector g of the normal field is always in the plane of a meridian, i. e., in a plane through the test point D and the Earth's spin axis SN (Figure 12.1). The vector g is thus described by two components: the radial component g_r (i. e., the projection

on the radius-vector joining the test point D with the Earth's center) and the meridional component g_m (in the plane of the meridian, at right angles to g_r). Positive g_r and g_m point to the Earth's center and to the north pole, respectively.

The normal potential function, i.e., the attraction to the reference ellipsoid, is generally obtained from a series expansion in spherical functions of geocentric latitude B (the angle between the radius-vector $\overline{OD}$ and the equatorial plane). Only the first three terms in this expansion are generally retained:

$$U(r,\ B) = \frac{a_{00}}{r} + \frac{a_{20}}{r^3} P_{20}(\sin B) + \frac{a_{40}}{r^5} P_{40}(\sin B), \qquad (12.6)$$

where a_{00}, a_{20}, a_{40} are constants, and $P_{20}(\sin B)$ and $P_{40}(\sin B)$ are the corresponding Legendre polynomials (the z o n a l h a r m o n i c s of the potential function):

$$\left. \begin{array}{l} P_{20}(\sin B) = \frac{3}{2}\sin^2 B - \frac{1}{2}, \\[2mm] P_{40}(\sin B) = \frac{35}{8}\sin^4 B - \frac{15}{4}\sin^2 B + \frac{3}{8}. \end{array} \right\} \qquad (12.7)$$

From (12.6) we see that the normal gravitational potential is a function of the distance r and the geocentric latitude B, but it is independent of the longitude L (the angle between the plane of the meridian through the test point D and the plane of some initial meridian). This property is attributable to the reference ellipsoid being a surface of revolution.

The constants a_{00}, a_{20}, and a_{40} can be determined from

$$\left. \begin{array}{l} a_{00} = fM = \gamma_e a_e^2 \left(1 - \alpha + \frac{3}{2}m - \frac{15}{14}m\alpha + \dots\right), \\[2mm] a_{20} = -\gamma_e a_e^4 \left(\frac{2}{3}\alpha - \alpha^2 - \frac{1}{3}m + \frac{10}{7}m\alpha + \dots\right), \\[2mm] a_{40} = \frac{8}{35}\gamma_e a_e^6 \left(\frac{7}{2}\alpha^2 - \frac{5}{2}m\alpha + \dots\right), \\[2mm] m = \frac{\Omega^2 a_e}{\gamma_e}, \quad \alpha = \frac{a_e - b_e}{a_e}, \end{array} \right\} \qquad (12.8)$$

where a_e and b_e are the semimajor and the semiminor axes of the general terrestrial geoid (i.e., the equatorial and the polar semidiameters), α the flattening of the ellipsoid, Ω the angular velocity of Earth's spin, γ_e gravitational acceleration at the equator of the geocentric reference ellipsoid (the so-called e q u a t o r i a l c o n s t a n t o f g r a v i t a t i o n a l a c c e l e r a t i o n), M the Earth's mass, f gravitational constant.

We substitute for the constants a_{00}, a_{20}, a_{40}

$$\mu = a_{00}, \quad \varepsilon = -\frac{3}{2}a_{20}, \quad \chi = \frac{35}{8}a_{40}. \qquad (12.9)$$

From (12.6) and (12.7) we then have

$$U(r,\ B) = \frac{\mu}{r} - \frac{\varepsilon}{r^3}\left(\sin^2 B - \frac{1}{3}\right) + \frac{\chi}{r^5}\left(\sin^4 B - \frac{6}{7}\sin^2 B + \frac{3}{35}\right). \qquad (12.10)$$

Thus, the normal gravitational potential of the Earth can be found if the four quantities a_e, α, γ_e and Ω are known. The spin rate Ω is known with a very high accuracy from astronomical measurements. The

198

determination of the constants a_e, α, and γ_e on the other hand, is one of the fundamental problems of gravimetry and the theory of Earth's figure. We shall use the following approximate values of these constants /33/:

$$
\left.
\begin{aligned}
a_e &= 6378.16 \text{km}, \\
\alpha &= 1 : 298.2, \\
\gamma_e &= 9.78031 \text{ m}/\text{sec}^2, \\
\Omega &= 7.29211 \cdot 10^{-5} \text{sec}^{-1}.
\end{aligned}
\right\}
\qquad (12.11)
$$

Then, from (12.8) and (12.9),

$$
\left.
\begin{aligned}
\mu &= 3.98602 \cdot 10^5 \text{ km}^3/\text{sec}^2, \\
\varepsilon &= 2.634 \cdot 10^{10} \text{ km}^5/\text{sec}^2, \\
\chi &= 6.773 \cdot 10^{15} \text{ km}^7/\text{sec}^2.
\end{aligned}
\right\}
\qquad (12.12)
$$

Making use of (12.2), (12.6), (12.7), and (12.9), we find expressions for the radial and the meridional components of the normal gravitational acceleration:

$$
\left.
\begin{aligned}
g_r &= -\frac{\partial U}{\partial r} = g_r^{(0)} + g_r^{(2)} + g_r^{(4)}, \\
g_m &= \frac{1}{r}\frac{\partial U}{\partial B} = g_m^{(2)} + g_m^{(4)},
\end{aligned}
\right\}
\qquad (12.13)
$$

where

$$
\left.
\begin{aligned}
g_r^{(0)} &= \frac{\mu}{r^2}, \\
g_r^{(2)} &= -2\frac{\varepsilon}{r^4}P_{20}(\sin B) = \frac{\varepsilon}{r^4}(1 - 3\sin^2 B), \\
g_r^{(4)} &= \frac{8}{7}\frac{\chi}{r^6}P_{40}(\sin B) = \\
&= \frac{\chi}{r^6}\left(5\sin^4 B - \frac{30}{7}\sin^2 B + \frac{3}{7}\right), \\
g_m^{(2)} &= -\frac{2}{3}\frac{\varepsilon}{r^4}\frac{\partial}{\partial B}P_{20}(\sin B) = \\
&= -2\frac{\varepsilon}{r^4}\sin B\cos B = -\frac{\varepsilon}{r^4}\sin 2B, \\
g_m^{(4)} &= \frac{8}{35}\frac{\chi}{r^6}\frac{\partial}{\partial B}P_{40}(\sin B) = \\
&= \frac{4}{7}\frac{\chi}{r^6}\sin B\cos B(7\sin^2 B - 3) = \\
&= \frac{1}{14}\frac{\chi}{r^6}(2\sin 2B - 7\sin 4B).
\end{aligned}
\right\}
\qquad (12.14)
$$

The term $g_r^{(0)}$ represents the gravitational pull of a spherical nonspinning Earth (having the same mass as the real Earth), while $g_r^{(2)}$, $g_r^{(4)}$, $g_m^{(2)}$, $g_m^{(4)}$ are the corrections introduced by the Earth's nonspherical figure and its spin. Let us assess the ratio of these corrections to the principal component $g_r^{(0)}$. We shall make use of relations (12.8) and (12.14). Since the Earth's flattening α is a very small quantity, we shall only retain terms of the lowest order of smallness. Moreover, on the basis of the numerical values (12.11), we take

$$
m = \frac{\Omega^2 a_e}{\gamma_e} \approx \alpha.
$$

Then,

$$
\frac{\varepsilon}{\mu} \approx \frac{a_e^2\alpha}{2}, \qquad \frac{\chi}{\mu} \approx a_e^4\alpha^2.
\qquad (12.15)
$$

199

We shall also apply the well-known property of Legendre polynomials /8/

$$|P_{l0}(\sin B)| \leqslant 1,$$ (12.16)

and the inequalities

$$|\sin 2B| \leqslant 1, \quad |2\sin 2B - 7\sin 4B| < 9.$$

Finally, in orbit

$$r > a_e.$$ (12.17)

In the result, we obtain the following estimates for the maximum values of the relevant ratios:

$$\left| \frac{g_r^{(2)}}{g_r^{(0)}} \right|_{max} \approx \left(\frac{a_e}{r} \right)^2 \alpha < \alpha \approx 0.003,$$

$$\left| \frac{g_m^{(2)}}{g_r^{(0)}} \right|_{max} \approx \left(\frac{a_e}{r} \right)^2 \frac{\alpha}{2} < \frac{\alpha}{2} \approx 0.0015,$$

$$\left| \frac{g_r^{(4)}}{g_r^{(0)}} \right|_{max} \approx \frac{8}{7} \left(\frac{a_e}{r} \right)^4 \alpha^2 < \frac{8}{7} \alpha^2 \approx 10^{-5},$$ (12.18)

$$\left| \frac{g_m^{(4)}}{g_r^{(0)}} \right|_{max} \approx \frac{9}{14} \left(\frac{a_e}{r} \right)^4 \alpha^2 < \frac{9}{14} \alpha^2 \approx 0.6 \cdot 10^{-5}.$$

We see from these estimates that the perturbing accelerations $g_r^{(2)}$, $g_m^{(2)}$, $g_r^{(4)}$, and $g_m^{(4)}$ are indeed small in comparison with the principal acceleration $g_r^{(0)}$. They rapidly decrease with the distance r from the Earth's center. The corrections $g_r^{(4)}$ and $g_m^{(4)}$ may further be treated as of second order of smallness relative to $g_r^{(2)}$ and $g_m^{(2)}$.

12.5. GRAVITY ANOMALIES

As we have previously observed, the geocentric reference ellipsoid is an approximation to the Earth's figure. Geoid undulations, i.e., the deviations Δh of the geoid from the reference surface, are introduced for the exact description of the geoid figure. According to the latest measurements, the undulations do not exceed some 150 m /6/, which is much less than the deviation of the reference ellipsoid from a sphere (the difference between the equatorial and the polar semidiameters of the geocentric reference ellipsoid is close to 22.1 km). The geoid undulations Δh can be represented as a function of the latitude B and the longitude l by series expansion in spherical functions /6, 21/:

$$\Delta h = \sum_{n=2}^{\infty} \sum_{m=0}^{n} (\alpha_{nm} \cos mL + \beta_{nm} \sin mL) P_{nm}(\sin B),$$ (12.19)

where α_{nm} and β_{nm} are the expansion coefficients, and $P_{nm}(\sin B)$ are the

associated Legendre functions, defined by

$$P_{nm}(\sin B) = \cos^m B \frac{d^m P_n(t)}{dt^m},$$
$$P_{n0}(\sin B) = P_n(t), \quad t = \sin B. \qquad (12.20)$$

Here

$$P_n(t) = \frac{1}{2^n n!} \frac{d^n (t^2 - 1)^n}{dt^n} \qquad (12.21)$$

is a Legendre polynomial (a zonal harmonic of the expansion).

The deviation of the geoid from the geocentric reference ellipsoid affects the gravitational potential U, which is written as

$$U = U_0 + \Delta U, \qquad (12.22)$$

where U_0 is the normal potential corresponding to the reference ellipsoid, and ΔU is the potential function of gravity anomalies.

The anomalous potential ΔU can be determined with the aid of Bruns' lemma /8, 21/: the anomalous potential on the reference surface is related with the geoid undulation Δh by the expression

$$\Delta \tilde{U} = \tilde{g} \Delta h, \qquad (12.23)$$

where $\tilde{g}$ is the gravitational acceleration on the reference surface.

Since the gravitational anomalies are small, the acceleration $\tilde{g}$ in (12.23) can be replaced with some mean g_0. Then, making use of (12.19),

$$\Delta \tilde{U} = g_0 \sum_{n=2}^{\infty} \sum_{m=0}^{n} (\alpha_{nm} \cos mL + \beta_{nm} \sin mL) P_{nm}(\sin B). \qquad (12.24)$$

To pass from the anomalies $\Delta \tilde{U}$ on the reference surface to the anomalies ΔU in the external space, we apply a well-known result of the potential theory /8, 21/. Let U_n be a potential whose value on a sphere of radius R is given by

$$\tilde{U}_n = \sum_{m=0}^{n} (a_{nm} \cos mL + b_{nm} \sin mL) P_{nm}(\sin B).$$

The potential in the external space is then

$$U_n = \frac{R^{n+1}}{r^{n+1}} \sum_{m=0}^{n} (a_{nm} \cos mL + b_{nm} \sin mL) P_{nm}(\sin B).$$

Seeing that the anomalous potential ΔU is small, and that the Earth's figure is close to a sphere of mean radius $R = 6371\,\text{km}$, we take expression (12.24) as defining the anomaly ΔU, not on the reference figure, but on the mean sphere. We thus obtain the following expression for the potential of gravity anomalies:

$$\Delta U = g_0 \sum_{n=2}^{\infty} \frac{R^{n+1}}{r^{n+1}} \sum_{m=0}^{n} (\alpha_{nm} \cos mL + \beta_{nm} \sin mL) P_{nm}(\sin B). \qquad (12.25)$$

201

From (12.2) and (12.22) it follows that the anomalous gravitational acceleration is

$$\Delta g = \text{grad } \Delta U. \qquad (12.26)$$

Since the potential ΔU is a function of r and B, but not of the longitude L, the vector Δg will in general deviate from the plane of the meridian (unlike the normal acceleration which is in this plane). The projections of the vector Δg on the radius-vector r, the normal B to the radius-vector in the plane of the meridian, and the normal L to the plane of the meridian are given by

$$\Delta g_r = -\frac{\partial}{\partial r}\Delta U, \quad \Delta g_m = \frac{1}{r}\frac{\partial}{\partial B}\Delta U, \quad \Delta g_L = \frac{1}{r\cos B}\frac{\partial}{\partial L}\Delta U.$$

Inserting (12.25) in the right-hand sides of these equalities and making use of (12.20), which give

$$\frac{d}{dB}P_{nm}(\sin B) = -\frac{m\sin B}{\cos B}P_{nm}(\sin B) + P_{n,\,m+1}(\sin B),$$

we find

$$\begin{aligned}
\Delta g_r &= \frac{g_0}{R}\sum_{n=2}^{\infty}(n+1)\left(\frac{R}{r}\right)^{n+2}\sum_{m=0}^{n}(\alpha_{nm}\cos mL + \beta_{nm}\sin mL)P_{nm}(\sin B), \\
\Delta g_m &= \frac{g_0}{R}\sum_{n=2}^{\infty}\left(\frac{R}{r}\right)^{n+2}\sum_{m=0}^{n}(\alpha_{nm}\cos mL + \beta_{nm}\sin mL)\left[P_{n,\,m+1}(\sin B) - \frac{m\sin B}{\cos B}P_{nm}(\sin B)\right], \\
\Delta g_L &= \frac{g_0}{R\cos B}\sum_{n=2}^{\infty}\left(\frac{R}{r}\right)^{n+2}\sum_{m=0}^{n}(-\alpha_{nm}\sin mL + \beta_{nm}\cos mL)mP_{nm}(\sin B).
\end{aligned} \right\} (12.27)$$

Gravity anomalies can be determined if the coefficients α_{nm} and β_{nm} in the expansion (12.19) are known. The reference surface is commonly the geocentric reference ellipsoid or some close biaxial oblate ellipsoid with its axis along the Earth's spin axis, and its center at the Earth's center of gravity. In determining the total gravitational field of the Earth, its normal component should be taken to coincide with the field of the reference figure.

Exact determination of the coefficients α_{nm} and β_{nm} is a complex problem, whose solution has not yet been completed. According to the latest data for these coefficients /6/, the components of the vector Δg calculated from (12.27) are not greater than $6 \cdot 10^{-4}$ m/sec^2, or $6 \cdot 10^{-5}$ $g_r^{(0)}$, at the Earth's surface. They rapidly decrease with the distance from the Earth's surface (as the fourth or higher power of $1/r$). Note that this applies to averaged gravity anomalies.

Direct measurements show that at some points of the Earth's surface (mainly on oceanic islands) gravity anomalies are higher by one order of magnitude /21/. These anomalies, however, are local, and have no effect on the motion of artificial satellites.

It follows from the preceding that the contribution of the Earth's nonspherical figure and its spin is mainly determined by the components $g_r^{(2)}$ and $g_m^{(2)}$ of the normal gravitational field. The higher normal-field components and $g_m^{(4)}$, as well as gravity anomalies, are of second order of smallness relative to the main perturbations. In the next chapter, we shall therefore concentrate on the effect of the principal perturbing accelerations $g_r^{(2)}$ and $g_m^{(2)}$.

202

Chapter 13

THE INFLUENCE OF THE SECOND ZONAL
HARMONIC OF THE GEOPOTENTIAL ON THE
MOTION OF ARTIFICIAL EARTH SATELLITES

13.1 THE PROJECTIONS OF PERTURBING
ACCELERATION ON AXES CONNECTED
WITH SATELLITE'S POSITION IN ORBIT

As we have shown in the previous chapter, the influence of the Earth's nonspherical figure and spin on its gravity is principally described by the second term in the series expansion of the normal gravitational potential (12.10) (the second zonal harmonic). From (12.18) it follows that the perturbing accelerations $g_r^{(2)}$ and $g_m^{(2)}$ produced by this zonal harmonic are small in comparison with the main part $g_r^{(0)}$ of the Earth's gravitational acceleration. In analyzing their effect, we shall therefore apply the methods developed in Chapters 2, 3, and 11 for small perturbing accelerations in circular and elliptical orbits. We first determine the projections S, T, W of the perturbing acceleration on the axes of a coordinate system connected with the satellite's position and the sense of its motion. The acceleration S is along the radius through the attracting center and the satellite's mass center, the acceleration T is at right angles to this radius in unperturbed orbital plane (it points in the direction of satellite's motion), and the acceleration W is normal to the orbital plane, completing the vectors S and T to a right-hand triad. Figure 13.1 depicts a hemisphere through

FIGURE 13.1. Normal gravitational acceleration of the Earth resolved along coordinate axes connected with the satellite's position in orbit.
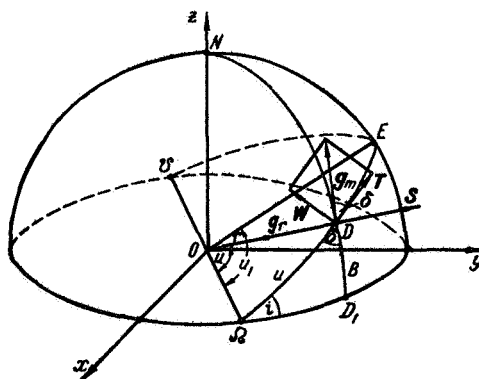
the satellite's position D, with its center O at the Earth's center. The projection of the orbit on this hemisphere is the great circle $\Omega DE\Upsilon$. The points Ω and Υ are the projections of the ascending and the descending nodes, and the point N is the north pole of the sphere.

The circles $\Omega D_1\Upsilon$ and NDD_1 represent the equator and the meridian through the point D, respectively. The figure also shows the perturbing accelerations g_r and g_m, as well as the projections S, T, and W.

We see from the figure that

$$S = -g_r, \quad T = g_m \cos \delta, \quad W = g_m \sin \delta, \tag{13.1}$$

where δ is the angle between the orbital plane $\Omega DE\Upsilon$ and the plane of the meridian D_1DN.

We substitute expressions (12.14) for the main components of the perturbing acceleration, $g_r^{(2)}$ and $g_m^{(2)}$. To eliminate the satellite's latitude B and the angle δ among the resulting expressions, we make use of the spherical right triangle ΩDD_1, where

$$\Omega\breve{D} = u, \quad D\breve{D}_1 = B, \quad \angle D\Omega D_1 = i, \quad \angle DD_1\Omega = \frac{\pi}{2},$$

u being the angular distance of the satellite from the ascending node Ω, and i the inclination of the orbit.

From the triangle ΩDD_1, we have

$$\left.\begin{aligned} \sin B &= \sin u \sin i, \\ \sin \delta &= \frac{\cos i}{\cos B}, \\ \cos \delta &= \frac{\sin i \cos u}{\cos B}. \end{aligned}\right\} \tag{13.2}$$

Substituting (12.14) and (13.2) in (13.1), we find

$$\left.\begin{aligned} S &= \frac{\varepsilon}{r^4}(3\sin^2 i \sin^2 u - 1) = \\ &= -\frac{\varepsilon}{2r^4}\left[3\sin^2 i \sin 2\left(u + \frac{\pi}{4}\right) + 2 - 3\sin^2 i\right], \\ T &= -\frac{\varepsilon}{r^4}\sin^2 i \sin 2u, \\ W &= -\frac{\varepsilon}{r^4}\sin 2i \sin u. \end{aligned}\right\} \tag{13.3}$$

13.2. SECULAR PERTURBATION OF THE CIRCULAR ORBIT PLANE

From (13.3) we see that these perturbing accelerations are a particular case of the periodic perturbations described by (3.5). Let u_0 be the distance of some initial position from the orbit's ascending node, and φ the angular distance of a current point from that initial position. Clearly,

$$u = u_0 + \varphi. \tag{13.4}$$

Substituting in (13.3) and comparing the result with (3.5), we find that in our case

$$
\begin{aligned}
&S_0 = -\frac{\varepsilon}{2r^4}(2 - 3\sin^2 i), \quad S_1 = 0, \\
&S_2 = -\frac{3}{2}\frac{\varepsilon}{r^4}\sin^2 i, \quad \varphi_{S_2} = -\left(\frac{\pi}{4} + u_0\right), \\
&T_0 = T_1 = 0, \quad T_2 = -\frac{\varepsilon}{r^4}\sin^2 i, \quad \varphi_{T_2} = -u_0, \\
&W_0 = W_2 = 0, \quad W_1 = -\frac{\varepsilon}{r^4}\sin 2i, \quad \varphi_{W_1} = -u_0, \\
&S_k = T_k = W_k = 0 \quad \text{при} \quad k \geqslant 3.
\end{aligned}
\tag{13.5}
$$

Let us first consider the secular perturbations of circular orbit produced by these perturbing accelerations. From Sec. 3.9 it follows that these perturbations are of two kinds:

(a) continuous rotation of the orbital plane due to W;

(b) variation of the orbital period due to S and T.

From (3.34) and (13.5) we see that the orbital plane is rotated around the axis OE (Figure 13.1), which makes an angle

$$
u_1 = \frac{\pi}{2}
\tag{13.6}
$$

with the line of nodes $O\Omega$.

Let $\delta\psi$ be the angle of rotation of the orbital plane during one circuit of revolution. Setting $\varphi = 2\pi$, $r_m = r$ in (3.35) and making use of (13.5), we find

$$
\delta\psi = -\frac{\pi}{r^2}\frac{\varepsilon}{\mu}\sin 2i.
\tag{13.7}
$$

The maximum linear displacement of the satellite per one circuit (at right angles to the orbital plane) clearly obtains upon passage through the ascending node Ω :

$$
\delta\xi = |r\,\delta\psi| = \frac{\pi}{r}\frac{\varepsilon}{\mu}|\sin 2i|.
\tag{13.8}
$$

We now calculate the corresponding secular variations in the inclination i and the node longitude Ω. Making use of (9.53), (13.6), and (13.7), we find

$$
\begin{aligned}
&\delta i = 0, \\
&\delta\Omega = -\frac{2\pi}{r^2}\frac{\varepsilon}{\mu}\cos i.
\end{aligned}
\tag{13.9}
$$

In (13.7), (13.8), and (13.9), we substitute for $\frac{\varepsilon}{\mu}$ its approximate expression (12.15), which gives:

$$
\begin{aligned}
&\delta\psi \approx -\frac{\pi}{2}\left(\frac{a_e}{r}\right)^2 \alpha \sin 2i, \\
&\delta\xi \approx \frac{\pi a_e^2}{2r}\alpha|\sin 2i|, \\
&\delta\Omega \approx -\pi\left(\frac{a_e}{r}\right)^2 \alpha \cos i.
\end{aligned}
\tag{13.10}
$$

It follows from the preceding that the Earth's nonspherical figure and spin cause continuous variation in the orientation of the circular orbit plane. The inclination i does not display secular variation, whereas the node monotonically moves in one direction (east-west for $0 \leqslant i < \pi/2$ and west-east for $\pi/2 < i \leqslant \pi$).

The node of polar orbits ($i = \pi/2$) shows no secular displacement. As the orbital plane is closer to the equator, the rate of secular displacement of the node increases. The instantaneous axis of secular rotation of the orbital plane, OE, is in this plane at right angles to the line of nodes. The maximum angular rate of rotation of the orbital plane about this axis is observed for $i = \pi/4$ and $i = 3\pi/4$ (maximum rate of rotation does not coincide with the maximum rate of node displacement: as the orbit approaches the equator, the ratio of these rates approaches zero). For polar and equatorial orbits ($i = 0$, $\pi/2$, π), the angular rate of secular rotation of the orbital plane around the instantaneous axis is zero. Maximum linear lateral displacement of the satellite is observed for nodal passage in orbits with $i = \pi/4$ and $i = 3\pi/4$. The angular displacements are inversely proportional to the square of the radius of the circular orbit, and the linear lateral displacements are inversely proportional to the radius to first power. The secular displacements are approximately proportional to the Earth's flattening α. For close satellites ($r \approx a_e$), maximum displacement per one circuit $\delta\Omega_{max} \approx 0°.6$, maximum rotation around instantaneous axis per one circuit $\delta\psi_{max} \approx 0°.3$, and maximum lateral displacement per one circuit $\delta\zeta_{max} = 33.5$ km. For distant satellites moving in the neighborhood of the Moon's orbit ($r \approx 384,000$ km), $\delta\Omega_{max} \approx 0''.6$, $\delta\psi_{max} \approx 0''.3$, $\delta\zeta_{max} \approx 0.5$ km.

13.3. PERTURBATION OF SATELLITE'S ORBITAL PERIOD IN CIRCULAR ORBIT

We now proceed with the perturbation of the period of revolution. From (3.10), (3.40), and (13.5), we have

$$\frac{\Delta P}{P} = \frac{r^2}{\mu}\left(2S_0 + \frac{3}{2}T_2\cos 2\varphi_{r_2}\right) = -\frac{1}{r^2}\frac{\varepsilon}{\mu}\left(2 - 3\sin^2 i + \frac{3}{2}\sin^2 i \cos 2u_0\right). \qquad (13.11)$$

Hence, making use of (1.5),

$$\Delta P = -\frac{2\pi}{\sqrt{\mu r}}\frac{\varepsilon}{\mu}\left(2 - 3\sin^2 i + \frac{3}{2}\sin^2 i \cos 2u_0\right). \qquad (13.12)$$

Note that, unlike the perturbations $\delta\psi$ and $\delta\Omega$, which represent monotonically growing displacement of the orbital plane, the variation ΔP is a constant correction to the satellite's orbital period: it is the difference between the sidereal and the osculating periods of revolution at the point of origin (see Sec. 13.6). The orbital period correction corresponds to a growing secular displacement of the satellite's position along the orbit. Making use of (1.4), we can calculate the displacement per circuit:

$$\delta l = -\Delta P w = \frac{2\pi}{r}\frac{\varepsilon}{\mu}\left(2 - 3\sin^2 i + \frac{3}{2}\sin^2 i \cos 2u_0\right). \qquad (13.13)$$

206

Substituting the approximate expression (12.15) in relations (13.11), (13.12), and (13.13), we find

$$\frac{\Delta P}{P} = -\frac{1}{2}\left(\frac{a_e}{r}\right)^2 \alpha \left(2 - 3\sin^2 i + \frac{3}{2}\sin^2 i \cos 2u_0\right),$$

$$\Delta P = -\frac{1}{2} P_E \sqrt{\frac{a_e}{r}} \alpha \left(2 - 3\sin^2 i + \frac{3}{2}\sin^2 i \cos 2u_0\right),$$

$$\delta l = \pi a_e \frac{a_e}{r} \alpha \left(2 - 3\sin^2 i + \frac{3}{2}\sin^2 i \cos 2u_0\right).$$

(13.14)

where

$$P_E = 2\pi \frac{a_e^{3/2}}{\sqrt{\mu}} \approx 84.5 \,\text{min}$$

(13.15)

is the period of revolution of a hypothetical satellite moving in circular orbit whose radius is equal to the semimajor axis of the geocentric reference ellipsoid.

The function of the angles i and u_0 in the right-hand sides of (13.14) attains its peak value for $i = u_0 = \frac{\pi}{2}$. Hence the peak values of the corresponding perturbations:

$$\left|\frac{\Delta P}{P}\right|_{\max} \approx \frac{5}{4}\left(\frac{a_e}{r}\right)^2 \alpha, \quad \Delta P_{\max} \approx \frac{5}{4} P_E \sqrt{\frac{a_e}{r}} \alpha,$$

$$|\delta l|_{\max} \approx \frac{5\pi}{2} a_e \frac{a_e}{r} \alpha.$$

(13.16)

For close satellites $(r \approx a_e)$, $\left|\frac{\Delta P}{P}\right|_{\max} \approx 0.0042$, $|\Delta P|_{\max} \approx 0.35$ min, $|\delta l|_{\max} \approx 167$ km. For distant satellites moving in the neighborhood of the lunar orbit $(r \approx 384,000 \,\text{km})$, $\left|\frac{\Delta P}{P}\right|_{\max} \approx 1.15 \cdot 10^{-6}$, $|\Delta P|_{\max} \approx 0.045$ min, $|\delta l|_{\max} \approx 2.8$ km.

The Earth's nonspherical figure and its spin thus produce a substantial secular displacement in the orbits of artificial satellites. The displacement is both along the orbit and at right angles to the orbital plane. It is larger for close satellites, but although it rapidly decreases with increasing flight altitude, it is nevertheless noticeable for satellites moving near the lunar orbit.

13.4. PERIODIC PERTURBATIONS OF CIRCULAR ORBIT

To determine the periodic perturbations of circular orbit, we substitute expressions (13.3) for the components of perturbing acceleration in relations (3.6). Making use of (3.7) and (13.4), we obtain the following expressions for the total perturbations Δr and Δl along the radius and along the orbit:

$$\Delta r = -\frac{1}{2r}\frac{\varepsilon}{\mu} \int_0^\varphi \{[2 - 3\sin^2 i + 3\sin^2 i \cos 2(\psi + u_0)] \sin(\varphi - \psi) +$$

$$+ 4\sin^2 i \sin 2(\psi + u_0)[1 - \cos(\varphi - \psi)]\} d\psi.$$

$$\Delta l = r \Delta u = \frac{1}{r}\frac{\varepsilon}{\mu} \int_0^\varphi \{[2 - 3\sin^2 i + 3\sin^2 i \cos 2(\psi + u_0)] \times$$

$$\times [1 - \cos(\varphi - \psi)] + \sin^2 i \sin 2(\psi + u_0)[3(\varphi - \psi) - 4\sin(\varphi - \psi)]\} d\psi.$$

207

These expressions can be written as

$$\Delta r = -\frac{1}{2r}\frac{\varepsilon}{\mu}\left[(2-3\sin^2 i)J_1+\sin^2 i\,(3J_2+4J_3-4J_4)\right],$$
$$\Delta l = \frac{1}{r}\frac{\varepsilon}{\mu}\big[(2-3\sin^2 i)J_5+$$
$$+\sin^2 i\,(3J_6-3J_7+3J_8-4J_9)\big],$$

(13.17)

where

$$J_1 = \int_0^{\varphi}\sin(\varphi-\psi)\,d\psi,$$

$$J_2 = \int_0^{\varphi}\cos 2\,(\psi+u_0)\sin(\varphi-\psi)\,d\psi.$$

$$J_3 = \int_0^{\varphi}\sin 2\,(\psi+u_0)\,d\psi,$$

$$J_4 = \int_0^{\varphi}\sin 2\,(\psi+u_0)\cos(\varphi-\psi)\,d\psi.$$

$$J_5 = \int_0^{\varphi}\left[1-\cos(\varphi-\psi)\right]d\psi,$$

$$J_6 = \int_0^{\varphi}\cos 2\,(\psi+u_0)\,d\psi,$$

$$J_7 = \int_0^{\varphi}\cos 2\,(\psi+u_0)\cos(\varphi-\psi)\,d\psi,$$

$$J_8 = \int_0^{\varphi}(\varphi-\psi)\sin 2\,(\psi+u_0)\,d\psi,$$

$$J_9 = \int_0^{\varphi}\sin 2\,(\psi+u_0)\sin(\varphi-\psi)\,d\psi.$$

(13.18)

Making use of (3.20), we obtain after some manipulations

$$J_1 = 1-\cos\varphi,$$

$$J_2 = \frac{1}{2}\int_0^{\varphi}\left[\sin(\psi+2u_0+\varphi)-\sin(3\psi+2u_0-\varphi)\right]d\psi =$$
$$=\frac{1}{6}\left[3\cos(2u_0+\varphi)-2\cos 2\,(u_0+\varphi)-\cos(2u_0-\varphi)\right],$$

$$J_3 = \frac{1}{2}\left[\cos 2u_0-\cos 2\,(\varphi+u_0)\right],$$

$$J_4 = \frac{1}{2}\int_0^{\varphi}\left[\sin(\psi+2u_0+\varphi)+\sin(3\psi+2u_0-\varphi)\right]d\psi =$$
$$=\frac{1}{6}\left[3\cos(2u_0+\varphi)-4\cos 2\,(u_0+\varphi)+\cos(2u_0-\varphi)\right],$$

$$J_5 = \varphi-\sin\varphi,$$

$$J_6 = \frac{1}{2}\left[\sin 2\,(\varphi+u_0)-\sin 2u_0\right],$$

$$J_7 = \frac{1}{2} \int_0^\varphi [\cos(\psi + 2u_0 + \varphi) + \cos(3\psi + 2u_0 - \varphi)]\, d\psi =$$

$$= \frac{1}{6} [4 \sin 2(u_0 + \varphi) - 3 \sin(2u_0 + \varphi) - \sin(2u_0 - \varphi)],$$

$$J_8 = (\varphi + u_0) \int_0^\varphi \sin 2(\psi + u_0)\, d\psi -$$

$$- \frac{1}{2} \int_0^\varphi 2(\psi + u_0) \sin 2(\psi + u_0)\, d\psi = \frac{1}{4} [2\varphi \cos 2u_0 - \sin 2(\varphi + u_0) + \sin 2u_0],$$

$$J_9 = \frac{1}{2} \int_0^\varphi [\cos(3\psi + 2u_0 - \varphi) - \cos(\psi + 2u_0 + \varphi)]\, d\psi =$$

$$= \frac{1}{6} [3 \sin(2u_0 + \varphi) - 2 \sin 2(u_0 + \varphi) - \sin(2u_0 - \varphi)].$$

Omitting the terms with φ (which describe the previously considered secular perturbations) from the expressions for J_5 and J_8, we substitute these relations in (13.17), which give the following equalities for the periodic perturbations:

$$\left.\begin{aligned}
\Delta_{\text{per}} r &= -\frac{1}{2r} \frac{\varepsilon}{\mu} \Big\{ (2 - 3 \sin^2 i)(1 - \cos\varphi) + \\
&\quad + \frac{\sin^2 i}{6} [12 \cos 2u_0 - 3 \cos(2u_0 + \varphi) - \\
&\quad - 2 \cos 2(u_0 + \varphi) - 7 \cos(2u_0 - \varphi)] \Big\}, \\
\Delta_{\text{per}} l &= -\frac{1}{r} \frac{\varepsilon}{\mu} \Big\{ (2 - 3 \sin^2 i) \sin\varphi + \\
&\quad + \frac{\sin^2 i}{12} [9 \sin 2u_0 + 6 \sin(2u_0 + \varphi) - \\
&\quad - \sin 2(u_0 + \varphi) - 14 \sin(2u_0 - \varphi)] \Big\}.
\end{aligned}\right\} \tag{13.19}$$

These relations can be written as

$$\Delta_{\text{per}} r = \Delta_0 r + A_1 \sin\varphi + A_2 \cos\varphi + A_3 \sin 2\varphi + A_4 \cos 2\varphi,$$
$$\Delta_{\text{per}} l = \Delta_0 l + A_5 \sin\varphi + A_6 \cos\varphi + A_7 \sin 2\varphi + A_8 \cos 2\varphi,$$

where $\Delta_0 r$, $\Delta_0 l$, A_i ($i = 1, 2, \ldots, 8$) are some functions of i, r, u_0. Seeing that

$$A_1 \sin\varphi + A_2 \cos\varphi = \sqrt{A_1^2 + A_2^2} \sin(\varphi - \varphi_1), \tag{13.19a}$$

where

$$\sin\varphi_1 = -\frac{A_2}{\sqrt{A_1^2 + A_2^2}}, \quad \cos\varphi_1 = \frac{A_1}{\sqrt{A_1^2 + A_2^2}}.$$

we write

$$\left.\begin{aligned}
\Delta_{\text{per}} r &= \Delta_0 r + \Delta_1 r \sin(\varphi - \varphi_1) + \Delta_2 r \sin 2(\varphi - \varphi_2), \\
\Delta_{\text{per}} l &= \Delta_0 l + \Delta_1 l \sin(\varphi - \varphi_3) + \Delta_2 l \sin 2(\varphi - \varphi_4),
\end{aligned}\right\} \tag{13.20}$$

where $\Delta_i r$, $\Delta_i l$, φ_k ($i = 0, 1, 2$; $k = 1, 2, 3, 4$) are some functions of i, r, u_0 which are constant for each given orbit.

The periodic perturbations of circular orbit thus reduce to some constant displacements of the satellite in the directions r and l, and also periodic distortions of the orbit whose frequency is equal to the satellite's orbital frequency and to twice that frequency.

To estimate the magnitude of these periodic perturbations, we consider the case of an equatorial satellite ($i = 0$). Expressions (13.19) take the form

$$\left.\begin{array}{l} \Delta_{\text{per}}r = -\frac{1}{r}\frac{\varepsilon}{\mu}(1 - \cos\varphi), \\[2mm] \Delta_{\text{per}}l = -\frac{2}{r}\frac{\varepsilon}{\mu}\sin\varphi. \end{array}\right\} \tag{13.21}$$

The peak magnitude of these perturbations is estimated with the aid of equality (12.15), which gives

$$|\Delta_{\text{per}}r|_{\max} = |\Delta_{\text{per}}l|_{\max} = \frac{2}{r}\frac{\varepsilon}{\mu} \approx \frac{a_\varepsilon}{r}a_\varepsilon\alpha. \tag{13.22}$$

For low-flying satellites ($r \approx a_\varepsilon$),

$$|\Delta_{\text{per}}r|_{\max} = |\Delta_{\text{per}}l|_{\max} \approx a_\varepsilon\alpha \approx 21 \text{ km}.$$

To find the periodic perturbation at right angles to the orbital plane, we substitute (3.7) and (13.5) in the first term in the right-hand side of the corresponding equality in (3.22). Thus,

$$\Delta_{\text{per}}z = -\frac{1}{2r}\frac{\varepsilon}{\mu}\sin 2i \cos u_0 \sin\varphi. \tag{13.23}$$

Hence, making use of the approximate relation (12.15), we obtain the peak magnitude of $\Delta_{\text{per}}z$:

$$|\Delta_{\text{per}}z|_{\max} = \frac{1}{2r}\frac{\varepsilon}{\mu} \approx \frac{1}{4}a_\varepsilon\frac{a_\varepsilon}{r}\alpha. \tag{13.24}$$

For low-flying satellites ($r \approx a_\varepsilon$),

$$|\Delta_{\text{per}}z|_{\max} \approx \frac{1}{4}a_\varepsilon\alpha \approx 5 \text{ km}. \tag{13.25}$$

Making use of (2.32), we can show that the periodic perturbation described by (13.23) rotates the orbital plane around an axis through the satellite's initial position, the angle of rotation being

$$\psi = -\frac{1}{2r^2}\frac{\varepsilon}{\mu}\sin 2i \cos u_0. \tag{13.26}$$

The peak magnitude of this angle is

$$|\psi|_{\max} = \frac{1}{2r^2}\frac{\varepsilon}{\mu} \approx \frac{1}{4}\left(\frac{a_\varepsilon}{r}\right)^2\alpha. \tag{13.27}$$

For low-flying satellites ($r \approx a_\varepsilon$),

$$|\psi|_{\max} \approx 2'.9. \tag{13.28}$$

The nonspherical figure of the Earth and its spin are thus seen to cause periodic as well as secular perturbations in the orbits of close satellites. The linear magnitudes of the periodic perturbations, however, are inversely proportional to the radius of the circular orbit.

13.5. SECULAR PERTURBATIONS OF ELLIPTICAL ORBIT

The secular perturbations in elements of elliptical orbit can be found from (4.19), (11.39), and (13.3). In calculating the small ratios $\frac{S}{g}$, $\frac{T}{g}$, and $\frac{W}{g}$, we take $g \approx \frac{\mu}{r^2}$. We thus obtain the following approximate expressions for the increments of the corresponding orbital elements per one circuit of revolution:

$$\delta p = -\frac{2}{p}\frac{\varepsilon}{\mu}\sin^2 i \int_0^{2\pi} (1+e\cos\vartheta)\sin 2u\, d\vartheta,$$

$$\delta e = \frac{1}{p^2}\frac{\varepsilon}{\mu}\int_0^{2\pi} \{\sin\vartheta\,(1+e\cos\vartheta)^2(3\sin^2 i \sin^2 u - 1) -$$

$$- [2\cos\vartheta + e(\cos^2\vartheta + 1)](1+e\cos\vartheta)\sin^2 i \sin 2u\}\, d\vartheta.$$

$$\delta\omega = \frac{1}{p^2}\frac{\varepsilon}{\mu}\int_0^{2\pi} \Big[-\frac{\cos\vartheta}{e}(1+e\cos\vartheta)^2(3\sin^2 i \sin^2 u - 1) -$$

$$- \frac{2+e\cos\vartheta}{e}(1+e\cos\vartheta)\sin\vartheta\sin 2u \sin^2 i +$$

$$+ 2(1+e\cos\vartheta)\sin^2 u \cos^2 i \Big]\, d\vartheta,$$

$$\delta\Omega = -\frac{2}{p^2}\frac{\varepsilon}{\mu}\cos i \int_0^{2\pi} (1+e\cos\vartheta)\sin^2 u\, d\vartheta,$$

$$\delta i = -\frac{1}{p^2}\frac{\varepsilon}{\mu}\sin 2i \int_0^{2\pi} (1+e\cos\vartheta)\cos u \sin u\, d\vartheta.$$

(13.29)

To facilitate the integration of the right-hand sides, we consider a definite integral of the form

$$J_1 = \int_0^{2\pi} \sin^n(x+\alpha)\cos^m(x+\alpha)\, dx,$$

where α is a constant, and n and m are arbitrary integers, at least one of which is odd. To avoid ambiguity, we put

$$m = 2k+1,$$

where k is an integer. Then

$$J_1 = \int_0^{2\pi} \sin^n(x+\alpha)[1-\sin^2(x+\alpha)]^k \cos(x+\alpha)\, dx = \int_{\sin\alpha}^{\sin\alpha} y^n(1-y^2)^k\, dy = 0.$$

It can be analogously shown that $J_1 = 0$ for $n = 2k+1$.

Thus,

$$\int_0^{2\pi} \sin^n(x+\alpha)\cos^m(x+\alpha)\,dx = 0, \qquad (13.30)$$

if at least one of the integers n or m is odd. In particular, this equality applies if the sum $(n+m)$ is odd.

Let us now consider an integral of the form

$$J_2 = \int_0^{2\pi} \sin^n x \cos^m x \sin^p(x+\alpha)\cos^q(x+\alpha)\,dx,$$

where n, m, p, q are integers, and α a constant. This integral may be represented as a sum of integrals:

$$J_2 = \sum_i A_i \int_0^{2\pi} \sin^{n_i} x \cos^{m_i} x\,dx,$$

where A_i $(i = 1, 2, \ldots)$ are some trigonometric functions of the constant α, and n_i and m_i are integers satisfying the equality

$$n_i + m_i = n + m + p + q.$$

Hence, applying (13.30), we find

$$\int_0^{2\pi} \sin^n x \cos^m x \sin^p(x+\alpha)\cos^q(x+\alpha)\,dx = 0 \qquad (13.31)$$

if the integer sum $n+m+p+q$ is odd.

Now, the angles u and ϑ in the right-hand sides of (13.29) are related by the well-known expression

$$u = \vartheta + \omega. \qquad (13.31')$$

The argument of the perigee ω (as well as the other orbital elements) is assumed to be constant during one circuit of revolution (this assumption holds true in our approximation). In calculating the right-hand sides of (13.29) we can therefore omit all terms which vanish in compliance with (13.30) and (13.31). Thus,

$$\delta p = \delta i = 0,$$

$$\delta e = \frac{1}{p^2}\frac{\varepsilon}{\mu} e \sin^2 i \int_0^{2\pi} (6\sin\vartheta\cos\vartheta\sin^2 u - 3\cos^2\vartheta\sin 2u)\,d\vartheta =$$

$$= -\frac{3}{2p^2}\frac{\varepsilon}{\mu} e \sin^2 i \int_0^{2\pi} (\sin 2\vartheta \sin 2u + \cos 2\vartheta \sin 2u)\,d\vartheta = 0,$$

$$\delta\omega = \frac{1}{p^2}\frac{\varepsilon}{\mu}\int_0^{2\pi} [-2\cos^2\vartheta\,(3\sin^2 i \sin^2 u - 1) - 3\cos\vartheta\sin\vartheta\sin 2u \sin^2 i + 2\sin^2 u \cos^2 i]\,d\vartheta =$$

$$= \frac{1}{p^2}\frac{\varepsilon}{\mu}\int_0^{2\pi} [-\sin^2 i\,(6\cos^2\vartheta\sin^2 u + 3\cos\vartheta\sin\vartheta\sin 2u) +$$

212

$$+ 2\cos^2 \vartheta + 2\cos^2 i \sin^2 u] \, d\vartheta = \frac{1}{p^2} \frac{\varepsilon}{\mu} \int_0^{2\pi} \left\{ -\frac{3}{2} \sin^2 i \left[(1 + \cos 2\vartheta)(1 - \cos 2u) + \right. \right.$$

$$\left. + \sin 2\vartheta \sin 2u \right] + 1 + \cos 2\vartheta + \cos^2 i (1 - \cos 2u) \left. \right\} d\vartheta =$$

$$= \frac{1}{p^2} \frac{\varepsilon}{\mu} \pi (- 3\sin^2 i + 2 + 2\cos^2 i) = \frac{\pi}{p^2} \frac{\varepsilon}{\mu} (5\cos^2 i - 1),$$

$$\delta\Omega = -\frac{3}{p^2} \frac{\varepsilon}{\mu} \cos i \int_0^{2\pi} \sin^2 u \, d\vartheta =$$

$$= -\frac{3}{p^2} \frac{\varepsilon}{\mu} \cos i \int_0^{2\pi} \frac{1 - \sin 2u}{2} \, d\vartheta = -\frac{2\pi}{p^2} \frac{\varepsilon}{\mu} \cos i.$$

The expressions for the increments of the elements of elliptical orbit per one circuit are thus written (to first approximation) as

$$\begin{matrix} \delta p = \delta e = \delta i = 0, \\ \delta\omega = \frac{\pi}{p^2} \frac{\varepsilon}{\mu} (5\cos^2 i - 1), \\ \delta\Omega = -\frac{2\pi}{p^2} \frac{\varepsilon}{\mu} \cos i. \end{matrix} \quad \right\} \qquad (13.32)$$

Making use of the approximate equality (12.15), we write

$$\begin{matrix} \delta\omega \approx \frac{\pi}{2} \left(\frac{a_e}{p} \right)^2 \alpha (5\cos^2 i - 1), \\ \delta\Omega \approx -\pi \left(\frac{a_e}{p} \right)^2 \alpha \cos i. \end{matrix} \quad \right\} \qquad (13.33)$$

Upon passing from elliptical to circular orbit, the parameter p equals the radius r of the orbit. The formulas for the secular displacement $\delta\omega$ of the perigee are then meaningless, and the formulas for the displacement $\delta\Omega$ of the node reduce to the corresponding equalities (13.9) and (13.10) derived for circular orbit. The qualitative analysis of the secular variation in the orientation of the elliptical orbit may therefore proceed from the results obtained for circular orbit in Sec. 13.2.

In analyzing the secular displacement of the perigee, $\delta\omega$, we note that for some critical inclinations,

$$i_{cr1} = \arccos \sqrt{\frac{1}{5}} \approx 63° 26' \quad \text{and} \quad i_{cr2} = \pi - i_{cr1} \approx 116° 34', \qquad (13.34)$$

we have $= 0$. For $i < i_{cr1}$ or $i > i_{cr2}$, $\delta\omega > 0$, i.e., the perigee moves in the direction of satellite's motion. For $i_{cr1} < i < i_{cr2}$, $\delta\omega < 0$ and the perigee regresses. The rate of perigee displacement (for $p = $ const) is maximal in equatorial orbit $(i = 0)$:

$$\delta\omega_{max} = 4 \frac{\pi}{p^2} \frac{\varepsilon}{\mu} \approx 2\pi \left(\frac{a_e}{p} \right)^2 \alpha. \qquad (13.35)$$

For low-flying satellites $(p \approx a_e)$, $\delta\omega_{max} \approx 2\pi\alpha \approx 1°.2$. It follows from (13.35) that the rate of secular displacement of the perigee point is inversely proportional to the square of the parameter p, decreasing as the size of the orbit increases. For satellites moving in the neighborhood of the lunar orbit $(p \approx 384,000 \text{ km})$, $\delta\omega_{max} \approx 1''.2$, which is a substantial figure.

Let n be the total number of circuits completed by a satellite in a certain time. The displacements $\Delta\Omega$ of the node and $\Delta\omega$ of the perigee are clearly given by

$$\Delta\Omega = n\,\delta\Omega, \quad \Delta\omega = n\,\delta\omega. \tag{13.36}$$

Let n_Ω and n_ω be the number of circuits for which the total displacements $\Delta\Omega$ and $\Delta\omega$ are 2π. Once the satellite has completed n_Ω and n_ω circuits, the orbital plane and the perigee point return to the original position. Therefore, essentially these are long-periodic perturbations. The periods $\bar{P}_\Omega$ and $\bar{P}_\omega$ of these disturbances are given by

$$\bar{P}_\Omega = n_\Omega P, \quad \bar{P}_\omega = n_\omega P, \tag{13.37}$$

where P is the orbital period of the satellite.

From (13.32), (13.33), and (13.36), we see that

$$
\left.
\begin{aligned}
n_\Omega &= \frac{2\pi}{|\delta\Omega|} = \frac{p^2}{|\cos i|}\frac{\mu}{\varepsilon} \approx \frac{2}{\alpha|\cos^2 i|}\left(\frac{p}{a_e}\right)^2, \\
n_\omega &= \frac{2\pi}{|\delta\omega|} = \frac{2p^2}{|5\cos^2 i - 1|}\frac{\mu}{\varepsilon} \approx \frac{4}{\alpha|5\cos^2 i - 1|}\left(\frac{p}{a_e}\right)^2.
\end{aligned}
\right\} \tag{13.38}
$$

Hence it follows that $n_\Omega \to \infty$ for $i \to \frac{\pi}{2}$, and $n_\omega \to \infty$ for $i \to i_{cr1}$ or $i \to i_{cr2}$.

The minimum circuit numbers n_Ω and n_ω obtain for a satellite in equatorial orbit $(i = 0)$, when

$$
\left.
\begin{aligned}
(n_\Omega)_{\min} &= p^2\frac{\mu}{\varepsilon} \approx \frac{2}{\alpha}\left(\frac{p}{a_e}\right)^2, \\
(n_\omega)_{\min} &= p^2\frac{\mu}{\varepsilon} \approx \frac{1}{\alpha}\left(\frac{p}{a_e}\right)^2.
\end{aligned}
\right\} \tag{13.39}
$$

Note that for $i = 0$ the evolution of the orbit's node is a meaningless effect (since the node in this case is an indeterminate concept). The expression for $(n_\Omega)_{\min}$ should therefore be considered as the limit for n_Ω as $i \to 0$.

For low-flying satellites $(p \approx a_e)$,

$$
\left.
\begin{aligned}
(n_\Omega)_{\min} &\approx \frac{2}{\alpha} \approx 600, \\
(n_\omega)_{\min} &\approx \frac{1}{\alpha} \approx 300.
\end{aligned}
\right\} \tag{13.40}
$$

To form a more detailed idea of the exact nature of long-periodic perturbations, we consider the example of nearly periodic orbits. Let r_{pert} and r_{unpert} be the distances of the satellite from the Earth's center in perturbed and unperturbed orbits, respectively. Making use of (2.38) and (2.41), we find

$$r_{\text{pert}} = r_m[1 - e\cos(\lambda t - \omega - n\delta\omega)],$$
$$r_{\text{unpert}} = r_m[1 - e\cos(\lambda t - \omega)],$$

where r_m, e, ω, λ are respectively the mean radius, the eccentricity, the argument of the perigee, and the mean angular velocity in unperturbed orbit, n the number of circuits from injection. The radial perturbation is thus

given by

$$\Delta r = r_{\text{pert}} - r_{\text{unpert}} = er_{\text{m}}[\cos(\lambda t - \omega) - \cos(\lambda t - \omega - n\delta\omega)] =$$
$$= -2er_{\text{m}}\sin\left(\lambda t - \omega - \frac{n\delta\omega}{2}\right)\sin\frac{n\delta\omega}{2}.$$

Seeing that

$$n = \frac{\lambda t}{2\pi} = \frac{t}{P},$$

we write for the preceding equality

$$\Delta r = -2er_{\text{m}}\sin\left[\lambda\left(1 - \frac{\delta\omega}{4\pi}\right)t - \omega\right]\sin\frac{\lambda\delta\omega}{4\pi}t.$$

Now, $\frac{\delta\omega}{4\pi} \ll 1$. We may therefore approximately take the perturbation Δr to vary with a frequency which is close to the orbital frequency of the satellite. The amplitude of these fluctuations is given by

$$A = 2er_{\text{m}}\left|\sin\frac{\lambda\delta\omega}{4\pi}t\right| = 2er_{\text{m}}\left|\sin\frac{\pi}{n_\omega P}t\right| = 2er_{\text{m}}\left|\sin\pi\frac{t}{P_\omega}\right|.$$

In other words, the radial perturbations Δr are in the nature of beats whose frequency is close to the satellite's orbital frequency. The peak amplitude of these beats is

$$A_{\max} = 2er_{\text{m}},$$

and it is observed at

$$t = \bar{P}_\omega\left(k + \frac{1}{2}\right),$$

where k is an integer. For $t = \bar{P}_\omega k$, the amplitude of these beats is $A = 0$.

The perturbations at right angles to the orbital plane can be shown to have the same form (with $\bar{P}_\Omega$ substituted for $\bar{P}_\omega$). The peak amplitude is $A_{\max} = r_{\text{m}}$.

13.6. PERTURBATIONS OF ORBITAL PERIOD IN ELLIPTICAL ORBIT.

Besides the secular perturbations which entail rotation of the orbital plane and movement of the perigee, there are also secular displacements of the satellite's position along the orbit (or, equivalently, perturbations of the time of arrival of the satellite at any given point). For the particular case of circular orbits, these perturbations were investigated in Sec. 13.3, where they were shown to cause a certain change in the orbital period.

We now proceed with the analysis of perturbations of the period of revolution in elliptical orbit. It should be noted, however, that in elliptical orbit the period of revolution is a very vague concept. Indeed, for unperturbed plane orbit, the period of revolution P is defined as the time in which a radius-vector OD through the Earth's center O and the satellite's center D returns to its initial position. In the presence of secular

perturbations, however, the orbital plane moves and the radius-vector OD cannot return to its precise initial position. The period of revolution is generally defined as the time between two successive passages of the satellite's center D across some fixed surface Σ. The length of the orbital period varies depending on the choice of the surface Σ. The following orbital periods are generally considered in connection with artificial Earth satellites:

nodical period of revolution P_Ω — the time between successive south-north passages of the satellite through the equatorial plane, i.e., the time it takes the satellite to revolve from ascending node Ω_0 to ascending node Ω_1 of two successive orbital circuits (Figure 13.2);

zonal period of revolution P_B — the time between successive passages of the satellite through the points D_0 and D_1 on a conical surface of constant geocentric latitude B (the satellite crosses the conical surface from south to north);

sidereal period of revolution P_s — the flight time from some point D_0 of the orbit to another point D' in the plane through the radius-vector OD_0, at right angles to the plane of the osculating orbit at the point D_0.

Some other orbital periods are also in use:

anomalistic period of revolution P_π — the time between two successive perigee passages;

osculating period of revolution P' — the time of revolution in osculating orbit.
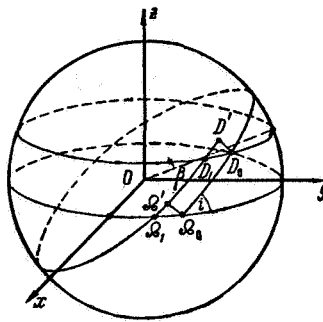
FIGURE 13.2. Illustrating the relationship between various orbital periods.

The osculating period is in fact the period of revolution in unperturbed orbit which would obtain if all the perturbing accelerations were to vanish starting from some instant. It is therefore also called the unperturbed orbital period. If the coordinates and the velocity components of a satellite at some point are known, the corresponding P' is easily found from (5.36) and (5.49). In practice, the other orbital periods do not differ much from the osculating (unperturbed) period P', and they are therefore conveniently described by formulas of the form

$$P = P' + \Delta P,$$

where ΔP is the perturbations of the orbital period, which is generally small in comparison with P and P'.

From the definitions of the periods P_B, P_s, and P' we see that these periods are not only different, but they actually depend on the choice of the initial position D_0 to which they are referred. As regards the periods P_Ω and P_π, they are referred to fixed points (the node and the perigee), and they are therefore unambiguously defined for each circuit of revolution. For orbits with $i \neq 0$, it is the nodical period of revolution P_Ω which is of the greatest significance: each passage of a satellite through the equatorial plane can be accurately recorded by tracking instruments. The time of perigee passage is more difficult to determine, especially for low-eccentricity orbits, where the position of the perigee point is fairly uncertain.

13.7. NODICAL PERIOD OF REVOLUTION

In deriving approximate relations for the nodical period P_Ω we should note that during the nodal passage of the satellite in its real orbit, the corresponding osculating orbit also passes through the node. Hence immediately

$$P_\Omega = \int_0^{2\pi} \frac{dt}{du} \, du, \tag{13.41}$$

where t is the flight time, and u is the angular distance from the current point to the node of the corresponding osculating orbit.

From (11.14) and (11.25) we have

$$\frac{du}{dt} = \frac{\sqrt{p\mu}}{r^2} - \cos i \, \frac{d\Omega}{dt}, \tag{13.42}$$

$$\frac{dt}{du} = \frac{r^2}{\sqrt{p\mu}} \left(1 - \frac{r^2}{\sqrt{p\mu}} \cos i \, \frac{d\Omega}{dt} \right)^{-1}. \tag{13.43}$$

From (11.14), (12.15), and (13.3) it follows that the second term in the right-hand side of (13.43) is a small quantity (of the same order as the Earth's flattening α). Therefore, neglecting terms of the order α^2, we write

$$\frac{dt}{du} \approx \frac{r^2}{\sqrt{p\mu}} + \frac{r^4}{p\mu} \cos i \, \frac{d\Omega}{dt}. \tag{13.44}$$

Substituting in (13.41) and applying (4.19), we find

$$P_\Omega = \frac{1}{\sqrt{\mu}} \int_0^{2\pi} \frac{p^{3/2}}{[1 + e \cos(u - \omega)]^2} \, du + \frac{1}{\mu} \int_0^{2\pi} \frac{p^3}{[1 + e \cos(u - \omega)]^4} \cos i \, \frac{d\Omega}{dt} \, du. \tag{13.45}$$

The osculating elements p, e, ω, i in the right-hand side of this equality are given by

$$p = p_0 + \Delta p, \quad e = e_0 + \Delta e, \quad \omega = \omega_0 + \Delta\omega, \quad i = i_0 + \Delta i, \tag{13.46}$$

where p_0, e_0, ω_0, i_0 are the nodical values of the corresponding osculating elements, and $\Delta p, \Delta e, \Delta \omega, \Delta i$ are small corrections to the nodical values, defined by

$$\Delta p = \int_0^u \frac{dp}{du}\, du, \quad \Delta e = \int_0^u \frac{de}{du}\, du, \left.\vphantom{\int_0^u}\right\}$$
$$\Delta \omega = \int_0^u \frac{d\omega}{du}\, du, \quad \Delta i = \int_0^u \frac{di}{du}\, du. \qquad (13.47)$$

Substituting (13.46) in (13.45), we have, to terms of the first order of smallness,

$$P_{\Omega} = P'_{\Omega} - (\Delta P_1 + \Delta P_2 + \Delta P_3 + \Delta P_4), \qquad (13.48)$$

where

$$P'_{\Omega} = \frac{1}{\sqrt{\mu}} \int_0^{2\pi} \frac{p_0^{3/2}}{[1 + e_0 \cos (u - \omega_0)]^2}\, du,$$

$$\Delta P_1 = -\frac{3}{2} \sqrt{\frac{p_0}{\mu}} \int_0^{2\pi} \frac{\Delta p}{[1 + e_0 \cos (u - \omega_0)]^2}\, du,$$

$$\Delta P_2 = \frac{2 p_0^{3/2}}{\sqrt{\mu}} \int_0^{2\pi} \frac{\cos (u - \omega_0)}{[1 + e_0 \cos (u - \omega_0)]^3}\, \Delta e\, du, \left.\vphantom{\int_0^{2\pi}}\right\} \qquad (13.49)$$

$$\Delta P_3 = \frac{2 p_0^{3/2}}{\sqrt{\mu}} \int_0^{2\pi} \frac{\sin (u - \omega_0)}{[1 + e_0 \cos (u - \omega_0)]^3}\, e_0 \,\delta\omega\, du,$$

$$\Delta P_4 = -\frac{p_0^3}{\mu} \cos i_0 \int_0^{2\pi} \frac{\frac{d\Omega}{dt}}{[1 + e_0 \cos (u - \omega_0)]^4}\, du.$$

P'_{Ω} is the osculating period at the node, and $\Delta P_1, \Delta P_2, \Delta P_3, \Delta P_4$ are corrections to this period. For small eccentricities $(e \ll 1)$, these corrections are also small. Therefore, terms of higher order of smallness can be ignored in calculating the derivatives $\frac{dp}{du}, \frac{de}{du}, \frac{d\omega}{du}$ for substitution in (13.47).

Proceeding as in the derivation of (13.29), we find

$$\frac{dp}{du} = -\frac{2}{p_0} \frac{\varepsilon}{\mu} \sin^2 i_0 (1 + e_0 \cos \vartheta) \sin 2u, \left.\vphantom{\frac{dp}{du}}\right\}$$

$$\frac{de}{du} = \frac{1}{p_0^2} \frac{\varepsilon}{\mu} \{\sin \vartheta (1 + e_0 \cos \vartheta)^2 (3 \sin^2 i_0 \sin^2 u - 1) -$$
$$- [2 \cos \vartheta + e_0 (\cos^2 \vartheta + 1)] \times$$
$$\times (1 + e_0 \cos \vartheta) \sin^2 i_0 \sin 2u\},$$

$$\frac{d\omega}{du} = \frac{1}{p_0^2} \frac{\varepsilon}{\mu} \left[-\frac{\cos \vartheta}{e_0} (1 + e_0 \cos \vartheta)^2 (3 \sin^2 i_0 \sin^2 u - 1) - \right. \qquad (13.50)$$
$$- \frac{2 + e_0 \cos \vartheta}{e_0} (1 + e_0 \cos \vartheta) \sin \vartheta \sin 2u \sin^2 i_0 +$$
$$\left. + 2 (1 + e_0 \cos \vartheta) \sin^2 u \cos^2 i_0 \right],$$

where

$$\vartheta = u - \omega_0. \qquad (13.51)$$

~ The determination of corrections to the orbital period from (13.49) reduces to evaluation of integrals of the form

$$J = \int_0^{2\pi} f(u)\,du \int_0^u \frac{dq}{du}\,du,$$

where $f(u)$ is a function of the angle u, and q one of the elements p, e or ω. Integrating by parts, we find

$$J = F(2\pi)\,\delta q - \int_0^{2\pi} F(u)\frac{dq}{du}\,du, \qquad (13.52)$$

where

$$F(u) = \int f(u)\,du, \quad \delta q = \int_0^{2\pi} \frac{dq}{du}\,du = \Delta q\,(2\pi).$$

Note that δq is secular perturbation of the corresponding elements per one orbital circuit, as defined by (13.32).

To simplify further manipulations, we shall consider low-eccentricity orbits, and all calculations will be carried out to terms of the first order of smallness in e. The subscript o for osculating orbital elements will be omitted. Then, applying (13.51), we have from (13.49) for the corrections ΔP_1, ΔP_2, ΔP_3

$$\left. \begin{aligned}
\Delta P_1 &= -\frac{3}{2}\sqrt{\frac{p}{\mu}}\int_0^{2\pi}(1 - 2e\cos\vartheta)\Delta p\,du, \\[2mm]
\Delta P_2 &= 2\frac{p^{3/2}}{\sqrt{\mu}}\int_0^{2\pi}(\cos\vartheta - 3e\cos^2\vartheta)\Delta e\,du, \\[2mm]
\Delta P_3 &= \frac{2p^{3/2}}{\sqrt{\mu}}\int_0^{2\pi}\left(\sin\vartheta - \frac{3}{2}e\sin 2\vartheta\right)e\,\Delta\omega\,du.
\end{aligned} \right\} \qquad (13.53)$$

Note that

$$\int (1 - 2e\cos\vartheta)\,du = u - 2e\sin\vartheta,$$

$$\int (\cos\vartheta - 3e\cos^2\vartheta)\,du = \sin\vartheta - \frac{3}{2}e\left(u + \frac{1}{2}\sin 2\vartheta\right),$$

$$\int \left(\sin\vartheta - \frac{3}{2}e\sin 2\vartheta\right)du = -\cos\vartheta + \frac{3}{4}e\cos 2\vartheta.$$

We apply transformation (13.52) to integrals (13.53). Making use of (13.32), (13.47), (13.50) and omitting all terms which contain the square of the eccentricity e, we find

$$\Delta P_1 = -\frac{3}{\sqrt{p\mu}}\frac{\varepsilon}{\mu}\sin^2 i \int_0^{2\pi}(u - 2e\sin\vartheta)(1 + e\cos\vartheta)\sin 2u\,du =$$

$$= -\frac{3}{\sqrt{p\mu}}\frac{\varepsilon}{\mu}\sin^2 i \int_0^{2\pi}[u\sin 2u +$$

$$+ e(u\cos\vartheta\sin 2u - 2\sin\vartheta\sin 2u)]\,du,$$

219

$$\Delta P_2 = -\frac{2}{\sqrt{p\mu}}\frac{\varepsilon}{\mu}\int_0^{2\pi}\Big[\sin\vartheta -$$

$$-\frac{3}{2}e\Big(u+\frac{1}{2}\sin 2\vartheta\Big)\Big]\Big\{\sin\vartheta\,(3\sin^2 i\,\sin^2 u-1)-$$

$$-2\cos\vartheta\,\sin 2u\,\sin^2 i + e\,[\sin 2\vartheta\,(3\sin^2 u\,\sin^2 i-1)-$$

$$-(3\cos^2\vartheta +1)\sin 2u\,\sin^2 i]\Big\}\,du =$$

$$=-\frac{2}{\sqrt{p\mu}}\frac{\varepsilon}{\mu}\int_0^{2\pi}\Big\{\sin^2\vartheta\,(3\sin^2 u\,\sin^2 i-1)-\sin 2\vartheta\,\sin 2u\,\sin^2 i +$$

$$+e\Big[\sin\vartheta\,\sin 2\vartheta\,(3\sin^2 u\,\sin^2 i-1)-$$

$$-\sin\vartheta\,(3\cos^2\vartheta +1)\sin 2u\,\sin^2 i -$$

$$-\frac{3}{2}\Big(u+\frac{1}{2}\sin 2\vartheta\Big)(3\sin\vartheta\,\sin^2 u\,\sin^2 i -$$

$$-\sin\vartheta -2\cos\vartheta\,\sin 2u\,\sin^2 i)\Big]\Big\}\,du,$$

$$\Delta P_3 = \frac{2p^{3/2}}{\sqrt{\mu}}\Big(\frac{3}{4}e\cos 2\omega-\cos\omega\Big)e\,\delta\omega +$$

$$+\frac{2}{\sqrt{p\mu}}\frac{\varepsilon}{\mu}\int_0^{2\pi}\Big(\cos\vartheta-\frac{3}{4}e\cos 2\vartheta\Big)\Big\{-\cos\vartheta\,(3\sin^2 u\,\sin^2 i-1)-$$

$$-2\sin\vartheta\,\sin 2u\,\sin^2 i + e\,[-2\cos^2\vartheta\,(3\sin^2 u\,\sin^2 i-1)-$$

$$-3\cos\vartheta\,\sin\vartheta\,\sin 2u\,\sin^2 i +2\sin^2 u\,\cos^2 i]\Big\}\,du =$$

$$=-\frac{2\pi}{\sqrt{p\mu}}\frac{\varepsilon}{\mu}e\,(5\cos^2 i-1)\cos\omega -$$

$$-\frac{2}{\sqrt{p\mu}}\frac{\varepsilon}{\mu}\int_0^{2\pi}\Big\{\cos^2\vartheta\,(3\sin^2 u\,\sin^2 i-1)+$$

$$+\sin 2\vartheta\,\sin 2u\,\sin^2 i + e\,[2\cos^3\vartheta\,(3\sin^2 u\,\sin^2 i-1)+$$

$$+3\cos^2\vartheta\,\sin\vartheta\,\sin 2u\,\sin^2 i -2\cos\vartheta\,\sin^2 u\,\cos^2 i -$$

$$-\frac{3}{4}\cos 2\vartheta\,(3\cos\vartheta\,\sin^2 u\,\sin^2 i -\cos\vartheta +2\sin\vartheta\,\sin 2u\,\sin^2 i)\Big]\Big\}\,du.$$

Omitting all terms of the order e^2, as well as those terms which vanish in virtue of (13.30) and (13.31), we find

$$\Delta P_1 = -\frac{3}{\sqrt{p\mu}}\frac{\varepsilon}{\mu}\sin^2 i\Big(\int_0^{2\pi}u\sin 2u\,du + e\int_0^{2\pi}u\cos\vartheta\,\sin 2u\,du\Big),$$

$$\Delta P_2 = -\frac{2}{\sqrt{p\mu}}\frac{\varepsilon}{\mu}\Big[\sin^2 i\Big(3\int_0^{2\pi}\sin^2\vartheta\,\sin^2 u\,du -\int_0^{2\pi}\sin 2\vartheta\,\sin 2u\,du\Big)-\int_0^{2\pi}\sin^2\vartheta\,du -$$

$$-e\sin^2 i\Big(\frac{9}{2}\int_0^{2\pi}u\sin\vartheta\,\sin^2 u\,du -3\int_0^{2\pi}u\cos\vartheta\,\sin 2u\,du\Big)+\frac{3}{2}e\int_0^{2\pi}u\sin\vartheta\,du\Big],$$

$$\Delta P_3 = -\frac{2\pi}{\sqrt{p\mu}}\frac{\varepsilon}{\mu}(4-5\sin^2 i)\,e\cos\omega -$$

$$-\frac{2}{\sqrt{p\mu}}\frac{\varepsilon}{\mu}\Big[\sin^2 i\Big(3\int_0^{2\pi}\cos^2\vartheta\,\sin^2 u\,du +\int_0^{2\pi}\sin 2\vartheta\,\sin 2u\,du\Big)-\int_0^{2\pi}\cos^2\vartheta\,du\Big].$$

$$(13.54)$$

In evaluating the integrals in the right-hand sides of these equalities, we make use of the identities

$$\int u \sin u\, du = \sin u - u \cos u,$$

$$\int u \cos u\, du = \cos u + u \sin u,$$

whence

$$\int_0^{2\pi} u \sin ku\, du = -\frac{2\pi}{k}, \quad \int_0^{2\pi} u \cos ku\, du = 0. \tag{13.55}$$

Hence, making use of (13.51), we have

$$\int_0^{2\pi} u \sin 2u\, du = -\pi,$$

$$\int_0^{2\pi} u \cos \vartheta \sin 2u\, du =$$

$$= \frac{1}{2} \left[\int_0^{2\pi} u \sin(3u - \omega)\, du + \int_0^{2\pi} u \sin(u + \omega)\, du \right] =$$

$$= \frac{\cos \omega}{2} \left[\int_0^{2\pi} u \sin 3u\, du + \int_0^{2\pi} u \sin u\, du \right] = -\frac{4}{3} \pi \cos \omega,$$

$$\int_0^{2\pi} \sin^2 \vartheta \sin^2 u\, du = \frac{1}{4} \int_0^{2\pi} (1 - \cos 2\vartheta)(1 - \cos 2u)\, du = \frac{\pi}{2} + \frac{1}{4} \int_0^{2\pi} \cos 2\vartheta \cos 2u\, du =$$

$$= \frac{\pi}{2} + \frac{1}{8} \int_0^{2\pi} [\cos(4u - 2\omega) + \cos 2\omega]\, du = \frac{\pi}{2} + \frac{\pi}{4} \cos 2\omega,$$

$$\int_0^{2\pi} \sin 2\vartheta \sin 2u\, du = \frac{1}{2} \int_0^{2\pi} [\cos 2\omega - \cos(4u - \omega)]\, du = \pi \cos 2\omega,$$

$$\int_0^{2\pi} \sin^2 \vartheta\, du = \frac{1}{2} \int_0^{2\pi} (1 - \cos 2\vartheta)\, du = \pi,$$

$$\int_0^{2\pi} u \sin \vartheta \sin^2 u\, du = \frac{1}{2} \int_0^{2\pi} u \sin \vartheta (1 - \cos 2u)\, du =$$

$$= -\pi \cos \omega - \frac{1}{4} \int_0^{2\pi} u [\sin(3u - \omega) -$$

$$- \sin(u + \omega)]\, du = -\pi \cos \omega - \frac{1}{3} \pi \cos \omega = -\frac{4}{3} \pi \cos \omega,$$

$$\int_0^{2\pi} u \sin \vartheta\, du = -2\pi \cos \omega,$$

$$\int_0^{2\pi} \cos^2 \vartheta \sin^2 u\, du = \int_0^{2\pi} \sin^2 u\, du - \int_0^{2\pi} \sin^2 \vartheta \sin^2 u\, du = \frac{\pi}{2} - \frac{\pi}{4} \cos 2\omega,$$

$$\int_0^{2\pi} \cos^2 \vartheta\, du = \pi.$$

Substituting in (13.54), we find

$$\Delta P_1 = \frac{2\pi}{\sqrt{p\mu}} \frac{\varepsilon}{\mu} \sin^2 i \left(\frac{3}{2} + 2e \cos \omega\right),$$

$$\Delta P_2 = \frac{2\pi}{\sqrt{p\mu}} \frac{\varepsilon}{\mu} \left(1 - \frac{3}{2} \sin^2 i + \frac{1}{4} \sin^2 i \cos 2\omega + \right.$$

$$\left. + 3e \cos \omega - 2e \sin^2 i \cos \omega\right),$$

$$\Delta P_3 = \frac{2\pi}{\sqrt{p\mu}} \frac{\varepsilon}{\mu} \left(1 - \frac{3}{2} \sin^2 i - \frac{1}{4} \sin^2 i \cos 2\omega - \right.$$

$$\left. - 4e \cos \omega + 5e \sin^2 i \cos \omega\right).$$
(13.56)

To calculate the correction ΔP_4 from (13.49), we make use of (4.19), (11.32), (13.3), and (13.31). Neglecting terms of the order e^2, we find

$$\Delta P_4 = \frac{2}{\sqrt{p\mu}} \frac{\varepsilon}{\mu} \cos^2 i \int_0^{2\pi} \frac{\sin^2 u}{1 + e \cos \vartheta} du \approx$$

$$\approx \frac{2}{\sqrt{p\mu}} \frac{\varepsilon}{\mu} \cos^2 i \int_0^{2\pi} (1 - e \cos \vartheta) \sin^2 u \, du =$$

$$= \frac{2}{\sqrt{p\mu}} \frac{\varepsilon}{\mu} \cos^2 i \int_0^{2\pi} \sin^2 u \, du = \frac{2\pi}{\sqrt{p\mu}} \frac{\varepsilon}{\mu} (1 - \sin^2 i).$$
(13.57)

Substituting (13.56) and (13.57) in (13.48), and seeing that to terms of the order e

$$p = a(1 - e^2) \approx a,$$

we find (with the aid of (5.36))

$$P_\Omega = P'_\Omega - \frac{2\pi}{\sqrt{\mu a}} \frac{\varepsilon}{\mu} \left[3 - \frac{5}{2} \sin^2 i - e \cos \omega (1 - 5 \sin^2 i)\right] =$$

$$= P'_\Omega \left\{1 - \frac{1}{a^2} \frac{\varepsilon}{\mu} \left[3 - \frac{5}{2} \sin^2 i - e \cos \omega (1 - 5 \sin^2 i)\right]\right\}.$$
(13.58)

Let ΔP_Ω be the difference between the nodical period of revolution and the osculating (unperturbed) period at the ascending node:

$$\Delta P_\Omega = P_\Omega - P'_\Omega.$$
(13.59)

Making use of the approximate relation (12.15), we write

$$\Delta P_\Omega \approx -\frac{1}{2} P_E \sqrt{\frac{a_e}{a}} a \left[3 - \frac{5}{2} \sin^2 i - e \cos \omega (1 - 5 \sin^2 i)\right],$$

$$\frac{\Delta P_\Omega}{P'_\Omega} \approx -\frac{1}{2} \left(\frac{a_e}{a}\right)^2 a \left[3 - \frac{5}{2} \sin^2 i - e \cos \omega (1 - 5 \sin^2 i)\right],$$
(13.60)

where P_E is defined by (13.15).

For close satellites in circular orbit ($e = 0$, $a \approx a_e$), the maximum value of this correction and its magnitude relative to the orbital period (for $i = 0$) are

$$|\Delta P_\Omega|_{max} \approx 0.42 \text{ min}, \quad \left|\frac{\Delta P_\Omega}{P'_\Omega}\right|_{max} \approx 0.005.$$

222

This correction is inversely proportional to $a^{1/2}$, and the correction-to-period ratio is inversely proportional to a^2.

The expression for ΔP_Ω contains a term which depends on the argument of perigee and increases with eccentricity (unlike the secular perturbations $\delta\omega$ and $\delta\Omega$, which are independent of ω). This property, established for low-eccentricity orbits, also applies for orbits with large e. More detailed investigations /7, 11, 12/ show that for higher e, this term increases more steeply. For $e \to 1$, it approaches infinity. In other words, highly elongated elliptical osculating orbits may correspond to open real orbits (and vice versa). This is so because for $e \approx 1$, comparatively small velocity perturbations near the perigee may convert an elliptical orbit into a hyperbolic one, or vice versa.

13.8. SIDEREAL PERIOD OF REVOLUTION BETWEEN ASCENDING NODES

Of all the various definitions of orbital period, the sidereal period P_s is the most accurate characteristic of the time required to complete one revolution around the Earth. Small perturbations of the period P_s displace the satellite in the direction of its motion. The sidereal period P_s in equatorial orbit ($i = 0$) is equal to the period of revolution in plane orbit.

To avoid the uncertainty introduced by the choice of the initial position, the sidereal period P_s will be reckoned from the orbit's ascending node (i.e., we measure this period of revolution at the ascending node of the orbit). From Figure 13.2 we see that in this case (to terms of higher order of smallness)

$$P_s = P_\Omega - \delta\Omega \left(\frac{dt}{du}\right)_\Omega \cos i,$$

where $\left(\frac{dt}{du}\right)_\Omega$ is the value of the corresponding derivative at the ascending node, $\delta\Omega = -\Omega\Omega_0$ is the perturbation of the ascending node per one circuit of revolution (in the west-east direction).

Applying (4.19), (13.32), (13.44) and omitting terms of higher order of smallness, we write

$$P_s = P_\Omega + \frac{2\pi}{p^2}\frac{e}{\mu}\frac{r_\Omega^2}{\sqrt{\mu p}}\cos^2 i = P_\Omega + \frac{2\pi}{\sqrt{\mu p}}\frac{e}{\mu}\frac{\cos^2 i}{(1+e\cos\omega)^2},$$

where r_Ω is the distance of the ascending node from the Earth's center. If we now omit terms of the order e^2, we find

$$P_s = P_\Omega + \frac{2\pi}{\sqrt{\mu p}}\frac{e}{p}[1 - \sin^2 i - 2e\cos\omega(1 - \sin^2 i)].$$

Inserting for P_Ω its expression from (13.58), we obtain

$$P_s = P_\Omega' - \frac{2\pi}{\sqrt{a\mu}}\frac{e}{\mu}\left[2 - \frac{3}{2}\sin^2 i + e\cos\omega(1 + 3\sin^2 i)\right] =$$
$$= P_\Omega'\left\{1 - \frac{1}{a^2}\frac{e}{\mu}\left[2 - \frac{3}{2}\sin^2 i + e\cos\omega(1 + 3\sin^2 i)\right]\right\}. \tag{13.61}$$

223

For $e = 0$, the correction from (13.61) is equal to the corresponding correction for circular orbit, (13.12) (if we put $u_0 = 0$, i.e., the ascending node is adopted as the point of origin).

In conclusion note that the last terms in the right-hand sides of (13.11) and (13.12) give the sidereal period P_s as a function of the initial position (for $e = 0$). In particular, for equatorial orbits ($i = 0$) this dependence on the choice of the initial point vanishes.

13.9. LONG-PERIOD PERTURBATIONS

From (13.58) and (13.61) we obtain a dependence of the orbital periods P_Ω and P_s on the argument of the perigee ω. P_Ω and P_s therefore experience long-period perturbations with a period $\bar{P}_\omega$ (the period of perigee movement). Of considerable practical significance are the long-period perturbations of the nodical period P_Ω, since they have a substantial influence on the epoch of nodal passage t_Ω (this epoch is commonly assumed as the starting point of each successive circuit).

The perturbations of the nodical period P_Ω are calculated, not from (13.58), but from a more exact formula derived by I. D. Zhongolovich /7/ by a similar technique to terms of the order e^2:

$$P_\Omega = P'_\Omega - \frac{P}{a^2}\frac{\varepsilon}{\mu}\left[3 - \frac{5}{2}\sin^2 i - e\cos\omega(1 - 5\sin^2 i) + \right.$$
$$\left. + \frac{17}{2}e^2\left(1 - \frac{10}{17}\sin^2 i\right) + \frac{9}{2}e^2\cos 2\omega\left(1 - \frac{5}{6}\sin^2 i\right)\right],$$

where $P = \text{const}$ is a mean orbital period of the satellite.

Applying the first relation in (12.15), we see that the relative correction to the osculating period P'_Ω at the ascending node is of the same order as the Earth's flattening α. As we have previously observed, the variation $\delta\omega$ in the argument of the perigee per one circuit is of the same order. We have also shown that the variation of a, e and i per one circuit of revolution is zero to terms of the order α. Hence it follows that to terms of the order α^2 we may write, making use of the first formula in (12.15) and the second formula in (13.32),

$$\delta P_\Omega = \delta P'_\Omega - \frac{P}{a^2}\frac{\varepsilon}{\mu}[1 - 5\sin^2 i - e\cos\omega(18 - 15\sin^2 i)]\, e\sin\omega\, \delta\omega, \qquad (13.62)$$

where δP_Ω and $\delta P'_\Omega$ are the increments of the corresponding periods per one circuit of revolution.

The second term in the right-hand side of this equality is of the order α^2. We now calculate, with the same accuracy, the first term in this equality, which gives the increment of the osculating period at the node per one circuit of revolution. We apply the energy integral, which in our case may be written in the form

$$\frac{v^2}{2} - U = \text{const},$$

where U is defined by (12.10). We shall retain terms of the order α only. Then, making use of (12.15), we omit the third term in the right-hand side of (12.10) and obtain the following relation for v and r at the node (i.e., for $B = 0$):

$$\frac{v^2}{2} - \frac{\mu}{r} - \frac{1}{3}\frac{\varepsilon}{r^3} = \text{const.}$$

Hence, making use of (4.19) and (5.15), we find

$$\frac{1}{a} + \frac{2}{3}\frac{\varepsilon}{\mu}\frac{(1 + e\cos\omega)^3}{p^3} = \text{const,}$$

where a, e and p are the nodical values of the corresponding osculating elements.

Applying (5.2) to this expression, we obtain to terms of the order α^2

$$\frac{\delta a}{a} = -2\frac{\varepsilon}{\mu}\frac{(1 + e\cos\omega)^2}{(1 - e^2)p^2}\, e\sin\omega\,\delta\omega, \qquad (13.63)$$

where δa and $\delta\omega$ are the increments of the corresponding osculating elements at the node per one circuit of revolution. Hence, making use of (5.36), we find

$$\frac{\delta P'_{\Omega}}{P'_{\Omega}} = \frac{3}{2}\frac{\delta a}{a} = -3\frac{\varepsilon}{\mu}\frac{(1 + e\cos\omega)^2}{(1 - e^2)p^2}\, e\sin\omega\,\delta\omega. \qquad (13.64)$$

From the above relations, and also from the first expression in (12.15) and the second expression in (13.32), we see that the increments δa and $\delta P'_{\Omega}$ are of the order α^2.

Substituting (13.64) in (13.62), we omit terms of the order α^3 and $\alpha^2 e^2$. We thus obtain the following expression for the variation of the nodical period per one circuit of revolution:

$$\delta P_{\Omega} = -\frac{\varepsilon}{\mu}\frac{P}{a^2}(4 - 5\sin^2 i)(1 - 3e\cos\omega)e\sin\omega\,\delta\omega. \qquad (13.65)$$

The increment δP_{Ω} is thus of the order α^2.

With the same accuracy, the elements P, a, e, and i in the right-hand side of (13.65) can be assumed constant. The period P_{Ω} may be treated as a function of the argument of the perigee ω. Now, seeing that all the quantities are smooth functions, we put $d\omega$ for $\delta\omega$ and write

$$P_{\Omega}(\omega) = P_{\Omega}(\omega_0) - \frac{\varepsilon}{\mu}\frac{P}{a^2}(4 - 5\sin^2 i)\int_{\omega_0}^{\omega}(1 - 3e\cos\omega)e\sin\omega\,d\omega,$$

where $P_{\Omega}(\omega)$ and $P_{\Omega}(\omega_0)$ are the values of P_{Ω} for some current ω and some initial ω_0.

Let the initial argument of the perigee be $\omega_0 = \pi/2$; the corresponding nodical period $P_{\Omega}(\pi/2)$ is denoted by P_1. Then integrating, we find

$$P_{\Omega} = P_1 + \frac{\varepsilon}{\mu}\frac{P}{a^2}(4 - 5\sin^2 i)e\cos\omega\left(1 - \frac{3}{2}e\cos\omega\right), \qquad (13.66)$$

225

i.e., the nodical period P_Ω experiences long-period fluctuations whose frequency is a multiple of the perigee movement frequency

$$v_\omega = \frac{1}{P_\omega},$$ (13.67)

where P_ω is defined by (13.37) and (13.38).

It follows from the first relation in (12.15) and from (13.66) that the amplitude of these long-period fluctuations of frequency v_ω is of the order $P\alpha e$, and the amplitude of the fluctuations of frequency $2v_\omega$ is of the order $P\alpha e^2$. Raising the order of the significant terms in the expansion in the eccentricity e in (13.66), we can recover long-period fluctuations of higher frequencies. The amplitude at any frequency kv_ω is of the order $P\alpha e^k$ (where k is an integer).

Let $\Delta_1 P$ be the amplitude of the fluctuations of frequency v_ω. From (12.15), (13.15), and (13.66) we have

$$\Delta_1 P \approx \frac{\alpha}{2} P_E \sqrt{\frac{a_e}{a}} (4 - 5 \sin^2 i) e \leqslant 2\alpha P_E \sqrt{\frac{a_e}{a}} \, e.$$

On the other hand, from relation (5.3) and the condition that the satellite must not touch the Earth's surface $(r_p > a_e)$, we have

$$a > \frac{a_e}{1 - e}.$$

Hence,

$$\Delta_1 P < 2\alpha P_E e \sqrt{1 - e}.$$

The factor $e \sqrt{1 - e}$ is maximal for $e = 2/3$. Hence, inserting the numerical values for α and P_E (see (12.11) and (13.15)), we find

$$\Delta_1 P < \frac{4}{3\sqrt{3}} P_E \alpha \approx 0.22 \, \text{min} \approx 13 \, \text{sec}.$$ (13.68)

This estimate is fairly accurate, since in reality the amplitude of the long-period fluctuations in the nodical period may reach 10 sec.

We now consider the fluctuations in the circuit starting time (the epoch of nodal passage). Let t_n be the epoch when the n-th circuit ends and the $(n+1)$-th circuit begins. Then

$$t_n = t_0 + \sum_{k=1}^{n} P_{\Omega k},$$

where t_0 is the initial epoch, $P_{\Omega k} = t_k - t_{k-1}$ is the nodical period for the k-th circuit of revolution. Hence, making use of (13.66), we have

$$t_n = t_0 + nP_1 + \frac{e}{\mu} \frac{P}{a^2} (4 - 5 \sin^2 i) e \sum_{k=1}^{n} \cos \omega_k \left(1 - \frac{3}{2} e \cos \omega_k\right),$$

where ω_k is the argument of the perigee during the k-th circuit. Now, applying (13.22) and omitting terms of the order e^3, we write

$$t_n = t_0 + nP_1 + \frac{P_e}{\pi} \sum_{k=1}^{n} \cos \omega_k \left(1 - \frac{3}{2} e \cos \omega_k\right) \delta\omega.$$

Putting $\delta\omega = d\omega$ and substituting integration for summation, we have

$$t_n = t_0 + nP_1 + \frac{Pe}{\pi} \int_{\omega_0}^{\omega_n} \cos\omega \left(1 - \frac{3}{2}e\cos\omega\right) d\omega =$$

$$= t_0 + nP_1 + \frac{Pe}{\pi} \left\{ \sin\omega_n - \sin\omega_0 - \right.$$

$$\left. - \frac{3}{4}e\left[\omega_n - \omega_0 + \frac{1}{2}(\sin 2\omega_n - \sin 2\omega_0)\right]\right\}.$$

Seeing that

$$\omega_n - \omega_0 = n\,\delta\omega, \quad P \approx P_1,$$

we have

$$t_n = t_0 + nP_1\left(1 - \frac{3}{4}e^2\frac{\delta\omega}{\pi}\right) +$$

$$+ \frac{Pe}{\pi}\left[\sin\omega_n - \sin\omega_0 - \frac{3}{8}e(\sin 2\omega_n - \sin 2\omega_0)\right]. \tag{13.69}$$

The first two terms in the right-hand side of this equality give the linear growth of the time t_n with the circuit number n, while the third term represents long-period perturbations whose frequencies are multiples of the perigee movement frequency ν_ω. The amplitudes of these perturbations are proportional to the orbital period, and may be quite substantial.

In conclusion, we consider the question of long-period perturbations of the osculating elements at the node. Making use of (13.63), we can show, by the same technique as for the period P, that

$$a = a_1\left[1 + \frac{2}{3}\frac{\varepsilon}{\mu}\frac{e\cos\omega}{p^2(1-e^2)}(3 + 3e\cos\omega + e^2\cos^2\omega)\right], \tag{13.70}$$

where a_1 is the nodical value of the osculating semimajor axis $\omega = \pi/2$. This expression is accurate to terms of the order α. However, unlike relations (13.66) and (13.69), its terms are all functions of the eccentricity e.

M. D. Kislik /11/ has shown that analogous expressions can be obtained for the osculating nodical values of the parameter p, the eccentricity e, and the inclination i. All the elements characterizing the shape, the size, and the inclination of the orbit to the equatorial plane are therefore seen to vary with frequencies which are multiples of the perigee movement frequency ν_ω. The net perturbation of the orbit observed after one complete revolution of its perigee point, $\bar{P}_\omega$, therefore reduces to a certain displacement of the ascending node, i.e., rotation of the orbit around the Earth's spin axis, all other orbital parameters remaining constant.

Chapter 14

THE EFFECT OF AIR DRAG ON MOTION OF
ARTIFICIAL EARTH SATELLITES IN
CIRCULAR AND NEARLY CIRCULAR ORBITS

14.1. STATEMENT OF THE PROBLEM

The orbits of artificial Earth satellites mostly lie at great altitudes (over $150-200$ km, excepting the injection and the reentry trajectories). At these heights, the air is highly rarefied and offers but a negligible resistance to the motion of the satellite. The effect of the aerodynamic drag, however, is distinctly secular and, although of small magnitude at any given time, it may eventually produce a substantial change in the principal parameters of motion of the space vehicle. This point is readily illustrated by the example of circular orbits. Indeed, in circular orbit, the air drag is constant to first approximation, pointing along the tangent to the orbit, against the satellite's motion. This force produces some constant perturbing deceleration T_0. As we have shown in Sec. 3.3, this perturbation will cause the satellite to move in a convolute spiral trajectory. The mean radius r_m of the orbit and the orbital period P will decrease monotonically, the longitudinal flight velocity v_u increasing. As the radius r_m diminishes, the satellite sinks into progressively denser layers of the atmosphere, and the secular perturbation is enhanced. The final outcome of persistent air drag is termination of satellite's life (i.e., the satellite falls on the ground).

This chapter analyzes the effects of air resistance on the motion of artificial Earth satellites in circular and nearly circular orbits. We mainly concentrate on the resulting secular perturbations. The effects of air drag on satellites in elliptical orbit will be considered in the next chapter.

14.2. DRAG AND AIR DENSITY

The drag R_x is directed against the velocity vector of the flying body relative to the air. Its magnitude is given by

$$R_x = c_x F_m \frac{\rho v_{rel}^2}{2},\qquad (14.1)$$

where c_x is the dimensionless drag coefficient, F_m the attack area (i.e., the area of the largest section perpendicular to the relative velocity vector), ρ air density, v_{rel} the magnitude of the relative velocity vector.

At great altitudes, where the free path of air molecules is comparable with, or much greater than, the size of the satellite, the drag coefficient c_x is virtually independent of the satellite figure: it is mainly determined by the mechanism of reflection of air molecules from the surface of the satellite /18/. The drag coefficient in the upper atmosphere is commonly assumed to have the value

$$c_x \approx 2 - 2.5. \tag{14.2}$$

The attack area F_m can be found without difficulty for oriented satellites, i.e., satellites which maintain a constant attitude in orbit. For nonoriented satellites, the inertial trihedron is generally assumed to move at random, so that

$$F_m = \frac{F_{tot}}{4}. \tag{14.3}$$

This relation applies for convex satellites (whose surface is on one side of any tangent plane), if all attitudes are equiprobable /18/. Formula (14.3) is also used for the attack area of a nonoriented satellite whose surface is not convex. In these cases, however, the real surface is replaced with a corresponding convex surface.

It should be remembered that (14.3) is suitable only for the calculation of some mean air resistance, with the averaging interval much greater than the period of oscillation of the satellite axes. This condition is generally satisfied in the analysis of secular perturbations. Over parts of the orbit, however, the condition of attitude equiprobability may break down, and the parameters F_m and R_x fluctuate.

In calculations of air density, vertical motions are generally neglected, and one proceeds from the so-called equation of vertical equilibrium of the atmosphere

$$dp = - g\rho \, dh. \tag{14.4}$$

Here dp is the change in air pressure p as the height changes by dh; g is the gravitational acceleration.

The relation between the air pressure p and the density ρ is expressed by the Clapeyron equation

$$\rho = \frac{pM}{R_0 T}, \tag{14.5}$$

where M is the molecular weight of air, T its absolute kinetic temperature (i.e., the temperature as determined by the mean velocity of air molecules at the given height), and

$$R_0 = 8.31 \cdot 10^7 \, g \cdot cm^2 / sec^2 \cdot deg \cdot mol \tag{14.5a}$$

is the universal gas constant.

Substituting (14.5) in (14.4), we find

$$\frac{dp}{p} = - \frac{gM}{R_0 T} \, dh. \tag{14.6}$$

229

Integrating from some initial height $h = h_1$ to current height h and making use of (14.5), we find

$$p(h) = p_1 \exp\left(-\int_{h_1}^{h} \frac{gM}{R_0 T}\, dh\right),$$

$$\rho(h) = \rho_1 \frac{M T_1}{M_1 T} \exp\left(-\int_{h_1}^{h} \frac{gM}{R_0 T}\, dh\right),$$

$$(14.7)$$

where p_1, ρ_1, M_1, and T_1 are the values of the corresponding parameters at the height $h = h_1$.

The vertical variation of temperature T and molecular weight M is thus required for the calculation of the function $\rho(h)$. The actual values of T and M depend on many different geophysical factors. At great heights, where the artificial Earth satellites fly ($h > 180 - 200$ km), the temperature and the molecular weight are highly sensitive to the state of the upper atmosphere, which is in turn a function of solar activity. At the relevant altitudes, the principal parameters of the upper atmosphere therefore depend, not only on height, but also on the geographical coordinates of the point, the time of day and year, and the general and local solar activity. The periodic march of atmospheric parameters linked with the diurnal and the annual periods of the Earth, the Sun's period of rotation about its axis relative to the Sun—Earth line (some 27 days), and the solar activity cycle (some 11 years) is a characteristic manifestation of this dependence. The parameters of the upper atmosphere are often perturbed by local solar phenomena, which are quite unpredictable at present. For heights of some $200 - 250$ km, the density of the atmosphere may vary by as much as $\pm(30 - 50)\%$ about the mean due to changes in insolation (as determined by the Earth's spin and its orbital motion). Solar phenomena may cause a temporary rise by as much as 50% in air density (persisting for a few days). In years of minimum solar activity, the mean air density at these altitudes is found to be $1/2 - 1/3$ of the corresponding density in years of maximum activity. As the height increases, the dependence on solar activity becomes more pronounced, and for heights above 500 km the air density may change by as much as a factor of 10, and even more, due to these factors.

It follows from the preceding that d y n a m i c m o d e l a t m o s p h e r e s must be devised, which take into consideration the dependence of the principal atmospheric parameters on all the above factors, as well as on height. There are, however, no satisfactory dynamic model atmospheres at present, since the relationships are much too complicated to be analyzed theoretically, and the experimental data are scant. The effect of air drag on artificial Earth satellites is therefore commonly calculated for s t a t i c (or s t e a d y - s t a t e) m o d e l a t m o s p h e r e s , which only allow for the height variation of the atmospheric parameters. The accuracy of these model atmospheres is often quite inadequate, and they should be adjusted with the aid of various experimental data. This adjustment is made by introducing various correction coefficients, which are generally derived from measurements of the elements of real orbits.

Appendix 1 lists the fundamental parameters of one of the latest static model atmospheres, the so-called CIRA 1961 (the COSPAR International

Reference Atmosphere for 1961) /36/. It should be noted that this reference atmosphere is based on the results of measurements obtained in a period of maximum solar activity. In periods of minimum solar activity, the density of the upper atmosphere may be several times less than the CIRA 1961 derived density /10, 14, 17, 20, 35/. The density ρ in Appendix 1 is given in g/cm^3. Engineers, however, make their calculations in the technical system of units, where ρ is determined in $kg \cdot sec^2/m^4$. To pass from one system of units to another, we use the equality

$$1 \, kg \cdot sec^2/m^4 = 9.807/1000 \, g/cm^3.$$

It follows from the preceding that the main factors which determine the drag R_x, namely the drag coefficient c_x, the effective attack area F_m(for nonoriented satellites), and the air density ρ, cannot be determined with any accuracy at present. Exact prediction of the influence of air drag on the motion of artificial Earth satellite is therefore impossible for practical reasons, and the results of the calculations must be continually refined as new measurements of the actual orbital elements become available.

14.3. LOCAL MODEL ATMOSPHERES

Local model atmospheres are generally used in adjusting the theoretical calculations to measurements of the actual orbital elements. These model atmospheres hold true in a limited range of heights for a limited time only. The air density ρ is determined from expressions of the form

$$\rho = \tilde{\rho}(h, q_i), \quad i = 1, 2, \ldots, n, \tag{14.8}$$

where q_i are some free parameters of the model atmosphere (adjustment parameters) which are obtained from the conditions of best fit between the theoretical and the experimental results.

One of the simplest model atmospheres of this kind (the so-called isothermal atmosphere) is easily derived if the quantities g, M, and T in (14.7) are assumed to be constant. Taking the integral in the right-hand side of (14.7), we find

$$\rho = \rho_1 \exp\left(-\frac{h - h_1}{H}\right), \tag{14.9}$$

where

$$H = \frac{R_0 T}{g M}. \tag{14.10}$$

The adjustment parameters of this local atmosphere are ρ_1 — the density of air at some height $h = h_1$, and the so-called density scale height, H. From the Clapeyron equation (14.5) we see that H is equal to the height of a hypothetical homogeneous column of constant density ρ_1, where the pressure at the altitude $h = h_1$ is equal to the pressure of the particular atmosphere being considered.

231

If a static model atmosphere $\rho = \tilde{\rho}(h)$ is to approximate to the real function $\rho(h)$ satisfactorily, its adjustment parameters should be selected from the conditions

$$\tilde{\rho}(h_1) = \rho(h_1), \quad \frac{d\tilde{\rho}}{dh}(h_1) = \frac{d\rho}{dh}(h_1). \tag{14.11}$$

These conditions are satisfied for

$$\rho_1 = \rho(h_1), \quad H = -\frac{\rho(h_1)}{\frac{d\rho}{dh}(h_1)} = -\frac{1}{\frac{d\ln\rho}{dh}(h_1)}. \tag{14.12}$$

We introduce the "molecular" temperature

$$T' = T\frac{M_0}{M}, \tag{14.13}$$

where $M_0 = 28.97$ g/mol is the molecular weight of air near the ground. Expression (14.7) takes the form

$$\rho = \rho_1 \frac{T_1'}{T'} \exp\left(-\int\limits_{h_1}^{h} \frac{g}{RT'}\, dh\right), \tag{14.14}$$

where R is the specific gas constant of air, defined by

$$R = \frac{R_0}{M_0} = 287 \text{ m}^2/\text{deg}\cdot\text{sec}^2, \tag{14.15}$$

and T_1' is the value of the temperature T' at the height $h = h_1$.

From (14.14) it follows that

$$\frac{d\rho}{dh} = -\frac{\rho}{T'}\left(\frac{dT'}{dh} + \frac{g}{R}\right).$$

Hence, making use of (14.12), we find

$$H = \frac{T_1'}{\frac{dT'}{dh}(h_1) + \frac{g(h_1)}{R}}. \tag{14.16}$$

For $\frac{dT'}{dh}(h_1) = 0$, this formula coincides with equality (14.10).

Relations (14.12) and (14.16) define an isothermal atmosphere which provides the best approximation to the actual variation of air density near a given height $h = h_1$. From (14.16), the scale height H can be determined as a function of the height h for any static model atmosphere. The corresponding scale height H characterizes the rate of vertical decrease of the air density ρ. Assuming H to be constant in the interval $h_1 \leqslant h < h_1 + H$, we find that as the height h increases by H, the density ρ decreases approximately by a factor of $e \approx 2.718$.

Figure 14.1 and Appendix 2 illustrate the function $H(h)$ for CIRA 1961. We see from the graph and the table that for $h < 120$ km, the parameter H is between 5 and 10 km, which corresponds to a sharp drop of air density with height. For heights of from 120 to 200 km, the rate of decrease in

air density levels out, H increasing to $30-40$ km. For $h > 200$ km, H slowly increases, and for $h = 800$ km, $H = 115$ km. We see from the table in Appendix 1 that this reduction in the rate of decrease of air density and the corresponding increase in H are related to the increase in temperature and the decrease in the molecular weight of air at high altitudes.
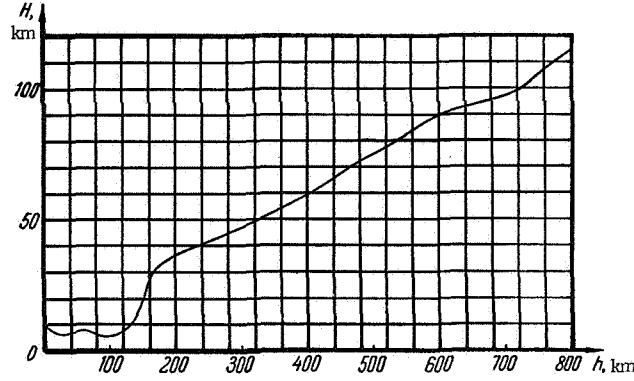
FIGURE 14.1. Density scale height H vs. the height h above the Earth's surface for CIRA 1961.

We now estimate the errors introduced by the isothermal model atmosphere. Seeing that the relative change in the "molecular" temperature T' with height is much greater than the corresponding change in the gravitational acceleration g, we shall assume that the latter is constant (a variable g will not affect the results of our analysis in a noticeable degree). We moreover assume that in the relevant altitude range the "molecular" temperature T' is a linear function of the height h:

$$T' = T'_1 + a(h - h_1),$$
(14.17)

where T'_1 is the value of the temperature T' at the height h_1, and a a coefficient characterizing the rate of vertical growth of T'. Clearly,

$$a = \frac{dT'}{dh}.$$
(14.18)

Substituting (14.17) in (14.14), we find

$$\rho = \rho_1 \frac{T'_1}{T'} \exp\left\{ -\int_{h_1}^{h} \frac{g\, dh}{R[T'_1 + a(h - h_1)]} \right\} =$$

$$= \rho_1 \left(\frac{T'}{T'_1} \right)^{-\left(1 + \frac{g}{Ra}\right)} = \rho_1 \left[1 + \frac{a(h - h_1)}{T'_1} \right]^{-\left(1 + \frac{g}{Ra}\right)}.$$
(14.19)

It is easily seen that for $a \to 0$ this expression gives the isothermal atmosphere (14.9). Indeed, from (14.16) and (14.18) it follows that in this case

$$H = \frac{T'_1}{a + \frac{g}{R}}, \quad 1 + \frac{g}{Ra} = \frac{T'_1}{Ha}.$$
(14.20)

233

Substituting the second equality in (14.19), we find

$$\rho = \rho_1 \left[1 + \frac{a(h-h_1)}{T_1'} \right]^{-\frac{T_1'}{Ha}} = \rho_1 \left\{ \left[1 + \frac{a(h-h_1)}{T_1'} \right]^{\frac{T_1'}{a(h-h_1)}} \right\}^{-\frac{h-h_1}{H}}.$$

Now, since

$$\lim_{\varepsilon \to 0} (1 + \varepsilon)^{\frac{1}{\varepsilon}} = e,$$

we have

$$\lim_{a \to 0} \rho = \rho_1 \exp\left(-\frac{h-h_1}{H}\right).$$

From expressions (14.9), (14.19), and (14.20), the relative error introduced by the isothermal atmosphere is

$$\delta\rho = \frac{\rho - \tilde{\rho}}{\rho_1} = \left[1 + \frac{a(h-h_1)}{T_1'} \right]^{-\left(1 + \frac{g}{Ra}\right)} - \exp\left(-\frac{h-h_1}{H}\right) =$$

$$= (1+\xi)^{-\left(1+\frac{g}{Ra}\right)} - \exp\left[-\xi\left(1 + \frac{g}{Ra}\right)\right], \qquad (14.21)$$

where

$$\xi = \frac{a(h-h_1)}{T_1'} = \frac{h-h_1}{H_T}, \quad H_T = \frac{T_1'}{a}. \qquad (14.22)$$

Note that H_T is the height increment corresponding to a two-fold increase in the initial temperature T_1', as extrapolated from (14.17).
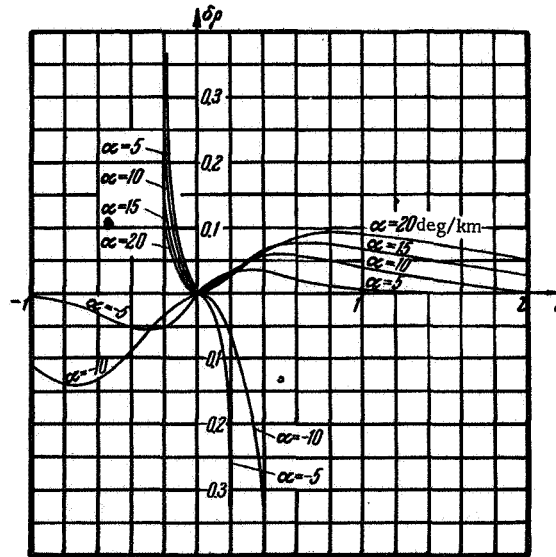
FIGURE 14.2. Relative error $\delta\rho$ introduced by the isothermal model atmosphere in air density determination vs. ξ for various $a = \frac{dT'}{dh}$.

Figure 14.2 plots the relative error $\delta\rho$ of the isothermal atmosphere as a function of ξ for various temperature gradients α (in deg/km). In calculations of the function $\delta\rho(\xi)$, the acceleration g was taken equal to its mean value at the height of 200 km, $g_m = 9.22$ m/sec^2. When examining these graphs, we must remember that for $\alpha > 0$, $\xi > 0$ correspond to $h > h_1$ and $\xi < 0$ to $h < h_1$. Conversely, for $\alpha < 0$, $\xi > 0$ correspond to $h < h_1$ and $\xi < 0$ to $h > h_1$. We see from the graphs that at the heights $h \gg h_1$, for temperature gradients α in the interval -5 deg/km $\leqslant \alpha \leqslant 20$ deg/km, the absolute value

of the relative error $|\delta\rho| = \left|\frac{\rho - \tilde{\rho}}{\rho_1}\right|$ does not exceed 10%. The error $|\delta\rho|$

decreases with decreasing $|\alpha|$. For $h < h_1$, the error $|\delta\rho|$ sharply increases with increasing $|\xi|$. The isothermal atmosphere is therefore adequate for "upward" extrapolation of the real atmosphere (to heights $h \gg h_1$). "Downward" extrapolation (to heights $h < h_1$), however, involves gross errors. If the isothermal scale atmosphere is applied in assessing the air drag on artificial Earth satellites, the parameter h_1 is generally taken as the height of the lowest point in orbit. Note that the foregoing discussion of the relative error $\delta\rho$ is inseparably connected with its definition (14.21). If the error is defined as

$$\delta\rho' = \frac{\rho - \tilde{\rho}}{\rho},$$

its behavior will be entirely different (it will increase monotonically for extrapolation in either direction).

The next higher approximation (after the isothermal atmosphere) to the real atmosphere is provided by a local model where the "molecular" temperature T' varies linearly as in (14.17). Making use of (14.19), (14.20), and (14.22), we write for the air density in this model atmosphere

$$\bar{\rho} = \rho_1 \left(1 + \frac{h - h_1}{H_T}\right)^{-\frac{H_T}{H}}. \tag{14.23}$$

As we have previously shown, for $\alpha \to 0$ $(H_T \to \infty)$, expression (14.23) reduces to (14.9). We come to the same conclusion if (14.9) and (14.23) are expanded in powers of $\frac{h - h_1}{H_T}$ and $\frac{h - h_1}{H}$:

$$\begin{aligned}
\tilde{\rho} &= \rho_1 \left[1 - \frac{h - h_1}{H} + \frac{1}{2!}\left(\frac{h - h_1}{H}\right)^2 - \right. \\
&\qquad\qquad \left. - \frac{1}{3!}\left(\frac{h - h_1}{H}\right)^3 + \ldots\right], \\
\bar{\rho} &= \rho_1 \left[1 - \frac{h - h_1}{H} + \frac{1}{2!}\left(\frac{h - h_1}{H}\right)^2\left(1 + \frac{H}{H_T}\right) - \right. \\
&\qquad\qquad \left. - \frac{1}{3!}\left(\frac{h - h_1}{H}\right)^3\left(1 + \frac{H}{H_T}\right)\left(1 + 2\frac{H}{H_T}\right) + \ldots\right].
\end{aligned} \tag{14.24}$$

We see from the expansions that the functions $\tilde{\rho}(h)$ and $\bar{\rho}(h)$ coincide to terms of the first order: differences are observed in terms of second and higher orders only. The parameter H in both model atmospheres should therefore be determined from the equality (14.11), while H_T is obtained from the condition

$$\frac{d^2\bar{\rho}}{dh^2}(h_1) = \frac{d^2\tilde{\rho}}{dh^2}(h_1). \tag{14.25}$$

235

Expression (14.23), unlike (14.9), has three free parameters (ρ, H and H_T), and not two; the adjustment with the real atmosphere can therefore be carried out to terms of the order $\left(\frac{h - h_1}{H}\right)^2$.

In previous integration of (14.14), we neglected the variability of the gravitational acceleration g. The inaccuracy introduced by this simplification can be eliminated if the air density ρ is determined, not as a function of the height h above the Earth's surface, but as a function of the so-called geopotential height

$$\Phi = \frac{R_E h}{R_E + h} = h\left(1 + \frac{h}{R_E}\right)^{-1},$$ (14.26)

where $R_E = 6371$ km is the mean radius of the Earth.

Expression (1.2) for the gravitational acceleration can be written as

$$g = g_0 \frac{R_E^2}{(R_E + h)^2},$$ (14.27)

where $g_0 \approx 9.807$ m/sec^2 is the mean gravitational acceleration on the Earth's surface. Now, differentiating (14.26), we find

$$d\Phi = \frac{R_E^2}{(R_E + h)^2} dh = \frac{g}{g_0} dh, \quad dh = \frac{g_0}{g} d\Phi.$$

Substituting in (14.14), we find

$$\rho = \rho_1 \frac{T_1'}{T'} \exp\left(-\int_{\Phi_1}^{\Phi} \frac{g_0}{RT'} d\Phi\right),$$ (14.27a)

where Φ_1 is the value of Φ at the height h_1.

Thus, when Φ is substituted for h as the independent variable, all the previous arguments pertaining to local model atmospheres remain in force. The variable g is replaced with the constant g_0, so that the uncertainty introduced by the variation of g is eliminated (the uncertainty contributed by the approximate relation (14.27) is negligible). From (14.26) it follows that for $h \ll R_E$, the difference between h and Φ is comparatively small. It is therefore often desirable to retain the height h as the independent variable of local model atmospheres, substituting for the variable g some constant mean value in the relevant layer.

14.4. THE EFFECT OF AIR DRAG ON MOTION IN CIRCULAR ORBIT

As we have previously observed, the magnitude and the direction of the drag force R_x are a function of the satellite's velocity relative to the air, v_{rel}, which is defined by the equality

$$v_{rel} = v - v_1,$$ (14.28)

where v is the velocity of the satellite in some inertial frame, and v_1 the velocity of air in the same frame.

If the attraction of the Sun, the Moon, and the planets is ignored, a system of nonrotating axes with its origin at the Earth's center may be assumed as the inertial frame. The motion of air relative to this frame is determined, on the one hand, by its rotation with the Earth and, on the other, by various local winds. Since the question of winds at high altitudes is fairly uncertain, their influence on the motion of artificial Earth satellites is ignored. As regards the atmospheric rotation, it is obvious that the lower layers are completely entrained by the Earth. We may further assume that starting with some altitude, the atmosphere virtually does not rotate with the Earth (otherwise, the velocity v_1 should increase monotonically with height). The rotation of the intermediate layers of the upper atmosphere is undecided. Anyhow, the magnitude of the vector v_1 is not greater than the velocity of the completely entrained atmosphere. At heights of 1000 km (where the air drag on satellites is still noticeable), this velocity does not exceed 540 m/sec, whereas the circular velocity at that height is close to 7350 m/sec. In circular motion, the magnitude of the velocity vector v_1 is thus no more than 7.5% of the magnitude of the satellite velocity v. In our preliminary analysis of drag effects we shall therefore take $v_{\text{rel}} \approx v$. The contribution from atmospheric rotation will be considered in the following.

With this simplification, the drag R_x in circular orbit (as treated in Sec. 1.1) is directed at right angles to the radius-vector joining the artificial satellite with the Earth's center, i.e., against the acceleration T (see Figure 2.1). Making use of (1.4) and (14.1), we may write the following expression for the corresponding perturbing acceleration at the height h:

$$T = -\frac{R_x}{m} = -c\rho w^2 = -c\rho \frac{\mu}{R_E + h} = -\frac{c\rho\mu}{r}, \qquad (14.29)$$

where m is the satellite's mass, $R_E = 6371$ km the mean radius of the Earth, $r = R_E + h$ the radius of the circular orbit, c a coefficient defined by

$$c = \frac{c_x F_m}{2m}. \qquad (14.30)$$

In particular, for a spherical satellite

$$c = \frac{c_x g_0 \pi D^2}{8G} = \frac{3}{4} \frac{c_x g_0}{\gamma D} \cdot 10^{-3}, \qquad (14.31)$$

where D is the satellite's diameter in meters, $G = mg_0$ its weight in kg, γ mean specific gravity of the satellite defined by

$$\gamma = \frac{6G}{\pi D^3} \cdot 10^{-3}.$$

According to the latest data for the recent American satellites (excluding the Echo-series satellites), the mean specific gravity γ ranges between 0.1 and 1 kg/dm³, the diameter D between 0.5 and 5 m, the drag coefficient, c_x, as mentioned previously, between 2 and 2.5. The coefficient c of spherical satellites may therefore range between 0.003 and 0.4 m³/kg·sec².

237

Table 14.1 lists the magnitude of the acceleration T for various heights h of circular orbit. The accelerations were computed from (14.29) for $c = 0.1 \, \text{m}^3/\text{kg} \cdot \text{sec}^2$ (i.e., for a comparatively small light-weight satellite), making use of the air densities ρ from the appendix. The table also gives the drag force R_x per square meter of attack section F_m (for $c_x = 2.4$).

TABLE 14.1

Height, h	Acceleration, $\lvert T \rvert$	Drag per unit area, R_x/F_m	Height, h	Acceleration, $\lvert T \rvert$	Drag per unit area, R_x/F_m
km	m/sec^2	kg/m^2	km	m/sec^2	kg/m^2
100	$3.0 \cdot 10^{-1}$	3.6	350	$7.4 \cdot 10^{-6}$	$8.9 \cdot 10^{-5}$
120	$1.5 \cdot 10^{-2}$	$1.8 \cdot 10^{-1}$	400	$3.1 \cdot 10^{-6}$	$3.7 \cdot 10^{-5}$
150	$1.1 \cdot 10^{-3}$	$1.3 \cdot 10^{-2}$	500	$6.9 \cdot 10^{-7}$	$8.3 \cdot 10^{-6}$
200	$2.2 \cdot 10^{-4}$	$2.7 \cdot 10^{-3}$	600	$2.0 \cdot 10^{-7}$	$2.4 \cdot 10^{-6}$
250	$6.3 \cdot 10^{-5}$	$7.6 \cdot 10^{-4}$	700	$6.8 \cdot 10^{-8}$	$8.2 \cdot 10^{-7}$
300	$2.0 \cdot 10^{-5}$	$2.4 \cdot 10^{-4}$	800	$2.6 \cdot 10^{-8}$	$3.1 \cdot 10^{-7}$

We see from the table that at the relevant heights ($h > 100 - 150 \, \text{km}$), the acceleration produced by the drag force is small in comparison with the gravitational acceleration. The perturbations due to air drag are therefore small, and they can be analyzed by the method of linearized equations of motion, described in Chapter 2 and 3 for circular orbits.

From (14.29) it follows that in unperturbed circular orbit ($r = \text{const}$), the air drag is constant. In other words,

$$T = T_0 = \text{const.}$$

In our case, the satellite therefore experiences a certain constant deceleration. The resulting slow-down can be analyzed from the results of Sec. 3.3. As we have shown in that section, this perturbation causes a monotonic reduction in flight height and in orbital period, i.e., the satellite will trace a convolute spiral, moving with an ever increasing velocity. *

All the resulting perturbations are proportional to $\dfrac{T_0}{g_m}$, where g_m is the gravitational acceleration at the relevant height. From (1.2) and (14.29) it follows that

$$\frac{T_0}{g_m} = -c\rho r = -c\rho(R_E + h). \tag{14.32}$$

Applying (3.7), (3.13), and (14.32), we obtain for the change in orbital period per circuit

$$\delta P = -\frac{12\pi^2}{\sqrt{\mu}} c\rho r^{5/2} \quad \text{or} \quad \frac{\delta P}{P} = -6\pi c\rho r, \tag{14.33}$$

---

* This seemingly paradoxical effect of "acceleration" by air drag is explained in Sec. 3.3.

238

where $P = 2\pi \dfrac{r^{3/2}}{\sqrt{\mu}}$ is the period of revolution in unperturbed orbit.

Making use of (3.12) and (3.14), we obtain expressions for the secular variations of the radius and the longitudinal flight velocity during one circuit, δr and δv_u, and for the displacement δl along the orbit corresponding to the variation δP of the orbital period:

$$\left.\begin{array}{ll}
\delta r = -4\pi c \rho r^2, & \dfrac{\delta r}{r} = \dfrac{2}{3}\dfrac{\delta P}{P}, \\[2mm]
\delta v_u = 2\pi c\rho \sqrt{\mu r}, & \dfrac{\delta v_u}{w} = -\dfrac{1}{3}\dfrac{\delta P}{P}, \\[2mm]
\delta l = -w\,\delta P = 12\pi^2 c\rho r^2, & \dfrac{\delta l}{r} = -2\pi\dfrac{\delta P}{P},
\end{array}\right\} \qquad (14.34)$$

where $w = \sqrt{\dfrac{\mu}{r}}$ is the velocity in unperturbed motion.

Satellite moving in perturbed orbit dips into atmospheric layers of progressively increasing density as the flight height $h \approx r - R_E$ decreases. This in turn leads to an increase in $|T|$, $|\delta P|$, $\delta l, |\delta r|$ and δv_u, i.e., the orbital perturbations grow monotonically. However, for small δr(which is generally the case in practice), the variation of $\delta P, \delta l,\ \delta r,$ and δv_u during a limited period can be neglected, and some mean values can be substituted. Making use of (3.8), (3.12), and (3.13) we then write expressions for the corresponding secular perturbations $(\Delta P)_{\text{sec}},\ (\Delta l)_{\text{sec}},\ (\Delta r)_{\text{sec}},\ (\Delta v_u)_{\text{sec}}$ of the orbital elements in n circuits, and also for the rate of secular radial displacement $(\Delta v_r)_{\text{sec}}$:

$$\left.\begin{array}{ll}
(\Delta P)_{\text{sec}} = \dfrac{2n-1}{2}\delta P, & (\Delta l)_{\text{sec}} = \dfrac{n^2}{2}\delta l, \\[2mm]
(\Delta r)_{\text{sec}} = n\,\delta r, & (\Delta v_u)_{\text{sec}} = n\,\delta v_u, \\[2mm]
(\Delta v_r)_{\text{sec}} = -2c\rho\sqrt{\mu r} = -\dfrac{\delta v_u}{\pi}.
\end{array}\right\} \qquad (14.35)$$

In these formulas, the circuit number n runs from 1, and not from 0. The increments $(\Delta l)_{\text{sec}},\ (\Delta r)_{\text{sec}},$ and $(\Delta v_u)_{\text{sec}}$ therefore give the corresponding perturbations at the end of the n-th circuit, while $(\Delta P)_{\text{sec}}$ is the perturbation of the orbital period during the n-th circuit (the time between the starting points of the $(n+1)$-th and n-th circuits). For $n = 1$,

$$(\Delta P)_{\text{sec}} = \dfrac{\delta P}{2}, \quad (\Delta l)_{\text{sec}} = \dfrac{\delta l}{2},$$
$$(\Delta r)_{\text{sec}} = \delta r, \quad (\Delta v_u)_{\text{sec}} = \delta v_u.$$

Air drag produces periodic, as well as secular, perturbations of circular orbit. The peak magnitudes of the periodic perturbations can be estimated from (3.11), (14.32), and (14.33), which give

$$\left.\begin{array}{ll}
|\Delta r|_{\max} = 2c\rho r^2, & \dfrac{|\Delta r|_{\max}}{r} = \dfrac{1}{3\pi}\left|\dfrac{\delta P}{P}\right|, \\[2mm]
|\Delta l|_{\max} = 8c\rho r^2, & \dfrac{|\Delta l|_{\max}}{r} = \dfrac{4}{3\pi}\left|\dfrac{\delta P}{P}\right|, \\[2mm]
|\Delta v_r|_{\max} = 4c\rho\sqrt{\mu r}, & \dfrac{|\Delta v_r|_{\max}}{w} = \dfrac{2}{3\pi}\left|\dfrac{\delta P}{P}\right|, \\[2mm]
|\Delta v_u|_{\max} = 2c\rho\sqrt{\mu r}, & \dfrac{|\Delta v_u|_{\max}}{w} = \dfrac{1}{3\pi}\left|\dfrac{\delta P}{P}\right|.
\end{array}\right\} \qquad (14.36)$$

239

We see from the above relations that the perturbation along the orbit is the largest. Indeed, from (14.34) and (14.36) we have

$$|\delta r|_{max} = \frac{\delta l}{3\pi} \approx \frac{\delta l}{9.4}, \quad |\Delta l|_{max} = \frac{2\,\delta l}{3\pi^2} \approx \frac{\delta l}{14.8}, \\ |\Delta r|_{max} = \frac{\delta l}{6\pi^2} \approx \frac{\delta l}{59}.$$

(14.37)

It should be kept in mind that the secular perturbation along the orbit, $(\Delta l)_{sec}$, is proportional to the square of the circuit number n, and the secular displacement along the radius, $(\Delta r)_{sec}$, varies as the first power of n; the maximum periodic perturbations $|\Delta l|_{max}$ and $|\Delta r|_{max}$, however, remain constant (if the increase of air drag resulting from the secular orbit contraction is neglected).

Table 14.2 lists the values of $\left|\frac{\delta P}{P}\right|$, $|\delta P|$, δl, $|\delta r|$, $|\Delta r|_{max}$, $|\Delta l|_{max}$, $|\delta v_u|$, and $|(\Delta v_r)_{sec}|$, calculated for the case $c = 0.1$ m³/kg· sec² and 120 km $\leqslant h \leqslant 800$ km.

TABLE 14.2

Height, h	Perturbations of circular orbit due to air drag for $c = 0.1$ m³/k·sec²							
	$\left\|\frac{\delta P}{P}\right\|$	$\|\delta P\|$	δl	$\|\delta r\|$	$\|\Delta r\|_{max}$	$\|\Delta l\|_{max}$	$\|\delta v_u\|$	$\|(\Delta v_r)_{sec}\|$
km		sec	km	km	km	km	m/sec	m/sec
120	$3.0 \cdot 10^{-2}$	158	1240	132	21	84	79	25
150	$2.1 \cdot 10^{-3}$	11	87	9.2	1.5	5.9	5.5	1.8
200	$4.6 \cdot 10^{-4}$	2.4	19	2.0	$3.2 \cdot 10^{-1}$	1.3	1.2	$3.7 \cdot 10^{-1}$
250	$1.3 \cdot 10^{-4}$	$7.0 \cdot 10^{-1}$	5.5	$5.8 \cdot 10^{-1}$	$9.2 \cdot 10^{-2}$	$3.7 \cdot 10^{-1}$	$3.4 \cdot 10^{-1}$	$1.1 \cdot 10^{-1}$
300	$4.3 \cdot 10^{-5}$	$2.3 \cdot 10^{-1}$	1.8	$1.9 \cdot 10^{-1}$	$3.0 \cdot 10^{-2}$	$1.2 \cdot 10^{-1}$	$1.1 \cdot 10^{-1}$	$3.5 \cdot 10^{-2}$
350	$1.6 \cdot 10^{-5}$	$8.7 \cdot 10^{-2}$	$6.7 \cdot 10^{-1}$	$7.1 \cdot 10^{-2}$	$1.1 \cdot 10^{-2}$	$4.5 \cdot 10^{-2}$	$4.1 \cdot 10^{-2}$	$1.3 \cdot 10^{-2}$
400	$6.6 \cdot 10^{-6}$	$3.7 \cdot 10^{-2}$	$2.8 \cdot 10^{-1}$	$3.0 \cdot 10^{-2}$	$4.8 \cdot 10^{-3}$	$1.9 \cdot 10^{-2}$	$1.7 \cdot 10^{-2}$	$5.4 \cdot 10^{-3}$
500	$1.5 \cdot 10^{-6}$	$8.6 \cdot 10^{-3}$	$6.7 \cdot 10^{-2}$	$7.1 \cdot 10^{-3}$	$1.1 \cdot 10^{-3}$	$4.5 \cdot 10^{-3}$	$3.9 \cdot 10^{-3}$	$1.3 \cdot 10^{-3}$
600	$4.6 \cdot 10^{-7}$	$2.7 \cdot 10^{-3}$	$2.0 \cdot 10^{-2}$	$2.1 \cdot 10^{-3}$	$3.4 \cdot 10^{-4}$	$1.4 \cdot 10^{-3}$	$1.2 \cdot 10^{-3}$	$3.7 \cdot 10^{-4}$
700	$1.6 \cdot 10^{-7}$	$9.6 \cdot 10^{-4}$	$7.2 \cdot 10^{-3}$	$7.6 \cdot 10^{-4}$	$1.2 \cdot 10^{-4}$	$4.9 \cdot 10^{-4}$	$4.0 \cdot 10^{-4}$	$1.3 \cdot 10^{-4}$
800	$6.3 \cdot 10^{-8}$	$3.8 \cdot 10^{-4}$	$2.9 \cdot 10^{-3}$	$3.0 \cdot 10^{-4}$	$4.8 \cdot 10^{-5}$	$1.9 \cdot 10^{-4}$	$1.6 \cdot 10^{-4}$	$5.0 \cdot 10^{-5}$

We see from the table that the effect of air drag on artificial Earth satellites sharply drops with increasing flight altitude. The periodic perturbations of the orbit virtually vanish at heights of some 400 km. The influence of secular perturbations can be ignored in predicting the motion of the satellite several circuits in advance at altitudes of 600 — 700 km and higher. In long-range forecasting, however, drag forces are by no means negligible even at greater altitudes. For example, at heights of 800 km, the secular displacement along the orbit is $\delta l = 3$ m per circuit. From (14.35) we thus have $(\Delta l)_{sec} = 1500$ km in 1000 circuits.

14.5. HEIGHT OF CIRCULAR ORBIT
AS A FUNCTION OF AIR DRAG

We see from Table 14.2 that as the flight height decreases, the effects of air drag become progressively more pronounced. The linear variation of the orbital period P and the radius r, and the quadratic variation of the displacement Δl along the orbit with the circuit number n (see (14.35)) break down, and the perturbations are enhanced. Starting with some height, the perturbing influence of the atmosphere is so large that the satellite cannot orbit. For $h = 120$ km, the reduction in flight height per one circuit is $|\delta h| = |\delta r| = 132$ km (see Table 14.2), i.e., the satellite hits the ground already in the course of its first orbital circuit. The final outcome of drag forces is to make the satellite fall to the Earth's surface. It is therefore important to establish the variation of the secular perturbations in the elements of circular orbit due to drag forces and to calculate the lifetime of satellites.

As we have shown in Sec. 1.1, all the parameters of motion in the plane of circular orbit are uniquely defined by flight height $h = r - R_E$. We shall therefore consider secular perturbations in flight height only, which are given by

$$\frac{dh}{dt} = (\Delta v_r)_{\text{sec}} = -2c\rho \sqrt{\mu r},$$

where $(\Delta v_r)_{\text{sec}}$ is the rate of secular displacement along the radius (see (14.35)). Hence, introducing the relative time

$$\tau = ct, \tag{14.38}$$

we have

$$d\tau = -\frac{dh}{2\rho \sqrt{\mu r}}. \tag{14.39}$$

If the air density ρ is calculated for a static model atmosphere (i.e., ρ is a function of flight height h only), integration of (14.39) gives

$$\tau - \tau_1 = F(h_1) - F(h), \tag{14.40}$$

where τ_1 and τ are the relative times corresponding to the initial height h_1 and the current height h, $F(h)$ is a function of height defined by

$$F(h) = \frac{1}{2\sqrt{\mu}} \int_0^h \frac{dh}{\rho(h) r^{1/2}}. \tag{14.41}$$

The function $F(h)$ is clearly determined by the particular model atmosphere used. If this function is known, then, from (14.38) and (14.40), we find the time required for the satellite to drop from the height h_1 to h:

$$t - t_1 = \frac{F(h_1) - F(h)}{c}. \tag{14.42}$$

We now proceed to derive the function $F(h)$ for different model atmospheres. The quantity $\sqrt{r} = \sqrt{R_E + h}$ entering the right-hand side of

(14.41) varies with the height h much more slowly than the density function $\rho(h)$. In our approximate calculations of $F(h)$ we therefore ignore the variation of $\sqrt{r}$, substituting for this quantity its initial value. Making use of (14.9) and (14.41), we find for the isothermal atmosphere

$$F(h) = \frac{1}{2\rho_1 \sqrt{\mu r}} \int_0^h \exp\left(\frac{h-h_1}{H}\right) dH =$$
$$= \frac{H}{2\rho_1 \sqrt{\mu r}}\left[\exp\left(\frac{h-h_1}{H}\right) - \exp\left(\frac{-h_1}{H}\right)\right] =$$
$$= \frac{H}{2\sqrt{\mu r}}\left(\frac{1}{\rho} - \frac{1}{\rho_0}\right), \tag{14.43}$$

where ρ_0 is air density at $h = 0$.

We see from this expression that $F(0) = 0$ and that this function increases rapidly with the height h. The first term in the right-hand side of this equality is much greater than the second term, and we therefore write

$$F(h) \approx \frac{H \exp\left(\frac{h-h_1}{H}\right)}{2\rho_1 \sqrt{\mu r}} = \frac{H}{2\rho \sqrt{\mu r}}. \tag{14.44}$$

Making use of (14.23), we similarly find for an atmosphere with a constant "molecular" temperature gradient:

$$F(h) = \frac{1}{2\rho_1 \sqrt{\mu r}} \int_0^h \left(1 + \frac{h-h_1}{H_T}\right)^{\frac{H_T}{H}} dh =$$
$$= \frac{H_T}{2\rho_1 \sqrt{\mu r}\left(\frac{H_T}{H} + 1\right)}\left[\left(1 + \frac{h-h_1}{H_T}\right)^{\frac{H_T}{H}+1} - \left(1 - \frac{h_1}{H_T}\right)^{\frac{H_T}{H}+1}\right]. \tag{14.45}$$

On the other hand, from (14.17), (14.22), and (14.23), we have

$$\left(1 + \frac{h-h_1}{H_T}\right)^{\frac{H_T}{H}+1} = \frac{\rho_1 T'}{\rho T_1'}.$$

Hence

$$F(h) = \frac{H}{2\sqrt{\mu r}\left(1 + \frac{H}{H_T}\right)}\left(\frac{T'}{T_1'\rho} - \frac{T_0'}{T_1'\rho_0}\right), \tag{14.46}$$

where T', T_1', and T_0' are the "molecular" temperatures at the heights h, h_1, and $h_0 = 0$, respectively. Neglecting the second term in the right-hand side of this relation, we write

$$F(h) \approx \frac{H}{2\rho \sqrt{\mu r}} \frac{T'}{T_1'\left(1 + \frac{H}{H_T}\right)}. \tag{14.47}$$

For $\alpha \to 0, H_T \to \infty$, and $T' = \text{const}$, relations (14.46) and (14.47) reduce to the corresponding expressions (14.43) and (14.44) for isothermal atmosphere.

The height h_1 for which the parameters ρ_1, H, and H_T are determined in this model can always be made equal to the height h for which the function

242

$F(h)$ is computed. Then $T' = T_1'$, and (14.47) takes the form

$$F(h) \approx \frac{H}{2\rho\sqrt{\mu r}} \frac{1}{1 + \frac{H}{H_T}}. \qquad (14.48)$$

The parameters H and H_T in the right-hand side are functions of the height h. From (14.20) and (14.22) it follows that these functions are given by

$$H(h) = \frac{T'(h)}{\alpha + \frac{g}{R}}, \quad H_T(h) = \frac{T'(h)}{\alpha}.$$

Hence, taking α and g to be constant, and applying (14.18), we write

$$\frac{dH}{dh} = \frac{\alpha}{\alpha + \frac{g}{R}} = \frac{H\alpha}{T'} = \frac{H}{H_T}. \qquad (14.48a)$$

Expression (14.48) takes the form

$$F(h) \approx \frac{H}{2\rho\sqrt{\mu r}} \frac{1}{1 + \frac{dH}{dh}}. \qquad (14.49)$$

The parameters of the upper atmosphere are sometimes determined making use of multilayer models, each of which is characterized by a constant "molecular" temperature gradient (some of these layers may actually be isothermal). Applying (14.41) and (14.47), we write for this model

$$F(h) = \sum_{i=1}^{n-1} [F_i(h_{i+1}) - F_i(h_i)] + F_n(h) - F_n(h_n), \qquad (14.50)$$

where $F_i(h)$ is the function $F(h)$ in some i-th layer, defined by (14.47), h_i and h_{i+1} are the base and the summit heights of the i-th layer, n is the number of the layer corresponding to the current height h.

Appendix 2 lists the values of the function $F(h)$ calculated from (14.41) for CIRA 1961. The values of $F(h)$ are given in $(m^3/kg \cdot sec^2) \times s.d.$, so that when they are divided by the coefficient c, which is expressed in $m^3/kg \cdot sec^2$, the quotient gives the flight time in mean solar days (s.d.).

Applying the data from Appendix 2 and relations (14.40) and (14.42), we can find the height h as a function of τ and t. Figures 14.3 and 14.4 plot the functions $h(\tau)$ for different initial heights h_1 ($h_1 = 200$ and 500 km). We see from the graphs that the rate of orbit contraction gradually increases in time. Finally, the satellite sinks down and falls on the ground.

The functions $F(h)$ can be conveniently determined from the foregoing expressions. The accuracy of these expressions can be assessed by examining the figures in Table 14.3, which gives the ratios $\frac{\tilde{F}(h)}{F(h)}$ and $\frac{\bar{F}(h)}{F(h)}$, where $F(h)$ is the value from Appendix 2, $\tilde{F}(h)$ and $\bar{F}(h)$ are the approximate values calculated from (14.44) and (14.49). The values of $\rho(h)$ and $H(h)$

243
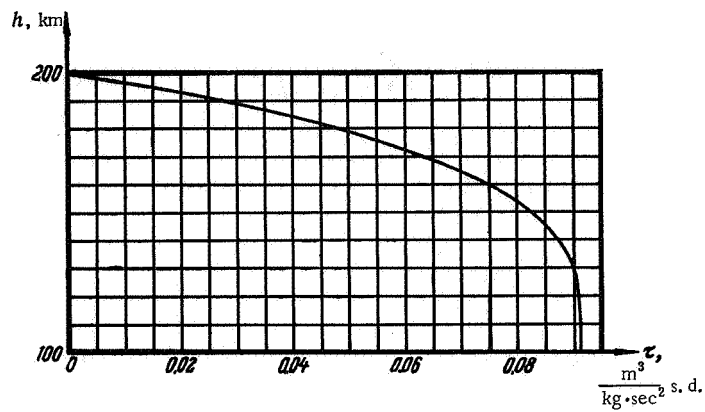
FIGURE 14.3. Flight height h vs. relative time τ for initial circular-orbit height h_1= 200 km.
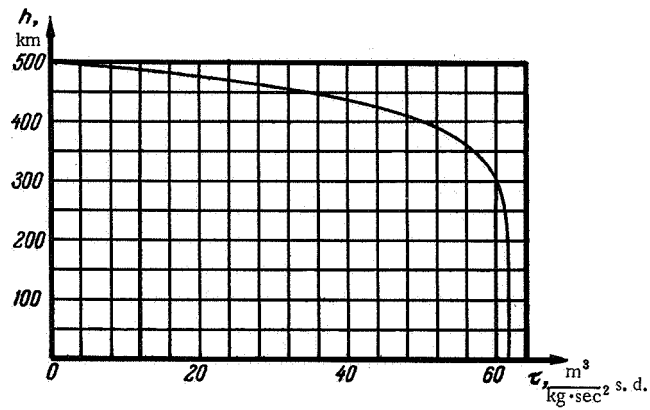
FIGURE 14.4. Flight height h vs. relative time τ for initial circular-orbit height h_1= 500 km.

TABLE 14.3

h, km	$\dfrac{\tilde{F}}{F}$	$\dfrac{\bar{F}}{F}$	h, km	$\dfrac{\tilde{F}}{F}$	$\dfrac{\bar{F}}{F}$
150	1.44	0.98	500	1.13	0.98
200	1.25	1.02	550	1.14	0.99
250	1.12	1.02	600	1.14	0.99
300	1.10	1.00	650	1.11	0.99
350	1.11	1.00	700	1.08	1.01
400	1.12	0.99	750	1.11	1.00
450	1.13	0.99	800	1.14	0.97

are taken from Appendices 1 and 2; the derivative $\frac{dH}{dh}$ is replaced with the mean

$$\left(\frac{dH}{dh}\right)_m = \frac{H(h) - H(h-\Delta)}{\Delta},$$

where Δ is a parameter so chosen that the satellite moves in the height range from h to $h-\Delta$ during most of its lifetime. This is easily seen to be equivalent to the condition $F(h) \gg F(h-\Delta)$. Moreover, between these heights, the function $H(h)$ should be as close to linear as possible (see Figure 14.1). In view of these considerations, we have chosen the following values of Δ:

for $\quad 300 \text{ km} \leqslant h \leqslant 800 \text{ km} \quad \Delta = 100 \text{ km},$

for $\quad\qquad\qquad h = 250 \text{ km} \quad \Delta = 50 \text{ km},$

for $\quad\qquad\qquad h = 200 \text{ km} \quad \Delta = 40 \text{ km},$

for $\quad\qquad\qquad h = 150 \text{ km} \quad \Delta = 20 \text{ km}.$

We see from this table that the relative error in $F(h)$ as calculated from (14.49) does not exceed 3%. This accuracy is quite satisfactory considering that all the numerical data are highly approximate. Formula (14.44) is slightly less accurate: the values of $F(h)$ are too high on account of the monotonic growth of H in the entire range of flight heights h. The last expression can be used in approximate estimates if no reliable information is available on the derivative $\frac{dH}{dh}$.

14.6. SATELLITE LIFETIME AND THE CRITICAL VALUES OF CIRCULAR-ORBIT ELEMENTS

From (14.41) we see that toward the end of the satellite lifetime (as $h \to 0$), $F(h) \to 0$. Hence, applying (14.42), we find an expression for the total lifetime of a satellite in circular orbit:

$$t_{\text{life}} = \frac{F(h_0)}{c}, \tag{14.51}$$

where h_0 is the initial flight height. In particular, from (14.35) and (14.47), we find for an atmosphere with constant temperature gradient

$$t_{\text{life}} = \frac{H}{2c\rho_0 \sqrt{\mu r_0}} \frac{T_0'}{T_1'\left(1 + \frac{H}{H_T}\right)} = \frac{H}{|(\Delta v_r)_{\text{sec}}|_0} \frac{T_0'}{T_1'\left(1 + \frac{H}{H_T}\right)}, \tag{14.52}$$

where r_0, ρ_0, T_0', $|(\Delta v_r)_{\text{sec}}|_0$ are the values of the corresponding quantities at the height $h = h_0$.

For isothermal atmosphere ($T_0' = T_1'$, $H_1 = \infty$), we have

$$t_{\text{life}} = \frac{H}{2c\rho_0 \sqrt{\mu r_0}} = \frac{H}{|(\Delta v_r)_{\text{sec}}|_0}. \tag{14.53}$$

245

Making use of (5.36) and (14.33), we write for (14.51)

$$t_{\text{life}} = k(h_0) \frac{P_0^2}{|\delta P_0|},$$ (14.54)

where

$$k(h_0) = 3F(h)\rho(h)\sqrt{\frac{\mu}{r}},$$ (14.55)

and P_0 and δP_0 are the initial values of the orbital period P and of its change during one circuit δP. Making use of (14.44) and (14.49), we find

$$k(h) = \begin{cases} \dfrac{3}{2}\dfrac{H}{r} & \text{for isothermal atmosphere,} \\ \dfrac{3}{2}\dfrac{H}{r}\dfrac{1}{1+\dfrac{dH}{dh}} & \text{for constant temperature-gradient atmosphere.} \end{cases}$$ (14.56)

The derivative $\frac{dH}{dh}$ in the right-hand side of the last expression can be found from (14.48a).

Expression (14.54) is convenient for calculating the lifetime of real satellites whose P_0, δP_0, and h_0 are known with fair accuracy. Using this formula, we avoid the errors connected with the uncertainty in c and ρ, but there are still the inaccuracies due to the deviation of the actual $k(h)$ from the calculated figures.

Appendix 2 lists the values of $k(h)$ calculated from (14.55) for CIRA 1961.

From (14.51), (14.52), and (14.53) it follows that the lifetime t_{life} in circular orbit (for a given static model atmosphere) is a function of the initial flight altitude h_0 and the coefficient c. It rapidly increases with increasing h_0 and decreasing c.

In some cases, we are interested in the variations of lifetime, Δt_{life}, for small changes in c and h_0. We have the obvious variational equation

$$\Delta t_{\text{life}} = \frac{\partial t_{\text{life}}}{\partial c}\Delta c + \frac{\partial t_{\text{life}}}{\partial h_0}\Delta h_0,$$

where Δc and Δh_0 are small increments in the corresponding parameters. From (14.41) and (14.51), we have

$$\frac{\partial t_{\text{life}}}{\partial c} = -\frac{F(h_0)}{c^2} = -\frac{t_{\text{life}}}{c},$$

$$\frac{\partial t_{\text{life}}}{\partial h_0} = \frac{1}{2c\rho_0\sqrt{\mu r_0}} = \frac{1}{|(\Delta v_r)_{\text{sec}}|_0} = \frac{\varphi(h_0)}{c},$$

where $\varphi(h)$ is a function of height:

$$\varphi(h) = \frac{1}{2\rho\sqrt{\mu r}}.$$

The values of this function for various heights are given in Appendix 2.

We now determine the conditions under which the satellite ceases its existence. These conditions correspond to some critical elements of the so-called critical orbit (minimum allowed flight altitude h_{crit},

246

minimum orbital period P_{crit}, maximum flight velocity w_{crit}, etc.). By
critical orbit we mean an orbit in which the satellite completes just
one revolution around the Earth, so that

$$P_{crit} = t_{life}.$$

Substituting (1.5) and (14.51), we obtain an equality for the critical height:

$$\frac{2\pi \ (R_E + h_{crit})^{3/2}}{\sqrt{\mu}} = \frac{F \ (h_{crit})}{c}.$$

Hence it follows that for a given atmosphere, the critical height h_{crit} is a
function of the coefficient c. If h_{crit} is known, the other critical elements
can be calculated fairly simply from the formulas of Chapter 1.

Figure 14.5 plots the critical flight altitude h_{crit} and the critical orbital
period P_{crit} as a function of the coefficient c for the previously introduced
model atmosphere. As c varies between wide limits ($0.001\,\mathrm{m^3/kg \cdot sec^2} \leq$
$\leq c \leq 1.0\,\mathrm{m^3/kg \cdot sec^2}$), the parameters h_{crit} and P_{crit} remain fairly constant
($108\,\mathrm{km} \leq h_{crit} \leq 188\,\mathrm{km}$, $86.5\,\mathrm{min} \leq P_{crit} \leq 88.1\,\mathrm{min}$). Here the parameters
h_{crit} and P_{crit} increase with c.
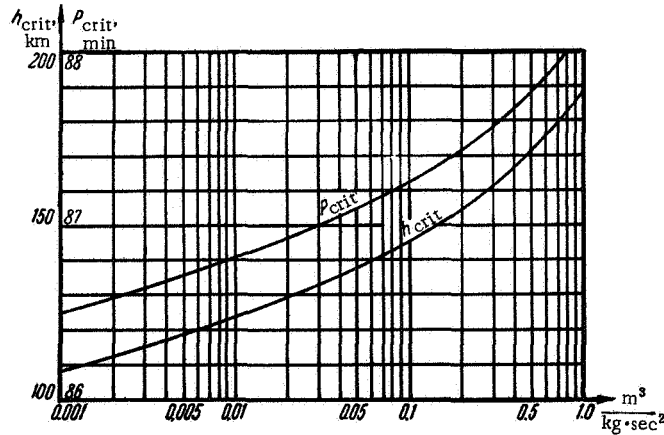
FIGURE 14.5. Critical flight altitude h_{crit} and critical orbital
period P_{crit} vs. the coefficient c for motion in circular orbit.

Comparison of the graphs in Figures 14.1 and 14.5 shows that satellites
cannot exist at altitudes of less than $110 - 120$ km because at these heights H
sharply decreases, i.e., the rate of change of air density with height becomes
very steep. Heights of some $110-120$ km are therefore the minimum allowed
flight altitudes of modern artificial Earth satellites, whose minimum orbital
period is $86.5 - 86.7$ min.

The plots of h_{crit} and P_{crit} vs. c in Figure 14.5 do not change noticeably
if a different model atmosphere is introduced. This is so because any
change in air density is equivalent to a certain change in the coefficient c,
and P_{crit} and h_{crit} are insensitive to these changes.

14.7. THE EFFECT OF ATMOSPHERIC ROTATION ON MOTION IN CIRCULAR ORBIT

In our analysis of atmospheric rotation, we shall proceed from relation (14.28). The vector v_1 — the velocity of air in an inertial frame — points from west to east, and its magnitude is given by

$$v_1 = k\Omega r \cos B, \tag{14.57}$$

where Ω is the angular velocity of rotation of the Earth, r the distance from the Earth's center to the satellite, B geocentric latitude, and k a coefficient characterizing the degree of entrainment of the atmosphere by the Earth. This coefficient varies between the limits

$$0 \leqslant k \leqslant 1. \tag{14.58}$$

We determine the projections of the satellite's relative velocity on the continuation of the radius-vector r from the Earth's center to the satellite, on the normal u to this radius-vector in the orbital plane, and on the normal
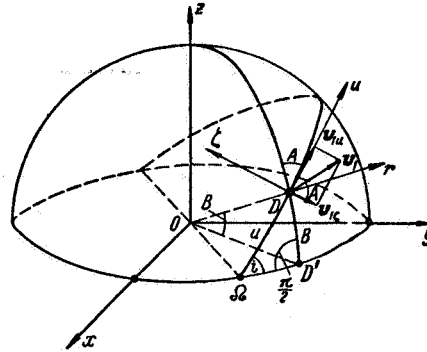
FIGURE 14.6. Determining satellite's velocity components relative to rotating atmosphere.

ζ to the orbital plane ($Dru\zeta$ constitute a right-hand triad). Making use of Figure 14.6, we can derive expressions for the projections v_{1u} and $v_{1\zeta}$ of the relative air velocity v_1 on the corresponding directions. Substituting (14.57) in (14.28), we find

$$\left. \begin{array}{l} v_{rel\,r} = v_r, \\ v_{rel\,u} = v_u - k\Omega r \cos B \sin A, \\ v_{rel\,\zeta} = k\Omega r \cos B \cos A, \end{array} \right\} \tag{14.59}$$

where $v_{rel\,r}$, $v_{rel\,u}$, $v_{rel\,\zeta}$ and v_r, v_u are the corresponding projections of the vectors v_{rel} and v; A is the azimuth of the line Du.

248

Consider a spherical right triangle $D\Omega D'$ $(O\Omega$ is the line of nodes, OD' is the intersection line of the meridional plane through the satellite D with the equatorial plane). In this triangle

$$\widehat{\Omega D} = u, \quad \widehat{DD'} = B, \quad \angle\, D\,\Omega\, D' = i,$$

$$\angle\,\Omega\, DD' = A, \quad \angle\,\Omega\, D'D = \frac{\pi}{2}.$$

Hence

$$\cos i = \sin A \cos B,$$

$$\cos \angle\,\Omega\, D'D = 0 = -\cos i \cos A + \sin i \sin A \cos u,$$

$$\cos A = \frac{\sin i \sin A \cos u}{\cos i},$$

$$\cos B \cos A = \sin i \cos u.$$

Substituting the first and the fourth of these relations in (14.59), we find

$$\left. \begin{aligned} v_{\mathrm{rel}\,r} &= v_r, \\ v_{\mathrm{rel}\,u} &= v_u - k\Omega r \cos i, \\ v_{\mathrm{rel}\,\zeta} &= k\Omega r \sin i \cos u. \end{aligned} \right\} \tag{14.60}$$

Hence an expression for the magnitude of the vector $\boldsymbol{v}_{\mathrm{rel}}$:

$$v_{\mathrm{rel}} = \sqrt{v_r^2 + (v_u - k\Omega r \cos i)^2 + k^2\Omega^2 r^2 \sin^2 i \cos^2 u} =$$

$$= \sqrt{v^2 - 2v_u k\Omega r \cos i + k^2\Omega^2 r^2 (1 - \sin^2 i \sin^2 u)}. \tag{14.61}$$

Let S, T, W be the projections of the perturbing acceleration produced by air drag on the directions Dr, Du and $D\zeta$. From (14.1) and (14.30) we have

$$\left. \begin{aligned} S &= -c\rho v_{\mathrm{rel}} v_{\mathrm{rel}\,r}, \\ T &= -c\rho v_{\mathrm{rel}} v_{\mathrm{rel}\,u}, \\ W &= -c\rho v_{\mathrm{rel}} v_{\mathrm{rel}\,\zeta}. \end{aligned} \right\} \tag{14.62}$$

The quantities v_{rel}, $v_{\mathrm{rel}\,r}$, $v_{\mathrm{rel}\,u}$, and $v_{\mathrm{rel}\,\zeta}$ are determined from (14.60) and (14.61). For circular orbit ($v_r = 0$, $v_u = v = w$),

$$\left. \begin{aligned} S &= 0, \\ T &= -c\rho\,(w - k\Omega r \cos i) \times \\ &\quad \times \sqrt{w^2 - 2wk\Omega r \cos i + k^2\Omega^2 r^2 (1 - \sin^2 i \sin^2 u)}, \\ W &= -c\rho k\Omega r \sin i \cos u \times \\ &\quad \times \sqrt{w^2 - 2wk\Omega r \cos i + k^2\Omega^2 r^2 (1 - \sin^2 i \sin^2 u)}. \end{aligned} \right\} \tag{14.63}$$

Calculations show that as the flight altitude $h = r - R_{\mathrm{E}}$ varies between the limits

$$120\ \mathrm{km} \leqslant h \leqslant 1000\ \mathrm{km} \tag{14.64}$$

the parameter $\dfrac{\Omega r}{w} = \dfrac{\Omega r^{3/2}}{\sqrt{\mu}}$ varies between the limits

$$0.06 < \frac{\Omega r}{w} < 0.073. \tag{14.65}$$

249

Since this ratio is small, we write (14.63) to terms of the first order of smallness as

$$T \approx - c\rho w^2 \left(1 - 2k \frac{\Omega r}{w} \cos i\right),$$
$$W \approx - c\rho w^2 k \frac{\Omega r}{w} \sin i \cos u. \qquad \qquad (14.66)$$

The rotation of the upper atmosphere thus produces perturbing accelerations not only along the orbit, but also at right angles to the orbital plane.

Comparison of the first expression in (14.66) with relation (14.29) shows that if atmospheric rotation is introduced, the perturbing acceleration T directed along the orbit varies in proportion to $\Phi = 1 - 2k \frac{\Omega r}{w} \cos i$, which is constant for a given orbit. From (14.58) and (14.65) it follows that for flight altitudes $h < 1000\,\text{km}$, this factor may vary between the limits

$$0.854 < \Phi < 1.146. \qquad \qquad (14.67)$$

Previously considered perturbations of circular orbit are clearly proportional to this factor, while the lifetime t_{life} is inversely proportional to Φ. West-east flight $(0 < i < \pi/2)$ corresponds to a decrease in the perturbing influence of drag forces $(\Phi < 1)$, while east-west flight $(\pi/2 < i \leqslant \pi)$ involves an increase in these perturbations $(\Phi > 1)$.

As we have previously observed, the total secular perturbations attributable to air drag eventually grow to a substantial level. The variations in these perturbations when multiplied by the factor Φ may also be large. In practice, however, it must be kept in mind that the effect introduced by this factor may be offset by changes in the coefficient c or in air density ρ. Since the accuracy of the numerical data for these quantities is not high, we are unable at present to differentiate between the errors introduced by incorrect approximation to atmospheric rotation and errors attributable to the uncertainty in the parameters c and ρ. The atmospheric entrainment coefficient k therefore cannot be determined from measurements of perturbations in the orbital plane (this problem could be solved, however, if two identical satellites were launched simultaneously in westerly and easterly directions).

Let us now consider the contribution from the acceleration W which is normal to the orbital plane. From (14.66) we see that this acceleration is proportional to $\cos u$, i.e., varies periodically during the period of satellite's revolution in orbit. We have shown in Sec. 3.7 that, aside from periodic perturbations (which are ignored as being small), there is also secular rotation of the orbital plane in this case. From (3.34), (3.35), and (14.66), seeing that $\cos u = \sin [u - (- \pi/2)]$, we find that the orbital plane rotates about the axis

$$u_1 = 0, \qquad \qquad (14.68)$$

i.e., around the line of nodes.

The angle of rotation per one circuit, i.e., the angle ψ for $\varphi = 2\pi$, is obtained from the expression

$$\delta\psi = -\pi \frac{c\rho w^2}{g} \frac{k\Omega r}{w} \sin i = -\pi c\rho r \frac{k\Omega r}{w} \sin i. \qquad (14.69)$$

Making use of (1.4), (9.53), (14.33), and (14.68), we find that the orbit's node remains fixed ($\delta\Omega = 0$), while the inclination changes by

$$\delta i = \delta\psi = -\pi c\rho r \frac{k\Omega r}{w} \sin i = \frac{k\Omega \sin i}{12\pi} \delta P, \qquad (14.70)$$

where δP is the change per circuit in the orbital period, calculated ignoring atmospheric rotation (if atmospheric rotation is taken into consideration, a correction of the order $\left(\frac{k\Omega r}{w}\right)^2$ is introduced in the right-hand side of (14.70), which is neglected in our analysis).

From (14.70) it follows that for any inclination i (which, as we have observed in Sec. 1.2, may vary from 0 to π), $\delta i \leqslant 0$. In other words, atmospheric rotation displaces the orbital plane toward a position with $i = 0$, i.e., the orbit approaches the equatorial plane with the satellite traveling from west to east. The rotation of the orbit in this direction, however, is extremely slow. For the data in Table 14.2, the maximum inclination decrement per one circuit (for $i = \pi/2$ and $k = 1$) varies from $|\delta i| \approx 1''.5 \cdot 10^{-4}$ at $h = 800$ km to $|\delta i| \approx 1''$ at $h = 200$ km and $|\delta i| \approx 4''.5$ at $h = 150$ km. We see that in the great majority of cases, $\delta i \ll 1''$.

Relation (14.70) can be applied to estimate the total inclination increment Δi during the satellite's lifetime. We assume that the parameters i and k in the right-hand side of (14.70) are constant, substituting their mean values i_m and k_m. Summing over the variations δi and δP during the satellite's lifetime, we find

$$\Delta i = -\frac{k_m \Omega \sin i_m}{12\pi}(P_0 - P_{crit}), \qquad (14.71)$$

where P_0 and P_{crit} are the initial and the critical periods of revolution.

As an example, consider a satellite injected into orbit at $h = 500$ km. Calculations with (14.71) show that the inclination of the satellite's orbit during its entire lifetime (which is several years long in this case) is at most some $3'$.

It follows from the preceding that the effect of atmospheric rotation on the motion of artificial Earth satellites is very difficult to detect in practice. For in-plane motion, this effect is obscured by variations in c and ρ. The rotation of the orbital plane, on the other hand, is highly insignificant. The coefficient k characterizing the degree of entrainment of the atmosphere by the rotating Earth may therefore be assigned any value from 0 to 1 in the analysis of air drag.

14.8. THE EFFECT OF AIR DRAG ON MOTION IN NEARLY CIRCULAR ORBIT

In previous sections we analyzed the air drag on satellites moving in circular orbits at a constant height h. In reality, however, the orbit

height is never constant, and the drag forces are therefore variable along the orbit. To make this point, consider the relation

$$h = r - r_E. \tag{14.72}$$

where r and r_E are the distances from the Earth's center to the satellite and to the satellite's projection on the geoid surface.* As the satellite moves in orbit, the distance r displays periodic fluctuations due to the deviations of the injection conditions from the conditions of ideal circular motion, and also due to various perturbing factors. The main perturbations are attributed to the second zonal harmonic of the geopotential (the expansion of the Earth's gravitational potential in spherical functions, (12.6)).

From (2.16) it follows that for small deviations from circular orbit, the perturbations due to inaccuracies in the initial conditions vary with a frequency which is equal to the satellite's orbital frequency. The perturbations produced by the second zonal harmonic, according to (13.20), vary with a frequency which is equal to the first two multiples of the satellite's orbital frequency.

The distance r_E can be determined from the well-known approximate expression /21/

$$r_E = a_e (1 - \alpha \sin^2 B), \tag{14.73}$$

where a_e is the semimajor axis of the geocentric reference ellipsoid, α its flattening, and B the geocentric latitude of the point under consideration. Hence, making use of (13.2), we find

$$r_E = a_e (1 - \alpha \sin^2 u \sin^2 i) = a_e \left[1 - \frac{\alpha \sin^2 i}{2} (1 - \cos 2u) \right]. \tag{14.74}$$

To sum up, the parameter r_E varies with a frequency which is equal to twice the orbital frequency of the satellite.

Comparing these results with (14.72), we conclude that the flight altitude h varies with a frequency which is equal to the first two multiples of the satellite's orbital frequency. Hence, by analogy with (13.20), we can show that

$$h = h_m + \Delta_1 \sin (u - u_1) + \Delta_2 \sin 2(u - u_2), \tag{14.75}$$

where Δ_1, Δ_2, u_1, and u_2 are some constants which depend on the initial conditions of motion and the fundamental parameters of the Earth's gravitational field, h_m is the mean flight altitude defined by

$$h_m = r_m - a_e \left(1 - \frac{\alpha \sin^2 i}{2} \right). \tag{14.76}$$

Here r_m is the mean radius of the nearly circular orbit under consideration. Integrating (14.75) with respect to u from 0 to 2π we find

$$h_m = \frac{1}{2\pi} \int_0^{2\pi} h(u) du. \tag{14.76'}$$

---

* The projection of a satellite on the geoid surface is often called the subsatellite point.

252

From (13.22), (14.72), and (14.74) we see that if the deviations from the initial conditions of circular motion are small, the amplitudes Δ_1 and Λ_2 of fluctuations in flight altitude may reach $a_e\alpha\approx21\,\mathrm{km}$. If the deviations in injection parameters are large, the amplitude Δ_1 of the first harmonic may increase substantially.

If the higher harmonics of the geopotential from the expansions (12.22) and (12.25) (i.e., gravity anomalies) are taken into consideration, higher-frequency terms should be included in expression (14.75). They will be much smaller, however, than the first three terms of the expansion.

From Appendix 2 we see that the air density changes considerably for any $10-20\,\mathrm{km}$ of flight altitude. The fluctuations of orbit height therefore must not be neglected in the analysis of drag forces. We shall consider only those cases when the amplitudes Δ_1 and Δ_2 of orbit-height fluctuations are not greater than the height of the homogeneous atmosphere H (the problem of air drag in largely noncircular orbits is considered in the next chapter). Moreover, in determining the drag force, we substitute the velocity of the satellite in the mean circular orbit for its actual orbital velocity. The relative errors resulting from this substitution are of the order $\dfrac{r-r_m}{r_m}$, whereas the relative change in drag force due to a change in flight altitude is of the order of $\dfrac{h-h_m}{H}$, and $H\ll r_m$.

We derive the air density as a function of height for the previously introduced constant-temperature-gradient atmosphere. The reference height h_i in (14.23) and (14.24) is the mean height h_m of the orbit. Then, making use of (14.29) and retaining the first three terms in the expansion of the air density ρ in powers of $\dfrac{h-h_i}{H}$, we obtain the following expression for the drag-induced acceleration:

$$T = -c\rho(h_m)\,w_m^2\left[1-\frac{h-h_m}{H}+\frac{1}{2}\left(\frac{h-h_m}{H}\right)^2\left(1+\frac{H}{H_T}\right)-\cdots\right], \qquad (14.77)$$

where w_m is the circular velocity for $r=r_m$.
From (14.75) we have

$$\left.\begin{aligned}
h-h_m &= \Delta_1\sin(u-u_1)+\Delta_2\sin2(u-u_2),\\
(h-h_m)^2 &= \tfrac{1}{2}\{\Delta_1^2[1-\cos2(u-u_1)]+\\
&\quad +\Delta_2^2[1-\cos4(u-u_2)]+\\
&\quad +2\Delta_1\Delta_2[\cos(u-2u_2+u_1)-\cos(3u-2u_2-u_1)]\}.
\end{aligned}\right\} \qquad (14.78)$$

Expression (14.77) is thus made up from a constant term plus periodic terms whose frequency is a multiple of the satellite's orbital frequency. The constant term is given by

$$T_0 = -c\rho(h_m)\,w_m^2\left[1+\frac{\Delta_1^2+\Delta_2^2}{4H^2}\left(1+\frac{H}{H_T}\right)+\cdots\right]. \qquad (14.79)$$

As we have previously shown, T_0 produces secular perturbations in the orbital period P and in the mean orbit radius r_m, i.e., the mean flight altitude h_m. Comparison of (14.29) and (14.79) shows that in nearly circular orbits the parameters P, r_m, and h_m vary just as in circular

orbit with a constant height $h = h_m$. The initial value of the coefficient c should be replaced with a corrected expression

$$c' = c \left[1 + \frac{\Delta_1^2 + \Delta_2^2}{4H^2} \left(1 + \frac{H}{H_r} \right) + \cdots \right]. \tag{14.80}$$

The factor following the coefficient c in the right-hand side of (14.80) is always greater than unity. On passing to a nearly circular orbit, we speed up the contraction of the orbital period P and of the mean flight altitude h_m (and therefore shorten the satellite lifetime) in comparison with those obtaining for the mean circular orbit.

From (14.77) and (14.78) it follows that in nearly circular orbit, the expression for the acceleration produced by air drag contains periodic, as well as constant, terms. The frequency of one of these terms is equal to the satellite's orbital frequency, and all the other frequencies are "overtones". Applying the results of Secs. 3.6 and 3.8, we can thus show that, in addition to the previously mentioned secular perturbations in P and h_m, there will be also perturbations connected, generally speaking, with variations in eccentricity, in the position of the perigee point, and with some constant increment of the orbital period P. A more detailed analysis shows, however, that the effect of these secular perturbations of nearly circular orbits is small in comparison with the previously described perturbations in P and h_m (this can be easily proved by the results of the next chapter). To first approximation, the nearly circular orbit can therefore be replaced with the mean circular orbit for the analysis of air drag. The coefficient c, however, should be modified to c' as indicated in (14.80).

Chapter 15

THE EFFECT OF AIR DRAG ON MOTION
IN ELLIPTICAL ORBIT

15.1. FUNDAMENTAL RELATIONS

In the previous chapter we considered the effect of air drag on motion
in circular and nearly circular orbits (nearly circular orbit is an orbit
where the flight altitude fluctuations are not greater than the density scale
height H, i.e., a few tens of kilometers). The results of Chapter 14,
however, do not apply to elliptical orbit, where the flying height changes
by as much as a few hundreds of kilometers. In the present chapter we
therefore proceed with an analysis of air drag in elliptical orbit. We
shall only consider secular variations of orbital elements, and the problem
is solved neglecting atmospheric rotation, i.e., putting $k = 0$ and $v_{rel} = v$
(see Sec. 14.4 and 14.7). We moreover ignore the change in flight altitude
due to the Earth's flattening and the noncentral components of its
gravitational field (these factors may have a substantial influence on the
determination of air density, but they are small in comparison with the
contribution from orbit's ellipticity). Making use of (14.1) and (14.30),
we now write for the components of the perturbing acceleration

$$S = -c\rho v v_r, \quad T = -c\rho v v_u, \quad W = 0, \tag{15.1}$$

where v_r and v_u are the projections of the velocity vector on the directions
Dr and Du (see Figure 14.6), and $v = \sqrt{v_r^2 + v_u^2}$ is the magnitude of the velocity
vector.

Applying (5.11) and (5.13), we write (15.1) in the form

$$\left.\begin{aligned}
S &= -\frac{c\rho\mu}{p} e \sin\vartheta \sqrt{1 + 2e\cos\vartheta + e^2}, \\
T &= -\frac{c\rho\mu}{1p}(1 + e\cos\vartheta)\sqrt{1 + 2e\cos\vartheta + e^2}, \quad W = 0,
\end{aligned}\right\} \tag{15.2}$$

where p is the parameter of the elliptical orbit, e its eccentricity, μ the
coefficient in expression (1.2) for the force of gravity, ϑ the current true
anomaly of the satellite.

Thus, if the atmospheric rotation is ignored, the perturbing acceleration
does not have a component normal to the orbital plane. Air drag therefore
does not alter the orientation of that plane.

Substituting (15.2) in (11.39) and making use of (1.2) and (4.19), we
obtain approximate expressions for the secular variations of the elements

which describe in-plane motion:

$$\delta p = -2cp^2 \int_0^{2\pi} \rho \frac{\sqrt{1+2e\cos\vartheta+e^2}}{(1+e\cos\vartheta)^2}\,d\vartheta,$$

$$\delta e = -2cp \int_0^{2\pi} \rho \frac{(e+\cos\vartheta)\sqrt{1+2e\cos\vartheta+e^2}}{(1+e\cos\vartheta)^2}\,d\vartheta, \qquad\qquad (15.3)$$

$$\delta\omega = -\frac{2cp}{e} \int_0^{2\pi} \rho \frac{\sin\vartheta\sqrt{1+2e\cos\vartheta+e^2}}{(1+e\cos\vartheta)^2}\,d\vartheta,$$

where δp, δe, and $\delta\omega$ are the variations of the parameter p, the eccentricity e, and the argument of the perigee ω per one circuit of revolution.

Let us consider the third relation in greater detail. We shall assume a steady-state atmosphere, i.e., $\rho = \rho(h)$. Then, making use of (4.19), we write

$$\delta\omega = -\frac{2cp}{e} \int_0^{2\pi} \Phi(\vartheta)\,d\vartheta,$$

where

$$\Phi(\vartheta) = \rho\left(\frac{p}{1+e\cos\vartheta} - R_E\right)\frac{\sin\vartheta\sqrt{1+2e\cos\vartheta+e^2}}{(1+e\cos\vartheta)^2},$$

and R_E is the mean radius of the Earth.

Since

$$\Phi(2\pi - \vartheta) = -\Phi(\vartheta),$$

we have

$$\int_0^{2\pi} \Phi(\vartheta)\,d\vartheta = \int_0^{\pi} \Phi(\vartheta)\,d\vartheta + \int_\pi^{2\pi} \Phi(\vartheta)\,d\vartheta = \int_0^{\pi} \Phi(\vartheta)\,d\vartheta - \int_0^{\pi} \Phi(\xi)\,d\xi = 0,$$

where $\xi = 2\pi - \vartheta$.

In other words, under our simplifying assumptions,

$$\delta\omega = 0. \qquad\qquad (15.4)$$

As a first approximation, the argument of the perigee ω is thus free from secular perturbations due to aerodynamic drag forces.

15.2. EXPANSION OF δp AND δe IN TERMS OF ECCENTRICITY

To simplify further manipulations, we substitute the eccentric anomaly E for the true anomaly ϑ in (15.3). From (5.39)

$$\cos\vartheta = \frac{\cos E - e}{1 - e\cos E}, \quad \sin\vartheta = \frac{\sqrt{1-e^2}\,\sin E}{1 - e\cos E}. \qquad\qquad (15.5)$$

Hence

$$d\vartheta = \frac{\sqrt{1-e^2}}{1-e\cos E}\,dE, \quad 1+e\cos\vartheta = \frac{1-e^2}{1-e\cos E},$$

$$1+2e\cos\vartheta+e^2 = \frac{1+e\cos E}{1-e\cos E}(1-e^2),$$

$$e+\cos\vartheta = \frac{\cos E}{1-e\cos E}(1-e^2).$$

(15.6)

Substituting in (15.3), we find

$$\delta p = -\frac{2cp^2}{1-e^2}\cdot\int_0^{2\pi}\rho\,\sqrt{1-e^2\cos^2 E}\,dE,$$

$$\delta e = -2cp\int_0^{2\pi}\rho\,\frac{\cos E\sqrt{1-e^2\cos^2 E}}{1-e\cos E}\,dE.$$

(15.7)

Series-expanding these expressions in terms of eccentricity and seeing that

$$\frac{\sqrt{1-e^2\cos^2 E}}{1-e\cos E} = (1-e^2\cos^2 E)^{\frac{1}{2}}(1-e\cos E)^{-1} =$$

$$= \left(1 - \frac{e^2}{2}\cos^2 E - \frac{e^4}{8}\cos^4 E - \dots\right)\times$$

$$\times(1+e\cos E + e^2\cos^2 E + e^3\cos^3 E + \dots) =$$

$$= 1 + e\cos E + \frac{e^2}{2}\cos^2 E + \frac{e^3}{2}\cos^3 E + \dots,$$

we find

$$\delta p = -\frac{2cp^2}{1-e^2}\int_0^{2\pi}\rho\left(1-\frac{e^2}{2}\cos^2 E - \frac{e^4}{8}\cos^4 E - \dots\right)dE,$$

$$\delta e = -2cp\int_0^{2\pi}\rho\left(\cos E + e\cos^2 E + \right.$$

$$\left. + \frac{e^2}{2}\cos^3 E + \frac{e^3}{2}\cos^4 E + \dots\right)dE.$$

(15.8)

These series converge for

$$0 \leqslant e < 1,$$

i.e., for any elliptical orbit. However, as the eccentricity e approaches unity, the number of significant terms increases. It is therefore advisable to establish in what interval of e-values the number of explicit terms in (15.8) is sufficient. The problem in fact reduces to estimating the accuracy of the evaluation of integrals of the form

$$J = \int_0^{2\pi}\rho F(E)\,dE$$

(15.9)

with expressions

$$\tilde{J} = \int_0^{2\pi}\rho\tilde{F}(E)\,dE,$$

257

where $\bar{F}(E)$ is an approximation to $F(E)$.

To find the relative error ε which obtains when $\bar{J}$ is substituted for J, we make use of the fact that $\rho > 0$. Hence,

$$\varepsilon = \frac{|J - \bar{J}|}{|J|} = \frac{1}{|J|} \left| \int_0^{2\pi} \rho [F(E) - \bar{F}(E)] dE \right| \leqslant \frac{1}{|J|} \int_0^{2\pi} \rho |F(E) - \bar{F}(E)| dE. \quad (15.10)$$

Now, suppose that a certain a has been found, which satisfies the condition

$$a \geqslant \frac{|F(E) - \bar{F}(E)|}{|F(E)|} \quad \text{for} \quad 2\pi \geqslant E \geqslant 0. \quad (15.11)$$

Then, making use of inequality (15.10), we obtain

$$\varepsilon \leqslant a \frac{\int_0^{2\pi} \rho |F(E)| dE}{\left| \int_0^{2\pi} \rho F(E) dE \right|}. \quad (15.12)$$

In particular, if the function $F(E)$ does not reverse its sign in the relevant interval, i.e.,

$$\operatorname{sgn} F(E) = \text{const} \quad \text{for} \quad 0 \leqslant E \leqslant 2\pi, \quad (15.13)$$

then

$$\varepsilon \leqslant a. \quad (15.14)$$

From (15.7) it follows that condition (15.13) is satisfied for δp. For δe, however,

$$F(E) > 0 \quad \text{for} \quad \frac{\pi}{2} > E > -\frac{\pi}{2},$$
$$F(E) < 0 \quad \text{for} \quad \frac{\pi}{2} < E < \frac{3}{2}\pi.$$

Hence

$$\left| \int_0^{2\pi} \rho F(E) dE \right| = \int_0^{2\pi} \rho |F(E)| dE - 2 \int_{\frac{\pi}{2}}^{\frac{3\pi}{2}} \rho |F(E)| dE. \quad (15.15)$$

For highly eccentric orbits $\left(e \gg \frac{H}{a} \right)$, the limits of the second integral in the right-hand side of (15.15) correspond to a range of flight altitudes which are much greater than the perigee height h_p of the orbit. The air density ρ in this range is very low. Therefore,

$$\int_0^{2\pi} \rho |F(E)| dE \gg \int_{\frac{\pi}{2}}^{\frac{3\pi}{2}} \rho |F(E)| dE$$

and

$$\left| \int_0^{2\pi} \rho F(E)\,dE \right| \approx \int_0^{2\pi} \rho \,|F(E)|\,dE.$$

Hence it follows that the accuracy with which δe is determined can be estimated from inequality (15.14).

The problem thus reduces to the determination of a parameter α which satisfies (15.11). From (15.7) and (15.8) it follows that in both cases, i.e., in estimating the accuracy of δp and δe, the ratio $\dfrac{|F(E)-\bar{F}(E)|}{|F(E)|}$ is a function of $e\cos E$. Therefore,

$$\varepsilon_p \leqslant \alpha_p = \left| 1 - \frac{1-\frac{e^2}{2}-\frac{e^4}{8}}{\sqrt{1-e^2}} \right| =$$

$$= \left| 1 - \left(1-\frac{e^2}{2}-\frac{e^4}{8}\right)\left(1+\frac{e^2}{2}+\frac{3}{8}e^4+\frac{5}{16}e^6+\frac{35}{128}e^8+\cdots\right) \right| =$$

$$= \frac{e^6}{16} + \frac{9}{128}e^8 + \cdots$$

$$\varepsilon_a \leqslant \alpha_e = \left| 1 - \sqrt{\frac{1-e}{1+e}}\left(1+e+\frac{e^2}{2}+\frac{e^3}{2}\right) \right| =$$

$$= \left| 1 - \sqrt{1-e^2}\left(1+\frac{e^2}{2}\right) \right| =$$

$$= \left| 1 - \left(1-\frac{e^2}{2}-\frac{e^4}{8}-\frac{e^6}{16}-\cdots\right)\left(1+\frac{e^2}{2}\right) \right| = \frac{3}{8}e^4 + \frac{1}{8}e^6 + \cdots,$$

where the subscripts p and e denote the corresponding values of the parameters ε and α in accuracy estimates of δp and δe.

Table 15.1 lists the coefficients α_p and α_e calculated from these formulas. We see from the table that for

$$0 \leqslant e \leqslant 0.5 \tag{15.16}$$

expression (15.8) is quite satisfactory for the determination of δp and δe.

TABLE 15.1

e	0	0.1	0.2	0.3	0.4	0.5	0.6	0.7
α_p	0	$6\cdot10^{-8}$	$4\cdot10^{-6}$	$5\cdot10^{-5}$	$3\cdot10^{-4}$	$1.3\cdot10^{-3}$	$4.8\cdot10^{-3}$	$1.5\cdot10^{-2}$
α_e	0	$4\cdot10^{-5}$	$6\cdot10^{-4}$	$3\cdot10^{-3}$	$1.0\cdot10^{-2}$	$2.6\cdot10^{-2}$	$5.6\cdot10^{-2}$	0.11

The air density $\rho(h)$ entering (15.8) will be calculated assuming an isothermal atmosphere (14.9). The reference height h_t is the perigee altitude h_p, so that at any point of the orbit $h \geqslant h_1$. As we have shown in Sec. 14.3, the corresponding error in air density ρ of the isothermal atmosphere is not greater than 10% of the peak density actually observed in orbit. This is satisfactory accuracy, seeing that our estimates of the

effect of drag forces on satellite motion are fairly crude. In isothermal atmosphere,

$$\rho(h) = \rho_p \exp\left(-\frac{h-h_p}{H}\right). \tag{15.17}$$

where ρ_p is the air density at the height h_p.

Let r and r_p be the distances of the current point and of the perigee from the Earth's center. Making use of (5.30) and seeing that in perigee $E=0$, we write

$$h - h_p = r - r_p = ae(1 - \cos E).$$

Substituting in (15.17), we have

$$\rho(h) = \rho_p \exp(-\nu + \nu \cos E), \tag{15.18}$$

where

$$\nu = \frac{ae}{H}. \tag{15.19}$$

Inserting for ρ in (15.18) its expression from (15.18), we have

$$\left.\begin{array}{l} \delta p = -\frac{2c\rho_p p^2}{1-e^2}\exp(-\nu)\left(F_0 - \frac{e^2}{2}F_2 - \frac{e^4}{8}F_4 - \cdots\right), \\[2mm] \delta e = -2c\rho_p p \exp(-\nu) \times \\[2mm] \qquad \times \left(F_1 + eF_2 + \frac{e^2}{2}F_3 + \frac{e^3}{2}F_4 + \cdots\right), \end{array}\right\} \tag{15.20}$$

where

$$F_n = \int_0^{2\pi} \exp(\nu \cos E) \cos^n E \, dE, \qquad n = 0, 1, 2, \ldots \tag{15.21}$$

F_n are clearly functions of ν. They can be expressed in terms of Bessel functions of an imaginary argument, $I_n(\nu)$. Making use of the well-known relations /1/

$$I_n(\nu) = \frac{1}{2\pi} \int_0^{2\pi} \exp(\nu \cos E) \cos nE \, dE, \tag{15.22}$$

$$I_{n-1}(\nu) - I_{n+1}(\nu) = \frac{2nI_n(\nu)}{\nu}, \tag{15.23}$$

we find

$$F_0(\nu) = \int_0^{2\pi} \exp(\nu \cos E) \, dE = 2\pi I_0(\nu),$$

$$F_1(\nu) = \int_0^{2\pi} \exp(\nu \cos E) \cos E \, dE = 2\pi I_1(\nu),$$

$$F_2(\nu) = \int_0^{2\pi} \exp(\nu \cos E) \cos^2 E \, dE =$$

$$= \int_0^{2\pi} \exp(\nu \cos E) \frac{1+\cos 2E}{2} \, dE = \frac{I_0(\nu) + I_2(\nu)}{2} \, 2\pi,$$

On the other hand, from the recursion relation (15.23), we have

$$I_2(v) = I_0(v) - \frac{2I_1(v)}{v}, \quad I_3(v) = I_1(v) - \frac{4I_2(v)}{v},$$

$$I_4(v) = I_2(v) - \frac{6I_3(v)}{v}.$$

Hence

$$F_2(v) = 2\pi \left[I_0(v) - \frac{I_1(v)}{v} \right].$$

Similarly,

$$F_3(v) = \int_0^{2\pi} \exp(v \cos E) \cos^3 E \, dE =$$

$$= \int_0^{2\pi} \exp(v \cos E) \frac{3 \cos E + \cos 3E}{4} \, dE =$$

$$= \frac{2\pi}{4} [3I_1(v) + I_3(v)] = 2\pi \left[I_1(v) - \frac{I_2(v)}{v} \right] =$$

$$= 2\pi \left[I_1(v) \left(1 + \frac{2}{v^2} \right) - \frac{I_0(v)}{v} \right],$$

$$F_4(v) = \int_0^{2\pi} \exp(v \cos E) \cos^4 E \, dE =$$

$$= \int_0^{2\pi} \exp(v \cos E) \frac{3 + 4 \cos 2E + \cos 4E}{8} \, dE =$$

$$= \frac{2\pi}{8} [3I_0(v) + 4I_2(v) + I_4(v)] = \frac{2\pi}{8} \left[3I_0(v) + 5I_2(v) - \frac{6I_3(v)}{v} \right] =$$

$$= \frac{2\pi}{8} \left[8I_0(v) - \frac{10I_1(v)}{v} - \frac{6I_1(v)}{v} + \frac{24I_2(v)}{v^2} \right] =$$

$$= 2\pi \left[I_0(v) - \frac{2I_1(v)}{v} + \frac{3I_2(v)}{v^2} \right] =$$

$$= 2\pi \left[I_0(v) - \frac{2I_1(v)}{v} + \frac{3I_0(v)}{v^2} - \frac{6I_1(v)}{v^3} \right] =$$

$$= 2\pi \left(1 + \frac{3}{v^2} \right) \left[I_0(v) - \frac{2I_1(v)}{v} \right].$$

To sum up, we have

$$\left. \begin{array}{l} F_0(v) = 2\pi I_0(v), \\ F_1(v) = 2\pi I_1(v), \\ F_2(v) = 2\pi \left[I_0(v) - \frac{I_1(v)}{v} \right], \\ F_3(v) = 2\pi \left[I_1(v) \left(1 + \frac{2}{v^2} \right) - \frac{I_0(v)}{v} \right], \\ F_4(v) = 2\pi \left(1 + \frac{3}{v^2} \right) \left[I_0(v) - \frac{2I_1(v)}{v} \right]. \end{array} \right\} \tag{15.24}$$

The variations δp and δe of the orbital elements can be calculated from relations (15.19), (15.20), and (15.24) with the aid of tables of Bessel functions. This technique is convenient for orbits with moderate eccentricity, satisfying inequalities (15.16).

261

15.3. ASYMPTOTIC EXPRESSIONS FOR δp AND δe IN HIGHLY ECCENTRIC ORBITS

From (15.20) and (15.24) we see that the secular perturbations δp and δe in elliptical orbit are functions of the parameter v. From (15.19) and (5.3) it follows that the parameter v is the ratio of the amplitude of orbit height fluctuations to the density scale height. The technique developed in the previous chapter for nearly circular orbits therefore applies when $v < 1$ (see Sec. 14.8). Here we shall deal with the case

$$v \gg 1. \tag{15.25}$$

Bessel functions $I_0(v)$ and $I_1(v)$ can therefore be determined from the asymptotic expansions /1/

$$
\begin{aligned}
I_0(v) &= \frac{\exp(v)}{\sqrt{2\pi v}} \left(1 + \frac{1}{8} \cdot \frac{1}{v} + \frac{9}{128} \cdot \frac{1}{v^2} + \frac{75}{1024} \cdot \frac{1}{v^3} + \cdots \right) \\
I_1(v) &= \frac{\exp(v)}{\sqrt{2\pi v}} \left(1 - \frac{3}{8} \cdot \frac{1}{v} - \frac{15}{128} \cdot \frac{1}{v^2} - \frac{105}{1024} \cdot \frac{1}{v^3} - \cdots \right).
\end{aligned}
\tag{15.26}
$$

Table 15.2 lists the relative errors of these expansions for various v (the calculations were made retaining four terms in each series, as shown in (15.26)). We see from the table that for

$$v > 1.5 \tag{15.27}$$

the functions $I_0(v)$ and $I_1(v)$ calculated from the asymptotic expansions are accurate to within 1%. This is more than adequate for the solution of our problem.

TABLE 15.2

v	1.5	2	3	4	5	6	7
$\left\|\frac{\delta I_0}{I_0}\right\|$	$7.3 \cdot 10^{-3}$	$4.2 \cdot 10^{-3}$	$2.7 \cdot 10^{-3}$	$9 \cdot 10^{-4}$	$3 \cdot 10^{-4}$	$1 \cdot 10^{-4}$	$1 \cdot 10^{-4}$
$\left\|\frac{\delta I_1}{I_1}\right\|$	$7.3 \cdot 10^{-3}$	$9.6 \cdot 10^{-3}$	$4.4 \cdot 10^{-3}$	$1.3 \cdot 10^{-3}$	$3 \cdot 10^{-4}$	$2 \cdot 10^{-4}$	$8 \cdot 10^{-5}$

Making use of (15.19) and putting $H \approx 100$ km and $a > 6500$ km, we substitute for (15.27) the inequality

$$e > 1.5 \frac{H}{a} \approx 0.023. \tag{15.28}$$

From (15.24) and (15.26) we have

$$P_n = \sqrt{\frac{2\pi}{v}} \exp(v) f_n \quad (n = 0, 1, 2, 3, 4), \tag{15.29}$$

where

$$f_0 = 1 + \frac{1}{8} \cdot \frac{1}{\nu} + \frac{9}{128} \cdot \frac{1}{\nu^2} + \frac{75}{1024} \cdot \frac{1}{\nu^3} + \cdots,$$

$$f_1 = 1 - \frac{3}{8} \cdot \frac{1}{\nu} - \frac{15}{128} \cdot \frac{1}{\nu^2} - \frac{105}{1024} \cdot \frac{1}{\nu^3} + \cdots,$$

$$f_2 = 1 - \frac{7}{8} \cdot \frac{1}{\nu} + \frac{57}{128} \cdot \frac{1}{\nu^2} + \frac{195}{1024} \cdot \frac{1}{\nu^3} + \cdots, \quad (15.30)$$

$$f_3 = 1 - \frac{11}{8} \cdot \frac{1}{\nu} + \frac{225}{128} \cdot \frac{1}{\nu^2} - \frac{945}{1024} \cdot \frac{1}{\nu^3} + \cdots,$$

$$f_4 = 1 - \frac{15}{8} \cdot \frac{1}{\nu} + \frac{489}{128} \cdot \frac{1}{\nu^2} - \frac{5445}{1024} \cdot \frac{1}{\nu^3} + \cdots$$

Substituting (15.29) in (15.20), we find

$$\delta p = -\frac{2c\rho_p p^2}{1-e^2} \sqrt{\frac{2\pi}{\nu}} \left(f_0 - \frac{e^2}{2} f_2 - \frac{e^4}{8} f_4 - \cdots \right),$$

$$\delta e = -2c\rho_p p \sqrt{\frac{2\pi}{\nu}} \left(f_1 + ef_2 + \frac{e^2}{2} f_3 + \frac{e^3}{2} f_4 + \cdots \right). \quad (15.31)$$

For orbits which satisfy conditions (15.16) and (15.27) or (15.28), expressions (15.30) and (15.31) are clearly adequate for calculating the variations δp and δe. In this case, we need not even refer to tables of Bessel functions.

A serious shortcoming of (15.31) is that it is an expansion in powers of e, and is therefore inconvenient for calculating secular perturbations of highly eccentric orbits. To eliminate this deficiency, we rewrite the series in the right-hand sides of these expressions as

$$f_0 - \frac{e^2}{2} f_2 - \frac{e^4}{8} f_4 - \cdots$$

$$\cdots = f_0 \left(1 - \frac{e^2}{2} - \frac{e^4}{8} - \cdots \right) + R_1,$$

$$f_1 + ef_2 + \frac{e^2}{2} f_3 + \frac{e^3}{2} f_4 + \cdots \quad (15.32)$$

$$\cdots = f_1 \left(1 + e + \frac{e^2}{2} + \frac{e^3}{2} + \cdots \right) + R_2,$$

where

$$R_1 = \frac{e^2}{2} (f_0 - f_2) + \frac{e^4}{8} (f_0 - f_4) + \cdots$$

$$\cdots = \frac{e^2}{2} \left(\frac{1}{\nu} - \frac{3}{8} \cdot \frac{1}{\nu^2} - \frac{15}{128} \cdot \frac{1}{\nu^3} + \cdots \right) +$$

$$+ \frac{e^4}{8} \left(\frac{2}{\nu} - \frac{15}{4} \cdot \frac{1}{\nu^2} + \frac{345}{64} \cdot \frac{1}{\nu^3} + \cdots \right) + \cdots,$$

$$R_2 = e(f_2 - f_1) + \frac{e^2}{2} (f_3 - f_1) + \frac{e^3}{2} (f_4 - f_1) + \cdots \quad (15.33)$$

$$\cdots = e \left(-\frac{1}{2} \cdot \frac{1}{\nu} + \frac{9}{16} \cdot \frac{1}{\nu^2} + \frac{75}{256} \cdot \frac{1}{\nu^3} + \cdots \right) +$$

$$+ \frac{e^2}{2} \left(-\frac{1}{\nu} + \frac{15}{8} \cdot \frac{1}{\nu^2} - \frac{105}{128} \cdot \frac{1}{\nu^2} + \cdots \right) +$$

$$+ \frac{e^3}{2} \left(-\frac{3}{2} \cdot \frac{1}{\nu} + \frac{63}{16} \cdot \frac{1}{\nu^2} - \frac{1335}{256} \cdot \frac{1}{\nu^3} + \cdots \right) + \cdots$$

Now,

$$1 - \frac{e^2}{2} - \frac{e^4}{8} - \cdots = \sqrt{1-e^2},$$

$$1 + e + \frac{e^2}{2} + \frac{e^3}{2} + \cdots = \sqrt{\frac{1+e}{1-e}}. \quad (15.34)$$

263

These equalities are exact (remaining in force for any number of terms in the expansions), since they are obtained from the expansions applied in the derivation of the original relations (15.8) if we put $\cos E = 1$.

To estimate the residuals R_1 and R_2, we retain terms of the order $\frac{1}{v}$ in (15.33). Thus, making use of (15.19), we find

$$
\left.\begin{array}{l}
R_1 \approx \frac{e}{2} \frac{H}{a} \left(1 + \frac{e^2}{4} + \ldots\right), \\
R_2 \approx -\frac{1}{2} \cdot \frac{H}{a} \left(1 + e + \frac{3}{2} e^2 + \ldots\right).
\end{array}\right\} \tag{15.35}
$$

We see from these expressions that the residuals are of the order $\frac{H}{a}$.

This ratio is known to be small (not greater than 0.01). The maximum allowed value of this ratio decreases with increasing eccentricity e (since with increasing e, the minimum allowed semimajor axis a increases). In (15.32) we may therefore omit the residual terms R_1 and R_2. Applying (15.19), (15.31), and (15.34), we obtain the following approximate finite relations

$$
\left.\begin{array}{l}
\delta p \approx -\frac{2c\rho_p p^2}{\sqrt{1-e^2}} f_0 \sqrt{\frac{2\pi}{v}} = -2\sqrt{2\pi} \frac{p^{3/2}}{\sqrt{e}} f_0(v) c\rho_p \sqrt{H}, \\
\delta e \approx -2c\rho_p p \sqrt{\frac{1+e}{1-e}} f_1 \sqrt{\frac{2\pi}{v}} = -2\sqrt{2\pi p} \frac{1+e}{\sqrt{e}} f_1(v) c\rho_p \sqrt{H}.
\end{array}\right\} \tag{15.36}
$$

From (15.30) it follows that at further simplification (for large v), we may put in (15.36)

$$
f_0 \approx f_1 \approx 1. \tag{15.37}
$$

The above relations can be applied, in particular, for analyzing the motion in highly elongated elliptical orbits, whose eccentricity is beyond the limits specified by (15.16). For e close to unity, the second expression in (15.36) becomes meaningless, however, since the residual term R_2 is represented in (15.35) by a divergent series. Expressions (15.36) do not apply for orbits of very low eccentricity, which do not meet conditions (15.27) or (15.28). In particular, for $e = 0$, from (15.19), (15.20), and (15.21) we have

$$
\left.\begin{array}{l}
v = 0, \quad F(0) = 2\pi, \quad F_1 = 0, \\
\delta p = -2c\rho_p p^2 F_0 = -4\pi c\rho_p p^2, \\
\delta e = -2c\rho_p p F_1 = 0.
\end{array}\right\} \tag{15.38}
$$

Relations (15.38) cannot be derived from the asymptotic expressions (15.31) and (15.36) by taking the limit as $e \to 0$. On the other hand, the above expression for δp coincides with relation (14.34) which has been derived for the radial variation δr in circular orbit (upon substituting p for r).

264

15.4. SECULAR PERTURBATIONS OF LOW-ECCENTRICITY ORBITS

In determining the secular perturbations of low-eccentricity orbits, which do not satisfy condition (15.27), we may conveniently apply the well-known expansions of $I_0(v)$ and $I_1(v)$ in powers of v /1/:

$$
\left.
\begin{aligned}
I_0(v) &= \sum_{k=0}^{\infty} \frac{\left(\frac{v}{2}\right)^{2k}}{(k!)^2} = 1 + \frac{v^2}{4} + \frac{v^4}{64} + \frac{v^6}{2304} + \cdots, \\
I_1(v) &= \sum_{k=0}^{\infty} \frac{\left(\frac{v}{2}\right)^{2k+1}}{k!\,(k+1)!} = \frac{v}{2} + \frac{v^3}{16} + \frac{v^5}{384} + \cdots
\end{aligned}
\right\}
\tag{15.39}
$$

For

$$ v \leqslant 2 \tag{15.40} $$

the relative error introduced by expansions (15.39) is not greater than 0.2% and 0.7% for the first and the second series, respectively. This accuracy is more than adequate.

We shall only consider orbits which satisfy inequality (15.40), which for $H \approx 100$ km and $a \approx 6500$ km reduces to the condition

$$ e \leqslant 0.03. \tag{15.41} $$

In (15.20) we therefore omit all terms whose order is higher than e. From (15.24) and (15.39) we also have

$$ F_2 = 2\pi \left(\frac{1}{2} + \frac{3}{16} v^2 + \frac{5}{384} v^4 + \cdots \right). \tag{15.42} $$

Substituting (15.24), (15.39), and (15.42) in (15.20), we obtain to terms of the order e

$$
\left.
\begin{aligned}
\delta p &= -4\pi c \rho_m p^2 \left(1 + \frac{v^2}{4} + \frac{v^4}{64} + \frac{v^6}{2304} + \cdots \right), \\
\delta e &= -2\pi c \rho_m p \left[v \left(1 + \frac{v^2}{8} + \frac{v^4}{192} + \cdots \right) + \right. \\
&\quad \left. + e \left(1 + \frac{3}{8} v^2 + \frac{5}{192} v^4 + \cdots \right) \right].
\end{aligned}
\right\}
\tag{15.43}
$$

where

$$ \rho_m = \rho_p \exp(-v). \tag{15.44} $$

From (15.17) and (15.19) it directly follows that ρ_m is the air density at the mean flying height

$$ h_m = h_p + ae = a - R_E. \tag{15.45} $$

For $e = 0$, relations (15.43) reduce to (15.38) or (14.34). For small e, the first relation in (15.34) coincides with the corresponding expression for nearly circular orbit, which can be derived from inequality (14.80) if the Earth's nonspherical figure is ignored and an isothermal atmosphere is adopted, i.e., if we put $\Delta_1 = ae$, $\Delta_2 = 0$, $H_T = \infty$.

Comparison of (15.16), (15.27), and (15.40) shows that the approximate relations of this and previous sections for the secular perturbations of elliptical orbit elements cover the entire range of allowed elliptical orbit eccentricities. In the interval $0 \leqslant e \leqslant \frac{2H}{a}$, relations (15.43) should be used, for $\frac{1.5H}{a} \leqslant e \leqslant 0.5$, relations (15.31) apply, and for $0.5 < e < 1$, relations (15.36).

15.5. SECULAR PERTURBATIONS OF SEMIMAJOR AXIS, ORBITAL PERIOD, AND PERIGEE AND APOGEE HEIGHTS

Previously considered secular perturbations in p and e completely describe the variation of orbital shape during comparatively long periods. In various applied problems, the perturbations of other orbital elements are also required. Under this category we have

     (i)   the semimajor axis a,
     (ii) the orbital period P,
     (iii) the perigee height h_p,
     (iv) the apogee height h_a.

For elliptical orbits and a spherical Earth, we can show, making use of (5.36), that

$$\delta P = \frac{3}{2}\frac{P}{a}\delta a, \quad \delta h_p = \delta r_p, \quad \delta h_a = \delta r_a, \tag{15.46}$$

where δP, δa, δh_p, δh_a, δr_p, δr_a are the variations of P, a, h_p, h_a, r_p, r_a per circuit, and r_p and r_a are respectively the perigee and the apogee distances from the Earth's center.

To find the variations δa, δr_p, and δr_a, we make use of relations (5.2) and (5.3):

$$a = \frac{p}{1-e^2}, \quad r_p = a(1-e), \quad r_a = a(1+e),$$

whence

$$\left.\begin{array}{l} \delta a = \dfrac{\delta p}{1-e^2} + \dfrac{2pe\,\delta e}{(1-e^2)^2}, \\[2mm] \delta r_p = (1-e)\delta a - a\,\delta e, \\[2mm] \delta r_a = (1+e)\delta a + a\,\delta e. \end{array}\right\} \tag{15.47}$$

Substituting (15.7) in the right-hand sides of these relations, we find

$$\left.\begin{array}{l} \delta a = -2ca^2 \displaystyle\int_0^{2\pi} \rho\,\dfrac{1+e\cos E}{1-e\cos E}\sqrt{1-e^2\cos^2 E}\,dE, \\[5mm] \delta r_p = -2ca^2(1-e)\displaystyle\int_0^{2\pi}\rho\,\dfrac{1-\cos E}{1-e\cos E}\times\sqrt{1-e^2\cos^2 E}\,dE, \\[5mm] \delta r_a = -2ca^2(1+e)\displaystyle\int_0^{2\pi}\rho\,\dfrac{1+\cos E}{1-e\cos E}\times\sqrt{1-e^2\cos^2 E}\,dE. \end{array}\right\} \tag{15.48}$$

266

Series-expanding the integrand, we obtain, as in (15.8),

$$
\begin{aligned}
\delta a &= -2ca^2 \int_0^{2\pi} \rho \left(1 + 2e\cos E + \frac{3}{2} e^2 \cos^2 E + \right. \\
&\quad \left. + e^3 \cos^3 E + \frac{7}{8} e^4 \cos^4 E + \ldots \right) dE, \\
\delta r_p &= -2ca^2(1-e) \int_0^{2\pi} \rho (1-\cos E)\left(1 + e\cos E + \right. \\
&\quad \left. + \frac{e^2}{2} \cos^2 E + \frac{e^3}{2} \cos^3 E + \ldots \right) dE, \\
\delta r_a &= -2ca^2(1+e) \int_0^{2\pi} \rho (1+\cos E)\left(1 + e\cos E + \right. \\
&\quad \left. + \frac{e^2}{2} \cos^2 E + \frac{e^3}{2} \cos^3 E + \ldots \right) dE.
\end{aligned}
\qquad (15.49)
$$

Assuming the isothermal atmosphere (14.9) and making use of (15.7) — (15.19), (15.21), we find

$$
\begin{aligned}
\delta a &= -2c\rho_p a^2 \exp(-\nu)\left(F_0 + 2eF_1 + \frac{3}{2} e^2 F_2 + e^3 F_3 + \frac{7}{8} e^4 F_4 + \ldots\right), \\
\delta r_p &= -2c\rho_p a^2 (1-e)\exp(-\nu)\left[(F_0 - F_1) + \right. \\
&\quad \left. + e(F_1 - F_2) + \frac{e^2}{2}(F_2 - F_3) + \frac{e^3}{2}(F_3 - F_4) + \ldots\right], \\
\delta r_a &= -2c\rho_p a^2 (1+e)\exp(-\nu)\left[(F_0 + F_1) + \right. \\
&\quad \left. + e(F_1 + F_2) + \frac{e^2}{2}(F_2 + F_3) + \frac{e^3}{2}(F_3 + F_4) + \ldots\right].
\end{aligned}
\qquad (15.50)
$$

All F_i ($i = 0, 1, 2, 3, 4$) are expressed in terms of Bessel functions of imaginary argument with the aid of relations (15.24).

For highly eccentric orbits, which satisfy conditions (15.27) and (15.28), we make use of asymptotic expansions (15.29) and (15.30), writing (15.50) as

$$
\begin{aligned}
\delta a &= -2c\rho_p a^2 \sqrt{\frac{2\pi}{\nu}}\left(f_0 + 2ef_1 + \frac{3}{2} e^2 f_2 + e^3 f_3 + \frac{7}{8} e^4 f_4 + \ldots\right), \\
\delta r_p &= -2c\rho_p a^2 (1-e)\sqrt{\frac{2\pi}{\nu}}\left[(f_0 - f_1) + \right. \\
&\quad \left. + e(f_1 - f_2) + \frac{e^2}{2}(f_2 - f_3) + \frac{e^3}{2}(f_3 - f_4) + \ldots\right], \\
\delta r_a &= -2c\rho_p a^2 (1+e)\sqrt{\frac{2\pi}{\nu}}\left[(f_0 + f_1) + \right. \\
&\quad \left. + e(f_1 + f_2) + \frac{e^2}{2}(f_2 + f_3) + \frac{e^3}{2}(f_3 + f_4) + \ldots\right].
\end{aligned}
\qquad (15.51)
$$

Proceeding with (15.51) as in the derivation of (15.36), we obtain the approximate relations

$$
\begin{aligned}
\delta a &\approx -2c\rho_p a^2 \frac{1+e}{1-e}\sqrt{1-e^2}\, f_0 \sqrt{\frac{2\pi}{\nu}} = -2\sqrt{2\pi}\, \frac{a^{3/2}}{\sqrt{e}}\frac{1+e}{1-e}\sqrt{1-e^2}\, f_0(\nu)\, c\rho_p \sqrt{H}, \\
\delta r_p &\approx -c\rho_p a^2 \sqrt{1-e^2}\, \frac{f'}{\nu}\sqrt{\frac{2\pi}{\nu}} = -\sqrt{2\pi}\, \frac{a^{3/2}}{e^{3/2}}\sqrt{1-e^2}\, f'(\nu)\, c\rho_p H^{3/2}, \\
\delta r_a &\approx -2c\rho_p a^2 \frac{1+e}{1-e}\sqrt{1-e^2}\, (f_0 + f_1)\sqrt{\frac{2\pi}{\nu}} = \\
&= -2\sqrt{2\pi}\, \frac{a^{3/2}}{\sqrt{e}}\frac{1+e}{1-e}\sqrt{1-e^2}\, [f_0(\nu) + f_1(\nu)]\, c\rho_p \sqrt{H}.
\end{aligned}
\qquad (15.52)
$$

where

$$f'(v) = 2v(f_0 - f_1) = 1 + \frac{3}{8} \cdot \frac{1}{v} + \frac{45}{128} \cdot \frac{1}{v^2} + \cdots \qquad (15.53)$$

For fairly large v (or if no high accuracy is required), we may achieve further simplification by putting

$$f_0 \approx f_1 \approx f' \approx 1.$$

From (5.36), (15.46), and (15.52) we have

$$\delta P = -\frac{6\pi}{\sqrt{\mu}} c\rho_p a^{3/2} \frac{1+e}{1-e} \sqrt{1-e^2} f_0 \sqrt{\frac{2\pi}{v}} =$$

$$= -6\pi \sqrt{\frac{2\pi}{\mu}} \frac{a^2}{\sqrt{e}} \frac{1+e}{1-e} \sqrt{1-e^2} f_0(v) c\rho_p \sqrt{H}. \qquad (15.54)$$

For low-eccentricity orbits which satisfy conditions (15.40) or (15.41), we retain only terms of the order e in (15.50). Then, making use of (5.36), (15.24), (15.39), (15.42), (15.44), and (15.46), we find

$$\begin{aligned}
\delta a &= -4\pi c\rho_m a^2 \left[1 + \frac{v^2}{4} + \frac{v^4}{64} + \frac{v^6}{2304} + \cdots + \right. \\
&\quad \left. + ev\left(1 + \frac{v^2}{8} + \frac{v^4}{192} + \cdots\right)\right], \\
\delta r_p &= -4\pi c\rho_m a^2 (1-e)\left[1 - \frac{v}{2} + \frac{v^2}{4} - \frac{v^3}{16} + \right. \\
&\quad + \frac{v^4}{64} - \frac{v^5}{384} + \frac{v^6}{2304} - \cdots - \\
&\quad - e\left(\frac{1}{2} - \frac{v}{2} + \frac{3}{16}v^2 - \frac{v^3}{16} + \right. \\
&\quad \left.\left. + \frac{5}{384}v^4 - \frac{v^5}{384} + \cdots\right)\right], \\
\delta r_a &= -4\pi c\rho_m a^2 (1+e)\left[1 + \frac{v}{2} + \frac{v^2}{4} + \right. \\
&\quad + \frac{v^3}{16} + \frac{v^4}{64} + \frac{v^5}{384} + \frac{v^6}{2304} + \cdots + \\
&\quad + e\left(\frac{1}{2} + \frac{v}{2} + \frac{3}{16}v^2 + \frac{v^3}{16} + \frac{5}{384}v^4 + \right. \\
&\quad \left.\left. + \frac{v^5}{384} + \cdots\right)\right], \\
\delta P &= -\frac{12\pi^2}{\sqrt{\mu}} c\rho_m a^{5/2}\left[1 + \frac{v^2}{4} + \frac{v^4}{64} + \right. \\
&\quad \left. + \frac{v^6}{2304} + \cdots + ev\left(1 + \frac{v^2}{8} + \frac{v^3}{192} + \cdots\right)\right].
\end{aligned} \qquad (15.55)$$

In conclusion, note that the range of e-values where the formulas of this section apply coincides with the corresponding range for the variations δp and δe (see Sec. 15.4).

15.6. ANALYSIS OF SECULAR PERTURBATIONS OF ELLIPTICAL ORBIT

The previous results enable us to analyze the character of the secular perturbations produced by drag forces in elliptical orbits. From (15.1),

(15.4), (15.36), (15.43), (15.52), and (15.55) it follows that, under the assumptions introduced at the beginning of this chapter, the orientation of the orbital plane and the position of the perigee point remain fixed, the secular perturbations leading to a monotonic reduction in the semimajor axis and the eccentricity of the orbit. On account of air drag, the satellite is thus seen to describe a convolute elliptical spiral, which gradually approaches a circular orbit. The period of revolution P monotonically decreases, and the mean orbital velocity increases. The flying height monotonically decreases along the entire trajectory. The loss of orbit height is maximal near the apogee point and minimal near the perigee.

We see from the aforementioned relations that the secular orbit perturbations resulting from air drag are directly proportional to air density at some characteristic altitude. For low-eccentricity orbits, which satisfy condition (15.40), this reference level is the mean orbit height $h_m = a - R_E$, whereas for highly eccentric orbits, where condition (15.27) is satisfied, the perigee height $h_p = r_p - R_E$ is adopted as reference. This is so because for low-eccentricity orbits, the air density is approximately a linear function of height in the relevant range of flight altitudes, i.e., only the first two terms need be retained in expansions (14.24). The mean deceleration in this case is determined by the mean air density at the mean flying height. For highly eccentric orbits, however, the air density is no longer a linear function of height, since over a greater part of the orbit the air density is much less than the density at the perigee point. It is therefore the deceleration near the perigee that has the decisive effect on secular perturbations of orbital elements.

It follows from the preceding that the secular orbit perturbations resulting from air drag rapidly decrease as the characteristic flying height increases. To analyze this dependence, we consider two families of orbits with different eccentricities: a family of orbits with constant perigee height, where

$$r_p = \text{const}, \quad a = \frac{r_p}{1 - e},$$ (15.56)

and a family of orbits with constant mean flight altitude, where

$$a = \text{const}, \quad r_p = a(1 - e).$$ (15.57)

We shall analyze the following secular perturbations:
  (i) change of orbital period per circuit, δP;
  (ii) mean rate of change of orbital period, $P' = \frac{\delta P}{P}$;
  (iii) change of perigee height per circuit, δr_p;
  (iv) change of apogee height per circuit, δr_a.

For the family of orbits (15.56), we shall seek the eccentricity dependence of the ratios

$$\frac{\delta P}{\delta P_{cir}}, \quad \frac{P'}{P'_{cir}}, \quad \frac{\delta r_p}{\delta r_a}, \quad \frac{\delta r_p}{\delta r_{cir}}, \quad \frac{\delta r_a}{\delta r_{cir}},$$

where δP_{cir}, P'_{cir}, δr_{cir} are the corresponding perturbations in circular orbit of radius $r = r_p$.

269

Clearly, for $e = 0$,

$$\frac{\delta P}{\delta P_{\text{cir}}} = \frac{P'}{P'_{\text{cir}}} = \frac{\delta r_{\text{p}}}{\delta r_{\text{a}}} = \frac{\delta r_{\text{p}}}{\delta r_{\text{cir}}} = \frac{\delta r_{\text{a}}}{\delta r_{\text{cir}}} = 1.$$

(15.58)

For highly eccentric orbits, which satisfy condition (15.27), we may write, making use of (5.36), (14.33), (14.34), (15.19), (15.52), (15.54), and (15.56):

$$\left.\begin{aligned}
\frac{\delta P}{\delta P_{\text{cir}}} &= \sqrt{\frac{H}{2\pi r_{\text{p}}}}\, \frac{(1+e)^{\frac{1}{2}}}{(1-e)^{\frac{3}{2}}e^{\frac{1}{2}}}\, f_0(v), \\
\frac{P}{P_{\text{cir}}} &= \sqrt{\frac{H}{2\pi r_{\text{p}}}}\, \frac{(1+e)^{\frac{1}{2}}}{(1-e)\,e^{\frac{1}{2}}}\, f_0(v), \\
\frac{\delta r_{\text{p}}}{\delta r_{\text{a}}} &= \frac{H}{2r_{\text{p}}}\, \frac{(1-e)^2}{(1+e)\,e}\, \frac{f'(v)}{f_0(v)+f_1(v)}, \\
\frac{\delta r_{\text{p}}}{\delta r_{\text{cir}}} &= \pi\left(\frac{H}{2\pi r_{\text{p}}}\right)^{\frac{1}{2}}\frac{1}{e}\sqrt{1+\frac{1}{e}}\, f'(v), \\
\frac{\delta r_{\text{a}}}{\delta r_{\text{cir}}} &= \sqrt{\frac{H}{2\pi r_{\text{p}}}}\, \frac{(1+e)^{\frac{1}{2}}}{(1-e)^2\,e^{\frac{1}{2}}}\, [f_0(v)+f_1(v)], \\
v &= \frac{r_{\text{p}}e}{H(1-e)}
\end{aligned}\right\}$$

(15.59)

Making use of (15.55), we can write analogous expressions for low-eccentricity orbits, too.

Applying (15.30) and (15.53), we see that the ratios $\frac{\delta r_{\text{p}}}{\delta r_{\text{a}}}$ and $\frac{\delta r_{\text{p}}}{\delta r_{\text{cir}}}$ monotonically decrease with increasing eccentricity e. Here

$$\lim_{e \to 1} \frac{\delta r_{\text{p}}}{\delta r_{\text{a}}} = 0, \qquad \lim_{e \to 1} \frac{\delta r_{\text{p}}}{\delta r_{\text{cir}}} = \frac{\pi}{2}\left(\frac{H}{\pi r_{\text{p}}}\right)^{\frac{1}{2}}.$$

The ratios $\frac{\delta P}{\delta P_{\text{cir}}}$, $\frac{P'}{P'_{\text{cir}}}$, and $\frac{\delta r_{\text{a}}}{\delta r_{\text{cir}}}$, on the other hand, first decrease with increasing eccentricity, then start increasing, and for $e \to 1$, they tend to infinity. These ratios are minimal for moderately eccentric orbits, where

$$f_0(v) \approx f_1(v) \approx 1.$$

Substituting in (15.59), we see that the minima approximately correspond to the solutions of the equations

$$\frac{d}{de}\ln\frac{(1+e)^{\frac{1}{2}}}{(1-e)^{\frac{3}{2}}e^{\frac{1}{2}}} = \frac{3}{2(1+e)} + \frac{5}{2(1-e)} - \frac{1}{2e} = 0,$$

$$\frac{d}{de}\ln\frac{(1+e)^{\frac{1}{2}}}{(1-e)\,e^{\frac{1}{2}}} = \frac{3}{2(1+e)} + \frac{1}{1-e} - \frac{1}{2e} = 0,$$

$$\frac{d}{de}\ln\frac{(1+e)^{\frac{1}{2}}}{(1-e)^2\,e^{\frac{1}{2}}} = \frac{3}{2(1+e)} + \frac{2}{1-e} - \frac{1}{2e} = 0.$$

It follows from these equations that the ratios $\frac{\delta P}{\delta P_{\text{cir}}}$, $\frac{P'}{P'_{\text{cir}}}$, $\frac{\delta r_{\text{a}}}{\delta r_{\text{cir}}}$ are minimal for the eccentricities

$$e_1 = \frac{\sqrt{19}-4}{3} \approx 0.120, \quad e_2 = 0.2, \quad e_3 = \frac{\sqrt{57}-7}{4} \approx 0.1375.$$

Substituting these eccentricities in the corresponding relations in (15.59), we obtain the minimum values

$$\left(\frac{\delta P}{\delta P_{\text{cir}}}\right)_{\min} \approx 4.7 \sqrt{\frac{H}{2\pi r_{\text{p}}}}, \quad \left(\frac{P'}{P'_{\text{cir}}}\right)_{\min} \approx 3.7 \sqrt{\frac{H}{2\pi r_{\text{p}}}},$$

$$\left(\frac{\delta r_{\text{a}}}{\delta r_{\text{cir}}}\right)_{\min} \approx 8.8 \sqrt{\frac{H}{2\pi r_{\text{p}}}}.$$

The existence of these minima is attributable to the combined influence of two factors which act in opposite directions. On the one hand, increasing e for constant r_{p} raises the flying height, which reduces the effect of air drag. On the other hand, any increase in the eccentricity raises the perigee velocity, and the effect of the impulsive deceleration at the perigee point on the apogee height and the orbital period becomes more pronounced.

Figures 15.1 and 15.2 plot the ratios $\frac{\delta P}{\delta P_{\text{cir}}}$, $\frac{P'}{P_{\text{cir}}}$, $\frac{\delta r_{\text{a}}}{\delta r_{\text{cir}}}$, $\frac{\delta r_{\text{p}}}{\delta r_{\text{a}}}$, and $\frac{\delta r_{\text{p}}}{\delta r_{\text{cir}}}$ vs. the eccentricity e, for $r_{\text{p}} = 6500\,\text{km}$ ($h_{\text{p}} = 229\,\text{km}$) and $H = 50\,\text{km}$. For eccentricities not satisfying condition (15.27), the calculations were made from (15.55). We see from the graphs that for moderate eccentricities ($e < 0.05$), the secular perturbations resulting from air drag rapidly decrease with increasing e. Note that δr_{p} decreases at a much higher rate than δr_{a} does.

For $0.05 < e < 0.3$, δP and δr_{a} remain fairly constant, and we have $\frac{\delta P}{\delta P_{\text{cir}}} \approx$

$\approx 0.15 - 0.23$, $\frac{\delta r_{\text{a}}}{\delta r_{\text{cir}}} \approx 0.3 - 0.4$. Further increase in e produces a steep increase in δP and δr_{a}. P' does not change much for $0.05 < e < 0.5$, fluctuating between $0.13\,P'_{\text{cir}}$ to $0.18\,P'_{\text{cir}}$. For $e \to 1$, δP, δr_{a}, and P' tend to infinity. δr_{p}, on the other hand, monotonically decreases for $0 < e < 1$. As the orbit approaches a parabola ($e \to 1$), this monotonic decrease proceeds at a somewhat reduced rate.

For the second family of orbits, which satisfy condition (15.57), we only consider the eccentricity dependence of the ratio

$$\frac{\delta P}{\delta P_{\text{m}}} = \frac{P'}{P'_{\text{m}}} = \frac{\delta a}{\delta r_{\text{m}}},$$

where δP_{m}, P'_{m}, and δr_{m} are the values of δP, P', and δr for the mean circular orbit of radius $r_{\text{m}} = a$.

Making use of (14.33), (15.54), and (15.55), we write

$$\frac{\delta P}{\delta P_{\text{m}}} = 1 + \frac{v^2}{4} + \frac{v^4}{64} + \frac{v^6}{2304} + \ldots + ev\left(1 + \frac{v^2}{8} + \frac{v^4}{192} + \ldots\right) \qquad (15.60)$$

for orbits satisfying condition (15.40), and

$$\frac{\delta P}{\delta P_{\text{m}}} = \frac{1+e}{1-e} \sqrt{1-e^2}\, \frac{I_0(v)}{\sqrt{2\pi v}}\, e^v \qquad (15.61)$$

for orbits satisfying condition (15.27).

The ratios in the left-hand sides of (15.60) and (15.61) increase monotonically with the eccentricity e. Hence, for any elliptical orbit we have

$$\delta P > \delta P_{\text{m}}, \quad P' > P'_{\text{m}}, \quad \delta a > \delta r_{\text{m}}. \qquad (15.62)$$

271
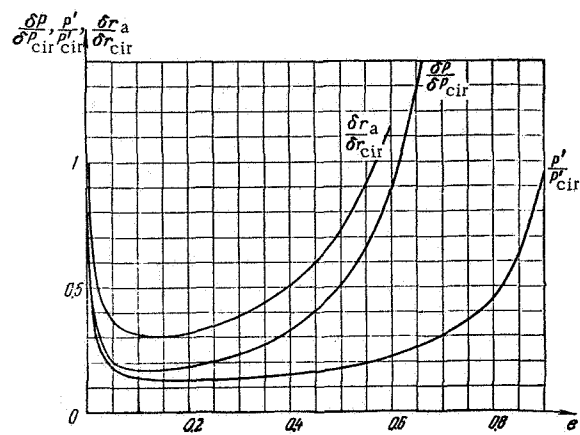
FIGURE 15.1. The ratios $\dfrac{\delta P}{\delta P_{cir}}$, $\dfrac{P'}{P'_{cir}}$, and $\dfrac{\delta r_a}{\delta r_{cir}}$ vs. eccentricity e of elliptical orbit.
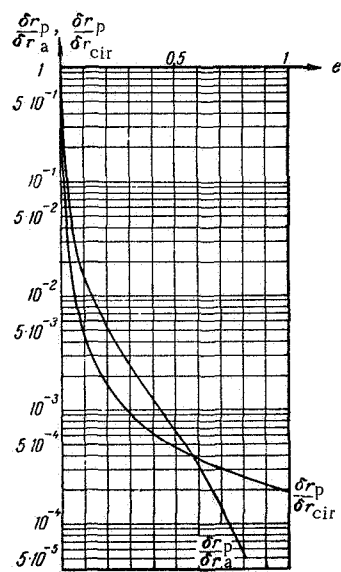
FIGURE 15.2. The ratios $\dfrac{\delta r_p}{\delta r_a}$ and $\dfrac{\delta r_p}{\delta r_{cir}}$ vs. eccentricity e of elliptical orbit.

Figure 15.3 plots the ratio $\frac{\delta P}{\delta P_m}$ vs. the eccentricity e for $H= 50\,\text{km}$, $a = 7000\,\text{km}$. We see from the graph that this ratio increases steeply with e. Therefore, even for comparatively low eccentricities ($e > 0.02 - 0.03$), the secular perturbations of elliptical orbit are much larger than the secular perturbations of corresponding circular orbit.
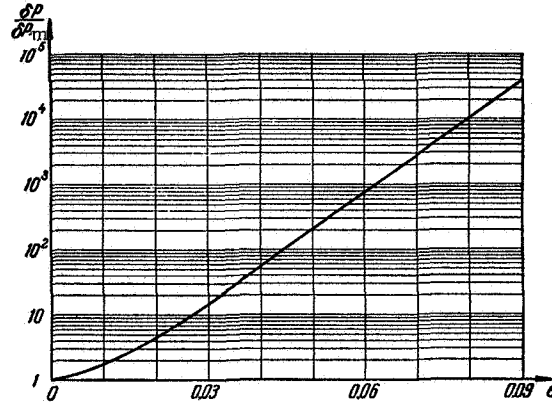
FIGURE 15.3. The ratio $\frac{\delta P}{\delta P_m}$ vs. the eccentricity e of elliptical orbit.

The foregoing relations give the perturbations of orbital elements during one circuit of revolution. In various applied problems, when analyzing the secular orbit perturbations during comparatively short periods, which comprise a few circuits of revolution, these perturbations may be assumed constant. The orbital elements are thus linear functions of time, where the variation $(\Delta t)_{\text{sec}}$ in the time of arrival at a given point displays a square-law variation, like the secular displacement $(\Delta t)_{\text{sec}}$ in circular orbit (see the second equality in (14.35)). Indeed,

$$(\Delta t)_{\text{sec}}(n) = \sum_{i=1}^{n} \Delta P_i,$$

where $(\Delta t)_{\text{sec}}(n)$ is the displacement $(\Delta t)_{\text{sec}}$ at the end of the n-th circuit, ΔP_i the variation of the orbital period during the i-th circuit.

ΔP_1 can be approximately determined as the arithmetic average of the variations in the osculation period at the beginning and the end of the first circuit, i.e., $\Delta P_1 = \frac{\delta P}{2}$. Hence,

$$\Delta P_2 = \Delta P_1 + \delta P = \frac{3}{2}\,\delta P,$$

$$\Delta P_3 = \Delta P_2 + \delta P = \frac{5}{2}\,\delta P,$$

$$\cdots \cdots \cdots \cdots$$

$$\Delta P_n = \Delta P_{n-1} + \delta P = \frac{2n-1}{2}\,\delta P$$

273

and then

$$(\Delta t)_{sec}(n) = \delta P \left(\frac{1}{2} + \frac{3}{2} + \frac{5}{2} + \cdots + \frac{2n-1}{2} \right) = \frac{n^2}{2} \delta P.$$

The general trend of secular perturbations as described above is eventually distorted as the satellite dips into progressively denser atmospheric layers. The rates of change of the orbital elements increase, and their variation approaches the curve plotted in Figure 14.4 for the contraction of circular orbit.

We should always bear in mind that the results obtained in this chapter are approximate on account of our simplifying assumptions. The principal simplifications are the following:

(i) the rotation of the Earth's atmosphere is ignored;
(ii) a steady-state (static) atmosphere is introduced;
(iii) the air density is calculated for the isothermal atmosphere;
(iv) the Earth's flattening is neglected.

Therefore, in reality, secular perturbations include various disturbances which are not apparent in our idealized scheme. Atmospheric rotation, for instance, gives rise to a certain slow variation in the orientation of the orbital plane (see Sec. 14.7). The dynamic properties of the atmosphere, in general, may alter the position of the perigee point, since in this case our proof of equality (15.4) is meaningless. Earth's flattening superimposes long-periodic fluctuations on the monotonic loss of perigee height h_p, since the perigee point moves in the noncentral gravitational field of the Earth (see Sec. 13.5). For some orbits, h_p may even temporarily increase (this upward trend is of course eventually offset by the monotonic loss of altitude), which results in a temporary reduction in the rate of secular orbit perturbations.

The scheme analyzed in this chapter therefore brings out the main regularities attributable to air drag, but obscures the finer features. To obtain a more accurate picture of flight conditions in the gravitational field of the nonspherical Earth, we should preferably proceed with numerical integration of the complete set of differential equations of motion of the satellite's mass center.

If the calculations are carried out with the aid of the approximate relations derived for nearly circular orbits, it is advisable to apply the method of Sec. 14.8, which employs a constant-temperature-gradient atmosphere and takes into consideration the effect of the Earth's flattening. For highly eccentric orbits, the characteristic parameter ρ_p is determined as the air density at the minimum flying height h_{min}, calculated with allowance for the Earth's flattening and the noncentral components of its field of gravity. The total change δP_{tot} in orbital period during one circuit of revolution should be calculated from

$$\delta P_{tot} = \delta P_{drag} + \delta P', \tag{15 63}$$

where δP_{drag} is the change in orbital period due to air resistance, which can be calculated from the formulas of this chapter, and $\delta P'$ is the change in orbital period in drag-free space ($c = 0$). The latter component is contributed by long-periodic perturbations of orbital period attributable to the Earth's nonspherical figure (see Sec. 13.9).

In conclusion note that in calculations of highly eccentric orbits we often have to consider the combined influence of atmospheric drag and the pull of other celestial bodies (see Sec. 16.12).

15.7. THE CHANGE IN ORBIT ECCENTRICITY DURING SATELLITE LIFETIME

To establish the variation of eccentricity during the entire lifetime of the satellite, we consider the relationship between the secular perturbations of eccentricity (δe) and of perigee height (δr_p). Making use of (15.19), (15.36), and (15.52), we may write for highly eccentric orbits

$$\frac{\delta e}{\delta r_p} = 2 \frac{(1+e)e}{H} \frac{f_1(v)}{f'(v)}.$$

We shall only seek an approximate dependence between the different perturbations. Therefore, substituting the differentials de and dr_p for the finite increments δe and δr_p and putting

$$f_1(v) \approx f'(v) \approx 1,$$

we obtain the differential equation

$$\frac{2\,dr_p}{H} = \frac{de}{e(1+e)} = \frac{de}{e} - \frac{de}{1+e}.$$

Integrating from some initial values r_{p0} and e_0 to the current r_p and e, we find

$$\left.\begin{aligned}
\ln\frac{e(1+e_0)}{e_0(1+e)} &= \frac{2(r_p - r_{p0})}{H}, \\
\frac{e}{1+e} &= \frac{e_0}{1+e_0} \exp\left(-2\frac{r_{p0}-r_p}{H}\right), \\
e &= \frac{e_0 \exp\left(-2\frac{r_{p0}-r_p}{H}\right)}{1+e_0\left[1-\exp\left(-2\frac{r_{p0}-r_p}{H}\right)\right]} < e_0 \exp\left(-2\frac{r_{p0}-r_p}{H}\right).
\end{aligned}\right\}$$
(15.64)

We see that as the perigee height decreases, the orbit eccentricity asymptotically approaches zero. When the perigee drops by $r_{p0}-r_p=H$, the eccentricity decreases more than 7-fold; for $r_{p0}-r_p=2H$, the reduction in eccentricity is more than 54-fold. As we have previously shown (see Sec. 14.6), the allowed flying height of artificial Earth satellites is limited by a certain critical value, which is mostly $120-150$ km. On the other hand, the initial perigee height h_{p0} is commonly $180-220$ km; the parameter H at altitudes of $150-200$ km varies between $25-40$ km (see Figure 14.1). Therefore, during the satellite's entire lifetime, the perigee height h_p decreases by no less than $2H$. Hence it follows that the eccentricity commonly changes by as much as one order of magnitude during the satellite's lifetime, and in the last stages the satellite's orbit is almost circular.

We see from relations (15.52) and (15.55) and from the graph in Figure 15.2 that the rate of change of perigee height sharply increases

with the decrease in e and r_p. Therefore, satellites which have been injected into highly eccentric orbits spend but a small fraction of their lifetime in the terminal nearly circular orbit. In other words, the conversion of the satellite's orbit into a circular one is a sign of its imminent fall on the ground.

15.8. DETERMINATION OF SATELLITE LIFETIME IN ELLIPTICAL ORBIT

To establish the lifetime of a satellite, we must trace the secular variations of its orbital elements during a comparatively long period. Since the orbital period of a satellite generally occupies a minor fraction of its lifetime, and since the secular variations of orbital elements are essentially smooth, we shall substitute differentials for the finite increments of orbital elements per circuit. In other words, we take

$$\left. \begin{aligned} \frac{dp}{d\tau} &\approx \frac{\delta p}{cP} = \frac{\sqrt{\mu}}{2\pi c a^{3/2}}\, \delta p, \\ \frac{de}{d\tau} &\approx \frac{\delta e}{cP} = \frac{\sqrt{\mu}}{2\pi c a^{3/2}}\, \delta e, \end{aligned} \right\} \qquad (15.65)$$

where P is the orbital period, τ the relative time defined by (14.38).

Making use of (15.36) and (15.43), we obtain the following set of differential equations

$$\frac{dp}{d\tau} = \left\{ \begin{aligned} &-\sqrt{\frac{2\mu}{\pi}}\, \frac{(1-e^2)^{3/2}}{\sqrt{e}}\, f_0(v)\rho(h_p)\, \sqrt{H(h_p)} \quad \text{for } v \geqslant 2, \\ &-2\sqrt{\mu p}\,(1-e^2)^{3/4}\rho(h_m) \times \left(1+\frac{v^2}{4}+\frac{v^4}{64}+\frac{v^6}{2304}+\ldots\right) \quad \text{for } v < 2, \end{aligned} \right.$$

$$\frac{de}{d\tau} = \left\{ \begin{aligned} &-\sqrt{\frac{2\mu}{\pi}}\, \frac{1+e}{\sqrt{e}}(1-e^2)^{3/2}\frac{f_1(v)}{p}\rho(h_p)\, \sqrt{H(h_p)} \quad \text{for } v \geqslant 2\cdot \\ &-\sqrt{\frac{\mu}{p}}\,(1-e^2)^{3/2}\rho(h_m) \times \left[v\left(1+\frac{v^2}{8}+\frac{v^4}{192}+\ldots\right)+ \right. \\ &\left. +e\left(1+\frac{3}{8}v^2+\frac{5}{192}v^4+\ldots\right)\right] \quad \text{for } v < 2, \end{aligned} \right.$$

$$(15.66)$$

where

$$h_p = \frac{p}{1+e} - R_E, \quad h_m = \frac{p}{1-e^2} - R_E, \quad v = \frac{pe}{(1-e^2)H(h_p)},$$

$f_0(v)$ and $f_1(v)$ are determined from (15.30), and $\rho(h_p)$, $H(h_p)$, $\rho(h_m)$ are borrowed from appropriate tables.

Numerical integration of these differential equations will provide us with a detailed picture of variation of the orbital elements of the satellite to its eventual fall (which can be identified in practice as the epoch when the perigee height h_p will have dropped to the critical value $h_{crit} \approx 100\,\text{km}$).

276

The corresponding relative time τ_{life} is a function of the initial conditions of motion:

$$\tau_{\text{life}} = F(p_0, \ e_0),$$

where p_0 and e_0 are the initial values of the corresponding elements.
Making use of (14.38), we find that

$$t_{\text{life}} = \frac{F(p_0, \ e_0)}{c}. \tag{15.67}$$

For any static model atmosphere, the function $F(p_0, \ e_0)$ can be calculated by numerical integration of the differential equations (15.66) for various initial conditions. The function F need not be determined for p_0 and e_0: any other pair of initial conditions which specify the size and the eccentricity of the orbit will do, such as $(r_{p\,0}, \ r_{a\,0})$, $(r_{p\,0}, \ e_0)$, $(p_0, \ e_0)$, etc. /22/.

15.9. ESTIMATING THE SATELLITE LIFETIME IN HIGHLY ECCENTRIC ORBITS

Various errors connected with the inaccuracy of the model atmosphere and with the variability of its parameters during long periods creep in when the lifetime of an artificial Earth satellite is determined by the method outlined in the previous section. The expected lifetime cannot be calculated with any accuracy in practice, and the best that we can hope for is some estimate of this time.

In deriving approximate formulas for these estimates, we shall proceed from the local isothermal atmosphere, whose parameters are determined from (14.12) and (14.16), where h_1 is the initial perigee height $h_{p\,0}$ of the orbit under consideration. This approach is justified, since during most of the satellite's lifetime, the perigee height is fairly close to the initial value.

For highly eccentric orbits, which satisfy conditions (15.27) or (15.28), we may write (making use of (5.1) and (15.66))

$$\frac{de}{d\tau} = -\sqrt{\frac{2\mu H}{\pi}} \ \frac{(1-e^2)^{3/2}}{\sqrt{e}} \ \frac{f_1(v)}{r_p} \ \rho(h_p). \tag{15.68}$$

We seek an approximate solution, and we may therefore put $f_1(v) = 1$. Moreover, from (14.9) and (15.64) we have

$$\rho(h_p) = \rho_{p0} \exp\left(\frac{r_{p\,0} - r_p}{H}\right) = \rho_{p0} \sqrt{\frac{e_0(1+e)}{e(1+e_0)}}, \tag{15.69}$$

where r_{p0} and e_0 are the initial values of r_p and e, and ρ_{p0} is the air density at the initial perigee altitude.
Equation (15.68) thus takes the form

$$\frac{de}{d\tau} = -\frac{\rho_{p0}}{r_p e} \sqrt{\frac{2\mu H e_0(1+e)(1-e^2)^3}{\pi(1+e_0)}}.$$

The parameter r_p in the right-hand side of this equation is fairly constant, and we may therefore substitute the initial value r_{p0} for it. Then

$$\frac{\rho p_0}{r_{p0}} \sqrt{\frac{2\mu H}{\pi}}\, d\tau = -\sqrt{\frac{1+e_0}{e_0}}\, \frac{e\, de}{\sqrt{(1+e)(1-e^2)^3}}. \qquad (15.70)$$

As we have shown in Sec. 15.8, the eccentricity of the satellite's orbit toward the end of its life is practically zero. Therefore, integrating equation (15.70) over the satellite's lifetime, we find

$$\frac{\rho p_0}{r_{p0}} \sqrt{\frac{2\mu H}{\pi}}\, \tau_{\text{life}} = \sqrt{\frac{1+e_0}{e_0}} \int_0^{e_0} \frac{e\, de}{\sqrt{(1+e)(1-e^2)^3}}.$$

Hence, making use of (14.38), we obtain a final expression for the lifetime

$$t_{\text{life}} = \frac{\tau_{\text{life}}}{c} = \frac{\Phi(h_{p0})\, \psi(e_0)}{c}, \qquad (15.71)$$

where

$$\left.\begin{aligned}
\Phi(h) &= \frac{r}{\rho} \sqrt{\frac{\pi}{2\mu H}}, \\
\psi(e_0) &= \sqrt{\frac{1+e_0}{e_0}} \int_0^{e_0} \frac{e\, de}{\sqrt{(1+e)(1-e^2)^3}}.
\end{aligned}\right\} \qquad (15.72)$$

In deriving this relation, we have knowingly admitted an inaccuracy: the integration of (15.70) with respect to e from 0 to e_0 is justified only for highly eccentric orbits. The resulting error in t_{life}, however, is comparatively small, since the flight time in low-eccentricity orbits is short in comparison with the total lifetime.

When the lifetime is calculated by substituting (15.72) in (15.71), the right-hand side of the explicit expression contains a factor

$$k = \frac{1}{c\rho_{p0}\sqrt{H(h_{p0})}}.$$

Making use of (15.54) and putting $f_0(\nu) \approx 1$, we find

$$\frac{1}{c\rho_{p0}\sqrt{H(h_{p0})}} = \frac{1}{|\delta P_0|} 6\pi \sqrt{\frac{2\pi}{\mu}} \frac{a_0^2}{\sqrt{e_0}} \frac{1+e_0}{1-e_0} \sqrt{1-e_0^2},$$

where δP_0 and a_0 are the initial values of the orbital period perturbation per circuit, δP, and of the semimajor axis a. Substituting this relation in (15.71), (15.72) and applying the second equality in (5.3), we find

$$t_{\text{life}} = \frac{6\pi^2}{|\delta P_0|} \frac{a_0^3}{\mu} \frac{(1+e_0)\sqrt{1-e_0^2}}{\sqrt{e_0}} \psi(e_0).$$

Hence, making use of (5.36), we write

$$t_{\text{life}} = \frac{P_0^2}{|\delta P_0|} \psi_1(e_0), \qquad (15.73)$$

where

$$\psi_1(e_0) = \frac{3(1+e_0)\sqrt{1-e_0^2}}{2\sqrt{e_0}} \quad \psi(e_0) = \frac{3(1+e_0)^2\sqrt{1-e_0}}{2e_0} \int_0^{e_0} \frac{e\,de}{\sqrt{(1+e)(1-e^2)^3}}, \quad (15.74)$$

and P_0 is the initial orbital period of the satellite.

The above formula is convenient for estimating the lifetime of orbited satellites, since it gives the unknown quantity as a function of the parameters P_0, $|\delta P_0|$ and e_0 which can be obtained with fairly high accuracy.

To calculate the functions $\psi(e_0)$ and $\psi_1(e_0)$ from (15.72) and (15.74), we should evaluate the indefinite integral

$$J = \int \frac{e\,de}{\sqrt{(1+e)(1-e^2)^3}} = \int \frac{e\,de}{(1+e)^2\sqrt{(1-e)^3}}.$$

Substitution of variables

$$x = \sqrt{1-e}, \quad dx = -\frac{de}{2\sqrt{1-e}}, \quad e = 1 - x^2 \quad (15.75)$$

gives

$$J = -2 \int \frac{1-x^2}{(2-x^2)^2 x^2}\,dx = \int \left[\frac{1}{(2-x^2)^2} - \frac{1}{2(2-x^2)} - \frac{1}{2x^2} \right] dx. \quad (15.76)$$

We now make use of the well-known relation /25/

$$\int \frac{dx}{a-bx^2} = \frac{1}{2\sqrt{ab}} \ln \frac{a+x\sqrt{ab}}{a-x\sqrt{ab}},$$

$$\int \frac{dx}{(a-bx^2)^2} = \frac{x}{2a(a-bx^2)} + \frac{1}{2a} \int \frac{dx}{a-bx^2}$$

and note that in our case

$$a = 2, \quad b = 1.$$

Expression (15.76) then takes the form

$$J = \frac{x}{4(2-x^2)} + \frac{1}{2x} - \frac{1}{4} \int \frac{dx}{2-x^2} = \frac{4-x^2}{4(2-x^2)x} - \frac{1}{8\sqrt{2}} \ln \frac{\sqrt{2}+x}{\sqrt{2}-x}$$

or, making use of (15.75),

$$J = \int \frac{e\,de}{\sqrt{(1+e)(1-e^2)^3}} = \frac{3+e}{4(1+e)\sqrt{1-e}} - \frac{1}{8\sqrt{2}} \ln \frac{\sqrt{2}+\sqrt{1-e}}{\sqrt{2}-\sqrt{1-e}}.$$

Hence

$$\int_0^{e_0} \frac{e\,de}{\sqrt{(1+e)(1-e^2)^3}} = \frac{3+e_0}{4(1+e_0)\sqrt{1-e_0}} - \frac{3}{4} + \frac{1}{8\sqrt{2}} \ln \frac{(\sqrt{2}+1)(\sqrt{2}-\sqrt{1-e_0})}{(\sqrt{2}-1)(\sqrt{2}+\sqrt{1-e_0})}. \quad (15.77)$$

For moderate eccentricities, expression (15.77) is preferably replaced with a series expansion of the integral in powers of e. From the standard

expansion of functions of the form $(1+e)^h$, we have

$$\frac{e}{\sqrt{(1+e)(1-e^2)^3}} = e(1+e)^{-1}(1-e^2)^{-1}(1-e)^{-\frac{1}{2}} = e\left(1 - \frac{1}{2}e + \frac{15}{8}e^2 - \frac{17}{16}e^3 + \dots\right).$$

Then

$$\int_0^{e_0} \frac{e\,de}{\sqrt{(1+e)(1-e^2)^3}} = \frac{e_0^2}{2}\left(1 - \frac{1}{3}e_0 + \frac{15}{16}e_0^2 - \frac{17}{40}e_0^3 + \dots\right). \tag{15.78}$$

Substituting in (15.72) and (15.74), we obtain after elementary manipulations

$$\left.\begin{aligned}
\psi(e_0) &= \frac{e_0^{3/2}}{2}\left(1 + \frac{1}{6}e_0 + \frac{31}{48}e_0^2 + \frac{71}{480}e_0^3 + \dots\right), \\
\psi_1(e_0) &= \frac{3e_0}{4}\left(1 + \frac{7}{6}e_0 + \frac{5}{16}e_0^2 + \frac{101}{480}e_0^3 + \dots\right).
\end{aligned}\right\} \tag{15.79}$$

Appendix 2 tabulates the function $\Phi(h)$ as calculated from (15.72) for the model atmosphere used in this book. Appendix 3 tabulates the functions $\psi(e_0)$ and $\psi_1(e_0)$ as calculated from (15.72), (15.74), and (15.77).

15.10. SATELLITE LIFETIME IN LOW-ECCENTRICITY ORBITS

To find the lifetime of low-eccentricity orbits, we make use of expressions (15.20), (15.24), and (15.50) for the secular perturbations of the semimajor axis (δa) and eccentricity (δe). Omitting terms proportional to e, we find

$$\left.\begin{aligned}
\delta a &= -4\pi c \rho_m a^2 I_0(\nu), \\
\delta e &= -4\pi c \rho_m a I_1(\nu),
\end{aligned}\right\} \tag{15.80}$$

where

$$\rho_m = \rho_p \exp(-\nu) \tag{15.81}$$

is the air density at the mean height

$$h_m = a - R_E. \tag{15.82}$$

Making use of (15.19), we obtain an expression for the change per circuit in ν:

$$\delta\nu = \frac{a}{H}\delta e + \frac{e}{H}\delta a = -4\pi c \rho_m \frac{a^2}{H}[I_1(\nu) + eI_0(\nu)].$$

For small eccentricities, the second term in the right-hand side of this expression is much less than the first term. This follows from the expansion (15.39), which gives

$$I_1(\nu) \approx \frac{\nu}{2} = e\frac{a}{2H}, \qquad eI_0(\nu) \approx e.$$

Since $a \gg 2H$, we have

$$\delta v \approx -4\pi c \rho_m \frac{a^2}{H} I_1(v). \tag{15.83}$$

Moreover, from (15.80) and (15.82) we see that the change per circuit in mean orbit height is

$$\delta h_m = \delta a = -4\pi c \rho_m a^2 I_0(v). \tag{15.84}$$

Orbit perturbations vary smoothly, and we may therefore write

$$\frac{dv}{dh_m} \approx \frac{\delta v}{\delta h_m} = \frac{1}{H} \frac{I_1(v)}{I_0(v)}, \quad \frac{I_0(v)}{I_1(v)} dv = \frac{dh_m}{H}. \tag{15.85}$$

We now make use of expression (15.22), which gives

$$I_0(v) = \frac{1}{2\pi} \int_0^{2\pi} \exp(v \cos E) \, dE,$$

$$I_1(v) = \frac{1}{2\pi} \int_0^{2\pi} \exp(v \cos E) \cos E \, dE,$$

$$I_2(v) = \frac{1}{2\pi} \int_0^{2\pi} \exp(v \cos E) \cos 2E \, dE,$$

whence

$$\frac{dI_1(v)}{dv} = \frac{1}{2\pi} \int_0^{2\pi} \exp(v \cos E) \cos^2 E \, dE = \frac{I_0(v) + I_2(v)}{2}.$$

On the other hand, from (15.23) we have

$$\frac{I_1(v)}{v} = \frac{I_0(v) - I_2(v)}{2}.$$

Adding the last two equalities, we find

$$I_0(v) = \frac{dI_1(v)}{dv} + \frac{I_1(v)}{v}.$$

Equation (15.85) now takes the form

$$\frac{dI_1(v)}{I_1(v)} + \frac{dv}{v} = \frac{dh_m}{H}.$$

Integrating, we obtain

$$\ln \frac{v I_1(v)}{v_0 I_1(v_0)} = \frac{h_m - h_{m0}}{H}, \quad v I_1(v) = v_0 I_1(v_0) \exp\left(\frac{h_m - h_{m0}}{H}\right), \tag{15.86}$$

where h_{m0} and v_0 are the initial values of the corresponding parameters. From this relation and from expansion (15.39) we see that v monotonically decreases in time as the mean flying height diminishes. Since invariably

$h_{m0} \gg H$, we may take for the final value of v, obtaining toward the end of the satellite lifetime $(h_m = 0)$,

$$v_h \approx 0. \qquad (15.86a)$$

We now write a differential equation between v and the relative time τ. Making use of (5.36), (14.38), and (15.83), we have

$$\frac{dv}{d\tau} \approx \frac{\delta v}{cP} = -\frac{2\sqrt{\mu a}}{H} \rho_m I_1(v).$$

On the other hand, from (14.9) and (15.86) we find

$$\rho_m = \rho_{m0} \exp\left(-\frac{h_m - h_{m0}}{H}\right) = \frac{v_0 I_1(v_0)}{v I_1(v)} \rho_{m0},$$

where ρ_{m0} is the air density at the height h_{m0}. Substituting this expression in the right-hand side of the differential equation, we find

$$v\, dv = -\frac{2\sqrt{\mu a}}{H} \rho_{m0} v_0 I_1(v_0)\, d\tau.$$

We integrate this equation from the initial epoch to the end of the satellite's lifetime. Seeing that the semimajor axis varies slowly, we substitute the initial value a_0 for the actual a. In the result, making use of (15.86a), we find

$$\frac{v_0^2}{2} = \frac{2\sqrt{\mu a_0}}{H} \rho_{m0} v_0 I_1(v_0)\, \tau_{life}$$

Hence, applying (14.38) and (15.39), we obtain an expression for the lifetime of low-eccentricity orbits:

$$t_{life} = \frac{H}{2\rho_{m0} c \sqrt{\mu a_0}} \frac{v_0}{2 I_1(v_0)} = \frac{H}{2\rho_{m0} c \sqrt{\mu a_0}} \frac{1}{1 + \dfrac{v_0^2}{8} + \dfrac{v_0^4}{192} + \cdots} \qquad (15.87)$$

or, making use of (14.44) and (15.82),

$$t_{life} = \frac{F(h_{m0})}{c} \frac{v_0}{2 I_1(v_0)} = \frac{F(h_{m0})}{c} \frac{1}{1 + \dfrac{v_0^2}{8} + \dfrac{v_0^4}{192} + \cdots}. \qquad (15.88)$$

Applying (5.36), (15.19), (15.39), (15.46), and (15.80), we can eliminate the factor $c\rho_m$ from (15.87), writing

$$t_{life} = \frac{3}{4} \frac{P_0^2}{|\delta P_0|} e_0 \frac{I_0(v_0)}{I_1(v_0)} = \frac{3}{2} \frac{H}{a_0} \frac{P_0^2}{|\delta P_0|} \frac{1 + \dfrac{v_0^2}{4} + \dfrac{v_0^4}{64} + \dfrac{v_0^6}{2304} + \cdots}{1 + \dfrac{v_0^2}{8} + \dfrac{v_0^4}{192} + \cdots}. \qquad (15.89)$$

For $e_0 \rightarrow 0$, relations (15.87), (15.88), and (15.89) clearly reduce to the corresponding equations (14.51), (14.53), and (14.54) for circular orbits.

15.11. COMPARATIVE ANALYSIS OF LIFETIME FORMULAS

We have derived two groups of expressions that can be used in calculating the lifetime of an elliptical orbit. The formulas of Sec. 15.9 apply for orbits of high initial eccentricity e_0. When e_0 is small, they are obviously in error ($t_{\text{life}} \to 0$ as $e \to 0$). The formulas of Sec. 15.10 were derived for small initial eccentricities. For $e_0 \to 0$, these relations give a solution which in the limit coincides with the circular orbit solution.

Let us now consider the question of "matching" of these two distinct groups of formulas. Making use of the asymptotic expansions (15.26) and relations (15.19) and (15.81), we write expressions (15.87) and (15.89) as

$$
\left.
\begin{aligned}
t^{\text{I}}_{\text{life}} &= \frac{r_{p0}}{c\rho_{p0}}\sqrt{\frac{\pi}{2\mu H}}\,\frac{e_0^{3/2}}{2}\,\frac{1}{1-e_0} \times \frac{1+O_{\text{I}}(e_0)}{1-\dfrac{3}{8}\cdot\dfrac{1}{v_0}-\dfrac{15}{128}\cdot\dfrac{1}{v_0^2}-\dfrac{105}{1024}\cdot\dfrac{1}{v_0^3}-\cdots}, \\[2ex]
t^{\text{II}}_{\text{life}} &= \frac{3}{4}\,\frac{P_0^2}{|\delta P_0|}\times e_0\,\frac{1+\dfrac{1}{8}\cdot\dfrac{1}{v_0}+\dfrac{9}{128}\cdot\dfrac{1}{v_0^2}+\dfrac{75}{1024}\cdot\dfrac{1}{v_0^3}+\cdots}{1-\dfrac{3}{8}\cdot\dfrac{1}{v_0}-\dfrac{15}{128}\cdot\dfrac{1}{v_0^2}-\dfrac{105}{1024}\cdot\dfrac{1}{v_0^3}-\cdots}[1+O_{\text{II}}(e_0)],
\end{aligned}
\right\} \quad (15.90)
$$

where $O_{\text{I}}(e_0)$ and $O_{\text{II}}(e_0)$ are the corresponding errors: they have the order of the initial eccentricity, since in the derivation of the respective formulas we ignored terms of this order.

On the other hand, for high eccentricities, we may write from (15.71), (15.72), (15.73), and (15.79)

$$
\left.
\begin{aligned}
t^{\text{III}}_{\text{life}} &= \frac{r_{p0}}{c\rho_{p0}}\sqrt{\frac{\pi}{2\mu H}}\,\frac{e_0^{3/2}}{2}\times\left(1+\frac{1}{6}e_0+\frac{31}{48}e_0^2+\frac{71}{480}e_0^3+\cdots\right)\left[1+O_{\text{III}}\left(\frac{1}{v_0}\right)\right], \\[2ex]
t^{\text{IV}}_{\text{life}} &= \frac{3}{4}\,\frac{P_0^2}{|\delta P_0|}\,e_0\times\left(1+\frac{7}{6}e_0+\frac{5}{16}e_0^2+\frac{101}{480}e_0^3+\cdots\right)\left[1+O_{\text{IV}}\left(\frac{1}{v_0}\right)\right],
\end{aligned}
\right\} \quad (15.91)
$$

where $O_{\text{III}}\left(\frac{1}{v_0}\right)$ and $O_{\text{IV}}\left(\frac{1}{v_0}\right)$ are the corresponding errors, which have the order $\frac{1}{v_0}=\frac{H}{ae_0}$.

Equating the lifetimes t_{life} from (15.90) and (15.91), we obtain, to terms of first order in e_0 and $\frac{1}{v_0}$,

$$
\frac{1+O_{\text{I}}(e_0)}{(1-e_0)\left(1-\dfrac{3}{8}\cdot\dfrac{1}{v_0}\right)}\approx\left(1+\frac{1}{6}e_0\right)\left[1+O_{\text{III}}\left(\frac{1}{v_0}\right)\right],
$$

$$
\frac{1+\dfrac{1}{8}\cdot\dfrac{1}{v_0}}{1-\dfrac{3}{8}\cdot\dfrac{1}{v_0}}[1+O_{\text{II}}(e_0)]\approx\left(1+\frac{7}{6}e_0\right)\left[1+O_{\text{IV}}\left(\frac{1}{v_0}\right)\right].
$$

Hence, equating terms of the first order of smallness in e_0 and $\frac{1}{v_0}$, we find

$$
\left.
\begin{aligned}
O_{\text{I}}(e_0) &\approx -\frac{5}{6}e_0, \\[1ex]
O_{\text{II}}(e_0) &\approx \frac{7}{6}e_0, \\[1ex]
O_{\text{III}}\left(\frac{1}{v_0}\right) &\approx \frac{3}{8}\cdot\frac{1}{v_0}=\frac{3}{8}\frac{H}{a_0e_0}, \\[1ex]
O_{\text{IV}}\left(\frac{1}{v_0}\right) &\approx \frac{1}{2}\cdot\frac{1}{v_0}=\frac{1}{2}\frac{H}{a_0e_0}.
\end{aligned}
\right\} \quad (15.92)
$$

The errors of (15.90) increase and the errors of (15.91) decrease as e_0 grows. Let us determine the critical initial eccentricity e_{cr}, for which a switch should be made from one set of formulas to the other. This critical parameter is clearly defined by the conditions

$$|O_1(e_{cr})| = O_{III}\left(\frac{H}{a_0 e_{cr}}\right) \quad \text{or} \quad O_{II}(e_{cr}) = O_{IV}\left(\frac{H}{ae_{cr}}\right).$$

Making use of (15.92) we see that the solutions of both equations give close results:

$$e_{cr} \approx 0.66 \sqrt{\frac{H}{a_0}} = 0.66 \sqrt{\frac{H}{r_{p0}}(1 - e_{cr})} =$$

$$= \sqrt{0.44 \frac{H}{r_{p0}} + 0.05 \left(\frac{H}{r_{p0}}\right)^2} - 0.22 \frac{H}{r_{p0}} \approx$$

$$\approx 0.66 \sqrt{\frac{H}{r_{p0}}} - 0.22 \frac{H}{r_{p0}}. \tag{15.93}$$

Table 15.3 lists the values of e_{cr} calculated from this relation for various initial perigee heights $h_{p0} = r_{p0} - R_E$. The parameter H for various h_{p0} was taken from the graph in Figure 14.1.

TABLE 15.3.

h_{p0} km	100	110	120	130	140	150	160	170	180
e_{cr}	0.019	0.021	0.022	0.025	0.029	0.035	0.042	0.044	0.046
h_{p0}, km	190	200	300	400	500	600	700	800	–
e_{cr}	0.047	0.048	0.054	0.060	0.067	0.072	0.074	0.080	–

Expressions (15.92) can be used in estimating the order of magnitude of the errors contributed by the approximate approach to the derivation of the foregoing formulas. From (15.92) and from Table 15.3 it follows that a maximum error of some $5 - 10\%$ obtains in t_{life} for $e_0 = e_{cr}$ if low-eccentricity formulas are applied when $e_0 \leqslant e_{cr}$ or high-eccentricity formulas are used for $e_0 \geqslant e_{cr}$.

However, the inaccuracy of our simplifying assumptions introduces additional errors in the determination of t_{life}. These errors are attributable to the following factors:

(a) introduction of the isothermal atmosphere as a basis for the derivation of the relevant formulas;

(b) deviation of the actual initial values of the atmospheric parameters from the theoretical values and inaccuracies in the coefficient c;

(c) dynamic state of the atmosphere;

(d) failure to allow for the Earth's flattening and the noncentral components of its field of gravity;

(e) failure to allow for other astrophysical and geophysical factors (lunisolar attraction, radiation pressure, gravity anomalies, etc.).

• To reduce the influence of errors under (a) above, the function $F(h_{m0})$ for nearly circular orbits should be calculated from (14.41), and not (14.44).

284

For highly eccentric orbits, however, this method is inadequate since the air drag in these orbits is mainly determined by the comparatively dense atmosphere near the perigee point. A local isothermal atmosphere should be chosen, which provides the best approximation to the actual variation of air density near the perigee. The adjustment parameters of this atmosphere are calculated from (14.12), putting $h_i = h_{p0}$. It is therefore advisable to change over from relations which express t_{life} in terms of $F(h_{m0})$ to those linking t_{life} with $\Phi(h_{p0})$ (see Sec. 15.9).

The errors under (b) above are successfully eliminated for orbited satellites by calculating δP_0 from actual orbital measurements. In this case formulas which give t_{life} in terms of δP_0 should be used.

The errors under (c) above cannot be eliminated unless a fairly accurate and reliable dynamic model of the atmosphere is available.

To reduce the effect of the errors under (d) above, the initial perigee height h_{p0} in all the relations should be replaced with the minimum height $h_{min\,0}$ during the first circuit, which is calculated with allowance for the Earth's flattening and the noncentral components of the geopotential (both these factors should be introduced jointly, since their effects are of the same order of magnitude). The mean flying height is then obtained from the formula

$$h_{m\,0} = h_{min\,0} + a_0 e_0.$$

In calculating the lifetime from experimental values of the initial orbital-period perturbation δP_0, we should remember that the reduction of orbital measurements actually gives the total perturbation $\delta P_{tot\,0}$. In accordance with (15.63), this is a sum of two components, δP_{drag0} and $\delta P_0'$. For fairly eccentric persisting orbits (with lifetimes of a few years), the long-periodic component $\delta P_0'$ resulting from the Earth's flattening may turn to be comparable with the secular component δP_{drag0} conditioned by air drag. If, however, the satellite lifetime is considerably longer than the period of perigee movement $\bar{P}_\omega$ (which is equal to the period of the component $\delta P'$), the effect of the long-periodic component $\delta P'$ on t_{life} can be ignored. The increment δP_0 in the right-hand sides of (15.73) and (15.89) is then replaced with δP_{drag0}, which is calculated from

$$\delta P_{drag0} = \delta P_{tot\,0} - \delta P_0'.$$

The effect of various astrophysical factors (lunisolar attraction, radiation pressure, etc.) is considered in the next chapters. We only note that for high-flying satellites these factors may have a decisive influence on t_{life} (see Chapters 16 and 17).

On the whole, given the state of our present-day knowledge of the upper atmosphere, we cannot obtain reliable data for satellite lifetimes: the best we can hope for is a crude estimate with errors ranging from 10 to 50%. These errors may be substantially reduced once the satellite has been actually injected into orbit and the parameter δP_0 has been measured experimentally (this is particularly significant for short-living satellites).

In conclusion, we consider to what extent the eccentricity of the orbit affects its lifetime. Take a family of orbits with a constant initial semi-major axis a_0, i.e., constant initial mean flying height h_{m0} or constant

initial period P_0; the initial eccentricity e_0 is variable. Let us establish the dependence on of the coefficient

$$k_1(e_0) = \frac{t_{\text{life}}}{t_{\text{life}(a_0)}}, \qquad (15.94)$$

where $t_{\text{life}}(a_0)$ is the lifetime of a circular orbit with initial radius $r_0 = a_0$. Making use of (14.44), (14.51), (15.19), (15.26), (15.39), (15.71), (15.79), and (15.88), we write for an isothermal atmosphere

$$k_1(e_0) = \begin{cases} \dfrac{v_0}{2I_1(v_0)} = \dfrac{1}{1 + \frac{v_0^2}{8} + \frac{v_0^4}{192} + \cdots} = 1 - \frac{v_0^2}{8} - \cdots & \text{for } v_0 < 2, \ e_0 < \dfrac{2H}{a_0}, \\[4mm] \dfrac{v_0}{2I_1(v_0)} = \sqrt{\dfrac{\pi}{2}} \exp(-v_0) \times \dfrac{v_0^{3/2}}{1 - \frac{3}{8}\cdot\frac{1}{v_0} - \frac{15}{128}\cdot\frac{1}{v_0^2} - \cdots} & \text{for } \dfrac{2H}{a_0} \leqslant e_0 \leqslant e_{\text{cr}}, \\[4mm] \dfrac{\sqrt{\pi}}{2} \exp(-v_0) v_0^{3/2}(1 - e_0) \times \left(1 + \frac{1}{6} e_0 + \frac{31}{48} e_0^2 + \cdots\right) & \text{for } e_0 \geqslant e_{\text{cr}}. \end{cases} \qquad (15.95)$$

It follows from these relations that for $a_0 = \text{const}$, the lifetime monotonically decreases with increasing e_0. This shortening of lifetime is comparatively slow for small e_0. For nearly circular orbits we may therefore put with fair accuracy $t_{\text{life}} \approx t_{\text{life}}(a_0)$. However, as e_0 increases, the lifetime falls off sharply due to the steep drop in $\exp(-v_0)$.

Let us now consider a family of orbits with constant initial perigee height h_{p0} (or constant r_{p0}). The dependence of lifetime on eccentricity for this family is characterized by the coefficient

$$k_2(e_0) = \frac{t_{\text{life}}}{t_{\text{life}(h_{p0})}}, $$

where $t_{\text{life}}(h_{p0})$ is the lifetime of circular orbit with initial radius $r_0 = r_{p0} = R_E + h_{p0}$.

Making use of (14.44) and (15.94), we write

$$k_2(e_0) = k_1(e_0)\frac{t_{\text{life}(a_0)}}{t_{\text{life}(h_{p0})}} = k_1(e_0)\sqrt{1 - e_0}\exp(v_0). \qquad (15.96)$$

From (15.95) and (15.96) it follows that for $h_{p0} = \text{const}$ the lifetime rapidly increases with initial eccentricity (for moderately eccentric orbits, the increase is approximately proportional to $e_0^{3/2}$).

15.12. LIST OF APPROXIMATE LIFETIME FORMULAS

In keeping with the foregoing results, the orbits of artificial Earth satellites should be divided into three groups for purposes of lifetime determination:

(a) low-eccentricity (nearly circular) orbits, which are investigated using the series expansions (14.24) of the functions $\tilde{\rho}(h)$ and $\bar{\rho}(h)$, this

being equivalent to the condition

$$v_0 < 1, \quad e_0 < \frac{H}{a_0};$$

(b) moderately eccentric orbits, satisfying the condition

$$\frac{H}{a_0} \leqslant e_0 \leqslant e_{\mathrm{cr}};$$

(c) highly eccentric orbits, having

$$e_0 \gg e_{\mathrm{cr}}.$$

For each of these groups, we can write approximate expressions of two kinds:

        (i) formulas for the determination of t_{life} from known c and ρ;

        (ii) formulas for the determination of t_{life} from known δP_0.

The formulas under (i) are conveniently used in a preliminary estimate of the satellite lifetime before launch, whereas the formulas under (ii) can be applied for orbited satellites.

As we have previously remarked, the t_{life} for orbits of groups (a) and (b) should be calculated from (15.88) and (15.89), and for orbits of group (c) from (15.71) and (15.73). For orbits of group (a) relation (15.89) should be preferably written in a form analogous to (14.54). Then, making use of (14.54) and (15.19), we can show that

$$t_{\mathrm{life}} = k(h_{\mathrm{m}0}) \frac{P_0^2}{|\delta P_0|} \frac{v_0 I_0(v_0)}{2 I_1(v_0)}.$$

For orbits of group (b), it is advisable to replace the air density at the height $h_{\mathrm{m}0}$ in (15.88) with air density at the height $h_{\mathrm{p}0}$. Making use of (15.19), (15.72), (15.81), and (15.87), we find

$$t_{\mathrm{life}} = \frac{\Phi(h_{\mathrm{p}0})}{c} \frac{e_0^{3/2}}{2(1-e_0)} \frac{\exp(v_0)}{\sqrt{2\pi v_0} \, I_1(v_0)}.$$

We thus obtain the following approximate formulas for t_{life}:

for $v_0 < 1$ and $e_0 < \dfrac{H}{a_0}$

$$t_{\mathrm{life}} = \frac{F(h_{\mathrm{m}0}) F_1(v_0)}{c} = \frac{P_0^2}{|\delta P_0|} k(h_{\mathrm{m}0}) F_2(v_0), \tag{15.97}$$

for $\dfrac{H}{a_0} \leqslant e_0 \leqslant e_{\mathrm{cr}}$

$$t_{\mathrm{life}} = \frac{\Phi(h_{\mathrm{p}0}) \psi_2(e_0) F_3(v_0)}{c} = \frac{P_0^2}{|\delta P_0|} e_0 F_4(v_0), \tag{15.98}$$

for $e_0 \gg e_{\mathrm{cr}}$

$$t_{\mathrm{life}} = \frac{\Phi(h_{\mathrm{p}0}) \psi(e_0)}{c} = \frac{P_0^2}{|\delta P_0|} \psi_1(e_0). \tag{15.99}$$

287

Here

$$F_1(v) = \frac{v}{2I_1(v)}, \qquad F_2(v) = \frac{vI_0(v)}{2I_1(v)},$$

$$F_3(v) = \frac{\exp(v)}{I_1(v)\sqrt{2\pi v}}, \qquad F_4(v) = \frac{3}{4}\frac{I_0(v)}{I_1(v)},$$

$$\psi_2(e_0) = \frac{e_0^{3/2}}{2(1-e_0)},$$

\hfill (15.100)

and v_0, $F(h_{m0})$, $k(h_{m0})$, $\psi(e_0)$, $\psi_1(e_0)$, $\Phi(h_{p0})$, e_{cr} are determined from (14.41), (14.55), (15.19), (15.72), (15.74), (15.77), and (15.93).

Note that for isothermal atmosphere ($H = \text{const}$), relations (15.97) and (15.98) are identical. If H is variable, they give different results. With variable H, it is advisable to calculate the functions $F(h)$ and $k(h)$ entering (15.97), not from (14.44) and (14.56), but preferably from (14.41) and (14.55).

Appendices 2 through 5 tabulate all the auxiliary functions entering the right-hand sides of (15.97)—(15.99). However, in machine computations, it is better to determine these functions directly from the analytical expressions listed above. The functions $\psi(e)$ and $\psi_1(e)$ are then conveniently computed from expansions (15.79). For $F_i(v)$ ($i = 1, 2, 3, 4$), by substituting (15.26) and (15.39) in (15.100), we find

for $v \leqslant 2$

$$F_1(v) = \frac{1}{1 + \frac{v^2}{8} + \frac{v^4}{192} + \cdots},$$

$$F_2(v) = \frac{1 + \frac{v^2}{4} + \frac{v^4}{64} + \frac{v^6}{2304} + \cdots}{1 + \frac{v^2}{8} + \frac{v^4}{192} + \cdots},$$

$$F_3(v) = \frac{2\exp(v)}{\left(1 + \frac{v^2}{8} + \frac{v^4}{192} + \cdots\right)\sqrt{2\pi v^3}},$$

$$F_4(v) = 1.5\frac{1 + \frac{v^2}{4} + \frac{v^4}{64} + \frac{v^6}{2304} + \cdots}{v\left(1 + \frac{v^2}{8} + \frac{v^4}{192} + \cdots\right)},$$

\hfill (15.101)

for $v \geqslant 1.5$

$$F_3(v) = \frac{1}{1 - \frac{3}{8}\cdot\frac{1}{v} - \frac{15}{128}\cdot\frac{1}{v^2} - \frac{105}{1024}\cdot\frac{1}{v^3} - \cdots},$$

$$F_4(v) = 0.75\frac{1 + \frac{1}{8}\cdot\frac{1}{v} + \frac{9}{128}\cdot\frac{1}{v^2} + \frac{75}{1024}\cdot\frac{1}{v^3}\cdots}{1 - \frac{3}{8}\cdot\frac{1}{v} - \frac{15}{128}\cdot\frac{1}{v^2} - \frac{105}{1024}\cdot\frac{1}{v^3}\cdots}.$$

\hfill (15.102)

Chapter 16

THE EFFECT OF LUNISOLAR ATTRACTION ON THE MOTION OF ARTIFICIAL EARTH SATELLITES

16.1. EQUATIONS OF MOTION OF A SPACE VEHICLE

In analyzing the gravitational pull of the Sun and the Moon on artificial Earth satellites, we shall use the general equations of motion of a space vehicle in the field of gravity of several attracting bodies /2/. Since all the attracting bodies in the solar system are nearly spherical, their gravitational forces will be determined from expressions of the form (4.3) (with some corrections introduced if absolutely necessary).

Let ρ be the vector defining the position of the space vehicle in some interial frame. Making use of (4.3), we write its equation of motion in this frame as

$$\ddot{\rho} = \sum_{i=0}^{n} \mu_i \frac{\rho_i - \rho}{|\rho_i - \rho|^3} + \frac{F}{m}, \tag{16.1}$$

where ρ_i ($i = 0, 1, 2, \ldots, n$) are the vectors which define the gravitational centers of the attracting bodies, μ_i coefficients equal to the product of the gravitational constant and the mass of the corresponding attracting body, m the mass of the space vehicle, F the resultant of all the additional forces on the vehicle, attributable to the nonspherical figure of the attracting bodies, atmospheric drag, radiation pressure, etc.

The motion of space vehicles is generally analyzed, not in an inertial frame, but in some nonrotating frame having its origin at the center of one of the attracting bodies. We call this body the p r i m a r y, and assign to it the subscript $i = 0$. For artificial Earth satellites, the Earth is commonly chosen as the primary. Note that we are dealing with the motion of space vehicles whose mass is negligible in comparison with the mass of the primaries. In the following, we therefore ignore all possible influence of the space vehicle on the primary. The equation of motion of the primary in an inertial frame is then written in the form

$$\ddot{\rho}_0 = \sum_{i=1}^{n} \mu_i \frac{\rho_i - \rho_0}{|\rho_i - \rho_0|^3} + \frac{F_0}{m_0}, \tag{16.2}$$

where F_0 is the resultant of all the additional forces on the primary, and m_0 its mass.

289

Let r be the vector which defines the position of the space vehicle in a frame connected with the primary. Clearly,

$$r = \rho - \rho_0. \qquad (16.3)$$

Subtracting (16.2) from (16.1) and making use of (16.3), we obtain the equation of motion of the space vehicle in a noninertial frame connected with the primary:

$$\ddot{r} = -\mu_0 \frac{r}{|r|^3} + \sum_{i=1}^{n} \mu_i \left(\frac{r_i - r}{|r_i - r|^3} - \frac{r_i}{|r_i|^3} \right) + \frac{F}{m} - \frac{F_0}{m_0}, \qquad (16.4)$$

where $r_i = \rho_i - \rho_0$ are the vectors which define the position of the other attracting bodies relative to the primary.

For most attracting bodies in the solar system, we may safely take $F_i = 0$. One of the principal exceptions is the Moon, whose motion must be calculated with allowance for the Earth's nonspherical figure.

We shall show in what follows that for motion in a certain neighborhood of the primary, the first term in the right-hand side of (16.4) is considerably greater than the sum total of the other terms. In particular, this is true for the great majority of coasting artificial Earth satellites. The first term in the right-hand side of (16.4) is therefore called the unperturbed (normal) acceleration, whereas the sum of the other terms is the perturbing acceleration. All the attracting bodies, with the exception of the primary, are referred to as the perturbing bodies.

16.2. SERIES EXPANSION OF THE PERTURBING ACCELERATION IN POWERS OF r/r_i

Let r and r_i $(i = 1, 2, \ldots, n)$ be the magnitudes of the corresponding vectors; we consider the case of motion close to the primary, when

$$r \ll r_i. \qquad (16.5)$$

To simplify the discussion, a system with a single perturbing body is assumed $(n = 1)$. All the results of this section can be easily generalized to the case of several perturbing bodies. We also take

$$F = F_0 = 0.$$

Under these assumptions, equations (16.4) take the form

$$\ddot{r} = -\mu_0 \frac{r}{r^3} + f_1, \qquad (16.6)$$

where f_1 is the perturbing acceleration:

$$f_1 = \mu_1 \left(\frac{r_1 - r}{|r_1 - r|^3} - \frac{r_1}{r_1^3} \right) = \mu_1 [r_1 (|r_1 - r|^{-3} - r_1^{-3}) - r |r_1 - r|^{-3}]. \qquad (16.7)$$

290

We remember that

$$|\boldsymbol{r}_1 - \boldsymbol{r}|^{-3} = [(\boldsymbol{r}_1 - \boldsymbol{r})(\boldsymbol{r}_1 - \boldsymbol{r})]^{-3/2} = r_1^{-3}\left(1 - 2\frac{\boldsymbol{r}\cdot\boldsymbol{r}_1}{r_1^2} + \frac{r^2}{r_1^2}\right)^{-3/2},\qquad (16.8)$$

and also that, in accordance with (16.5),

$$\varepsilon = \frac{2\boldsymbol{r}\cdot\boldsymbol{r}_1}{r_1^2} - \frac{r^2}{r_1^2} \ll 1.$$

In writing the right-hand side of (16.8), we therefore make use of Newton's binomial expansion

$$(1 - \varepsilon)^{-3/2} = 1 + \frac{3}{2}\varepsilon + \frac{15}{8}\varepsilon^2 + \cdots \qquad (16.9)$$

Retaining terms of the second order of smallness relative to r/r_1, we write

$$|\boldsymbol{r}_1 - \boldsymbol{r}|^{-3} = \frac{1}{r_1^3}\left[1 + \frac{3}{2}\left(\frac{2\boldsymbol{r}\cdot\boldsymbol{r}_1}{r_1^2} - \frac{r^2}{r_1^2}\right) + \frac{15}{8}\left(\frac{2\boldsymbol{r}\cdot\boldsymbol{r}_1}{r_1^2} - \frac{r^2}{r_1^2}\right)^2 + \cdots\right] =$$

$$= \frac{1}{r_1^3}\left[1 + 3\frac{\boldsymbol{r}\cdot\boldsymbol{r}_1}{r_1^2} + \frac{15}{2}\left(\frac{\boldsymbol{r}\cdot\boldsymbol{r}_1}{r_1^2}\right) - \frac{3}{2}\frac{r^2}{r_1^2} + \cdots\right].$$

Substituting in (16.7) and retaining terms of the second order of smallness, we find

$$\boldsymbol{f}_1 = \boldsymbol{f}_{11} + \boldsymbol{f}_{12} + \cdots, \qquad (16.10)$$

where

$$\left.\begin{aligned}
\boldsymbol{f}_{11} &= \frac{\mu_1}{r_1^2}\left(3\frac{\boldsymbol{r}_1}{r_1}\frac{\boldsymbol{r}\cdot\boldsymbol{r}_1}{r_1^2} - \frac{\boldsymbol{r}}{r_1}\right), \\
\boldsymbol{f}_{12} &= \frac{\mu_1}{r_1^2}\left\{\frac{\boldsymbol{r}_1}{r_1}\left[\frac{15}{2}\left(\frac{\boldsymbol{r}\cdot\boldsymbol{r}_1}{r_1^2}\right)^2 - \frac{3}{2}\frac{r^2}{r_1^2}\right] - 3\frac{\boldsymbol{r}}{r_1}\frac{\boldsymbol{r}\cdot\boldsymbol{r}_1}{r_1^2}\right\}.
\end{aligned}\right\} \qquad (16.11)$$

The vectors $\boldsymbol{f}_{11}$ and $\boldsymbol{f}_{12}$ are perturbing accelerations of first and second order, respectively. Let $\boldsymbol{r}^0$ and $\boldsymbol{r}_1^0$ be the unit vectors in the directions $\boldsymbol{r}$ and $\boldsymbol{r}_1$, and α the angle between these directions. Then (16.11) is written as

$$\left.\begin{aligned}
\boldsymbol{f}_{11} &= \frac{\mu_1}{r_1^2}\frac{r}{r_1}(3\cos\alpha\cdot\boldsymbol{r}_1^0 - \boldsymbol{r}^0), \\
\boldsymbol{f}_{12} &= \frac{\mu_1}{r_1^2}\frac{r^2}{r_1^2}\left[\left(\frac{15}{2}\cos^2\alpha - \frac{3}{2}\right)\boldsymbol{r}_1^0 - 3\cos\alpha\cdot\boldsymbol{r}^0\right].
\end{aligned}\right\} \qquad (16.12)$$

Putting

$$\boldsymbol{g} = \mu_0\frac{\boldsymbol{r}}{r^3} \qquad (16.13)$$

for the normal acceleration, and g, f_{11}, and f_{12} for the magnitudes of the corresponding vectors, we can easily show that

$$\left.\begin{aligned}
g &= \frac{\mu_0}{r^2}, \qquad f_{11} = \frac{\mu_1}{r_1^2}\frac{r}{r_1}\varphi_1(\alpha), \qquad f_{12} = \frac{\mu_1}{r_1^2}\frac{r^2}{r_1^2}\varphi_2(\alpha), \\
\varphi_1(\alpha) &= \sqrt{(3\cos\alpha\cdot\boldsymbol{r}_1^0 - \boldsymbol{r}^0)^2} = \sqrt{3\cos^2\alpha + 1}, \\
\varphi_2(\alpha) &= \sqrt{\left[\left(\frac{15}{2}\cos^2\alpha - \frac{3}{2}\right)\boldsymbol{r}_1^0 - 3\cos\alpha\cdot\boldsymbol{r}^0\right]^2} = \frac{3}{2}\sqrt{5\cos^4\alpha - 2\cos^2\alpha + 1}.
\end{aligned}\right\} \qquad (16.14)$$

Hence

$$\frac{f_{11}}{g} = \frac{\mu_1}{\mu_0}\left(\frac{r}{r_1}\right)^3 \varphi_1(\alpha), \quad \frac{f_{12}}{g} = \frac{\mu_1}{\mu_0}\left(\frac{r}{r_1}\right)^4 \varphi_2(\alpha). \tag{16.15}$$

Furthermore, from (16.14) we have

$$1 \leqslant \varphi_1(\alpha) \leqslant 2, \quad \frac{3}{\sqrt{5}} \leqslant \varphi_2(\alpha) \leqslant 3. \tag{16.16}$$

Note that for close satellites $(r \ll r_1)$, the perturbing acceleration produced by the gravitational pull of the second body is much less than the gravitational acceleration of that body, $g_1 = \mu_1/r_1^2$. Indeed, from (16.14) and (16.16), we have

$$\frac{f_{11}}{g_1} = \frac{r}{r_1}\varphi_1(\alpha) \leqslant 2\frac{r}{r_1}, \quad \frac{f_{12}}{g_1} = \frac{r^2}{r_1^2}\varphi_2(\alpha) \leqslant 3\left(\frac{r}{r_1}\right)^2.$$

This is so because, in accordance with equation (16.4), the perturbing acceleration is a geometrical difference between the gravitational accelerations set up by the perturbing body at the center of the primary and at the point occupied by the space vehicle.

16.3. THE SPHERE OF ACTION OF ATTRACTING BODIES

From (16.15) and (16.16) it follows that the ratio of perturbing-to-normal accelerations steeply increases as we move away from the primary. In the first approximation, this increase is proportional to $(r/r_1)^3$. Hence, in the vicinity of each attracting body there is always a region where the attraction of that body is prevalent, while the contribution from other attracting bodies reduces to comparatively small perturbing accelerations, which can often be ignored.

There are several different techniques for the definition of these regions /13, 32/. We shall consider one of the definitions, which introduces the so-called sphere of action. The gravitational system will comprise only two attracting bodies M_0 and M_1, the mass of the body M_0 being much less than the mass of the body M_1, i.e.,

$$\mu_0 \ll \mu_1. \tag{16.17}$$

This is a typical case encountered in the analysis of motion of a space vehicle in the solar system. By considering the pair "natural satellite — planet", we can establish the effective region of gravitational pull of the natural satellite, by considering the pair "planet — Sun", we establish the region of planetary pull and by considering the pair "Sun — Galaxy", we find the effective range of the Sun.

Let O_0 and O_1 be the centers of the two attracting bodies, and D the center of the space vehicle. We also put (Figure 16.1)

$$\overline{O_0 D} = r_0, \quad \overline{O_1 D} = r_1, \quad \overline{O_1 O_0} = c,$$
$$|r_0| = r_0, \quad |r_1| = r_1, \quad |c| = c.$$

From (16.6) it follows that the equation of motion of the vehicle D in a frame connected with the body M_0 is

$$\ddot{r}_0 = g_0 + f_1, \qquad (16.18)$$

and in a frame connected with the body M_1,

$$\ddot{r}_1 = g_1 + f_0, \qquad (16.19)$$

where g_0 and g_1 are the respective normal gravitational accelerations, and f_1 and f_0 the corresponding perturbing accelerations.
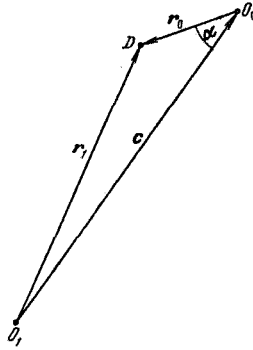
FIGURE 16.1. Mutual disposition of the space vehicle D and the attracting centers O_0 and O_1.

The sphere of action of the body M_0 is defined as the region where

$$\frac{f_1}{g_0} < \frac{f_0}{g_1},$$

and the sphere of action of the body M_1 is the region where

$$\frac{f_1}{g_0} > \frac{f_0}{g_1}.$$

Here

$$g_0 = |g_0|, \quad g_1 = |g_1|,$$
$$f_0 = |f_0|, \quad f_1 = |f_1|.$$

The sphere of action of an attracting body is thus the region of space where the perturbing-to-normal accelerations ratio is minimal if that attracting body is selected as the primary.

The boundary of the spheres of action of the two attracting bodies is clearly given by the equality

$$\frac{f_1}{g_0} = \frac{f_0}{g_1}. \qquad (16.20)$$

293

From condition (16.17) it follows that this boundary is much closer to M_0 than to M_1. In other words, on the boundary of the spheres of action, we have

$$r_0 \ll r_1, \quad c \approx r_1.$$

Hence, making use of (16.7) and (16.14) and remembering that $r_1 = c + r_0$, we write the following expressions for the magnitudes of the corresponding accelerations ($g_1, f_0,$ and f_1 are given to first approximation):

$$\left.\begin{array}{l}
g_0 = \dfrac{\mu_0}{r_0^2}, \quad g_1 = \dfrac{\mu_1}{r_1^2} \approx \dfrac{\mu_1}{c^2}, \\[2mm]
f_1 = \dfrac{\mu_1 r_0}{c^3} \varphi_1(\alpha) = \dfrac{\mu_1 r_0}{c^3} \sqrt{1 + 3\cos^2 \alpha}, \\[2mm]
f_0 = \mu_0 \left| \dfrac{c - r_1}{|c - r_1|^3} - \dfrac{c}{c^3} \right| = \mu_0 \left| \dfrac{r_0}{r_0^3} + \dfrac{c}{c^3} \right| \approx \dfrac{\mu_0}{r_0^2},
\end{array}\right\}$$

(16.21)

where α is the angle between the vectors r_0 and $\overline{O_0 O_1} = -c$.

Substituting in (16.20), we obtain an approximate equation for the boundary of the spheres of action:

$$\left.\begin{array}{l}
\dfrac{\mu_1 r_0^3}{\mu_0 c^3} \sqrt{1 + 3\cos^2 \alpha} = \dfrac{\mu_0 c^2}{\mu_1 r_0^2}, \\[3mm]
r_0 = \left(\dfrac{\mu_0}{\mu_1}\right)^{2/5} (1 + 3\cos^2 \alpha)^{-1/10} c.
\end{array}\right\}$$

(16.22)

Note that

$$1 \geqslant (1 + 3\cos^2 \alpha)^{-1/10} \geqslant \dfrac{1}{\sqrt[5]{2}} \approx 0.87.$$

This term is maximal for $\alpha = \pm \pi/2$ and minimal for $\alpha = 0; \pi$.

The sphere of action of the lesser body is thus close to a spherical surface: it is a slightly oblate figure of revolution, whose minor axis points to the greater attracting body.

Table 16.1 lists the maximum radii of the spheres of action for various pairs of attracting bodies, according to G. A. Chebotarev /32/.

TABLE 16.1

Attracting bodies		Maximum radius of the sphere of action of the lesser body, km	Maximum perturbing-to-normal accelerations ratio
lesser	greater		
Moon	Earth	$62.5 \cdot 10^3 - 69.8 \cdot 10^3$	0.55
Venus	Sun	$612 \cdot 10^3 - 621 \cdot 10^3$	0.099
Earth	Sun	$913 \cdot 10^3 - 944 \cdot 10^3$	0.104
Mars	Sun	$524 \cdot 10^3 - 631 \cdot 10^3$	0.066
Jupiter	Sun	$45.9 \cdot 10^6 - 50.5 \cdot 10^6$	0.35
Sun	Galaxy	$9 \cdot 10^{12}$	0.008

The limits indicated in the table for the maximum radii of the spheres of action correspond to different distances between the attracting bodies.

If the primary is always that attracting body in whose sphere of action the space vehicle moves at the particular time, the perturbing-to-normal

accelerations ratio is maximal when the vehicle crosses the common
boundary of the two spheres of action. From (16.21) and (16.22) it follows
that on the boundary

$$\frac{f_1}{g_0} = \frac{f_0}{g_1} = \left(\frac{\mu_0}{\mu_1}\right)^{1/5}(1 + 3\cos^2\alpha)^{1/5}.$$

For $\alpha = 0$, the ratio is maximal:

$$\left(\frac{f_1}{g_0}\right)_{max} = \left(\frac{f_0}{g_1}\right)_{max} \approx 1.32\left(\frac{\mu_0}{\mu_1}\right)^{1/5}.$$

The maximum perturbing-to-normal accelerations ratio thus depends
only on the mass ratio of the attracting bodies: it is independent of the
distance between them. This ratio decreases with decreasing μ_0/μ_1. In
other words, the greater the mass ratio of M_1 to M_0, the smaller the
perturbing influence of one body on motion in the sphere of action of its
counterpart. Table 16.1 lists the maximum perturbing-to-normal
accelerations ratios for various pairs of attracting bodies.

From (16.21) it follows that as we move away from the boundary of the
spheres of action, the perturbing-to-normal accelerations ratio decreases.
As we approach M_0, the ratio f_1/g_0 decreases, to first approximation, as r_0^3,
and as we recede beyond the sphere of action of this body, the ratio f_0/g_1
is seen to vary as $1/r_0^2$.

The sphere of action of the lesser body M_0 also comprises regions where
the gravitational pull of M_1 is actually greater than that of M_0 (i. e., $g_1 > g_0$).
For example, the gravitational pull of the Sun exceeds the gravitational
pull of the Earth already at distances of $256 \cdot 10^3 - 265 \cdot 10^3$ km from the
Earth's center, while the maximum radius of the Earth's sphere of action
is $913 \cdot 10^3 - 944 \cdot 10^3$ km /32/. In particular, in the Moon's orbit, the pull
of the Sun is much greater than the pull of the Earth, and yet the real lunar
orbit is much closer to the unperturbed orbit of Earth's satellite than to
the unperturbed orbit of an independent planet. This is so because the
Moon is far inside the Earth's sphere of action.

16.4. LUNISOLAR PERTURBATIONS IN THE MOTION
OF ARTIFICIAL EARTH SATELLITES

We shall only consider the motion of satellites orbiting at heights
$h \leqslant 100,000$ km above the Earth's surface. From relations (16.14), we
can show that for these satellites the perturbing effect of all celestial
bodies, with the exception of the Sun and the Moon, is invariably negligible.
Preliminary estimates of the lunisolar perturbations can be obtained from
Table 16.2. This table lists the maximum perturbing accelerations f, and
their ratios to the gravitational acceleration g of the Earth at various
heights h. The calculations were made from the first-order relations
(16.14). For purposes of comparison, the table also gives the magnitude
(relative to g) of the maximum perturbations produced by the second zonal
harmonic of the geopotential and by gravity anomalies. The perturbations
due to the second zonal harmonic are obtained from the approximate

expressions (12.18), and the gravity anomalies are estimated from

$$f_{max}(h) = f_{max}(0)\left(\frac{R}{R+h}\right)^4,$$

where $f_{max}(h)$ is the maximum perturbing acceleration at the height h, $f_{max}(0)$ the maximum gravity anomaly at the ground, R the mean radius of the Earth. We take $f_{max}(0) = 6 \cdot 10^{-4}\,m/sec^2$. This estimate is much too high, since most of the terms in the expansion (12.27) decrease with the height h much faster than $\left(\frac{R}{R+h}\right)^4$.

TABLE 16.2

Height h, km	Maximum perturbing acceleration		Maximum perturbing acceleration-to-g ratio			
	solar, $m/sec^2 \cdot 10^{-6}$	lunar, $m/sec^2 \cdot 10^{-6}$	for solar perturbation	for lunar perturbation	for the perturbation due to the second zonal harmonic of geopotential	for gravity anomalies
0	0,50	1.1	$5.1 \cdot 10^{-8}$	$1.1 \cdot 10^{-7}$	$3.4 \cdot 10^{-3}$	$6.0 \cdot 10^{-5}$
2,000	0.66	1.4	$1.2 \cdot 10^{-7}$	$2.5 \cdot 10^{-7}$	$1.9 \cdot 10^{-3}$	$3.5 \cdot 10^{-5}$
10,000	1.3	2.8	$8.6 \cdot 10^{-7}$	$1.9 \cdot 10^{-6}$	$5.1 \cdot 10^{-4}$	$9.1 \cdot 10^{-6}$
20,000	2.1	4.5	$3.6 \cdot 10^{-6}$	$7.9 \cdot 10^{-6}$	$2.0 \cdot 10^{-4}$	$3.5 \cdot 10^{-6}$
50,000	4.4	9.8	$3.5 \cdot 10^{-5}$	$7.7 \cdot 10^{-5}$	$4.3 \cdot 10^{-5}$	$7.8 \cdot 10^{-7}$
100,000	8.3	18	$2.4 \cdot 10^{-4}$	$5.2 \cdot 10^{-4}$	$1.2 \cdot 10^{-5}$	$2.2 \cdot 10^{-7}$

We see from the table that the perturbing acceleration produced by the gravitational pull of the Moon is some 2.2 times as large as the solar perturbing acceleration. For satellites flying at heights of a few thousands of kilometers and less, these perturbations are much less than gravity anomalies, which are commonly ignored even in exact calculations. For heights above the 20,000 km level, the lunisolar perturbations are greater than gravity anomalies, and above the 50,000 km, they exceed all the other geopotential perturbations.

The influence of the second and higher terms in the expansion (16.10) can be estimated from relations (16.14). The ratio of each successive term to its predecessor is found to be of the order r/r_t. Hence it follows that the series which describes the effect of solar perturbations on the motion of artificial Earth satellite converges very rapidly, and all terms but the first can be omitted in most cases. The analogous series representing the lunar perturbations converges much more slowly. Already at heights of $50,000 - 100,000$ km, the second term constitutes a few tens of percent of the first term. The first term is suitable for crude estimates only.

16.5. PROJECTIONS OF THE PERTURBING ACCELERATION ON THE SATELLITE'S ORBITAL AXES

Since the perturbing accelerations for the artificial Earth satellites under consideration are invariably small, we shall only consider the secular and the long-periodic perturbations of orbital elements, i.e., we calculate the resultant change in orbital elements during one circuit of revolution. The perturbing effects attributable to the Moon and to the Sun will be treated independently, and the corresponding perturbing accelerations will be found from the first-order relations (16.11). In our analysis, we follow the treatment of M. L. Lidovich /19/.

To calculate the secular orbit perturbations from (2.16) or (11.39), we should first find the projections S, T, W of the perturbing accelerations on the satellite's orbital axes (see Figure 2.1). We shall operate in the rectangular frame $O\xi\eta\zeta$ introduced in Sec. 5.5 (see Figure 5.5). Let i, j, k be the unit vectors along these axes, S^0, T^0, W^0 the unit vectors in the directions of S, T, W and $\varkappa_1$, $\varkappa_2$, $\varkappa_3$ the direction cosines of the vector r_1 relative to the axes ξ, η, ζ. Then, from Figure 16.2,

$$\left.\begin{aligned}
r_1 &= r_1(\varkappa_1 i + \varkappa_2 j + \gamma_3 k), \\
r &= r(i\cos\vartheta + j\sin\vartheta), \\
S^0 &= i\cos\vartheta + j\sin\vartheta, \\
T^0 &= -i\sin\vartheta + j\cos\vartheta, \\
W^0 &= k,
\end{aligned}\right\} \tag{16.23}$$

where ϑ is the true anomaly of the position D.
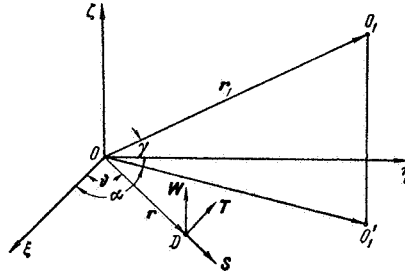
FIGURE 16.2. Resolution of perturbing acceleration along the satellite's orbital axes.

Let γ be the angle between the vector r_1 and its projection OO_1' on the orbital plane $\xi\eta$, and α the angle between this projection and the orbit's major axis $O\xi$ (see Figure 16.2). Clearly,

$$\left.\begin{aligned}
\varkappa_1 &= \cos\gamma\cos\alpha, \quad \varkappa_2 = \cos\gamma\sin\alpha, \\
\varkappa_3 &= \sin\gamma, \quad \cos\gamma = \sqrt{\varkappa_1^2 + \varkappa_2^2}.
\end{aligned}\right\} \tag{16.24}$$

Making use of (16.23) and (16.24), we find

$$
\left.\begin{aligned}
\boldsymbol{r}_1 \cdot \boldsymbol{r} &= r_1 r\, (\varkappa_1 \cos \vartheta + \varkappa_2 \sin \vartheta) = \\
&= r_1 r \cos \gamma \cos (\vartheta - \alpha), \\
\boldsymbol{r}_1 \cdot \boldsymbol{S}^0 &= r_1\, (\varkappa_1 \cos \vartheta + \varkappa_2 \sin \vartheta) = \\
&= r_1 \cos \gamma \cos (\vartheta - \alpha), \\
\boldsymbol{r}_1 \cdot \boldsymbol{T}^0 &= r_1\, (- \varkappa_1 \sin \vartheta + \varkappa_2 \cos \vartheta) = \\
&= - r_1 \cos \gamma \sin (\vartheta - \alpha), \\
\boldsymbol{r}_1 \cdot \boldsymbol{W}^0 &= r_1 \varkappa_3 = r_1 \sin \gamma, \\
\boldsymbol{r}_1 \cdot \boldsymbol{S}^0 &= r, \quad \boldsymbol{r} \cdot \boldsymbol{T}^0 = \boldsymbol{r} \cdot \boldsymbol{W}^0 = 0.
\end{aligned}\right\} \qquad (16.24\mathrm{a})
$$

Substituting in the first-order expression for the perturbing acceleration, (16.11), and applying relation (4.19), we find

$$
\left.\begin{aligned}
S &= f_{11} S^0 = g_1 \frac{r}{r_1}\, [3 \cos^2 \gamma \cos^2 (\vartheta - \alpha) - 1] = \\
&= 3 g_1 \frac{p}{r_1}\left(\beta_1 \cos^2\vartheta + 2\beta_3 \cos\vartheta \sin\vartheta + \beta_2 \sin^2\vartheta - \tfrac{1}{3}\right)\frac{1}{\Delta}, \\
T &= f_{11} T^0 = -3 g_1 \frac{r}{r_1}\cos^2 \gamma \cos (\vartheta - \alpha) \sin (\vartheta - \alpha) = \\
&= 3 g_1 \frac{p}{r_1}\, [(\beta_2 - \beta_1) \cos\vartheta \sin\vartheta + \beta_3 (\cos^2\vartheta - \sin^2\vartheta)]\frac{1}{\Delta}, \\
W &= f_{11} W^0 = 3 g_1 \frac{r}{r_1}\cos \gamma \sin \gamma \cos (\vartheta - \alpha) = \\
&= 3 g_1 \frac{p}{r_1}\, (\beta_4 \sin\vartheta + \beta_5 \cos\vartheta)\frac{1}{\Delta},
\end{aligned}\right\} \qquad (16.25)
$$

where p is the parameter of unperturbed orbit, and Δ, g_1, β_i ($i = 1, 2, \ldots, 5$) are defined by

$$
\left.\begin{aligned}
\Delta &= 1 + e \cos \vartheta, \quad g_1 = \frac{\mu_1}{r_1^2}, \\
\beta_1 &= \varkappa_1^2, \quad \beta_2 = \varkappa_2^2, \quad \beta_3 = \varkappa_1 \varkappa_2, \quad \beta_4 = \varkappa_2 \varkappa_3, \quad \beta_5 = \varkappa_1 \varkappa_3.
\end{aligned}\right\} \qquad (16.26)
$$

Note that g_1 is the magnitude of the acceleration imparted to the primary by the perturbing body.

In the following, we shall only consider satellites whose orbital period around the Earth is small in comparison with the period of the Moon, as well as with the period of the Earth's revolution around the Sun. For these satellites, the direction of the vector $\boldsymbol{r}_1$, to first approximation, is constant during one complete revolution around the Earth. In our determination of the change in the orbital elements during one circuit, the parameters $\varkappa_1$, $\varkappa_2$, $\varkappa_3$, α, and γ are therefore assumed constant. The problem with variable parameters is considered by M. L. Lidov /19/.

16.6. CIRCULAR ORBIT PERTURBATIONS DURING ONE CIRCUIT

In our analysis of motion in circular orbit of radius r, the axis $O\xi$ (Figure 16.2) points to some initial position D_0. The angle ϑ entering expressions (16.23) —(16.25) is then replaced with the angle φ reckoned from the point D_0. Expressions (16.25) are written in the form (3.5),

putting for the expansion coefficients

$$S_0 = g_1 \frac{r}{r_1} \left(\frac{3}{2} \cos^2 \gamma - 1 \right), \quad S_1 = 0,$$

$$S_2 = \frac{3}{2} g_1 \frac{r}{r_1} \cos^2 \gamma, \quad \varphi_{S_2} = \alpha - \frac{\pi}{4},$$

$$T_0 = T_1 = 0, \quad T_2 = \frac{3}{2} g_1 \frac{r}{r_1} \cos^2 \gamma, \quad \varphi_{T_2} = \alpha + \frac{\pi}{2}, \qquad (16.27)$$

$$W_0 = W_2 = 0, \quad W_1 = \frac{3}{2} g_1 \frac{r}{r_1} \sin 2\gamma, \quad \varphi_{W_1} = \alpha - \frac{\pi}{2}.$$

$$S_i = T_i = W_i = 0 \quad \text{for} \quad i \geqslant 3.$$

Comparing these expressions with the conclusions of Sec. 3.9, we see that the perturbations of circular orbit during one circuit alter the orbital period and rotate the orbital plane. The perturbation in orbital period is specified by the coefficients S_0 and T_2, and the orbit plane rotation is determined by the coefficient W_1.

The deviation ΔP of the real (sidereal) period from the unperturbed period is determined from (3.10) and (3.40), which give

$$\frac{\Delta P}{P} = \left(2 \frac{S_0}{g_0} + \frac{3}{2} \frac{T_2}{g_0} \cos 2\varphi_{T_2} \right),$$

where P is the period of revolution in unperturbed orbit. Hence, making use of (16.21) and (16.27), we find

$$\frac{\Delta P}{P} = \frac{\mu_1 r^3}{\mu_0 r_1^3} \left[3 \cos^2 \gamma \left(1 - \frac{3}{4} \cos 2\alpha \right) - 2 \right]. \qquad (16.28)$$

The corresponding displacement δl along the orbit, per one circuit of revolution, is given by

$$\frac{\delta l}{r} = - 2\pi \frac{\Delta P}{P}, \qquad (16.29)$$

which follows directly from (1.4) and (1.5).

From relations (3.34), (16.27) and Figure 16.2 we see that during one circuit, the orbital plane rotates about an axis which is the projection of the vector $r_1 = \overline{OO}_1$ on the orbital plane $\xi\eta$, i. e., about the axis OO_1' (Figure 16.2). If viewed from the tip O_1' of the projection, the plane appears to rotate counterclockwise for $\gamma > 0$ and clockwise for $\gamma < 0$.

The angle of rotation $\delta\psi$ during one circuit and the corresponding maximum lateral displacement δz are determined from (3.35) and (16.26), which give

$$\delta\psi = \frac{\delta z}{r} = \frac{3}{2} \pi \frac{\mu_1 r^3}{\mu_0 r_1^3} \sin 2\gamma. \qquad (16.30)$$

From (16.28) —(16.30) we see that the relative perturbations of orbital elements $\left(\frac{\Delta P}{P}, \frac{\delta l}{r}, \delta\psi = \frac{\delta z}{r} \right)$ increase in proportion to r^3. The absolute values of these perturbations increase even faster (δl and δz as r^4, and δP as $r^{9/2}$).

From (16.27) and (16.29) it follows that for constant r, the perturbations ΔP and δl are maximal at $\alpha = \pi/2$, $\gamma = 0$, whereas $\delta\psi$ and δz are maximal

299

for $\gamma = \pi/4$. Making use of (16.15), (16.16), (16.28), and (16.30), we find

$$
\left.\left|\frac{\Delta P}{P}\right|\right._{max} = 3.25 \frac{\mu_1 r^3}{\mu_0 r_1^3} = \frac{13}{8}\left.\left|\frac{f_{11}}{g_0}\right|\right._{max} ,
$$

$$
\left.\left|\frac{\delta l}{r}\right|\right._{max} = 6.5\pi \frac{\mu_1 r^3}{\mu_0 r_1^3} = 3.25\pi\left.\left|\frac{f_{11}}{g_0}\right|\right._{max} ,
$$
(16.31)

$$
\left.\left|\frac{\delta z}{r}\right|\right._{max} = \frac{3}{2}\pi \frac{\mu_1 r^3}{\mu_0 r_1^3} = \frac{3}{4}\pi\left.\left|\frac{f_{11}}{g_0}\right|\right._{max} ,
$$

where $\left.\left|\frac{f_{11}}{g_0}\right|\right._{max}$ is the maximum perturbing-to-normal accelerations ratio listed in Table 16.2.

Table 16.3 gives the peak perturbations ΔP, δl, δz, and $\delta\psi$ produced by the Moon's gravitational pull, as calculated from these formulas (to obtain the corresponding solar perturbations, the figures of Table 16.3 should be divided approximately by 2.2). We see from the table that for satellites flying in circular orbits at altitudes of a few thousands of kilometers and less, the lunisolar perturbations are negligible. At altitudes of the order of 10,000 km, these perturbations, however, become noticeable. Further increase of orbit height results in a steep rise of these perturbations, which eventually reach substantial magnitudes.

TABLE 16.3

Circular orbit height h, km	Maximum perturbations			
	ΔP, sec	δl, m	δz, m	$\delta\psi$, sec of arc
0	$9.1\cdot10^{-4}$	7.3	1.7	0.05
2,000	$3.2\cdot10^{-3}$	21	5	0.12
10,000	$6.3\cdot10^{-2}$	310	72	0.9
20,000	0.55	$2.1\cdot10^3$	490	3.8
50,000	16	$49\cdot10^3$	$10\cdot10^3$	38.0
100,000	290	$570\cdot10^3$	$130\cdot10^3$	250.0

16.7. ELLIPTICAL ORBIT PERTURBATIONS DURING ONE CIRCUIT

We calculate the elliptical orbit perturbations from the approximate relations (11.39). Making use of (11.28), we can write a similar approximate formula for the change in the semimajor axis during one circuit:

$$
\delta a = \frac{2a}{1-e^2}\int_0^{2\pi}\left(\frac{S}{g}e \sin\vartheta + \frac{T}{g}\frac{p}{r}\right)d\vartheta.
$$
(16.32)

In evaluating the right-hand sides of (11.39) and (16.32), we shall assume that the orbital elements and the vector r_1 remain constant during the particular circuit of revolution. Under these assumptions, applying

relations (4.19) and (16.25), we see that the problem reduces to integrals of the form

$$J_{nml} = \int_0^{2\pi} \frac{\cos^m \vartheta \sin^l \vartheta}{\Delta^n} \, d\vartheta,$$

where n, m, l are some positive integers, and $\Delta = \Delta(\vartheta) = \frac{p}{r}$ is determined from (16.26).

It is easily seen that $J_{nml} = 0$ for odd l (since in this case the integrand is an odd function of the angle ϑ). Thus, upon substituting (16.25) in (11.39) and (16.32), we find

$$\delta a = \frac{6a}{1-e^2} \frac{\mu_1 p^3}{\mu_0 r_1^3} \beta_3 \int_0^{2\pi} \left(2e \frac{\cos \vartheta \sin^2 \vartheta}{\Delta^3} + \frac{\cos^2 \vartheta - \sin^2 \vartheta}{\Delta^2} \right) d\vartheta,$$

$$\delta e = 3 \frac{\mu_1 p^3}{\mu_0 r_1^3} \beta_3 \int_0^{2\pi} \left[\frac{2 \cos \vartheta \sin^2 \vartheta}{\Delta^3} + \left(1 + \frac{1}{\Delta}\right) \frac{\cos \vartheta (\cos^2 \vartheta - \sin^2 \vartheta)}{\Delta^3} + e \frac{\cos^2 \vartheta - \sin^2 \vartheta}{\Delta^4} \right] d\vartheta,$$

$$\delta \Omega = 3 \frac{\mu_1 p^3}{\mu_0 r_1^3} \frac{1}{\sin i} \times \left(\beta_5 \sin \omega \int_0^{2\pi} \frac{\cos^2 \vartheta}{\Delta^4} \, d\vartheta + \beta_4 \cos \omega \int_0^{2\pi} \frac{\sin^2 \vartheta}{\Delta^4} \, d\vartheta \right),$$

$$\delta i = 3 \frac{\mu_1 p^3}{\mu_0 r_1^3} \left(\beta_5 \cos \omega \int_0^{2\pi} \frac{\cos^2 \vartheta}{\Delta^4} \, d\vartheta - \beta_4 \sin \omega \int_0^{2\pi} \frac{\sin^2 \vartheta}{\Delta^4} \, d\vartheta \right),$$

$$\delta \omega = 3 \frac{\mu_1 p^3}{\mu_0 r_1^3} \frac{1}{e} \left\{ -\beta_1 \int_0^{2\pi} \left[\left(1 + \frac{1}{\Delta}\right) \frac{\cos \vartheta \sin^2 \vartheta}{\Delta^3} + \right. \right.$$

$$\left. \left. + \frac{\cos^3 \vartheta}{\Delta^3} \right] d\vartheta + \beta_2 \int_0^{2\pi} \frac{\cos \vartheta \sin^2 \vartheta}{\Delta^4} \, d\vartheta + \frac{1}{3} \int_0^{2\pi} \frac{\cos \vartheta}{\Delta^3} \, d\vartheta \right\} - \delta \Omega \cos i. \tag{16.33}$$

We substitute $1 - \cos^2 \vartheta$ for $\sin^2 \vartheta$ in the right-hand sides and also apply expression (16.26) for Δ, which gives

$$\cos^m \vartheta = \left(\frac{\Delta - 1}{e} \right)^m. \tag{16.34}$$

The right-hand sides of (16.33) thus reduce to integrals of the form

$$J_n = \int_0^{2\pi} \frac{d\vartheta}{\Delta^n(\vartheta)} \qquad (n = 0, 1, 2, 3, 4).$$

We now make use of the well-known formulas /25/

$$\int \frac{d\vartheta}{1 + e \cos \vartheta} = \frac{2}{\sqrt{1 - e^2}} \arctan \sqrt{\frac{1 - e}{1 + e}} \tan \frac{\vartheta}{2},$$

$$\int \frac{d\vartheta}{(1 + e \cos \vartheta)^n} = \frac{1}{(n-1)(1-e^2)} \left[-\frac{e \sin \vartheta}{(1 + e \cos \vartheta)^{n-1}} + \right.$$

$$\left. + (2n - 3) \int \frac{d\vartheta}{(1 + e \cos \vartheta)^{n-1}} - (n - 2) \int \frac{d\vartheta}{(1 + e \cos \vartheta)^{n-2}} \right].$$

Then

$$J_1 = \frac{2\pi}{(1 - e^2)^{1/2}}, \tag{16.35}$$

$$J_n = \frac{2n - 3}{(n-1)(1-e^2)} J_{n-1} - \frac{n-2}{(n-1)(1-e^2)} J_{n-2}. \tag{16.36}$$

From the recursion formula (16.36) and from equality (16.35), we find

$$
\left.\begin{array}{l}
J_2 = \dfrac{2\pi}{(1-e^2)^{5/2}}, \\[2mm]
J_3 = \dfrac{\pi\,(2+e^2)}{(1-e^2)^{5/2}}, \\[2mm]
J_4 = \dfrac{\pi\,(2+3e^2)}{(1-e^2)^{7/2}}.
\end{array}\right\}
\qquad (16.37)
$$

Making use of (16.34) and (16.37), we reduce equalities (16.33) to final expressions for the perturbations of orbital elements during one circuit:

$$
\left.\begin{array}{l}
\delta a = 0, \\[2mm]
\delta e = -\,15\pi\dfrac{\mu_1}{\mu_0}\left(\dfrac{a}{r_1}\right)^3 e\,\sqrt{1-e^2}\,\beta_3, \\[2mm]
\delta\Omega = 3\pi\dfrac{\mu_1}{\mu_0}\left(\dfrac{a}{r_1}\right)^3 \dfrac{1}{\sqrt{1-e^2}\,\sin i}\,[(1+4e^2)\,\beta_5\sin\omega + \\[2mm]
\qquad\qquad\qquad\qquad\qquad + (1-e^2)\,\beta_4\cos\omega], \\[2mm]
\delta i = 3\pi\dfrac{\mu_1}{\mu_0}\left(\dfrac{a}{r_1}\right)^3 \dfrac{1}{\sqrt{1-e^2}}\,[(1+4e^2)\,\beta_5\cos\omega - \\[2mm]
\qquad\qquad\qquad\qquad\qquad - (1-e^2)\,\beta_4\sin\omega], \\[2mm]
\delta\omega = 3\pi\dfrac{\mu_1}{\mu_0}\left(\dfrac{a}{r_1}\right)^3 \sqrt{1-e^2}\,(4\beta_1-\beta_2-1)-\delta\Omega\,\cos i.
\end{array}\right\}
\qquad (16.38)
$$

In deriving these formulas, we retained only the first term in the expansion (16.10) of the perturbing acceleration and neglected the variation in the vector r_1 during one revolution of the satellite. In calculating the effect of the lunar pull for comparatively low-flying Earth satellites (with orbit heights of some $50{,}000-100{,}000$ km), either of these assumptions involves a considerable inaccuracy. Higher precision can be achieved by using M. L. Lidov's formulas, which have been derived on the basis of second-order expressions, assuming a variable r_1 /19/.

16.8. AN ANALYSIS OF ELLIPTICAL ORBIT PERTURBATIONS DURING ONE CIRCUIT

From (16.38) we see that, as a first approximation, the semimajor axis is free from secular perturbations $(\delta a = 0)$. This is a direct consequence of our assumption that the vector r_1 and the orbital elements are all constant. Indeed, in this case the motion is in a conservative field of force, so that the total mechanical energy of the satellite in orbit is conserved. Upon completing one revolution around the Earth, the satellite returns to its initial position (the orbital elements being constant), so that its flight velocity also remains constant. Hence, making use of (5.15), we find $\delta a = 0$. Lidov /19/ has shown that this equality does not apply if the vector r_1 is variable. However, calculations show that for the artificial Earth satellites under consideration, the increment δa is small in comparison with the variations in other orbital elements.

The increments δe, δi, and $\delta\Omega$ derived in the previous section are related by an additional expression. If the perturbing body is fixed in space, the projection of the angular momentum vector L of the space vehicle about the

point O on the direction $r_1 = \overline{OO_1}$ is constant in time. Indeed, putting L_1 for this projection, we have

$$L_1 = r_1^0 \cdot (r \times \dot{r}), \quad \dot{L_1} = r_1^0 \cdot (r \times \ddot{r}),$$

where r_1^0 is the unit vector along r_1. On the other hand, from (16.4) we have that for $n = 1$ and $F = F_0 = 0$,

$$\ddot{r} = Ar + Br_1,$$

where A and B are some scalar factors. Substituting this equality in the expression for $\dot{L_1}$, we find

$$\dot{L_1} = 0, \quad L_1 = \text{const.}$$

Making use of (4.4) and (5.10), we write the following expression for the magnitude of the angular momentum vector:

$$L = |r \times v| = c = \sqrt{\mu p} = \sqrt{\mu a (1 - e^2)}.$$

Since the angular momentum vector L is perpendicular to the orbital plane, i.e., points along the axis $O\zeta$, we have

$$L_1 = L \varkappa_3 = \varkappa_3 \sqrt{\mu a (1 - e^2)} = \text{const.}$$

Seeing that $\delta a = 0$, we write

$$-\varkappa_3 \frac{e\, \delta e}{1 - e^2} + \delta \varkappa_3 = 0. \tag{16.39}$$

To find an expression for $\delta \varkappa_3$, we make use of the nonrotating frame $Oxyz$ depicted in Figure 1.2. The matrix of the direction cosines for the axes x, y, z and ξ, η, ζ is given in Sec. 5.5. Let $\|A\|$ denote this matrix. Then

$$\begin{Vmatrix} \varkappa_1 \\ \varkappa_2 \\ \varkappa_3 \end{Vmatrix} = \|A\|^* \begin{Vmatrix} \alpha_1 \\ \alpha_2 \\ \alpha_3 \end{Vmatrix}, \tag{16.40}$$

$$\begin{Vmatrix} \alpha_1 \\ \alpha_2 \\ \alpha_3 \end{Vmatrix} = \|A\| \begin{Vmatrix} \varkappa_1 \\ \varkappa_2 \\ \varkappa_3 \end{Vmatrix}, \tag{16.41}$$

where α_1, α_2, α_3 are the cosines of the angles between the vector r_1 and the axes x, y, z, and $\|A\|^*$ is the transpose of the matrix $\|A\|$. Hence, if the vector r_1 is fixed in the frame $Oxyz$ ($\alpha_1 = \text{const}$, $\alpha_2 = \text{const}$, $\alpha_3 = \text{const}$), we find

$$\left. \begin{aligned} \varkappa_3 &= \alpha_1 \sin \Omega \sin i - \alpha_2 \cos \Omega \sin i + \alpha_3 \cos i, \\ \delta \varkappa_3 &= (\alpha_1 \cos \Omega \sin i + \alpha_2 \sin \Omega \sin i)\delta \Omega + \\ &\quad + (\alpha_1 \sin \Omega \cos i - \alpha_2 \cos \Omega \cos i - \alpha_3 \sin i)\delta i. \end{aligned} \right\} \tag{16.41a}$$

Substituting α_1, α_2, α_3, we find

$$\delta \varkappa_3 = (\varkappa_1 \cos \omega - \varkappa_2 \sin \omega)\delta \Omega \sin i - (\varkappa_1 \sin \omega + \varkappa_2 \cos \omega)\delta i, \tag{16.42}$$

whence, applying (16.39), we finally write

$$-\varkappa_3 \frac{e\,\delta e}{1-e^2} + (\varkappa_1 \cos\omega - \varkappa_2 \sin\omega)\delta\Omega \sin i - (\varkappa_1 \sin\omega + \varkappa_2 \cos\omega)\delta i = 0. \qquad (16.43)$$

Equality (16.43) is useful for verifying the results of a numerical calculation of $\delta e, \delta\Omega, \delta i$. Its validity can be established by substituting (16.38) in (16.43).

In particular, for circular orbit $(e=0)$, relation (16.39) takes the form $\delta\varkappa_3 = 0$. In other words, the change in the orientation of the orbital plane during one circuit reduces to its rotation around the vector $r_1 = \overline{OO_1}$. If this rotation is small, it can be resolved into two component rotations: around the normal to the orbital plane and around the projection of the vector r_1 on that plane. The former does not alter the orientation of the orbital plane, and the latter is equivalent to the rotation of the circular orbit plane derived in Sec. 16.6.

We now determine the position of the axis of rotation of the orbital plane in a general case. We introduce an angle χ, defined by

$$\begin{aligned}
\cos\chi &= \frac{(1+4e^2)\,\beta_5}{\sqrt{(1+4e^2)^2\,\beta_5^2 + (1-e^2)^2\,\beta_4^2}}, \\
\sin\chi &= \frac{(1-e^2)\,\beta_4}{\sqrt{(1+4e^2)^2\,\beta_5^2 + (1-e^2)^2\,\beta_4^2}}.
\end{aligned} \right\} \qquad (16.44)$$

Then expressions (16.38) for $\delta\Omega$ and δi can be written as

$$\begin{aligned}
\delta\Omega &= \frac{\sin(\omega+\chi)}{\sin i}\,\delta\psi, \quad \delta i = \cos(\omega+\chi)\,\delta\psi, \\
\delta\psi &= 3\pi\frac{\mu_1}{\mu_0}\left(\frac{a}{r_1}\right)^3 \frac{\sqrt{(1+4e^2)^2\,\beta_5^2 + (1-e^2)^2\,\beta_4^2}}{\sqrt{1-e^2}}.
\end{aligned} \right\} \qquad (16.45)$$

Making use of (9.53), we find that this perturbation of the orbital plane produces rotation through an angle $\delta\psi$ around an axis in the orbital plane, which makes an angle χ with the major axis $O\xi$.

From (16.24) and (16.26) we find that for $e \to 0$, the angle χ approaches the angle α between the axis $O\xi$ and the projection of the vector r_1 on the orbital plane. The expression for the angle of rotation $\delta\psi$ reduces to the corresponding equality for circular orbit, (16.30).

For $e \to 1$, $\chi \to 0$. In other words, the plane of highly-elongated elliptical orbits rotates around an axis which is close to $O\xi$. The angle of rotation $\delta\psi$ sharply increases as the eccentricity approaches unity (since $\sqrt{1-e^2} \to 0$).

The variation of perigee height h_p is of considerable significance in some problems. In particular, for low-perigee orbits, a substantial change in the perigee height h_p may result in termination of satellite's life. To find the change δh_p in perigee height during one revolution, we make use of (5.3), (16.24), (16.25), and (16.38), which give

$$\delta h_\mathrm{p} = \delta r_\mathrm{p} = -a\,\delta e = \frac{15}{2}\,\pi\,\frac{\mu_1}{\mu_0}\left(\frac{a}{r_1}\right)^3 e\,\sqrt{1-e^2}\,\cos^2\gamma\,\sin 2\alpha. \qquad (16.46)$$

We see from this formula that the perigee height increases when the projection of the vector r_1 on the orbital plane $\xi\eta$ is in the first or the third quadrant $(0 < \alpha < \pi/2$ or $\pi < \alpha < 3\pi/2)$ and decreases if this projection

is in the second or the fourth quadrant $(\pi/2 < a < \pi$ or $3\pi/2 < a < 2\pi)$. The maximum perturbation $|\delta h_p|_{max}$ is attained for $\gamma = 0$, $a = \pi/4 + n\pi/2$ (where n is an integer).

Table 16.4 lists the values of $|\delta h_p|_{max}$ attributable to the lunar pull for various perigee and apogee heights of the orbit (to obtain the corresponding solar perturbations, the figures of Table 16.4 should be divided approximately by 2.2). We see from the table that for the relevant satellites the variation δh_p is fairly insensitive to the minimum flying height h_p, and is principally determined by the maximum flight altitude h_a (excepting the case $h_p \to h_a$, when $\delta h_p \to 0$). For satellites orbiting at heights of a few thousands of kilometers and less, δh_p is small (a few meters). As h_a increases, this perturbation steeply rises, reaching a few kilometers or even tens of kilometers for $h_a = 50,000 - 100,000$ km.

TABLE 16.4.

h_p, km $\backslash$ h_a, km	200	2,000	10,000	20,000	50,000
2,000	2.5 m	0	—	—	—
10,000	34 m	37 m	0	—	—
20,000	181 m	206 m	243 m	0	—
50,000	2.4 km	2.8 km	4.1 km	5.1 km	0
100,000	21.5 km	24.6 km	36.2 km	47.7 km	65.5 km

To first approximation, these perturbations during one circuit alter the position and the height of the perigee point (the semimajor axis of the orbit remaining constant), and also rotate the orbital plane around some axis in that plane. All perturbations are proportional in magnitude to

$$\frac{\mu_1}{\mu_0}\left(\frac{a}{r_i}\right)^3.$$

Moreover, for $e \ll 1$, the perturbation δe is proportional to the eccentricity e, and the perturbation in perigee height is proportional to the linear eccentricity $ae = \frac{h_a - h_p}{2}$.

In addition to the above perturbations of orbital elements, there is also a certain deviation of the actual orbital period from the unperturbed period (see Sec. 16.6). This deviation of course leads to a growing discrepancy in the satellite's positions in actual and unperturbed orbits.

16.9. ELLIPTICAL ORBIT PERTURBATIONS DURING SEVERAL REVOLUTIONS

Let $q_j(j = 1, 2, \ldots, 6)$ be the orbital elements ($q_1 = a$. $q_2 = e$, $q_3 = i$, $q_4 = \omega$, $q_5 = \Omega$, $q_6 = r_p$). Expressions (16.38) for the perturbations in these elements during one revolution can be written as

$$\delta q_j = \sum_{k=0}^{5} \beta_k F_{jk}(q_1, q_2, q_3, q_4), \tag{16.47}$$

305

where the coefficients β_k $(k = 0, 1, 2, \ldots, 5)$ are defined by (16.26) $(\beta_0 = 1)$, and F_{jk} $(j = 1, 2, \ldots, 6;$ $k = 0, 1, 2, \ldots 5)$ are some functions of the orbital elements q_j.

We see from Tables 16.3 and 16.4 that the perturbations δq_j are comparatively small. Therefore, to first approximation, the orbital elements q_j can be assumed constant during several revolutions of the satellite around the Earth, and we put $F_{jk} = \mathrm{const}$. The coefficients β_k, however, are highly variable due to the comparatively fast motion of the perturbing body relative to the Earth. Hence it follows that the variation of the orbital elements in n circuits can be determined from formulas of the form

$$\Delta q_j = \sum_{k=0}^{5} F_{jk} \sum_{l=1}^{n} \beta_{kl}, \tag{16.48}$$

where l is the current circuit number, and β_{kl} are the values of the coefficients β_k during that circuit.

To calculate the sums $\sum_{k=1}^{n} \beta_{kl}$, we make use of the fact that the coefficients β_k vary smoothly from circuit to circuit, so that summation can be replaced with integration:

$$\sum_{l=1}^{n} \beta_{kl} = \frac{1}{P} \sum_{l=1}^{n} \beta_{kl} P \approx \frac{1}{P} \int_{0}^{t} \beta_k \, dt, \tag{16.49}$$

where P is the period of revolution around the Earth, and $t = nP$ the flight time. We obtain the following expressions for the perturbations of orbital elements during several circuits:

$$\Delta q_j = \frac{1}{P} \sum_{k=0}^{5} F_{jk} \int_{0}^{t} \beta_k \, dt, \tag{16.50}$$

where F_{jk} (a, e, i, ω) are the multipliers of β_k in expressions (16.38) for δq_j.

In determining the time-dependence of the coefficients β_k, we assume that the perturbing bodies (the Sun and the Moon) describe circular orbits around the Earth, moving with constant angular velocities. The principal characteristics of these orbits (the radius r_1, the orbital period P_1, the angular velocity of revolution around the Earth λ_1, and the coefficient μ) have the following numerical values:

$$\left. \begin{array}{l} r_\odot = 149.6 \cdot 10^6 \, \mathrm{km}, P_\odot = 365.26 \, \mathrm{s. \, d}, \lambda_\odot = \dfrac{2\pi}{P_\odot}, \\[2mm] \mu_\odot = 3.33 \cdot 10^5 \mu_0, \ r_{\mathbb{C}} = 384\,000 \, \mathrm{km}, \\[2mm] P_{\mathbb{C}} = 27.32 \, \mathrm{s. \, d}, \ \lambda_{\mathbb{C}} = \dfrac{2\pi}{P_{\mathbb{C}}}, \ \mu_{\mathbb{C}} = \dfrac{\mu_0}{81.3}. \end{array} \right\} \tag{16.51}$$

Here $\odot$ denotes the parameters of the Sun, and $\mathbb{C}$ the parameters of the Moon; μ_0 is the gravitational acceleration of the Earth, from (12.12).

Note that the results obtained in the following can be generalized to the case of perturbing bodies which describe elliptical orbits $/19/$.

306

We introduce a right-hand rectangular system of axes $Oxyz$, with its origin at the Earth's center O. The axis Ox points to the perturbing body O_1, so that the plane Oxy coincides with the orbital plane of the perturbing body, and the axis Oz is directed at right angles to this orbital plane (to the north). The orientation of the orbital plane and the position of the perigee point are defined by the inclination i, the longitude of the ascending node Ω, and the argument of the perigee ω, which are all reckoned from the plane Oxy and the line Ox (Figure 16.3).
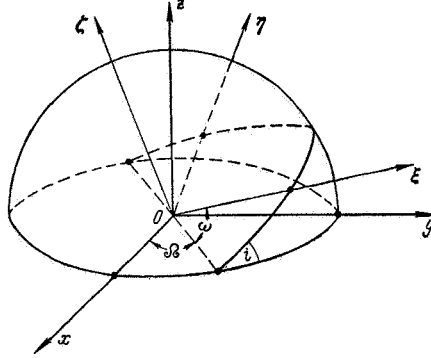
FIGURE 16.3. Transformation from the coordinates $Oxyz$ connected with the mutual disposition of the attracting bodies O and O_1 to the coordinates $O\xi\eta\zeta$ connected with the satellite's orbit.

It follows from our assumptions that in calculating the right-hand side of (16.50) we may take

$$\omega = \text{const}, \quad i = \text{const}, \quad \Omega = \Omega_0 - \lambda_1 t, \qquad (16.52)$$

where Ω_0 is the initial longitude Ω, and λ_1 is the angular velocity of the perturbing body in its relative orbit, from (16.51).

From Figure 16.3 we see that the angles Ω, i, ω specify the orientation of the axes $O\xi\eta\zeta$ relative to the frame $Oxyz$. The matrix of the corresponding direction cosines is given in Sec. 5.5. Since the vector $r_1 = \overline{OO_1}$ points along the axis Ox, then, applying this matrix, we write the following expressions for the direction cosines of r_1 relative to the frame $O\xi\eta\zeta$:

$$\left. \begin{array}{l} \varkappa_1 = \cos \Omega \cos \omega - \sin \Omega \cos i \sin \omega, \\ \varkappa_2 = -\cos \Omega \sin \omega - \sin \Omega \cos i \cos \omega, \\ \varkappa_3 = \sin \Omega \sin i. \end{array} \right\} \qquad (16.53)$$

Hence, making use of (16.26) and (16.52), we find that the expressions for β_k ($k = 0, 1, 2, \ldots, 5$) are sums of products of $\sin^2 \Omega$, $\cos^2 \Omega$, and $\sin \Omega \cos \Omega$ by some functions of the angles ω and i. Expressing $\sin^2 \Omega$, $\cos^2 \Omega$ and $\sin \Omega \cos \Omega$ in terms of $\sin 2\Omega$ and $\cos 2\Omega$ and applying equalities (13.19 a) and (16.52), we write

$$\beta_k = \beta_{k0} + \beta_{k2} \sin 2\lambda_1 (t - t_k), \qquad (16.54)$$

307

where β_{k0}, β_{k2}, t_k are some functions of ω, i, Ω_0. Substituting these equalities in (16.50) and seeing that $\Delta q_j = 0$ for $t = 0$, we obtain the following expression for the perturbations of orbital elements:

$$\Delta q_j = t\,\Delta q_{j0} + \Delta q_{j2}\,[\sin 2\,(\lambda_1 t - \Omega_j) + \sin 2\Omega_j], \qquad (16.55)$$

where Δq_{j0}, Δq_{j2}, Ω_j are some functions of a, e, ω, i, Ω_0.

The first term in the right-hand side of (16.55) clearly represents secular perturbations, while the second term corresponds to long-periodic perturbations of orbital elements. The frequency of the long-periodic perturbations is $2\lambda_1$ and their period is $P_1/2$, where P_1 is the period of revolution of the perturbing body relative to the Earth.

Lunisolar perturbations are thus reduced, in the first approximation, to the following effects:

(i) secular perturbations which are proportional to the flight time t;

(ii) long-periodic solar perturbations with a period $\dfrac{P_\odot}{2} = 182.63$ s. d.;

(iii) long-periodic lunar perturbations with a period $\dfrac{P_{\mathbb{C}}}{2} = 13.66$ s. d.

There are also short-period perturbations, whose frequency is a multiple of the satellite's orbital frequency.

All the foregoing is meaningful only if the orbital elements remain fairly constant during half a revolution of the perturbing body around the Earth. Moreover, it must be kept in mind that the rate of secular perturbations varies in time. In many cases, these are long-periodic variations /19/.

16.10. SECULAR PERTURBATIONS OF ORBITAL ELEMENTS

The mean rate of a secular perturbation is taken as the magnitude of a corresponding perturbation during one revolution of the satellite around the Earth, $\overline{\delta q_j}$. Clearly,

$$\overline{\delta q_j} = P\,\Delta q_{j0}.$$

Applying expression (16.52) for Ω, we write relation (16.55) in the form

$$\Delta q_j = \frac{\Omega_0 - \Omega}{\lambda_1 P}\,\overline{\delta q_j} + \Delta q_{j2}\,[\sin 2\,(\Omega_0 - \Omega_j - \Omega) + \sin 2\Omega_j]. \qquad (16.56)$$

On the other hand, from (16.50) and (16.52) we have

$$\Delta q_j = -\frac{1}{P\lambda_1}\sum_{k=0}^{5} F_{ik} \int_{\Omega_0}^{\Omega} \beta_k\,d\Omega. \qquad (16.57)$$

Equating the right-hand sides of (16.56) and (16.57) and putting $\Omega = \Omega_0 + \pi$, we find

$$\overline{\delta q_j} = \frac{1}{\pi}\sum_{k=0}^{5} F_{jk} \int_{\Omega_0}^{\Omega_0 + \pi} \beta_k\,d\Omega.$$

308

Hence, making use of (16.54), we have

$$\overline{\delta q}_j = \sum_{k=0}^{5} F_{jk} \beta_{k0}.$$ (16.58)

The mean rates $\overline{\delta q}_j$ can thus be obtained from (16.38) upon substituting β_{k0} for β_k. The coefficients β_{k0} are calculated from (16.26), (16.53), and (16.54), which give

$$\left. \begin{aligned} \beta_{00} &= 1, \\ \beta_{10} &= \frac{1}{2}(\cos^2 \omega + \cos^2 i \sin^2 \omega), \\ \beta_{20} &= \frac{1}{2}(\sin^2 \omega + \cos^2 i \cos^2 \omega), \\ \beta_{30} &= -\frac{1}{4}\sin^2 i \sin 2\omega, \\ \beta_{40} &= -\frac{1}{4}\sin 2i \cos \omega, \\ \beta_{50} &= -\frac{1}{4}\sin 2i \sin \omega. \end{aligned} \right\}$$ (16.59)

From (16.38), (16.46), (16.58), and (16.59) we obtain the following expressions for secular perturbations per one circuit:

$$\left. \begin{aligned} \overline{\delta a} &= 0, \\ \overline{\delta e} &= \frac{15}{4}\pi \frac{\mu_1}{\mu_0} \left(\frac{a}{r_1}\right)^3 e \sqrt{1-e^2} \sin^2 i \sin 2\omega, \\ \overline{\delta \Omega} &= -\frac{3}{2}\pi \frac{\mu_1}{\mu_0} \left(\frac{a}{r_1}\right)^3 \frac{\cos i}{\sqrt{1-e^2}}(1-e^2+5e^2 \sin^2 \omega), \\ \overline{\delta i} &= -\frac{15}{8}\pi \frac{\mu_1}{\mu_0} \left(\frac{a}{r_1}\right)^3 \frac{e^2}{\sqrt{1-e^2}}\sin 2i \sin 2\omega, \\ \overline{\delta \omega} &= \frac{3}{2}\pi \frac{\mu_1}{\mu_0} \left(\frac{a}{r_1}\right)^3 \frac{1}{\sqrt{1-e^2}} \times [5\cos^2 i \sin^2 \omega + (1-e^2)(2-5\sin^2 \omega)], \\ \overline{\delta h}_p &= -\frac{15}{4}\pi \frac{\mu_1}{\mu_0} \left(\frac{a}{r_1}\right)^3 ae \sqrt{1-e^2} \sin^2 i \sin 2\omega. \end{aligned} \right\}$$ (16.60)

These expressions enable us to proceed with an analysis of the secular orbit perturbations. For any given perturbing body, the perturbations are seen to depend entirely on the orbital elements a, e, i, ω of the satellite, being independent of the node position Ω, or of the epoch of nodal passage t_Ω (we recall that i, ω, Ω, t_Ω are measured in rotating frame $Oxyz$ connected with the position of the perturbing body relative to the Earth). Moreover, if the semimajor axis a changes, the variations in all the orbital elements are proportional to a^3. In other words, the rate of secular evolution of the orbit is altered, but its trend remains as before. The trend of the secular orbit evolutions is thus specified by the elements e, i, ω.

In particular, the perigee height h_p grows secularly if the perigee point is in the second or the fourth quadrant of the orbit (the quadrants are reckoned from the epoch of south-north passage of the satellite through the orbital plane of the perturbing body), i.e., if $\pi/2 < \omega < \pi$ or $3\pi/2 < \omega < 2\pi$; the perigee height displays a secular contraction if the perigee point is in the first or the third quadrant of the orbit, i.e., if $0 < \omega < \pi/2$ or $\pi < \omega < 3\pi/2$. If we examine the family of all orbits with constant perigee and apogee heights, h_p and h_a, and various angles ω and i, the maximum secular perturbation $|\overline{\delta h}_p|_{max}$ is recorded for $i = \pi/2$, $\omega = \pi/4 + n\pi/2$, where n is an integer. Comparison of (16.46) and (16.60) shows that

$$|\overline{\delta h}_p|_{max} = \frac{1}{2}|\delta h_p|_{max}.$$

Table 16.4 can therefore be applied to estimate the dependence of $|\overline{\delta h}_\text{p}|_\text{max}$ on the maximum and the minimum flight altitudes. The values of $|\delta h_\text{p}|_\text{max}$ from that table should be divided by 2 to obtain the corresponding estimates.

16.11. LONG-PERIOD PERTURBATIONS
OF ECCENTRICITY AND PERIGEE HEIGHT

Of the long-period orbit evolutions discussed in Sec. 16.9, we shall only analyze the variations in the eccentricity e and in the perigee height h_p, since these perturbations are highly significant in the solution of some applied problems (e. g., determination of satellite lifetimes). The techniques of this section can be successfully applied to the analysis of long-period perturbations in other orbital elements.

From (16.38), (16.46), (16.47), and (16.57) we see that the problem reduces to the evaluation of the integral

$$\int_{\Omega_0}^{\Omega} \beta_3 \, d\Omega.$$

Making use of (16.26) and (16.53), we find

$$\left. \begin{aligned} \beta_3 &= -\frac{\sin^2 i \sin 2\omega}{4} + \tilde{\beta}_3, \\ \tilde{\beta}_3 &= -\frac{1}{4}[(1 + \cos^2 i)\sin 2\omega \cos 2\Omega + 2\cos i \cos 2\omega \sin 2\Omega]. \end{aligned} \right\} \quad (16.61)$$

The first term in the right-hand side of the expression for β_3 represents the previously considered secular perturbations. In the analysis of long-period perturbations, we may therefore substitute $\tilde{\beta}_3$ for β_3 in (16.57). Thus,

$$\int \tilde{\beta}_3 \, d\Omega = \frac{1}{8}[2\cos i \cos 2\omega \cos 2\Omega - (1+\cos^2 i)\sin 2\omega \sin 2\Omega].$$

We introduce the parameters D and φ, defined by the equalities

$$\left. \begin{aligned} D &= \sqrt{4\cos^2 i \cos^2 2\omega + (1 + \cos^2 i)^2 \sin^2 2\omega}, \\ \cos\varphi &= \frac{2\cos i \cos 2\omega}{D}, \quad \sin\varphi = \frac{(1 + \cos^2 i)\sin 2\omega}{D}. \end{aligned} \right\} \quad (16.62)$$

Now,

$$\int \tilde{\beta}_3 \, d\Omega = \frac{D}{8}\cos(2\Omega + \varphi).$$

Hence

$$\int_{\Omega_0}^{\Omega} \tilde{\beta}_3 \, d\Omega = \frac{D}{8}[\cos(2\Omega + \varphi) - \cos(2\Omega_0 + \varphi)].$$

Making use of (16.38), (16.46), (16.47), and (16.57), we may write

$$
\left.\begin{array}{l}
\tilde{\delta e} = \frac{15}{16} C(a) D(\omega, i) e \sqrt{1-e^2} \left[\cos(2\Omega + \varphi) - \cos(2\Omega_0 + \varphi)\right], \\[2mm]
\delta h_{\mathrm{p}} = -a\, \tilde{\delta e}, \\[2mm]
C(a) = \frac{\mu_1}{\mu_0} \left(\frac{a}{r_1}\right)^3 \frac{P_1}{P} = \frac{\mu_1}{2\pi \sqrt{\mu_0}} \frac{a^{3/2}}{r_1^3} P_1.
\end{array}\right\}
\qquad (16.63)
$$

Here $\tilde{\delta e}$ and δh_{p} are the long-period perturbations, P and P_1 are the orbital periods of the satellite and of the perturbing body relative to the Earth, and the element Ω is determined from (16.51) and (16.52).

As a fairly accurate approximation, the orbital period of the perturbing body can be calculated from the equality /2/

$$
P_1 = 2\pi \frac{r_1^{3/2}}{\sqrt{\mu_0 + \mu_1}}.
$$

Hence, seeing that $\mu_\odot \gg \mu_0$, we may write approximate expressions for the orbital periods of the Sun and the Moon about the Earth:

$$
P_\odot \approx 2\pi \frac{r_\odot^{3/2}}{\sqrt{\mu_\odot}}, \qquad
P_{\mathbb{C}} \approx 2\pi \frac{r_{\mathbb{C}}^{3/2}}{\sqrt{\mu_0 + \mu_{\mathbb{C}}}}.
$$

Substituting in (16.33), we find the following expressions for the coefficient C of lunisolar perturbations:

$$
C_\odot = \frac{P}{P_\odot}, \qquad
C_{\mathbb{C}} = \frac{\mu_{\mathbb{C}}}{\mu_0 + \mu_{\mathbb{C}}} \frac{P}{P_{\mathbb{C}}} = \frac{1}{82.3} \frac{P}{P_{\mathbb{C}}}.
\qquad (16.64)
$$

Let E and H be the amplitudes of the long-periodic perturbations in the eccentricity and the perigee height, respectively. From (16.63) we have

$$
E = \frac{15}{16} C(a) D(\omega, i) e \sqrt{1-e^2}, \quad H = aE.
\qquad (16.65)
$$

Making use of (16.62), we can show that the coefficient $D(\omega, i)$ is maximal when $i = \omega = 0$, its peak value being

$$
D_{\max} = 2.
\qquad (16.66)
$$

Now, from (16.64) we obtain expressions for the peak amplitudes of the long-periodic lunisolar perturbations:

$$
\left.\begin{array}{l}
E_{\odot\,\max} = \frac{15}{8} \frac{P}{P_\odot} e \sqrt{1-e^2}, \\[2mm]
H_{\odot\,\max} = \frac{15}{8} \frac{P}{P_\odot} ae \sqrt{1-e^2}, \\[2mm]
E_{\mathbb{C}\,\max} = \frac{15}{8} \frac{P}{82.3 P_{\mathbb{C}}} e \sqrt{1-e^2}, \\[2mm]
H_{\mathbb{C}\,\max} = \frac{15}{8} \frac{P}{82.3 P_{\mathbb{C}}} ae \sqrt{1-e^2}.
\end{array}\right\}
\qquad (16.67)
$$

311

Inserting for $P_\odot$ and $P_{\mathbb{C}}$ their numerical values from (16.51), we obtain the ratio of the peak amplitudes of the lunar and the solar perturbations:

$$\frac{H_{\odot\,max}}{H_{\mathbb{C}\,max}} = \frac{E_{\odot\,max}}{E_{\mathbb{C}\,max}} = \frac{82.3P_{\mathbb{C}}}{P_\odot} \approx 6.16. \tag{16.68}$$

The peak amplitudes of the long-periodic solar perturbations are thus approximately 6.16 times as large as the amplitudes of the corresponding lunar perturbations. We recall that the maximum solar perturbations during one circuit (as well as the maximum secular solar perturbations) are approximately 1/2.18 of the corresponding lunar perturbations.

Table 16.5 lists the peak amplitudes of the solar perturbations, $E_{\odot\,max}$, $H_{\odot\,max}$, calculated for various perigee and apogee heights, h_p and h_a. The "numerator" of each fraction is the $E_{\odot\,max}$, and the "denominator" is the $H_{\odot\,max}$, in kilometers. We see from the table that the maximum amplitudes of the long-periodic solar perturbations are mainly determined by the apogee height h_a and are fairly insensitive to the perigee altitude h_p (except when $h_p \to h_a$, giving $H_{max} \to 0$, $E_{max} \to 0$). For satellites with apogee heights $h_a > 10^5$ km, the peak amplitude of apogee and perigee height fluctuations is quite substantial (of the order of tens and hundreds of kilometers).

TABLE 16.5

Apogee height h_a, km	Perigee height h_p, km				
	200	2,000	10,000	20,000	50,000
2,000	$\dfrac{5.1 \cdot 10^{-5}}{0.4}$	0	—	—	—
10,000	$\dfrac{2.8 \cdot 10^{-4}}{3.2}$	$\dfrac{2.5 \cdot 10^{-4}}{3.1}$	0	—	—
20,000	$\dfrac{6.0 \cdot 10^{-4}}{10.0}$	$\dfrac{6.0 \cdot 10^{-4}}{10.5}$	$\dfrac{4.2 \cdot 10^{-4}}{9.0}$	0	—
50,000	$\dfrac{1.6 \cdot 10^{-3}}{51}$	$\dfrac{1.7 \cdot 10^{-3}}{56}$	$\dfrac{1.9 \cdot 10^{-3}}{69}$	$\dfrac{1.7 \cdot 10^{-3}}{70}$	0
100,000	$\dfrac{3.3 \cdot 10^{-3}}{187}$	$\dfrac{3.6 \cdot 10^{-3}}{208}$	$\dfrac{4.5 \cdot 10^{-3}}{277}$	$\dfrac{4.9 \cdot 10^{-3}}{325}$	$\dfrac{4.0 \cdot 10^{-3}}{329}$

The maximum change in perigee (or apogee) height due to long-periodic perturbations is

$$\widetilde{\Delta h}_{max} = 2H_{max}. \tag{16.69}$$

This change occurs during one quarter of revolution of the perturbing body around the Earth $(t = P_1/4)$.

Making use of (16.60), (16.63), and (16.66), we find the maximum secular variation of the perigee height during that time:

$$\overline{\Delta h}_{max} = \frac{P_1}{4P} \frac{15}{4} \pi \frac{\mu_1}{\mu_0} \left(\frac{a}{r_1}\right)^3 ae \sqrt{1-e^2} = \frac{\pi}{2} H_{max}. \tag{16.70}$$

312

Hence, applying the above relations between the lunar and the solar perturbations, we arrive at the following estimate for the maximum variation of perigee (or apogee) height during one quarter $(P_\odot/4 = 91.31\,\text{s.d.})$ for the combined lunisolar perturbation:

$$\Delta h\left(\frac{P_\odot}{4}\right) < \left[2\left(1 + \frac{1}{6.16}\right) + \frac{\pi}{2}(1 + 2.18)\right] H_{\odot\,\text{max}} \approx 7.3 H_{\odot\,\text{max}}, \qquad (16.71)$$

where $H_{\odot\,\text{max}}$ is obtained from (16.67) or from Table 16.5.

This estimate is somewhat exaggerated. Indeed, from (16.60), (16.62), and (16.63) it follows that the maxima of the secular and the long-periodic perturbations never coincide (the secular perturbations are maximal when $i = 2\omega = \pi/2$ and the long-periodic perturbations when $i = 2\omega = 0$). In calculating satellite orbits with great apogee heights $(h_a > 10^4\,\text{km})$ we should nevertheless expect considerable variations of perigee height (tens and hundreds of kilometers) in comparatively short periods. For orbits with a small initial h_p, this may lead to a very rapid termination of the satellite life (if the orbit evolution tends to reduce the h_p). We see from (16.63) that the actual variation of the perigee height depends not only on the elements a, e, i, ω, but also on the longitude Ω_0, which specifies the initial phase of the long-period perturbations.

16.12. LONG-RANGE ORBIT EVOLUTION

In previous sections we only considered orbit evolution during comparatively short periods, when the orbital elements entering the right-hand sides of equations (11.32) remained fairly constant. The assumption of constant orbital elements clearly does not apply over long periods, since all the elements are subjected to growing secular perturbations. For satellites with apogee height $h_a > 10^4\,\text{km}$, these perturbations are mainly produced by the combined effects of air drag, Earth's flattening, and lunisolar perturbations (for perigee heights $h_p > 1000\,\text{km}$, the effect of air drag is mostly negligible). In the exact analysis of motion of artificial Earth satellites we are therefore dealing with equations (16.4) which allow for the various factors mentioned above. This set of equations is generally solved by numerical integration. This technique, however, is practicable only for comparatively short periods (no more than a few tens or at most hundreds of circuits). The machine time requirements for numerical integration of long-range orbit evolution (e.g., in satellite lifetime determinations) are formidable. Moreover, there is always a danger of error build-up in lengthy numerical integration. The method proposed in Sec. 15.8 is more suitable for these purposes. Since the secular and the long-periodic perturbations of the orbital elements q_j are essentially smooth functions, the finite increments of these elements during one circuit, δq_j, can be replaced with the corresponding differentials dq_j. We thus arrive at a set of differential equations

$$\left. \begin{aligned} \frac{dq_j}{dN} &= \delta q_{j1} + \delta q_{j2} + \delta q_{j3} + \delta q_{j4} \\ t &= \int_{N_0}^{N} P\,dN, \end{aligned} \right\} \qquad (16.72)$$

313

where q_j ($j = 1, 2, \ldots, 5$) is a set of elements which specify the size, the shape, and the orientation of the orbit (e.g., the elements a, e, ω, i, Ω), $\delta q_{j1}, \delta q_{j2}, \delta q_{j3}, \delta q_{j4}$ are the perturbations of orbital elements during one circuit produced by (1) air drag, (2) Earth's flattening, (3) lunar and (4) solar perturbations; P is the orbital period of the satellite. If the function $N(t)$ is not required with any precision, the period P can be calculated from (5.36). If higher accuracy is required, the orbital period should be corrected for the various perturbing factors, as indicated in the preceding. The increments $\delta q_{j1}, \delta q_{j2}, \delta q_{j3}, \delta q_{j4}$ should be calculated from (13.32), (15.66), and (16.38). For satellites with distant apogees (of the order of $5 \cdot 10^4 - 10^5$ km and more), the lunar perturbations should preferably be allowed for with the aid of second-order equations /19/.

If the effect of long-periodic lunisolar perturbations is negligible, relations (16.60) can be substituted for (16.38).

Because of the complexity of the expressions in the right-hand sides of (16.72), whose numerical values depend on the mutual position of the Earth, the Moon, and the Sun, no analytical methods of solution are available at present for this set of equations. It is therefore solved by numerical integration. Each step in the integration scheme corresponds to one complete circuit of revolution, which ensures maximum saving in machine time in comparison with the straightforward solution of the set (16.4). The computer time can be additionally reduced by using finite-difference techniques /29/. Each step in the numerical solution then corresponds to quite a few circuits (the number of circuits in each step is determined by the period during which the orbital elements may be assumed constant).

The solution of equations (16.72) is essentially simplified if only one perturbing center need be considered. In practice this is so when analyzing the motion of artificial Moon satellites, for which the Earth's pull is some 178 times as great as the Sun's pull. In this case, equations (16.72) have three integrals, and their solution reduces to two quadratures. The dependence of the solution on the initial conditions of motion can be analyzed in great detail /19/.

In conclusion we note that, aside from the previously mentioned perturbing factors influencing the motion of artificial Earth satellites, there are also other disturbing forces (terrestrial gravity anomalies, radiation pressure, electromagnetic forces, etc.). However, for the great majority of satellites (with the exception of some peculiar satellites, e.g., of the Echo series), the effect of these forces is inferior in comparison with the contribution from the factors considered in the last chapters.

Chapter 17

THE EFFECT OF RADIATION PRESSURE ON
MOTION OF ARTIFICIAL EARTH SATELLITES

17.1. RADIATION PRESSURE

Light (or other forms of radiant energy) impinging on a surface set up
a so-called r a d i a t i o n   p r e s s u r e .   Surfaces reflecting or emitting
radiation also experience this pressure. Radiation pressure is a vector
quantity, defined as the ratio of the force on a surface element to the area
of that element. In general, the radiation pressure vector is written as /16/

$$q = \pm \frac{\Sigma}{c} \tau,$$ (17.1)

where Σ is the flux intensity of radiant energy through unit area of the
surface element being considered, c the velocity of light, τ a unit vector
in the direction of incident (reflected or emitted) light; the sign + implies
incidence of radiation, while − reflection or emission. Since radiation
pressure is produced by the incident and the reflected luminous fluxes,
the magnitude of this pressure substantially depends on the mechanism
of light reflection. We consider the following three limiting cases:
        (i) total absorption of incident light,
        (ii) perfect specular reflection,
        (iii) perfect diffuse reflection.
If the incident flux is completely absorbed, there is no reflected radiation.
Expression (17.1) is then written in the form

$$q = \frac{S \cos \alpha}{c} \tau,$$ (17.2)

where S is the intensity of the radiant energy flux through unit surface area
at right angles to the flux, α the angle between the direction of the luminous
flux and the normal to the surface.

With perfect specular reflection, the intensity of the reflected flux is
equal to the intensity of the incident flux, and its direction is specified
by the equality of the angles of incidence and reflection. Hence it follows
that the radiation pressure vectors q_1 and q_2 of the incident and the reflected
fluxes are equal in magnitude and are symmetric about the normal to the
surface (Figure 17.1). From (17.2) we see that the magnitudes of the
vectors q_1 and q_2 are

$$q_1 = q_2 = \frac{S \cos \alpha}{c}.$$

Hence the resultant pressure vector in the case of perfect specular
reflection (Figure 17.1):

$$q = \frac{2S \cos^2 \alpha}{c} n,$$ (17.3)

where n is the unit vector in the direction of the inner normal to the surface.

In diffuse reflection, the radiation pressure q_1 of the incident flux is
determined by (17.2). To find the pressure q_2 of the reflected flux, we take
a unit surface area and assume Lambert-law scattering of energy /16/:

$$dS = \varkappa \cos \gamma \, d\Omega,$$ (17.4)

where $d\Omega$ is a solid angle element, γ the angle between the axis of the solid
angle and the normal to the surface, dS is the intensity of the reflected flux
in the solid angle $d\Omega$, $\varkappa$ a constant.
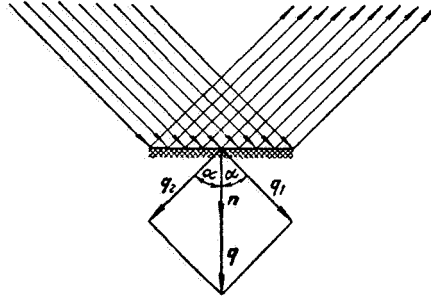
FIGURE 17.1. Specular reflection of a
luminous flux by a surface element.
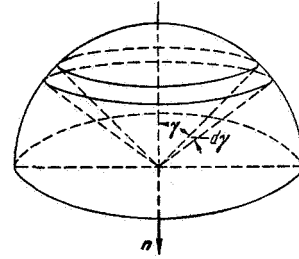
FIGURE 17.2. Diffuse reflection of a
luminous flux.

Consider a solid angle between two coaxial infinitesimally close circular
cones, whose common axis is normal to the reflecting surface. The angles
between the generatrices of these cones and their axis are γ and $\gamma + d\gamma$
(Figure 17.2). Then

$$d\Omega = 2\pi \sin \gamma \, d\gamma$$

and (17.4) takes the form

$$dS = 2\pi\varkappa \sin \gamma \cos \gamma \, d\gamma.$$ (17.5)

On the other hand, the total intensity of the energy flux through unit
surface element is $S \cos \alpha$. Hence, assuming perfect diffuse reflection,
we find

$$S \cos \alpha = \pi\varkappa \int_0^{\frac{\pi}{2}} \sin 2\gamma \, d\gamma = \pi\varkappa, \quad \varkappa = \frac{S \cos \alpha}{\pi}.$$

316

Substituting $\varkappa$ in (17.5), we find

$$dS = 2S \cos \alpha \sin \gamma \cos \gamma \, d\gamma. \tag{17.6}$$

From symmetry considerations it follows that the pressure components of the reflected flux tangent to the reflecting surface mutually cancel. There is only the normal component dq_2. From (17.1) and (17.6) we have

$$dq_2 = \frac{2S \cos \alpha}{c} n \sin \gamma \cos^2 \gamma \, d\gamma.$$

Integrating, we find the total radiation pressure set up by the reflected flux:

$$q_2 = \frac{2S \cos \alpha}{c} n \int_0^{\frac{\pi}{2}} \sin \gamma \cos^2 \gamma \, d\gamma = \frac{2S \cos \alpha}{3c} n. \tag{17.7}$$

Hence, making use of (17.2), we find the resultant radiation pressure in the case of perfect diffuse reflection:

$$q = \frac{S \cos \alpha}{c} \left(\tau + \frac{2}{3} n \right). \tag{17.8}$$

If the actual reflection mechanism is a combination of specular and diffuse reflections, the expression for the radiation pressure takes the form

$$q = \frac{S \cos \alpha}{c} \left[(1 - k_1) \tau + \left(2k_1 \cos \alpha + \frac{2}{3} k_2 \right) n \right], \tag{17.9}$$

where k_1 and k_2 are the coefficients of specular and diffuse reflection, varying from 0 to 1.

As we have previously observed, the pressure set up by the incident and reflected light adds to the pressure of emitted radiant energy (mainly infrared heat radiation). The pressure of the emitted radiation is determined like the pressure of reflected light. For diffuse emission according to Lambert's law (17.4), the radiation pressure is calculated from (17.7). If the space vehicle under consideration has no internal sources of energy, the emitted and the absorbed radiant fluxes are of course equal in a state of thermal equilibrium. If we furthermore ignore the redistribution of energy in the spacecraft interior, i.e., if each surface element is assumed to radiate the entire energy absorbed by it, we write

$$k_1 + k_2 = 1. \tag{17.10}$$

If energy transfer in the interior is not negligible, and if there are also internal sources of energy, the pattern is considerably complicated.

17.2. THE EFFECT OF RADIATION PRESSURE ON
THE MOTION OF A SPHERICAL ARTIFICIAL EARTH SATELLITE

The Sun is obviously the main source of radiant energy for space vehicles inside the solar system. If absorption of radiant energy in the interplanetary

space is neglected, the flux intensity per unit surface can be written as

$$S = S_0 \left(\frac{r_\odot}{r}\right)^2,$$
(17.11)

where r is the distance of the vehicle from the Sun, $r_\odot$ the mean radius of the Earth's orbit, S_0 the flux intensity of solar radiation at the distance of the Earth's orbit, whose numerical value is /24/

$$S_0 = 1.94 \, \text{cal/cm}^2 \cdot \text{min} = 1.35 \cdot 10^6 \, \text{erg/cm}^2 \cdot \text{sec}.$$

Applying (17.2) and taking $\alpha = 0$ for the angle of incidence, we find the solar radiation pressure in the case of total absorption:

$$q_1 = \frac{S}{c} = q_0 \left(\frac{r_\odot}{r}\right)^2,$$
(17.12)

where q_0 is the radiation pressure at the distance of the Earth's orbit, given by

$$q_0 = \frac{S_0}{c} = 4.5 \cdot 10^{-7} \, \text{kg/m}^2.$$
(17.13)

At present, of greatest applied significance is the analysis of solar radiation pressure on light-weight inflatable balloon satellites of the Echo type. We shall therefore confine the discussion to satellites of spherical geometry.

From (17.2) and (17.12) it follows that for total absorption, the perturbing acceleration f produced by the radiation pressure points along the luminous flux. Its magnitude is given by

$$f = \frac{q}{m} \int \cos\alpha \, d\sigma = \frac{q_1}{m} \int d\sigma' = \frac{\pi R_s^2}{m} q_1,$$
(17.14)

where R_s is the radius of the satellite, m its mass, $d\sigma$ the area of a surface element, $d\sigma' = \cos\alpha \, d\sigma$ the area of the element's projection on a plane normal to the luminous flux; the integral is taken over the entire illuminated surface of the satellite.

From symmetry considerations it follows that in specular and diffuse reflection, the total perturbing acceleration on a spherical satellite is also
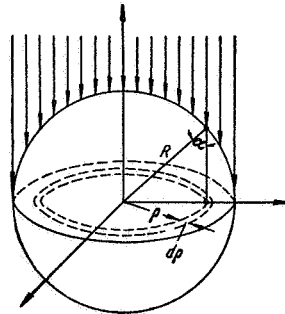

FIGURE 17.3. Distribution of luminous flux incident on a spherical satellite.

318

along the luminous flux. Making use of (17.3) and (17.12), we find that for
perfect specular reflection, the magnitude of the perturbing acceleration is

$$f = 2\frac{q_1}{m}\int \cos^3\alpha\, d\sigma = 2\frac{q_1}{m}\int \cos^2\alpha\, d\sigma'.$$

The element $d\sigma$ is a ring of radius ρ and width $d\rho$. From Figure 17.3
we see that the above expression for f takes the form

$$f = \frac{4\pi q_1}{m}\int_0^{R_s} \rho\cos^2\alpha\, d\rho = \frac{4\pi q_1}{mR_s^2}\int_0^{R_s} (R_s^2 - \rho^2)\rho\, d\rho = \frac{\pi R_s^2}{m}\, q_1. \qquad (17.15)$$

This expression coincides with (17.14), which has been derived for the
case of total absorption of radiant energy.

From (17.2), (17.8), and (17.14) it follows that for perfect diffuse
reflection, the perturbing acceleration is

$$f = \frac{\pi R_s^2}{m}\, q_1 + \frac{2}{3}\frac{q_1}{m}\int \cos\alpha\, d\sigma'. \qquad (17.16)$$

Referring to Figure 17.3, we see that

$$\int \cos\alpha\, d\sigma' = \frac{2\pi}{R_s}\int_0^{R_s} \sqrt{R_s^2 - \rho^2}\,\rho\, d\rho = \frac{\pi}{R_s}\int_0^{R_s^2} y^{1/2}\, dy = \frac{2}{3}\,\pi R_s^2,$$

where

$$y = R_s^2 - \rho^2.$$

Substituting in (17.16), we find

$$f = 1\frac{4}{9}\frac{\pi R_s^2}{m}\, q_1 \approx 1.44\frac{\pi R_s^2}{m}\, q_1. \qquad (17.17)$$

Comparing relations (17.9), (17.14), (17.15), and (17.17) we see that
in the general case of a spherical satellite without internal sources of
energy, the perturbing acceleration is given by

$$f = \frac{\pi R_s^2}{m}\, kq_1, \qquad (17.18)$$

where k is a coefficient depending on the mechanism of light reflection, and
also on the distribution of thermal emission over the satellite surface (the
latter factor is largely determined by heat transfer processes in the satellite).

$k = 1$ corresponds to a case of perfect specular reflection, and also to
the case of total absorption of luminous energy, for uniform distribution
of thermal radiation over the entire surface.

$k = 1.44$ corresponds to perfect diffuse reflection, and also to partial
diffuse reflection, on proviso that there is no heat transfer between
individual surface elements (i. e., the absorbed energy is diffusely radiated
by the same surface elements).

In most cases the actual value of the coefficient k is between these limits.
If solar radiation pressure produces substantial perturbation of the satellite's

319

orbit, the numerical value of the coefficient can be refined by means of theoretical calculations based on trajectory measurements.

Applying (17.12), we write (17.18) as

$$f = Akq_0 \frac{r_\odot^2}{r^2}, \quad A = \frac{\pi R_s^2}{m} = \frac{F}{m}, \quad F = \pi R_s^2, \tag{17.19}$$

where the coefficient A is the ratio of the satellite mean cross section F to its mass m. This expression is valid for satellites of arbitrary geometry. In some cases, F should be interpreted as some characteristic area of the satellite (e. g., for solar-oriented satellites this is the area of the cross section normal to the luminous flux, for nonoriented convex satellite it is one quarter of the total surface area, etc.). In general, the choice of F is fairly arbitrary, since the coefficient k can always be adjusted to offset any discrepancy. This coefficient should be calculated taking into consideration the conditions of absorption, reflection, and emission of radiant energy by the satellite, which is achieved by integrating equalities (17.2), (17.3), (17.7), and (17.8) for solar radiation pressure on a single surface element. The resultant radiation pressure, however, may prove to make a certain angle with the Sun — satellite direction.

17.3. RELATIVE MAGNITUDE OF SOLAR RADIATION PRESSURE AND OTHER PERTURBING FACTORS

We now calculate the ratio of the perturbing accelerations set up by solar radiation pressure (f) and by air drag (T) for a spherical satellite in circular orbit. Making use of (14.29), (14.31), and (17.19), and putting $r = r_\odot$, we write

$$\frac{f}{T} = \frac{2kq_0}{c_x \rho w^2}. \tag{17.20}$$

We see that this ratio is inversely proportional to air density ρ, and it therefore increases with flight altitude h.

TABLE 17.1

Height of circular orbit h, km	200	300	400	500	600	700	800
$\frac{f}{T}$	0.0002	0.003	0.018	0.08	0.27	0.8	2.1

Table 17.1 lists the values of $\frac{f}{T}$ as a function of the circular orbit height h; these values were calculated from (17.20) for the atmosphere of Appendix I, assuming $c_x = 2.4$, $k = 1.44$, and $q_0 = 4.5 \cdot 10^{-7} \, \text{kg/m}^2$ (see 17.13)). We see from that table that for flight heights $h < 500 \, \text{km}$, the

magnitude of solar radiation pressure is much less than the magnitude of air resistance. At these altitudes, radiation pressure is in fact less than the unaccountable fluctuations in air drag. Therefore, for $h < 500$ km, the effects of solar radiation pressure are commonly ignored. For $h > 500$ km, the radiation pressure is comparable in magnitude with the drag forces, and for $h > 700$ km it is even greater than the air drag (for the particular atmosphere being considered).

To compare the perturbing acceleration f due to solar radiation pressure with the perturbing acceleration $f_\odot$ of the solar attraction, we make use of relations (16.21) and (17.19). Putting

$$\frac{k}{\varphi_1(\alpha)} \approx 1 \quad \text{and} \quad c \approx r \approx r_\odot.$$

we find

$$\frac{f}{f_\odot} \approx \frac{Aq_0}{g_\odot} \frac{r_\odot}{r_0}, \qquad (17.21)$$

where $g_\odot = \dfrac{\mu_\odot}{r_\odot^2}$ is the Sun's gravitational acceleration at the distance of the Earth's orbit, r_0 the satellite's distance from the Earth's center.

Making use of (1.3) and (16.51), we find $g_\odot \approx 6 \cdot 10^{-3}$ m/sec². If the size and the weight of the satellite may vary between the limits indicated in Sec. 14.4, we find that A in this case varies from 0.003 to 0.3 m³/kg·sec². As we have shown in the previous chapter, solar attraction has a substantial influence on satellites flying at heights $h > 10^4$ km above the Earth's surface. Thus, $r_0 = 17 \cdot 10^3$ km. Substituting these numerical values in (17.21) and applying (16.51) and (17.13), we find that under our assumptions, the ratio $f/f_\odot$ varies from 0.002 (large heavy satellites) to 0.2 (small light-weight satellites).

It follows from the preceding that solar radiation pressure is noticeable only for small light-weight satellites orbiting at $h > 500$ km. For all other satellites, the perturbations produced by radiation pressure are small in comparison with the disturbing effects due to the other factors. Special classes of artificial Earth satellites, however, may provide an exception to this rule. Among these exceptions we have

(i) very small satellites (e. g., reflecting dipoles used in the West Ford project),

(ii) light-weight inflatable balloons (Echo-series satellites).

The perturbations set up by solar radiation pressure may be quite substantial for these special satellites. For Echo I, which was a sphere 30.5 m in diameter weighing 70.4 kg, $A = \dfrac{\pi R_s^2}{m} \approx 100$ m³/kg·sec /23/, which is some 300 times as large as the above maximum value of this coefficient for ordinary satellites (it follows from (17.19) that the magnitude of the perturbing acceleration produced by radiation pressure is proportional to A).

17.4. PROJECTIONS OF THE PERTURBING ACCELERATION ON THE SATELLITE'S ORBITAL AXES

In estimating the effect of solar radiation pressure on the motion of artificial Earth satellites, we shall proceed from the following assumptions.

(1) The resultant perturbing acceleration produced by radiation pressure points along the Sun — satellite central line. As we have previously shown, this is so for spherical satellites. The proposition obviously applies for all satellites which are symmetric about the Sun—satellite central line, and also for satellites of arbitrary geometry if the absorption of radiant energy is total, i.e., there is no reflection or emission of energy.

(2) Since the distance of the satellite from the Earth's center is small in comparison to its distance from the Sun, the perturbing acceleration can in fact be determined for a satellite hypothetically located at the Earth's center.

(3) The Sun travels around the Earth in a circular orbit of radius $r_\odot$.

Under these simplifying assumptions, making use of (17.19), we find an expression for the perturbing acceleration vector

$$f = - Q r_1^0,$$ (17.22)

where r_1^0 is the unit vector along the Earth—Sun line, and Q a coefficient given by

$$Q = A k q_0 = \frac{F}{m} k q_0 = \frac{\pi R_s^2}{m} k q_0.$$ (17.23)

The last of these equalities applies for spherical satellites only.

From (17.22), we can easily find the projections S, T, W of the perturbing acceleration on the satellite's orbital axes (see Figure 2.1 or Figure 16.2). We make use of equalities (16.23) and note that

$$r_1^0 = \varkappa_1 i + \varkappa_2 j + \varkappa_3 k,$$ (17.24)

where i, j, k are the unit vectors along the $O\xi\eta\zeta$ axes depicted in Figure 5.5 or Figure 16.2, and $\varkappa_1, \varkappa_2, \varkappa_3$ are the direction cosines of the Earth—Sun line in this frame. Thus,

$$\left.\begin{aligned} S &= - Q r_1^0 \cdot S^0 = - Q (\varkappa_1 \cos\vartheta + \varkappa_2 \sin\vartheta) = \\ &\qquad = - Q \cos\gamma \cos(\vartheta - \alpha), \\ T &= - Q r_1^0 \cdot T^0 = Q (\varkappa_1 \sin\vartheta - \varkappa_2 \cos\vartheta) = \\ &\qquad = Q \cos\gamma \sin(\vartheta - \alpha), \\ W &= - Q r_1^0 \cdot W^0 = - Q \varkappa_3 = Q \sin\gamma, \end{aligned}\right\}$$ (17.25)

where S^0, T^0, W^0 are the unit vectors along S, T and $W; \vartheta$ is the true anomaly of the satellite, α and γ are the angles which are determined from equality (16.24) or from Figure 16.2.

17.5. PERTURBATION OF CIRCULAR ORBIT DURING ONE REVOLUTION

In determining the perturbations of circular orbit per revolution, we make use of the fact that the satellite's orbital period is much less than a year, so that the displacement of the Sun relative to the Earth can be ignored during this period, i.e., the direction cosines $\varkappa_1, \varkappa_2, \varkappa_3$ remain constant. Our problem thus reduces to a particular case of the classical three-body problem, where a point moves in the field of attraction of two stationary centers (with repulsion substituted for the attraction of one of the centers). It is, however, hardly advisable to apply the complicated methods which are available for the solution of the general problem /3/, since our approach is fairly crude. We shall therefore seek an approximate solution by linearizing the effect of small perturbing accelerations.

Let the axis $O\xi$ (Figure 16.2) point to some initial position D_0, and let φ be the angular distance between the initial and the current positions in circular orbit. Then in (17.25) the true anomaly ϑ is replaced with φ, and the expressions take the form

$$\left.\begin{aligned} S &= Q\cos\gamma\sin\left(\varphi-\alpha-\tfrac{\pi}{2}\right), \\ T &= Q\cos\gamma\sin(\varphi-\alpha), \quad W=-Q\sin\gamma. \end{aligned}\right\} \tag{17.26}$$

We thus obtain a particular case of (3.5) with the assumptions

$$\left.\begin{aligned} S_0 &= 0, \quad S_1 = Q\cos\gamma, \quad \varphi_{S_1} = \alpha+\tfrac{\pi}{2}, \\ T_0 &= 0, \quad T_1 = Q\cos\gamma, \quad \varphi_{T_1} = \alpha, \\ W_0 &= -Q\sin\gamma, \quad W_1 = 0, \\ S_i &= T_i = W_i = 0 \quad \text{for} \quad i \geqslant 2. \end{aligned}\right\} \tag{17.27}$$

For simplicity, let us consider the case of a satellite which is constantly illuminated by the Sun — this satellite is never eclipsed by the Earth. It follows from (17.26) and (17.27) that the satellite experiences a constant perturbing acceleration at right angles to the orbital plane and an in-plane periodic acceleration, whose frequency is equal to the satellite's orbital frequency. As we have shown in Secs. 3.3 and 3.4, these accelerations are incapable of producing secular perturbations of the orbital plane, while in-plane secular perturbations reduce to a change in the orbital period and to a growing distortion of the orbit shape. A circular orbit is transformed into a nearly circular one with an increasing eccentricity and a constant mean radius.

The rate of distortion of the orbit can be described in terms of the change δr in the distance of the satellite from the Earth's center (or in flight altitude) during one circuit of revolution. Consider a point D of the orbit, located at an angular distance φ from the point of origin D_0. The increment δr at this point can be determined from

$$\delta r(\varphi) = \Delta r(\varphi+2\pi) - \Delta r(\varphi), \tag{17.28}$$

where $\Delta r(\varphi)$ and $\Delta r(\varphi+2\pi)$ are the radial perturbations for two successive passages of the satellite through the point D. Applying (3.22) to calculate

these perturbations and making use of (3.7), we find

$$\delta r(\varphi) = -2\pi \frac{r_m^3}{\mu}\left[\frac{S_1}{2}\cos(\varphi - \varphi_{S_1}) + T_1 \sin(\varphi - \varphi_{T_1})\right],$$

where r_m is the mean radius of the orbit. Substituting expressions (17.27) for S, φ_{S_1}, T_1, and φ_{T_1}, we find

$$\delta r(\varphi) = -3\pi \frac{r_m^3}{\mu} Q \cos\gamma \sin(\varphi - \alpha). \qquad (17.29)$$

The maximum change in flight altitude obtains at points with $\varphi = \alpha \pm \pi/2$, i.e., at points which are located on the normal to the projection of the Earth — Sun line onto the orbital plane. The magnitude of this change per circuit is

$$\delta r_{max} = 3\pi \frac{r_m^3}{\mu} Q \cos\gamma. \qquad (17.30)$$

With constant r_m and Q, the maximum perturbation is observed for $\gamma = 0$, i.e., when the Earth — Sun line is in the orbital plane.

This technique can also be applied to determine the growing perturbations along the orbit, as well as perturbations in orbital velocities. Making use of (3.32) and (17.27), we obtain the following expression for the relative perturbation of the orbital period:

$$\frac{\Delta P}{P} = \frac{3Q}{g_m}\cos\vartheta \cos\alpha, \quad g_m = \frac{\mu}{r_m^2}. \qquad (17.31)$$

As an example, consider a satellite which moves in circular orbit at a height $h = 1000$ km with $\gamma = \alpha = 0$. We shall determine the corresponding δr_{max} and ΔP for various values of the coefficient $A = \frac{F}{m}$. Making use of equalities (17.13), (17.23), (17.30), and (17.31), we put $k = 1.44$. The results are listed in Table 17.2.

TABLE 17.2

Orbit perturbations	Characteristic area-to-satellite mass ratio A, m^3/kg·sec^2		
	100	0.3	0.003
In orbital period ΔP, sec	0.16	$5\cdot10^{-5}$	$5\cdot10^{-7}$
Radial (in flight altitude) per circuit δr_{max}, m	600	2	0.02

We see from the table that for ordinary satellites, whose A is between 0.003 and 0.3 m^3/kg·sec^2, the perturbations produced by solar radiation pressure are small and mostly negligible. However, for large light-weight satellites of the Echo I type, having $A \approx 100$ m^3/kg·sec^2 (and also for very

small satellites), solar radiation pressure may cause substantial perturbations which must not be neglected.

The preceding analysis of circular orbit perturbations is for a non-eclipsing satellite which is constantly illuminated by the Sun. The problem is considerably complicated if the sunlight is screened by the Earth over part of the satellite orbit. Suitable expressions can nevertheless be obtained for determining, to first approximation, the resulting perturbations in orbital elements. To this end it suffices to integrate the right-hand sides of (3.6). For the angles ψ corresponding to the illuminated section of the orbit, the perturbing accelerations S, T, and W should be calculated from (17.26), with ψ substituted for φ. Over the eclipsed section,

$$S = T = W = 0.$$

17.6. PERTURBATION OF ELLIPTICAL ORBIT DURING ONE REVOLUTION

In determining the perturbations of elliptical orbit during one circuit of revolution, we shall proceed from the simplifying assumptions of the previous section. Substituting (17.25) in the right-hand sides of (11.39) and (16.32), we make use of (4.19) and the relation

$$\int_0^{2\pi} F(\cos\vartheta)\sin^l\vartheta\, d\vartheta = 0,$$

where $F(\cos\vartheta)$ is some function of $\cos\vartheta$, and l is an arbitrary odd number. The result is the following expressions for elliptical orbit perturbations during one revolution of the satellite:

$$
\begin{aligned}
\delta a &= -\frac{2a}{1-e^2}\frac{Qp^2}{\mu}\varkappa_2\int_0^{2\pi}\left(e\frac{\sin^2\vartheta}{\Delta^2}+\frac{\cos\vartheta}{\Delta}\right)d\vartheta, \\[2mm]
\delta e &= -\frac{Qp^2}{\mu}\varkappa_2\int_0^{2\pi}\left(\frac{1}{\Delta^2}+\frac{\cos^2\vartheta+e\cos\vartheta}{\Delta^3}\right)d\vartheta, \\[2mm]
\delta\Omega &= -\frac{Qp^2}{\mu}\varkappa_3\frac{\sin\omega}{\sin i}\int_0^{2\pi}\frac{\cos\vartheta}{\Delta^3}d\vartheta, \\[2mm]
\delta i &= -\frac{Qp^2}{\mu}\varkappa_3\cos\omega\int_0^{2\pi}\frac{\cos\vartheta}{\Delta^3}d\vartheta, \\[2mm]
\delta\omega &= \frac{Qp^2}{e\mu}\varkappa_1\int_0^{2\pi}\left(\frac{1}{\Delta^2}+\frac{\sin^2\vartheta}{\Delta^3}\right)d\vartheta-\cos i\,\delta\Omega,
\end{aligned}
\right\}
\qquad (17.32)
$$

where $\Delta = 1 + e\cos\vartheta$.

Substituting $1-\cos^2\vartheta$ for $\sin^2\vartheta$ in the right-hand sides of these relations and expressing $\cos\vartheta$ in terms of Δ, we reduce the problem to integrals of the form

$$J_n = \int_0^{2\pi}\frac{d\vartheta}{\Delta^n(\vartheta)}\qquad (n = 1, 2, 3).$$

325

From the previous evaluations of these integrals, (16.35) and (16.37), we obtain the final expressions for the perturbations of elliptical orbit per circuit:

$$\left.\begin{aligned}
&\delta a = 0, \\
&\delta e = -3\pi Q \varkappa_2 \frac{a^2}{\mu} \sqrt{1-e^2}, \\
&\delta \Omega = 3\pi Q \varkappa_3 \frac{a^2}{\mu} \frac{\sin \omega}{\sin i} \frac{e}{\sqrt{1-e^2}}, \\
&\delta i = 3\pi Q \varkappa_3 \frac{a^2}{\mu} \cos \omega \frac{e}{\sqrt{1-e^2}}, \\
&\delta \omega = 3\pi Q \varkappa_1 \frac{a^2}{\mu} \frac{\sqrt{1-e^2}}{e} - \cos i \, \delta \Omega.
\end{aligned}\right\} \qquad (17.33)$$

The perturbation of elliptical orbit thus changes the eccentricity, rotates the semimajor axis, and alters the orientation of the orbital plane (there is also a certain deviation of the sidereal period from the osculating period). The length of the semimajor axis a remains unaffected. As we have shown in Sec. 16.8, this is a consequence of our assumption that the Earth—Sun direction is fixed in space and that the orbital elements used in the calculation of the right-hand sides in (17.32) are constant. The proof offered in Sec. 16.8 for the constancy of the projection of the satellite's angular momentum vector about the Earth's center on the Earth—Sun direction also remains in force. The perturbations δe, $\delta \Omega$, and δi therefore satisfy identity (16.43), which can be verified by direct substitution.

Note that expressions (17.33) for the perturbations $\delta \Omega$ and δi can be written as

$$\delta \Omega = \delta \psi \frac{\sin \omega}{\sin i}, \qquad \delta i = \delta \psi \cos \omega,$$

where

$$\delta \psi = 3\pi Q \varkappa_3 \frac{a^2}{\mu} \frac{e}{\sqrt{1-e^2}}. \qquad (17.34)$$

Comparing these expressions with (9.35), we see that during one circuit of revolution the orbital plane is rotated around the semimajor axis through an angle $\delta \psi$, defined by (17.34). Since according to (16.24) $\varkappa_3 = \sin \gamma$, the maximum rotation angle $\delta \psi$, with constant Q, a, and e, is attained for $\gamma = \frac{\pi}{2}$, i.e., when the orbital plane of the satellite is perpendicular to the Earth—Sun direction.

As an example, let us consider the American satellite Echo I, which was launched into orbit with perigee and apogee heights $h_p = 1500$ km and $h_a = 1700$ km, having $A \approx 100 \, \text{m}^3/\text{kg} \cdot \text{sec}^2$. Making use of (17.13) and putting in (17.23) $k = 1.44$, we obtain the maximum rotation angle $\delta \psi$ for this satellite (with $\varkappa_3 = 1$):

$$\delta \psi \approx 0''.3.$$

This angle is small in comparison with the orbit plane rotation produced by the Earth's flattening (for Echo I the orbital plane might have been rotated by as much as 10' per circuit).

It can be proved that for $e \to 0$, the foregoing orbit perturbations approach as a limit the circular orbit perturbations derived in the previous section. Indeed, from (17.34) we have $\delta\psi \to 0$ for $e \to 0$. This corresponds to the circular orbit plane remaining unperturbed.

Let us now consider the perturbations of r in elliptical orbit. From (4.19) we have

$$\delta r = \frac{\delta p}{1 + e \cos \vartheta} + \frac{e \sin \vartheta \, \delta\vartheta - \cos \vartheta \, \delta\vartheta}{(1 + e \cos \vartheta)^2}. \tag{17.35}$$

Let the angular distance of the given point from the node be constant. Then, seeing that $p = a(1 - e^2)$ and $\vartheta = u - \omega$, we write

$$\delta p = \delta a \,(1 - e^2) - 2ae \, \delta e, \quad \delta\vartheta = - \delta\omega.$$

These equalities, together with relations (17.33), are substituted in (17.35). Now, applying (16.24) and seeing that $\lim_{e \to 0} a = \lim_{e \to 0} p = r_m$, we write

$$\lim_{e \to 0} \delta r = -3\pi Q \, \frac{r_m^3}{r} \cos \gamma \sin (\vartheta - a).$$

The right-hand side of this equality coincides with the corresponding expression in (17.29) for perturbation of circular orbit, with ϑ substituted for φ (which is fully admissible, since the choice of initial position in orbit is quite arbitrary).

The above expressions for orbit perturbations correspond to the case of a noneclipsing satellite which is continuously illuminated by the Sun. The formulas for satellites which are eclipsed by the Earth are much more complicated /23, 34/. In the general case, the previously considered perturbations of orbital elements are supplemented by a perturbation of the semimajor axis. To derive the corresponding expressions, we should make use of (11.39) and (16.32), inserting expressions (17.25) for the components of the perturbing acceleration (along the illuminated sections of the orbit). Making use of (16.34), we reduce the problem to integrals of the form

$$\int \frac{d\vartheta}{(1 + e \cos \vartheta)^n} \quad \text{and} \quad \int \frac{\sin \vartheta \, d\vartheta}{(1 + e \cos \vartheta)^n},$$

where n is an integer.

Integrals of the first kind are evaluated using the recursion formula from Sec. 16.7, while in integrals of the second kind we employ the substitution

$$1 + e \cos \vartheta = \Delta, \quad \sin \vartheta \, d\vartheta = - \frac{d\Delta}{e}.$$

17.7. LONG-RANGE PERTURBATIONS

In calculating orbit perturbations over considerable stretches of time, the Earth — Sun direction must not be assumed as fixed in space. If the assumption of constant orbital elements is retained in the evaluation of

the right-hand sides of (11.39) and (16.32), the problem can be solved by the method described in Sec. 16.9. The parameters $\varkappa_i$ ($i = 1, 2, 3$) entering the right-hand sides of (17.33) are correspondingly replaced with

$$\bar{\varkappa}_i = \frac{1}{P} \int_0^t \varkappa_i \, dt, \qquad (17.36)$$

where P is the satellite's orbital period.

Hence, making use of (16.52) and (16.53), we can obtain expressions for the coefficients $\bar{\varkappa}_i$ and, substituting these expressions for $\varkappa_i$ in the right-hand sides of (17.33), we write relations for long-range orbit perturbations. These are in fact long-periodic perturbations with a period of one year. We shall not discuss these relations in any detail, since in practice the problem is considerably complicated by the screening of sunlight by the Earth, and also by the superposition of other perturbing factors which have been considered in the preceding.

The derivation of finite formulas for long-range perturbations in the case of eclipsing satellites is a highly arduous task. The exact immersion and emersion times in and from the Earth's shadow cannot be found in finite form: they are calculated from some transcendental equation (see next section).

The problem of the combined influence of the Earth's flattening and of solar radiation pressure (neglecting the eclipses), however, can be reduced to finite expressions /23/. These expressions were derived for cases when the perturbation of the orbital plane due to solar radiation pressure was small in comparison with the perturbation due to the Earth's flattening. This and other assumptions introduced in the derivation of the finite formulas (mainly the omission of air drag and of lunisolar attraction) are justified for satellites orbiting at heights of some $10^3 - 10^4$ km. At these altitudes, however, the sunlight is commonly screened over the greater portion of the orbit, and this substantially reduces the region of applicability of the finite relations.

In practice, long-range perturbations due to the combined effect of solar radiation pressure and other disturbing factors can be determined by numerical integration of equations (16.72). Terms allowing for the perturbation due to solar radiation pressure during one circuit (with sunlight screened off by the Earth) must be introduced in the right-hand sides of these expressions.

If the orbit of the space vehicle is determined by numerical integration of equations (16.4) and solar radiation pressure points along the Sun—vehicle central line, the contribution from this pressure can be easily found. Seeing that in this case the gravitational acceleration of the Sun and the acceleration set up by the radiation pressure are colinear, we make use of relation (17.19) to introduce in the right-hand side of (16.4) the following combined expression for the effect of the two factors:

$$f_\odot = (\mu_\odot - Akq_0 r_\odot^2) \frac{r_1 - r}{(r_1 - r)^3} - \mu_\odot \frac{r_1}{r_1^3}, \qquad (17.37)$$

where r_1 and r are vectors which define the position of the Sun and of the space vehicle relative to the Earth, and $f_\odot$ is the acceleration produced by the combined action of solar radiation pressure and solar gravitational pull (in a nonrotating frame with its origin at the Earth's center).

328

17.8. IMMERSION AND EMERSION TIMES
OF A SATELLITE

As we have previously observed, the perturbations produced by solar radiation pressure cannot be calculated unless the time of satellite immersion in the Earth's shadow and the time of its emersion from the shadow cone are known. This problem lends itself to an approximate solution, since the effect of solar radiation pressure on the majority of artificial Earth satellites is slight and since the coefficient k in (17.19) and (17.23) is known with low accuracy. We therefore assume that the Earth is a sphere of radius R, and also neglect the tapering of the Earth's shadow due to atmospheric refraction and the finite size of the Sun. The Earth's shadow is thus a circular cylinder of radius R, whose axis is parallel to the Sun—Earth direction. The problem reduces to the determination of the crossing times of this cylinder by the satellite. Let z be the angle between the Earth—satellite line and the line through the centers of the Earth and the Sun (i.e., the zenith distance of the Sun as viewed from the satellite); ε is the angle between the Earth—satellite line and the tangent to the Earth's surface drawn from the satellite. Under our simplifying assumptions, the satellite crosses the Earth's shadow when

$$z = \varepsilon;\qquad (17.38)$$

for $z > \varepsilon$ the satellite is immersed in the shadow, and for $z < \varepsilon$ the satellite is insolated.

The angle ε is calculated from a formula, which is obvious from elementary geometric considerations:

$$\cos \varepsilon = -\sqrt{1 - \frac{R^2}{r^2}},\qquad (17.39)$$

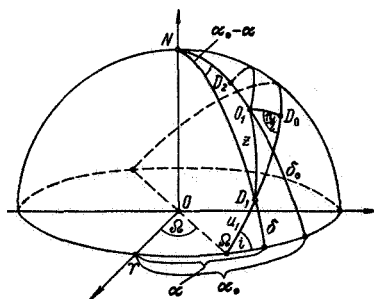where r is the distance of the satellite from the Earth's center.

FIGURE 17.4. Determining the zenith distance
of the Sun.

To find the angle z, we examine Figure 17.4, which shows a sphere centered at the Earth's center O; the point N is the north pole of this sphere, and the points D_1 and O_1 are the intersections of the sphere with

329

the lines from the Earth's center to the satellite and to the Sun. Consider the spherical triangle D_1NO_1, where

$$\overset{\frown}{O_1D_1} = z, \quad \overset{\frown}{ND_1} = \frac{\pi}{2} - \delta,$$

$$\overset{\frown}{NO_1} = \frac{\pi}{2} - \delta_\odot, \quad \angle D_1NO_1 = \alpha_\odot - \alpha;$$

here δ and α are the declination and the right ascension of the satellite, $\delta_\odot$ and $\alpha_\odot$ ditto for the Sun. From these equalities we have

$$\cos z = \sin\delta\sin\delta_\odot + \cos\delta\cos\delta_\odot\cos(\alpha_\odot - \alpha). \tag{17.40}$$

Substituting (17.39) and (17.40) in (17.38), we obtain the shadow equation, which is in fact the condition of satellite immersion (or emersion):

$$\sin\delta\sin\delta_\odot + \cos\delta\cos\delta_\odot\cos(\alpha_\odot - \alpha) = -\sqrt{1 - \frac{R^2}{r^2}}, \tag{17.41}$$

where $\delta_\odot$ and $\alpha_\odot$ are provided by astronomical measurements, and δ and α are determined from (1.12).

From geometrical considerations it follows that for each circuit of revolution the shadow equation may have two solutions, one solution, or no solutions at all. The first of the three cases corresponds to an orbit where the satellite is eclipsed for some time, and the third case represents continuous insolation.

For a satellite in circular orbit, when the change per circuit in $\delta_\odot$ and $\alpha_\odot$ is ignored, the shadow equation can be solved in finite form. Let D_0 be the point where the satellite's orbital plane meets the great circle through the point O_1, at right angles to the orbital plane. For given coordinates of the Sun $\alpha_\odot$, $\delta_\odot$, and for given orbital elements Ω, i, the position of the point D_0 is determined by elementary formulas from spherical trigonometry, which are used in calculating the arcs $\overset{\frown}{O_1D_0}$ and $\overset{\frown}{\Omega D_0}$. Now, from the spherical right triangle $D_1O_1D_0$ and from equality (17.39) we see that the shadow equation can be written as

$$\cos\overset{\frown}{D_1D_0} = -\frac{\sqrt{1 - \frac{R^2}{r^2}}}{\cos\overset{\frown}{O_1D_0}}. \tag{17.42}$$

The arc $\overset{\frown}{D_1D_0}$ can be calculated from this equality, and the angular distances of the points D_1 and D_2, where the satellite meets the shadow envelope, from the node Ω are given by

$$u_{1,2} = \overset{\frown}{\Omega D_0} \pm \overset{\frown}{D_1D_0}. \tag{17.43}$$

In elliptical orbit, r is variable, and equation (17.42) should be solved separately by the method of successive approximations. There is, however, a certain danger in adopting this course, as the method may lead to a false conclusion that the equation is unsolvable (if at any step too large a value is inserted for r in the right-hand side of the equation). A more reliable method for elliptical orbits calls for a graphical solution of the shadow equation or for a successive substitution-and-verification procedure for a sequence of orbit points (this, of course, cannot be carried out unless an electronic computer is available).

APPENDIX 1

TABLE OF THE BASIC PARAMETERS OF THE COSPAR REFERENCE ATMOSPHERE FOR 1961 (CIRA 1961)

Height h	Density ρ	Pressure p	Temperature T	Molecular weight M
km	g/m³	dyne/cm²	°K	g/mol
0	$1.23 \cdot 10^{-3}$	$1.02 \cdot 10^{6}$	289.25	28.97
10	$4.19 \cdot 10^{-4}$	$2.68 \cdot 10^{5}$	222.36	28.97
20	$8.89 \cdot 10^{-5}$	$5.54 \cdot 10^{4}$	217.07	28.97
30	$1.84 \cdot 10^{-5}$	$1.21 \cdot 10^{4}$	228.28	28.97
40	$4.07 \cdot 10^{-6}$	$2.90 \cdot 10^{3}$	247.86	28.97
50	$1.02 \cdot 10^{-6}$	$7.91 \cdot 10^{2}$	269.56	28.97
60	$3.04 \cdot 10^{-7}$	$2.25 \cdot 10^{2}$	257.82	28.97
70	$8.84 \cdot 10^{-8}$	$5.51 \cdot 10^{1}$	217.04	28.97
80	$1.94 \cdot 10^{-8}$	$1.03 \cdot 10^{1}$	184.60	28.97
90	$3.19 \cdot 10^{-9}$	1.62	181.14	28.97
100	$4.78 \cdot 10^{-10}$	$2.92 \cdot 10^{-1}$	212.10	28.85
110	$9.49 \cdot 10^{-11}$	$7.28 \cdot 10^{-2}$	265.02	28.72
120	$2.44 \cdot 10^{-11}$	$2.44 \cdot 10^{-2}$	342.96	28.60
130	$6.95 \cdot 10^{-12}$	$1.16 \cdot 10^{-2}$	569.44	28.43
140	$3.07 \cdot 10^{-12}$	$7.22 \cdot 10^{-3}$	799.13	28.25
150	$1.69 \cdot 10^{-12}$	$5.08 \cdot 10^{-3}$	1014.53	28.09
160	$1.11 \cdot 10^{-12}$	$3.81 \cdot 10^{-3}$	1155.26	27.90
170	$8.26 \cdot 10^{-13}$	$2.92 \cdot 10^{-3}$	1176.53	27.70
180	$6.59 \cdot 10^{-13}$	$2.25 \cdot 10^{-3}$	1193.17	27.47
190	$4.73 \cdot 10^{-13}$	$1.75 \cdot 10^{-3}$	1210.51	27.25
200	$3.61 \cdot 10^{-13}$	$1.36 \cdot 10^{-3}$	1226.77	27.00
210	$2.77 \cdot 10^{-13}$	$1.07 \cdot 10^{-3}$	1243.27	26.75
220	$2.14 \cdot 10^{-13}$	$8.48 \cdot 10^{-4}$	1259.05	26.48
230	$1.67 \cdot 10^{-13}$	$6.74 \cdot 10^{-4}$	1273.57	26.18
240	$1.30 \cdot 10^{-13}$	$5.40 \cdot 10^{-4}$	1287.72	25.87
250	$1.03 \cdot 10^{-13}$	$4.34 \cdot 10^{-4}$	1301.45	25.55
260	$8.11 \cdot 10^{-14}$	$3.51 \cdot 10^{-4}$	1314.20	25.21
270	$6.45 \cdot 10^{-14}$	$2.86 \cdot 10^{-4}$	1325.88	24.85
280	$5.15 \cdot 10^{-14}$	$2.34 \cdot 10^{-4}$	1338.01	24.50
290	$4.14 \cdot 10^{-14}$	$1.92 \cdot 10^{-4}$	1347.81	24.11
300	$3.34 \cdot 10^{-14}$	$1.59 \cdot 10^{-4}$	1358.51	23.74
310	$2.71 \cdot 10^{-14}$	$1.32 \cdot 10^{-4}$	1367.80	23.35
320	$2.21 \cdot 10^{-14}$	$1.10 \cdot 10^{-4}$	1376.74	22.96
330	$1.81 \cdot 10^{-14}$	$9.25 \cdot 10^{-5}$	1385.24	22.57
340	$1.49 \cdot 10^{-14}$	$7.79 \cdot 10^{-5}$	1392.61	22.17
350	$1.23 \cdot 10^{-14}$	$6.59 \cdot 10^{-5}$	1401.28	21.80
360	$1.02 \cdot 10^{-14}$	$5.60 \cdot 10^{-5}$	1409.97	21.44
370	$8.55 \cdot 10^{-15}$	$4.78 \cdot 10^{-5}$	1415.91	21.05

Height h	Density ρ	Pressure p	Temperature T	Molecular weight M
km	g/m^3	dyne/cm^2	°K	g/mol
380	$7.16 \cdot 10^{-15}$	$4.10 \cdot 10^{-5}$	1423.66	20.70
390	$6.03 \cdot 10^{-15}$	$3.52 \cdot 10^{-5}$	1430.46	20.35
400	$5.09 \cdot 10^{-15}$	$3.04 \cdot 10^{-5}$	1436.16	20.00
410	$4.32 \cdot 10^{-15}$	$2.63 \cdot 10^{-5}$	1444.26	19.70
420	$3.68 \cdot 10^{-15}$	$2.29 \cdot 10^{-5}$	1451.09	19.40
430	$3.15 \cdot 10^{-15}$	$2.00 \cdot 10^{-5}$	1456.45	19.10
440	$2.70 \cdot 10^{-15}$	$1.74 \cdot 10^{-5}$	1461.72	18.82
450	$2.33 \cdot 10^{-15}$	$1.53 \cdot 10^{-5}$	1465.97	18.55
460	$2.01 \cdot 10^{-15}$	$1.34 \cdot 10^{-5}$	1469.84	18.30
470	$1.75 \cdot 10^{-15}$	$1.18 \cdot 10^{-5}$	1471.54	18.05
480	$1.52 \cdot 10^{-15}$	$1.05 \cdot 10^{-5}$	1474.15	17.84
490	$1.33 \cdot 10^{-15}$	$9.20 \cdot 10^{-6}$	1474.15	17.68
500	$1.17 \cdot 10^{-15}$	$8.20 \cdot 10^{-6}$	1474.15	17.48
510	$1.02 \cdot 10^{-15}$	$7.28 \cdot 10^{-6}$	1474.15	17.18
520	$8.92 \cdot 10^{-16}$	$6.48 \cdot 10^{-6}$	1474.15	16.87
530	$7.88 \cdot 10^{-16}$	$5.78 \cdot 10^{-6}$	1474.15	16.64
540	$6.94 \cdot 10^{-16}$	$5.16 \cdot 10^{-6}$	1474.15	16.46
550	$6.15 \cdot 10^{-16}$	$4.62 \cdot 10^{-6}$	1474.15	16.31
560	$5.45 \cdot 10^{-16}$	$4.14 \cdot 10^{-6}$	1474.15	16.13
570	$4.85 \cdot 10^{-16}$	$3.71 \cdot 10^{-6}$	1474.15	16.00
580	$4.32 \cdot 10^{-16}$	$3.34 \cdot 10^{-6}$	1474.15	15.88
590	$3.87 \cdot 10^{-16}$	$3.00 \cdot 10^{-6}$	1474.15	15.79
600	$3.45 \cdot 10^{-16}$	$2.70 \cdot 10^{-6}$	1474.15	15.70
610	$3.09 \cdot 10^{-16}$	$2.43 \cdot 10^{-6}$	1474.15	15.56
620	$2.76 \cdot 10^{-16}$	$2.19 \cdot 10^{-6}$	1474.15	15.42
630	$2.47 \cdot 10^{-16}$	$1.98 \cdot 10^{-6}$	1474.15	15.27
640	$2.22 \cdot 10^{-16}$	$1.79 \cdot 10^{-6}$	1474.15	15.16
650	$2.00 \cdot 10^{-16}$	$1.62 \cdot 10^{-6}$	1474.15	15.10
660	$1.80 \cdot 10^{-16}$	$1.47 \cdot 10^{-6}$	1474.15	14.97
670	$1.62 \cdot 10^{-16}$	$1.33 \cdot 10^{-6}$	1474.15	14.86
680	$1.45 \cdot 10^{-16}$	$1.21 \cdot 10^{-6}$	1474.15	14.74
690	$1.32 \cdot 10^{-16}$	$1.10 \cdot 10^{-6}$	1474.15	14.70
700	$1.19 \cdot 10^{-16}$	$1.00 \cdot 10^{-6}$	1474.15	14.62
710	$1.07 \cdot 10^{-16}$	$9.10 \cdot 10^{-7}$	1474.15	14.42
720	$9.70 \cdot 10^{-17}$	$8.29 \cdot 10^{-7}$	1474.15	14.34
730	$8.77 \cdot 10^{-17}$	$7.56 \cdot 10^{-7}$	1474.15	14.22
740	$7.95 \cdot 10^{-17}$	$6.90 \cdot 10^{-7}$	1474.15	14.12
750	$7.22 \cdot 10^{-17}$	$6.31 \cdot 10^{-7}$	1474.15	14.02
760	$6.59 \cdot 10^{-17}$	$5.77 \cdot 10^{-7}$	1474.15	13.99
770	$6.00 \cdot 10^{-17}$	$5.28 \cdot 10^{-7}$	1474.15	13.93
780	$5.49 \cdot 10^{-17}$	$4.83 \cdot 10^{-7}$	1474.15	13.92
790	$5.02 \cdot 10^{-17}$	$4.42 \cdot 10^{-7}$	1474.15	13.92
800	$4.60 \cdot 10^{-17}$	$4.05 \cdot 10^{-7}$	1474.15	13.88

APPENDIX 2

TABLE OF THE FUNCTIONS $H(h)$, $F(h)$, $\varphi(h)$, $k(h)$, AND $\Phi(h)$ FOR CIRA 1961

Height h, km	Scale height H, km	F $\dfrac{m^3}{kg \cdot sec^2}$ s. d.	φ $\dfrac{m^3}{kg \cdot sec^2}$ $\dfrac{s. d.}{km}$	$k \cdot 10^3$	Φ $\dfrac{m^3}{kg \cdot sec^2}$ s. d.
100	5.5	$1.3 \cdot 10^{-5}$	$2.3 \cdot 10^{-6}$	1.30	1.30
110	6.5	$8.4 \cdot 10^{-5}$	$1.18 \cdot 10^{-5}$	1.64	6.03
120	7.5	$3.30 \cdot 10^{-4}$	$4.57 \cdot 10^{-5}$	1.67	21.9
130	9.5	$1.36 \cdot 10^{-3}$	$1.60 \cdot 10^{-4}$	1.96	68.4
140	13	$3.83 \cdot 10^{-3}$	$3.63 \cdot 10^{-4}$	2.43	128
150	19	$8.94 \cdot 10^{-3}$	$6.59 \cdot 10^{-4}$	3.12	197
160	28	0.0171	$1.00 \cdot 10^{-3}$	3.93	251
170	31	0.0289	$1.35 \cdot 10^{-3}$	4.93	318
180	33	0.0441	$1.69 \cdot 10^{-3}$	5.99	387
190	35	0.0642	$2.35 \cdot 10^{-3}$	6.26	525
200	37	0.0912	$3.07 \cdot 10^{-3}$	6.78	674
210	38	0.127	$4.00 \cdot 10^{-3}$	7.21	869
220	39	0.172	$5.18 \cdot 10^{-3}$	7.57	1110
230	40	0.231	$6.63 \cdot 10^{-3}$	7.92	1410
240	41	0.306	$8.51 \cdot 10^{-3}$	8.16	1790
250	42	0.402	0.0107	8.49	2240
260	43	0.523	0.0136	8.69	2810
270	44	0.676	0.0171	8.93	3500
280	45	0.868	0.0214	9.14	4340
290	46	1.11	0.0266	9.37	5350
300	47	1.40	0.0330	9.58	6570
310	48	1.77	0.0406	9.80	8020
320	49	2.22	0.0497	10.0	9750
330	51	2.77	0.0607	10.2	$1.17 \cdot 10^4$
340	52	3.44	0.0736	10.4	$1.41 \cdot 10^4$
350	53	4.26	0.0892	10.6	$1.69 \cdot 10^4$
360	54	5.23	0.107	10.9	$2.02 \cdot 10^4$
370	56	6.41	0.128	11.1	$2.37 \cdot 10^4$
380	57	7.81	0.153	11.4	$2.81 \cdot 10^4$
390	58	9.48	0.181	11.6	$3.32 \cdot 10^4$
400	60	11.5	0.215	11.8	$3.89 \cdot 10^4$
410	61	13.8	0.253	12.1	$4.53 \cdot 10^4$
420	62	16.5	0.297	12.3	$5.26 \cdot 10^4$
430	64	19.7	0.346	12.6	$6.08 \cdot 10^4$

Height h, km	Scale height H, km	Auxiliary functions			
		F $\dfrac{m^3}{kg \cdot sec^2}$ s. d.	φ $\dfrac{m^3}{kg \cdot sec^2} \dfrac{s. d.}{km}$	$k \cdot 10^8$	Φ $\dfrac{m^3}{kg \cdot sec^2}$ s. d.
440	66	23.5	0.404	12.8	$7.03 \cdot 10^4$
450	67	27.8	0.467	13.1	$8.03 \cdot 10^4$
460	69	32.9	0.541	13.3	$9.22 \cdot 10^4$
470	71	38.7	0.621	13.6	$1.05 \cdot 10^5$
480	72	45.3	0.715	13.9	$1.20 \cdot 10^5$
490	73	52.9	0.816	14.2	$1.36 \cdot 10^5$
500	75	61.7	0.927	14.5	$1.53 \cdot 10^5$
510	76	71.6	1.06	14.7	$1.74 \cdot 10^5$
520	77	83.0	1.21	14.9	$1.98 \cdot 10^5$
530	79	95.9	1.37	15.2	$2.22 \cdot 10^5$
540	80	111	1.56	15.4	$2.50 \cdot 10^5$
550	82	127	1.76	15.6	$2.79 \cdot 10^5$
560	84	146	1.98	15.9	$3.13 \cdot 10^5$
570	86	167	2.23	16.2	$3.48 \cdot 10^5$
580	87	190	2.50	16.5	$3.88 \cdot 10^5$
590	89	217	2.78	16.8	$4.30 \cdot 10^5$
600	90	246	3.12	17.0	$4.80 \cdot 10^5$
610	91	279	3.48	17.2	$5.35 \cdot 10^5$
620	92	316	3.90	17.4	$5.95 \cdot 10^5$
630	92	357	4.35	17.6	$6.64 \cdot 10^5$
640	93	403	4.84	17.8	$7.38 \cdot 10^5$
650	94	454	5.37	18.1	$8.16 \cdot 10^5$
660	94	511	5.96	18.3	$9.06 \cdot 10^5$
670	95	574	6.61	18.5	$1.01 \cdot 10^6$
680	96	643	7.39	18.6	$1.12 \cdot 10^6$
690	96	721	8.11	18.8	$1.23 \cdot 10^6$
700	97	806	8.99	19.0	$1.36 \cdot 10^6$
710	98	901	9.99	19.1	$1.51 \cdot 10^6$
720	99	1006	11.0	19.3	$1.66 \cdot 10^6$
730	101	1122	12.2	19.5	$1.82 \cdot 10^6$
740	103	1250	13.4	19.7	$1.99 \cdot 10^6$
750	105	1390	14.8	19.8	$2.16 \cdot 10^6$
760	107	1545	16.2	20.1	$2.36 \cdot 10^6$
770	109	1714	17.7	20.3	$2.56 \cdot 10^6$
780	111	1900	19.4	20.6	$2.79 \cdot 10^6$
790	113	2102	21.2	20.8	$3.02 \cdot 10^6$
800	115	2323	23.1	21.1	$3.28 \cdot 10^6$

APPENDIX 3

TABLE OF THE FUNCTIONS $\phi\,(e_0)$, $\phi_1\,(e_0)$, AND $\phi_2\,(e_0)$

e_0	ψ	ψ_1	ψ_2
0	0	0	0
0.001	$1.665 \cdot 10^{-5}$	$7.509 \cdot 10^{-4}$	$1.668 \cdot 10^{-5}$
0.002	$4.474 \cdot 10^{-5}$	$1.504 \cdot 10^{-3}$	$4.481 \cdot 10^{-5}$
0.003	$8.220 \cdot 10^{-5}$	$2.258 \cdot 10^{-3}$	$8.241 \cdot 10^{-5}$
0.004	$1.266 \cdot 10^{-4}$	$3.014 \cdot 10^{-3}$	$1.270 \cdot 10^{-4}$
0.005	$1.769 \cdot 10^{-4}$	$3.772 \cdot 10^{-3}$	$1.777 \cdot 10^{-4}$
0.006	$2.326 \cdot 10^{-4}$	$4.532 \cdot 10^{-3}$	$2.338 \cdot 10^{-4}$
0.007	$2.932 \cdot 10^{-4}$	$5.293 \cdot 10^{-3}$	$2.949 \cdot 10^{-4}$
0.008	$3.583 \cdot 10^{-4}$	$6.056 \cdot 10^{-3}$	$3.607 \cdot 10^{-4}$
0.009	$4.276 \cdot 10^{-4}$	$6.821 \cdot 10^{-3}$	$4.308 \cdot 10^{-4}$
0.010	$5.009 \cdot 10^{-4}$	$7.588 \cdot 10^{-3}$	$5.050 \cdot 10^{-4}$
0.011	$5.780 \cdot 10^{-4}$	$8.356 \cdot 10^{-3}$	$5.833 \cdot 10^{-4}$
0.012	$6.586 \cdot 10^{-4}$	$9.126 \cdot 10^{-3}$	$6.652 \cdot 10^{-4}$
0.013	$7.428 \cdot 10^{-4}$	$9.898 \cdot 10^{-3}$	$7.509 \cdot 10^{-4}$
0.014	$8.303 \cdot 10^{-4}$	$1.067 \cdot 10^{-2}$	$8.400 \cdot 10^{-4}$
0.015	$9.210 \cdot 10^{-4}$	$1.145 \cdot 10^{-2}$	$9.326 \cdot 10^{-4}$
0.016	$1.015 \cdot 10^{-3}$	$1.222 \cdot 10^{-2}$	$1.028 \cdot 10^{-3}$
0.017	$1.112 \cdot 10^{-3}$	$1.300 \cdot 10^{-2}$	$1.127 \cdot 10^{-3}$
0.018	$1.211 \cdot 10^{-3}$	$1.378 \cdot 10^{-2}$	$1.230 \cdot 10^{-3}$
0.019	$1.314 \cdot 10^{-3}$	$1.457 \cdot 10^{-2}$	$1.335 \cdot 10^{-3}$
0.020	$1.419 \cdot 10^{-3}$	$1.535 \cdot 10^{-2}$	$1.443 \cdot 10^{-3}$
0.021	$1.527 \cdot 10^{-3}$	$1.614 \cdot 10^{-2}$	$1.554 \cdot 10^{-3}$
0.022	$1.638 \cdot 10^{-3}$	$1.693 \cdot 10^{-2}$	$1.668 \cdot 10^{-3}$
0.023	$1.751 \cdot 10^{-3}$	$1.772 \cdot 10^{-2}$	$1.785 \cdot 10^{-3}$
0.024	$1.867 \cdot 10^{-3}$	$1.851 \cdot 10^{-2}$	$1.905 \cdot 10^{-3}$
0.025	$1.985 \cdot 10^{-3}$	$1.930 \cdot 10^{-2}$	$2.027 \cdot 10^{-3}$
0.026	$2.107 \cdot 10^{-3}$	$2.010 \cdot 10^{-2}$	$2.152 \cdot 10^{-3}$
0.027	$2.229 \cdot 10^{-3}$	$2.089 \cdot 10^{-2}$	$2.280 \cdot 10^{-3}$
0.028	$2.355 \cdot 10^{-3}$	$2.169 \cdot 10^{-2}$	$2.410 \cdot 10^{-3}$
0.029	$2.483 \cdot 10^{-3}$	$2.249 \cdot 10^{-2}$	$2.543 \cdot 10^{-3}$
0.030	$2.613 \cdot 10^{-3}$	$2.329 \cdot 10^{-2}$	$2.678 \cdot 10^{-3}$
0.031	$2.745 \cdot 10^{-3}$	$2.410 \cdot 10^{-2}$	$2.817 \cdot 10^{-3}$
0.032	$2.879 \cdot 10^{-3}$	$2.490 \cdot 10^{-2}$	$2.957 \cdot 10^{-3}$
0.033	$3.016 \cdot 10^{-3}$	$2.571 \cdot 10^{-2}$	$3.100 \cdot 10^{-3}$
0.034	$3.155 \cdot 10^{-3}$	$2.652 \cdot 10^{-2}$	$3.245 \cdot 10^{-3}$
0.035	$3.296 \cdot 10^{-3}$	$2.733 \cdot 10^{-2}$	$3.393 \cdot 10^{-3}$
0.036	$3.439 \cdot 10^{-3}$	$2.814 \cdot 10^{-2}$	$3.543 \cdot 10^{-3}$
0.037	$3.584 \cdot 10^{-3}$	$2.896 \cdot 10^{-2}$	$3.695 \cdot 10^{-3}$
0.038	$3.731 \cdot 10^{-3}$	$2.978 \cdot 10^{-2}$	$3.850 \cdot 10^{-3}$
0.039	$3.880 \cdot 10^{-3}$	$3.060 \cdot 10^{-2}$	$4.007 \cdot 10^{-3}$
0.040	$4.031 \cdot 10^{-3}$	$3.142 \cdot 10^{-2}$	$4.167 \cdot 10^{-3}$
0.041	$4.184 \cdot 10^{-3}$	$3.224 \cdot 10^{-2}$	$4.328 \cdot 10^{-3}$
0.042	$4.339 \cdot 10^{-3}$	$3.306 \cdot 10^{-2}$	$4.492 \cdot 10^{-3}$
0.043	$4.496 \cdot 10^{-3}$	$3.389 \cdot 10^{-2}$	$4.659 \cdot 10^{-3}$

e	ψ	ψ_1	ψ_2
0.044	$4.654 \cdot 10^{-3}$	$3.471 \cdot 10^{-2}$	$4.827 \cdot 10^{-3}$
0.045	$4.815 \cdot 10^{-3}$	$3.554 \cdot 10^{-2}$	$4.998 \cdot 10^{-3}$
0.046	$4.978 \cdot 10^{-3}$	$3.638 \cdot 10^{-2}$	$5.171 \cdot 10^{-3}$
0.047	$5.142 \cdot 10^{-3}$	$3.721 \cdot 10^{-2}$	$5.346 \cdot 10^{-3}$
0.048	$5.308 \cdot 10^{-3}$	$3.804 \cdot 10^{-2}$	$5.523 \cdot 10^{-3}$
0.049	$5.476 \cdot 10^{-3}$	$3.888 \cdot 10^{-2}$	$5.703 \cdot 10^{-3}$
0.050	$5.646 \cdot 10^{-3}$	$3.972 \cdot 10^{-2}$	$5.884 \cdot 10^{-3}$
0.051	$5.817 \cdot 10^{-3}$	$4.056 \cdot 10^{-2}$	$6.068 \cdot 10^{-3}$
0.052	$5.991 \cdot 10^{-3}$	$4.140 \cdot 10^{-2}$	$6.254 \cdot 10^{-3}$
0.053	$6.166 \cdot 10^{-3}$	$4.224 \cdot 10^{-2}$	$6.442 \cdot 10^{-3}$
0.054	$6.343 \cdot 10^{-3}$	$4.309 \cdot 10^{-2}$	$6.632 \cdot 10^{-3}$
0.055	$6.521 \cdot 10^{-3}$	$4.394 \cdot 10^{-2}$	$6.825 \cdot 10^{-3}$
0.056	$6.701 \cdot 10^{-3}$	$4.479 \cdot 10^{-2}$	$7.019 \cdot 10^{-3}$
0.057	$6.883 \cdot 10^{-3}$	$4.564 \cdot 10^{-2}$	$7.216 \cdot 10^{-3}$
0.058	$7.067 \cdot 10^{-3}$	$4.649 \cdot 10^{-2}$	$7.414 \cdot 10^{-3}$
0.059	$7.252 \cdot 10^{-3}$	$4.735 \cdot 10^{-2}$	$7.615 \cdot 10^{-3}$
0.060	$7.439 \cdot 10^{-3}$	$4.820 \cdot 10^{-2}$	$7.818 \cdot 10^{-3}$
0.061	$7.628 \cdot 10^{-3}$	$4.906 \cdot 10^{-2}$	$8.022 \cdot 10^{-3}$
0.062	$7.818 \cdot 10^{-3}$	$4.992 \cdot 10^{-2}$	$8.229 \cdot 10^{-3}$
0.063	$8.010 \cdot 10^{-3}$	$5.078 \cdot 10^{-2}$	$8.438 \cdot 10^{-3}$
0.064	$8.204 \cdot 10^{-3}$	$5.165 \cdot 10^{-2}$	$8.649 \cdot 10^{-3}$
0.065	$8.399 \cdot 10^{-3}$	$5.251 \cdot 10^{-2}$	$8.862 \cdot 10^{-3}$
0.066	$8.595 \cdot 10^{-3}$	$5.338 \cdot 10^{-2}$	$9.077 \cdot 10^{-3}$
0.067	$8.794 \cdot 10^{-3}$	$5.425 \cdot 10^{-2}$	$9.294 \cdot 10^{-3}$
0.068	$8.993 \cdot 10^{-3}$	$5.512 \cdot 10^{-2}$	$9.513 \cdot 10^{-3}$
0.069	$9.195 \cdot 10^{-3}$	$5.600 \cdot 10^{-2}$	$9.734 \cdot 10^{-3}$
0.070	$9.398 \cdot 10^{-3}$	$5.687 \cdot 10^{-2}$	$9.957 \cdot 10^{-3}$
0.071	$9.602 \cdot 10^{-3}$	$5.775 \cdot 10^{-2}$	$1.018 \cdot 10^{-2}$
0.072	$9.809 \cdot 10^{-3}$	$5.863 \cdot 10^{-2}$	$1.041 \cdot 10^{-2}$
0.073	$1.002 \cdot 10^{-2}$	$5.951 \cdot 10^{-2}$	$1.064 \cdot 10^{-2}$
0.074	$1.023 \cdot 10^{-2}$	$6.039 \cdot 10^{-2}$	$1.087 \cdot 10^{-2}$
0.075	$1.044 \cdot 10^{-2}$	$6.128 \cdot 10^{-2}$	$1.110 \cdot 10^{-2}$
0.076	$1.065 \cdot 10^{-2}$	$6.216 \cdot 10^{-2}$	$1.134 \cdot 10^{-2}$
0.077	$1.086 \cdot 10^{-2}$	$6.305 \cdot 10^{-2}$	$1.157 \cdot 10^{-2}$
0.078	$1.108 \cdot 10^{-2}$	$6.394 \cdot 10^{-2}$	$1.181 \cdot 10^{-2}$
0.079	$1.129 \cdot 10^{-2}$	$6.483 \cdot 10^{-2}$	$1.205 \cdot 10^{-2}$
0.080	$1.151 \cdot 10^{-2}$	$6.573 \cdot 10^{-2}$	$1.230 \cdot 10^{-2}$
0.081	$1.173 \cdot 10^{-2}$	$6.662 \cdot 10^{-2}$	$1.254 \cdot 10^{-2}$
0.082	$1.195 \cdot 10^{-2}$	$6.752 \cdot 10^{-2}$	$1.279 \cdot 10^{-2}$
0.083	$1.218 \cdot 10^{-2}$	$6.842 \cdot 10^{-2}$	$1.304 \cdot 10^{-2}$
0.084	$1.240 \cdot 10^{-2}$	$6.932 \cdot 10^{-2}$	$1.329 \cdot 10^{-2}$
0.085	$1.262 \cdot 10^{-2}$	$7.022 \cdot 10^{-2}$	$1.354 \cdot 10^{-2}$
0.086	$1.285 \cdot 10^{-2}$	$7.113 \cdot 10^{-2}$	$1.380 \cdot 10^{-2}$
0.087	$1.308 \cdot 10^{-2}$	$7.204 \cdot 10^{-2}$	$1.405 \cdot 10^{-2}$
0.088	$1.331 \cdot 10^{-2}$	$7.294 \cdot 10^{-2}$	$1.431 \cdot 10^{-2}$
0.089	$1.354 \cdot 10^{-2}$	$7.386 \cdot 10^{-2}$	$1.457 \cdot 10^{-2}$

e_0	ψ	ψ_1	ψ_2
0.090	$1.377 \cdot 10^{-2}$	$7.477 \cdot 10^{-2}$	$1.484 \cdot 10^{-2}$
0.091	$1.401 \cdot 10^{-2}$	$7.568 \cdot 10^{-2}$	$1.510 \cdot 10^{-2}$
0.092	$1.424 \cdot 10^{-2}$	$7.660 \cdot 10^{-2}$	$1.537 \cdot 10^{-2}$
0.093	$1.448 \cdot 10^{-2}$	$7.752 \cdot 10^{-2}$	$1.563 \cdot 10^{-2}$
0.094	$1.472 \cdot 10^{-2}$	$7.844 \cdot 10^{-2}$	$1.590 \cdot 10^{-2}$
0.095	$1.496 \cdot 10^{-2}$	$7.936 \cdot 10^{-2}$	$1.618 \cdot 10^{-2}$
0.096	$1.520 \cdot 10^{-2}$	$8.028 \cdot 10^{-2}$	$1.645 \cdot 10^{-2}$
0.097	$1.544 \cdot 10^{-2}$	$8.121 \cdot 10^{-2}$	$1.673 \cdot 10^{-2}$
0.098	$1.569 \cdot 10^{-2}$	$8.214 \cdot 10^{-2}$	$1.701 \cdot 10^{-2}$
0.099	$1.593 \cdot 10^{-2}$	$8.307 \cdot 10^{-2}$	$1.729 \cdot 10^{-2}$
0.100	$1.618 \cdot 10^{-2}$	$8.400 \cdot 10^{-2}$	$1.757 \cdot 10^{-2}$

e_0	ψ	ψ_1	e_0	ψ	ψ_1	e_0	ψ	ψ_1
0.10	0.01618	0.08402	0.41	0.1583	0.4768	0.72	0.5535	1.168
0.11	0.01872	0.09340	0.42	0.1655	0.4935	0.73	0.5773	1.198
0.12	0.02140	0.1030	0.43	0.1729	0.5104	0.74	0.6025	1.230
0.13	0.02421	0.1128	0.44	0.1805	0.5277	0.75	0.6292	1.260
0.14	0.02715	0.1228	0.45	0.1883	0.5452	0.76	0.6576	1.294
0.15	0.03022	0.1331	0.46	0.1964	0.5632	0.77	0.6879	1.328
0.16	0.03341	0.1435	0.47	0.2048	0.5814	0.78	0.7202	1.362
0.17	0.03674	0.1540	0.48	0.2134	0.5998	0.79	0.7548	1.398
0.18	0.04018	0.1648	0.49	0.2223	0.6188	0.80	0.7921	1.435
0.19	0.04376	0.1760	0.50	0.2315	0.6380	0.81	0.8323	1.472
0.20	0.04746	0.1872	0.51	0.2410	0.6574	0.82	0.8758	1.512
0.21	0.05129	0.1986	0.52	0.2508	0.6774	0.83	0.9232	1.551
0.22	0.05525	0.2103	0.53	0.2610	0.6976	0.84	0.9750	1.593
0.23	0.05934	0.2222	0.54	0.2715	0.7184	0.85	1.032	1.636
0.24	0.06355	0.2343	0.55	0.2824	0.7394	0.86	1.095	1.682
0.25	0.06791	0.2466	0.56	0.2936	0.7606	0.87	1.165	1.728
0.26	0.07240	0.2592	0.57	0.3053	0.7826	0.88	1.244	1.776
0.27	0.07703	0.2720	0.58	0.3175	0.8048	0.89	1.333	1.827
0.28	0.08180	0.2850	0.59	0.3300	0.8274	0.90	1.436	1.881
0.29	0.08671	0.2982	0.60	0.3431	0.8505	0.91	1.555	1.936
0.30	0.09177	0.3117	0.61	0.3567	0.8740	0.92	1.697	1.996
0.31	0.09697	0.3254	0.62	0.3709	0.8980	0.93	1.868	2.061
0.32	0.1023	0.3393	0.63	0.3857	0.9226	0.94	2.080	2.130
0.33	0.1079	0.3536	0.64	0.4011	0.9476	0.95	2.353	2.205
0.34	0.1135	0.3681	0.65	0.4171	0.9732	0.96	2.724	2.289
0.35	0.1194	0.3828	0.66	0.4339	0.9992	0.97	3.267	2.384
0.36	0.1254	0.3978	0.67	0.4515	1.026	0.98	4.181	2.496
0.37	0.1316	0.4131	0.68	0.4699	1.053	0.99	6.247	2.643
0.38	0.1380	0.4286	0.69	0.4893	1.081	1.00	∞	3.0
0.39	0.1446	0.4444	0.70	0.5096	1.109			
0.40	0.1515	0.4605	0.71	0.5309	1.138			

APPENDIX 4

TABLE OF THE FUNCTIONS $F_l (v)$ $(l=1, 2, 3, 4)$

v	F_1	F_2	F_3	F_4
0	1	1	∞	∞
0.1	0.998	1	27.838	15.007
0.2	0.995	1.005	10.847	7.538
0.3	0.989	1.011	6.480	5.056
0.4	0.980	1.020	4.613	3.825
0.5	0.969	1.031	3.607	3.093
0.6	0.956	1.044	2.991	2.611
0.7	0.941	1.060	2.582	2.271
0.8	0.924	1.078	2.293	2.021
0.9	0.905	1.098	2.081	1.830
1.0	0.885	1.120	1.919	1.680
1.1	0.863	1.144	1.792	1.560
1.2	0.840	1.170	1.692	1.462
1.3	0.815	1.198	1.610	1.382
1.4	0.790	1.227	1.543	1.315
1.5	0.764	1.258	1.487	1.258
1.6	0.737	1.291	1.440	1.210
1.7	0.710	1.324	1.400	1.169
1.8	0.683	1.360	1.366	1.133
1.9	0.656	1.396	1.336	1.102
2.0	0.629	1.433	1.310	1.075

v	F_3	F_4	v	F_3	F_4	v	F_3	F_4
2.0	1.310	1.075	3.4	1.143	0.897	4.8	1.093	0.844
2.1	1.288	1.051	3.5	1.138	0.892	4.9	1.090	0.842
2.2	1.268	1.030	3.6	1.133	0.886	5.0	1.088	0.839
2.3	1.251	1.012	3.7	1.128	0.881	5.1	1.086	0.837
2.4	1.235	0.995	3.8	1.124	0.877	5.2	1.084	0.835
2.5	1.221	0.980	3.9	1.120	0.872	5.3	1.082	0.833
2.6	1.209	0.967	4.0	1.116	0.869	5.4	1.080	0.832
2.7	1.198	0.955	4.1	1.113	0.865	5.5	1.078	0.830
2.8	1.188	0.944	4.2	1.109	0.861	5.6	1.077	0.828
2.9	1.178	0.935	4.3	1.106	0.858	5.7	1.075	0.826
3.0	1.170	0.926	4.4	1.103	0.855	5.8	1.074	0.825
3.1	1.163	0.918	4.5	1.100	0.852	5.9	1.072	0.824
3.2	1.156	0.910	4.6	1.098	0.849	6.0	1.071	0.822
3.3	1.149	0.904	4.7	1.095	0.846	6.1	1.070	0.821

ν	F_3	F_4	ν	F_3	F_4	ν	F_3	F_4
6.2	1.068	0.819	7.5	1.055	0.806	8.8	1.046	0.797
6.3	1.067	0.818	7.6	1.054	0.805	8.9	1.046	0.796
6.4	1.066	0.817	7.7	1.054	0.804	9.0	1.045	0.796
6.5	1.065	0.816	7.8	1.053	0.803	9.1	1.045	0.795
6.6	1.064	0.814	7.9	1.052	0.802	9.2	1.044	0.794
6.7	1.063	0.813	8.0	1.051	0.802	9.3	1.044	0.794
6.8	1.062	0.812	8.1	1.051	0.801	9.4	1.043	0.793
6.9	1.061	0.811	8.2	1.050	0.801	9.5	1.043	0.793
7.0	1.060	0.810	8.3	1.049	0.800	9.6	1.042	0.792
7.1	1.059	0.810	8.4	1.049	0.799	9.7	1.042	0.792
7.2	1.058	0.808	8.5	1.048	0.799	9.8	1.041	0.791
7.3	1.057	0.808	8.6	1.048	0.798	9.9	1.041	0.791
7.4	1.056	0.806	8.7	1.047	0.797	10.0	1.040	0.790

BIBLIOGRAPHY

1. WATSON, G. N. *A Treatise on the Theory of Bessel Functions.* — Cambridge. 1944.

2. DUBOSHIN, G. N. Nebesnaya mekhanika (Celestial Mechanics). — Fizmatgiz. 1963.

3. DUBOSHIN, G. N. Nebesnaya mekhanika. Analiticheskie i kachestvennye metody (Celestial Mechanics — Analytical and Qualitative Methods). — Izdatel'stvo Nauka. 1964.

4. DUBOSHIN, G. N. Teoriya priyazheniya (Theory of Potential). — Fizmatgiz. 1961.

5. DUBOSHIN, G. N. and D. E. OKHOTSIMSKII. *Nekotorye problemy astrodinamiki i nebesnoi mekhaniki* (Some Problems of Astrodynamics and Celestial Mechanics). — Kosmicheskie Issledovaniya, Vol. 1, No. 2. 1963.

6. ZHONGOLOVICH, I. D. Vneshnee gravitatsionnoe pole Zemli i fundamental'nye postoyannye, svyazannye s nim (External Gravitational Field of the Earth and Some Related Fundamental Constants). — Trudy Instituta Teoreticheskoi Astronomii AN SSSR, No. 3. 1952.

7. ZHONGOLOVICH, I. D. Nekotorye formuly, otnosyashchiesya k dvizheniyu material'noi tochki i pole tyagoteniya urovennogo ellipsoida vrashcheniya (Some Formulas Pertaining to the Motion of a Point Mass in the Gravitational Field of a Level Ellipsoid of Revolution). — Byulleten' Instituta Teoreticheskoi Astronomii AN SSSR, Vol. 7, No. 7(90). 1960.

8. IDEL'SON, N. I. Teoriya potentsiala i prilozheniya k voprosam geofiziki (Theory of Potential and Its Applications to Geophysics). — Gostekhizdat. 1932.

9. KAZAKOV, S. A. Kurs sfericheskoi astronomii (A Course of Spherical Astronomy). — Gostekhizdat. 1940.

10. KING-HELE, D. Artificial Satellites and Scientific Investigations. — [Russian translation. 1961.]

11. KISLIK, M. D. Analiz integralov dvizheniya iskusstvennogo sputnika v normal'nom gravitatsionnom pole Zemli (Analysis of the Integrals of Motion of an Artificial Satellite in the Normal Gravitational Field of the Earth). — In: "Iskusstvennye sputniki Zemli", No. 13. 1962.

12. KISLIK, M. D. Dvizhenie iskusstvennogo sputnika v normal'nom gravitatsionnom pole Zemli (Motion of an Artificial Satellite in the Normal Gravitational Field of the Earth). — In: "Iskusstvennye sputniki Zemli", No. 4. 1960.

13. KISLIK, M. D. Sfery vliyaniya bol'shikh planet i Luny (Effective Spheres of Attraction of the Major Planets and the Moon). — Kosmicheskie Issledovaniya, Vol. 2, No. 6. 1964.

14. KOLEGOV, G. A. Variatsii plotnosti verkhnei atmosfery (Density Variations in the Upper Atmosphere). — In: "Iskusstvennye sputniki Zemli", No. 4. 1960.

15. KOCHIN, N. E. Vektornoe ischislenie i nachala tenzornogo ischisleniya (Vector Analysis and Elements of Tensor Analysis). — Izdatel'stvo AN SSSR. 1961.

16. LANDSBERG, G. S. Optika (Optics). — Fizmatgiz. 1957.

17. LIDOV, M. L. Opredelenie plotnosti atmosfery po tormozheniyu pervykh iskusstvennykh sputnikov Zemli (Inference of Atmospheric Density from the Deceleration of First Artificial Earth Satellites). — In: "Iskusstvennye sputniki Zemli", No. 1. 1958.

18. LIDOV, M. L. Soprotivlenie neorientirovannogo tela pri dvizhenii v razrezhennom gaze (Aerodynamic Drag on a Nonoriented Body in a Rarefied Gas). — Izvestiya AN SSSR, geophys. series, No. 12. 1957.

19. LIDOV, M. L. Evolyutsiya orbit iskusstvennykh sputnikov planet pod deistviem gravitatsionnykh vozmushchenii vneshnikh tel (Evolution of Orbits of Artificial Planetary Satellites due to Gravitational Perturbations of External Bodies). — In: "Iskustvennye sputniki Zemli", No. 8. 1961.

20. MAROV, M. Ya. O Plotnosti verkhnei atmosfery v gody minimuma solnechnoi aktivnosti (Density of the Upper Atmosphere in Years of Minimum Solar Activity). — Kosmicheskie Issledovaniya, Vol. 2, No. 6. 1964.

21. MIKHAILOV, A. A. Kurs gravimetrii i teorii figury Zemli (A Course of Gravimetry and the Theory of Earth's Figure). — Izdatel'stvo Redbyuro GUGK pri SNK SSSR. 1939.

22. OKHOTSIMSKII, D. E., T. M. ENEEV, and G. P. TARATYNOVA. Opredelenie vremeni sushchestvovaniya iskusstvennogo sputnika Zemli i issledovanie vekovykh vozmushchenii ego orbity (Determination of Satellite Lifetime and a Study of Secular Orbit Perturbations). — Uspekhi Fizicheskikh Nauk, Vol. 63, No. 1a. 1957.

23. POLYAKHOVA, E. N. Svetovoe davlenie i dvizhenie sputnikov Zemli (Radiation Pressure and the Motion of Earth Satellites). — Byulleten' Instituta Teoreticheskoi Astronomii AN SSSR, Vol. 9, No. 1 (104). 1963.

24. POPOV, P. I. et al. Astronomiya (Astronomy). — Gostekhizdat. 1940.

25. RYZHIK, I. M. Tablitsy integralov, summ, ryadov i proizvedenii (Tables of Integrals, Sums, Series, and Products). — Gostekhizdat. 1948.

26. SUBBOTIN, M. F. Kurs nebesnoi mekhaniki (A Course of Celestial Mechanics), Vol. 1. — Gostekhizdat. 1933.

27. SUBBOTIN, M. F. Kurs Nebesnoi Mekhaniki (A Course of Celestial Mechanics), Vol. 3. — Gostekhizdat. 1949.

28. SUSLOV, G. K. Teoreticheskaya mekhanika (Theoretical Mechanics). — Gostekhizdat. 1946.

29. TARATYNOVA, G. P. Metody chislennogo resheniya uravnenii v konechnykh raznostyakh (Finite Difference Techniques of Numerical Solution of Equations). — In: "Iskusstvennye sputniki Zemli", No. 4. 1960.

30. FIKHTENGOL'TS, G. M. Osnovy matematicheskogo analiza (Elementary Calculus), Vol. 2. — Fizmatgiz. 1960.

31. CHARNYI, V. I. Ob izokhronnykh proizvodnykh (Time-Constant Derivatives). — In: "Iskusstvennye sputniki Zemli", No. 16. 1963.

32. CHEBOTAREV, G. A. Gravitatsionnye sfery bol'shikh planet, Luny i Solntsa (Gravitational Spheres of the Major Planets, the Moon, and the Sun). — Astronomicheskii Zhurnal, Vol. 10, No. 5. 1963.

33. KAULA, W. M. A Geoid and World Geodetic System Based on a Combination of Gravimetric, Astrogeodetic and Satellite Data. — Journal of Geophysical Research, Vol. 66, No. 6. 1961.

34. KOZAI, Y. Effects of Solar Radiation Pressure on the Motion of an Artificial Satellite. — Smithsonian Astrophys. Obs., Special Report 56. 1961.

35. MAY, B. R. The Estimation of Atmospheric Scale Heights from the Contraction of Satellites' Orbits. — Planetary and Space Science, Vol. 11, No. 6. 1963.

36. Report of the Preparatory Group for an International Reference Atmosphere. COSPAR Meeting in Florence, April, 1961.

SUBJECT INDEX

[1845]